The one-step function for discrete-time nonlinear switched singular systems

Sutrisno, Sutrisno; Trenn, Stephan

41^{st} Benelux Meeting on Systems and Control

July 5-7, 2022
Brussels, Belgium

Book of Abstracts

The 41st Benelux Meeting on Systems and Control is supported by

Alain Vande Wouwer, Michel Kinnaert, Emanuele Garone, Laurent Dewasme, and Guilherme A. Pimentel
Book of Abstracts 41st Benelux Meeting on Systems and Control

Université de Mons and Université Libre Bruxelles

A catalog record is available from Université de Mons.

Part 1
Programmatic Table of Contents

Tuesday, July 5, 2022

P0 UB5.132
Welcome and Opening

Chair:A. Vande Wouwer,M. Kinnaert 11.20-11.30

P1 UB5.132
Plenary 1 : Ilya Kolmanovsky
Perspectives, Challenges and Opportunities in Control of Systems with Constraints
Chair: Emanuele Garone 11.30-12.30

TuP01 UB5.132
System Theory 1
Chair: Wim Michiels 14:00-15:40

TuP01-1 **14:00-14:20**
Learning stability guarantees for data-driven constrained switching linear systems
Adrien Banse UCLouvain
Zheming Wang UCLouvain
Raphaël Jungers UCLouvain

TuP01-2 **14:20-14:40**
Stochastic Similarity Relations for Continuous State POMDPs
Maico H. W. Engelaar Eindhoven University of Technology
Sofie Haesaert Eindhoven University of Technology
Mircea Lazar Eindhoven University of Technology

TuP01-3 **14.40-15.00**
Controller-design for time-delay systems using TDS CONTROL
Pieter Appeltans KU Leuven
Haik Silm KU Leuven
Wim Michiels KU Leuven

TuP01-4 **15.00-15.20**
(γ,δ)-Conformance: A Notion of System Comparison
Armin Pirastehzad University of Groningen
Arjan van der Schaft University of Groningen
Bart Besselink University of Groningen

TuP01-5 **15.20-15.40**
Impulse-controllability of system classes of switched DAEs
Paul Wijnbergen University of Groningen
Stephan Trenn University of Groningen

TuP02 UB5.230
System Identification 1
Chair: John Lataire 14:00-15:40

TuP02-1 **14:00-14:20**
A square root filter for windowed recursive linear least squares regression
Ralf Peeters Maastricht University
Joël Karel Maastricht University
Pietro Bonizzi Maastricht University

TuP02-2 **14:20-14.40**
Learning separable decompositions of MIMO nonlinear systems
Koen Tiels Eindhoven University of Technology
Maciej Filinski Wroclaw University of Science and Technology
Pawel Wachel Wroclaw University of Science and Technology

TuP02-3 **14.40-15.00**
Data-driven modelling of unsteady fluid dynamics
Joshua A. Foster Vrije Universiteit Brussel
Jan Decuyper Vrije Universiteit Brussel
Tim De Troyer Vrije Universiteit Brussel
Mark C. Runacres

TuP02-4 **15.00-15.20**
Nonlinear System Identification Based on Linear Parameter-Varying Approximations by Gaussian Process in the Frequency Domain
Sadegh Ebrahimkhani Vrije Universiteit Brussel, Pleinlaan 2, Brussels, Belgium
John Lataire Vrije Universiteit Brussel, Pleinlaan 2, Brussels, Belgium

TuP02-5 **15.20-15.40**
Visualization of MIMO Uncertainty Structures for Robust Control
Paul Tacx Eindhoven University of Technology
Tom Oomen Eindhoven University of Technology

TuP03 UB4.132
Energy 1
Chair: Luis Daniel Couto 14:00-15.40

TuP03-1 **14:00-14:20**

Development of physics based control-oriented models for the heat exhaust in fusion power plants

Jesse Koenders DIFFER
Matthijs van Berkel DIFFER
Gijs Derks DIFFER
Holger Reimerdes, Egbert Westerhof

TuP03-2 **14:20-14.40**

On designing MPC controller with obstacle avoidance for a Parallel SCARA robot

Taranjitsingh Singh Flanders Make
Christophe Lauwerys Flanders Make
Quentin Docquier Flanders Make
Branimir Mrak

TuP03-3 **14.40-15.00**

A consensus approach to balancing the capacitor voltage for modular multilevel converters

Victor Daniel Reyes Dreke Eindhoven University of Technology
Mircea Lazar Eindhoven University of Technology

TuP03-4 **15.00-15.20**

Detection and Isolation of Small Faults in Lithium-Ion Batteries via the Asymptotic Local Approach

Luis D. Couto Universite libre de Bruxelles
John M. Reniers University of Oxford
David A. Howey University of Oxford
Michel Kinnaert

TuP03-5 **15.20-15.40**

Charge and Balance of a String of Li-ion Cells An Explicit Reference Governor approach

Alejandro Goldar Davila Université libre de Bruxelles
Emanuele Garone Université libre de Bruxelles

TuP04 UB4.136
Robotics 1
Chair: Matthias Pezzutto 14:00-15:40

TuP04-1 **14:00-14:20**

Point-to-point trajectory generation and control for vibration reduction of swinging products

Robbert van der Kruk Eindhoven University of Technology

TuP04-2 **14:20-14.40**

Collision-free Source Seeking Control of Unicycle Robot under Uncertain Environment

Tinghua Li University of Groningen
Bayu Jayawardhana University of Groningen

TuP04-3 **14.40-15.00**

A Hybrid-System Formalism to Verify Properties of Robot Swarms

Guillermo Legarda Herranz Université libre de Bruxelles
Emanuele Garone Université libre de Bruxelles
Mauro Birattari Université libre de Bruxelles

TuP04-4 **15.00-15:20**

Safe human-robot collaboration in mixed teams

Elise Verhees Eindhoven University of Technology
René van de Molengraft Eindhoven University of Technology
Michel Reniers Eindhoven University of Technology
Elena Torta

TuP04-5 **15.20-15.40**

Trajectory optimization of a high speed pick and place unit using soft switching multiple model predictive control

Babak Mehdizadeh Gavgani Ghent University
Arash Farnam Ghent University
Foeke Vanbecelaere Ghent University
Jeroen D. M. De Kooning, Guillaume Crevecoeur

TuP05 UB2.147
Koopman Operator - Deep Learning
Chair: Maarten Schoukens 14:00-15:40

TuP05-1 **14:00-14:20**

Deep Learning-based Identification of Koopman Models with Inputs

Lucian Cristian Iacob Eindhoven University of Technology
Gerben Izaak Beintema Eindhoven University of Technology
Maarten Schoukens Eindhoven University of Technology
Roland Tóth

TuP05-2 **14:20-14.40**

Constructing a Lyapunov function for nonlinear systems via the Koopman operator approach

Christian Mugisho Zagabe University of Namur
Alexandre Mauroy University of Namur

TuP05-3 **14.40-15.00**

Continuous-time system identification by deep subspace encoders

Gerben I. Beintema Eindhoven University of Technology
Roland Tóth TU/e and SZTAKI
Maarten Schoukens Eindhoven University of Technology

TuP05-4 **15.00-15.20**

Learning-Based Model-Augmentation of Nonlinear Approximative Models using the Sub-Space Encoder

Chris Verhoek Eindhoven University of Technology
Gerben Beintema Eindhoven University of Technology
Sofie Haesaert Eindhoven University of Technology
Maarten Schoukens and Roland Tóth

TuP05-5 **15.20-15.40**

Learning-based augmentation of mechatronic system models by deep subspace encoders

András Retzler KU Leuven
Gerben Izaak Beintema Eindhoven University of Technology
Maarten Schoukens Eindhoven University of Technology
Roland Tóth, Jan Swevers, Zsolt Kollár

TuP06 UB4.151
State Observers 1
Chair: Mihaela Sbarciog 14:00-15.40

TuP06-1 **14:00-14:20**

Sensor Data Fusion as an Alternative for Monitoring Oxychlorides in Electrochlorination Applications

E.A. Ross Wageningen University and Research
R.M. Wagterveld Wetsus
M. Mayer EasyMeasure
J.D. Stigter, B. Højris, Y. Li, K.J. Keesman

TuP06-2 **14:20-14.40**

Observability-Based Optimal Sensor Placement in Hydraulic Fluid Transport Networks

Caspar Geelen Wageningen University
Doekle Yntema Wetsus
Jaap Molenaar Wageningen University
Karel Keesman

TuP06-3 **14.40-15.00**

Joint Parameter and State Estimation: A Supervisory Multi-Observer Approach

Tomas Meijer Eindhoven University of Technology
Victor Dolk Eindhoven University of Technology
Michelle Chong Eindhoven University of Technology
Romain Postoyan, Bram de Jager, Dragan Nešić, Maurice Heemels

TuP06-4 **15.00-15.20**

Event-Based Estimation for POMDPs: Application to Remote Estimation in Precision Farming

R.M. Beumer Eindhoven University of Technology
M.J.G. van de Molengraft Eindhoven University of Technology
D.J. Antunes Eindhoven University of Technology

TuP06-5 **15.20-15.40**

A Multiple Observer Approach to Cyber-Attack Detection

Twan Keijzer Delft University of Technology
Riccardo M.G. Ferrari Delft University of Technology

TuP07 UA4.222
Optimization 1
Chair: Jan Swevers 14:00-15.40

TuP07-1 **14:00-14:20**

Exploiting Symbolic Linearization to Implement the Sequential Convex Quadratic Programming Method

Alejandro Astudillo MECO Research Team - KU Leuven
Joris Gillis MECO Research Team - KU Leuven
Moritz Diehl University of Freiburg
Wilm Decré, Goele Pipeleers, Jan Swevers

TuP07-2 **14:20-14.40**

Multiway data regression using a spline-type tensor decomposition

Raphaël Widdershoven KU Leuven
Lieven De Lathauwer KU Leuven
Nithin Govindarajan KU Leuven
Nico Vervliet, Martijn Boussé

TuP07-3 **14.40-15.00**

Online Unit Commitment Problem Solving using Dynamic Programming

Wim Van Roy KU Leuven
Joris Gillis KU Leuven
Goele Pipeleers KU Leuven
Jan Swevers

TuP07-4 **15.00-15.20**

An adaptive restart heavy-ball projected primal-dual method for solving constrained linear quadratic optimal control problems

Y.J.J. Heuts Eindhoven University of Technology
G.P. Padilla Eindhoven University of Technology
M.C.F. Donkers Eindhoven University of Technology

TuP07-5 **15.20-15.40**

E-Drive Specification Using Multi-fidelity Scalable Models

Olaf Borsboom Eindhoven University of Technology
Mauro Salazar Eindhoven University of Technology
Theo Hofman Eindhoven University of Technology

TuE01 UB5.132
Med. Bio Sys. 1
Chair: Simon Van Mourik 16.10-18.10

TuE01-1 **16.10-16.30**

A modular elementary flux mode reduction procedure for dynamic metabolic modelling

Maxime Maton University of Mons (FPMs)
Philippe Bogaerts University of Brussels
Alain Vande Wouwer University of Mons (FPMs)

TuE01-2 **16.30-16.50**

A general ODE-based model to describe pest populations dynamics

Nicolas Bono Rossello Université Libre de Bruxelles
Luca Rossini Università degli Studi della Tuscia
Stefano Speranza Università degli Studi della Tuscia
Emanuele Garone

TuE01-3 **16.50-17.10**

Control by state feedback of an age-dependent epidemiological model

Candy Sonveaux University of Namur
Joseph J. Winkin University of Namur

TuE01-4 **17.10-17.30**

Global Sensitivity Analysis of a Microkinetic Model of the Oxygen Evolution Reaction

Bart van den Boorn 1DIFFER - Dutch Institute for Fundamental Energy Research
Anja Bieberle-Hutter
Matthijs van Berkel

TuE01-5 **17.30-17.50**

The Effect of Vaccination and Human Behaviour in Epidemic Models

Kathinka Frieswijk University of Groningen
Lorenzo Zino University of Groningen
Ming Cao University of Groningen

TuE01-6 **17.50-18.10**

Optimising Photosynthetic Induction to control supplemental greenhouse lighting

Dominique Joubert Wagenignen University & Research
J.D. Stigter Wagenignen University & Research

TuE02 UB5.230
Data Driven Techniques
Chair: John Lataire 16.10-18.10

TuE02-1 **16.10-16.30**

Data-driven distributionally robust control of partially observable jump linear systems

Mathijs Schuurmans KU Leuven
Panagiotis Patrinos KU Leuven

TuE02-2 **16.30-16.50**

Spatio-temporal decoupling for system identification using SVD and recurrent neural networks

Carlos Jose Gonzalez Rojas TUe
Leyla Ozkan TUe
Mateus Dias Ribeiro German Aerospace Center

TuE02-3 **16.50-17.10**

Data-based batch process model using principle component analysis and Gaussian process regression

Maarten Vlaswinkel Eindhoven University of Technology
Bram de Jager Eindhoven University of Technology
Frank Willems Eindhoven University of Technology

TuE02-4 **17.10-17.30**

Data-driven tuning of rational feedforward controllers for noncommutative MIMO systems

Maurice Poot Eindhoven University of Technology
Jim Portegies Eindhoven University of Technology
Tom Oomen Eindhoven University of Technology

TuE02-5 **17.30-17.50**

Data-driven distributionally robust MPC for constrained stochastic systems

Peter Coppens KU Leuven
Panagiotis Patrinos KU Leuven

TuE02-6 **17.50-18.10**

Data–driven rate–based integral predictive control with estimated prediction matrices

P. C. N. Verheijen Eindhoven University of Technology
G. R. Goncalves da Silva
M. Lazar

TuE03 UB4.132
Process Control
Chair: Laurent Dewasme 16.10-18.10

TuE03-1 **16.10-16.30**

Control of Simulated Moving Bed Chromatographic Processes

Valentin P. Chernev University of Mons
Alain Vande Wouwer University of Mons
Achim Kienle Otto von Guericke University, Magdeburg
Lino de Oliveira Santos

TuE03-2 **16.30-16.50**

Improving hoist ergonomics by retrofitting automatic controllers

Joram Meskens Flanders Make
Abdellatif Bey-Temsamani Flanders Make
Bruno Depraetere Flanders Make

TuE03-3 **16.50-17.10**

Determination of Residence Time Distribution in Continuous Manufacturing line using data driven modeling

Pau Lapiedra Carrasquer KU Leuven
Carlos Andre Munoz KU Leuven
Satyajeet S. Bhonsale KU Leuven
Liang Li, Jan F.M. Van Impe

TuE03-4 **17.10-17.30**

Crystallization kinetics inference using Gaussian process regression

Michiel Busschaert KU Leuven
Steffen Waldherr KU Leuven

TuE03-5 **17.30-17.50**

A simulation-based method for design space exploration

Nick Paape Eindhoven University of Technology
Joost van Eekelen Eindhoven University of Technology
Michel Reniers Eindhoven University of Technology

TuE03-6 **17.50-18.10**

Real-time passenger-centric timetable scheduling for railway networks: A distributed control method

Xiaoyu Liu Delft University of Technology
Azita Dabiri
Bart De Schutter

TuE04 UB4.136
Learning-Based Control 1
Chair: Tom Oomen 16.10-18.30

TuE04-1 **16.10-16.30**

Learning constitutive laws in engineering systems

Sarvin Moradi Eindhoven University of Technology
Nick Jaensson Eindhoven University of Technology
Roland Toth Eindhoven University of Technology
Maarten Schoukens

TuE04-2 **16.30-16.50**

Total Energy Shaping with Neural Interconnection and Damping Assignment - Passivity Based Control

Santiago Sanchez-Escalonilla Plaza University of Groningen
Rodolfo Reyes-Baez University of Groningen
Bayu Jayawardhana University of Groningen

TuE04-3 **16.50-17.10**

On feedforward control using physics-guided neural networks: Training cost regularization and optimized training

Max Bolderman Eindhoven University of Technology
Mircea Lazar Eindhoven University of Technology
Hans Butler Eindhoven University of Technology

TuE04-4 **17.10-17.30**

Neural networks for motion feedforward: control-relevant training and non-causality

Leontine Aarnoudse Eindhoven University of Technology
Johan Kon Eindhoven University of Technology
Wataru Ohnishi The University of Tokyo
Maurice Poot, Paul Tacx, Nard Strijbosch, Tom Oomen

TuE04-5 **17.30-17.50**

Bridging Dynamic Neural Networks and Optimal Control

Edward Kikken Flanders Make
Bruno Depraetere Flanders Make
Jeroen Willems Flanders Make

TuE04-6 **17.50-18.10**
Combined MPC and reinforcement learning controller for traffic signal control in urban traffic networks
Dingshan Sun Delft University of Technology
Anahita Jamshidnejad
Bart De Schutter

TuE04-7 **18.10-18.30**
Learning-based Model Matching for Fault Detection and Isolation of Nonlinear Systems
Farhad Ghanipoor Eindhoven University of Technology
Carlos Murguia Eindhoven University of Technology
Nathan van de Wouw Eindhoven University of Technology
Peyman Mohajerin Esfahani

TuE05 UB2.147
System Theory 2
Chair: Joseph Winkin 16.10-18.10

TuE05-1 **16.10-16.30**
Consistency of behavioural assume-guarantee contracts
Brayan M. Shali University of Groningen
Arjan van der Schaft University of Groningen
Bart Besselink University of Groningen

TuE05-2 **16.30-16.50**
H infinity distributed synchronising controller for Euler-Lagrangian multi-agents under communication time-delay
Arash Farnam Ghent University
Babak Mehdizadeh Gavgani Ghent University
Guillaume Crevecoeur Ghent University

TuE05-3 **16.50-17.10**
Extended differential balancing for nonlinear systems
Arijit Sarkar University of Groningen, The Netherlands
Jacquelien M.A. Scherpen University of Groningen, The Netherlands

TuE05-4 **17.10-17.30**
Multirate Performance Quantification using Time-Lifting and Local Polynomial Modeling
Max van Haren Eindhoven University of Technology
Lennart Blanken Eindhoven University of Technology and Sioux Technologies
Tom Oomen Eindhoven University of Technology and Delft University of Technology

TuE05-5 **17.30-17.50**
Least-squares globally optimal misfit modelling for SISO systems
Sibren Lagauw KU Leuven
Bart De Moor KU Leuven

TuE05-6 **17.50-18.10**
Globally optimal least-squares misfit identification of multidimensional autonomous systems
Lukas Vanpoucke KU Leuven
Bart De Moor KU Leuven

TuE06 UB4.151
Vehicles 1
Chair: Alain Vande Wouwer 16.10-18.30

TuE06-1 **16.10-16.30**
S-drone: a novel aerial robotic swarm hardware
SINAN OGUZ ULB
Mary Katherine Heinrich ULB
Michael Allwright ULB

TuE06-2 **16.30-16.50**
Distributed MPC for mapping mission with multiple UAVs
Dora Novak Université Paris-Saclay
Alain Vande Wouwer University of Mons
Sihem Tebbani Université Paris-Saclay

TuE06-3 **16.50-17.10**
Implementation and Tests of an INDI Control Strategy with the Parrot Mambo Minidrone
Delansnay Gilles University of Mons
Vande Wouwer Alain University of Mons

TuE06-4 **17.10-17.30**
Multi-stage Optimal Motion Planning for Drone Racing
Mathias Bos KU Leuven
Wilm Decré KU Leuven
Jan Swevers KU Leuven
Goele Pipeleers

TuE06-5 **17.30-17.50**
MPC-based Imitation Learning for Autonomous Vehicles Lane Keeping from Human Demonstrations
Flavia Sofia Acerbo KU Leuven
Jan Swevers
Tinne Tuytelaars
Tong Duy Son

TuE06-6 **17.50-18.10**
Building avehicle digital twin for ADAS testing and control
Ludovico Ruga Siemens Digital Industries Software
Tong Duy Son Siemens Digital Industries Software
Theo geluk Siemens Digital Industries Software

TuE06-7 **18.10-18.30**
Implementation of collision avoidance for multi-UAVs system
Oscar Fabian Archila University of Mons/BTU
Alain Vande Wouwer University of Mons
Johannes Schiffer BTU Cottbus-Senftenberg

TuE07 UA4.222
Electromechanical Applications 1
Chair: Michel Kinnaert 16.10-18.30

TuE07-1 **16.10-16.30**
Modelling of a Primary Flight Electromechanical Actuator considering Temperature and Production Variability
Benjamin Wauthion Université Libre de Bruxelles
Michel Kinnaert Université Libre de Bruxelles
Paul Alexandre Société Anonyme Belge de Construction Aéronautique

TuE07-2 **16.30-16.50**
Control systems in Gravitational Wave detectors: A survey of the design challenges
Mathyn van Dael Eindhoven University of Technology, Nikhef
Gert Witvoet Eindhoven University of Technology, TNO
Bas Swinkels Nikhef
Tom Oomen

TuE07-3 **16.50-17.10**
Tool interoperability for efficient model-based system design
Sander Thuijsman Eindhoven University of Technology

TuE07-4 **17.10-17.30**
Hardware-in-the-loop testing for the Swalmen tunnel using automatically generated PLC code
Lars Moormann Eindhoven University Eindhoven
Asia van de Mortel-Fronczak Eindhoven University Eindhoven
Wan Fokkink Vrije Universiteit Amsterdam
Koos Rooda

TuE07-5 **17.30-17.50**
Non-collocated vibration suppression using delayed feedback
Haik Silm KU Leuven
Wim Michiels KU Leuven
Tomas Vyhlidal Czech Technical University in Prague

TuE07-6 **17.50-18.10**
A first hands-on mechatronics project for engineering students using active magnetic bearings
Laurens Jacobs KU Leuven
Jan Swevers KU Leuven
Goele Pipeleers KU Leuven

TuE07-7 **18.10-18.30**
Model based control of soft robots aiming for trajectory tracking
Mahboubeh Keyvanara Eindhoven University of Technology
Arman Goshtasbi University of Twente
Irene Kuling Eindhoven University of Technology

Wednesday, July 6, 2022

WeP01 UB5.132
Optimal Control 1
Chair: Emanuele Garone 9:00 - 11:00

WeP01-1 **9:00-9:20**
Hybrid Control Implementation Analysis based on the finite set model predictive control design
Shafaq Gul Ghent University, Member of Flanders Make
Frederik De Belie Ghent University, Member of Flanders Make

WeP01-2 **9:20-9:40**
Design Methods for Sampled-Data Systems
Luuk Spin Eindhoven University of Technology
Tijs Donkers Eindhoven University of Technology

WeP01-3 **9:40-10:00**
On the steady-state behavior of finite–control–set MPC with an application to high-precision switched amplifiers
Duo Xu Eindhoven University of Technology
Mircea Lazar Eindhoven University of Technology

WeP01-4 **10:00-10:20**
Data-driven distributionally robust iterative risk-constrained model predictive control
Alireza Zolanvari University of Groningen
Ashish Cherukuri University of Groningen

WeP01-5 **10:20-10:40**
Optimal Control and Design of Magnetic Spring-assisted Systems
Branimir Mrak Flanders Make
Jeroen Willems Flanders Make
Edward Kikken Flanders Make

WeP01-6 **10:40-11:00**
Identifying bang-bang type MPC using Support Vector Machines
Tony Dang Flanders Make
Frederik Debrouwere Flanders Make
Erik Hostens Flanders Make

WeP02 UB5.230
Interconnected Systems
Chair: Guilherme A. Pimentel 9:00 - 11:00

WeP02-1 **9:00-9:20**
Modelling Framework and Partitioning of Large-Scale Systems
Alessandro Riccardi Delft University of Technology
Luca Laurenti Delft University of Technology
Bart De Schutter Delft University of Technology

WeP02-2 **9:20-9:40**
Private Computation of Polynomials over Networks
Teimour Hosseinalizadeh University of Groningen
Fatih Turkmen University of Groningen
Nima Monshizadeh University of Groningen

WeP02-3 **9:40-10:00**
Abstracted Reduction of Interconnected Structural Models
Luuk Poort Eindhoven University of Technology
Rob Fey Eindhoven University of Technology
Bart Besselink University of Groningen
Nathan van de Wouw

WeP02-4 **10:00-10:20**
A priori error bounds for model reduction of interconnected systems
Lars Janssen Eindhoven University of Technology
Rob Fey Eindhoven University of Technology
Bart Besselink University of Groningen
Nathan van de Wouw

WeP02-5 **10:20-10:40**
Modelling of networks of memristords
Anne-Men Huijzer University of Groningen
Bart Besselink University of Groningen
Arjan van der Schaft University of Groningen

WeP02-6 **10:40-11:00**
Handling sensor and process noise in dynamic network identification
Stefanie Fonken Eindhoven University of Technology
Karthik Ramaswamy Eindhoven University of Technology
Paul Van den Hof Eindhoven University of Technology

WeP03 UB4.132
Nonlinear Control
Chair: Marcel Heertjes 9:00 - 11:00

WeP03-1 **9:00-9:20**
Nonlinear feedforward control for a class of tasks: A Gaussian Process approach applied to a printer
Max van Meer Eindhoven University of Technology
Maurice Poot Eindhoven University of Technology
Jim Portegies Eindhoven University of Technology

WeP03-2 **9:20-9:40**
Virtual systems in nonlinear control design
Rodolfo Reyes-Baez University of Groningen
Bayu Jayawardhana University of Groningen

WeP03-3 **9:40-10:00**
Analysis of Sampled-Data Hybrid Integrator-Gain-Based Control Systems
Bardia Sharif Eindhoven University of Technology
Marcel Heertjes Eindhoven University of Technology
Henk Nijmeijer Eindhoven University of Technology
Maurice Heemels

WeP03-4 **10:00-10:20**
Adaptive control without knowing what to adapt to
Rian Beck Flanders Make
Sudarsan Kumar Venkatesan Flanders Make
Bruno Depraetere Flanders Make

WeP03-5 **10:20-10:40**
Multi-layered simulation relations for linear stochastic systems
B.C. van Huijgevoort Eindhoven University of Technology
Sofie Haesaert Eindhoven University of Technology

WeP03-6 **10:40-11:00**
Implicit Fixed-Time ISS Safe CBFs
Ming Li TU/e
Zhiyong Sun Eindhoven University of Technology

WeP04 UB4.136
Learning-Based Control 2
Chair: Jan Swevers 9:00 - 11:00

WeP04-1 **9:00-9:20**
Learning-based Control for High-efficient PPC Engines with Gaussian Process
Wang Pan Eindhoven University of Technology
Frank Willems Eindhoven University of Technology

WeP04-2 **9:20-9:40**
Feedforward Control in the Presence of Input Nonlinearities: A Learning-based Approach
Jilles van Hulst Eindhoven University of Technology
Maurice Poot Eindhoven University of Technology
Jim Portegies Eindhoven University of Technology
Tom Oomen,Dragan Kostic and Kai Wa Yan

WeP04-3 **9:40-10:00**
MPC Informed Control via Neural Networks
Muhammed Bahadir Saltik University of Groningen
Bayu Jayawardhana University of Groningen
Ashish Cherukuri University of Groningen

WeP04-4 **10:00-10:20**
Iterative Learning Control based on Estimation and Control with Set-membership Uncertainty: ECOset-ILC.
Daniele Ronzani KU Leuven
Joris Gillis KU Leuven
Goele Pipeleers KU Leuven
Jan Swevers

WeP04-5 **10:20-10:40**
Reduction in calibration effort of diesel engine transient control by using LSTM-based methodology
Prasoon Garg Eindhoven University of Technology
Emilia Silvas Eindhoven University of Technology
Frank Willems Eindhoven University of Technology

WeP04-6 **10:40-11:00**
Safe Learning-Based Model Predictive Control
Filippo Airaldi Delft University of Technology
Bart De Schutter Delft University of Technology
Azita Dabiri Delft University of Technology

WeP05 UB2.147
Robotics 2
Chair: Bayu Jayawardhana 9:00 - 11:00

WeP05-1 **9:00-9:20**
Optimal motion planning sped up with LogSum-Exp for obstacle avoidance
Joris Gillis KU Leuven
Jan Swevers KU Leuven
Goele Pipeleers KU Leuven

WeP05-2 **9:20-9:40**
An adaptive MPC scheme for systems with variable topologies
Tony Dang Flanders Make
Taranjitsingh Singh Flanders Make
Frederik Debrouwere Flanders Make

WeP05-3 **9:40-10:00**
Reformulating Collision Avoidance Constraints for Multi-DOF Robotic Planning
Dries Dirckx KU Leuven
Jan Swevers KU Leuven
Wilm Decré KU Leuven
Goele Pipeleers

WeP05-4 **10:00-10:20**
Learning from demonstration for leader-follower robotic configurations
Busra Sen Eindhoven University of Technology
Elena Torta Eindhoven University of Technology
M.J.G. van de Molengraft Eindhoven University of Technology
Marco Alonso, Henry Stoutjesdijk

WeP05-5 **10:20-10:40**
Exploiting Plant Dynamics in Robotic Fruit Localization
Jordy Senden Eindhoven University of Technology
Lars Janssen Eindhoven University of Technology
Robbert van der Kruk Eindhoven University of Technology
Herman Bruyninckx, René van de Molengraft

WeP05-6 **10:40-11:00**
Remote Control of a Two-Wheeled Robot: Evidences from Experiments over Wi-Fi
Matthias Pezzutto University of Padova
Emanuele Garone Université Libre de Bruxelles

WeP06 UB4.151
Vehicles 2
Chair: Maarten Steinbuch 9:00 - 11:00

WeP06-1 **9:00-9:20**

Simulation-aided Verification of SLAM Algorithms

Anoosh Anjaneya Hegde Siemens Digital Industries Software
Michael Phillips Siemens Digital Industries Software
Herman Van der Auweraer Siemens Digital Industries Software
Tong Duy Son

WeP06-2 **9:20-9:40**

Hybrid Vehicle Models for Control of Evasive Maneuvers

Leila Gharavi Delft University of Technology
Bart De Schutter Delft University of Technology
Simone Baldi Southeast University

WeP06-3 **9:40-10:00**

Traffic control for AGVs on a grid layout

Karlijn Fransen Eindhoven University of Technology
Joost van Eekelen Eindhoven University of Technology
Michel Reniers Eindhoven University of Technology

WeP06-4 **10:00-10:20**

A Closed-Form Solution to Control Allocation in the Framework of Constrained Navigation of Autonomous Ships

Xavier Jordens Université libre de Bruxelles
Emanuele Garone Université libre de Bruxelles

WeP06-5 **10:20-10:40**

Motion planning and control for autonomous vehicles in lane merging scenarios

M.E. Geurts Eindhoven, University of Technology
E. Silvas Eindhoven, University of Technology
A. Katriniok Ford Research & Innovation Center
W.P.M.H. Heemels

WeP06-6 **10:40-11:00**

Safety Shell: Reducing performance-limits in autonomous vehicles

Caspar Hanselaar Eindhoven University of Technology
Emilia Silvas Eindhoven University of Technology / TNO
Andrei Terechko NXP Semiconductors N.V.
Maurice Heemels

WeP07 UA4.222

Optimization 2

Chair: Wilm Decré 9:00 - 11:00

WeP07-1 **9:00-9:20**

An online optimization approach to the random coordinate descent algorithm in open multi-agent systems

Charles Monnoyer de Galland UCLouvain
Renato Vizuete Université Paris-Saclay
Julien M. Hendrickx UCLouvain
Paolo Frasca, Elena Panteley

WeP07-2 **9:20-9:40**

Towards Memory-Optimal Traversal of Expression Graphs of Atomic Operations in CasADi

Alejandro Astudillo MECO Research Team - KU Leuven
Joris Gillis MECO Research Team - KU Leuven
Goele Pipeleers MECO Research Team - KU Leuven
Wilm Decré, Jan Swevers

WeP07-3 **9:40-10:00**

Extension of the Performance Estimation framework via a novel approach for convex interpolation

Anne Rubbens UCLouvain
Julien Hendrickx UCLouvain

WeP07-4 **10:00-10:20**

Towards Performance Estimation Problems on Quadratic Functions

N. Bousselmi Université catholique de Louvain
J. Hendrickx Université catholique de Louvain
F. Glineur Université catholique de Louvain

WeP07-5 **10:20-10:40**

Advances in Feasible SQP Methods for NMPC

David Kiessling KU Leuven
Jan Swevers KU Leuven
Moritz Diehl University of Freiburg
Joris Gillis

WeP07-6 **10:40-11:00**

Performance Estimation Problem for Decentralized Optimization Methods

Sebastien Colla UCLouvain
Julien M. Hendrickx UCLouvain

P2 UB5.132

Plenary lecture 2: David Howey

Data-driven battery health diagnosis in real-world applications

Chair:Michel Kinnaert 11:30-12:30

MC1 UB5.132

Mini-course 1: Mouhacine Benosman

A hybrid approach to control: classical control theory meets machine learning theory

Chair:Laurent Dewasme 14:00-15:30

WeE01 UB5.132

Optimal Control 2

Chair: Bojana Rosic 16:00 - 18:00

WeE01-1 **16:00-16:20**

On designing distributed consensus protocol for multi- Energy Storage Unit (ESU) system in a microgrid

Taranjitsingh Singh Flanders Make
Tony Dang Flanders Make
Frederik Debrouwere Flanders Make

WeE01-2 **16:20-16:40**

Industrial DC grids using MPC tweaked to be charge sustaining

Bruno Depraetere Flanders Make
Taranjitsingh Singh Flanders Make
Jeroen Willems Flanders Make

WeE01-3 **16:40-17:00**

Computing an FIR controller using an efficient iterative scheme

R. Haasjes University of Twente
A.P. Berkhoff 1. University of Twente & 2.TNO
B. Rosíc University of Twente

WeE01-4 **17:00-17:20**

Disturbance estimation to avoid the model mismatch effects in Model Predictive Control

Alvaro Florez KU Leuven
Jan Swevers KU Leuven

WeE01-5 **17:20-17:40**

Offset-free model predictive control of the electron density profile in a tokamak

T.O.S.J. Bosman DIFFER
M. van Berkel DIFFER
M.R. de Baar DIFFER

WeE01-6 **17:20-18:00**

Detecting floor surface changes using SNIS

Bastiaan Vandewal KU Leuven
Goele Pipeleers KU Leuven
Jan Swevers KU Leuven

WeE02 UB5.230

System Identification 2

Chair: Wouter Hakvoort 16:00 - 18:00

WeE02-1 **16:00-16:20**

A short review of finite-sample error analysis of linear system identification for control

Shengling Shi Delft University of Technology
Bart De Schutter Delft University of Technology

WeE02-2 **16:20-16:40**

Parameter estimation of multiple poles by subspace-based methods

Prabhu Vijayan KU Leuven
Mariya Ishteva KU Leuven
Ivan Markovsky VUB
Prabhu Vijayan

WeE02-3 **16:40-17:00**

Spectral network identification with generalized diffusive coupling

Marvyn Gulina University of Namur
Alexandre Mauroy University of Namur

WeE02-4 **17:00-17:20**

Sparse Learning In System Identification: Debiasing And Infinite-Dimensional Algorithms

M. Tolga Akan Eindhoven University of Technology
Mingzhou Yin ETH Zurich
Andrea Iannelli ETH Zurich
Mohammad Khosravi, ETH Zurich, Department of Information Technology and Electrical Engineering, khosravm@control.ee.ethz.ch

WeE02-5 **17:20-17:40**

Parameter estimation under periodic disturbances using the Maximum Likelihood algorithm

D.M.E. Kruijver University of Twente
W.B.J. Hakvoort University of Twente
M.A. Beijen DEMCON Advanced Mechatronics

WeE02-6 **17:40-18:00**

Identifying a highly nonlinear MIMO Volterra system including Bayesian confidence bounds in seconds on a laptop

Eva Memmel Delft University of Technology
Clara Menzen Delft University of Technology
Kim Batselier Delft University of Technology

WeE03 UB4.132
Med. Bio. Sys. 2
Chair: Karel Keesman 16:00 - 18:00

WeE03-1 **16:00-16:20**
Towards advanced model based control of bio-processes
Satyajeet S. Bhonsale KU Leuven
Wannes Mores KU Leuven
Jan F.M. Van Impe KU Leuven

WeE03-2 **16:20-16:40**
Assessment of microbial food safety risks due to climate change
Lydia Katsini KU Leuven
Satyajeet Bhonsale KU Leuven
Carlos Andre Munoz Lopez KU Leuven
Styliani Roufou, Sholeem Griffin, Vasilis Valdramidis, Simen Akkermans, Monika Polanska, Jan F.M. Van Impe

WeE03-3 **16:40-17:00**
Experimental modeling of a beer fermentation process
Jesús M. Zamudio Lara Université de Mons
Laurent Dewasme Université de Mons
Héctor Hernández Escoto Universidad de Guanajuato
Alain Vande Wouwer

WeE03-4 **17:00-17:20**
Towards large-scale observer design for Magnetic Resonance Thermometry in hyperthermia cancer treatments
Sven Nouwens TU eindhoven
Maarten Paulides TU eindhoven
Bram de Jager TU eindhoven
Maurice Heemels

WeE03-5 **17:20-17:40**
Patient-ventilator asynchrony detection in mechanical ventilation
Lars van de Kamp Eindhoven University of Technology
Joey Reinders Demcon Advanced Mechatronics
Bram Hunnekens Demcon Advanced Mechatronics
Nathan van de Wouw, Tom Oomen

WeE03-6 **17:40-18:00**
Dynamic model development for prediction of intracellular trehalose accumulation in baker's yeast
Antoine Huet ULB
Mihaela Sbarciog ULB
Philippe Bogaerts ULB

WeE04 UB4.136
Learning-Based Control 3
Chair: Bayu Jayawardhana 16:00 - 18:00

WeE04-1 **16:00-16:20**
Reinforcement learning for optimal control of linear systems with constraints via piecewise affine/quadratic approximation
Kanghui He Delft University of Technology
Ton van den Boom Delft University of Technology
Bart De Schutter Delft University of Technology

WeE04-2 **16:20-16:40**
Physics-Guided Neural Networks for Feedforward Control: An Orthogonal Projection-Based Approach
Johan Kon Eindhoven University of Technology
Marcel Heertjes Eindhoven University of Technology
Tom Oomen Eindhoven University of Technology
Dennis Bruijnen, Jeroen van de Wijdeven

WeE04-3 **16:40-17:00**
Simple Learning Control for Smooth Dog Clutch Engagements
Jeroen Willems Flanders Make
Stijn Goossens Dana Incorporated
Bruno Depraetere Flanders Make
Sorin Bengea

WeE04-4 **17:00-17:20**
Integrated optimization-based and learning-based control for PWA systems
Caio Fabio Oliveira da Silva Delft University of Technology
Azita Dabiri Delft University of Technology
Bart De Schutter Delft University of Technology

WeE04-5 **17:20-17:40**
Flexible learning with prior knowledge: iterative learning control with sampled-data characterized basis functions
Masahiro Mae The University of Tokyo
Max van Haren
Wataru Ohnishi
Tom Oomen, Hiroshi Fujimoto

WeE04-6 **17:40-18:00**

A Privacy Preserving Federated Learning Framework

Haleh Hayati Eindhoven University of Technology
Carlos Murguia

WeE05 UB2.147
Game Theory
Chair: Matthias Pezzutto 16:00 - 18:00

WeE05-1 **16:00-16:20**

Learning MPC for Interaction-Aware Autonomous Driving

Evens Brecht KU Leuven
Mathijs Schuurmans KU Leuven
Panagiotis Patrinos KU Leuven

WeE05-2 **16:20-16:40**

Stochastic stability of perturbed best-response dynamics for networked coordination games

Bo Jin University of Groningen
Ming Cao University of Groningen

WeE05-3 **16:40-17:00**

A passivity approach for consensus-based and rigid formation

Ningbo Li University of Groningen
Jacquelien Scherpen University of Groningen
A.J. van der Schaft University of Groningen
Zhiyong Sun

WeE05-4 **17:00-17:20**

Using dynamic norms to facilitate innovation diffusion in networks

Lorenzo Zino University of Groningen
Mengbin Ye Curtin University
Ming Cao University of Groningen

WeE05-5 **17:20-17:40**

Aggregating distributed energy resources for grid flexibility services A distributed game theoretic approach

Xiupeng Chen University of Groningen
Jacquelien M. A. Scherpen University of Groningen
Nima Monshizadeh University of Groningen

WeE05-6 **17:40-18:00**

Inverse Learning for Linear-quadratic Zero-sum Differential Games

Emin Martirosyan University of Groningen
Ming Cao University of Groningen

WeE06 UB4.151
Vehicles 3
Chair: Maarten Steinbuch 16:00 - 18:00

WeE06-1 **16:00-16:20**

Stochastic barrier functions for safety verification of autonomous vehicles and human agents

Frederik Baymler Mathiesen Delft University of Technology
Luca Laurenti Delft University of Technology
Simeon Calvert Delft University of Technology

WeE06-2 **16:20-16:40**

Sim2real for Autonomous Vehicle Control using Executable Digital Twin

Jean Pierre Allamaa Siemens Digital Industries Software and KU Leuven
Tong Duy Son Siemens Digital Industries Software
Panagiotis Patrinos KU Leuven
Herman Van der Auweraer

WeE06-3 **16:40-17:00**

Are we there yet? An Overview of Open Challenges in Trajectory Prediction for Autonomous Driving

M. Muñoz Sánchez Eindhoven University of Technology
E. SilvasEindhoven University of Technology and TNO
J. Elfring Eindhoven University of Technology and TomTom
R. van de Molengraft

WeE06-4 **17:00-17:20**

Link manipulation of mixed-vehicle cyclic platoon: A stability perspective

W. Jeong Gyeongsang National University
Y. Kim Gyeongsang National University
A. Vande Wouwer University of Mons

WeE06-5 **17:20-17:40**

Autonomous Driving of Articulated Vehicles at Distribution Centre

Viral Gosar Eindhoven University of Technology
Mohsen Alirezaei
I.J.M. Besselink

WeE06-6 **17:40-18:00**

The effect of varying demand on Breasśs paradox in traffic networks

Jasper Verbree University of Groningen
A.K. Cherukuri University of Groningen

WeE07 UA4.222
Optimization 3
Chair: Guilherme A. Pimentel 16:00 - 18:00

WeE07-1 **16:00-16:20**
Joint design and operation of an electric autonomous mobility-on-demand system
Fabio Paparella Eindhoven University of Technology
Theo Hofman Eindhoven University of Technology
Mauro Salazar Eindhoven University of Technology

WeE07-2 **16:20-16:40**
Tightening ambiguity sets characterizations for data-driven distributionally robust optimization
Lotfi Mustapha Chaouach TU Delft
Dimitris Boskos TU Delft
Tom Oomen TU Eindhoven and TU Delft

WeE07-3 **16:40-17:00**
A Pareto ellipsoids based algorithm for multi-objective optimisation under parametric uncertainty
Wannes Mores KU Leuven
Satyajeet S. Bhonsale KU Leuven
Ihab Hashem KU Leuven
Philippe Nimmegeers, Jan Van Impe

WeE07-4 **17:00-17:20**
Computational advantage for model predictive control by using multiprocessing libraries and artificial bee colony optimization
Jhonny Rodrigues Faculdade de Engenharia da Universidade do Porto
Alejandro Goldar Universitè libre de Bruxelles

WeE07-5 **17:20-17:40**
Alpaqa: A matrix-free solver for nonlinear MPC and large-scale nonconvex optimization
Pieter Pas KU Leuven
Mathijs Schuurmans KU Leuven
Panagiotis Patrinos KU Leuven

WeE07-6 **17:40-18:00**
Towards tight convergence rates of the gradient method on hypoconvex functions
Teodor Rotaru KU Leuven
François Glineur Université catholique de Louvain
Panagiotis Patrinos KU Leuven

IM UB5.132
In memoriam Rik Pintelon
John Lataire, Noël Hallemans, Dries Peumans
System Identification - a frequency domain approach
Chair: Michel Kinnaert 18:15-19:15

Thursday, July 7, 2022

MC2 UB5.132
Mini-course 2: Mouhacine Benosman
A hybrid approach to control: classical control theory meets machine learning theory
Chair: Laurent Dewasme 9:00-10:30

ThP01 UB5.132
Electromechanical Applications 2
Chair: Wouter Hakvoort 10:50 - 11:50

ThP01-1 **10:50-11:10**
Low frequency isolation of a six degrees of freedom platform using high precision inertial sensors
Mouhamad Haidar Lakkis ULg,ULB
Jennifer Watchi Université Libre de Bruxelles
Christophe Collette ULg,ULB
Rasa Jamshidi, Ameer Sider

ThP01-2 **11:10-11:30**
Wind farm power reserve for secondary frequency regulation through distributed yaw optimization
Younes Oudich Université Libre de Bruxelles
Michel Kinnaert Université Libre de Bruxelles
Frederik De Belie Ghent University

ThP01-3 **11:30-11:50**
On discretization of continuous-time LPV control solutions
Yorick Broens Eindhoven University of Technology
Hans Butler Eindhoven University of Technology
Roland Tóth Eindhoven University of Technology

ThP02 UB5.230
System Identification 3
Chair: Paul Van den Hof 10:50 - 11:50

ThP02-1 **10:50-11:10**

A frequency domain maximum likelihood Approach to Estimate Space-Dependent Parameters in heat and mass transport

Ricky van Kampen DIFFER
Siep Weiland Eindhoven University of Technology
Hans Zwart University of Twente
Matthijs van Berkel

ThP02-2 **11:10-11:30**

Flux fit method for estimating transport parameters in nuclear fusion reactors based on perturbation analysis

Jelle Slief DIFFER - Dutch Institute for Fundamental Energy Research
Ricky van Kampen DIFFER - Dutch Institute for Fundamental Energy Research
Matthijs van Berkel DIFFER - Dutch Institute for Fundamental Energy Research
Michael Brookman

ThP02-3 **11:30-11:50**

Subnetwork identification in diffusively coupled linear networks

E.M.M. (Lizan) Kivits Eindhoven University of Technology
Paul M.J. Van den Hof Eindhoven University of Technology

ThP03 UB4.132
Energy 2
Chair: Alejandro Goldar Davila 10:50 - 11:50

ThP03-1 **10:50-11:10**

Concurrent design of an electric fleet powertrain

Maurizio Clemente Eindhoven University of Technology
Mauro Salazar Eindhoven University of Technology
Theo Hofman Eindhoven University of Technology

ThP03-2 **11:10-11:30**

Modeling and State-Of-Health prediction of Lithium-Ion Batteries under dynamic, high-current Applications

Francis le Roux Eindhoven University of Technology
Ernst Ferg uYilo e-Mobility Programme
Theo van Niekerk Nelson Mandela University

ThP03-3 **11:30-11:50**

Combined cell-level estimation of state-of-charge and temperature in battery packs

Bjorn van de Ven Eindhoven University of Technology
Ron Sneijders Eindhoven University of Technology
Feye Hoekstra Eindhoven University of Technology
H.J. Bergveld, M.C.F. Donkers

ThP04 UB4.136
Mechatronics
Chair: Emanuele Garone 10:50 - 11:50

ThP04-1 **10:50-11:10**

Tuning the stability margin for passivity-based controllers for standard mechanical systems

Carmen Chan-Zheng University of Groningen
Pablo Borja TU Delft
Jacquelien M.A. Scherpen University of Groningen

ThP04-2 **11:10-11:30**

On Robust Fault Diagnosis of Complex Mechatronic Systems

Koen Classens Eindhoven University of Technology
Maurice Heemels Eindhoven University of Technology
Tom Oomen Eindhoven University of Technology

ThP04-3 **11:30-11:50**

A Saturation-Aware Trajectory-Based Explicit Reference Governor for a Robotic Manipulator

Michele Ambrosino Université libre de Bruxelles
Andres Cotorruelo Université libre de Bruxelles
Emanuele Garone Université libre de Bruxelles

ThP05 UB2.147
Vibration
Chair: Michel Kinnaert 10:50 - 11:50

ThP05-1 **10:50-11:10**

Spectrum optimization of time-delay systems applied to non-collocated vibration suppression

Adrian Saldanha KU Leuven
Haik Silm KU Leuven
Wim Michiels KU Leuven
Tomas Vyhlidal

ThP05-2 **11:10-11:30**

Constrained Optimal System Design for Active Vibration Isolation Systems

Sil Spanjer University of Twente
Wouter Hakvoort University of Twente

ThP05-3 **11:30-11:50**

Active Metamaterial Vibration Suppression in Flexure Mechanisms

Bram Seinhorst University of Twente
Wouter Hakvoort University of Twente

ThP06 UB4.151
State Observers 2
Chair: Joseph Winkin 10:50 - 11:50

ThP06-1 **10:50-11:10**

On a sliding mode observer for a reaction-convection-diffusion model

Mohet Judicaël University of Namur and naXys
Hastir Anthony University of Namur and naXys
Habib Dimassi University of Sousse
Joseph J. Winkin, Alain Vande Wouwer

ThP06-2 **11:10-11:30**

Sampling-free Linear Iterative Bayesian Updating of Non-linear Model States

Wouter van Dijk University of Twente
W.B.J. Hakvoort University of Twente
B. Rosic University of Twente

ThP06-3 **11:30-11:50**

Real-time fault estimation for a class of discrete-time linear parameter-varying systems

Chris van der Ploeg Eindhoven University of Technology
Emilia Silvas Eindhoven University of Technology
Nathan van de Wouw Eindhoven University of Technology
Peyman Mohajerin Esfahani

ThP07 UA4.222
Switched Systems
Chair: Bojana Rosic 10:50 - 11:50

ThP07-1 **10:50-11:10**

On contraction analysis of switched systems with mixed contracting-noncontracting modes via mode-dependent average dwell time

Hao Yin University of Groningen
Bayu Jayawardhana University of Groningen
Stephan Trenn University of Groningen
H. Yin

ThP07-2 **11:10-11:30**

Efficient Abstraction of Switched Stochastic Systems driven by Neural Networks

Steven Adams TU Delft
Luca Laurenti TU Delft
Morteza Lahijanian University of Colorado Boulder

ThP07-3 **11:30-11:50**

The one-step function for discrete-time nonlinear switched singular systems

Sutrisno University of Groningen
Stephan Trenn University of Groningen

P3 UB5.132
Plenary Lecture: Nicanor Quijano
The Role of Population Games and Evolutionary Dynamics in Control
Chair: Alain Vande Wouwer 12:00-13:00

CL UB5.132

Announcement of the Best Junior Presentation Prize
Chair:A.Vande Wouwer,M.Kinnaert13:00-13:15

Part 2
Contributed Lectures

Plenary Lecture 1: Ilya Kolmanovsky

Title: Perspectives, Challenges and Opportunities in Control of Systems with Constraints
Constraints represent bounds imposed on system state, output and control signals that must be satisfied during system operation. Examples of constraints include safety limits, comfort limits and obstacle avoidance requirements. Constraints are important considerations in many engineering systems such as aircraft, spacecraft and automotive vehicles. Achieving high performance in systems with constraints is challenging: The effective controllers must be nonlinear and often have to be based on prediction and optimization. The interest in handling computational (cyber-) constraints in addition to physical constraints has also been increasing concomitantly with the growing research in cyber-physical systems.

The speaker will present several perspectives on control of systems with constraints, drawn from his experience with the relevant theory and applications, and discuss the underlying challenges and opportunities. These include, in particular, the development of add-on schemes of various kind that could be augmented to the nominal system to protect it from constraint violation, the interplay between closed-loop stability, performance and computations in model predictive control, integration of constrained control and learning, and dealing with constraints in situations in which eventual constraint violation is unavoidable. Applications to spacecraft, aircraft and automotive systems will be considered throughout for illustration.

Short Biography: Professor Ilya V. Kolmanovsky has received his Ph.D. degree in Aerospace Engineering in 1995, his M.S. degree in Aerospace Engineering in 1993 and his M.A. degree in Mathematics in 1995, all from the University of Michigan, Ann Arbor. He is presently a full professor in the Department of Aerospace Engineering at the University of Michigan. Professor Kolmanovsky's research interests are in control theory for systems with state and control constraints, and in control applications to aerospace and automotive systems. Before joining the University of Michigan in January 2010, he was with Ford Research and Advanced Engineering in Dearborn, Michigan for close to 15 years. He is a Fellow of IEEE, an Associate Fellow of AIAA, a past recipient of the Donald P. Eckman Award of American Automatic Control Council, of 2002 and 2016 IEEE Transactions on Control Systems Technology Outstanding Paper Awards, of SICE Technology Award, of several technical achievement, innovation and publication awards of Ford Research and Advanced Engineering. His publication record includes over 200 journal articles, over 400 conference papers, 20 book chapters, 3 edited books, as well as 104 United States patents. He serves as a Senior Editor for IEEE Transactions on Control Systems Technology.

Plenary Lecture 2: David Howey

Title: Data-driven battery health diagnosis in real-world applications Accurate diagnostics and prognostics of battery health improves overall system performance. This allows industry to unlock value by detecting faults and improving maintenance and logistics, extending operational range, and understanding asset depreciation. However, battery aging is complex and caused by many interacting factors. Two key questions arise: first, how to handle modelling challenges, including parameter variability and nonlinearities, in methods for online estimation of state of health. Second, how to develop validated predictions of future health, where key issues include coping with variable usage scenarios, and cell-to-cell behavioural differences. This talk will discuss recent approaches to tackle some of these exciting topics, particularly focusing on diagnostics from field data, including the combining of non-parametric and parametric models to allow flexibility in model fitting from data, whilst retaining the benefits of equivalent circuit and physical models.

Short Biography: David Howey is Professor of Engineering Science at the University of Oxford, UK. He leads a group researching on modelling and control of energy storage systems, with a particular focus on Li-ion batteries for electric vehicles and grid/off-grid storage. He received the MEng degree in Electrical and Information Sciences from the University of Cambridge in 2002 and his PhD from Imperial College London in 2010. Since 2010 he has co-authored 80+ peer-reviewed journal and conference articles, and 5 patents. He is an editorial board member of IEEE Transactions on Industrial Informatics and the new OUP journal Oxford Open Energy, and is co-founder of the Oxford Battery Modelling Symposium. He is the recipient of recent funding from EPSRC, InnovateUK, UKRI, Faraday Institution, Continental AG and Siemens, and he co-leads control and estimation tasks in the Faraday Institution Multiscale Modelling project. Howey is also academic lead for the £40m Energy Superhub Oxford that is building a transmission connected 50 MWh hybrid battery. He previously led the Faraday Institution "UK EV and Battery Production Potential" project (with McKinsey), and was academic lead in InnovateUK projects on battery re-use (EP/P510737/1) and solar home systems in Africa (EP/R035822/1), and a $1.2m Korean project on microgrids, plus Co-I in EPSRC projects TRENDS, FUTURE vehicles, STABLE-NET and RHYTHM. Professor Howey is co-founder of Brill Power Ltd., a company spun-out of his lab in 2016 focused on advanced battery management system topologies. They have raised significant early stage funding and adopted several patents from his group. Howey also won a Samsung GRO Award on modelling leading to two R&D contracts and a multi-year collaboration, with results patented by Samsung Electronics.

Plenary Lecture 3: Nicanor Quijano

Title: The Role of Population Games and Evolutionary Dynamics in Control Recently, there has been in the control community an increasing interest in studying large-scale distributed systems (LSDS). Several techniques have been developed, wishing to address the main challenges found in LSDS. One way to approach this type of problems is to use game-theoretical methods. Game theory shares some common points with control systems problems, in particular of distributed topology, where the interconnection of different elements (agents) leads to a global behavior depending on the local interaction of these agents. Evolutionary game theory (EGT) is one type of dynamic games that has been used to design distributed controllers for different applications like control of water systems, charging of electric vehicles, and synchronization of isolated microgrids. The aim of this talk is to present and discuss relevant advances and analytical methodologies in population games and evolutionary dynamics, and its applications for solving control problems.

Short Biography: Nicanor Quijano (IEEE Senior Member) received his B.S. degree in Electronics Engineering from Pontificia Universidad Javeriana (PUJ), Bogotá, Colombia, in 1999. He received the M.S. and PhD degrees in Electrical and Computer Engineering from The Ohio State University, in 2002 and 2006, respectively. In 2007, he joined the Electrical and Electronics Engineering Department, Universidad de los Andes (UAndes), Bogotá, Colombia as an Assistant Professor. He is currently a Full Professor, the director of the research group in control and automation systems (GIAP, UAndes), and an associate editor for the IEEE Transactions on Control Systems Technology, the Journal of Modern Power Systems and Clean Energy, and Energy Systems. He has been a member of the Board of Governors of the IEEE Control Systems Society (CSS) for the 2014 period, and he was the chair of the IEEE CSS, Colombia for the 2011-2013 period. He has published more than 100 scientific papers (journal papers, international conference papers, book chapters), he has co-advised the best European PhD thesis in the control systems area in 2017, and he is the co-author of the best paper of the ISA Transactions, 2018. In 2021, he obtained the Experienced Research Award from the School of Engineering, UAndes. Currently his research interests include hierarchical and distributed network optimization methods for control using learning, bio-inspired, and game-theoretical techniques for dynamic resource allocation problems, especially those in energy, water, agriculture, and transportation.

Mini-course: Mouhacine Benosman

Title: A hybrid approach to control: classical control theory meets machine learning theory Until recently, one could classify control approaches into two main paradigms. The first is the classical machine learning (ML) control paradigm that heavily relies on data, e.g., classical approximate dynamic programming (ADP), reinforcement learning (RL) methods, deep neural networks (DNN), and deep RL. The main advantages of these methods are efficiency and flexibility due to the increased availability of data and computation power. On the other hand, these methods lack performance guarantees, such us stability, boundedness of signals, a.k.a., safety, and general robustness.

The second paradigm is the classical control theory approach, which relies on dynamical systems theory, e.g., robust control theory, adaptive control theory, Lyapunov-based design, etc. In this case the pros and cons are somewhat reversed. Some examples of advantages of this paradigm include the rigor of mathematical analysis and the performance guarantees in term of stability, boundedness of signals, and robustness. However, one of the main disadvantages of this approach is the lack of flexibility or generalizability since the model of the system must satisfy very specific properties.

In the past 10 or so years, several efforts have attempted to merge these two paradigms. The result is what we refer to as Learning-based control methods. These methods use tools from classical control theory together with tools from ML theory. The aim is to design 'hybrid' learning-based controllers that take advantage of the flexibility of ML data-driven methods, while maintaining the stability, safety, and robustness guarantees from control theory.

This short course will concentrate on learning-based control methods. We first present recent results in the field of learning-based adaptive control, where classical model-based adaptive control methods are merged with data-driven estimation methods, e.g., extremum seeking control (ESC), Gaussian processes (GP) optimization, and reinforcement learning (RL). We then discuss some recent results on robust constrained model-based RL that use tools from nonlinear control theory to guarantee stability, robustness and safety. We will cover the main theoretical aspects of these approaches and finish the course with a few examples of industrial applications.

Short Biography: Before coming to Mitsubishi Electric Research Laboratories (MERL) in 2010, Mouhacine worked at universities in Reims University, France and Strathclyde University, Scotland, and the National University of Singapore. His research interests include modeling and control of flexible robotic manipulators, nonlinear robust and fault tolerant control, multi-agent control with applications to smart-grid and robotics, estimation and control of partial differential equations with applications to thermo-fluid models, learning-based adaptive control for nonlinear systems, and control-theory based optimization algorithms with application to machine learning. Mouhacine has published more than 50 peer-reviewed journal articles and conference papers, and has more than 20 patents in the field of mechatronics systems control. He is a senior member of the IEEE, Associate Editor of the Journal of Optimization Theory and Applications, Associate Editor of the Journal of Advanced Control for Applications, Associate Editor of the IEEE Control Systems Letters, and Senior Editor of the International Journal of Adaptive Control and Signal Processing.

In memoriam Rik Pintelon

John Lataire, Noël Hallemans, Dries Peumans

System Identification - a frequency domain approach. Prof. Rik Pintelon passed away last year in September 2021. He was an exceptional person, both from a scientific and from a human perspective. In this plenary talk, a selection of Rik's achievements as a person and as a scientist will be given, and on-going research work along the lines he initiated will be presented.

Rik played a key role in elevating frequency domain based system identification to a mature data-driven modelling tool. His work was highly recognised in the scientific community. He has been the recipient of the Joseph F. Keithley award in 2012 from the IEEE Instrumentation and Measurement society, he received the degree of Doctor of Science (DSc) from the University of Warwick where he has also been honorary professor from 2013 to 2018, and received multiple awards for publications including the 2008 IOP outstanding paper award in Measurement Science & Technology, the 2014 Martin Black prize in Physiological Measurement and the 2014 Andy Chi award in IEEE transactions on Instrumentation and Measurement.

Rik's work revolved around parametric and non-parametric identification of dynamic systems, with a very special attention to the estimation of uncertainties. Specifically, he played a leading and profound role in developing detection and quantification techniques of non-idealities – noise, nonlinear distortions and time-varying contributions – in Frequency Response Function measurement techniques. He successfully transferred this expertise to many colleagues and researchers in Belgium and across the globe, while remaining open minded and meticulous in his derivations.

Rik attached a warm attention to the human aspects of research and education. As the chairman of the Doctoral Committee at the Engineering Faculty of the VUB he vice-chaired between 30 and 40 PhD defenses per year, assessing the scientific integrity and the fair evaluations of the candidates. During that time, he instigated exemplary initiatives to improve and maintain the well-being of PhD researchers, amongst others by monitoring their educational and administrative load and equal chances, in all confidentiality.

Rik has been a role model to many of us, a great colleague and friend, always to be remembered.

Speakers Biography:

John Lataire (S'06–M'11) was born in Brussels, Belgium, in 1983. He received the Electrical Engineer degree in electronics and information processing and the Ph.D. degree in engineering sciences (Doctor in de Ingenieurswetenschappen) from the Vrije Universiteit Brussel, Brussels, in 2006 and 2011, respectively. From October 2007 to October 2011, he was on a Ph.D. fellowship from the Research Foundation—Flanders (FWO). Since August 2006, he has been working as a Researcher with the Department ELEC-VUB, Brussels. Dr. Lataire is the coauthor of more than 40 articles in refereed international journals. He received the 2008 IOP outstanding paper award (best paper in Measurement Science & Technology), the Best Junior Presentation Award 2010 at the 29th Benelux Meeting on Systems and Control, was the co-recipient of the 2014 Andy Chi award (best paper in IEEE Trans. on Instrumentation and Measurement), and was the recipient of the 2016 J. Barry Oakes Advancement Award (from the IEEE Instrumentation and Measurement society). His main interests include the frequency domain formulation of the identification of dynamic systems, with a specific focus on the identification of time-varying systems, and the use of kernel-based regression in system identification.

Noël Hallemans was born in Brussels in 1996. In 2019, he obtained his master's degree in Electrical Engineering with the highest distinction from both the Vrije Universiteit Brussel (VUB) and the Université Libre de Bruxelles (ULB). His master thesis dissertation, entitled 'Nonparametric

Identification of Linear Time-Varying Systems using Gaussian Processes', won that year's Brussels Engineering Alumni prize for best master thesis. Since September 2019 he has been working as a researcher with the ELEC department (VUB) under supervision of professors Rik Pintelon and John Lataire. His research focuses on frequency domain data-driven modelling of dynamical systems, in particular on the best linear time-varying approximations and kernel-based FRF estimators. Recently, he obtained an Eutopia grant for a scientific research stay at the University of Warwick, to apply these data-driven methods to energy storage devices.

Dries Peumans (Member, IEEE) was born in Brussels, Belgium, in 1992. He received the M.Sc. degree and the Ph.D. degree in Electrical Engineering (Electronics and Information Technology) from the Vrije Universiteit Brussel (VUB), Belgium, in 2015 and 2020, respectively. Since 2021, he is a postdoctoral researcher at the VUB and at the Advanced RF group of imec. Broadband characterization and modelling of mm-wave and sub-THz circuits and transceivers currently involve his research activities.

Tuesday - July 5, 2022
14:00 - 15:40 (TuP)

Learning stability guarantees for data-driven constrained switching linear systems

Adrien Banse, Zheming Wang, Raphaël Jungers
ICTEAM, Université Catholique de Louvain, Louvain-la-Neuve, Belgium
Email: adrien.banse@student.uclouvain.be,
{zheming.wang, raphael.jungers}@uclouvain.be

Introduction

We focus on stability analysis of *constrained switching linear systems* in which the dynamics are unknown and whose switching signal is constrained by an automaton. We propose a *data-driven* Lyapunov framework for providing probabilistic stability guarantees based on data harvested from observations of the system. Moreover, we show that the *entropy* of the language accepted by the automaton allows to bound the number of samples needed in order to reach some pre-specified accuracy.

1 Constrained switching linear systems

We consider discrete-time *switching linear systems* defined by a set $\mathscr{A} = \{A_i\}_{i\in\{1,\dots,m\}}$ of m matrices. Their dynamics, for any $t \in \mathbb{N}$, is given by the following equation:

$$x_{t+1} = A_{\sigma(t)} x_t. \tag{1}$$

A *constrained switching linear system* (*CSLS*) is a switching linear system with logical rules on its switching signal. We represent these rules by an *automaton* i.e., a strongly connected, directed and labelled graph $\mathscr{G}(V,E)$ with V the set of nodes and E the set of edges. The edge $(v,w,\sigma) \in E$ between two nodes $v,w \in V$ carries the *label* $\sigma \in \{1,\dots,m\}$, which maps to a mode of the switching system.

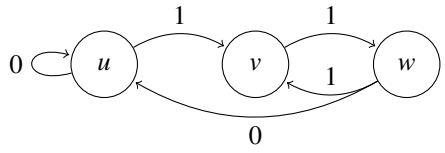

Figure 1: An automaton defined by two modes (0 and 1), and the following logical rule. If mode 1 is chosen, then it has to be chosen at least twice in a row.

The *constrained joint spectral radius* $\rho(\mathscr{G},\mathscr{A})$ of a given CSLS is defined as follows:

$$\rho(\mathscr{G},\mathscr{A}) = \lim_{t\to\infty} \max\{\|A_{\sigma(t-1)}\dots A_{\sigma(0)}\|^{1/t} : \sigma(0),\dots,\sigma(t-1) \text{ is accepted by } \mathscr{G}\}. \tag{2}$$

The stability of a CSLS defined by $\mathscr{A}$ and $\mathscr{G}$ is ruled by its constrained joint spectral radius. It is asymptitocally stable if and only if $\rho(\mathscr{G},\mathscr{A}) < 1$ (see [2], Corollary 2.8).

Finally, the *entropy* $h(\mathscr{G})$ of an automaton $\mathscr{G}$ is the growth rate of $|\mathscr{L}_{\mathscr{G},l}|$ where $\mathscr{L}_{\mathscr{G},l}$ is the language accepted by $\mathscr{G}$ restricted to length l (see [3], Definition 4.1.1). It is given by the equation

$$h(\mathscr{G}) = \lim_{l\to\infty} \frac{\log_2 |\mathscr{L}_{\mathscr{G},l}|}{l}. \tag{3}$$

2 Data-driven approach

In many practical applications, the engineer cannot rely on having a model, but rather has to analyse stability in a *data-driven* fashion. In this setting, we have acces to a set of observations $\omega_N = \{(x_{i,0}, A_i), i = 1,\dots,N\}$, where $x_{i,0} \in \mathbb{S}$, the unit sphere, and $A_i = A_{\sigma_i(l-1)}\dots A_{\sigma_i(0)}$ with $\sigma_i(0),\dots,\sigma_i(l-1)$ accepted by $\mathscr{G}$.

In order to tackle hybrid behaviors in arbitrary switching linear systems, novel data-driven stability analysis methods have been recently developed based on scenario optimization. For example, [1] provides a data-driven method for approximating the *joint spectral radius* of an unknown switching linear system. In this work, we generalize this method to CSLS. We derive a probabilistic Lyapunov method to approximate the *constrained joint spectral radius* in order to give probabilistic certificates on stability.

We then analyze further the obtained result. We show that a lower entropy allows for a better probablistic guarantee for the stability of a given CSLS.

References

[1] Guillaume O. Berger, Raphaël M. Jungers, and Zheming Wang. Chance-constrained quasi-convex optimization with application to data-driven switched systems control. *arXiv:2101.01415 [cs, eess, math]*, 01 2021.

[2] Xiongping Dai. A gel'fand-type spectral radius formula and stability of linear constrained switching systems. *arXiv:1107.0124 [cs, math]*, 07 2011.

[3] Douglas Lind and Brian Marcus. *An Introduction to Symbolic Dynamics and Coding*. Cambridge University Press, 1995.

Stochastic Similarity Relations for Continuous State POMDPs

Maico H. W. Engelaar[1], Mircea Lazar[1], and Sofie Haesaert[1]

1 Introduction

With emerging applications in robotics, and especially autonomous vehicles, a high demand exists for control systems capable of performing complex tasks in a safe manner. Many of these control systems are inherently uncertain and evolve over continuous spaces. For such classes of control systems, Partially Observable Markov Decision Processes (POMDPs) provide a suitable modelling and analysis framework [4]. For these systems, safe functioning can be specified rigorously via temporal logic specifications [1, 2]. Such safety specifications include, amongst others, reachability, repeatability, invariance and combinations thereof, all with pregiven minimal probabilities explaining to which extent a stochastic system needs to satisfy these tasks.

Unfortunately, POMDPs evolving over continuous spaces can generally not be studied analytically and are computationally expensive to approximate numerically [3]. Hence, to mitigate this complexity of POMDPs, the objective of this study is to find (simplified) abstractions of POMDPs, by means of (approximate) stochastic similarity relations, while preserving the safety features, i.e., the temporal logic specifications. More precisely, this study will develop a new tailored approach for POMDPs that is based on earlier work for MDPs [1] and belief MDPs [2], and that enables the design and verification of controllers.

2 Problem Statement

Given a model $\mathbf{M}$ and a temporal logic specification ϕ, we want to find a controller $\mathbf{C}$, such that the controlled system satisfies ϕ with probability at least B, that is

$$\mathbb{P}(\mathbf{C} \times \mathbf{M} \models \phi) \geq B. \tag{1}$$

More specifically, we will define $\mathbf{M}$ as a POMDP, that is, $\mathbf{M} := (\mathbb{X}, \pi, \mathbb{T}, \mathbb{U}, \mathbb{Z}, r)$ where $\mathbb{U}$ is the input space; $\mathbb{X}$ is a Polish[2] state space; $\mathbb{T}$ is a conditional stochastic state kernel that assigns to each state $x \in \mathbb{X}$ and control $u \in \mathbb{U}$ a probability measure $\mathbb{T}(\cdot|x,u) \in \mathscr{P}(\mathbb{X}, \mathscr{B}(\mathbb{X})^3)$; $\mathbb{Z}$ is a Polish output space; r is a conditional stochastic observation kernel that assigns to each state $x \in \mathbb{X}$ a probability measure $r(\cdot|x) \in \mathscr{P}(\mathbb{Z}, \mathscr{B}(\mathbb{Z}))$; and π is the initial probability distribution defined as $\pi : \mathscr{B}(\mathbb{X}) \to [0,1]$.

In this study, we want to develop abstractions to mitigate complexity in POMDPs. More precisely, we want to design abstractions of POMDPs that are suitable for the efficient design and verification of controllers, that is abstractions $\hat{\mathbf{M}}$ based on which we can design a controller $\mathbf{C}$ such that

$$\exists \hat{\mathbf{C}} : \mathbb{P}\left(\hat{\mathbf{C}} \times \hat{\mathbf{M}} \models \phi\right) \geq \hat{B} \Leftrightarrow \exists \mathbf{C} : \mathbb{P}(\mathbf{C} \times \mathbf{M} \models \phi) \geq B. \tag{2}$$

To achieve this objective, a better type of (approximate) stochastic bisimulation has to be developed that can fully relate the dynamics of both systems.

3 Specific Example

To illustrate the importance of this study, consider the following two discrete linear time-invariant stochastic control systems. These systems can be equivalently represented as POMDPs, but are given here as the following stochastic difference equations:

$$\Sigma_1 : \begin{cases} x_1(t+1) = e_1(t) \\ x_2(t+1) = x_1(t) \\ x_3(t+1) = x_2(t) + u(t) \\ y(t) = \left[x_1(t)^T \; x_2(t)^T \; x_3(t)^T\right]^T \end{cases} \qquad \Sigma_2 : \begin{cases} x_1(t+1) = e_1(t) \\ x_2(t+1) = x_1(t) \\ x_3(t+1) = x_2(t) + u(t) \\ y(t) = \left[x_2(t)^T \; x_3(t)^T\right]^T \end{cases}$$

For a specification ϕ defined solely over x_3, we can trivially ascertain that if a controller C_1 exists for system Σ_1 such that $\mathbb{P}(C_1 \times \Sigma_1 \models \phi) \geq B$ this implies that there will also exists a controller C_2 such that $\mathbb{P}(C_2 \times \Sigma_2 \models \phi) \geq B$ and vice versa. We are investigating exact and approximate stochastic bisimulation relations that cover this example and more involved examples such as high dimensional POMDPs.

[1] Electrical Engineering, Control Systems group, Eindhoven University of Technology, Email: {m.h.w.engelaar, m.lazar, s.haesaert}@tue.nl

[2] A Polish space is a separable completely metrizable topological space.

[3] $\mathscr{B}(\mathbb{X})$ is the Borel σ-algebra of the topological space $\mathbb{X}$.

References

[1] S. Haesaert, S. Soudjani, and A. Abate. "Verification of general Markov decision processes by approximate similarity relations and policy refinement." *SIAM Journal on Control and Optimization*, 2017.

[2] S. Haesaert, P. Nilsson, C. I. Vasile, R. Thakker, A. Agha-mohammadi, A. D. Ames and R. M. Murray. "Temporal logic control of POMDPs via label-based stochastic simulation relations." *IFAC-PapersOnLine, 51*(16), 271-276, 2018.

[3] K. Lesser, and M. Oishi. "Reachability for partially observable discrete time stochastic hybrid systems." *Automatica, 50*(8), 1989-1998, 2014.

[4] M. Svoreňová, M. Chmelík, K. Leahy, H. F. Eniser, K. Chatterjee, I. Černá and C. Belta. "Temporal logic motion planning using POMDPs with parity objectives: case study paper". *In Proceedings of the 18th International Conference on Hybrid Systems: Computation and Control*, 2015, 233–238.

Controller-design for time-delay systems using TDS CONTROL

Pieter Appeltans, Haik Silm, and Wim Michiels
NUMA, Department of Computer Science, KU Leuven,
Celestijnenlaan 200a - box 2402, 3001 Leuven, Belgium
Email: pieter.appeltans@kuleuven.be

1 Introduction

We present TDS CONTROL, a MATLAB package for the analysis, and design of controllers for linear time-invariant (LTI) systems with discrete delays [1]. More specifically, the code considers systems of the following form:

$$\begin{cases} E\dot{x}(t) = \sum_{i=0}^{m} A_i x(t-\tau_i) + \sum_{i=0}^{m} B_i u(t-\tau_i) - \sum_{i=0}^{m} H_i \dot{x}(t-\tau_i) \\ y(t) = \sum_{i=0}^{m} C_i x(t-\tau_i) + \sum_{i=0}^{m} D_i u(t-\tau_i) \end{cases} \quad (1)$$

with $0 = \tau_0 < \tau_1 < \cdots < \tau_m < \infty$ the delay values and $x(t) \in \mathbb{R}^n$, $u(t) \in \mathbb{R}^p$, and $y(t) \in \mathbb{R}^q$. The matrix $E \in \mathbb{R}^{n\times n}$ is potentially singular. The other matrices are real-valued matrices with appropriate dimensions. Note that systems of the form (1) can represent a broad class of LTI time-delay systems, including neutral systems and delay description systems (under certain assumptions on the system matrices to avoid advanced systems).

Compared to undelayed LTI systems, it is well known that systems with delay are in some sense "infinite dimensional". For instance, the stability of a LTI delay system can be examined in terms of the roots of an associated characteristic function which has infinitely many roots. As such, the existing analysis methods for undelayed systems need to be extended. The presented software can be used to analyze several control measures such as the spectral abscissa, the $\mathscr{H}_\infty$-norm, and the distance to instability for systems of the form (1).

2 Controller design

Besides analysis, TDS CONTROL can also be used to design dynamic output feedback controllers with a chosen order n_c:

$$\begin{cases} \dot{x}_c(t) = A_c x_c(t) + B_c y(t) \\ u(t) = C_c x_c(t) + D_c y(t) \end{cases} \quad (2)$$

in which $x_c(t)$ belongs to $\mathbb{R}^{n_c}$, and A_c, B_c, C_c, and D_c are real-valued matrices with appropriate dimensions. The controller design algorithm consists of minimizing one of the control measures mentioned above, with respect to entries of the matrices in (2). For example, in an attempt to design a stabilizing controller the spectral abscissa, i.e., the real part of the right-most characteristic root, is minimized. As a strictly negative spectral abscissa is a necessary and sufficient condition for stability, the presented design method is not conservative and a stabilizing controller can be computed whenever it exits, although different initial values have to be sampled until a satisfactory controller is found.

3 Additional features

TDS CONTROL allows to design robust controllers either with respect to structured uncertainties, including delay uncertainties, in the plant's model [2], or by $\mathscr{H}_\infty$-norm optimization [3]. It is also possible to impose structure on the matrices in (2), i.e., certain entries can be fixed to a given value. This allows the design of structured controllers such as decentralized, overlapping and PID(-like) controllers [4].

The software package takes the sensitivity of certain quantities, such as the spectral abscissa and the $\mathscr{H}_\infty$-norm, with respect to infinitesimal delay perturbations into account, which is relevant for particular classes of systems that can be modeled by (1).

TDS CONTROL is freely available for download at gitlab.kuleuven.be/u0011378/tds-control.

References

[1] W. Michiels and S.-I. Niculescu, *Stability, Control, and Computation for Time-Delay Systems: An Eigenvalue-Based Approach*, 2nd ed., SIAM, 2014.

[2] F. Borgioli and W. Michiels, "A novel method to compute the structured distance to instability for combined uncertainties on delays and system matrices," *IEEE Transactions on Automatic Control*, vol. 65, no. 4, pp. 1747–1754, 2020.

[3] S. Gumussoy and W. Michiels, "Fixed-order H-infinity control for interconnected systems using delay differential algebraic equations," *SIAM J. Control Optim.*, vol. 49, no. 5, pp. 2212–2238, 2011.

[4] D. Dileep, R. Van Parys, G. Pipeleers, L. Hetel, J.-P. Richard, and W. Michiels, "Design of robust decentralised controllers for MIMO plants with delays through network structure exploitation," *International Journal of Control*, vol. 93, no. 10, pp. 2275–2289, 2020.

$(\gamma,\delta)-$Conformance: A Notion of System Comparison

Armin Pirastehzad Arjan van der Schaft Bart Besselink

Systems, Control, and Optimization Group
Bernoulli Institute for Mathematics, Computer Science and Artificial Intelligence
University of Groningen
Nijenborgh 9, 9747 AG Groningen, The Netherlands
Email: a.pirastehzad@rug.nl,a.j.van.der.schaft@rug.nl,b.besselink@rug.nl

1 Introduction

The analysis and synthesis of modern engineering systems have become arduous, as these systems often comprise numerous interconnected components. More specifically, it is prohibitively difficult to address and verify many control design objectives. These challenges motivate one to seek ways of abstracting systems into less complex ones which somehow replicate their behavior. Towards this end, a crucial step is to conceive a notion of system comparison addressing the input-output equivalence of two systems. We propose a notion of system comparison which measures to what extend two systems behave similarly in an input-output sense. Moreover, we fully characterize the notion in terms of linear matrix inequalities.

2 The notion of $(\gamma,\delta)-$conformance

Consider continuous-time linear systems of the form

$$\mathbf{\Sigma}_i : \begin{cases} \dot{x}_i = A_i x_i + B_i u_i + E_i d_i, \\ y_i = C_i x_i, \end{cases} \tag{1}$$

where $x_i \in \mathbb{R}^{n_i}$, $u_i \in \mathbb{R}^{m_i}$, $d_i \in \mathbb{R}^{q_i}$, and $y_i \in \mathbb{R}^{p_i}$ represent system state, input, disturbance, and output, respectively, and the matrix A_i is Hurwitz. While the system state x_i is considered as an internal variable, the input u_i and the output y_i are regarded as external variables through which $\mathbf{\Sigma}_i$ interacts with its environment. The presence of the disturbance d_i leads to non-determinism in the sense that trajectories do not solely depend on the initial condition $x_i(0)$ and the external input u_i.

Definition 1. For $\gamma,\delta > 0$, the system $\mathbf{\Sigma}_2$ is said to $(\gamma,\delta)-$conform system $\mathbf{\Sigma}_1$, denoted by $\mathbf{\Sigma}_1 \preccurlyeq_{\gamma,\delta} \mathbf{\Sigma}_2$, if there exist constants $\varepsilon,\eta,\mu > 0$ such that for every input $u_1,u_2 \in \mathscr{L}_2$ and every disturbance $d_1 \in \mathscr{L}_2$, there exists a disturbance $d_2 \in \mathscr{L}_2$ such that for initial conditions $x_1(0) = 0$ and $x_2(0) = 0$,

$$\begin{aligned} \|y_1 - y_2\|_{\mathscr{L}_2}^2 \leq \gamma \|u_1 - u_2\|_{\mathscr{L}_2}^2 + (\delta - \varepsilon) \left\| \begin{bmatrix} u_1 \\ u_2 \end{bmatrix} \right\|_{\mathscr{L}_2}^2 \\ + (\mu - \varepsilon) \|d_1\|_{\mathscr{L}_2}^2 - \eta \|d_2\|_{\mathscr{L}_2}^2 . \end{aligned} \tag{2}$$

For each trajectory of system $\mathbf{\Sigma}_1$, the notion of $(\gamma,\delta)-$conformance seeks a trajectory of $\mathbf{\Sigma}_2$ that is closest to it. Parameters γ and δ measure how close these two trajectories are. Hence, the notion of $(\gamma,\delta)-$conformance measures the capability of system $\mathbf{\Sigma}_2$ in replicating the input-output behavior of system $\mathbf{\Sigma}_1$. For this reason, this notion provides us a criterion which measures how similar the input-output behaviors of two systems are.

3 Main Results

Inspired by H_∞ control theory and dissipativity theory, we characterize the notion of $(\gamma,\delta)-$conformance as an LMI feasibility problem.

Theorem 1. Given $\gamma,\delta > 0$, system $\mathbf{\Sigma}_2$ $(\gamma,\delta)-$conforms system $\mathbf{\Sigma}_1$ if and only if there exist a positive definite matrix X, a matrix Π, and positive scalars κ and ν such that

$$\begin{bmatrix} XA^T + AX + \Pi^T B^T + B\Pi & E & XC^T + \Pi^T D^T \\ E^T & -\begin{bmatrix} Q & 0 \\ 0 & \kappa I \end{bmatrix} & 0 \\ CX + D\Pi & 0 & -\begin{bmatrix} I & 0 \\ 0 & \nu I \end{bmatrix} \end{bmatrix} \prec 0,$$

where

$$A = \begin{bmatrix} A_1 & 0 \\ 0 & A_2 \end{bmatrix}, \quad B = \begin{bmatrix} 0 \\ E_2 \end{bmatrix},$$
$$C = \begin{bmatrix} C_1 & -C_2 \\ 0 & 0 \end{bmatrix}, \quad D = \begin{bmatrix} 0 \\ I \end{bmatrix},$$
$$E = \begin{bmatrix} B_1 & 0 & E_1 \\ 0 & B_2 & 0 \end{bmatrix}, \quad Q = \begin{bmatrix} (\gamma+\delta)I & -\gamma I \\ -\gamma I & (\gamma+\delta)I \end{bmatrix}.$$

4 Conclusion

The notion of $(\gamma,\delta)-$conformance measures to what extent two systems behave similarly in an input-output sense. This notion admits an LMI-type necessary and sufficient condition for which several fast computational tools exist. The notion of $(\gamma,\delta)-$conformance can be utilized for such purposes as system abstraction in contract-based design frameworks.

Impulse-controllability of system classes of switched DAEs

P. Wijnbergen
Bernoulli Institute, RUG
Email: p.wijnbergen@rug.nl

S. Trenn
Bernoulli Institute, RUG
Email: s.trenn@rug.nl

Introduction

In this note we study system classes containing *switched differential algebraic equations* (switched DAEs) of the following form:

$$E_\sigma \dot{x} = A_\sigma x + B_\sigma u, \tag{1}$$

where $\sigma : \mathbb{R} \to \mathbb{N}$ is the switching signal and $E_p, A_p \in \mathbb{R}^{n\times n}$, $B_p \in \mathbb{R}^{n\times m}$, for $p,n,m \in \mathbb{N}$. In general, trajectories of switched DAEs exhibit jumps (or even impulses), which may exclude classical solutions from existence. Therefore, we adopt the *piecewise-smooth distributional solution framework* introduced in [1]. We study impulse controllability of system classes where a class is said to be strongly impulse controllable if every system contained in it is impulse controllable.

System Classes

In particular, we study classes of switched DAEs with a switching signal in the class $\mathcal{S}_\mathtt{n}$ defined as follows.

Definition 1 *The class of (arbitrary) switching signals $\mathcal{S}_\mathtt{n}$ is defined as the set of all $\sigma : \mathbb{R} \to \{0,1,...,\mathtt{n}\}$ of the form*

$$\sigma(t) = q_p \quad t \in [t_p, t_{p+1}) \tag{2}$$

where $\mathbf{q} := (q_0, q_1, \ldots, q_\mathtt{n}) \in \{0,1,\ldots,\mathtt{n}\}^{\mathtt{n}+1}$ is the mode sequence *of σ and $t_1 < t_2 < ... < t_\mathtt{n}$ are the $\mathtt{n} \in \mathbb{N}$ switching times in $(0,\infty)$ with $t_0 := 0$ and $t_{\mathtt{n}+1} := \infty$ for notational convenience. Furthermore, for a given sequence of switching times, let $\tau_i := t_{i+1} - t_i$, $i = 0,1,\ldots,\mathtt{n}-1$ such that $\tau := (\tau_0, \tau_1, \ldots, \tau_{\mathtt{n}-1}) \in \mathbb{R}^\mathtt{n}_{>0}$, defines the sequence of (finite) mode-durations.*

Note that in the above definition, we do not exclude the situation that $q_p = q_{p+1}$ for some p, effectively leading to a switching signal with less then $\mathtt{n}$ switches. Consequently, for such a switching signal the mode duration τ is not uniquely defined, as the switching time t_{p+1} can be altered without changing the actual switching signal. Nevertheless, this does not lead to any technical problems.

Definition 2 (System classes) *For a family of matrix triplets $\{(E_p, A_p, B_p)\}_{p=0}^\mathtt{n}$ with regular pairs (E_p, A_p), the* system class $\Sigma_\mathtt{n}$ *of associated switched (regular) DAEs* (1) *under arbitrary switching is given by*

$$\Sigma_\mathtt{n} := \{(E_\sigma, A_\sigma, B_\sigma) \mid \sigma \in \mathcal{S}_\mathtt{n}\},$$

where $(E_\sigma, A_\sigma, B_\sigma)$ is understood as a triple of (piecewise-constant) time-varying matrices for each specific switching signal $\sigma : (t_0, \infty) \to \{0,1,\ldots,\mathtt{n}\}$.

Equipped with the notion of a system class, we state the definition of impulse controllability of (1) based on [2] and define strong impulse controllability of a system class. Before doing so, recall that for mode i the augmented consistency space is defined as

$$\mathcal{V}_{(E_i,A_i,B_i)} := \left\{ x_0 \in \mathbb{R}^n \;\middle|\; \begin{array}{l} \exists \text{ smooth solutions } (x,u) \text{ of} \\ E_i\dot{x} = A_i x + B_i u \text{ and } x(0) = x_0 \end{array} \right\}.$$

Definition 3 (Impulse controllability) *The (individual) switched DAE $(E_\sigma, A_\sigma, B_\sigma)$ is called* impulse controllable *iff for all $x_0 \in \mathcal{V}_{[E_0,A_0,B_0]}$, there exists a solution $(x,u) \in \mathbb{D}^{n+m}_{pwC^\infty}$ with $x(t_0^+) = x_0$ which is impulse free.*

The whole system class $\Sigma_\mathtt{n}$ associated to the family $\{(E_p, A_p, B_p)\}_{p=0}^\mathtt{n}$ is called strongly impulse controllable, if $(E_\sigma, A_\sigma, B_\sigma)$ is impulse controllable for all $\sigma \in \mathcal{S}_\mathtt{n}$.

Main result

If all systems in the system class are impulse controllable, then all the systems that are effectively single switched system. This observation leads to the following result.

Theorem 1 *Consider the system class $\Sigma_\mathtt{n}$ associated to $\{E_p, A_p, B_p\}_{p=0}^\mathtt{n}$ with corresponding (individual) consistency projectors Π_p, impulse controllable spaces $\mathcal{C}_p^{imp}$ and reachability spaces $\mathcal{R}_p$. Then $\Sigma_\mathtt{n}$ is strongly impulse controllable if, and only if,*

$$\mathcal{V}_{[E_i,A_i,B_i]} \subseteq \mathcal{C}_j^{imp} + \mathcal{R}_i \tag{3}$$

for all $i, j \in \{0,1,...,\mathtt{n}\}$.

The result of Theorem 1 shows that impulse controllability of a system class can be determined in finitely many steps. A future direction of reasearch is the study of system classes containing switched DAEs with a fixed mode sequence.

References

[1] Stephan Trenn. *Distributional differential algebraic equations*. PhD thesis, Institut für Mathematik, Technische Universität Ilmenau, Universitätsverlag Ilmenau, Germany, 2009.

[2] Paul Wijnbergen and Stephan Trenn. Impulse controllability of switched differential-algebraic equations. In *2020 European Control Conference (ECC)*, pages 1561–1566. IEEE, 2020.

A square root filter for windowed recursive linear least squares regression

Ralf Peeters
Dept. Data Science & Knowledge Engineering, Maastricht University
ralf.peeters@maastrichtuniversity.nl

Joël Karel
Dept. Data Science & Knowledge Engineering, Maastricht University
joel.karel@maastrichtuniversity.nl

Pietro Bonizzi
Dept. Data Science & Knowledge Engineering, Maastricht University
pietro.bonizzi@maastrichtuniversity.nl

1 Abstract

Linear least squares regression is a well-known modeling technique with many applications in system identification, filtering, signal processing, and data analysis. Computation of the model parameters can be organized in a highly efficient way, e.g. by making it recursive in the data, which is useful for real-time applications. In some applications, such as the Levinson algorithm for auto-regressive modeling, it can even be made recursive in the regressors [2, 3]. Adding to the versatility of the method is the option to include exponential forgetting, by which past data are made increasingly obsolete, rendering the method of interest for time-varying parameter estimation as well as detection applications.

The use of exponential forgetting implies that the total sum of the weights received by past data remains bounded, but to have very old data still play a role in the estimate, however small, can be considered unwanted. An alternative to such an approach is to use a sliding window of finite size. This can also be implemented recursively, with or without exponential forgetting; see [4, 5, 6]. Some renewed interest in this topic was sparked in [7, 8] and is also seen more recently in areas involving edge computing. There it is important to have lightweight and efficient yet powerful algorithms on board of devices with limited power and memory storage resources.

In this paper we start from the recursive square root filter for linear least squares regression presented in [1], which is recursive in the data, with the square root filter aiming to improve numerical robustness. It admits a Bayesian interpretation so that it can be combined with prior information on the parameters should this be available. By first deriving its time-reversed version, which can be used for deleting data rather than adding it, we extend it to the finite size sliding window situation with exponential forgetting having similar complexity as the original algorithm. We then analyze and demonstrate its numerical behavior. We conclude the paper by presenting an example in which the algorithm is used for real-time heart rate detection, motivated by an application in remote patient monitoring of cardiac function. It employs a finite window of varying size, and uses test data from the public PhysioNet database [9].

References

[1] Vaclav Peterka, A Square Root Filter for Real Time Multivariate Regression, Kybernetika, Volume 11, Number 1, 1975, pp. 53-67.

[2] L. Ljung, System Identification: Theory for the User, Prentice-Hall, 1987.

[3] Torsten Söderström and Petre Stoica, System Identification. New York: Prentice-Hall, 1989.

[4] B.-Y. Choi and Z. Bien, Sliding-windowed weighted recursive least-squares method for parameter estimation, Electronics Letters, Volume 25, Issue 20, 1989, pp. 1381-1382.

[5] Hanyu Liu and Zhenya He, A sliding-exponential window RLS adaptive filtering algorithm: Properties and applications, Signal Processing, Volume 45, 1995, pp. 357-368.

[6] Hideaki Sakai and Hiroshi Nakaoka, A fast sliding window QRD-RLS algorithm, Signal Processing, Volume 78, 1999, pp. 309-319.

[7] Jin Jiang and Youmin Zhang, A revisit to block and recursive least squares for parameter estimation, Computers and Electrical Engineering, Volume 30, 2004, pp. 403-416.

[8] Kiyoshi Nishiyama, A New Formalism of the Sliding Window Recursive Least Squares Algorithm and Its Fast Version, IEICE Transactions on Fundamentals of Electronics, Communications and Computer Sciences, Volume E94.A, Number 6, 2011, pp. 1394-1400.

[9] PhysioNet, see: https://physionet.org

Learning separable decompositions of MIMO nonlinear systems

Koen Tiels
Eindhoven University of Technology
Department of Mechanical Engineering
Email: k.tiels@tue.nl

Maciej Filiński and Paweł Wachel
Wrocław University of Science and Technology
Department of Control Systems and Mechatronics
Email: maciej.filinski@pwr.edu.pl
and pawel.wachel@pwr.edu.pl

1 Introduction

Identification of nonlinear phenomena is challenging, especially for multiple input multiple output (MIMO) systems. We present a new structure exploration technique for MIMO dynamical systems with finite memory and address the following questions: 1) Which system inputs contribute to which system outputs? 2) Can the nonlinear characteristic be separated into additive sub-characteristics?

2 Problem setup

Consider a MIMO nonlinear system with p inputs $u_n = [u_n^1 u_n^2, \ldots, u_n^p]^T$, q outputs $y_n = [y_n^1 y_n^2, \ldots, y_n^q]^T$, and known finite memory d, where n is the time index:

$$y_n = g(v_n^1, v_n^2, \ldots, v_n^p) + e_n \tag{1}$$

$$v_n^k = [u_n^k, u_{n-1}^k, \ldots, u_{n-d}^k]^T \tag{2}$$

The nonlinear characteristic $g : \mathbb{R}^{p\times(d+1)} \to \mathbb{R}^q$ is unknown and such that $\sup_{u\in[0,1]^p} g(u) \leq c_g < \infty$. We assume that the input u_n is i.i.d. uniformly distributed on $[0,1]^p$, the output noise e_n is i.i.d., zero-mean, has covariance matrix $\sigma_e^2 I$ and bounded fourth-order moments, and the noise and input signals are mutually independent sequences.

3 Double separation algorithm

The first stage of the proposed algorithm is based on the distance correlation (DC) coefficient. In contrast to Pearson correlation, the DC between two signals is zero if and only if these signals are independent [2]. Making use of the finite memory of the system, a careful selection of the input-output data is made such that the data set contains mutually independent measurements of the system outputs and the corresponding system inputs. Next, the DC between each input and output is estimated. Fig. 1 shows a typical result.

The second stage of the proposed algorithm estimates projection coefficients that are sensitive to the existence of additive system sub-characteristics. Let ξ_1 be an arbitrary set of indices of preselected inputs and let ξ_2 be its complement. We say that a characteristic $g^\kappa(\cdot)$ is separable with respect to ξ_1 and ξ_2 if $g^\kappa = g^\kappa_{\xi_1} + g^\kappa_{\xi_2}$, where $g^\kappa_{\xi_1}$ and $g^\kappa_{\xi_2}$ are functions that depend only on inputs with indices in ξ_1 and ξ_2, respectively [3]. Recursive extension of this rule leads to separability with respect to arbitrary partitions of the set of input

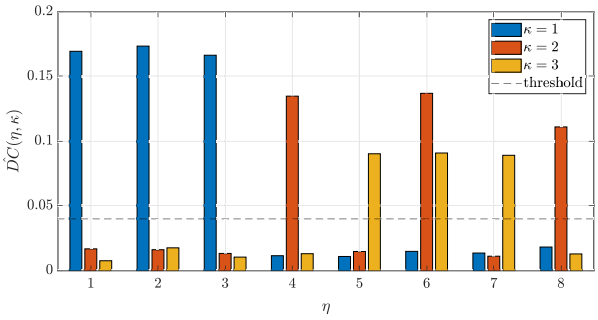

Figure 1: Estimated DC coefficients between ηth input and κth output of a system with 8 in- and 3 outputs. Large coefficients indicate dependence, zero (or small) coefficients indicate independence. We can correctly deduce that output 1 only depends on the first three inputs, output 2 only depends on inputs 4, 6, and 8, and output 3 only depends on inputs 5, 6, and 7.

indices. We can then estimate if a characteristic is fully separable, e.g., $g^1(v_n^1, v_n^2, v_n^3) = g^{1a}(v_n^1) + g^{1b}(v_n^2) + g^{1c}(v_n^3)$, partially separable, e.g., $g^2(v_n^4, v_n^6, v_n^8) = g^{2a}(v_n^4, v_n^6) + g^{2b}(v_n^8)$, or not separable, without identifying these characteristics.

4 Conclusion

The proposed method allows for exploration of the internal system structure and thus may support further modelling or identification tasks. A numerical experiment illustrates the ability of the proposed approach to indicate which of the system inputs contribute to which outputs and illustrates the ability of the approach to detect separable lower-dimensional sub-characteristics in the system.

References

[1] P. Wachel, K. Tiels, and M. Filiński, "Learning low-dimensional separable decompositions of MIMO nonlinear systems," International Journal of Control, doi: 10.1080/00207179.2021.2019315, 2021.

[2] G.J. Székely, M.L. Rizzo, and N.K. Bakirov, "Measuring and testing dependence by correlation of distances," The Annals of Statistics, 35(6), 2769–2794, 2007.

[3] T. Goda, "On the separability of multivariate functions," Mathematics and Computers in Simulation, 159, 210–219, 2019.

Data-driven modelling of unsteady fluid dynamics

Joshua A. Foster * jfoster@vub.be
Jan Decuyper * jan.decuyper@vub.be
Tim De Troyer * tim.de.troyer@vub.be
Mark C. Runacres * mark.runacres@vub.be

* *Department of Engineering Technology, Vrije Universiteit Brussel, Brussels Institute for Thermal-Fluid Systems and Clean Energy, Pleinlaan 2, 1050 Brussels, Belgium*

1 Abstract

Recent advances in nonlinear system identification and machine learning have resulted in a plethora of data-driven modelling tools. A number of them have already been successfully applied in the context of fluid dynamics, e.g. polynomial nonlinear state-space models, dictionary methods such as Sparse Identification of Nonlinear Dynamics (SINDy), as well as linear Dynamic Mode Decomposition (DMD) models. Knowing what model structure is best suited for a given task is non-trivial.
In this work DMD and SINDy are applied to unsteady fluid dynamics. Both methods enable to gain insight into system dynamics. The canonical system of the flow field in the wake of a periodically oscillating cylinder is studied.

DMD decomposes periodic data into dynamic modes (DM). These consist of spatial mode fields and corresponding temporal behaviour, as shown in Figure 1. The spatial modes and their temporal behaviour are respectively defined by the eigenvectors and corresponding eigenvalues of transformation matrix **A** of the periodic data. These are derived without directly calculating **A** and can be linearly combined to reconstruct the data and make future state predictions [1].

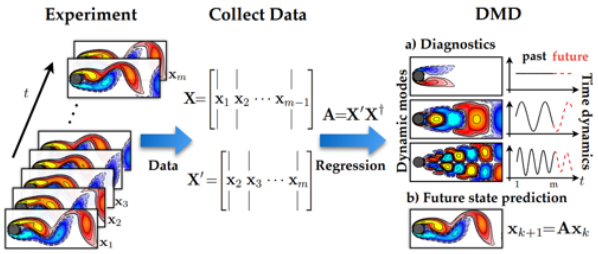

Figure 1: Illustration demonstrating the dynamic modes which consist of the eigenvector-eigenvalue pairs of transformation matrix **A**. **Source:** Brunton and Kutz [1].

SINDy can be used to identify nonlinear ordinary differential equations (ODE's) that approximate the dynamics of systems with multiple variables, as shown in Figure 2. The dynamics of flow fields are identified in the space spanned by their proper orthogonal decomposition (POD) basis. The fields are then reconstructed by multiplying the identified dynamics with the POD modes that match the basis [1].

Both methods are applied to the vorticity field of a lock-in experiment using the first 10 modes.
DMD achieves a relative RMS error of 16 % using 10 DM's. SINDy captures the dynamics of the field in terms of its first 10 POD modes and identifies them as a set of nonlinear difference equations, achieving a relative RMS error of 4.5 %.

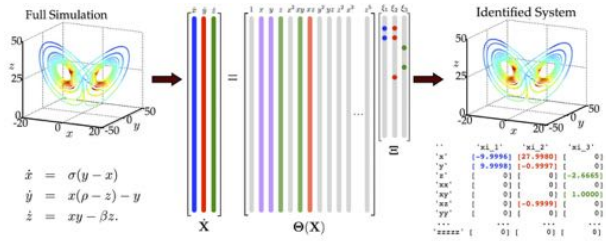

Figure 2: Demonstration of how a sparse selection of terms from function library Θ is used to reconstruct the ODE's on the left which generated the training data. **Source:** Brunton and Kutz [1].

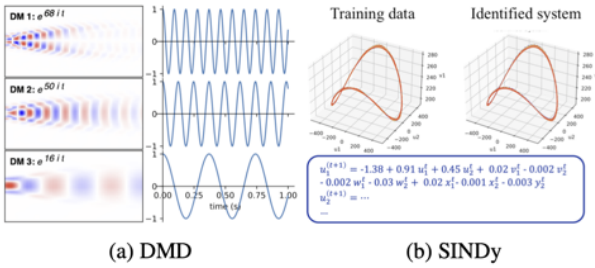

Figure 3: Dynamics in terms of the first three DMD modes (a) and as identified by SINDy in the space spanned by the first three POD modes, including the first DE (b).

Both methods analyse periodic data in terms of modes. DMD gives insight into dynamics through the individual dynamic modes and their sum. These are derived from the POD modes of the data. SINDy uses the POD modes directly and translates their relationships into (nonlinear) difference equations. It captures the dynamics of the studied system more efficiently than DMD.

References

[1] Steven L. Brunton and Nathan J. Kutz. *Data-Driven Science and Engineering: Machine Learning, Dynamical Systems and Control.* Cambridge University Press, 2017

Nonlinear System Identification Based on Linear Parameter-Varying Approximations by Gaussian Process in the Frequency Domain

Sadegh Ebrahimkhani, John Lataire
ELEC dept., Vrije Universiteit Brussel, Pleinlaan 2, 1050 Brussels, Belgium.
Email: Sadegh.Ebrahimkhani@vub.be

1 Problem Setting and Assumptions

In the real world, nonlinear (NL) behavior exists in most applications. While these NL systems can be locally approximated by linear systems, their global behavior is generally expressed by nonlinear differential equations. On the other hand, for many of these NL systems, the governing equations are unknown or hard to find from first principles. Data-driven approaches could be a good choice for modeling such problems.

This research deals with the problem of the identification of a class of NL systems in the frequency domain. A general form of the NL differential equation is considered as

$$f\left(y(t),\dots,y^{(n_a)}(t),u(t),\dots,u^{(n_b)}(t)\right)=0 \qquad (1)$$

where $u(t)$ and $y(t)$ are the input and output signals of the system, $\bullet^{(n)}$ denotes the nth derivative operator with respect to t, and $f(\bullet)$ is an NL static function of the instantaneous values of $(y(t),\dots,y^{(n_a)}(t),u(t),\dots,u^{(n_b)}(t))$.

The NL system is working on a stable slow time-varying setpoint $p(t)=(y_L(t),\dots,y_L^{(n_a)}(t),u_L(t),\dots,u_L^{(n_b)}(t))$. Then a small-fast input perturbation is used to perturb the system trajectory slightly. When the perturbation $\tilde{p}(t)=(\tilde{y}(t),\dots,\tilde{y}^{(n_a)}(t),\tilde{u}(t),\dots,\tilde{u}^{(n_b)}(t))$ is small and the nonlinearities are sufficiently smooth, then the NL system can be approximated by a linear-parameter-varying (LPV) system:

$$\sum_{n=0}^{n_a}\alpha_n(p(t))\frac{d^n\tilde{y}(t)}{dt^n}+\sum_{m=0}^{n_b}\beta_m(p(t))\frac{d^m\tilde{u}(t)}{dt^m}=0 \qquad (2)$$

where the parameter varying (PV) coefficients $\alpha_n(p(t))$ and $\beta_m(p(t))$ are defined by $\alpha_n(p(t))=\frac{\partial f}{\partial y^{(n)}}|_{p(t)}$ and $\beta_m(p(t))=\frac{\partial f}{\partial u^{(m)}}|_{p(t)}$ with $n=0,1,\dots,n_a$ and $m=0,1,\dots,n_b$. Indeed, the LPV (2) is the NL system (1) linearized at each point of $p(t)$.

In [1] the NL system is linearized around a periodic motion and in [2] about an arbitrary time-varying trajectory. Both [1] and [2] are based on LTV approximations, while in this paper a direct LPV modeling approach is proposed. In the proposed method we exploit the known relations among the PV coefficients and between LPV and NL models. Which is often the key to obtaining better performance and coping with a lack of data. On the other hand, in addition to using the perturbed motion, the proposed method can use measured data outside this perturbed trajectory as well.

This research was supported by the Fund for Scientific Research (FWO Vlaanderen, grant G005218N) and by the Flemish Government (Methusalem Grant METH1).

2 Proposed method

A multi-input multi-output (MIMO) Gaussian process (GP) is used to model the vector of PV coefficients of the LPV system (2):

$$\begin{aligned}&(\alpha_0(p(t)),\dots,\alpha_n(p(t)),\beta_0(p(t)),\dots,\beta_m(p(t)))\\&\sim\mathcal{GP}(m(p(t)),K(p(t),p'(t)))\end{aligned} \qquad (3)$$

where $m(\bullet),K(\bullet,\bullet')$ are the mean and kernel to be designed. We show that these PV coefficients are related. The relation between these PV coefficients is considered in the designed kernel. After modeling the LPV system, by integration, the NL system is reconstructed. The obtained NL system is an ordinary differential equation (ODE) in which the coefficients are GPs. The relation among PV coefficients and the relation between PV coefficients and coefficients of the reconstructed NL ODE are considered in the designed kernel. Finally, the joint LPV and NL systems are identified by a frequency domain estimator.

In this research, the identification of NL and corresponding LPV system is reformulated as a Gaussian process regression with value and integral observations. The value corresponds to LPV region measurements, and integral measurements are related to the NL response.

References

[1] M. W. Sracic and M. S. Allen, "Method for identifying models of nonlinear systems using linear time periodic approximations'," *Mech. Syst. Signal Process.*, vol. 25, no. 7, pp. 2705–2721, 2011.

[2] John Lataire, Rik Pintelon, Tom Oomen, "An LTV Approach to Identifying Nonlinear Systems-with Application to an RRR Robot11", IFAC-PapersOnLine, 54 (7), pp. 445-450, 2021

Visualization of MIMO Uncertainty Structures for Robust Control

Paul Tacx[1] and Tom Oomen[1,2]
[1]Eindhoven University of Technology, Department of Mechanical Engineering
[2]Delft University of Technology, Delft Center for Systems and Control, Delft, The Netherlands
Email: p.j.m.m.tacx@tue.nl, t.a.e.oomen@tue.nl

1 Background

The availability of reliable and systematic robust control algorithms has spurred the development of uncertainty structures of multivariable model sets for robust control [1], [3]. Over de last decades uncertainty structures have developed from additive and multiplicative structures to more advanced structures specifically tailored for multivariable systems [2], [3]. The multivariable aspect and the more advanced uncertainty structures complicate uncertainty structure comparison, understanding, controller design, and performance analysis of uncertain systems.

2 Problem Formulation

The Bode plot is a critical tool for understanding, controller design, and performance analysis of control systems. In the scalar case, uncertainty structures for robust control reduce to a Möbius transformation from which the magnitude and phase can be computed. However, extending to multivariable systems is not straightforward, inducing the notion of phase of a multivariable uncertain system. The aim is to develop a unified approach for generating multivariable Bode plots for both the magnitude and phase of multivariable uncertain systems.

3 Approach

The key observation is that the Bode plot of scalar systems is based on the polar decomposition which naturally connects the Nyquist plot and Bode magnitude and phase plot. The key idea is to extend the polar description to the multivariable case which leads to a multivariable magnitude and phase definition [4]. The resulting multivariable magnitude and phase are extended to the uncertain case by reformulation through the S-procedure to a feasibility problem.

4 Results

The developed approach is applied to a multivariable motion system based on the uncertainty structure in [3]. The resulting multivariable Bode magnitude and phase are shown in Fig. 1, 2. The figures reveal that for frequencies in the vicinity of the bandwidth, the model set is tight. This specific behavior is attributed to the control-relevant structure. Overall, the example shows that the proposed approach offers additional insight and understanding by generating multivariable Bode plots of uncertain systems.

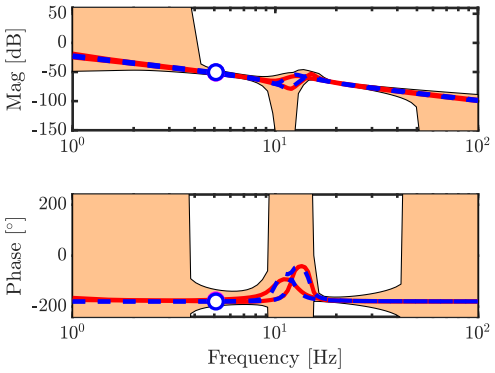

Figure 1: Multivariable Bode magnitude (top) and phase (bottom). True system P_o (——), nominal model $\hat{P}$ (——), model set (■), and target bandwidth (○).

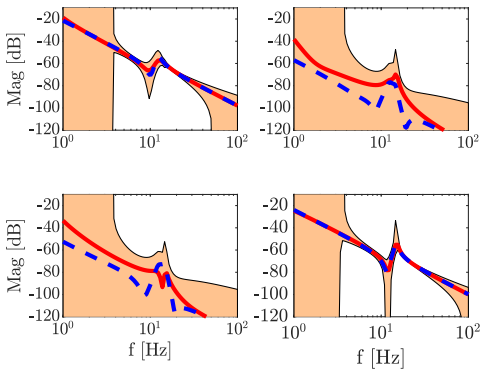

Figure 2: Element-wise Bode magnitude. True system P_o (——), nominal model $\hat{P}$ (——), model set (■).

This work is part of the research programme VIDI with project number 15698, which is (partly) financed by the Netherlands Organisation for Scientific Research (NWO).

References

[1] M. Gevers, "Identification for control: From the early achievements to the revival of experiment design," Eur. J. of Contr., vol. 11, no. 4-5, pp. 335–352, 2005.

[2] J. Doyle and G. Stein, "Multivariable feedback design: Concepts for a classical/modern synthesis," IEEE Trans. on Autom. Control, vol. 26, no. 1, pp. 4–16, 1981.

[3] T. Oomen, R. van Herpen, S. Quist, M. van de Wal, O. Bosgra, and M. Steinbuch, "Connecting system identification and robust control for next-generation motion control of a wafer stage," IEEE Trans. on Contr. Sys. Tech., vol. 22, no. 1, pp. 102–118, 2013.

[4] I. Postlethwaite, J. Edmunds, and A. MacFarlane, "Principal gains and principal phases in the analysis of linear multivariable feedback systems," IEEE Trans. on Autom. Contr., vol. 26, no. 1, pp. 32–46, 1981.

Development of physics based control-oriented models for the heat exhaust in fusion power plants

J.T.W. Koenders[1,3], M. van Berkel[1], G.L. Derks[3], H. Reimerdes[2], E. Westerhof[1] and the TCV Team*

[1] DIFFER - Dutch Institute for Fundamental Energy Research, Eindhoven, the Netherlands

[2] Ecole Polytechnique Fédérale de Lausanne (EPFL), Swiss Plasma Center (SPC), Lausanne, Switzerland

[3] Eindhoven University of Technology, Control Systems Technology, Eindhoven, the Netherlands

* See author list of S. Coda et al. 2019 Nucl. Fusion 59 112023

1 Introduction

The heat and particle exhaust in tokamaks is guided to a dedicated region called *the divertor*. Unmitigated, the expected power fluxes impacting the divertor targets during reactor relevant operation exceed present-day engineering limits [1]. Real-time feedback control of *plasma detachment*, a regime characterized by a large reduction in plasma temperature and pressure at the divertor target, is required to maintain a sufficient reduction of these fluxes [2, 3]. Control of detachment is presently achieved by puffing specific amounts of deuterium or nitrogen gas into the system. We aid detachment controller design by developing control-oriented models of the dynamic processes at play, with the aim to develop a physics based dynamic model to guide the tokamak heat exhaust control efforts.

2 Results of system identification experiments

System identification experiments have been performed on the Tokamak à Configuration Variable (TCV) [4, 5, 6]. In these experiments impurity emission fronts are used to diagnose the divertor plasma. Such an emission front is defined as follows. During plasma detachment a temperature gradient along the divertor leg is established. This gradient gives rise to a sharp optical emission fall-off, frequently referred to as a front. These fronts are indicative of a local electron temperature, and their location can be used as a measure of detachment strength. Their position is used as a control parameter which is referred to as L_{pol} as depicted in Figure 1. The emission front positions are measured using a real-time detection algorithm [7] applied to camera images from the multi-spectral imaging diagnostic MANTIS [8]. The identification experiments show phase behavior reminiscent of a diffusive, or fractional system. Using additional data from the CFD like code SOLPS-ITER to complement the experiments, it was found that a 1D diffusion transport model can accurately describe the obtained FRF measurements [9]. The physics responsible for the diffusive like behavior was hypothesized to be caused by plasma-neutral collisions the injected gas molecules undergo until they are ionised. In this talk we investigate the validity of this hypothesis by analyzing results from monte-carlo style neutral particle simulations by the code EIRENE.

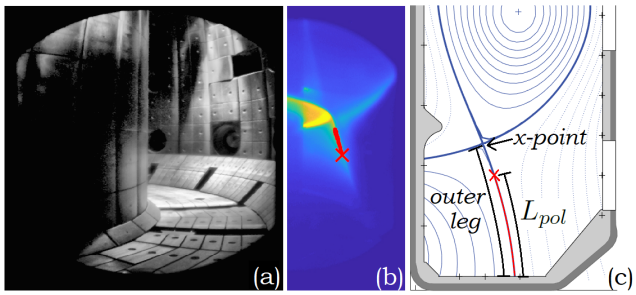

Figure 1: (a) MANTIS camera view in the TCV Tokamak [6]. (b) Identified CIII front location by the detection algorithm, indicated by the red X [5]. (c) Geometric representation of the front location L_{pol} along the outer leg.

3 Modeling based on system identification experiments

The results of the neutral particle simulations show a clear exponential decay, while an algebraic or fractional decay would be expected based on the system identification experiments. After further investigation into possible parallel processes, we find two parallel exponential time-scales could be responsible for the measured dynamics. Such a parallel dynamic system closely resembles an algebraic or fractional dynamic response. We postulate a control-oriented particle inventory model with different confinement time-scales of particles in the main and divertor plasma, which is able to reproduce experimental findings. This model opens a new direction for the further investigation of the physical processes dominating the divertor plasma response to gas injection, gaining new insights in the scaling of these dynamics to future tokamak power plants.

References

[1] R. Pitts et al., Nucl. Mat. Ener. **20**, (2019)
[2] B. Lipschultz et al., Nuclear Fusion **56**, (2016)
[3] A. Leonard, Plasma Phys. Control. Fusion **60**, (2018)
[4] T. Ravensbergen et al., Nat. Commun. **12**, (2021)
[5] M. van Berkel et al., PPCF **62**, (2020)
[6] S. Coda et al., Nucl. Fusion **59**, (2019)
[7] T. Ravensbergen et al., Nucl. Fusion **60**, (2020)
[8] A. Perek et al., Rev. Sci. Instrum. **90**, (2019)
[9] Koenders et al., Nucl. Fusion, (submitted)

On designing MPC controller with obstacle avoidance for a Parallel SCARA robot

Taranjitsingh Singh, Christophe Lauwerys, Branimir Mrak and Quentin Docquier
Flanders Make
Lommel, Belgium
Email: firstname.lastname@flandersmake.be

1 Introduction

There has been an increasing demand in manufacturing industries for fast motion tasks like pick and place. In hindsight, steady decrease in the cost of computing power gives closed kinematic structured robots like parallel SCARA a mechanical advantage for such tasks [1]. Advanced technique like model predictive control (MPC) is one of the favourable techniques that allows formulation of optimal trajectory planning that minimizes energy or time for sunc fast motion tasks. This article presents an energy-optimal based MPC design for trajectory optimization of a parallel SCARA robot with obstacle avoidance.

2 Approach

Our MPC control algorithm is computed by solving the following optimization problem:

$$\begin{aligned} &\text{optimize:} && \text{end-effector trajectory from starting to end} \\ &\text{subject to:} && \text{Model} \\ & && \text{end-effector speed constraint} \\ & && \text{end-effector initial and final constraints} \\ & && \text{obstacle avoidance} \end{aligned} \tag{1}$$

The objective of the MPC controller is to find a trajectory for the end-effector from an initial position to the final position while avoiding obstacle. The obstacle avoidance constraints are handled by the existence of a hyperplane between the end-effector and obstacle at each time instant. This approach can easily accommodate moving obstacles. We consider readily available variants of kinematic and dynamic models in the Joint and Cartesian space. The optimization problem 1 is formulated and solved using an ongoing high-level toolbox on top of CasADi framework [2].

Figure 1 shows the results with considering kinematic models in Cartesian space. We found out that our algorithm optimizes the trajectory from the starting point to the end point in 0.25[s] by avoiding the obstacle and without violating the end-effector speed limits (also shown in the figure). The computation time is approximately 179[ms] for the considered model variant. Simulations were also performed with

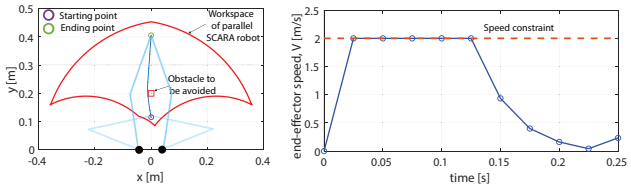

Figure 1: (left) End-effector trajectory from starting point to the final point with obstacle avoidance. (right) End-effector speed satisfying constraints.

the rest of the variants of model and they show satisfactory results.

3 Future Work

Future works include the design of our MPC algorithm in the presence of a moving obstacle. The main aim of our research is to bring the advanced controller to the manufacturing industries. Hence, the implementation of MPC algorithms on industrial platforms online is required to overcome the drawback related to the computation time. We also aim at developing computationally feasible plug-and-play MPC algorithms for industrial platforms and validate it on parallel SCARA robot.

References

[1] A. Burisch, S. Soetebier, J. Wrege, and R. Slatter, "Design of a parallel hybrid micro-scara robot for high precision assembly," in *Mechatronics and Robotics*, vol. 4. Citeseer, 2004, pp. 1370–1380.

[2] J. A. Andersson, J. Gillis, G. Horn, J. B. Rawlings, and M. Diehl, "CasADi: a software framework for nonlinear optimization and optimal control," *Mathematical Programming Computation*, vol. 11, no. 1, pp. 1–36, 2019.

Acknowledgement: This work is supported by Flanders Make SBO project: DIRAC: Deterministic and Inexpensive Realizations of Advanced Control.

A consensus approach to balancing the capacitor voltage for modular multilevel converters

Victor Daniel Reyes Dreke[1], Mircea Lazar[1]
[1] Control Systems Group, Eindhoven University of Technology, 5600 MB Eindhoven, The Netherlands
Email: v.d.reyes.dreke@tue.nl

1 Introduction

Modular multilevel converters (MMCs) are leading the way to improve the performance of the power converters in many industrial applications [1]. Their higher efficiency, their lower harmonic distortion content, their transformerless operational capability, and their fault tolerance make the MMCs a better solution than most voltage-source-converters (VSCs) in many applications. Consequently, this hardware has been used as a core element to develop more efficient and sustainable solutions for industrial applications, like renewable energy generation, high-voltage direct-current (HVDC) transmission and ultra-fast charging stations (UFCS).

2 Motivation

To achieve the expected performance or even to improve it, accurate control techniques for the MMC are needed. In this case, as presented in Figure 1, the MMCs have a modular structure, which implies that coordinated actions among the modules (SM) are required to operate the MMC efficiently. The controller implemented in this system should steer all the capacitors voltage to a common value during its entire operation for guaranteeing safety and reliability.

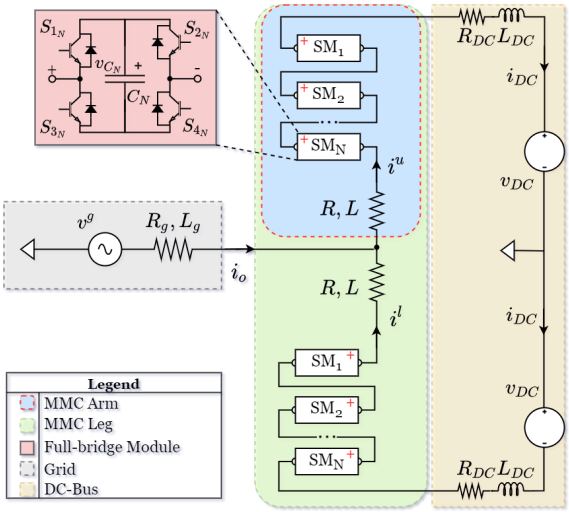

Figure 1: Modular multilevel converter schematic.

The discrete-time dynamic of the i^{th} module is formulated as

$$\Sigma_i : x_i(k+1) = x_i(k) + \frac{T_s}{C} \cdot w(k) \cdot u_i(k), \qquad (1)$$

where T_s is the sampling time, C is the modules capacitance, $x_i \in \mathbb{R}$ is the i^{th} module capacitor voltage, $w \in \mathbb{R}$ is the current going through the i^{th} module and $u_i \in \{-1, 0, 1\}$ is the control input. This dynamic offers two main challenges for controlling the system: *(i)* bilinear behaviour, and *(ii)* finite-discrete control inputs.

3 Approach

Aiming to overcome the challenge of controlling the MMC, we propose a consensus control approach to balance the capacitor voltages. In this case, we based our solution on the framework presented in [2, 3]. Different from the literature, we design a communication network with a leader-ring-followers architecture that ensures convergence to a consensus state set by the leader regardless of the number of modules connected. This solution offers higher robustness than [1] due to its distributed implementation and the fact that the leader only needs to be virtually connected to one follower. Figure 2 shows partial results of the proposed solution.

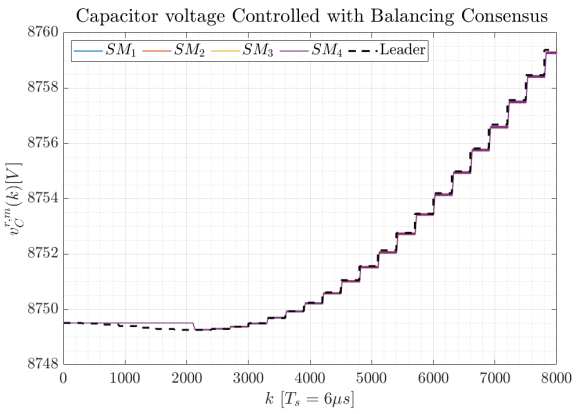

Figure 2: Capacitor voltage behaviour under consensus control.

References

[1] L. Mathe, P. D. Burlacu, and R. Teodorescu, "Control of a modular multilevel converter with reduced internal data exchange," *IEEE Transactions on Industrial Informatics*, vol. 13, no. 1, pp. 248–257, 2017.

[2] J. Lunze, *Networked Control of Multi-Agent Systems*, vol. 1. Bookmundo, 1 ed., 2019.

[3] Y. Koyama and T. Isobe, "Current control of modular multilevel converters using a daisy-chained distributed control system with communication path redundancy," in *IECON 2019 - 45th Annual Conference of the IEEE Industrial Electronics Society*, vol. 1, pp. 6108–6113, 2019.

Detection and Isolation of Small Faults in Lithium-Ion Batteries via the Asymptotic Local Approach

Luis D. Couto[1], Jorn M. Reniers[2], David A. Howey[2], Michel Kinnaert[1]
[1]Department of Control Engineering and System Analysis
Université libre de Bruxelles (ULB), B-1050 Bruxelles, Belgium
Email: lcoutome@ulb.ac.be, michel.kinnaert@ulb.ac.be

[2]Department of Engineering Science
University of Oxford, Oxford OX1 3PJ, UK
Email: jorn.reniers@eng.ox.ac.uk, david.howey@eng.ox.ac.uk,

Lithium-ion batteries are the most promising energy storage systems due to their high energy and power density. Indeed, they power up a wide spectrum of applications from mobile phones to electric cars. However, the better performance of lithium-ion batteries is at the expense of possible safety concerns when these batteries are mishandled. Possible safety hazards are commonly prevented through battery oversizing, but this yields bigger, more expensive and underused batteries. An alternative approach is to build less conservative batteries while relying on battery diagnostics for detection and isolation of possible faults affecting battery behaviour.

The supervision of lithium-ion batteries is carried out by a battery-management system, which is in charge of monitoring the state of the battery notably including state-of-charge (SoC) and state-of-health (SoH). The SoH is the battery condition in a given sense (e.g. capacity) with respect to its condition at the beginning-of-life. Popular approaches for SoC & SoH estimation rely on state observers (e.g. Kalman filters) exploiting a model of the battery, where SoH involves model parameters that evolve slowly with time as the battery ages. However, identifiability issues may arise from the state/parameter interplay, and an additional decision system is needed to analyse the evolution of the model parameters as well as evaluate their significance with respect to estimation error. In contrast with state/parameter estimation, another model-based approach resorts to residual generation, which involves state observers or parity relations. One should notice that the obtained methods were initially developed for additive faults. However, changes in model parameters (i.e. multiplicative faults) belong to another category. In this case, parity relation residuals will exhibit patterns that depend on the operating conditions. Besides, observer-based residuals consisting of the innovation sequence are not a sufficient statistic to detect multiplicative faults.

In this work, we want to achieve early change detection and isolation of lithium-ion battery degradation (multiplicative faults) from standard battery operation data. To this end, we design a diagnosis scheme (see Fig. 1) that exploits a specific type of residual (the so-called primary residual) in the context of the asymptotic local approach [1]. It must be stressed that this residual represents a sufficient statistic for parametric change detection. The diagnosis scheme relies on three aspects. First, a reduced-order electrochemical model of the battery under both healthy and faulty conditions was used. Secondly, a state observer was used to notably generate the primary residuals. Finally, the residuals were exploited by statistical tests for FDI. In contrast with previous contributions [2], a wide faulty parameter space is explored, including single and multiple faults acting simultaneously. Moreover, a statistical test based on Nikiforov's method [3] was studied via Monte Carlo simulations under two possible fault magnitudes. This test is able to detect small faults and discriminate between them. The detection and isolation accuracy of Nikiforov's method improves with increasing fault magnitudes, although parameters with possibly low sensitivity and faults involving them are more difficult to diagnose. Since the proposed fault detection and isolation (FDI) scheme is able to handle small faults, it could unlock the possibility of sorting batteries according to their quality (strong vs weak cells) at the very beginning of battery life after few cycling operations. Having battery packs with low cell-to-cell variability would potentially extend the pack useful life.

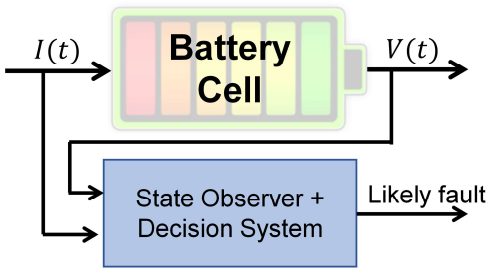

Figure 1: Block diagram of the FDI scheme.

Acknowledgement

This research is supported by the Fonds de la Recherche Scientifique - FNRS under grant n°T.0142.20 and the Wiener-Anspach Foundation.

References

[1] M. Basseville, "Model-based statistical signal processing and decision theoretic approaches to monitoring", IFAC Proceedings, 2003. 36: p. 1-12.

[2] L.D. Couto, J.M. Reniers, D.A. Howey and M. Kinnaert, "Detection and Isolation of Small Faults in Lithium-Ion Batteries via the Asymptotic Local Approach", American Control Conference, 2021, p. 4434-4440.

[3] I. V. Nikiforov, "A simple recursive algorithm for diagnosis of abrupt changes in signals and systems", ACC Proceedings, 1998. 3, p. 1938-1942.

Charge and Balance of a String of Li-ion Cells: An Explicit Reference Governor approach

Alejandro Goldar
SAAS - ULB
alejandro.goldar.davila@ulb.be

Emanuele Garone
SAAS - ULB
emanuele.garone@ulb.be

Some battery-powered devices sometimes require a series-parallel arrangement of Lithium-ion cells, *a battery pack*, to fulfill voltage, power and capacity demands. Although, all the cells within the pack should have identical dynamics for a given charging profile, cells might not react in the same way, showing operational imbalances.

A Battery Management System (BMS) should be able to counteract possible imbalances occurring within the pack in order to avoid undesirable degradation phenomena. Thus far, imbalances between cells are equalized either by dissipating the excess of energy or by transferring the energy from one cell to another. Most of these currently-available equalization strategies are empirically designed to counteract voltage imbalances without accounting for the charging process. In fact, the imbalances are equalized during idle times, when the current is assumed to be constant.

For a string of cells, the charging and balancing problem is addressed by some authors by making use of Model Predictive Control (MPC), resulting in nonlinear and complex-to-solve policies. The main challenge to solve an MPC for the charge and balance of the battery string underlies in the configuration of the balancing grid. To equalize possible imbalances, each cell within the string might be connected, or disconnected, to the grid. Therefore, the description of the connection scenarios within the MPC builds a nonlinear mixed-integer problem that, to the best of our knowledge, is not solvable in polynomial time. Although in [1] we propose a max-min to reduce the complexity of this mixed-integer problem, it is not implementable from a computational viewpoint for a large number of cells (Fig. 1, dash-dotted line with triangle markers).

A better approach, as showed in [2], is to consider pulse-width modulation (PWM) for the shunting switches of the balancing grid. Thus, both the duty cycles of switches and the charging current of the string can be determined by a continuous nonlinear optimization. However, the computational intensiveness of such nonlinear optimization explodes when a large number of cells forms the string (Fig. 1, dotted line with plus markers).

The computational burden of the resulting nonlinear MPC can be nevertheless reduced (Fig. 1, dash-dotted line with diamond markers) by evaluating individual optimization sub-problems, that find the charging current for each cell to calculate afterwards the duty cycles as the ratios between the individual current of each cell and the maximum current (Alg. 2 [1]). However, the computational capabilities of some BMS might not allow solving a high number of optimization problems at each time instant. Therefore, charging protocols with a few –and less complex– number of operations are more convenient and time saving. A possible way to further reduce the computational burden of the MPC is by replacing it in each sub-problem with a cascade architecture whose inner loop ensures stability and fast tracking, and its outer loop enforces constraints satisfaction by finding a suitable reference.

This work proposes a modification of the ratio-based algorithm of [1] that makes use of a cascade architecture for each cell, where the outer loop is an Explicit Reference Governor (ERG). The ERG is a variant of the reference governors that relies on the invariance of Lyapunov level-sets to ensure constraint satisfaction. This means that neither prediction nor online optimization is required, making it very efficient due to a reduced required number of operations. When this scheme is implemented (Fig. 1, continuous line with star markers), the computational time does not increase significantly when more cells are considered within the string.

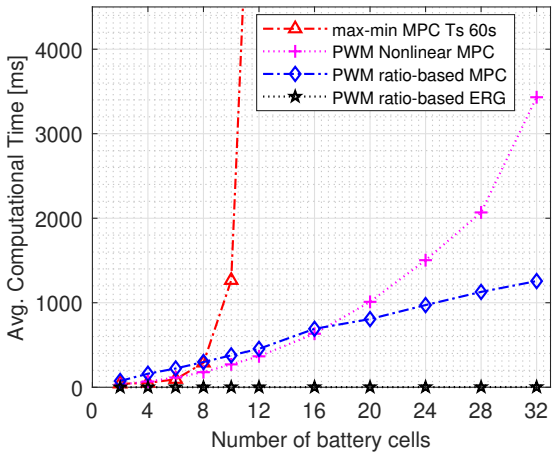

Figure 1: Effects on the Computational time of the cell number

References

[1] Goldar, A., Kinnaert, M., Garone, E. (2020). A comparison of low-complexity charging and balancing protocols with degradation awareness for a string of Li-ion cells. In 21st IFAC World Congress, 53(2), 11570-11576.

[2] Pozzi, A., Zambelli, M., Ferrara, A., Raimondo, D. (2020). Balancing-aware charging strategy for series-connected lithium-ion cells: A nonlinear model predictive control approach. IEEE Trans. on Control Syst. Tech., 28(5), 1862-1877.

Point-to-point trajectory generation and motion control for vibration reduction of swinging products

Robbert van der Kruk
Mechanical Engineering Control Systems Technology Technical University Eindhoven
r.j.v.d.kruk@tue.nl

1 Abstract

Input shaping can effectively reduce residual vibrations of flexible systems induced by the reference signal. It requires a trade off of increased travel time versus reduced overshoot. In this paper a new method is introduced to relate the relative overshoot to the ratio of vibration time and travel time. Practical applications of robotics point to point control of swinging products include case packing of food in liquid contained bags such as soap and cheese.

For fast pick and placement of swinging products input shaping provides significant reduction of the overshoot, without additional time, when the travel time is less than 1.8 times and larger than 2.5 times the natural vibration time. The classic input shaper ZV provides best performance. Combined with matching the feedback controller bandwidth to the vibration frequency of the swinging product the input shaper provides similar performance while providing a smoother acceleration of the object to reduce peel-off. An experimental validation on a delta robot system confirms the performance improvement obtained by an zero vibration input shaper for a cheese product packed in a liquid bag suspended by means of a suction cup.

In extreme accurate applications for flexible joint systems which require minimal overshoot, input shaping has the potential to reduce the residual vibration in case the travel time is longer than twice the vibration time. For faster flexible joint applications where the travel time approaches the vibration time, the additional travel time of the ZV shaper does significantly trade off with the obtained overshoot reduction.

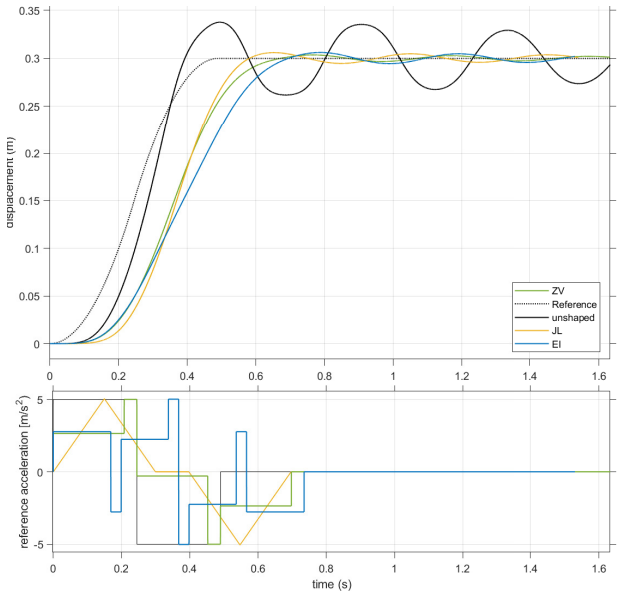

Figure 1: Displacement and reference acceleration for input shaped parabolic shaped trajectories. Frequency well tuned, damping mismatch: 10%. Ratio $vibrationtime/traveltime = 0.7$

Collision-free Source Seeking Control of Unicycle Robot under Uncertain Environment

Tinghua Li [1] t.li@rug.nl
Bayu Jayawardhana[1] b.jayawardhana@rug.nl

[1] DTPA, ENTEG, Faculty of Science and Engineering, University of Groningen, The Netherlands

1 Abstract

In this work, we proposed a collision-free source seeking control of unicycle robot in an unknown cluttered environment, where the obstacle avoidance is guided by the control barrier functions (CBF) embedded in quadratic programming, and the source seeking control relies solely on the use of on-board sensors that measure signal strength of the source. To tackle the mixed relative degree of the CBF, we proposed three different CBF, namely the zeroing control barrier functions (ZCBF), reciprocal control barrier functions (RCBF) and exponential control barrier functions (ECBF), that can directly be integrated with our recent gradient-ascent source-seeking control law. We provide rigorous analysis of the three different methods and show the efficacy of the approaches in simulation using realistic virtual environment of Gazebo/ROS.

2 Problem Formulation and Control Design

For the safety-guaranteed source seeking control problem, we consider an unknown dynamic environment where the source emanates laminar flow, and it decays with the distance to the source. The unicycle robot is equipped with sensors for real-time signal strength and obstacle distance measurements. The robot can drive forward with a longitudinal velocity u and rotate with an angular velocity ω.

Consider the nonlinear system

$$\dot{x} = f(x) + g(x)u \tag{1}$$

where state $x \in \mathbb{R}^n$, control input $u \in \mathbb{R}^m$, and $f, g : \mathbb{R}^n \to \mathbb{R}^n$ assumed to be locally Lipschitz continuous. The aim of the collision-free source seeking problem is to design a control law which generates admissible states such that keep the system within the safe set $\mathscr{X}_s$ for all $t \geq 0$, gradually approach and finally stabilize within the close range of the unknown source's location. The safe set is described as

$$\mathscr{X}_s = \left\{ \left\| x - x_{obs,i} \right\| - d \geq 0 \right\} \tag{2}$$

where i is the sequence number of the obstacles which is currently with the closest Euclidean distance to the robot, d is the pre-set minimum safe distance between robot and obstacle's boundary, (x, y) and $(x_{obs,i}, y_{obs,i})$ denote the center coordinates of robot and the boundary coordinate of the i-th obstacle, respectively.

To clarify, the safe set denotes the closest Euclidean distance between robot and obstacles' boundary (which can be the fixed static obstacles, moving objects, or walking person).

In particular, to combine the source seeking control [1] with the barier function, we solve the mixed relative degree of the control inputs v and ω by three methods, which applied with ZCBF, RCBF and ECBF, respectively. The control barrier functions are constructed by considering the distance and orientation of the robot to the closest obstacle's boundary.

The optimal safe control input u^* can thereby be obtained by solving the quadratic programming problem with three various constraints:

$$u^* = \underset{u \in \mathscr{U}}{\operatorname{argmin}} \frac{1}{2} \left\| u - u_s \right\|^2 \tag{3}$$

where the reference control input u_s comes from the source seeking algorithm [1].

3 Main Results

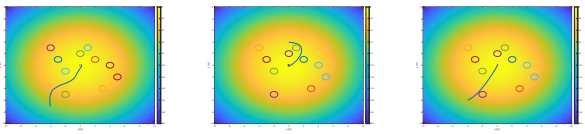

(a) ZCBF (b) ECBF (c) RCBF

Figure 1: Simulation results based on the three control barrier functions h, where both the longitudinal and angular velocity are controlled. The source is set at the origin $(0,0)$, surrounded by multiple circular-shape obstacles, and the signal strength is distributed as $J(x,y) = -x^2 - y^2$. The robot is set at three various initial positions (noted as $'o'$) to search the source (noted as $'*'$) while avoiding the collision with obstacles, the minimum safe distance between robot and the obstacle's boundary is set as 0.1.

References

[1] T. Li, B. Jayawardhana, A.M. Kamat and A.G.P. Kottapalli, "Source-Seeking Control of Unicycle Robots With 3-D-Printed Flexible Piezoresistive Sensors," *IEEE Transactions on Robotics*, 2021.

A Hybrid-System Formalism to Verify Properties of Robot Swarms

Guillermo Legarda Herranz[1], Emanuele Garone[2], Mauro Birattari[1]
[1]IRIDIA-CoDE, [2]SAAS, Université libre de Bruxelles
Av. F. D. Roosevelt 50, 1050 Bruxelles, Belgium
{guillermo.legarda.herranz, emanuele.garone, mauro.birattari}@ulb.be

1 Abstract

Robot swarms constitute an attractive solution to carry out tasks where the environment may pose a threat to human operators or where single robots would not be able to perform efficiently. Their robustness and scalability arise from a fully decentralised control architecture and make them preferable in such scenarios to multi-robot systems controlled in a centralised fashion. While interest in this field has been growing steadily over the past twenty years, a systematic method to design the control software for each of the individual robots in a way that guarantees some desired properties of the resulting collective behaviour is still missing. This is one of the main limitations that hinders the use of robot swarms in real-world applications. In this project, we aim to develop a framework that allows to describe the desired properties of a swarm and automatically generate control software that ensures such properties.

Robot swarms consist of relatively simple robots (see Figure 1), which frequently interact with each other in their pursuit of a common goal. Together with the systematic uncertainties introduced by imperfect sensors and actuators, this makes the resulting system behaviour highly unpredictable. A common approach to the verification problem has been to model robot swarms as Markov chains and use model-checking tools. We argue that the use of hybrid systems to model robot swarms allows for a desirable abstraction of the swarm dynamics and may therefore be used to formally verify a richer variety of their properties. For previous work that followed the same motivation, see [1].

In our approach, we define the properties of a robot swarm as constraints on appropriate state variables, such as inter-robot distances and velocities. Such properties reflect characteristics of the swarm behaviour that may be required or desired for a given task, such as collision avoidance or aggregation at a given location. A review of swarm robotics tasks can be found in [2]. This approach, while more common in the field of control theory than in swarm robotics, allows us to systematically produce inequality constraints that are platform-agnostic and, thus, generalisable.

Through these constraints, we define differential invariants, which may be used to either complement bounded model checking tools or for deductive verification. In particular, we explore the use of differential dynamic logic (d$\mathscr{L}$), which

Figure 1: The e-puck robot, a swarm robotics platform of widespread use for research purposes.

follows the grammar

$$\phi, \psi ::= p(\theta_1, ..., \theta_n) | \neg\phi | \phi \wedge \psi | \phi \vee \psi | \phi \rightarrow \psi | \forall x \psi | \exists x \psi | [\alpha]\phi | \langle\alpha\rangle, \quad (1)$$

where ϕ and ψ are formulas, θ_1 and θ_2 are terms, p is a predicate symbol, x is a logical variable and α is a hybrid program [3]. Extensions of d$\mathscr{L}$, including differential dynamic temporal logic (dTL) and quantified differential dynamic logic (Qd$\mathscr{L}$), provide tools for reasoning about the temporal behaviour of hybrid systems and about distributed hybrid systems, respectively.

Acknowledgements

The project has received funding from the European Research Council (ERC) under the European Union's Horizon 2020 research and innovation programme (DEMIURGE Project, grant agreement No 681872) and from Belgium's Wallonia-Brussels Federation through the ARC Advanced Project GbO—Guaranteed by Optimization. M. Birattari acknowledges support from the Belgian Fonds de la Recherche Scientifique—FNRS, of which he is a Research Director.

References

[1] F. Leofante, S. Schupp, E. Ábrahám, and A. Tacchella (2019). "Engineering Controllers for Swarm Robotics via Reachability Analysis in Hybrid Systems". ECMS Proceedings, pp. 407-413.

[2] M. Brambilla, E. Ferrante, M. Birattari, and M. Dorigo (2013). "Swarm robotics: A review from the swarm engineering perspective". Swarm Intelligence, 7(1):1-41.

[3] A. Platzer (2012). "Logical Analysis of Hybrid Systems". Descriptional Complexity of Formal Systems. DCFS 2012. Lecture Notes in Computer Science, vol 7386. Springer, Berlin, Heidelberg.

Safe Human-Robot Collaboration in Mixed Teams

Elise Verhees, Elena Torta, Michel Reniers, and René van de Molengraft
Control Systems Technology, Eindhoven University of Technology
P.O. Box 513, 5600 MB Eindhoven, The Netherlands
Email: e.d.t.verhees@tue.nl

1 Introduction

Due to the many recent developments in autonomous robotic solutions, close interaction with people to accomplish a shared goal has become reasonably common [1]. Robot coworkers possess qualities like strength, endurance, and precision. This makes them valuable team members, that complement human's flexibility and decision making. This project aims to address safe human-robot collaboration, while explicitly targeting mixed teams, and in the presence of learning and adaptation.

2 Challenges

While a lot of research has already been done with regard to Human Robot Interaction, existing work is mainly focused on a single robot interacting with a single human [2]. Moreover, the environment is often controlled and the considered time horizon short. It thus remains to be seen whether current approaches could be adopted in dynamic settings involving mixed teams.

3 Method

The focus of this research lies on context awareness, learning and adaptation, and supervisory control for ensuring both safety and task progression (Fig. 1); all are considered from a human-robot mixed team perspective. Robots that are aware of their context are able to observe and interpret the state of their environment, as well as use this to infer their team members' intentions. The contextual cues important for mixed team tasks and the sharing of information between team members will be investigated. This will be complemented by a literature study about existing world modelling architectures. Furthermore, mutual learning is relevant for behavior adaptation and improving coordination between team members. Therefore, a study to identify which learning method is best suited for mixed team tasks in a dynamic environment will be conducted. Lastly, a *safe* progression towards the goal is essential. Supervisory control theory will be researched to determine whether it can be used to ensure meaningful progression of the task, while at the same time achieve predictive and thus preventive safety. This allows smooth collaboration in the team, as opposed to incorporating safety switches that are triggered when a threshold is violated.

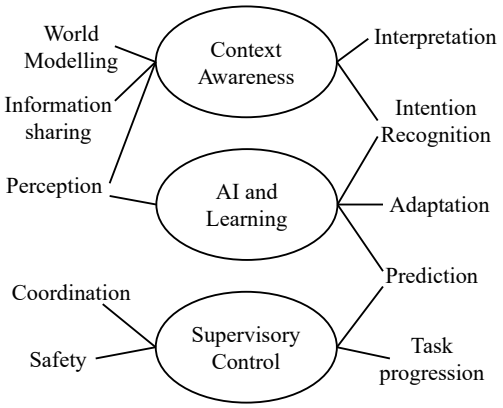

Figure 1: Research topics

The literature research on the above mentioned topics should highlight current limitations with respect to mixed teams. Based on these limitations, new modelling approaches for the design of world models and supervisory controllers for mixed teams in the presence of learning and adaptation will be devised. The new methods will be validated on a research integrator consisting of at least two robots and two humans.

4 Conclusion

Our presentation will introduce the initial ideas of the project on safe human-robot collaboration in mixed teams. We will discuss the goal and challenges, and introduce the topics relevant for tackling the problem. Hopefully, this will trigger an open discussion about relevant methods and insights to advance the state of the art in world modelling, learning, and supervisory control theory for collaboration in mixed teams.

References

[1] Villani, V., Pini, F., Leali, F., & Secchi, C. (2018). Survey on human–robot collaboration in industrial settings: Safety, intuitive interfaces and applications. *Mechatronics*, 55, 248-266.

[2] Park, H. W., Grover, I., Spaulding, S., Gomez, L., & Breazeal, C. (2019, July). A model-free affective reinforcement learning approach to personalization of an autonomous social robot companion for early literacy education. In *Proceedings of the AAAI Conference on Artificial Intelligence* (Vol. 33, No. 01, pp. 687-694).

Trajectory optimization of a high speed pick and place unit using soft switching multiple model predictive control

Babak Mehdizadeh Gavgani[1,2*], Arash Farnam[1,2], Foeke Vanbecelaere[1,3], Jeroen D. M. De Kooning[1,3], and Guillaume Crevecoeur[1,2]

[1]Department of Electromechanical, Systems and Metal Engineering, Ghent University, Belgium
[2]FlandersMake@UGent – corelab EEDT-DC, Flanders Make, Belgium
[3]FlandersMake@UGent – corelab EEDT-MP, Flanders Make, Belgium
[*]Email: babak.mehdizadehgavgani@ugent.be

1 Introduction

Considering the increasing trend in energy consumption and its consequent negative impacts on global warming, the development of energy efficient industrial machines is highly valued. Moreover, industry desires techniques which are applicable to current manufacturing infrastructures with limited to no hardware adaptations. Within this scope, trajectory optimization is a promising cost-effective alternative with no necessity for further investments. In trajectory optimization, the machine user only needs to define the starting position (θ_{start}) and ending position (θ_{final}) of the machine as shown in Fig. 1. The time duration (Δt) of the motion task can also be provided with the aim to optimize the energy efficiency. Up to now, a wide range of trajectory optimization techniques have been reported in literature amongst which the prevalent MPC paradigm. Nonlinear MPC allows to find setpoints for motion control systems but when facing fast dynamic systems, the setpoints need to be delivered in bounded time. In this work, an online optimal trajectory design strategy based on Soft Switching Multiple Model Predictive Control (SSM-MPC) for an industrial pick-and-place machine is proposed. By using the SSM-MPC, the generated trajectory will be adaptive to system parameters variations such as load inertia, etc.

2 System modeling and trajectory optimization

Due to the inherent optimization nature of MPC while handling system constraints, it seems promising to design not only an optimal but also a robust trajectory. Nonlinear MPC is an interesting candidate to generate optimal trajectories considering the nonlinear behaviour of the industrial application. However, calculating the optimal trajectory is not guaranteed in terms of the computational time for nonlinear MPC while during nonlinear operation the computational load needs to be bounded in time. To tackle these challenges, this work presents the SSM-MPC to design optimal trajectories for motion control systems. We first linearize the nonlinear system model around various operating points to build up a model bank [1]. We use the gap metric tool to optimize the model bank size by assessing the similarity between the two neighboring linear models. Figure 1 depicts the pick and place unit and its simplified model based on a two mass spring damper system. The governing dynamics of

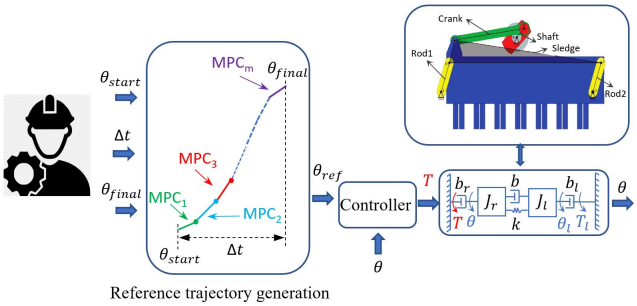

Figure 1: Schematic overview of the SSM-MPC trajectory generation strategy

this model are summarized in (1) where J_r is the rotor-side inertia and J_l is the load-side inertia, which depends on the load position θ_l. The coupling parameters are stiffness k and damping b. b_l and b_m are the load and motor-side external dampings, respectively. The motor torque T is the control input and the machine position θ is the system output. T_l is the load side torque which is a function of θ_l.

$$\begin{cases} T - b_m\dot{\theta} - b(\dot{\theta} - \dot{\theta}_l) - k(\theta - \theta_l) = J_r\ddot{\theta} \\ T_l - b_l\dot{\theta}_l + b(\dot{\theta} - \dot{\theta}_l) + k(\theta - \theta_l) = \frac{1}{2}\dot{J}_l\dot{\theta}_l + J_l\ddot{\theta}_l \end{cases} \quad (1)$$

In a chosen operating point $\theta = \theta^*$, $J_l(\theta^*)$ and $T_l(\theta^*)$ are constant values. By applying frequency domain analysis, the nonlinear system model behavior around θ^* can be approximated by $G(s) = \frac{\dot{\theta}(s)}{T(s)}$. The model bank is constructed by applying the gap metric technique on this approximation in various operating points. Next, the linear MPCs are defined according to the obtained model bank. As shown in Fig. 1, by varying the operating point, the switching unit will switch between the linear MPCs to generate the optimal trajectory. Each linear MPC will generate the optimal trajectory for the operating region in which it was designed.

3 Acknowledgments

This work was supported by the Flanders Make SBO project DIRAC.

References

[1] B.M. Gavgani, A. Farnam, J. D. M. De Kooning, and G. Crevecoeur "Efficiency Enhancements of Wind Energy Conversion Systems using Soft Switching Multiple Model Predictive Control," IEEE Transactions on Energy Conversion, October 2021 (Early access).

Deep Learning-based Identification of Koopman Models with Inputs

Lucian Cristian Iacob[a], Gerben Izaak Beintema[a], Maarten Schoukens[a] and Roland Tóth[a,b]
[a]Control Systems Group, Eindhoven University of Technology, Eindhoven, The Netherlands
[b]Systems and Control Laboratory, Institute for Computer Science and Control, Budapest, Hungary
Email: {l.c.iacob, g.i.beintema, m.schoukens, r.toth}@tue.nl

1 Introduction

In recent years, there has been a growing interest in the development of global linear embeddings of nonlinear dynamical systems. A possible solution is given by the Koopman framework. The main idea is to lift the nonlinear system to a possibly infinite dimensional, but linear, space where the dynamics are governed by a so-called Koopman operator. In practice, only a limited number of lifting functions (called observables) can be used. However, as the choice is generally ad-hoc, there is no guarantee on the approximation capability. Furthermore, in its original formulation, the Koopman framework only addresses autonomous systems. In the present work, we aim to address these shortcomings.

2 Proposed method

To learn the lifting from data, we employ deep Artificial Neural Networks (deep-ANNs) and develop an encoder based on the concept of reconstructability [1]. The model structure is selected as control affine, leading to a linear form, with a varying input matrix.

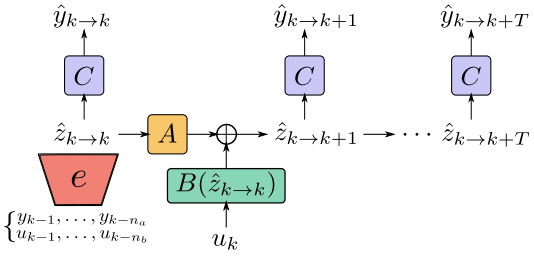

Figure 1: Network structure

The data generating system is considered to have a nonlinear control affine representation:

$$x_{k+1} = f(x_k) + g(x_k)u_k, \qquad y_k = h(x_k) + v_k, \qquad (1)$$

where f, g, h are nonlinear maps, $x_k \in \mathbb{R}^{n_x}$ is the state, $u_k \in \mathbb{R}^{n_u}$ is the input, $y_k \in \mathbb{R}^{n_y}$ is the output and $v_k \in \mathbb{R}^{n_y}$ is an additive zero-mean noise. The selected model structure is defined next:

$$\hat{z}_{k+1} = A_\theta \hat{z}_k + B_\theta(\hat{z}_k)u_k, \qquad \hat{y}_k = C_\theta \hat{z}_k, \qquad (2)$$

with A being the Koopman matrix, $B(z)$ is a nonlinear function of the lifted state $z \in \mathbb{R}^{n_z}$ and C denotes the linear output map. The control affine model structure is chosen as it offers more flexibility in the learning process, providing a better approximation capability than using a constant input matrix [1]. The subscript θ denotes the parameters (weights and biases) of the ANN. The initial lift to $\hat{z}_{k\to k}$ is achieved using the encoder function e_θ:

$$\hat{z}_{k\to k} := e_\theta(y_{k-n_a:k-1}, u_{k-n_b:k-1}), \qquad (3)$$

where e_θ is a combination of the inverse of the constructability map and a set of nonlinear constraints. The indentification approach assumes an Output Error (OE) noise model structure and uses a T-step ahead prediction based identification criterion. The parameters θ are tuned using batch optimization, allowing for the parallelization of the computations.

3 Example

To illustrate the capabilities of the proposed method, we use the Silverbox benchmark [2], which is an electrical implementation of a mass-spring-damper system with a cubic spring nonlinearity, showing a similar behaviour to a forced Duffing oscillator. As can be seen in Fig. 2, when a multisine test input is applied, the identified model can accurately represent the dynamics of the true system. When a linearly increasing filtered Gaussian (arrowhead) input is applied, the error increases towards the end, due to the extrapolation region (where data was not available for training). If this region is discarded, the obtained results are comparable to the state of the art.

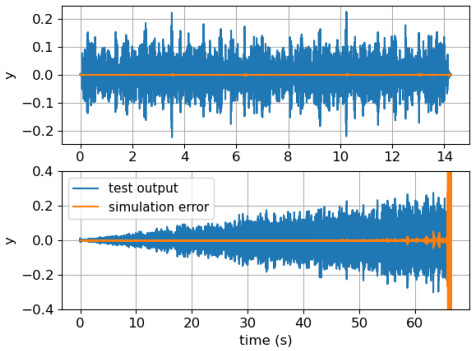

Figure 2: Multisine test (top) and arrowhead (bottom)

References

[1] L. C. Iacob, G. I. Beintema, M. Schoukens and R. Tóth, *Deep Identification of Nonlinear Systems in Koopman Form*, Conference on Decision and Control, 2021

[2] T. Wigren and J. Schoukens, *Three free data sets for development and benchmarking in nonlinear system identification*, European Control Conference, 2013

This work has received funding from the European Research Council (ERC) under the European Union's Horizon 2020 research and innovation programme (grant agreement nr. 714663).

Constructing a Lyapunov function for nonlinear systems via the Koopman operator approach

Christian Mugisho Zagabe and Alexandre Mauroy
Namur Institute for Complex Systems (naXys), Department of Mathematics
University of Namur, Rue J. Grafé 2, B-5000 Namur, Belgium
Email: christian.mugisho@unamur.be and alexandre.mauroy@unamur.be

1 Introduction

Characterizing global stability remains a challenge in dynamical systems theory. Thanks to the Lyapunov's second method, the existence of a Lyapunov function guarantees global stability, but there is no general method to construct it. The Koopman operator approach can be seen as a "global linearization" of the dynamics and therefore can be used to induce global properties such as global stability. For a given nonlinear system, the associated infinitesimal generator of the semigroup of Koopman operators (Koopman generator in short) acts linearly on observables (see [3]). This action can be seen as a linear infinite-dimensional representation of the nonlinear system that is amenable to spectral analysis. In particular, the existence of specific Koopman eigenfunctions yields necessary and sufficient conditions for the global stability of hyperbolic attractors [1].

Using the Kooopman operator approach, we proposed in [2] a novel method for constructing a common Lyapunov function for particular switched nonlinear systems. Our goal is to extend the constructive method of [2] to linear infinite-dimensional cases and induce Lyapunov function for the original nonlinear system. Regarding theoritical aspects in Koopman theory (see e.g.[3]) we will focus on vector fields on polydiscs, so the Koopman generator is defined in the Hardy space of polydiscs $\mathbb{H}^2(\mathbb{D}^n)$.

2 Koopman operator on $\mathbb{H}^2(\mathbb{D}^n)$

The *Hardy space* on the polydisc $\mathbb{D}^n$ is the Hilbert space

$$\mathbb{H}^2(\mathbb{D}^n) = \left\{ f : \mathbb{D}^n \longrightarrow \mathbb{C}, \text{holomorphic} : \|f\|^2 < +\infty \right\},$$

with the norm $\|f\|^2 = \sum_{\alpha\in\mathbb{N}^n} |a_\alpha|^2$ and the scalar product $\langle f,g\rangle = \sum_{\alpha\in\mathbb{N}^n} a_\alpha \bar{b}_\alpha$ for $f(z) = \sum_{\alpha\in\mathbb{N}^n} a_\alpha z^\alpha$ and $g(z) = \sum_{\alpha\in\mathbb{N}^n} b_\alpha z^\alpha$. The set of monomials $\{z^\alpha : \alpha \in \mathbb{N}^n\}$ is the standard orthonormal basis for $\mathbb{H}^2(\mathbb{D}^n)$, and its elements will be denoted by e_α and ordered with the lexicographic order. Note that $\mathbb{H}^2(\mathbb{D}^n)$ is a reproducing Kernel Hilbert space (RKHS) and its (Cauchy) Kernel allows us to define the *evaluation functional* $\langle k_z, f\rangle = f(z)$. See [4] for more details.

Consider the continuous-time dynamical system

$$\dot{z} = F(z), \qquad z \in \mathbb{D}^n, \quad F \in \mathscr{C}^1,$$

which generates a flow $\varphi^t : \mathbb{D}^n \to \mathbb{D}^n$, with $t \in \mathbb{R}^+$. The *semigroup of Koopman operators* on $\mathbb{H}^2(\mathbb{D}^n)$ is the family of operators $(U^t)_{t\geq 0}$:

$$U^t : \mathbb{H}^2(\mathbb{D}^n) \to \mathbb{H}^2(\mathbb{D}^n) : U^t f = f \circ \varphi^t.$$

The *Koopman generator* of $(U^t)_{t\geq 0}$ is the operator

$$L_F f = F \cdot \nabla f, f \in \mathscr{D} \subset \mathbb{H}^2(\mathbb{D}^n),$$

where the domain $\mathscr{D} = \left\{ f \in \mathbb{H}^2(\mathbb{D}^n) : F \cdot \nabla f \in \mathbb{H}^2(\mathbb{D}^n) \right\}$ is dense on $\mathbb{H}^2(\mathbb{D}^n)$. The Koopman operator U^t and its associated infinitesimal generator L_F are both linear on $\mathbb{H}^2(\mathbb{D}^n)$. See [3] for more details. In this study we assume the vector field F is polynomial and the origin 0 is a unique (hyperbolic) equilibrum point in $\mathbb{D}^n$.

3 The main result

Under some conditions, the Koopman operator framework allows us to construct a Lyapunov function for polynomial vector fields.

Theorem 1 *Let*

$$\dot{z} = F(z), z \in \mathbb{D}^n \quad \text{and} \quad \dot{f} = L_F f, f \in \mathscr{D} \subset \mathbb{H}^2(\mathbb{D}^n)$$

be a nonlinear system and its corresponding Koopman system. Let assume that

- *the jacobian $JF(0)$ is triangularisable and Hurwitz*
- *and $\exists Q \in]0,1[$ which bounds the double sequence*

$$\left\{ \frac{4D^2 \left|\langle e_j, L_F e_k\rangle\right|^2}{\left|\Re\left(\langle e_j, L_F e_j\rangle\right)\right| \left|\Re\left(\langle e_k, L_F e_k\rangle\right)\right|} \right\}_{1\leq k\leq j-1,\, j\geq 2},$$

where D is the number of nonlinear terms of F.

Then there exists a sequence $\varepsilon_k \sim Q^k$ such that,

1. *the series $\mathscr{V}(f) = \sum_{|\alpha|\geq 1} \varepsilon_\alpha \left|\langle f, e_\alpha\rangle\right|^2$ is a Lyapunov functional of the Koopman system*
2. *and the function $V(z) = \mathscr{V}(k_z) = \sum_{k=1}^{\infty} \varepsilon_k |z|^{2\alpha(k)}$ is a Lyapunov function for the nonlinear system in $\mathbb{D}^n$.*

References

[1] A. Mauroy and I. Mezić, *Global stability analysis using the eigenfunctions of the Koopman operator*, IEEE TAC, vol. 61, pp. 3356-3369, 2016.

[2] C. M. Zagabe and A. Mauroy, *Switched nonlinear systems in the Koopman operator framework : Toward a Lie-algebraic condition for uniform stability*, ECC, IEEE, pp. 281-286, 2021.

[3] A. Mauroy, I. Mezić and Y. Susuki, *The Koopman Operator in Systems and Control Concepts, Methodologies and Applications*, Springer, 2020.

[4] W. Rudin, *Function Theory in Polydiscs*, Benjamin, New York, 1969.

Continuous-time system identification by deep subspace encoders

Gerben Izaak Beintema[a], Roland Tóth[a,b], Maarten Schoukens[a]
[a]Control Systems Group, Electrical Engineering, Eindhoven University of Technology
[b]Systems and Control Laboratory, Institute for Computer Science and Control, Budapest, Hungary.
Emails: g.i.beintema@tue.nl, r.toth@tue.nl, m.schoukens@tue.nl

1 Introduction

Nonlinear continuous-time models are widely used in control, but identification methods for continuous-time systems are relatively underdeveloped. The subspace encoder method [1] has shown to be a successful and robust state-space model identification method. This work extends this method to the continuous-time setting.

2 Continuous-time subspace encoder method

By integrating the state-space equations given by

$$\dot{\hat{x}}(t) = f_\theta(\hat{x}(t), u(t)),$$
$$\hat{y}(t) = h_\theta(\hat{x}(t)),$$

using an RK4 integrator with a ZOH condition on the input signal $u(t)$ one is in principle able to compute the simulation loss. However, due to the linear scaling of the computational complexity and numerical instabilities of the simulation loss, this often becomes infeasible. These issues are avoided by the encoder method which employs any number of small subsections of truncation length T. This improves computational complexity since the loss can be computed in parallel on each subsection individually and instabilities have less time to develop.

On each subsection the network structure as seen in Figure 1 is applied. This structure employs an encoder function ψ_θ parameterized by a neural network that aims to approximate the reconstructability map from a set of past inputs and outputs to the current state. This encoder function is optimized together with f_θ and h_θ and does not require the introduction of any additional loss functions since if ψ_θ provides a better initial state approximation it also lowers the previously derived loss function.

3 Benchmark Results

We applied the proposed method on the cascade tank dataset [2] which has square root nonlinearities and hard saturations due to overflow. The dataset consists of only two short datasets of lengths 1024 samples ($\Delta t = 4$ sec). We use the first dataset to train models parameterized by 2 hidden layer networks with 64 nodes per layer for f_θ, h_θ and ψ_θ, $T = 60$, $n_x = 2$ using the Adam optimizer.

The resulting simulations on the test set can be viewed in Figure 2. This figure illustrates that all estimated models are

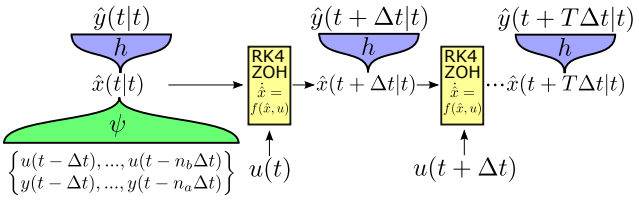

Figure 1: The continuous-time subspace encoder method applied on a subsection of length T starting from t. Here the $t|t$ notation indicates (current time|starting time) to be able to distinguish between different subsections.

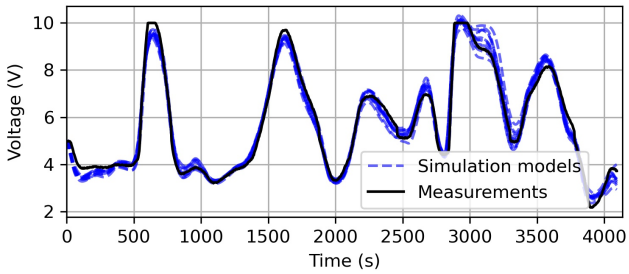

Figure 2: Simulations on the test set obtained from 11 models with different initial parameters estimated by the proposed method on the cascade tank dataset.

able to closely emulate the complex nonlinear behaviour of the system. The mean RMS simulation is 0.315 ± 0.016 V which is a the state-of-the-art result similar to the 0.33 RMS obtained by [3]. We argue that our method is more robust as it only employs a single loss function and the computational complexity does not scale with the number of data samples.

References

[1] G. Beintema, R. Toth, and M. Schoukens, "Nonlinear state-space identification using deep encoder networks," in *Learning for Dynamics and Control*, pp. 241–250, PMLR, 2021.

[2] M. Schoukens, P. Mattson, T. Wigren, and J.-P. Noel, "Cascaded tanks benchmark combining soft and hard nonlinearities," in *Workshop on nonlinear system identification benchmarks*, pp. 20–23, 2016.

[3] M. Forgione and D. Piga, "Continuous-time system identification with neural networks: model structures and fitting criteria," *European Journal of Control*, vol. 59, pp. 69–81, 2021.

Learning-Based Model-Augmentation of Nonlinear Approximative Models using the Sub-Space Encoder

Chris Verhoek[1], Gerben Beintema[1], Sofie Haesaert[1], Maarten Schoukens[1], and Roland Tóth[1,2]
[1] Control Systems Group, Eindhoven University of Technology, The Netherlands
[2] Systems and Control Laboratory, Institute for Computer Science and Control, Budapest, Hungary
{c.verhoek, g.i.beintema, s.haesaert, m.schoukens, r.toth}@tue.nl

1 Introduction

The class of *Linear Time-Invariant* (LTI) systems provide a rich framework for modeling dynamical systems and has been successful to meet the needs of industrial applications. However, with the ever-growing complexity and increasing performance requirements of high-tech systems, *nonlinear* (NL) system analysis has become essential in engineering problems. Due to the complexity of these considered systems, modeling them via first principles is often too complicated or even impossible. Therefore, we focus in this work on *data-driven modeling*, i.e, identification of NL systems.

Despite the tremendous progress in automating and optimizing the identification procedure [3], identification of systems beyond the linear class is still immature and lacks theoretical understanding. Moreover, due to the growing system complexity, the identification algorithms often *waste* a lot of resources on identifying *simple* dynamic relationships, such as rigid body dynamics. In this work, we aim to leverage the effectiveness of NL data-driven modeling by augmenting *a priori system knowledge* with powerful *learning* methods. *Model-Augmentation* (MA) has already been explored in the LTI case, but is in a rather immature state for NL systems.

Our MA concept focuses on *augmenting* a known approximative *state-space* (SS) model of the NL system with an *Artificial Neural Network* (ANN), i.e., a universal approximator. In this way, the ANN *completes* the dynamic behavior of the approximative NL SS model, and thus we obtain an accurate model of the *actual* NL system. The approximative SS model can be obtained via, e.g., first principles knowledge. There are numerous ANN methods available in literature that we can use in our MA concept. In this work, we augment our approximative model with the *Sub-Space Encoder Network* (SUBNET)[1] [1]. The SUBNET method is particularly suited when considering SS models. We implement the aforementioned MA concept with the SUBNET on a 3 Degree-of-Freedom *Control Moment Gyroscope* (CMG) usecase.

2 Methods

We obtain the approximative SS model by converting the first principles model of the CMG, found in [2], to a *gridded Linear Parameter-Varying* SS (gLPV-SS) model. The resulting gLPV-SS approximates the NL behavior of the CMG. This gLPV-SS model now serves as our approximate SS model, which we now augment with an ANN. With the SUBNET, we can consider multiple augmentation configurations. In order to retain the state-dimension of the approximate NL SS model, we augment the ANN via an additive term in the SS equations, i.e.,

$$x_k^+ = f_{\text{Approx}}(x_k, u_k) + f_{\text{ANN}}(x_k),$$
$$y_k = h_{\text{Approx}}(x_k, u_k) + h_{\text{ANN}}(x_k).$$

The additive ANN *completes* the dynamics of the gLPV-SS model, and hence resembles the dynamic behavior of the CMG. Thus, the ANN learns the dynamics that have been disregarded in the conversion step towards an approximative model of the NL system, which significantly reduces the required resources to obtain an accurate model of the system.

3 Results

The results of this method are shown in Fig. 1, where blue is the original data of the CMG, orange is the simulation data and green is the difference between the original and the simulation data. The left plot shows the behavior of the gLPV-SS model, while the right plot depicts the augmented model. The results show that the ANN truly completes the behavior of the gLPV-SS model.

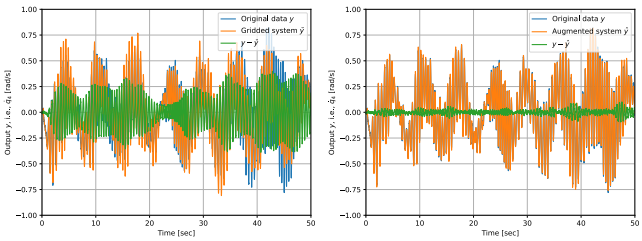

Fig. 1: gLPV-SS model with (r) & without (l) SUBNET augmentation.

This work has received funding from the European Research Council (ERC) under the European Union's Horizon 2020 research and innovation programme (grant agreement nr. 714663), and financial support in the scope of the AI4GNC project with SENER Aeroespacial S.A., contract nr. 4000133595/20/NL/CRS

[1] See tinyurl.com/SUBNETdeepSI for a Python toolbox.

References

[1] G. I. Beintema, R. Tóth, and M. Schoukens (2021). "Nonlinear state-space model identification from video data using deep encoders," in *Proc. of the 19th Symposium on System Identification*, vol. 54, p. 697-701.

[2] T. Bloemers, and R. Tóth (2019). "Equations of motion of a control moment gyroscope," Tech. Rep., Eindhoven University of Technology.

[3] J. Schoukens, and L. Ljung. (2019) "Nonlinear system identification: A user-oriented road map," *IEEE Control Systems Magazine*, vol. 39, no. 6, p. 28–99.

Learning-based augmentation of mechatronic system models by deep subspace encoders

András Retzler[1,2,5], Gerben Izaak Beintema[3], Maarten Schoukens[3], Roland Tóth[3,4], Jan Swevers[1,2], and Zsolt Kollár[5]

[1]MECO Research Team, Dept. of Mechanical Engineering, KU Leuven, Heverlee, Belgium
[2]DMMS-M laboratory, Flanders Make, Heverlee, Belgium
[3]Dept. of Electrical Engineering, Eindhoven University of Technology, Eindhoven, The Netherlands
[4]Systems and Control Laboratory, Institute for Computer Science and Control, Budapest, Hungary
[5]Dept. of Measurement and Inf. Systems, Budapest Univ. of Technology and Economics, Budapest, Hungary
Email addresses: andras.retzler@kuleuven.be, g.i.beintema@tue.nl

1 Problem statement

Our goal is to estimate the parameters of grey-box models of mechatronic systems, where the continuous-time model is augmented with artificial neural network elements included as additional terms. This black-box part is to improve the original model derived from first principles, physics (e.g. rigid body dynamics), in order to have better accuracy in simulation. The estimation task can be formulated as a nonlinear optimization problem with a least-squares objective, acting on the multi-step prediction error of the model that has been computed by numerical integration, assuming zero-order hold. However, such problems can be hard to solve if the objective function has multiple local minima. Regions in the parameter space where the computation of the model response becomes non-contractive are also a challenge. Thus, there is a need for robust identification methods that can overcome these difficulties and are computationally tractable.

2 Related work

The subspace encoder method [1] has previously been used to estimate black-box state-space models with fully connected neural networks as nonlinear functions for the state and output equations. As in multiple shooting, the subspace encoder method computes the loss on multiple, possibly overlapping, short subsections, which improves computation speed and reduces the effects of local minima. Furthermore, on these subsections, a third network, the so-called encoder function was used to provide an estimate of the initial state based on historical input and output samples. This resulted in an unconstrained optimization problem. The method is available in the open-source deepSI toolbox [2], and in [1] it was shown to obtain state-of-the-art performance on multiple challenging benchmarks.

3 Proposed solution

In the current study, we combine parameter estimation of first-principle laws-based models of the system with the subspace encoder method (see Figure 1). Starting from the setting in [1], we replace the state and output equations with the equations of the resulting grey-box model augmented with neural networks, and we also include physical knowledge into the encoder (e.g. some states are in a fixed relation with other states, like position with velocity). We use Adam batch optimization, as in [1]. Compared to traditional multiple shooting, no additional decision variables are needed for the initial states, as those are provided by the encoder structure, so the required computational resources scale linearly with the length of the dataset. We compare the accuracy and robustness of this method with existing traditional shooting methods for grey-box identification (single shooting, multiple shooting).

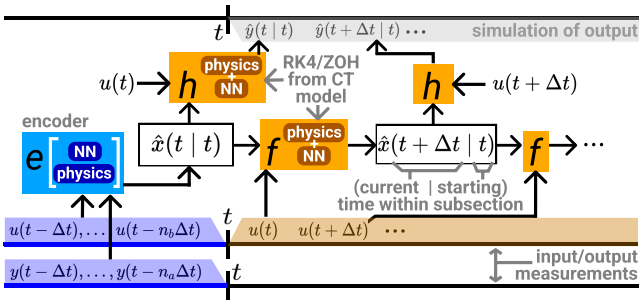

Figure 1: Simulation within a subsection.

4 Acknowledgements

This research is supported by Flanders Make: ICON project ID2CON: Integrated IDentification for CONtrol.

References

[1] G. Beintema, R. Tóth, and M. Schoukens, "Nonlinear state-space identification using deep encoder networks," in Proceedings of the 3rd Conference on Learning for Dynamics and Control, May 2021, pp. 241–250.

[2] G. Beintema, deepSI. [Online]. Available: https://github.com/GerbenBeintema/deepSI

Sensor Data Fusion as an Alternative for Monitoring Oxychlorides in Electrochlorination Applications

Ross, E.A. [1,2] Edwin.Ross@wetsus.nl
Wagterveld, R.M. [1] Martijn.Wagterveld@wetsus.nl
Mayer, M. [3] Mateo.Mayer@easymeasure.nl
Stigter, J.D. [2] Hans.Stigter@wur.nl
Højris, B. [4] bhoejris@grundfos.com
Keesman, K.J. [1,2] Karel.Keesman@wur.nl

[1] Wetsus, European Centre of Excellence for Sustainable Water Technology Oostergoweg 9, 8911 MA, Leeuwarden, the Netherlands

[2] Mathematical and Statistical Methods - Biometris, Wageningen University and Research, PO Box 16, 6700 AA, Wageningen, the Netherlands

[3] EasyMeasure B.V., Breestraat 22, 3811 BJ, Amersfoort, the Netherlands

[4] Grundfos Holding A/S, Poul Due Jensens Vej 7, DK-8850, Bjerringbro, Denmark

1 Abstract

As oxychloride concentrations have been found harmful to human and animal health [1, 2, 3], governments are increasingly demanding strict control of such chemical species in drinking water [4, 5]. As not all oxychlorides can be directly monitored using hardware sensors, in this work, Sensor Data Fusion (SDF) was investigated as an alternative approach. In contrast to manual laboratory analysis it is capable of providing estimates in real time using affordable sensors [6, 7, 8].

In this study, an SDF algorithm was developed for an electrochlorination process, based on classical observer theory, with the aim of monitoring chlorate formation. Starting from time-scale analysis, a reduced-order nonlinear state-space model of the electrochlorination and mixing process was formulated. A novel UV-a absorption sensor was used as part of the sensor suite, to track the hypochlorite concentration.

It was found that, while the system was not fully observable, it was detectable. Using the Extended Kalman Filter an effective observer was made. The algorithm was verified experimentally and was found to be capable of accurately estimating chlorate concentrations in real-time. In addition, a Monte Carlo analysis was performed on the unobservable states to determine their uncertainty over the course of the experiment.

References

[1] World Health Organization. *Guidelines for drinking-water quality: fourth edition incorporating first addendum*, 4th ed.; 2017.

[2] Snyder, S. Perchlorate in Drinking-water. Background document WHO/FWC/WSH/16.46, World Health Organization, 2016.

[3] Cotruvo, J.; Fawell, J.K. Chlorine Dioxide, Chlorite and Chlorate in Drinking-water. Background document WHO/FWC/WSH/16.49, World Health Organization, 2016.

[4] The European Parliament and the Council of the European Union. Directive (EU) 2020/2184 of the European Parliament and of the Council of 16 December 2020 on the Quality of Water Intended for Human Consumption (recast), 2020.

[5] The European Commission. Commission Recommendation (EU) 2015/682 of 29 April 2015 on the Monitoring of the Presence of Perchlorate in Food, 2015.

[6] Hall, D.L.; Llinas, J. An introduction to multisensor data fusion. *Proceedings of the IEEE* **1997**, 85, 6–23.

[7] Fortuna, L.; Graziani, S.; Rizzo, A.; Xibilia, M. *Soft Sensors for Monitoring and Control of Industrial Processes*, 1st ed.; Advances in Industrial Control, Springer-Verlag London, 2007.

[8] Mohd Ali, J.; Ha Hoang, N.; Hussain, M.A.; Dochain, D. Review and classification of recent observers applied in chemical process systems. *Computers and Chemical Engineering* **2015**, 76, 27–41.

Observability-Based Optimal Sensor Placement in Hydraulic Fluid Transport Networks

Geelen, Caspar V.C.[1,2]
Email: caspar.geelen@wur.nl
Yntema, Doekle R.[2]
Email: doekle.yntema@wetsus.nl
Molenaar, Jaap[1]
Email: jaap.molenaar@wur.nl
Keesman, Karel J.[1,2] (corresponding author)
Email: karel.keesman@wur.nl
[1]Biometris, Wageningen University, PO Box 16, 6700AA, Wageningen, The Netherlands
[2]Wetsus, PO Box 1113, 8900CC, Leeuwarden, The Netherlands

1 Introduction

Conduit bursts or leakages present an ongoing problem for hydraulic fluid transport grids, such as oil or water conduit networks. Measurements from additional sensors increase the accuracy of burst detection methods, but the position of a sensor within a network is critical in order to maximize the additional information provided by the sensor. Although sensor placement and operation costs have decreased in recent years, there remains a tradeoff between information gain and sensor costs (Scozzari et al., 2021). Traditional sensor placement methodologies focus on burst detectability as the criteria for optimal placement of additional pressure sensors and utilize a sensitivity-based approach to determine those placements (Boatwright et al., 2018). Most current methodologies do not incorporate pressure dynamics into the calculations for optimal sensor placement (Boatwright et al., 2018; Giustolisi et al., 2008). These pressure transients, or water hammers, are often caused by pipe bursting and are an important indicator of bursts. It has been shown that detection of these transients plays a crucial role in burst detection (Lee et al., 2016). Therefore, there is a need for optimal sensor placement methodologies capable of including fast pressure dynamics.

2 Methodology

We present a linearized state-space model of hydraulic fluid transport networks suited for optimal sensor placement, based on the continuity and momentum equation for unsteady, nonuniform flow of a slightly compressible fluid through slightly elastic pipes:

$$\frac{\partial}{\partial t}\begin{pmatrix}p\\V\end{pmatrix}+\begin{bmatrix}V & \rho c^2\\ \rho^{-1} & V\end{bmatrix}\frac{\partial}{\partial x}\begin{pmatrix}p\\V\end{pmatrix}=\begin{pmatrix}0\\ -g\,sin(\theta)-\dfrac{fV|V|}{2D}\end{pmatrix}$$

Here, p is the pressure in Pa, V is the flow velocity in $\frac{m}{s}$, ρ is the mass density of the transported fluid in $\frac{kg}{m^3}$, c is the elastic wave velocity in $\frac{m}{s}$, g is the acceleration due to gravity in $\frac{m}{s^2}$, θ is the angle the conduit makes with the horizontal, with the angle taken positive if the conduits slopes upwards in the flow direction, f is the Darcy-Weisbach friction factor (dimensionless), and D is the diameter of the inside of the conduit in m.

This approach does not rely on model simulation of hydraulic burst scenarios or on burst sensitivity matrices, but instead determines optimal sensor placement solely from the model structure, taking into account the pressure dynamics and hydraulics of the network. Observability Gramians can be used to identify the optimal sensor configuration by maximizing observability functionals based on robust optimality criteria. For linear, time-invariant systems, the sensitivity of output y with respect to initial states x(0) is given by Ce^{At}, thus the observability Gramian can be interpreted as a Fisher Information Matrix and thus be understood as a measure of information content (Grubben and Keesman, 2018).

3 Results

Observability-based sensor placement was applied to multiple water distribution networks, showing its capacity in determining the most suitable sensor locations. We also show the results from a comparison between sequential and simultaneous sensor placement routines. The results show that the best sensor locations for these networks can be accurately determined and explained.

References

Boatwright, S., Romano, M., Mounce, S., Woodward, K., Boxall, J., 2018. Optimal Sensor Placement and Leak/Burst Localisation in a Water Distribution System Using Spatially-Constrained Inverse-Distance Weighted Interpolation 3, 282–273. https://doi.org/10.29007/37cp

Giustolisi, O., Savic, D., Kapelan, Z., 2008. Pressure-Driven Demand and Leakage Simulation for Water Distribution Networks. J. Hydraul. Eng. 134. https://doi.org/10.1061/(asce)0733-9429(2008)134:5(626)

Grubben, N.L.M., Keesman, K.J., 2018. Controllability and observability of 2D thermal flow in bulk storage facilities using sensitivity fields. Int. J. Control 91, 1554–1566. https://doi.org/10.1080/00207179.2017.1321782

Lee, S.J., Lee, G., Suh, J.C., Lee, J.M., 2016. Online Burst Detection and Location of Water Distribution Systems and Its Practical Applications. J. Water Resour. Plan. Manag. 142, 04015033. https://doi.org/10.1061/(asce)wr.1943-5452.0000545

Scozzari, A., Mounce, S., Han, D., Soldovieri, F., 2021. ICT for Smart Water Systems: Measurements and Data Science.

Joint Parameter and State Estimation: A Supervisory Multi-Observer Approach

T. J. Meijer[1,†], V. S. Dolk[1], M. S. Chong[1], R. Postoyan[2], B. de Jager[1], D. Nešić[3], W. P. M. H. Heemels[1]
[1] Department of Mechanical Engineering, Eindhoven University of Technology, Eindhoven, The Netherlands
[2] Université de Lorraine, CNRS, CRAN, F-54000 Nancy, France
[3] Department of Electrical and Electronic Engineering, the University of Melbourne, Parkville, VIC 3010, Australia
[†] Email: t.j.meijer@tue.nl

1 Introduction

Joint state and parameter estimation problems are relevant in many contexts including control and digital twinning. A typical approach is to augment the state with the parameters and formulate the joint estimation problem as a (nonlinear) state estimation problem. Doing so, however, can destroy the underlying structure of the problem and often complicates the derivation of theoretical convergence guarantees. Dedicated techniques have thus been developed in the literature but these generally only apply to specific classes of systems. We follow a different sampling-based approach to jointly estimate states and parameters for general nonlinear systems, while guaranteeing convergence of state and parameter estimates to within a margin of the true values [1].

In particular, we consider a discrete-time nonlinear system

$$\begin{aligned} x_{k+1} &= f(x_k, p, u_k, v_k), \\ y_k &= h(x_k, p, u_k, w_k), \end{aligned} \tag{1}$$

where $x_k \in \mathbb{R}^{n_x}$, $u_k \in \mathbb{R}^{n_u}$ and $y_k \in \mathbb{R}^{n_y}$ denote the state to be estimated, known input and measured output, respectively. The input, process noise $v_k \in \mathbb{R}^{n_v}$ and measurement noise $w_k \in \mathbb{R}^{n_w}$ are bounded and unknown. The state x_k is assumed to be uniformly bounded and the parameter vector p is constant, unknown and belongs to a given compact set $\mathbb{P}$, i.e., $p \in \mathbb{P} \subset \mathbb{R}^{n_p}$. Our objective is to jointly estimate the parameters p and the state x_k of the system (1) (within guaranteed margins) subject to bounded process and measurement noise, given the input and measured output.

2 Proposed solution: Supervisory multi-observer

The proposed supervisory multi-observer scheme, shown in Fig. 1, consists of (a) the *multi-observer*, a bank of state observers, and (b) the *supervisor*, which at any time selects one of the observers to provide the state and parameter estimates.

The multi-observer consists of N observers–each corresponding to a parameter sample $\hat{p}_i \in \mathbb{P}$, $i \in \mathcal{N} := \{1, 2, \ldots, N\}$–given by

$$\begin{aligned} \hat{x}_{i,k+1} &= \hat{f}(\hat{x}_{i,k}, \hat{p}_i, u_k, y_k), \\ \hat{y}_{i,k} &= h(\hat{x}_{i,k}, \hat{p}_i, u_k, 0), \end{aligned} \tag{2}$$

where $\hat{x}_{i,k} \in \mathbb{R}^{n_x}$ and $\hat{y}_{i,k} \in \mathbb{R}^{n_y}$ denote the state and output estimate of the i-th observer. Each observer is designed such that its estimation error satisfies a robust stability property with respect to v, w and $\tilde{p}_i := \hat{p}_i - p$, $i \in \mathcal{N}$. We propose a static scheme to obtain the parameter samples $\{\hat{p}_i\}_{i\in\mathcal{N}}$ and a dynamic scheme, which iteratively refines the set of samples to typically achieve more accurate estimates.

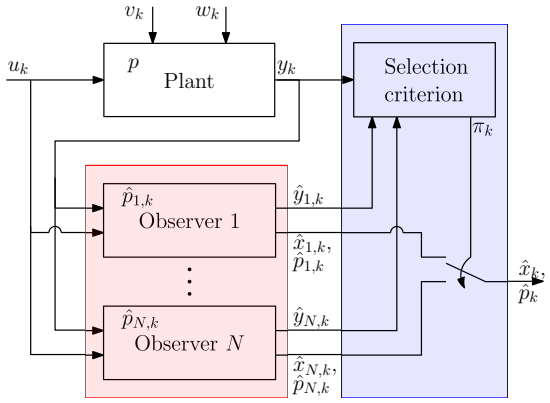

Figure 1: Supervisory observer scheme consisting of the (□) multi-observer and (□) supervisor.

The supervisor selects, at every time $k \in \mathbb{N}$, one of the observers, $\pi_k \in \mathcal{N}$, to produce estimates $\hat{x}_k = \hat{x}_{\pi_k,k}$ and $\hat{\pi}_k = \hat{p}_{\pi_k}$, $k \in \mathbb{N}$. The following selection criterion is used:

$$\pi_k \in \arg\min_{i\in\mathcal{N}} \sum_{j=0}^{k-1} \lambda^{k-1-j} (\hat{y}_{i,j} - y_j)^2, \quad k \in \mathbb{N}, \tag{3}$$

where $\lambda \in [0, 1)$ is a design parameter.

3 Convergence guarantees

We can guarantee the following convergence result for the proposed multi-observer scheme under a persistency of excitation condition: For any desired margins $\nu_{\tilde{p}}, \nu_{\tilde{x}} \in \mathbb{R}_{>0}$, there exist $\upsilon_{\tilde{p}}, \upsilon_{\tilde{x}}, \omega_{\tilde{p}}, \omega_{\tilde{x}} \in \mathcal{K}_\infty$, a sufficient number of observers N and time $M \in \mathbb{N}_{\geqslant 1}$ such that

$$\begin{aligned} &\|\hat{p}_k - p\| \leqslant \nu_{\tilde{p}} + \upsilon_{\tilde{p}}(\sup_{j\in\mathbb{N}} \|v_j\|) + \omega_{\tilde{p}}(\sup_{j\in\mathbb{N}} \|w_j\|), \text{ for } k \geqslant M, \\ &\lim_{k\to\infty} \|\hat{x}_k - x_k\| \leqslant \nu_{\tilde{x}} + \upsilon_{\tilde{x}}(\sup_{j\in\mathbb{N}} \|v_j\|) + \omega_{\tilde{x}}(\sup_{j\in\mathbb{N}} \|w_j\|). \end{aligned} \tag{4}$$

The convergence margins are dependent on the noise and design parameters $\nu_{\tilde{p}}$ and $\nu_{\tilde{x}}$, which can be made arbitrarily small (at the cost of requiring more observers N). The estimation scheme is demonstrated using a numerical example.

References

[1] T. J. Meijer, V. S. Dolk, M. S. Chong, R. Postoyan, B. de Jager, D. Nešić, and W. P. M. H. Heemels. Joint parameter and state estimation of noisy discrete-time nonlinear systems: A supervisory multi-observer approach. In *60th IEEE Conf. Decis. Control*, pages 5163–5168, 2021.

Event-Based Estimation for POMDPs: Application to Remote Estimation in Precision Farming[1]

Ruben Beumer, René van de Molengraft and Duarte J. Antunes
Control Systems Technology
Eindhoven University of Technology
P.O. Box 513, 5600 MB Eindhoven, The Netherlands
Email: {r.m.beumer,m.j.g.v.d.molengraft,d.antunes}@tue.nl

1 Introduction

The number of applications that rely on remote sensing and estimation has increased tremendously in the past decade, spurred by the availability of inexpensive sensors and processors and proper communication networks. Remote sensing and estimation is now ubiquitous in surveillance, industrial inspection, and agriculture, among many other applications. In many of these applications the sensors can work as a proxy to detect events (faults, issues) that need to be confirmed by closer inspection; inspection may require other (more expensive) sensors, mobile robots, or personnel. For instance in the case of precision farming diseases or weed can be inferred to some extent from a few sensors placed in the field (e.g., cameras and moisture or temperature sensors). However, for achieving full situational awareness the number of these sensors would be impractical. Thus, farmer or mobile robot inspection is required for full situational awareness. Still, these sensors can provide very useful information on when to inspect. From a high level perspective the problem tackled in the present research is to provide a policy for if and when these (expensive) inspections should take place based on the limited sensor information.

2 Proposed approach

We propose to tackle this problem as an event-based estimation problem for Partially Observable Markov Decision Processes (POMDPs). The framework of event-based estimation is used since decisions (when to inspect) rely on measurements (events) rather than on time (e.g. periodic inspection); in fact some of the present ideas are inspired by previous work on event-based estimation and control [1]. However, differently from what is common in the context of event-based control we consider finite state spaces for the variables to be measured. This greatly reduces the mathematical complexity of the results and can be motivated by the fact that in many of the intended applications the state is already discrete or can be quantized. For instance in the context of precision farming, the state could be a vector of binary variables indicating if there is weed or not in a given area of the field. The state could also include an interval where the actual temperature lies (rather that the exact value), which is often enough for decision making in these contexts. While precision farming applications are our main motivation, the results are general and can be useful in other event-based problems for POMDPs.

We formulate the problem as a POMDP with a general average cost and with two sets of measurements: regular (inexpensive) sensors available at every time step and expensive sensors, whose use needs to be considered at each time step and thus determined by a decisions variable. Both the case where obtaining expensive measurements is costly (penalized in the cost) and where the trade-off problem is considered as a multi-objective optimization problem are tackled. The information available to make decision includes the data from the regular and expensive sensors (only when used). Under some assumptions justified for the applications intended, we show that the average cost problem can be tackled as a shortest path problem, which is actually a stopping time problem. We show that an optimal policy can be obtained, for which the complexity does however grow exponentially with the time horizon and thus it is impractical. This motivates us to propose two classes of approximate policies. First, we propose a class of policies resulting from relaxed dynamic programming, see [2]. These policies guarantee a cost within a constant factor of the cost of the optimal policy. In practice the complexity of the approximate policy is by far smaller than that of the optimal policy. However, there are no formal guarantees that this is the case. Second, inspired by [1], we propose a class of policies that (under mild assumptions) leads to a strictly better cost than that of periodic inspection for the same inspection rate. The two proposed policies are compared in numerical simulations for meaningful applications in precision farming.

[1] This research is part of the research program SYNERGIA (project number 17626), which is partly financed by the Dutch Research Council (NWO).

References

[1] D. J. Antunes and M. H. Balaghi I., "Consistent event-triggered control for discrete-time linear systems with partial state information," *IEEE Control Systems Letters*, vol. 4, no. 1, pp. 181–186, Jan 2020.

[2] B. Lincoln and A. Rantzer, "Relaxing dynamic programming," *IEEE Trans. on Automatic Control*, vol. 51, no. 8, pp. 1249–1260, Aug 2006.

A Multiple Observer Approach to Cyber-Attack Detection

Twan Keijzer
Delft Center for Systems and Control
Delft University of Technology
Mekelweg 2, 2628 CD Delft
The Netherlands
Email: T.Keijzer@tudelft.nl

Riccardo M.G. Ferrari
Delft Center for Systems and Control
Delft University of Technology
Mekelweg 2, 2628 CD Delft
The Netherlands
Email: R.Ferrari@tudelft.nl

1 Introduction

Following the ever growing adoption of automation technologies, also spatially distributed systems such as energy distribution and road transportation systems, become increasingly automated. In such systems communication between subsystems is often beneficial, if not critical, to the efficient operation of the system. The use of such long range, often wireless, communication however comes with an increased vulnerability to cyber-attacks, which can cause major disruptions to safe operation if they go undetected [1].

It is therefore essential to protect these systems against such attacks. Broadly, one can either apply measures on the communicated signal itself, such as is done with encryption [2], or one can analyse the system behaviour using either a data-driven or model based methods for detection of anomalies [1]. In this work we will consider model based methods for anomaly detection, specifically the Sliding Mode Observer (SMO) based detection from [3].

The SMO based detection method from [3] uses the so-called Equivalent Output Injection (EOI) of an SMO as residual for detection. In [3] a robust detection threshold is designed as a bound on the EOI in healthy conditions. By constructing the threshold in this way it is guaranteed there are no false attack detections. However, depending on the size of the uncertainties, sufficiently small and/or fast attacks can result in missed detections.

2 Multiple Observer Cyber-Attack Detection

In this work we propose to use multiple SMO based detectors in parallel to reduce the rate of missed detections. The idea to use multiple observers in parallel is not new and has been used before in the field of fault detection. Here a bank of observers is designed where each one uses a fixed or adaptive model of the fault scenario to be detected [4]. Such an approach is however not applicable to cyber-attacks as these can be maliciously designed with unlimited possibilities.

The multiple observer approach to cyber-attack detection proposed in this work utilizes the flexibility of the detector behaviour that can be achieved by gain tuning. Specifically, for the robust SMO based detector from [3] the gains can be changed to obtain a trade-off between detection time and minimal detectable attack magnitude. Therefore, by using multiple detectors with different gains the amount of missed detections can be significantly decreased.

To demonstrate the effectiveness of the scheme we use the model of a collaborative vehicle platoon from [3] where the communication of the acceleration input is being disturbed by an additive attack. We have implemented the SMO based detector with six different sets of gains to this model. The solid lines in figure 1 show the detection time of each of these detector designs to step attacks of varying magnitude. Furthermore, the time before a crash occurs due to the attack is shown with the red dashed line. One can see that with multiple detectors a larger range of attacks can be detected in time for a crash to be avoided.

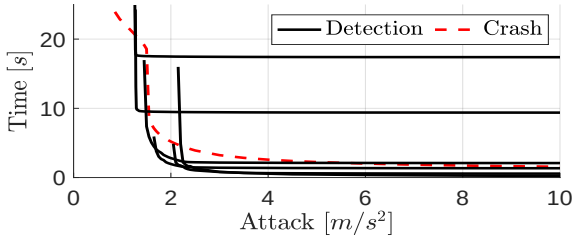

Figure 1: Detection performance of multiple SMO based cyber-attack detection for step attacks of varying magnitude.

References

[1] R. M. G. Ferrari and A. M. H. Teixeira, Eds., *Safety, security, and privacy for cyber-physical systems*, ser. Lecture Notes in Control and Information Sciences. Springer, 2021.

[2] J. Kim, H. Shim, H. Sandberg, and K. H. Johansson, "Method for Running Dynamic Systems over Encrypted Data for Infinite Time Horizon without Bootstrapping and Re-encryption," in *60th IEEE Conference on Decision and Control*, 2021, pp. 5614–5619.

[3] T. Keijzer, F. Jarmolowitz, and R. M. G. Ferrari, "Detection of cyber-attacks in collaborative intersection control," in *European Control Conference*, 2021.

[4] P. M. Frank, "Fault Diagnosis in Dynamic Systems Using Analytical and Knowledge-based Redundancy A Survey and Some New Results," *Automatica*, vol. 26, no. 3, pp. 459–474, 1990.

Exploiting Symbolic Linearization to Implement the Sequential Convex Quadratic Programming Method

Alejandro Astudillo[1*], Joris Gillis[1], Moritz Diehl[2], Wilm Decré[1], Goele Pipeleers[1], Jan Swevers[1]
[1]MECO Research Team, Dept. of Mechanical Engineering, KU Leuven, Leuven, Belgium.
[1]DMMS Lab, Flanders Make, Leuven, Belgium.
[2]Dept. of Microsystems Engineering (IMTEK) and Dept. of Mathematics, University of Freiburg, Freiburg, Germany.
[*]Email: alejandro.astudillovigoya@kuleuven.be

1 Introduction

Sequential quadratic programming (SQP) is a method to solve nonconvex optimal control problems (OCP) like those emerging, for instance, in nonlinear model predictive control of robot manipulators. For the following OCP

$$\min_{w} \quad \phi_0(c_0(w)) \tag{1a}$$
$$\text{s.t.} \quad h_i(w) = 0, \qquad i = 1,\dots,n_h, \tag{1b}$$
$$\phi_i(c_i(w)) \leq 0, \ \ i = 1,\dots,n_g, \tag{1c}$$

the SQP method iteratively solves quadratic programming (QP) subproblems to generate a sequence of iterates w_k that converges to a local minimizer w^* as $k \to \infty$. The objective function of such QP subproblems depends on the exact Hessian of the Lagrangian of OCP (1), which is costly to evaluate. However, if the functions $\phi_i(c_i(w))$, $i = [0, n_g]$, have a convex-over-nonlinear structure, i.e., ϕ_i is a convex function and c_i is a nonlinear function, their convexity can be exploited by variants of the SQP method such as the sequential convex quadratic programming (SCQP) method, in order to reduce the complexity of the Hessian.
The SCQP method replaces the exact Hessian of the Lagrangian in the QP subproblem by an approximation that ignores the contribution of the purely nonlinear constraints and the second order derivatives of $c_i(w)$. The SCQP Hessian approximation is defined as follows.

$$B_k^{\text{SCQP}}(w,\mu) := \frac{\partial c_0}{\partial w}(w)^\top \nabla^2_{c_0}\phi_0(c_0(w))\frac{\partial c_0}{\partial w}(w) + \sum_{i=1}^{n_g} \mu_i \frac{\partial c_i}{\partial w}(w)^\top \nabla^2_{c_i}\phi_i(c_i(w))\frac{\partial c_i}{\partial w}(w), \tag{2}$$

where μ_i are the Lagrange multipliers of the inequality constraints (1c).

2 Problem

Setting the SCQP method to solve (1) requires several steps. Within a numerical optimization framework, the modeler would need to (i) find the index i of the Lagrange multiplier μ_i corresponding to ψ_i, (ii) compute the Hessians of ϕ_i and the Jacobians of c_i, (iii) construct the expression of $B_k^{\text{SCQP}}(w,\mu)$ (2), and (iv) replace the exact Hessian of the Lagrangian with the SCQP approximation within the execution of the SQP method. This modeling and implementation effort increases the engineering time needed to prepare and solve an OCP and involves the modification of solver plugins in the optimization framework, which is not desirable.

3 Approach

To reduce the engineering time required to implement the SCQP method, we propose a novel operator lin defined as

$$\text{lin}(f(w)) := \begin{cases} \tilde{f}(w) := f_{\text{lin}}(w,w) = f(w) \\ \frac{\partial \tilde{f}}{\partial w}(w) = \frac{\partial f_{\text{lin}}}{\partial \hat{w}}(w,w) = \frac{\partial f}{\partial w}(w) \\ \frac{\partial^2 \tilde{f}}{\partial w^2}(w) = \frac{\partial^2 f_{\text{lin}}}{\partial \hat{w}^2}(w,w) = \mathbf{0} \end{cases} \tag{3}$$

where $f_{\text{lin}}(\hat{w},\overline{w}) := f(\overline{w}) + \frac{\partial f}{\partial \hat{w}}(\overline{w})(\hat{w}-\overline{w})$ represents the symbolic linearization of a function $f(\hat{w})$, i.e., the application of a first-order Taylor expansion to $f(\hat{w})$ around a symbolic equilibrium point $\overline{w}$. The lin operator replaces the second-order derivative of a symbolic expression with a zero matrix. Applying the lin operator to $c_i(w)$, $i = [0, n_g]$ in (1a) and (1c), and to h_i, $i = [1, n_h]$ in (1b), we build the following alternative OCP

$$\min_{w} \quad \phi_0(\text{lin}(c_0(w))) \tag{4a}$$
$$\text{s.t.} \quad \text{lin}(h_i(w)) = 0, \qquad i = 1,\dots,n_h, \tag{4b}$$
$$\phi_i(\text{lin}(c_i(w))) \leq 0, \ \ i = 1,\dots,n_g. \tag{4c}$$

whose exact Hessian of the Lagrangian is equal to the SCQP Hessian approximation (2) [1]. Therefore, directly applying the SQP method to (4) is equivalent to applying the SCQP method to (1), reducing the steps required to set the SCQP method to solve (1).

Acknowledgement This work is supported by Flanders Make SBO MULTIROB: "Rigorous approach for programming and optimal control of multi-robot systems" and by the FWO project G0A6917N of the Research Foundation - Flanders (FWO - Flanders). Flanders Make is the Flemish strategic research centre for the manufacturing industry.

References

[1] A. Astudillo, J. Gillis, M. Diehl, W. Decré, G. Pipeleers and J. Swevers, "Position and orientation tunnel-following NMPC of robot manipulators based on symbolic linearization in sequential convex quadratic programming," in IEEE Robotics and Automation Letters, 2022.

Multiway data regression using a spline-type tensor decomposition

Raphaël Widdershoven Nithin Govindajaran Nico Vervliet Martijn Boussé
Lieven De Lathauwer
Kasteelpark Arenberg 10 - bus 2446, 3001 Leuven
Etienne Sabbelaan 53 - bus 7657, 8500 Kortrijk
{first name}.{last name}@kuleuven.be[1]

1 Multivariate polynomials and splines

Polynomials and splines are often used to approximate univariate functions, but are not as effective in the multivariate case. This is caused by the curse of dimensionality that increases the amount of coefficients exponentially with the number of input variables. These all need to be estimated, which requires a lot of data and computation power. In the context of multiway data regression you obtain an overfitting model due to the multicolinearity of the coefficients [6].

2 Tensors

An important research trend is the transition from vector and matrix based mathematical engineering to generalizations that make use of higher-order tensors. Tensor algorithms have revolutionised high-dimensional computations. This development also stumbled upon the same problem, the curse of dimensionality, but managed to overcome it and harness it. In machine learning or more specifically supervised learning, this potential still largely has to be unleashed [5].

3 Combining both

Tensor decompositions allow for a compact representation of multivariate polynomials and splines. The compactness of these representations avoids overfitting and allows computation in a linear time by tensor algorithms, but is still general enough to represent most naturally occurring functions well [1].

4 Splines versus polynomials

Previously, a similar model was studied specifically with polynomials [4]. These are easy to represent and allow for a uniform approximation of continuous functions, but may lead to high-oscillatory behaviour. In this research [7] splines are used. These give the same advantages, but are compactly supported, making them more adaptive for local approximation and thus even allow the approximation of isolated nonlinearities [3]. The extra difficulty is the placement of the spline-knots.

[1]The email addresses are raphael.widdershoven@kuleuven.be, nithin.govindarajan@kuleuven.be, nico.vervliet@kuleuven.be, martijn.bousse@kuleuven.be and lieven.delathauwer@kuleuven.be.

5 Contributions

The contribution of this research is a general solution method to approximate an unknown map, based on noisy data [2]. Different implementations have been compared. Without imposing additional structure, classical multivariate splines have exponential time and memory complexity with respect to the number of input variables. With this model it is reduced to a linear complexity. Finally, a few heuristic methods for placing the spline-knots are compared.

References

[1] G. Beylkin, J. Garcke, M. J. Mohlenkamp, *Multivariate Regression and Machine Learning with Sums of Separable Functions*, SIAM, (2009) pp. 1840-1857.

[2] M. Boussé, N. Sidiropoulos, L. De Lathauwer, *NLS Algorithm for Kronecker-Structured Linear Systems with a CPD Constrained Solution*, EUSIPCO, (2019) pp. 1-5.

[3] N. Govindarajan, N. Vervliet, L. De Lathauwer, *Regression and classification with spline-based separable expansions*, Technical Report 21-67, ESAT-STADIUS, KU Leuven (Leuven, Belgium), 2021

[4] S. Hendrikx, M. Boussé, N. Vervliet, L. De Lathauwer, *Algebraic and optimization based algorithms for multivariate regression using symmetric tensor decomposition*, Proceedings of CAMSAP 20195, IEEE, Guadeloupe, (2019) pp. 475-479.

[5] N. Sidiropoulos, L. De Lathauwer, X. Fu, K. Huang, E. Papalexakis, C. Faloutsos, *Tensor Decomposition for Signal Processing and Machine Learning*, IEEE, (2017) pp. 3551-3582.

[6] P. Sinha, *Multivariate polynomial regression in data mining: Methodology, problems and solutions*, Int. J. Sci. Eng. Res., (2013) pp. 962–965.

[7] R. Widdershoven, *Spline-type tensorontbindingen voor gesuperviseerd leren*, Leuven : KU Leuven. Faculteit Ingenieurswetenschappen, Leuven, 2021.

Online Unit Commitment Problem Solving using Dynamic Programming

Wim Van Roy*, Joris Gillis, Goele Pipeleers and Jan Swevers
MECO Research Team, KU Leuven DMMS lab, Flanders Make
*Email: wim.van.roy@kuleuven.be

1 Overview

Unit Commitment problems (UCMs) are problems in which a set of generators need to work together to achieve a common goal. Examples of such problems are the energy grid, heating systems or production of compressed air. The nature of these problems are NP-hard as it combines nonlinearities together with discrete states of the generators[1]. Due to this complexity, achieving the global optimum often takes a very long time and warmstarting is often impossible making the solvers limited to offline scheduling approaches. This abstract proposes a new solution technique based on Dynamic Programming (DP), a recursive solution technique. The technique can achieve a near-optimal solution in short amount of time making it feasible to run online on embedded targets.

2 Background

The goal of a UCM is to generate a demand flow of electricity, heat or air as efficiently as possible over a given time horizon using the given set of generators. Equation 1 [2] formulates the UCM for a horizon of T and a set of generators $\mathbb{G}$.

$$\begin{aligned} \min & \sum_{g\in\mathbb{G}}\sum_{t=0}^{T} p_g(c_{g,t}, s_{g,t}) \\ \text{s.t.} & \sum_{g\in\mathbb{G}} q_g(c_{g,t}, s_{g,t}) = D(t) \quad \forall t \in [0,1,...,T] \\ & (c_{g,t}, s_{g,t}) \in \Pi_g(t) \qquad\qquad \forall g \in \mathbb{G}, \\ & \qquad\qquad\qquad\qquad \forall t \in [0,1,...,T] \end{aligned} \tag{1}$$

In this equation $c_{g,t}$ and $s_{g,t}$ are the capacity and the machine state of generator g at time t. The consumed power and the produced flow of the generator g are given by p_g and q_g. The machine state can be *on*, *off* or *idling* and are constraint by the feasible set Π_g. The demand flow is given by $D(t)$. In literature, both the consumed power and produced flow formulas are often simplified to piecewise linear functions[1]. As a result, this formulation becomes a Mixed Integer Linear Problem (MILP). Existing solvers for MILP-problems are often hard to warmstart and take a long calculation time, especially when there are many feasible solutions.

3 Contribution

The proposed DP solution technique divides the original problem from Equation 1 into smaller subproblems for which the state and the capacity for each generator only has to be solved for one time instance given the required costs to go to a next iteration. Each iteration solves the problem given by Equation 2.

$$\begin{aligned} \min & \sum_{g\in\mathbb{G}} p_g(c_{g,t_i}, s_{g,t_i}) \\ & \quad + C_{g,t_{i+1}}(s_{g,t_i}) + C_{g,t_{i-1}}(s_{g,t_i}) \\ \text{s.t.} & \sum_{g\in\mathbb{G}} q_g(c_{g,t_i}, s_{g,t_i}) = D(t_i) \\ & (c_{g,t_i}, s_{g,t_i}) \in \Pi_g(t_i | c_{g,t_{i-1}}, s_{g,t_{i-1}}) \quad \forall g \in \mathbb{G} \end{aligned} \tag{2}$$

In this equation a lumped cost to go to the next state is given by $C_{g,t_{i+1}}$ as well as an additional cost $C_{g,t_{i-1}}$ due to the state of a previous time step. The feasible set of states for the generator is based on the previous time step. The algorithm alternately solves these subproblems in a backwards sweep and updates the feasible set of states for the generators in a forward sweep in time. This process continues until no further improvements can be made. After each iteration, the solvers guaranties a feasible solution. Since the algorithm can be stopped at any given time after the first iterate and allows warmstarting, it is able to run in an online system. A comparison with MILP-based approaches from literature is performed. The results show that the proposed technique achieves a near-optimal solution while reducing the calculation time. The proposed technique can run in an online system.

References

[1] Tiwari, S., Dwivedi, B., Dave, M. P., Shrivastava, A., Agrawal, A., & Bhadoria, V. S. (2021). Unit commitment problem in renewable integrated environment with storage: A review. *International Transactions on Electrical Energy Systems*, e12775.

[2] Knueven, B., Ostrowski, J., & Watson, J. P. (2020). On mixed-integer programming formulations for the unit commitment problem. *INFORMS Journal on Computing*, 32(4), 857-876.

An Adaptive Restart Heavy-Ball Projected Primal-Dual Method for Solving Constrained Linear Quadratic Optimal Control Problems[1]

Y.J.J. Heuts G.P. Padilla M.C.F. Donkers
Control Systems Group, Eindhoven University of Technology
Email: {y.j.j.heuts, g.p.padilla, m.c.f.donkers}@tue.nl

1 Introduction

In order to apply numerical optimal control to nonlinear systems or problems with integer decisions. Sequential quadratic programming, e.g., [1] can be used to solve the problem, while in the latter branch-and-bound methods, e.g., [2] can be applied. In both cases, a linear-quadratic subproblem has to be solved repeatedly. This calls for solvers for linear quadratic (LQ) optimal control problems (OCPs) that have a low computational effort that scales well when the number of states/inputs and time horizon increases. [3]

2 Problem formulation

We aim to solve a linear quadratic reference tracking problem, which can be reformulated in the static optimization problem

$$\begin{aligned} \min_{w} \quad & \tfrac{1}{2}\omega^\top \mathbf{G}\omega + \mathbf{F}^\top \omega + \iota_\Omega(\omega) \\ \text{s.t.} \quad & \mathbf{A}\omega - \mathbf{b} = 0, \end{aligned}$$

where $\mathbf{G}$ contains the quadratic and, $\mathbf{F}$ the linear costs, ι_Ω indicated the box constrained feasible set $\Omega := \{\omega \in \mathbb{R} \mid \underline{\omega} \leqslant \omega \leqslant \overline{\omega}\}$. $\mathbf{A}$ and $\mathbf{b}$ capture the system dynamics. It should be noted that all matrices are sparse, i.e., $\mathbf{G}$ is a diagonal matrix and $\mathbf{A}$ is a sparse block-banded-matrix. This structure and sparsity will also be exploited in the following section to propose a computationally efficient optimization algorithm.

3 Heavy-Ball Projected Primal-Dual Algorithm

In order to find a KKT point of the static optimization problem, we propose a primal-dual method with preconditioning matrices chosen such that the unconstrained solution is obtained in one step. The obtained iteration then reduces to

$$\begin{cases} \omega^{i+1} = \max\{\underline{\omega}, \min\{\overline{\omega}, \{-\mathbf{G}^{-1}\mathbf{F} - \mathbf{G}^{-1}\mathbf{A}^\top \lambda^i\}\} \\ \lambda^{i+1} = \lambda^i + \alpha(\mathbf{A}\mathbf{G}^{-1}\mathbf{A}^\top)^{-1}(\mathbf{A}\omega^{i+1} - \mathbf{b}) + \beta(\lambda^i - \lambda^{i-1}). \end{cases}$$

As an algorithm is unreliable to use if convergence is not guaranteed, we assess the iteration based on the observation that it can be rewritten as a dynamic system that admits a Lur'e structure, i.e., a linear/affine system with states λ with a static nonlinearity.

[1]This work has received financial support under the grant LONGRUN

By then defining a Lyapunov function and applying a LaSalle's invariance argument, it is possible to show that for a set of parameters, the iteration is asymptotically stable, which means that the algorithm converges to the solution of the original problem.

4 Illustrative Examples

The algorithm is compared to some commercial and open-source solvers. In Fig. 1 the computational times for each are reported for two examples. It can be seen that, although the algorithm has been coded in MATLAB (and the others are compiled code), we are able to achieve computational times which are close to solvers that have already proven their performance.

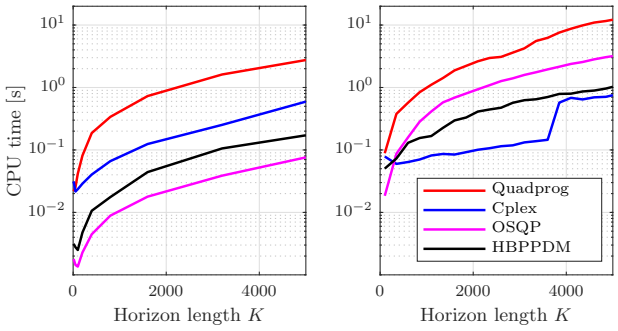

Figure 1: CPU time as function of horizon length using different solvers for an inverted pendulum model (left) and an ATFI-16 airplane model (right).

References

[1] P. T. Boggs and J. W. Tolle, "Sequential quadratic programming," *Acta numerica*, 1995.

[2] S. Boyd and J. Mattingley, "Branch and bound methods," *Notes for EE364b, Stanford University*, 2007.

[3] Y. Heuts, G. Padilla Cazar, and M. Donkers, "An adaptive restart heavy-ball projected primal-dual method for solving constrained linear quadratic optimal control problems," *CDC*, 2021.

E-Drive Specification Using Multi-fidelity Scalable Models

Olaf Borsboom
Eindhoven University of Technology
PO Box 513, 5600 MB,
Eindhoven, The Netherlands
o.j.t.borsboom@tue.nl

Mauro Salazar
Eindhoven University of Technology
PO Box 513, 5600 MB,
Eindhoven, The Netherlands
m.r.u.salazar@tue.nl

Theo Hofman
Eindhoven University of Technology
PO Box 513, 5600 MB,
Eindhoven, The Netherlands
t.hofman@tue.nl

1 Abstract

Electric vehicles are increasingly pervading the market [1]. When designing the powertrain system of electric vehicles, researchers typically aim to jointly optimize the hardware design and control of the system, which is often referred to as a co-design problem. The electric vehicle powertrain system investigated in this study can be decomposed into several components, namely the battery, the power electronics, the electric motor (EM) and the transmission. These components can then be further subdivided into elements such as battery cells, stator and rotor, etc. This results in a very high-dimensional and complex co-design problem.

Typically, the co-design problem is solved using model-based computer-aided engineering tools. However, there is a large disparity between the high-level vehicle requirements that electric car manufacturers might specify (in terms of performance, cost and energy efficiency) and the low-level component design questions that are raised in this context. Moreover, in modeling and design approaches, there exists a trade-off between the accuracy, the scalability, and the speed of the computational procedure. To this day, this powertrain co-design problem is generally approached by using significant simplifications and assumptions to ensure the problem is computationally tractable. This is achieved, for instance, by linearly scaling the EM and its losses in the maximum torque and the mass, sacrificing accuracy [2]. However, implementing an optimization algorithm using accurate but computationally expensive models, such as finite element (FE) methods, is not amenable to system level optimization [3].

This work presents an outlook on a scalable, convex optimization model of the EM, based on multi-fidelity surrogate modeling techniques, that can predict high level outputs with lower level design inputs. After selecting the relevant design inputs, we first create an EM training data set, consisting of two subsets. The first subset is a smaller set of (computationally expensive) high-fidelity samples that are locally accurate. The second subset is a larger set of (computationally inexpensive) low-fidelity samples that can capture the general trend of the outputs of interest [4]. Carefully selecting the locations of these data points in the design space maximizes the amount of knowledge we can accumulate from a limited number of sample evaluations. Second, we use a surrogate modeling technique that corrects the regression model of the low-fidelity samples with high-fidelity local accuracy. This results in a parametric EM model that predicts the following objectives: the efficiency, the maximum torque and power, the geometric dimensions, the weight and the cost. Third, we implement the scalable EM model in a full powertrain model that consists of similar models of the remaining components (the battery, the power electronics and the transmission) depending on the specific powertrain architecture, and optimize the design and control over a drive cycle. Additionally, we can set performance requirements on the powertrain, such as a maximum speed or acceleration. Overall, this approach has the potential to reduce the amount of effort from EM design experts, the number of design variables, and the computational time, whilst maintaining a good prediction accuracy over the full design space.

References

[1] "Electric vehicle statistics in the netherlands," Netherlands Enterprise Agency, 2022.

[2] E. Silvas, T. Hofman, N. Murgovski, P. Etman, and M. Steinbuch, "Review of optimization strategies for system-level design in hybrid electric vehicles," *IEEE Transactions on Vehicular Technology*, vol. 66, no. 1, pp. 57–70, 2016.

[3] G. Lei, J. Zhu, Y. Gou, C. Liu, and B. Ma, "A review of design optimization methods for electrical machines," *Energies*, vol. 10, no. 12, 2017.

[4] M. G. Fernández-Godino, C. Park, N. H. Kim, and R. T. Haftka, "Issues in deciding whether to use multifidelity surrogates," *AIAA Journal*, vol. 57, pp. 1–16, 2019.

Tuesday - July 5, 2022
16:10 - 18:30 (TuE)

A Modular Elementary Flux Mode Reduction Procedure for Dynamic Metabolic Modelling

Maton Maxime[1*], Philippe Bogaerts[2], Alain Vande Wouwer[1]
[1]Systems, Estimation, Control and Optimization, University of Mons, Belgium
[2]3BIO - Modeling and Control of Bioprocesses, University of Brussels, Belgium
[*]Email: Maxime.Maton@umons.ac.be

1 Abstract

Elementary flux modes (EFMs) are a powerful concept in metabolic engineering for the derivation of macroscopic dynamic models, which are useful for the design of bioprocess monitoring and control strategies. However, for detailed metabolic networks, the number of modes increases significantly leading to an intractable initial set of EFMs. In that context, systematic procedures for the generation or selection of subsets of EFMs are required. In a preliminary study [1], the authors proposed such a procedure, which is improved in the current study by including additional features, including the computation of the initial set of elementary vectors, the differentiate consideration of positivity constraints on the fluxes and the prediction error of reduced macroscopic reaction sets (reduced below the number of measured components). The procedure proceeds in several steps including minimal generation algorithms and geometric and optimization-based criteria for the reduction while ensuring a biological interpretation of the reduced set of modes. This work makes use of experimental data of CHO-cells in batch cultures on the basis of a detailed network and proposes different measurement configurations to highlight the performance of the procedure. Finally, a simple dynamic model including the prediction of the biomass is built on the basis of the resulting macroscopic bioreaction scheme.

2 Methods and results

Fig.1 illustrates the reduction procedure aimed at systematically reducing the number of elementary flux modes up to a number Λ chosen below the number of measured extracellular species. It starts from an initial set of modes generated by complete enumeration or subset selection and is made of several steps which can all be activated or bypassed as necessary. The reduction ensures (i) the removal of modes leading to macroreactions without a biological interpretation, (ii) the elimination of collinear modes based on a cosine-criterion and (iii) the respect of positivity constraints and the satisfaction of a least-squares deviation from experimental data by means of a series of optimization problems.

This study relies on a detailed metabolic network leading to

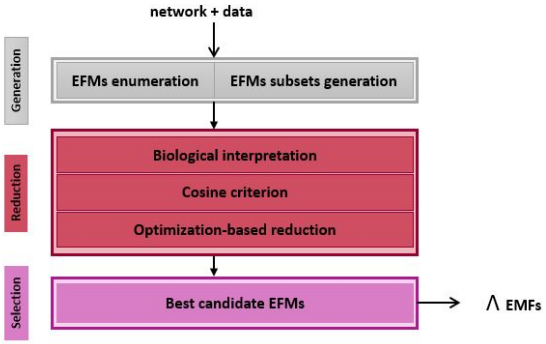

Figure 1: The reduction procedure

almost one billion EFMs, giving to the reduction procedure all its significance. In this case, a fast generation algorithm is used to identify an initial subset of modes and the reduction is executed to select a number of elementary flux vectors below the number of measured components. Different case studies are addressed, i.e., either 6 or 20 extracellular measurements. Validations are provided and show very satisfactory results. Fig.2 depicts the evolution of the measured concentrations as compared to the prediction of a dynamic simulator built on the basis of the bioreaction scheme obtained with the EFM reduction procedure.

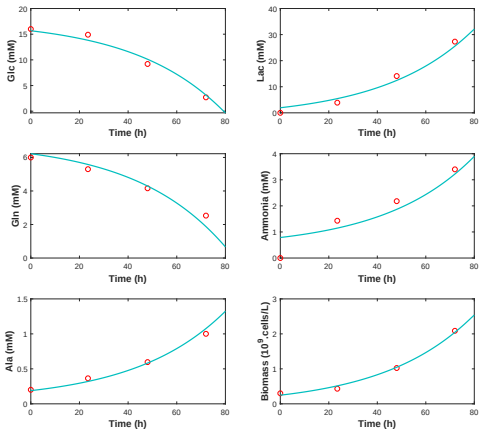

Figure 2: Time evolution of measured concentrations

References

[1] M. Maton, Ph. Bogaerts, and A. Vande Wouwer, "Selection of a suboptimal minimal set of EFMs for dynamic metabolic modelling," IFAC-PapersOnLine, 2021. Vol.54(3) 667-672

A General ODE-based Model to Describe Pest Populations Dynamics

Nicolás Bono Rosselló, Emanuele Garone
Service d'Automatique et d'Analyse des Systèmes
Université libre de Bruxelles
50, av. F.D. Roosevelt, CP 165/55
1050 Bruxelles, Belgique
nbonoros@ulb.ac.be, egarone@ulb.ac.be

Luca Rossini, Stefano Speranza
Dipartimento di Scienze Agrarie e Forestali
Università degli Studi della Tuscia
Camillo De Lellis
01100 Viterbo, Italy
luca.rossini@unitus.it

1 Introduction

Integrated Pest Management (IPM) systems aim at providing an effective and environmentally sensitive approach to pest management [1]. IPM schemes use as inputs information on the pests life cycles and environmental conditions. This information, in combination with available pest control tools, is used to define and manage pest damage actions by the most economical means, and with the least possible impact on the environment.

The development of automated detection technologies of pests is fundamental in IPM systems, but not sufficient. Measuring in agriculture is still expensive and many treatments require not only the current status but the future evolution of the infestations. In this context, the use of pest population models is particularly important. Particularly, when pest management is performed by release of natural enemies the effectiveness of strategies is highly dependant on the pest life cycle and more susceptible to certain life stages.

Several pest populations models have been proposed on the literature, but most of them are *ad hoc* models developed and tailored for specific insect species. The aim of this work is precisely to propose a general model able to describe the life cycle of most insect species of agricultural interest.

2 Model formulation

The model proposed is a physiologically-based model. Conceptually, physiologically-based models can be defined as the union between "phenological models" and "population dynamics models". This type of models describes the development of ectotherm populations over time while considering the stage development driven by environmental factors. This popular approach is based on the fact that insects, like most ectotherms, progress through their life stages with development rates that are highly dependent on the environmental parameters, temperature mainly [2].

The ectotherms' life cycle is divided into discrete age classes, each representing an "identifiable" life stage. Based on this we define the life cycle as a series of interconnected stages whose population varies based on environmentally dependant *rate functions* such as development rate, fertility rate or mortality rate. Figure 1 provides a schematic representation of this idea.

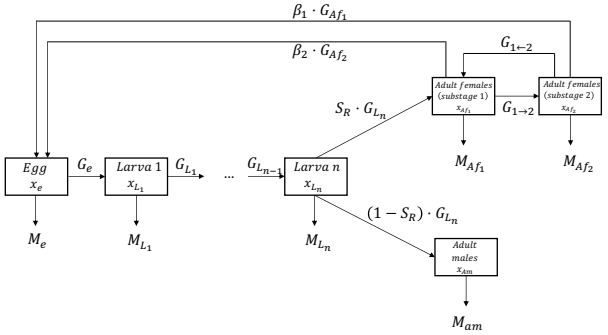

Figure 1: Schematic representation of the pest life cycle.

Accordingly, we associate to each stage a scalar state $x_i(t)$ $i = e, L_1, \ldots, L_n, A_m, A_{f1}, A_{f2}$ which represents the number of individuals in the population at time t at the stage i. Each stage population variation over time is then represented by an ODE which depends on the inflows and outflows of individuals associated to that stage. Mathematically,

$$\frac{d}{dt}x_i(t) = G_{i-1}(t)x_{i-1}(t) - G_i(t)x_i(t) - M_i(t)x_i(t) \qquad (1)$$

where $x_i(t)$ is the number of insects at the life stage i, $G_i(t)$ is a generic development rate function, in other words, the population that goes from stage i to stage $i+1$, and $M_i(t)$ is the mortality rate function associated to stage i.

References

[1] M. Barzman, P. Bàrberi, A. N. E. Birch, P. Boonekamp, S. Dachbrodt-Saaydeh, B. Graf, B. Hommel, J. E. Jensen, J. Kiss, P. Kudsk, J. R. Lamichhane, A. Messéan, A.-C. Moonen, A. Ratnadass, P. Ricci, J.-L. Sarah, and M. Sattin, "Eight principles of integrated pest management," *Agronomy for Sustainable Development*, vol. 35, pp. 1199–1215, Oct. 2015.

[2] D. G. Harcourt, "Development and use of life tables in study of natural insect populations," *Annual Review of Entomology*, vol. 14, no. 1, p. 175, 1969.

Control by state feedback of an age-dependent epidemiological model

Candy Sonveaux and Joseph J. Winkin

Namur Institute for Complex Systems (naXys) and Department of Mathematics
University of Namur, rue de Bruxelles 61, B-5000 Namur, Belgium
Email: candy.sonveaux@unamur.be, joseph.winkin@unamur.be

Epidemic models are crucial to have a better understanding of the evolution of diseases and to act effectively on them. One possible control policy in epidemic models is the vaccination. This is the one considered in this work.

In the following, an adapted version of the well-known SIR model of Kermack and McKendrick [1] is used. In this model the population is divided in three distinct groups: the group S of susceptible individuals who can catch the disease, the group I of infected individuals who can transmit the disease and the group R of recovered indivdiuals who have permanent immunity. Moreover, in this work, the importance of the age, a, of individuals is taken into account since several factors in epidemic models are age-dependent, vaccination being one of them.

The evolution of the disease propagation is described, using densities, by a set of nonlinear partial-integro differential equations (PIDE), as mentionned in [2],

$$\begin{aligned}(\partial_t+\partial_a)S(t,a) &= -(\Theta(t,a)+\mu(a))S(t,a)\\ &\quad -\beta(a)S(t,a)\int_0^L I(t,b)\,db,\\ (\partial_t+\partial_a)I(t,a) &= -(\mu(a)+\gamma(a))I(t,a)\\ &\quad +\beta(a)S(t,a)\int_0^L I(t,b)\,db,\\ (\partial_t+\partial_a)R(t,a) &= \Theta(t,a)S(t,a)+\gamma(a)I(t,a)\\ &\quad -\mu(a)R(t,a)\end{aligned} \tag{1}$$

under non-negative initial conditions $S(0,a)=S_0(a)$, $I(0,a)=I_0(a)$, $R(0,a)=R_0(a)$ and boundary conditions $S(t,0)=B, I(t,0)=0, R(t,0)=0$, where B denotes the birth rate. The population is assumed to be closed, therefore, only birth and mortality can change the total size of the population $P(t)$. Their respective rates are given by B, assumed to be constant, and $\mu(a)$. Moreover, the mode of transmission of the disease is assumed to be by contact between S-individuals and I-individuals. The transmission coefficient is given by $\beta(a)$. In addition, the I-individuals recover at a rate denoted by $\gamma(a)$. It is assumed that $\beta(\cdot)$ and $\gamma(\cdot)$ are in $L^\infty([0,L])$. Finally, the term $\Theta(t,a)$ is the input variable representing the rate of S-individuals being vaccinated at time t and age a. The vaccination is assumed to work perfectly: once vaccinated, an individual never catches the disease again.

The dynamical analysis of the open-loop system shows that, when the basic reproduction number of infection given by

$$R(0)=\int_0^L c(b)\Gamma(b)\int_0^b \frac{\beta(\sigma)}{\Gamma(\sigma)}\exp\left(-\int_0^\sigma \Theta^\star(\eta)\,d\eta\right)d\sigma db,$$

where $\Gamma(b)=\exp\left(-\int_0^b \gamma(\eta)\,d\eta\right)$, is greater than 1, then the disease-free equilibrium is unstable. In view of this, the aim of this work is to design a feedback control-law of vaccination $\Theta(t,a)$ that implies the convergence of the states trajectories to the disease-free equilibrium.

To answer this question, an approximation of Model 1 obtained by discretizing (1) in n classes of age is considered. This methodology is inspired by [3] and leads to a set of $2n$ ordinary differential equations. Then, by applying Isidori's theory developed in [4, chap.5] it is shown that, by an appropriate choice of the control tuning parameters, the state feedback law $(\theta_1(t)...\theta_n(t))^T$ implies the exponential convergence towards zero of the infected population $i_k(t)$ of the ODE Model, for $k=1,...,n$, as time tends to infinity, see [5]. Moreover, assuming that $\theta_k(t)$ is greater than 0, it is shown that the states trajectories remain positive for the closed-loop system, as is to be expected. Numerical simulations corroborate those results.

In addition a state-feedback law has been designed directly on Model 1, see [5]. This law is deduced from the one obtained on the ODE Model. Since the designed state-feedback control law is not applicable in practice because it requires the knowledge of all the state variables, we aim also to develop a state observer. Finally, in view of the current sanitary situation, it seems natural to perform numerical simulations on real data.

References

[1] W. Kermack and A. Mckendrick. Contributions to the mathematical theory of epidemics—II. The problem of endemicity. *Bulletin of Mathematical Biology*, 53(1-2):57–87, 1991.

[2] G. Bastin and J-M. Coron. *Stability and boundary stabilization of 1-D hyperbolic systems*, pages 40-43. coll. PNLDE Subseries in Control. Birkhauser. Switzerland, 2016.

[3] D. W. Tudor. An age-dependent epidemic model with application to measles. *Mathematical Biosciences*, 73(1):131–147, 1985.

[4] A. Isidori. *Nonlinear control systems*. Springer, 3rd edition, 1995.

[5] C. Sonveaux and J. J. Winkin. State feedback control law design for an age-dependant SIR model, submitted.

Global Sensitivity Analysis of a Microkinetic Model of the Oxygen Evolution Reaction

Bart van den Boorn[1] b.f.h.vandenboorn@differ.nl
Anja Bieberle-Hütter[1] a.bieberle@differ.nl
Matthijs van Berkel[1,2] m.vanberkel@differ.nl

[1]DIFFER - Dutch Institute for Fundamental Energy Research, De Zaale 20, 5612 AJ Eindhoven, The Netherlands
[2]Control Systems Technology, Mechanical Engineering, Eindhoven University of Technology, PO Box 513, 5600 MB, Eindhoven, The Netherlands

1 Introduction

Water-splitting in photo-electrochemical cells (PECs) to generate hydrogen can provide a key contribution to the increased need for energy storage in the shift towards renewables. However, solar water-splitting is not yet able to achieve the efficiencies required for commercial use. The oxygen generating reaction occurring at the photo-anode, the oxygen evolution reaction (OER), is commonly regarded as the performance limiting reaction. Microkinetic modelling of the OER, represented by a non-linear state-space model, provides an opportunity as it enables investigation of the OER process in the PEC, for example through impedance spectra [1]. This model has applied potential as input and current density as output and 14 physical model parameters. To improve the OER process investigation effort, characterisation of the contribution of the 14 parameters to the model output is required. Not with the aim of model reduction, but to uncover how the uncertainty of these parameters affects the model, as this could dictate the relevance of further research into these parameters.

Hence in this work, we perform Sobol's variance-based sensitivity analysis method on the OER model in [1], using this method for the first time on a photo-electrochemical system. Prior to the sensitivity analysis, a literature review is conducted into the values of the physical parameters relevant to the microkinetic model. Using the results from parameter literature study in the sensitivity analysis allows us to assess the relevance of a parameter's uncertainty from the perspective of the model.

2 Sensitivity Analysis

In Sobol's method [2], the fractional contribution of each of the physical parameters to the model output variance is represented in sensitivity indices, which allows for identification of a parameters' direct contribution and its interaction with other parameters. The analysis constitutes of Monte-Carlo-style model simulations where the physical parameters are sampled from the value ranges of our literature study, following the quasi-random Sobol's sampling sequence. We analyse parameter sensitivity for three different levels of sensitivity index convergence; screening, ranking and full convergence, which each provide distinct information.

3 Results

In this presentation, we show the primary results of our two-part study: (1) The literature analysis of the physical parameters and their value ranges and (2) the OER model sensitivity analysis, which includes the identification of the most and least influential parameters. For example, we show the first order (direct influence) and total effect (including interactions) indices of each physical parameter on the OER model output. Here we discover that, out of 14 parameters, the valance band energy level E_V has the largest influence, while six parameters have approximately no influence, see Figure 1. Furthermore, we find that a large intrinsic parameter uncertainty does not necessarily translate to large model output uncertainty, and vice versa. Additionally, we employ computationally low-cost sample visualisation methods to show the tendency of the model output with regards to each of the parameters, which can be used to identify more optimal OER conditions and improve the modelled system.

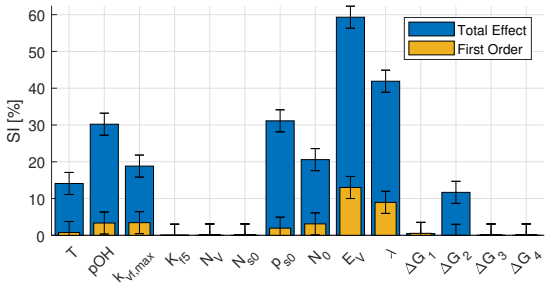

Figure 1: First order and total effect sensitivity indices of the OER model input parameters.

[1] K. George, M. van Berkel, X. Zhang, R. Sinha, and A. Bieberle-Hutter. In: *J. Phys. Chem. C* 123.15 (2019), pp. 9981–9992.

[2] A. Saltelli, P. Annoni, I. Azzini, F. Campolongo, M. Ratto, and S. Tarantola. In: *Comput. Phys. Comm.* 181.2 (2010), pp. 259–270.

The Effect of Vaccination and Human Behaviour in Epidemic Models

Kathinka Frieswijk, Lorenzo Zino, Ming Cao
Discrete Technology & Production Automation, University of Groningen
Nijenborgh 4, 9747 AG Groningen, The Netherlands
Email: {k.frieswijk,lorenzo.zino,m.cao}@rug.nl

1 Introduction

Inspired by the surge of COVID-19 cases that have been observed around the globe after the introduction of vaccination campaigns and the relaxation of non-pharmaceutical interventions, we propose a mathematical model on a temporal network for the spread of infections in a population that is partially vaccinated. The proposed model focuses on recurrent infections, such as those that do not provide permanent immunity (e.g. COVID-19) or infections that are caused by fast mutating viruses (e.g. influenza).

2 Model

The infection is spread via physical encounters in close proximity on an undirected network $(\mathscr{V},\mathscr{E}(t))$, where $\mathscr{V} = \{1,\dots,n\}$ and $t \in \mathbb{R}_{\geq 0}$. The encounters are generated via a mechanism inspired by continuous-time activity-driven networks [1], which incorporates human behaviour by including a responsibility level $\sigma \in [0,1]$, reflecting the probability that an individual will opt for the protection of others when only mild symptoms are present. By adding a compartment to the traditional susceptible–infected–susceptible (SIS) model, we separate infectious mildly symptomatic individuals from infected individuals who are quarantined. The model includes three control measures: i) *testing campaigns*, where individuals are triggered to get tested according to a Poisson clock with rate $c_t \in \mathbb{R}_{\geq 0}$; ii) *non-pharmaceutical interventions* (NPIs), modelled by introducing a parameter $\eta \in [0,1]$; and iii) *vaccination*, where $v \in [0,1]$ denotes the vaccination coverage. Here, we include two parameters, one for the effect of vaccination on transmission ($\gamma_t \in [0,1]$), and the other for its effect on the development of severe illness ($\gamma_q \in [0,1]$). Other parameters are the per-contact infection probability $\lambda \in [0,1]$, the probability to develop severe symptoms $p_q \in [0,1]$, and the recovery rate $\beta \in \mathbb{R}_{>0}$.

3 Results

Employing a mean-field approach, we derive that the system is governed by

$$\begin{aligned}\dot{y}_i &= 2(1-\eta)\lambda\,(1-\gamma_t v)\left[1-p_q\left(1-\gamma_q v\right)\right](1-\sigma)y_i - (\beta+c_t)y_i,\\ \dot{y}_q &= \left[2(1-\eta)\lambda\,(1-\gamma_t v)\,p_q\left(1-\gamma_q v\right)(1-\sigma)+c_t\right]y_i - \beta y_q.\end{aligned} \tag{1}$$

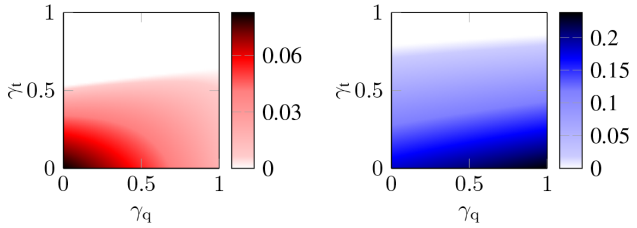

(a) Prevalence of severe illness (b) Epidemic threshold $\bar{c}_t$

Figure 1: (a) Prevalence of severe illness and (b) epidemic threshold for different levels of the effectiveness against severe illness γ_q and the effectiveness against transmission γ_t.

From the analysis of (1), we establish that the *epidemic threshold* is given by

$$\bar{c}_t := 2(1-\eta)(1-\sigma)\lambda\,(1-\gamma_t v)\left[1-p_q\left(1-\gamma_q v\right)\right]-\beta. \tag{2}$$

If $c_t > \bar{c}_t$, then a local outbreak will be extinguished and not escalate into a pandemic. If $c_t \leq \bar{c}_t$, the system converges to an endemic equilibrium. Simulations are used to illustrate our theoretical results, and to further investigate the role of vaccination and individuals' responsibility in epidemic spreading. Our results show that effective testing practices and a high level of responsibility are key toward the prevention of outbreaks. Interestingly, we discovered that vaccination is beneficial in the mitigation of an epidemic by reducing the prevalence of seriously ill individuals (Figure 1a), but it could in some cases favour resurgent outbreaks, as the epidemic threshold increases for a higher level of effectiveness against severe illness γ_q (Figure 1b). To obtain eradication of the disease, this calls for a higher level of cautiousness in the population and higher testing rates. All details and analytical derivations can be found in the preprint on arXiv [2].

References

[1] L. Zino, A. Rizzo, and M. Porfiri, "Continuous-Time Discrete-Distribution Theory for Activity-Driven Networks," *Phys. Rev. Lett.*, vol. 117, no. 228302, 2016.

[2] K. Frieswijk, L. Zino, and M. Cao, 'Modelling the Effect of Vaccination and Human Behaviour on the Spread of Epidemic Diseases on Temporal Networks," *arXiv preprint*, arXiv:2111.05590, 2021.

Optimising Photosynthetic Induction to control supplemental greenhouse lighting

Dominique Joubert
Dept. of Mathematical and Statistical Methods
Wageningen University and Research
P.O. Box 16, 6700 AV Wageningen
The Netherlands
Email: dominique.joubert@wur.nl

J.D. Stigter
Dept. of Mathematical and Statistical Methods
Wageningen University and Research
P.O. Box 16, 6700 AV Wageningen
The Netherlands

1 Introduction

Conventional greenhouse supplemental lighting practices are often guided by decreases in observed natural light. For such strategies however, the conversion of supplemental light energy into photosynthesis may not always be efficient.

Here, the inefficiency of photosynthesis is addressed using a model-based approach. More concisely, supplemental light is added to optimise a leaf's photosynthetic induction, a physiological measure of its photosynthetic efficiency.

2 The problem

Consider the net photosynthetic rate (A_n), modelled to account for plant physiology under natural fluctuating light ($PAR_{natural}$) in Fig.1. A leaf's photosynthetic efficiency at

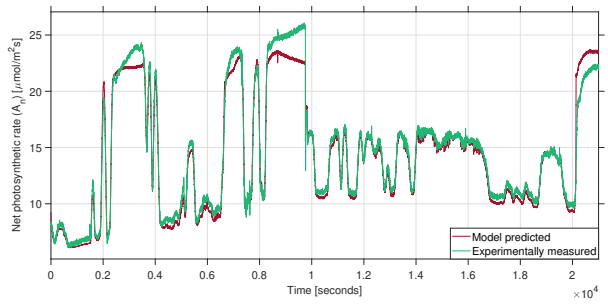

Figure 1: Net photosynthetic rate (A_n) - both modelled and measured - under natural fluctuating light ($PAR_{natural}$).

$PAR_{natural}$(t) can be expressed as an induction percentage,

$$\%\ induction(PAR_{natural}(t)) = \frac{A_n(PAR_{natural}(t))}{A_{n_{ss}}(PAR_{natural}(t))} \times 100 \quad (1)$$

$A_{n_{ss}}(PAR_{natural}(t))$ is the steady-state photosynthetic rate obtainable at a specific $PAR_{natural}$. Due to stomatal and enzymatic limitations, a leaf may not reach $A_{n_{ss}}$ during rapid fluctuations in $PAR_{natural}$. Accordingly, photosynthetic efficiency decreases.

The aim here is to boost a leaf's photosynthetic efficiency by using a set-point of 100% induction as control guide, thereby implementing physiology driven supplemental lighting.

3 Results

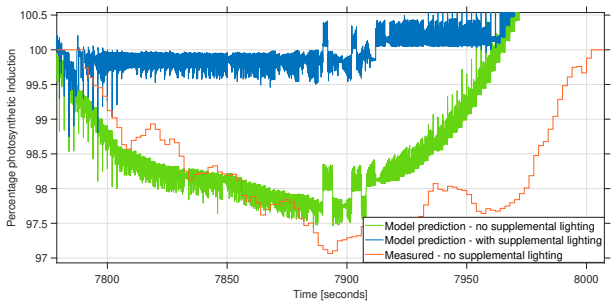

Figure 2: A drop in photosynthetic induction over a 3 minute period coincides with an increase in $PAR_{natural}$. An optimised induction level is achieved by introducing supplemental light ($PAR_{supplemental}$), shown in green in Fig.3.

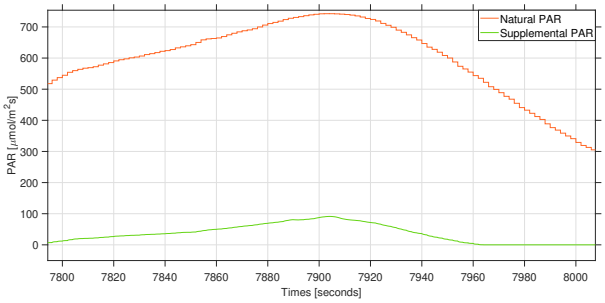

Figure 3: $PAR_{natural}$ and the required $PAR_{supplemental}$.

4 Conclusion

A leaf's photosynthetic capacity can be optimised by adding intermittent low levels of supplemental lighting. The use of dimmable LEDs make this application feasible. The belief is that whilst both conventional and physiology driven lighting practices will produce similar crop yields, the latter will be associated with lower energy costs.

Data-driven distributionally robust control of partially observable jump linear systems

Mathijs Schuurmans Panagiotis Patrinos
ESAT-STADIUS, KU Leuven — Kasteelpark Arenberg 10, 3001, Leuven, Belgium
{mathijs.schuurmans, panos.patrinos}@esat.kuleuven.be

1 Introduction and motivation

We consider discrete-time Markov jump linear systems (MJLS), which are described by dynamics of the form

$$x_{t+1} = A_{\theta_t} x_t + B_{\theta_t} u_t, \qquad y_t = C_{\theta_t} x_t,$$

where $x_t \in \mathbb{R}^{n_x}$, $u_t \in \mathbb{R}^{n_u}$, $y_t \in \mathbb{R}^{n_y}$ and $\theta_t \in W = \{1, \dots, d\}$ are the (continuous) state, the control, the output and the discrete mode at time t, respectively. The (discrete-valued) mode θ_t is governed by a Markov chain, with transition probabilities $P_{ij} = \mathbb{P}[\theta_t = j \mid \theta_{t-1} = i]$. This class of systems finds applications in a myriad of different fields, including energy systems [2] and automated driving [3].

Our main objective is to design controllers for MJLS, while simultaneously learning the transition matrix P, which is initially assumed to be completely unknown. For the purpose of control, it is often assumed that the mode is directly measurable [4, 3]. In practice, however, the mode typically represents some latent internal system state which needs to be inferred from measurements of the continuous state (if known) or from output measurements directly. Given output measurements y_t, the task is thus to (i) recursively estimate the active mode, in order to continually learn the transition probabilities of the underlying Markov chain, and (ii) integrate this procedure with an online controller design which leverages this information to gradually improve performance. By adopting a DR framework, we can do so while retaining system theoretic guarantees. We illustrate this by means of a linear controller design, while keeping in mind more advanced applications, requiring for instance model predictive control (MPC)-based approaches [3].

2 Mode estimation

In order to learn the transition probabilities, we develop a procedure to estimate underlying modes, based on output measurements. Traditional solutions to this problem require knowledge of the so-called *mode-observability index* N, i.e., the number of previous output measurements $(y_{t-k})_{k=1}^{N}$ required to uniquely determine (a subsequence of) the corresponding modes $(\theta_{t-k})_{k=1}^{N}$. Although it was shown that this number can theoretically be determined offline, the procedure to do so is often prohibitively expensive, even for small-scale systems [1]. To address this shortcoming, we develop a mode estimation procedure which adaptively selects the length of the observation horizon and show that for any mode-observable system, this length is upper-bounded by N. Moreover, we experimentally illustrate that this upper bound tends to be strict, suggesting more efficient memory usage than traditional approaches requiring the offline determination of N.

3 Distributionally robust output-feedback control

Since the mode observer does not provide exact knowledge of the continuous state x_t, we show how a time-varying output feedback controller can be designed that stabilizes the system in the mean-square sense.

The described mode estimation scheme outputs mode transitions (θ_t, θ_{t+1}), which can be used to construct empirical distributions $\hat{P}_i = (\hat{P}_{ij})_{j \in W}$, $i \in W$: $\hat{P}_{ij} = \frac{1}{n_i} \sum_{k=1}^{n_i} \mathbf{1}(\theta_k = i \wedge \theta_{k+1} = j)$, with n_i the number of observed transitions originating in mode i at time t (dependence on t is suppressed to ease notation). Using concentration inequalities, we can construct *ambiguity sets* $\mathscr{A}_i = \left\{ \mu \in \Delta_d \mid \|\mu - \hat{P}_i\|_1 \leq r_i \right\}$, where Δ_d the d-dimensional probability simplex and r_i is selected to ensure that $\mathbb{P}[P_i \in \mathscr{A}_i] \geq 1 - \beta_t$ for a given $\beta_t \in (0,1)$. Exploiting the polytopic structure of $\mathscr{A}_i = \mathbf{conv}\{P_i^{(1)}, \dots, P_i^{(M)}\}$, we construct a (time-varying) control law $u_t = K_t y_t$ such that there exists a mode-dependent matrix $V_i \succ 0$, $i \in W$ satisfying the Lyapunov-type stability condition

$$\sum_{j \in W} P_{ij}^{(q)} (A_j + B_j K_t C_j)^\top V_j (A_j + B_j K_t C_j) - V_i \prec 0,$$

for all $q \in \{1, \dots, M\}$, $i \in W$, and $t \in \mathbb{N}$. Extending the results from [5], we cast this problem to a linear matrix inequality, which can be solved efficiently. Provided that the sequence $(\beta_t)_{t \in \mathbb{N}}$ is square-summable, we finally show mean-square stability of the closed-loop system.

Acknowledgements This work was supported by the Ford-KU Leuven Research Alliance. The work of P. Patrinos was supported by: FWO projects: No. G086318N; No. G086518N; FNRS, FWO under EOS Project No. 30468160 (SeLMA), Research Council KU Leuven C1 project No. C14/18/068.

References

[1] M. Babaali and M. Egerstedt. Pathwise observability and controllability are decidable. In *42nd IEEE International Conference on Decision and Control (IEEE Cat. No.03CH37475)*, volume 6, pages 5771–5776 Vol.6, Dec. 2003.

[2] C. A. Hans, P. Sopasakis, J. Raisch, C. Reincke-Collon, and P. Patrinos. Risk-Averse Model Predictive Operation Control of Islanded Microgrids. *IEEE Transactions on Control Systems Technology*, 28(6):2136–2151, Nov. 2020.

[3] M. Schuurmans, A. Katriniok, H. E. Tseng, and P. Patrinos. Learning-Based Risk-Averse Model Predictive Control for Adaptive Cruise Control with Stochastic Driver Models. In *IFAC 2020 World Congress*, pages 15337–15342, Berlin, 2020.

[4] M. Schuurmans and P. Patrinos. A General Framework for Learning-Based Distributionally Robust MPC of Markov Jump Systems. *arXiv:2106.00561*, 2021.

[5] Z. Shu, J. Lam, and J. Xiong. Static output-feedback stabilization of discrete-time Markovian jump linear systems: A system augmentation approach. *Automatica*, 46(4):687–694, Apr. 2010.

Spatio-temporal decoupling for system identification using SVD and recurrent neural networks

Carlos J. G. Rojas, L. Özkan
Control Systems Group
Eindhoven University
Email: {c.j.gonzalez.rojas,l.ozkan}@tue.nl

Mateus Dias Ribeiro
Institute of Aerodynamics and Flow Technology
German Aerospace Center
Email: mateus.diasribeiro@dlr.de

1 Introduction

Distributed parameter systems (DPS) are ubiquitous in industrial processes and nature. These systems are described by partial differential equations (PDEs) and generally represent complex nonlinear dynamics with solutions constituting an infinite-dimensional vector space. Depending on the phenomenon and the purpose of the model, the resulting mathematical description of the system can have uncertainties in terms of unknown dynamics, parameters, constitutive equations, or coupling between different scales. In this work, we explore a system identification approach to approximate uncertainties in the form of undefined model structures using a non-intrusive method. The approach combines classical spatio-temporal decomposition techniques with recurrent neural network models.

2 Problem formulation and Methodology

Consider a DPS described by the following PDE:

$$\frac{\partial z}{\partial t} = N\big(z, \mathbf{x}, t, \nabla z, t, u\big), \tag{1}$$

where z is the variable of interest (state of the system), N represents the dynamics (combination of linear and nonlinear terms), $\mathbf{x}$ represents the spatial coordinates, t is the continuous time, and u is the control action. The initial and boundary conditions are given and the full state and control signals are available. A simple approach to address these DPS is to use the canonical linear discrete representation as follows:

$$\mathbf{z}_{k+1} \approx \mathbf{A}\mathbf{z}_k + \mathbf{B}\mathbf{u}_k, \tag{2}$$

where the dynamic and input matrices ($\mathbf{A}$ and $\mathbf{B}$) can be approximated using methods such as the dynamic mode decomposition with control (DMDc) [1].

The approach proposed in Fig. 1 is related to the DMDc, but goes beyond the linear approximation on the reduced space. The steps are the following:

1. Collect the state $\mathbf{z}_k$ and control measurements $\mathbf{u}_k$ across the sampled times from $k = 1, 2, ..., m$ and form the data matrix $\mathbf{Z}'$ with the states $\mathbf{z}_k$ as columns.
2. Apply the SVD on $\mathbf{Z}'$, define a truncation dimension r , and then project the states $\mathbf{z}$ using the left singular vectors in U ($z = \mathbf{U}\tilde{z}$).

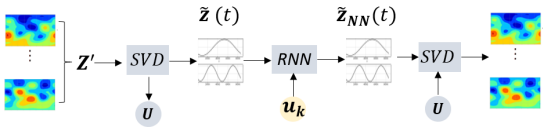

Figure 1: Methodology proposed

3. Model the temporal evolution of the time coefficients $\tilde{z}$ using a recurrent neural network (RNN) as in [2], but including the control measurements $\mathbf{u}_k$ as input of the neural network:

$$\tilde{z}_{t+1} = RNN(\tilde{z}_t, u_k, h_t, \theta), \tag{3}$$

where h_t, θ are the parameters of the RNN.

It has been shown that the modeling of latent space dynamics with RNNs can provide closure for unresolved reduced spaces while taking advantage of the sequential nature of the problem [2]. The last step proposed here is an extension from autonomous dynamics to systems with control inputs.

3 Conclusion and Future work

We proposed an extension of RNN latent-state modeling of autonomous systems to problems with control inputs. Modeling the temporal evolution on the reduced space simplifies the identification problem and allows to move back and forth to the full space using a simple linear encoding-decoding operation. This formulation can be extended to applications where the behavior of the system in a latent space is partially known or for the development of physics-informed parametric model surrogates. Another important consideration would be to model the errors derived from the truncated linear projection and optimize the neural network model in terms of the reconstruction in the full space.

References

[1] Joshua L. Proctor, Steven L. Brunton and J. Nathan Kutz, "Dynamic mode decomposition with control", SIAM, 2016.

[2] Maulik, et al., "Time-series learning of latent-space dynamics for reduced-order model closure", Physica D: Nonlinear Phenomena 405 , 2020.

Data-based batch process model using principle component analysis and Gaussian process regression

Maarten Vlaswinkel* Bram de Jager* Frank Willems*,†
*Dept. of Mechanical Eng., Eindhoven University of Technology (TU/e), The Netherlands
†TNO Automotive, Helmond, The Netherlands

Batch control systems are systems that only have a single set of control actions at the start of each cycle. However, the inter-cycle dynamics are complex and need to follow a predefined trajectory. Examples of such systems are certain processing steps in manufacturing processes or the combustion in internal combustion engines. Physics-based models are often too complex and computationally expensive or too simple and not accurate enough.

In this paper, we present a data-based method to model the inter-cycle dynamics of such systems. In the presented method, the inter-cycle dynamics are seen as a mapping $f : \mathcal{U} \times \mathcal{C} \times \mathcal{T} \to \mathbb{R}$, where $\mathcal{U}$ is the input space, $\mathcal{C}$ is the initial condition space and $\mathcal{T}$ is the inter-cycle time space.

The presented method uses a training set of n_e experiments collected in the measured operation space $(\bar{\mathcal{U}} \times \bar{\mathcal{C}}) \subset (\mathcal{U} \times \mathcal{C})$ over the full inter-cycle time $\mathcal{T}$. Using Principle Component Analysis (PCA) [1], it is possible to separate $(\bar{\mathcal{U}} \times \bar{\mathcal{C}})$ from $\mathcal{T}$ such that

$$f(u,\, c,\, t) = \sum_{i=1}^{n_\mathrm{e}-1} w_i(u,\, c) x_i(t) \tag{1}$$

with the Principle Component (PC) $x_i(t)$ and related weight $w_i(u,\, c)$ for $i \in \{1,\, 2,\, \ldots,\, n_\mathrm{e} - 1\}$, input $u \in \bar{\mathcal{U}}$, initial condition $c \in \bar{\mathcal{C}}$ and time $t \in \mathcal{T}$. To reduce the required number of PCs, we approximate the sum in (1) with $n_\mathrm{pc} < n_\mathrm{e} - 1$ PCs. This results in

$$f(u,\, c,\, t) \approx \sum_{j=1}^{n_\mathrm{pc}} w_j(u,\, c) x_j(t). \tag{2}$$

Eq. (2) is only defined for the measured operation space. However, this needs to be expanded to the full operation space $(\mathcal{U} \times \mathcal{C})$. This is done by applying Gaussian Process Regression (GPR) on $w_j(u,\, c)$ $\forall j \in \{1,\, 2,\, \ldots,\, n_\mathrm{pc}\}$ [2].

The above presented method is applied to model the in-cylinder pressure trace during combustion of a duel-fuel combustion engine fuelled with diesel and E85 [3]. The inputs are the injected mass of diesel and E85 and start-of-injection of diesel. The initial conditions are the pressure and temperature at intake valve close, the ratio of recirculated exhaust gas and the air-to-fuel ratio.

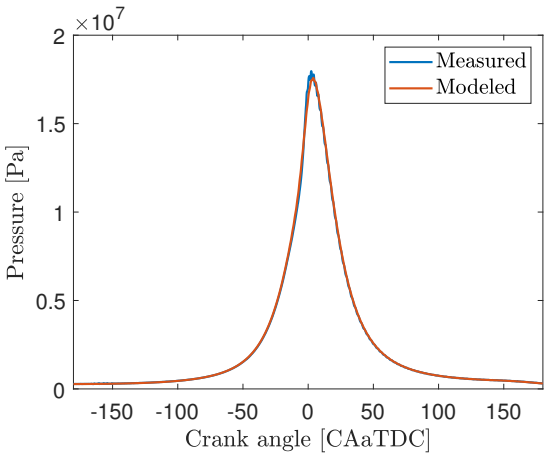

Figure 1: Measured and modelled in-cylinder pressure at the same operating conditions not part of the training data

Fig. 1 shows the measured and modelled in-cylinder pressure trace $f(u,\, c,\, t)$ of an operating point not included in the training data. In the example, $n_\mathrm{pc} = 7$ and the inter-cycle time space is represented by the crank angle.

During the presentation we will give more insight into selecting n_pc and the limitation of the model regarding the selected experiments. Furthermore, we will discuss the possibility of modelling cycle-to-cycle variations using the above presented method.

References

[1] J. Shlens, "A Tutorial on Principal Component Analysis," *arXiv:1404.1100 [cs, stat]*, Apr. 2014.

[2] C. E. Rasmussen and C. K. I. Williams, *Gaussian Processes for Machine Learning*, ser. Adaptive Computation and Machine Learning. Cambridge, Mass: MIT Press, 2006.

[3] R. Willems, F. Willems, N. Deen, and B. Somers, "Heat release rate shaping for optimal gross indicated efficiency in a heavy-duty RCCI engine fueled with E85 and diesel," *Fuel*, p. 119656, Nov. 2020.

Data-Driven Tuning of Rational Feedforward Controllers for Noncommutative MIMO Systems[1]

Maurice Poot[2,*], Jim Portegies[3], Tom Oomen[2,4]

[2]Control Systems Technology Group, Dept. of Mechanical Engineering, Eindhoven University of Technology, The Netherlands

[3]CASA, Dept. of Mathematics and Computer Science, Eindhoven University of Technology, The Netherlands

[4]Delft Center for Systems and Control, Delft University of Technology, The Netherlands

[*]Email: m.m.poot@tue.nl

1 Background

Feedforward control is essential in mechatronic systems that perform varying motion tasks with extreme accuracy requirements. In [1], iterative learning control (ILC) with rational basis functions (RBFs) is introduced to enable high tracking accuracy with extrapolation of the motion tasks for rational SISO systems. The rational parameterizations result in a non-convex optimization problem and is solved by using SK-iterations, i.e., solving a sequence of weighted least-squares problems. These algorithms are experimentally efficient due to the fact that the system is commutative and since almost all iterative aspects involve computational steps and not experimental steps.

2 Problem formulation

The aim of this research is to develop a solution method for RBF ILC for MIMO systems that do not commute.

3 Approach

The developed MIMO RBF approach exploits the idea from input shaping [2] to avoid exploitation of the commutation property. By rewriting the optimization problem into an input shaping solution with a compensatory input, a single weighted least-squares problems is obtained that can be solved after each experiment. Instead of solving a sequence of weighted least-squares problems offline, only a single weighted least-squares problem is solved each experiment. This avoids the exploitation of the commutation property at the cost of only slightly slower convergence.

4 Results

Preliminary results, shown in Fig. 1, for positioning of a wire bonder in one-direction only, i.e., SISO, shows indeed that the convergence rate of the cost of the developed MIMO RBF method is slower than the RBF-SK method while attaining the same final cost. As expected, the convergence rate equals that of one-step-only RBF-SK method, i.e., performing only one SK optimization per experiment.

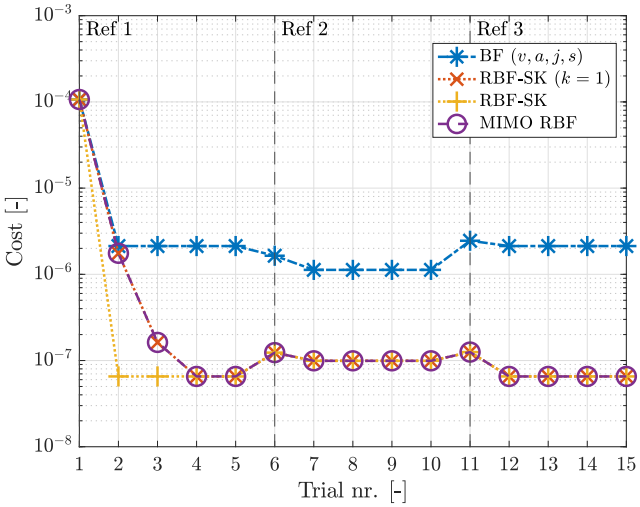

Figure 1: Comparison of cost per trial, i.e., experiment, in SISO ILC simulation of traditional polynomial BF (—), the one-step-only ($k = 1$) RBF-SK (—), standard RBF-SK (—), and the proposed MIMO RBF method (—).

5 Conclusion and outlook

The MIMO RBF framework will enable accurate rational feedforward control for noncommutative MIMO systems. Initial result show that the commutation property can be avoided at the cost of only slightly slower convergence. Ongoing research focuses on the analysis of the convergence properties and experimental validation.

References

[1] J. Bolder and T. Oomen, "Rational basis functions in iterative learning control - With experimental verification on a motion system," *IEEE Trans. Control Syst. Technol.*, vol. 23, no. 2, pp. 722–729, 2015.

[2] F. Boeren, D. Bruijnen, N. Van Dijk, and T. Oomen, "Joint input shaping and feedforward for point-to-point motion: Automated tuning for an industrial nanopositioning system," *Mechatronics*, vol. 24, no. 6, pp. 572–581, 2014.

[1]This work is supported by ASM Pacific Technology. The authors thank Dragan Kostić, Robin van Es, and Jilles van Hulst for their contributions to this research.

Data-driven distributionally robust MPC for constrained stochastic systems

Peter Coppens[†]
peter.coppens@kuleuven.be

Panagiotis Patrinos[†]
panos.patrinos@kuleuven.be

[†]STADIUS, Department of Electrical Engineering (ESAT), KU Leuven, Leuven, Belgium.

1 Abstract

We develop an MPC scheme for stochastic dynamics with chance constraints. The disturbances $\{w_t\}_{t=0}^{N}$ are i.i.d. random vectors, the distribution of which is unknown, usually introducing the need for robust approaches. *Distributionally robust optimization* improves upon classical robust control by using available data to infer properties of the distribution, while retaining guarantees.

To describe the distribution $\mu_\star$ of w_t we use data-driven ambiguity sets $\mathscr{A} \subseteq \mathfrak{P}(\mathscr{W})$ of probability measures s.t.

$$\mathbb{P}[\mu_\star \in \mathscr{A}] \geq 1 - \varepsilon.$$

The randomness enters $\mathscr{A}$ through the data that is used to estimate it. We then synthesize a controller that is optimal for the worst case distribution in $\mathscr{A}$. The maximization over measures is reformulated using results from semi-infinite conic duality [1].

Since the random variables of interest like the cost and chance constraints depend on multiple realizations of w_t we show how the classical conic duality results can be extended to ambiguity set over product measures and when chance constraints are involved. To do so, we need to consider a tight convex relaxation of the problem. We illustrate how the resulting scheme can be applied both with offline data or while gathering data after deployment. Moreover, we show when recursive feasibility holds

Similar results were achieved in [2] for a tube-based approach with Wasserstein ambiguity, the radius of which is not data-driven; in [3] for moment-based ambiguity which is not data-driven and does not guarantee recursive feasibility; and [4] for discrete distributions.

All developments hold for general continuous dynamics, the reformulation however is a semi-infinite optimization problem. So, for tractability's sake, we consider the simplified setting of linear dynamics with additive noise and quadratic cost and chance constraints. The policy is parametrized using affine disturbance feedback [5]. The fully data-driven ambiguity set constrains the second moment and mean of the additive disturbance using a matrix Hoeffding concentration inequality [6]. To do so we need to assume that $\|w_t\|_2 \leq r$ a.s. The resulting optimal control problem is then a *semidefinite program (SDP)*. We validate the scheme's performance through numerical experiments. Fig. 1 shows a state trajectory for a system with one state and one input. The cost is such that the state should be as close to the dashed line – depicting the chance constraint – as possible, without crossing it. Each time step a new observation of w_t is used to update the ambiguity, which is initialized from 10 samples. It is clear that as data is gathered, the online scheme becomes less conservative compared to the robust scheme which only uses $\|w_t\|_2 \leq r$. The bottom offline scheme used 10 000 samples to generate an ambiguity set.

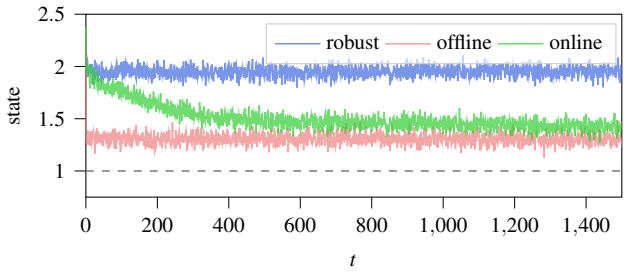

Figure 1: Evaluation of online learning scheme.

Acknowledgements

This work was supported by: the Research Foundation Flanders (FWO) PhD grant 11E5520N and research projects G0A0920N, G086518N and G086318N; Research Council KU Leuven C1 project No. C14/18/068; Fonds de la Recherche Scientifique – FNRS and the FWO – Vlaanderen under EOS project no 30468160 (SeLMA); EU's Horizon 2020 research and innovation programme: Marie Skłodowska-Curie grant No. 953348.

References

[1] Alexander Shapiro. On Duality Theory of Conic Linear Problems. In *Semi-Infinite Programming. Nonconvex Optimization and Its Applications, vol 57*. Springer, Boston, MA, 2001.

[2] Christoph Mark and Steven Liu. Stochastic MPC with Distributionally Robust Chance Constraints. 2020.

[3] Bart P. G. Van Parys, Daniel Kuhn, Paul Goulart, and Manfred Morari. Distributionally Robust Control of Constrained Stochastic Systems. *IEEE TAC*, 61(2), 2015.

[4] M. Schuurmans and P. Patrinos. Learning-based distributionally robust model predictive control of markovian switching systems with guaranteed stability and recursive feasibility. In *CDC*. IEEE, 2020.

[5] P. Goulart, E. Kerrigan, and J. Maciejowski. Optimization over state feedback policies for robust control with constraints. *Automatica*, 42(4), 2006.

[6] Joel A. Tropp. An Introduction to Matrix Concentration Inequalities. *Found. Trends Mach. Learn.*, 8(1-2), 2015.

Data–driven rate–based integral predictive control with estimated prediction matrices

P. C. N. Verheijen, G. R. Gonçalves da Silva, M. Lazar
Eindhoven University of Technology, The Netherlands
{p.c.n.verheijen, g.goncalves.da.silva, m.lazar}@tue.nl

1 Introduction

Model predictive control (MPC) is a control strategy that computes the optimal control input by predicting the future response over a finite time horizon [1]. Hereby, the performance of the controller is dictated by the accuracy of the prediction, which is usually derived from a model of the system. Data–driven control eliminates the modelling step by directly identifying the prediction matrices from I/O data. Indirect data–driven predictive control was originally proposed in [2], where an unconstrained subspace predictive control (SPC) algorithm was derived based on off-line I/O data. On-line, the controller estimates the future outputs as a linear combination of the estimated prediction matrices and previously applied inputs and measured outputs. [3] made an attempt to add integral action by assuming a particular ARIMAX model structure, which allows using the discrete output derivative for feedback, and by summing up terms in the SPC prediction matrices. A data–driven correspondent of standard, rate–based (also called velocity form) integral model predictive control [1], has not yet been developed, to the best of our knowledge.

2 Approach

In rate-based MPC, the optimal control input sequence ΔU_k^* is computed every time instant k by minimizing a cost function, e.g.,

$$J := (Y_k - \mathcal{R}_k)^T \Omega (Y_k - \mathcal{R}_k) + \Delta U_k^T \Psi \Delta U_k. \qquad (1)$$

Y_k is predicted as a linear combination of the rate–based prediction matrices, the state at time k and ΔU_k. Through the steps of SPC, we can estimate the data–driven prediction matrices of the system $\begin{bmatrix} P_1 & P_2 & \Gamma \end{bmatrix}$, such that,

$$Y_k = P_1 \mathbf{u}_{k-N} + P_2 \mathbf{y}_{k-N+1} + \Gamma U_k. \qquad (2)$$

However, this is not the rate–based representation. In our previous research, we propose that using the same experiment data U and Y, the corresponding rate–based prediction matrices can be obtained by creating a manipulated input sequence ΔU, where $\Delta u(k) = u(k) - u(k-1)$ and using that sequence together with Y in the estimation procedure. Therefore, the rate–based prediction matrices estimate the same output Y_k as,

$$Y_k = P_{1_I} \Delta \mathbf{u}_{k-N} + P_{2_I} \mathbf{y}_{k-N+1} + \Gamma_I \Delta U_k, \qquad (3)$$

3 Results

Fig. 1 presents the closed–loop simulation results on a linear actuator model for the developed i-DPC and the standard SPC as presented in [2]. Also, between $t = 2$ s and $t = 4$ s we apply a constant disturbance force.

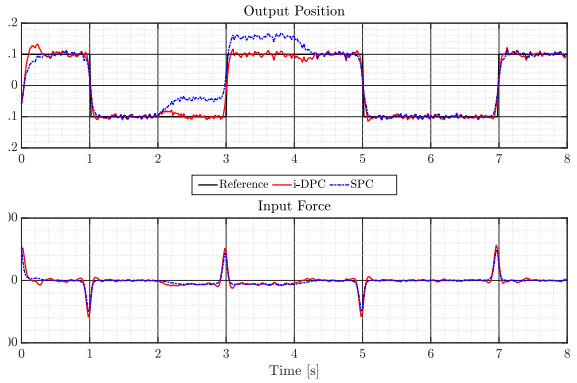

Figure 1: Linear motor example: closed–loop response comparison between SPC and i-DPC.

The benefits of the integral action can be observed by the response to the disturbance.

References

[1] L. Wang, *Model predictive control system design and implementation using MATLAB®*. Springer Science & Business Media, 2009.

[2] W. Favoreel, B. De Moor, and M. Gevers, "SPC: Subspace predictive control," *IFAC Proceedings Volumes*, vol. 32, no. 2, pp. 4004–4009, 1999.

[3] R. Kadali, B. Huang, and A. Rossiter, "A data driven subspace approach to predictive controller design," *Control engineering practice*, vol. 11, no. 3, pp. 261–278, 2003.

Control of Simulated Moving Bed Chromatographic Processes

Valentin Plamenov Chernev[1], Alain Vande Wouwer[1], Achim Kienle[2,3] and Lino de Oliveira Santos[4]

[1]Systems, Estimation, Control and Optimization, University of Mons, Mons, Belgium
valentinplamenov.chernev@umons.ac.be; alain.vandewouwer@umons.ac.be

[2]Max Planck Institute for Dynamics of Complex Technical Systems and [3]Institut für Automatisierungstechnik, Otto von Guericke University, Magdeburg, Germany; kienle@mpi-magdeburg.mpg.de

[4]Department of Chemical Engineering, University of Coimbra, Coimbra, Portugal; lino@eq.uc.pt

1 Introduction

Simulated moving bed (SMB) chromatographic processes are used for continuous separation of mixtures of components with very close physical properties which are difficult to be separated by other processes. These processes have application in the petrochemical, biotechnological and pharmaceutical industries. The process configuration for binary separation consists of preparative chromatographic columns connected to each other forming a ring (Figure 1). The mixture to be separated is fed into the SMB plant through the feed port. The more adsorbed component travels to the extract port while the less adsorbed one travels to the raffinate port. Fresh solvent is introduced through the desorbent port. In order to achieve countercurrent movement of the liquid and solid phases the columns are repositioned in direction opposite to the liquid flow after some time period called switching time. Usually these processes are operated in open-loop mode due to their complexity and because of the high sensitivity to the disturbances at the optimum operating point with minimum solvent consumption, often suboptimal operating conditions are applied. Here, to hold the process close to the optimal operating point and to reject the disturbances we propose different feedback control strategies.

2 Modelling and Simulation

Mathematical modelling of the SMB chromatographic process leads to a system of partial differential alegbraic equations (PDAEs):

$$\begin{cases} \varepsilon \frac{\partial C_{i,k}}{\partial t} + (1-\varepsilon)\frac{\partial q_{i,k}}{\partial t} + \varepsilon v_k \frac{\partial C_{i,k}}{\partial z} = \varepsilon D_{ax} \frac{\partial^2 C_{i,k}}{\partial z^2} \\ \frac{\partial q_{i,k}}{\partial t} = k_{m_{i,k}} \left(q^*_{i,k}(\boldsymbol{C}) - q_{i,k} \right) \\ q^*_{i,k} = f(\boldsymbol{C}) \end{cases} \tag{1}$$

where the first equation describes the change of the concentration of the components in the liquid phase, the second in the solid phase, and the third one describes the thermodynamic equilibrium between the two phases and it is called adsorption isotherm. For the solution of this system in our previous work [1] we used a numerical algorithm based on the conservation element/solution element (CE/SE) method.

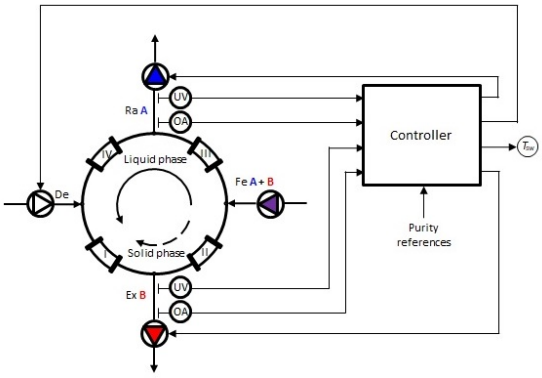

Figure 1: SMB process with the control configuration

Results showed that this method is faster than the popular cell method used in some commercial chromatographic simulators which makes it a suitable choice for use in on-line optimizing control such as model predictive control (MPC).

3 Control Strategy

For the control of the SMB process, classical PID control, as well as MPC, are developed and discussed, highlighting their respective advantages and disadvantages. The goal of the controller is to maintain the product purities at the specified reference values while at same time minimizing the solvent consumption. To achieve this in real time, information from the SMB plant is needed. The product purities are measured by an online analytical analyzer and the concentration front movements inside the columns are detected by two UV sensors on each of the outlet ports. Manipulated variables are the cycle duration T_{sw} and the liquid flow rates inside every column which are maintained by the pumps on each of the outlet ports as well as on the desorbent port. The feed flow rate is specified from the upstream operations and acts as a disturbance which has to be rejected by the controller.

References

[1] Chernev; Vande Wouwer; Kienle, *Efficient Simulation of Chromatographic Processes Using the Conservation Element/Solution Element Method*. Processes 2020, 8, 1316.

Improving hoist ergonomics by retrofitting automatic controllers

Joram Meskens, Abdellatif Bey-Temsamani & Bruno Depraetere
† Flanders Make, Belgium. E-mail: firstname.lastname@flandersmake.be

Motivation

A wide variety of cranes is used in industry, ranging from big autonomous ones, over ones electronically driven by operators using joysticks or command buttons, to completely passive hoists for smaller loads. These latter only support the weight in the vertical direction, and operators still have to manually move it in the horizontal direction. Since there is always some friction in the overhead guides, the load will need to be pushed or pulled to a certain angle to put tension on the cable, before the overhead support moves along. Even without friction, there will still need to be sufficient tension to accelerate the inertia of all the moving parts overhead. Since angles are always needed to initiate motion, the loads also often swings, which makes it harder to bring the load to standstill when desired. For loads in the 10-100kg range this leads to muscles issues and to low productivity in operators. Especially since for such loads operators tend to prefer productivity, and cut corners while not using the support systems sufficiently slow, whereas for heavier loads the correct and slow use of supportive systems is hard to avoid.

Implementation and results

In this paper we retrofit a hoist to combat these issues. Motors were added to actuate the X-Y motion of the overhead guides on a life-size crane in the Flanders Make lab in Leuven. We also added a sensor to detect the cable angle, so that when an operator moves the load and the angle is not zero, we can move the overhead support in the direction of the load to assist the operator. Figure 1 shows the principle in a schematic way. Many works have focused on controlling swinging cranes. Since we here control from angle to

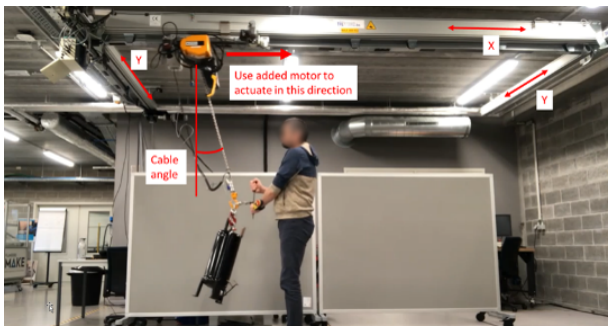

Figure 1: Implementation on life-size crane in Leuven.

speed of the overhead motor, the control is fairly straightforward, and a proportional-derivative feedback control (PD-controller) suffices to yield a good performance.

Experimental results

The approach has been experimentally tested using real operators to move various loads. Figure 2 shows results for two payloads that needed to be moved from one position to another while ending at standstill, which is the task operators typically need to perform in industrial practice. It can be seen that for both payloads the amplitude of the forces is much lower, but also that the total motion time (the length of the signal) is much lower and the task can thus be completed faster with the added control mechanism.

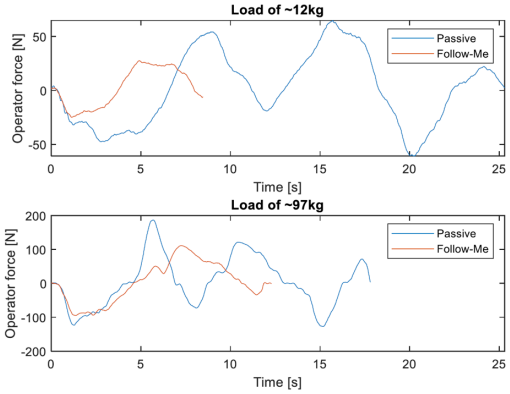

Figure 2: Forces with and without the support system, for completing a point to standstill task.

We have made an extensive evaluation of this support system on several operators and for various payloads. To improve performance further, we made an adaptive version in which the cable is connected through a load cell to estimate the payload mass. With that knowledge we then adjust the tuning, to provide more support for heavier loads. Figure 3 shows the results: compared to the passive system, both the normal and especially the adaptive version significantly reduce the operator forces.

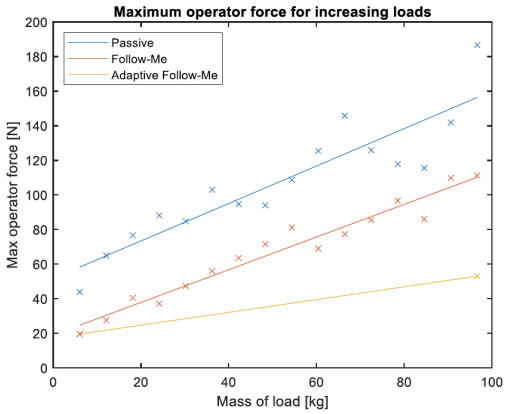

Figure 3: Comparison for various payloads.

Acknowledgements: This work was carried out in the framework of Flanders Make's ICON project Smarthandler, funded by the agency Flanders Innovation & Entrepreneurship (VLAIO) and Flanders Make. Flanders Make is the Flemish strategic research centre for the manufacturing industry.

Determination of Residence Time Distribution in Continuous Manufacturing line using data driven modeling

Pau Lapiedra Carrasquer,
Carlos Andre Munoz,
Satyajeet S. Bhonsale, Jan Van Impe
BioTeC+, KU Leuven, Belgium
Email: jan.vanimpe@kuleuven.be

Liang Li
Janssen Pharmaceutica, Belgium
Email: lli110@its.jnj.com

1 Introduction

The recent introduction of continuous manufacturing processes in the pharmaceutical industry has increased the need for a deeper process understanding to improve its monitoring and control capabilities. Identifying and better understanding the relationships between Critical Process Parameters, Critical Material Attributes and Critical Quality Attributes is crucial to guarantee quality of the final drug. In continuous manufacturing, the product needs to be traceable throughout the entire line to ensure a robust control at all times. Developing a clear connection between the different inline measurements (i.e., process parameters and PAT data) and the product characteristics at specific locations is a key aspect. Residence time distribution (RTD) is a commonly used methodology that defines the probability distribution of the time that a particle stays inside a system. The RTD is specific for a given geometry and materials and it has to be experimentally determined for every new drug formulation. For this reason, there is a high interest in making RTD determination more efficient and less experimentally consuming.

2 Methods

In this contribution, a Direct Compression continuous system is studied. A step change was used as an input signal for RTD determination and the model was implemented as a combination of an ideal plug flow reactor model with two CSTR in series (PFR+2TIS). To determine the RTD experimentally, the distribution function is normalized in terms of API concentration:

$$C(t) = C_0 + (C_f - C_0) \times \delta(t-\theta) \times \left(1 - \frac{\tau_1 \times e^{\frac{\theta - t}{\tau_1}} - \tau_2 \times e^{\frac{\theta - t}{\tau_2}}}{\tau_1 - \tau_2}\right) \quad (1)$$

Where C_0 is initial concentration, C_f is concentration at the end of the step change experiment, δ is the heaviside function, θ is delay, τ_1 is time constant from tank 1 and τ_2 is time constant from tank 2. The parameters are estimated by a least squares optimization.

The concentration data used to fit the RTD model is usually obtained from samples collected at the exit of the tablet press. What we proposed in this study was to use directly the spectral data from the NIR tool located in the feed frame of the tablet press, which offers a much higher measuring frequency, to predict the final concentration of the tablet. Principal Component Analysis and PLS-DA were applied to the NIR spectral data. Both techniques were compared to see which one was able to capture better the dynamic response of the step change so it could be used for RTD modeling.

3 Results

In both PCA and PLS-DA approaches the results indicated that the majority of the system variation was captured with 3 Latent Variables (LV), being the first two the ones capturing the dynamic response of the step change. To summarize the step change variation in only one variable, a rotation of the scores matrix was performed.

The fit of the RTD model was done using content uniformity data (CU), and also the data obtained from the scores of PLS-DA. The results showed significant similarities between the two approaches. However, in both cases, the model is not identifiable. Different constraints were tested to tackle this issue.

References

[1] P. Bhalode, H. Tian, S. Gupta et al.,"Using residence time distribution in pharmaceutical solid dose manufacturing – A critical review," International Journal of Pharmaceutics, 2021.

[2] T. Pedersen, A. Karttunen, O. Korhonen et al., "Determination of Residence Time Distribution in a Continuous Powder Mixing Process With Supervised and Unsupervised Modeling of In-line Near Infrared (NIR) Spectroscopic Data," Journal of Pharmaceutical Sciences, 2021.

[3] S. Tanimura, R. Singh, A. Roman-Ospino et al., "Residence time distribution modelling and in line monitoring of drug concentration in a tablet press feed frame containing dead zones," International Journal of Pharmaceutics, 2021.

[4] A. Vanarase, M. Alcala, J. Jerez Rozo et al., "Real-time monitoring of drug concentration in a continuous powder mixing process using NIR spectroscopy," Chemical Engineering Science, 2010.

Crystallization kinetics inference using Gaussian process regression[1]

Michiel Busschaert[a] and Steffen Waldherr[a,b]

[a]Department of Chemical Engineering, KU Leuven. Celestijnenlaan 200F, 3001 Leuven, Belgium.
E-mail: {michiel.busschaert,steffen.waldherr}@kuleuven.be
[b]Division of Molecular Systems Biology, University of Vienna. Djerassiplatz 1, 1030 Vienna, Austria.
E-mail: steffen.waldherr@univie.ac.at

Introduction: Crystallization process are often modeled using a Population Balance Model (PBM) [1]. The population members are individual crystals, which are only distinguished by their size x in simple models. The crystals are dispersed in a medium with solute concentration C. The number density function (NDF), $n(t,x)$, represents the estimated amount of crystals per size[2]. Changes in the population are induced by growth (by which size x increases by solute uptake) and nucleation (by which new crystals are formed), denoted with kinetic rates $G(x,C)$ and $B(C)$, respectively.

Estimating kinetic rates for $G(x,C)$ and $B(C)$ is often difficult in practice. In this abstract, we propose the use of non-parametric regression using Gaussian processes to infer kinetic behavior from population moment measurements.

The PBM for a continuous crystallization process, where for further purpose, the growth rate $G(x,C)$ is assumed to be independent of the crystal size x, is given by [2]

$$\begin{aligned} \frac{\partial n(t,x)}{\partial t} + \frac{\partial G(C)n(t,x)}{\partial x} &= -dn(t,x), \\ G(C)n(t,0) &= B(C), \\ \frac{dC(t)}{dt} &= -3k_v\rho_C \int_0^\infty G(C)x^2 n(t,x)dx + d(C_{\text{in}} - C(t)), \end{aligned} \tag{1}$$

where d is a dilution rate, C_{in} is the concentration of the inflow and $k_v\rho_C$ is a constant factor which relates to shape and mass density of individual crystals.

The moment dynamics of the population are obtained via integration, $\mu_k(t) = \int_0^\infty n(t,x)x^k dx$. Consequently, (1) is reduced into a set of four ordinary differential equations

$$\begin{aligned} \frac{dC(t)}{dt} &= -3k_v\rho_C G(C)\mu_2(t) + d(C_{\text{in}} - C(t)), \\ \frac{d\mu_0(t)}{dt} &= -d\mu_0(t) + B(C), \\ \frac{d\mu_1(t)}{dt} &= -d\mu_1(t) + G(C)\mu_0(t), \\ \frac{d\mu_2(t)}{dt} &= -d\mu_2(t) + 2G(C)\mu_1(t). \end{aligned} \tag{2}$$

[1]This work has been funded by Fonds voor Wetenschappelijk Onderzoek Vlaanderen (FWO), grant number G066621N.

[2]Such that the estimated amount of crystals with size in the interval $[x, x+dx]$ is equal to $n(t,x)dx$.

Gaussian process regression (GPR) [3] is a tool to perform non-parametric regression. A latent function, here both $G(C)$ and $B(C)$, is assumed to be a Gaussian process, which can be regarded as an extension to an infinite dimensional Gaussian distribution. The Gaussian process is specified by a so-called covariance kernel. By supplying training data, determined from measurements of the moments $\mu_{0,1,2}$ for different concentrations C by transforming (2), the Gaussian process can be conditioned (also termed learning).

A numerical case study, based on aspirin crystallization, is used to test the procedure. Measurements are generated following dynamics and conditions described in [2]. Artificial measurement noise is added to replicate real life conditions. An example of such GPR result is given in Figure 1.

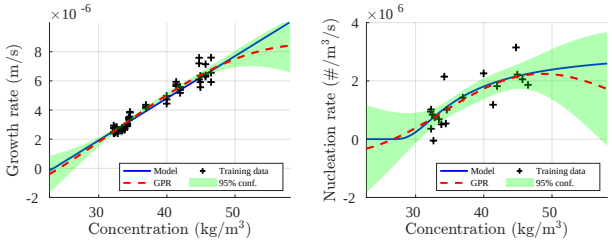

Figure 1: GPR result of growth rate $G(C)$ (left) and nucleation rate $B(C)$ (right).

For further work, it will be attempted to include particle size x along with concentration C as input in growth rate $G(x,C)$ inference.

Note: This abstract is based on an elsewhere submitted paper by the authors [4].

References

[1] Ramkrishna, D. (2000). *Population Balances: Theory and Applications to Particulate Systems in Engineering*. Academic Press, San Diego.

[2] Savvopoulos, S.V., *et al.*, (2019). *A mathematical model of the ultrasound-assisted continuous tubular crystallization of aspirin*. Crystal Growth & Design, 19(9), 5111-5122.

[3] Rasmussen, C.E. and Williams, C.K.I. (2006). *Gaussian processes for machine learning*. MIT Press. URL: http://www.gaussianprocess.org/gpml/.

[4] Busschaert, M. and Waldherr, S. (2021). *Inference of Kinetics in Population Balance Models using Gaussian Process Regression* [submitted].

A simulation-based method for design space exploration of production systems

N. Paape*, J.A.W.M. van Eekelen, M.A. Reniers
Control Systems Technology, Eindhoven University of Technology
Email corresponding author*: n.paape@tue.nl

1 Introduction

The design process of a production system is often an intricate process, with many iterations of (re)design. Using simulation to explore the design space allows design alternatives to be evaluated [1]. However, much of design space exploration is still manual: iterating on the design, constructing the model, and interpreting the simulation results.

Our goal is to develop a simulation-based method for design space exploration of production systems. Figure 1 shows the four steps that this method utilizes, and the inputs and outputs for each step. This procedure by itself is not new, but our plan is to develop novel ideas for how these steps can be automated. In the next sections we explain the four steps of the method, and what novel ideas we plan to introduce.

2 Explore design space

The first step is explore the design space, and propose a system design. The design space includes specifications such as which machines are available, how production is controlled, and constraints on the design. We plan to use heuristic search algorithms for design space exploration, similar to [2]. One of our goals is to investigate how feedback from the 'evaluate' step can be utilized to improve design exploration. For example: when a specific bottleneck is identified, then the design could be adjusted to reduce this bottleneck.

3 Construct model

The model construction step takes the system design and uses a model library to construct a simulation model. Using a model library places the restriction on the design space that all possible system components, must have a corresponding model component in the model library (this relation is indicated by the dotted line in Figure 1). We plan on investigating on how the model library can be developed, and how it can be used to automatically construct simulation models.

4 Simulate

Production systems are often required to operate in a wide variety of conditions. To determine the performance of the system in these conditions, the system is simulated for a range of production scenarios. A scenario specifies the conditions under which the production system operate. For example, a scenario can specify the characteristics of the incoming flow of unprocessed products, and the orders which must be produced. In this method simulation would be automated in a simulation environment such as Anylogic.

5 Evaluate

In the evaluation phase the performance of the design is evaluated according to selected performance indicators. We plan to investigate how this performance evaluation can be used to automatically identify in which direction the design exploration should continue. This 'evaluation report' is then returned as feedback to the heuristic for design space exploration. After performance evaluation the stop condition for design space exploration is checked (e.g. stop if the performance targets are met). When reached, the method outputs a selection of recommended designs.

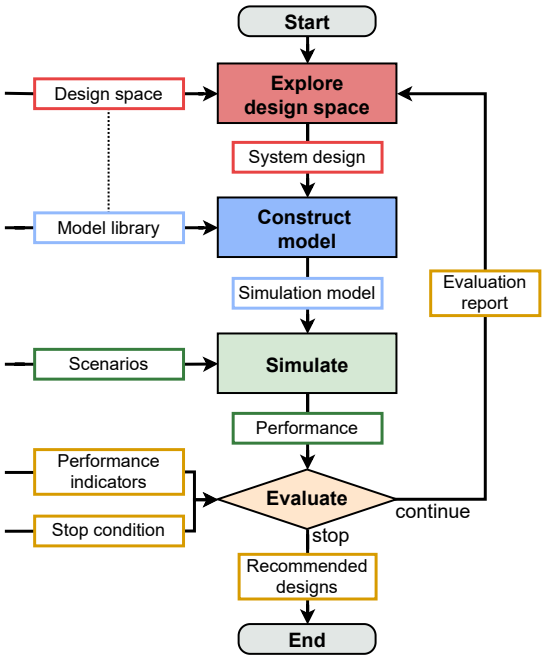

Figure 1: The proposed simulation-based method for design space exploration of production systems.

References

[1] Owens, S. F. and Levary, R. R. (2002). "Evaluating design alternatives of an extruded food production line using simulation," Simulation, 78(10), 626–632.

[2] Wang, G., Yan, Y., Zhang, X., Shangguan, J., and Xiao, Y. (2008). A simulation optimization approach for facility layout problem. IEEM 2008, 734–738.

Real-time passenger-centric timetable scheduling for railway networks: A distributed control method [1]

Xiaoyu Liu, Azita Dabiri, and Bart De Schutter
Delft Center for Systems and Control
Delft University of Technology
Delft, The Netherlands
{x.liu-20,a.dabiri,b.deschutter}@tudelft.nl

1 Introduction

Timetable scheduling plays a key role in daily operations of railway networks, as it influences the operational costs and the quality of service provided to passengers. With the rapidly growing passenger demands and the increasing scale of railway networks, advanced railway traffic network models and the corresponding control approaches are crucial to generate efficient timetables and to improve the performance of railway transportation services.

Formulating the railway timetable scheduling problem generally leads to a constrained control problem. Model predictive control (MPC) is a well recognized effective real-time method to control constrained systems [1]. The passenger-centric timetable scheduling problem for railway networks is challenging because of its complexity and scale. For large-scale systems, many researchers have been developing non-centralized methods that coordinate subsystems in a decentralized, distributed, or hierarchical manner to achieve fast and efficient solutions for the overall system [2]. In our research, we develop new distributed model predictive control methods for timetable scheduling for railway networks where the problem feasibility, optimality, and computational efficiency are comprehensively considered.

2 A novel timetable scheduling model

Passenger demands are generally represented by time-varying origin-destination matrices. Incorporating time-varying passenger demands is a challenging task in real-time timetable scheduling problems, as it greatly increases the computational burden. Passenger demands usually change gradually throughout the day. Therefore, in the developed model, we discretize the planning time span into several periods, where passenger demands in each period are assumed to be constant. The numbers of trains departing at each platform during each period are the decision variables in this model. By optimizing the number of trains visiting a given platform during each period, an upper bound of the transport capacity per period is determined, so that passengers can be absorbed by trains at the platform.

[1] This work is supported by the China Scholarship Council under Grant 202007090003.

3 Distributed MPC for real-time timetable scheduling

In general, the MPC optimization problem for railway timetable scheduling is a nonlinear nonconvex problem. We can use the method in [3] to transform the nonlinear terms into linear terms. The MPC optimization problem is then transformed into a mixed-integer linear programming (MILP) problem, which can be solved efficiently using existing solvers, provided the railway network is not too large.

In our research, we propose distributed model predictive control approaches to deal with the computational complexity issues arising in large-scale railway networks. In distributed model predictive control methods, the original large-scale MILP problem is divided into several small-scale subproblems that can be solved sequentially or in parallel to reduce the computational burden. The distributed-robust-safe-but-knowledgeable (DRSBK) algorithm [4] is a promising method for real-time control of large-scale systems, as it enables the use of much shorter planning horizons while maintaining the robust feasibility of the original MPC method. Therefore, the DRSBK algorithm will be adopted and further improved to fulfill the requirement of real-time passenger-centric timetable scheduling in railway networks. The convergence, optimality, and recursive feasibility of the proposed distributed MPC method will also be investigated.

References

[1] D. Q. Mayne, "Model predictive control: Recent developments and future promise," *Automatica*, vol. 50, no. 12, pp. 2967–2986, 2014.

[2] J. M. Maestre and R. R. Negenborn, *Distributed Model Predictive Control Made Easy*. Springer, 2014, vol. 69.

[3] A. Bemporad and M. Morari, "Control of systems integrating logic, dynamics, and constraints," *Automatica*, vol. 35, no. 3, pp. 407–427, 1999.

[4] Y. Kuwata, A. Richards, T. Schouwenaars, and J. P. How, "Distributed robust receding horizon control for multivehicle guidance," *IEEE Transactions on Control Systems Technology*, vol. 15, no. 4, pp. 627–641, 2007.

Learning Constitutive Laws in Engineering Systems

Sarvin Moradi[a,c] s.moradi@tue.nl
Nick Jaensson[b,c] n.o.jaensson@tue.nl
Roland Toth[a,c,d] r.toth@tue.nl
Maarten Schoukens[a,c] m.schoukens@tue.nl

[a] Control Systems and [b]Polymer Technology Group, Eindhoven University of Technology, Eindhoven, the Netherlands
[c] Eindhoven Artificial Intelligence Systems Institute, Eindhoven, the Netherlands
[d] Systems and Control Laboratory, Institute for Computer Science and Control, Budapest, Hungary

1 Introduction and Motivation

Despite significant developments in modeling and system identification methods, learning complex and chaotic systems is still a challenging problem. Development of classical physics-based (white-box) models need deep detailed knowledge of the system dynamics which is often not completely available or tedious and expensive to obtain. On the other hand, data-driven (black-box) methods are capable to reconstruct complex unknown dynamics from data, but the estimated models often lack generalizability and are hard to interpret. As a remedy, this project aims to use an ANN-based Hamiltonian modeling framework to develop comprehensive and reliable models for engineering systems. Hamiltonian Neural Networks (HNNs) are a state-of-the-art grey-box modeling tool in which Hamiltonian mechanics is embedded as prior knowledge in the neural network (see Figure 1).

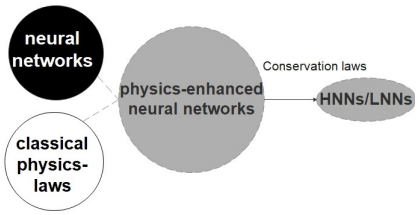

Figure 1: Physics-enhanced ANNs (such as HNNs and LNNs) embed physics laws in neural network based models.

2 Hamiltonian and Lagrangian ANNs

In Hamiltonian mechanics, the total energy, E_{tot}, of the system is conserved and defined as the Hamiltonian of the generalized position ($\mathbf{q}$) and momenta ($\mathbf{p}$) vectors, i.e. $E_{\text{tot}} = H(\mathbf{q},\mathbf{p})$. The Hamiltonian is a scalar function, satisfying

$$\frac{d\mathbf{q}}{dt} = \frac{\partial H}{\partial \mathbf{p}} \ , \frac{d\mathbf{p}}{dt} = -\frac{\partial H}{\partial \mathbf{q}}. \tag{1}$$

Greydanus et al. proposed to learn H, as an energy-like scalar value in an unsupervised manner [1]. They formulated H as an ANN H_θ and trained it under the loss function:

$$L_{HNN} = \left\| \frac{\partial H_\theta}{\partial \mathbf{p}} - \frac{\partial \mathbf{q}}{\partial t} \right\|_2 + \left\| \frac{\partial H_\theta}{\partial \mathbf{q}} + \frac{\partial \mathbf{p}}{\partial t} \right\|_2. \tag{2}$$

In this way, the conservation law, equation (1), is embedded in the trained ANN. The identified H fully defines a continuous-time motion model of the system, which can be calculated directly. Furthermore, their ability to learn conservation laws, makes HNNs more interpretable. The main drawback of HNNs is their use of so-called canonical coordinates. Cranmer et al. generalized HNNs by introducing the Lagrangian equation of motion to the ANNs [2]. Unlike HNNs, the use of canonical coordinates is not required in Lagrangian Neural Networks (LNNs). LNNs enforce the conservation law to the ANNs for arbitrary coordinates, hence they can surpass HNNs in modeling more complex systems.

3 Conclusions

Physics-enhanced neural networks are a forefront research topic with a high potential in various engineering fields. In this work, the applicability of HHNs and LNNs together with the recently introduced port-Hamiltonian ANNs (pHNNs) [3] for modeling engineering systems is studied and compared to other classical system identification methods. Envisaged benchmarking systems include a gyroscope and pendulum setup in which conservation of energy is important.

This work is part of the DAMOCLES research project which received funding from the Eindhoven Artificial Intelligence Systems Institute, as part of the EMDAIR funding programme.

References

[1] Greydanus, S. J., Dzumba, M., Yosinski, J., "Hamiltonian Neural Networks," *Proc. of the 33rd Conference on Neural Information Processing Systems*, Vancouver, Canada, 2019.

[2] Cranmer, M., Greydanus, S., Hoyer, S., Battaglia, P., Spergel, D. and Ho, S.,"Lagrangian Neural Networks," *arXiv*:2003.04630, July 2020.

[3] Desai, S., Mattheakis, D., Sondak, S., Protopapas, P., Roberts, S.,"Port-Hamiltonian Neural Networks for Learning Explicit Time-Dependent Dynamical Systems," *Physical Review E*, vol. 104, no. 3, p. 034312-1, 2021.

Total Energy Shaping with Neural Interconnection and Damping Assignment - Passivity Based Control

Santiago Sanchez-Escalonilla Plaza
University of Groningen
santiago.sanchez@rug.nl

Rodolfo Reyes-Baez
University of Groningen
r.reyes.baez@rug.nl

Bayu Jayawardhana
University of Groningen
b.jayawardhana@rug.nl

1 Abstract

The universal approximation property of Neural Networks (NNs) [1] make them capable of representing very complex functions. Generally, in control theory we study and manipulate the properties of dynamical systems using an input function (the control law) that shape the dynamics of the closed-loop system. However, using learning in control of complex systems is often discouraged due to the lack of explainability of the approach, frequently referred as "black-box" approaches. Recent progress in the regularization of NNs has allowed to obtain parametric functions that satisfy predefined restrictions in the form of a PDE. This is the case for physics-informed neural networks (PINNs) [2], where the learned function can be interpreted as an approximated solution of the PDE.

In many nonlinear control methods for complex systems, the corresponding control law requires the solution of an auxiliary differential equation that embed the control requirements or specifications. Interconnection and damping assignment passivity-based control (IDA-PBC)[3], is an energy shaping method for stabilization of an affine nonlinear system around a desired equilibrium. IDA-PBC focuses in finding a static state feedback control law of the form,

$$u(x) = \beta(x) + v, \tag{1}$$

such that the open-loop port-Hamiltonian (pH) system,

$$\Sigma_1 : \begin{cases} \dot{x} = [J(x) - R(x)]\frac{\partial H}{\partial x}(x) + g(x)u(x) \\ y = g^\top(x)\frac{\partial H}{\partial x}(x) \end{cases} \tag{2}$$

is transformed into a closed-loop target passive pH system,

$$\Sigma_2 : \begin{cases} \dot{x} = [J_d(x) - R_d(x)]\frac{\partial H_d}{\partial x}(x) + g(x)v \\ y = g^\top(x)\frac{\partial H_d}{\partial x}(x) \end{cases} \tag{3}$$

where $J_d(x)$, $R_d(x)$ and $H_d(x)$ are the desired interconnection, damping and energy functions of the target closed-loop system and are found by the addition of an auxiliary term to the open-loop respective functions: $J_d(x) := J(x) + J_a(x)$, $R_d(x) := R(x) + R_a(x)$ and $H_d(x) := H(x) + H_a(x)$.

Theorem 2 in (Ortega et al.) [3] indicates that such a control law myst satisfy the following matching equation,

$$g^\perp(x)[J_d(x) - R_d(x)]\frac{\partial H_d}{\partial x}(x) = g^\perp(x)[J(x) - R(x)]\frac{\partial H}{\partial x}(x) \tag{4}$$

and a set of other implicit assumptions (structure preservation, integrability, equilibrium assignment and Lyapunov stability) [3] that impose additional structure to the appropriate solution.

We propose solving the PDE matching equations (4), using NNs in the PINN scheme [2], by systematically constructing a loss function that encodes the requirements in the form of residuals,

$$\begin{aligned} &\mathscr{L}(\theta; x, x^\star) := f_{\text{transient}} + f_{\text{eq}} + f_{\text{lyap}} + f_{\text{matching}} \\ &\theta^\star = \text{argmin}_\theta \mathscr{L}(\theta; x, x^\star) \end{aligned} \tag{5}$$

The NN is then used to solve the non-parameterized IDA-PBC problem by approximating H_a and R_a (Figure 1).

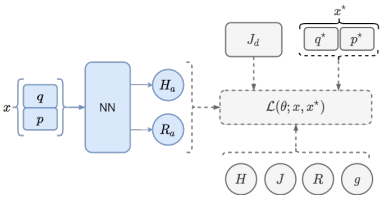

Figure 1: Neural IDA-PBC diagram.

This methodology allows to reformulate the IDA-PBC control technique as an adaptive problem (5), providing flexibility for cases where analytical solutions are not easily avaiblable. The approach has been validated in the settings of Fully-actuated Mechanical systems and simulation data was obtained for the Simple pendulum and the Double pendulum cases. The results show that this design methodology can stabilize both systems around any arbitrary equilibrium point.

References

[1] K. Hornik, et al. "Multilayer Feedforward Networks Are Universal Approximators." Neural Networks, 1989.

[2] G. Em Karniadakis, et al. "Physics-Informed Machine Learning." Nature Reviews Physics, 2021.

[3] R. Ortega, et al. "Interconnection and Damping Assignment Passivity-Based Control of Port-Controlled Hamiltonian Systems." Automatica, 2002.

On feedforward control using physics–guided neural networks: Training cost regularization and optimized initialization

Max Bolderman[1], Mircea Lazar[1] and Hans Butler[1,2]
[1] Control Systems Group, Eindhoven University of Technology, 5600 MB Eindhoven, The Netherlands
[2] ASML, 5504DR Veldhoven, The Netherlands
Email: {m.bolderman, m.lazar, h.butler}@tue.nl

1 Introduction

The physics–guided neural network (PGNN), which employs a physics–based model in parallel to a black–box neural network (NN), is proposed in [1] for identification of inverse system dynamics with the aim to obtain a high performing feedforward controller. The framework already showed significant improvements in tracking performance with respect to conventional methods on a practical application. However, the flexible nature of NNs create an overparameterization when simultaneously training the parameters corresponding to the physical and NN model [2]. The resulting parameter drift yields uninterpretability of the physical model, as well as a decreased generalizability of the PGNN to conditions that were not present in the training data.

2 Nonlinear inverse system identification using PGNNs

We consider the discrete–time inverse dynamical system

$$u(t) = \theta_0^T T_{\text{phy}}\big(\phi(t)\big) + g\big(\phi(t)\big), \tag{1}$$

which describes the relation between the input $u(t)$ and the regressor $\phi(t) = [y(t+n_a),\dots,y(t-n_b),u(t-1),\dots,u(t-n_c)]^T$ for a system that is not affected by noise. Here, $y(t)$ is the output and n_a, n_b, n_c describe the order of the dynamics. We assume that the part $\theta_0^T T_{\text{phy}}\big(\phi(t)\big)$ is a linear–in–the–parameters model that is derived from physics, and $g\big(\phi(t)\big)$ denotes the *unknown dynamics* resulting from parasitic friction, electromagnetic disturbances, and other effects.

The PGNN is used for identification of (1), i.e., we predict

$$\hat{u}\big(\theta,\phi(t)\big) = f_{\text{NN}}\big(\theta_{\text{NN}},\phi(t)\big) + \theta_{\text{phy}}^T T_{\text{phy}}\big(\phi(t)\big), \tag{2}$$

with $\theta = \{\theta_{\text{NN}},\theta_{\text{phy}}\}$ the PGNN parameters, θ_{NN} the NN weights and biases, and θ_{phy} the physical model parameters. Then, θ is identified using an input–output data set Z^N as:

$$\hat{\theta} = \arg\min_{\theta} V\big(\theta,Z^N\big). \tag{3}$$

Typically, a MSE cost function is chosen, i.e., $V\big(\theta,Z^N\big) = V_{\text{MSE}}\big(\theta,Z^N\big) = \frac{1}{N}\sum_{t=0}^{N-1}\big(u(t)-\hat{u}\big(\theta,\phi(t)\big)\big)^2$. However, this yields an overparameterization of the PGNN (2) that results in a parameter drift during training. The effect is observed from the competition between the feedforward signals corresponding to the NN and the physics–based (PG) part of the PGNN (2) in the middle plot of Fig. 1.

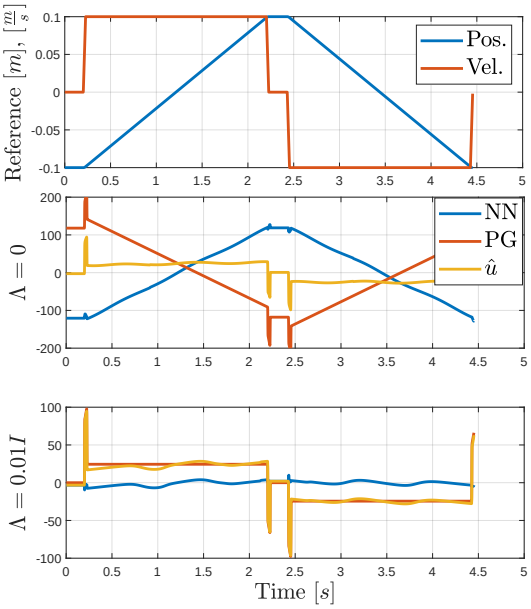

Figure 1: Feedforward signals resulting from the different terms in the PGNN (2) for the reference shown in the top.

3 Results

The parameter drift is prevented, as shown in the bottom plot in Fig. 1, via the use of the regularized cost function

$$V\big(\theta,Z^N\big) = V_{\text{MSE}}\big(\theta,Z^N\big) + (\theta_{\text{phy}} - \hat{\theta}_{\text{LIP}})^T \Lambda (\theta_{\text{phy}} - \hat{\theta}_{\text{LIP}}), \tag{4}$$

where $\hat{\theta}_{\text{LIP}}$ are priorly identified parameters of the LIP model using the MSE, and Λ is a positive definite regularization matrix. Moreover, we propose a method to ensure that the non–convex PGNN training converges to a set of parameters that improve on the cost function with respect to the physics–based model, i.e., $V\big(\hat{\theta},Z^N\big) < V\big(\hat{\theta}_{\text{LIP}},Z^N\big)$.

References

[1] M. Bolderman, M. Lazar, and H. Butler, "Physics–guided neural networks for inversion–based feedforward control applied to linear motors," *IEEE Conference on Control Technology and Applications*, pp. 1115–1120, 2021.

[2] O. Nelles, *Nonlinear System Identification*. Springer, 2001.

Neural Networks for Motion Feedforward: Control-Relevant Training and Non-Causality

Leontine Aarnoudse[1*], Johan Kon[1], Wataru Ohnishi[2], Maurice Poot[1], Paul Tacx[1], Nard Strijbosch[1], Tom Oomen[1,3]

[1]Control Systems Technology, Eindhoven University of Technology, Eindhoven, The Netherlands

[2]Graduate School of Engineering, The University of Tokyo, Tokyo, Japan

[3]Delft Center for Systems and Control, Delft University of Technology, Delft, The Netherlands

[*]Email: l.i.m.aarnoudse@tue.nl

1 Background

Neural networks are universal function approximators and, as such, offer large potential for flexible and accurate motion feedforward. Motion feedforward involves several important aspects, including control-relevance [2] and non-causal feedforward for non-minimum phase systems that require pre-actuation to achieve zero error [1].

2 Problem formulation

Consider a SISO control system with error $e \in \mathbb{R}$ given by

$$e = Sr - SPf \tag{1}$$

with reference $r \in \mathbb{R}$, feedforward signal $f \in \mathbb{R}$ and system sensitivity $S = (1 + PC)^{-1}$ with plant P and controller C. The feedforward signal for which $e = 0$ is given by

$$f = (SP)^{-1}Sr \tag{2}$$

Neural networks are used to find a mapping $f_{\text{nn}} = \mathcal{F}(r)$ such that the error e in (1) is minimized for $f = f_{\text{nn}}$. The aim is to investigate the implications of the invertibility of P, in particular when P has non-minimum phase zeros, and the use of closed-loop data, i.e., the role of SP in (1).

3 Approach

The training data needed to find the mapping from r to f consists of a representative set of ten references with corresponding feedforward signals f_{train}, found using iterative learning control [3]. The neural network-based feedforward f_{nn} that minimizes the error in terms of the squared 2-norm is the minimizer of the control-relevant loss function

$$\mathcal{J}_{\text{CR}}(f_{\text{nn}}) = \|SP(f_{\text{train}} - f_{\text{nn}})\|_2^2, \tag{3}$$

to which a term $w\|f_{\text{train}} - f_{\text{nn}}\|_2^2$ with weighting $w = 1e^{-3}$ is added as regularization.

Non-causal mappings between r and f_{nn} are generated by two types of networks. Non-causal time-delay neural networks (TDNN) take a shifted finite sequence of reference samples as input, resulting in finite preview. Bi-directional long short-term memory (biLSTM) layers in recurrent neural networks (RNN) receive both forward and time-reversed data, giving infinite preview.

Figure 1: Arizona flatbed printer

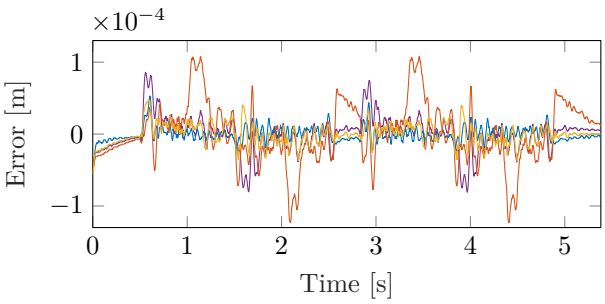

Figure 2: Errors for a reference outside of the training set resulting from f_{train} (—), polynomial basis functions (—), a non-causal TDNN (—) and a non-causal RNN (—).

4 Results

Neural networks for motion feedforward are applied to the industrial flatbed printer shown in Figure 1. The input of the networks consists of a fourth-order reference with its derivatives. Non-causal TDNNs reduce the loss by a factor 3 compared to a linear feedforward neural network (FNN) that is equivalent to polynomial basis functions. RNNs are sensitive to overfitting, reducing the performance, see Figure 2.

References

[1] J. van Zundert and T. Oomen, "On inversion-based approaches for feedforward and ILC," *Mechatronics*, vol. 50, no. November 2016, pp. 282–291, 2018.

[2] F. Boeren, A. Bareja, T. Kok, and T. Oomen, "Frequency-Domain ILC Approach for Repeating and Varying Tasks: With Application to Semiconductor Bonding Equipment," *IEEE/ASME Trans. Mechatronics*, vol. 21, no. 6, pp. 2716–2727, 2016.

[3] D. A. Bristow, M. Tharayil, and A. G. Alleyne, "A survey of iterative learning control," *IEEE Control Syst.*, vol. 26, no. 3, pp. 96–114, 2006.

Bridging Dynamic Neural Networks and Optimal Control

Edward Kikken, Bruno Depraetere & Jeroen Willems
Flanders Make, Lommel, Belgium. E-mail: firstname.lastname@flandersmake.be

Optimal control problems (OCP) are powerful methods that enable optimization of system states and inputs given a cost function and constraints [1]. However, their real world performance is typically hampered by insufficient model accuracy. In the field of machine learning, dynamic neural networks have been proposed as a generic and performant method to model dynamic systems in a data-driven fashion. In this paper, we will propose a method that bridges the current gap between the two research fields, paving the way for further studies.

The Mass-Spring-Damper Toy Case

A mass-spring-damper system with state $x = [x_1, x_2]$, spring and damper constant k and d is considered, see Eq. 1. It is integrated using a forward Euler integrator, i.e., $x_{k+1} = x_k + T_s \dot{x}_k$ with a sampling time $T_s = 0.001$ and input u.

$$\begin{bmatrix} \dot{x_1} \\ \dot{x_2} \end{bmatrix} = \begin{bmatrix} x_2 \\ \frac{1}{m}(-kx_1 - dx_2 + u) \end{bmatrix} \tag{1}$$

The Recurrent Neural Network Model

In this section, we will train a data-driven model: a Recurrent Neural Net (RNN). A 1-layer fully connected RNN consisting of 10 neurons was selected since the dynamics to fit are of low (linear) complexity. Furthermore, the sigmoid ($S(y) = 1/(1+e^{-y})$) activation was used for its continuous differentiability, which is not the case for e.g., ReLU activations. This differentiability is expected to be key for convergence in the gradient-based control optimization later. The RNN equations, see 2, were formulated manually for usage in the OCP, but it is planned to use model export tools (e.g., ONNX [3]) in future work.

$$\begin{aligned} z &= S\left(W_1 \begin{bmatrix} \hat{x} \\ u \end{bmatrix} + b_1\right) \\ \hat{x} &= W_2 z + b_2 \end{aligned} \tag{2}$$

Training the RNN was done by forward Euler integration ($\hat{x}_{k+1} = \hat{x}_k + T_s \hat{\dot{x}}_k$), denoted by $\int$ in Fig. 1, combined with a mean squared error cost on $\hat{x}$ using the PyTorch [2] framework. See Fig. 2 for the open-loop simulation of the trained RNN on the training and validation data.

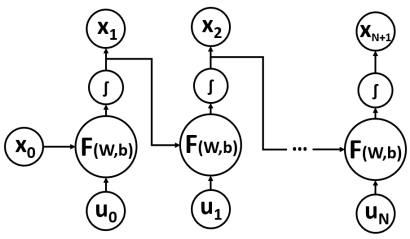

Figure 1: RNN architecture

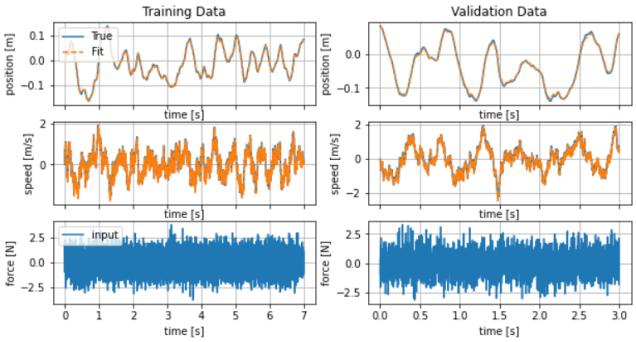

Figure 2: RNN training and validation fit.

The Optimal Control Problem

A control task was defined for the RNN model: perform a point-to-point motion with minimal input force, see Eq. 3. The optimization was performed using Rockit [1].

$$\begin{aligned} \min_{u} \quad & u^2 \\ \text{s.t.} \quad & \hat{x}_{k+1} = \hat{x}_k + T_s \hat{\dot{x}}_k \; \forall k \in [1, 1001] \\ & \hat{x}_0 = [0,0], \; \hat{x}_{t_f} = [0.5, 0] \end{aligned} \tag{3}$$

Results and Outlook

In Fig. 3 the state evolution of both the RNN ($\hat{x}$) and original model (x) when open-loop simulated with the OCP inputs are displayed. The target position error $\hat{x}_1(t_f) - x_1(t_f)$ is 0.002m and the RMS state errors are $[0.011, 0.16]$. For comparison, the OCP inputs were calculated with the original model, which resulted in an RMS error on the input of 0.02N. To the authors this first exploration is promising and indicates various directions for future work.

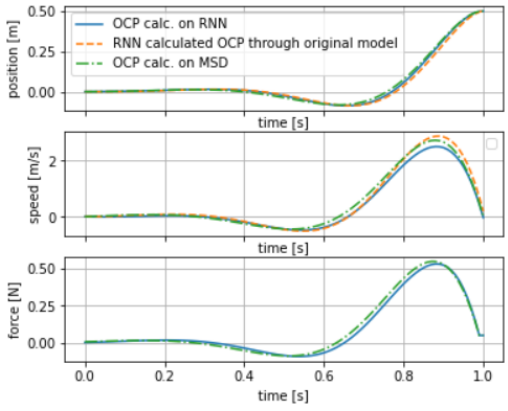

Figure 3: OCP results on RNN and original model.

References

[1] Gillis, Joris ; Vandewal, Bastiaan ; Pipeleers, Goele ; Swevers, Jan, "Effortless modeling of optimal control problems with rockit", 39th Benelux Meeting on Systems and Control 2020, Elspeet, The Netherlands.

[2] https://pytorch.org

[3] https://onnx.ai

Combined MPC and reinforcement learning controller for traffic signal control in urban traffic networks [1]

Dingshan Sun
Delft Center for Systems and Control
Delft University of Technology
d.sun-1@tudelft.nl

Anahita Jamshidnejad
Department of Control and Operations
Faculty of Aerospace Engineering, TU Delft
a.jamshidnejad@tudelft.nl

Bart De Schutter
Delft Center for Systems and Control
Delft University of Technology
b.deschutter@tudelft.nl

1 Motivation

MPC has shown to be a very effective and popular control approach for urban traffic control [1], due to its flexible and robust nature. However, the use of MPC has some disadvantages as well. Centralized control of large-scale systems can become computationally infeasible. Besides, when the system (model) suffers from disturbances and uncertainties, the control performance will become sub-optimal. In recent years the use of data-driven reinforcement learning (RL) for control of urban traffic systems has gained great interest [2]. Model-free RL algorithms do not need a model to obtain a well-performing control law and they are of adaptive nature, i.e., they can change their control solution according to changing traffic situations. This makes them very capable of dealing with disturbances in the system. However, the performance of such algorithms does not converge to an optimal solution without a sufficient training process. In addition, the stability of a RL-based controlled system is generally not guaranteed. MPC and RL methods excellently complement each other. Therefore, it is of great interest to investigate the possibility to combine MPC and RL to exploit the advantages of both methods.

2 Proposed framework combining MPC and RL

We propose a framework that combines MPC and RL inspired by [3]. As shown in Figure 1, the combined MPC and RL framework is illustrated. The nominal traffic system can be represented by a macroscopic traffic model (e.g., the BLX model), while the real system can be approximated by a microscopic simulation model, such as SUMO. This framework can potentially mitigate the drawbacks of both MPC and RL control. The adaptive framework may be able to reduce the negative effect that uncertainties have on the performance of an MPC controller. Moreover, the addition of an adaptive law in the form of an RL controller may also reduce the computational complexity in comparison to a conventional MPC controller because an RL algorithm can operate with a very low online computational effort. The improvement of performance in the presence of uncertainties will potentially be the largest advantage of the application of the framework in traffic signal control compared to a normal MPC controller in a traffic signal control setting.

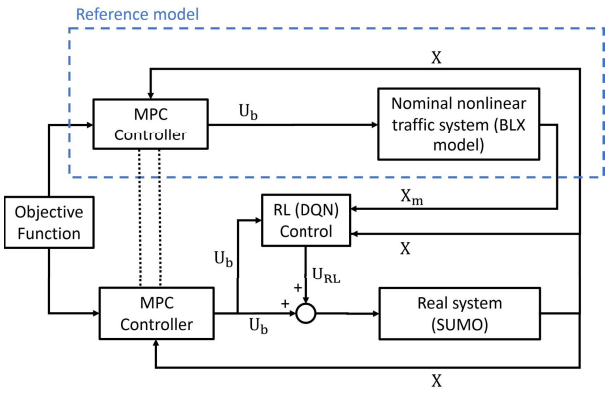

Figure 1: The combined model predictive control and reinforcement learning model-reference framework.

As regards the possible improvements of the framework compared to a conventional RL controller, the MPC control law offers a baseline control law, which might result in improved system performance during training of the RL agent compared to the conventional RL strategy. This might also make the framework more sample-efficient. Compared to the model-reference RL control scheme in [3], this framework will also be robust through the rolling horizon scheme of the MPC controller.

[1] This project has received funding from the European Research Council (ERC) under the European Union's Horizon 2020 research and innovation programme (Grant agreement No. 101018826), and also from the China Scholarship Council (CSC Grant No. 201806230254).

References

[1] B. L. Ye et al., "A survey of model predictive controlmethods for traffic signal control," IEEE/CAA Journalof Automatica Sinica, vol. 6, no. 3, pp. 623–640, 2019.

[2] A. Haydari and Y. Yılmaz, "Deep reinforcement learning for intelligent transportation systems: A survey," IEEE Transactions on Intelligent Transportation Systems, vol. 23, no. 1, pp. 11–32, 2022.

[3] Q. Zhang, W. Pan, and V. Reppa, "Model-reference reinforcement learning control of autonomous surface vehicles with uncertainties," arXiv preprint arXiv:2003.13839, Mar. 2020.

Learning-based Model Matching for Fault Detection and Isolation of Nonlinear Systems

Farhad Ghanipoor[1], Carlos Murguia[1], Peyman Mohajerin Esfahani[2], Nathan van de Wouw[1]

[1]Department of Mechanical Engineering, Eindhoven University of Technology, Eindhoven, The Netherlands

[2]Delft Center for Systems and Control, Delft University of Technology, Delft, The Netherlands

Emails: {f.ghanipoor, C.G.Murguia, N.v.d.Wouw}@tue.nl
P.MohajerinEsfahani@tudelft.nl

1 Introduction

The reliable functioning of high-tech systems can only be achieved through predictive maintenance, for which techniques for fault detection (is a fault occurring?) and fault isolation (what is the fault source?) are essential prerequisites [1]. We aim to develop a hybrid (physics-learning) fault detection and isolation (FDI) scheme that provides superior monitoring performance by leveraging cutting-edge machine learning (ML) algorithms and first-principles physics-based models.

2 Problem Formulation

Consider a nonlinear dynamical system of the form:

$$\begin{cases} \dot{x}(t) = g(x(t),u(t)) + \eta(x(t),u(t)) + \omega(t) + \phi(x(t),u(t),t), \\ y(t) = x(t) + \nu(t), \end{cases} \tag{1}$$

where t, x, y, u are time, state, measured output, and known input vectors, respectively. Function $g(\cdot)$ is a known nonlinear function. Function $\eta(\cdot)$ represents unknown model uncertainty. Functions $\omega(\cdot), \nu(\cdot)$ are unknown disturbances, and function $\phi(\cdot)$ is the unknown process fault.

3 Methodology

The proposed methodology has two stages: 1. offline uncertainty learning, and 2. online FDI scheme. First, in the offline learning stage, a static map for unstructured uncertainty is trained on the basis of the healthy system input and output data (i.e., for the system with $\phi = 0$). We use a supervised method (i.e., linear regression in this abstract) to find the static map from system input and output to uncertainty in the training phase. Labeled data for the supervised learning of the model uncertainty is obtained using the known part of the system dynamics and healthy system input and output historical data. Then, in the online stage, we estimate the fault by matching the faulty model and the approximately known model of the healthy system (which is constituted by a physics-based model and the trained uncertainty model). Based on the estimated fault signal, the fault can be detected and isolated using the CUSUM-based procedure [2] as a change detection method.

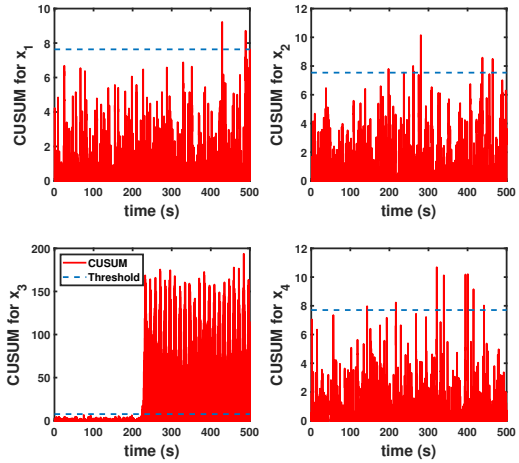

Figure 1: The CUSUM sequences and the thresholds.

4 Simulation Results

In what follows, the methodology is applied to a nonlinear benchmark system (a single-link robotic arm with a revolute elastic joint). In the simulation, a fault occurs abruptly at 225 seconds. The CUSUM-based thresholds and sequences for each state are depicted in Fig. 1. It is clear from the left-down plot of the figure that the fault can be detected by the proposed method since the CUSUM sequence exceeds the threshold after the fault occurrence.

Acknowledgment

This publication is part of the project Digital Twin project 4.3 with project number P18-03 of the research programme Perspectief which is (mainly) financed by the Dutch Research Council (NWO).

References

[1] Ding, S. X. (2008). Model-based fault diagnosis techniques: design schemes, algorithms, and tools. Springer Science & Business Media.

[2] Murguia, C., & Ruths, J. (2016). Cusum and chi-squared attack detection of compromised sensors. In 2016 IEEE Conference on Control Applications (CCA).

Consistency of behavioural assume-guarantee contracts

B. M. Shali, b.m.shali@rug.nl
A. J. van der Schaft, a.j.van.der.schaft@rug.nl
B. Besselink, b.besselink@rug.nl
Bernoulli Institute, University of Groningen, The Netherlands

1 Introduction

Behavioural assume-guarantee contracts are introduced in [1] as an alternative to common methods for providing specifications on control systems, such as dissipativity theory and set invariance. While the specifications expressed by the latter are typically static, contracts express specifications on *dynamic* behaviour. Furthermore, contracts take the environment of the system explicitly into account. Incorporating knowledge about this environment can ease the design burden on the system. It is also essential in facilitating modular design and analysis of interconnected systems.

We are only interested in contract specifications that can actually be satisfied by some system. In other words, so-called *consistent* contracts are the only ones of practical relevance. Motivated by this, we present necessary and sufficient conditions for consistency of assume-guarantee contracts.

2 Contract consistency

Consider a linear system of the form

$$\Sigma : \begin{cases} \dot{x} = Ax + Bu, \\ y = Cx + Du. \end{cases} \tag{1}$$

In the context of an interconnected system, Σ interacts with other components via the external variables u and y. Thus, we identify Σ by its *external behaviour*

$$\mathfrak{B}(\Sigma) = \{(u,y) \mid \exists x \text{ s.t. (1) holds}\}. \tag{2}$$

The contracts presented in [1] are used as specifications for the external behaviour of Σ. A characteristic feature of these contracts is that they take the environment of Σ explicitly into account. The environment of Σ is a linear system that generates the input u. The available information about the behaviour of the environment of Σ is captured by the *assumptions* A, defined as a linear system of the form

$$\mathrm{A} : 0 = A\left(\tfrac{\mathrm{d}}{\mathrm{d}t}\right)u, \tag{3}$$

where $A(s)$ is a polynomial matrix. On the other hand, the *guarantees* Γ capture the desired external behaviour of Σ when interconnected with a relevant environment. They are defined as a linear system of the form

$$\Gamma : G\left(\tfrac{\mathrm{d}}{\mathrm{d}t}\right)y = H\left(\tfrac{\mathrm{d}}{\mathrm{d}t}\right)u, \tag{4}$$

where $G(s)$ and $H(s)$ are polynomial matrices.

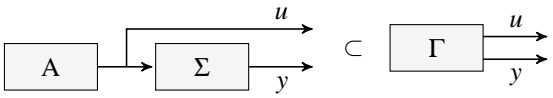

Figure 1: Σ implements $\mathscr{C} = (\mathrm{A}, \Gamma)$

A *contract* $\mathscr{C} = (\mathrm{A}, \Gamma)$ is a pair of assumptions and guarantees. A system Σ *implements* $\mathscr{C} = (\mathrm{A}, \Gamma)$ if and only if

$$\mathfrak{B}(\mathrm{A} \wedge \Sigma) \subset \mathfrak{B}(\Gamma), \tag{5}$$

where $\mathrm{A} \wedge \Sigma$ is obtained by feeding the input generated by A to Σ. This is illustrated in Figure 1. If there exists a system Σ that implements the contract $\mathscr{C}$, then $\mathscr{C}$ is called *consistent*. Not every contract is consistent. Indeed, u is an input in Σ, hence u is free in $\mathfrak{B}(\Sigma)$, which implies that any restrictions on u imposed by the guarantees must already be present in the assumptions. In other words, the contract $\mathscr{C} = (\mathrm{A}, \Gamma)$ is consistent only if $\mathfrak{B}_{\mathrm{i}}(\mathrm{A}) \subset \mathfrak{B}_{\mathrm{i}}(\Gamma)$, where the behaviour $\mathfrak{B}_{\mathrm{i}}(\,\cdot\,)$ is with respect to the input u only.

The condition that $\mathfrak{B}_{\mathrm{i}}(\mathrm{A}) \subset \mathfrak{B}_{\mathrm{i}}(\Gamma)$ is not sufficient. However, we can obtain the following necessary and sufficient condition in a special case of the guarantees Γ.

Lemma 1. *If $G(s)$ is square and invertible, then $\mathscr{C} = (\mathrm{A}, \Gamma)$ is consistent if and only if there exists a polynomial matrix $M(s)$ such that $G(s)^{-1}(H(s) - M(s)A(s))$ is proper.*

A suitable polynomial matrix $M(s)$ can easily be obtained in the following special case, where we utilize the properties of row-reduced polynomial matrices [2].

Lemma 2. *If $G(s)$ and $A(s)$ are square, invertible, and in row-reduced form, then $\mathscr{C} = (\mathrm{A}, \Gamma)$ is consistent if and only if $G(s)^{-1}(H(s) - \bar{M}(s)A(s))$, where $\bar{M}(s)$ is given by the polynomial part of $H(s)A(s)^{-1}$.*

Lemma 2 can be generalized to the case where $G(s)$ and $A(s)$ are not a priori row-reduced. Using the result, we can obtain necessary and sufficient conditions for contract consistency in the most general case.

References

[1] B. M. Shali, A. J. van der Schaft, and B. Besselink, "Behavioural assume-guarantee contracts for linear dynamical systems," in *IEEE Proceedings of the Conference on Decision and Control*, 2021.

[2] T. Kailath, *Linear Systems*. Prentice-Hall, 1980.

H_∞ distributed synchronising controller for Euler-Lagrangian multi-agents under communication time-delay

Arash Farnam[1,2] Babak Mehdizadeh Gavgani[1,2] Guillaume Crevecoeur[1,2]

[1]Department of Electromechanical, Systems and Metal Engineering, Ghent University, Belgium
[2]FlandersMake@UGent – corelab EEDT-DC, Flanders Make, Belgium
Email: arash.farnam@ugent.be

1 Introduction

In this abstract, we consider the issue of synchronising multiple agents whose dynamics can be described by Euler-Lagrangian equations. An H_∞ distributed controller algorithm is developed to guarantee the synchronisation of multi-agents with respect to unknown time-varying time-delays in the communication channels between the agents. Instead of considering static controllers, we propose dynamic controllers that behave as second-order linear systems. The proposed sufficient criterions for the asymptotic convergence and synchronisation with respect to time-delays follow from the Lyapunov-Krasovskii functional using linear matrix inequalities framework. The sufficient conditions only depend on the upper bounds of time-delays, and are independent from the dynamics of agents. This makes the proposed method suitable for systems with multiple agents that are each subject to different dynamics.

2 Problem definition and distributed synchronising controller

Multi-agent systems consisting of agents interconnected with communication networks have the potential to tackle tasks more effectively than single systems. They can cooperate with each other while executing pre-determined tasks like multi-agent robotic manipulators that together need to carry a heavy load. Besides cooperation, distributed control systems can significantly improve the robustness and performance of the overall system. It is worth mentioning that the concept of synchronisation has readily shown its advantages and usefulness for coordinating of multi-agents in several works existing in literature [1].

The multiple agents in distributed control systems need to come to an agreement on the determined command, i.e. the so-called consensus problem between agents needs to be solved. Realizing consensus can help many applications and is therefore a heavily investigated research topic at the moment. Furthermore, it seems that consensus between different agents probably is the most investigated research topic because of its various applications. In this study we focus on the synchronisation problem between agents that are subject to time-varying time-delays in the communication channels. It is well-known already that a communication delay leads to worse performance or even instability in dynamical systems controlled over the communication channels. We consider here communication delays in an alternative approach using linear matrix inequalities (LMIs) that rely on the delays upper bounds.

We consider a networked system with N agents, in which we suppose all agents ($i \in 1,2,...,N$) are modelled by Euler-Lagrange equations as follows

$$A_i(x_i)\ddot{x}_i + B_i(x_i,\dot{x}_i)\dot{x}_i + C_i(x_i) \quad = \quad \tau_i + \omega_i \qquad (1)$$

in which the vector $x_i \in \mathbb{R}^n$ denotes the group of angular positions of the joints; $A_i(x_i) \in \mathbb{R}^{n\times n}$, $B_i(x_i,\dot{x}_i) \in \mathbb{R}^{n\times n}$ and $C_i(x_i)$ denote the inertia matrix, the matrix of coriolis and centripetal forces, and gravitational forces, respectively. $\tau_i \in \mathbb{R}^m$ and $\omega_i \in \mathbb{R}^w$ indicate the torques as control input and disturbance input acting on the *i*th agent, respectively.

The group of interconnected agents (1) are synchronised if the following relation holds

$$\lim_{t\to\infty} || x_j(t) - x_i(t) || = 0 \ \ \forall i \in \{1,...,N\}, \forall j \in N_i, \qquad (2)$$

We propose the following dynamical distributed synchronising H_∞ controller with constants k_{1i}, k_{2i}, k_{3i}

$$\begin{aligned} D_i\ddot{u}_i \quad = \quad & k_{1i}\text{sign}(\alpha_i\bar{x}_i) - k_{2i}\sum_{j=1}^{N}\beta_{ij}(u_i(t) - \qquad (3)\\ & -u_j(t-\eta_{ij}(t)) - k_{3i}\dot{u}_i \ \ \forall i \in \{1,...,N\}, \forall j \in N_i, \end{aligned}$$

in which $\bar{x}_i = x_i - u_i$ and $\eta_{ij}(t)$ is the communication time-delay between the i*th* and j*th* agents. Furthermore, the constant β_{ij} indicates the coupling gain between the i*th* and j*th* agents.

In order to meet the actuator limit, we define the input of i*th* agent as follows

$$\tau_i = -k_{1i}\text{sign}(\alpha_{1i}\bar{x}_i(t)) - k_{4i}\text{sign}(\alpha_{2i}\dot{x}_i(t)) + C_i(x_i) \qquad (4)$$

It is worth mentioning that the input signal (4) is bounded with an upper bound that is equal to $k_{1i} + k_{4i} + || C_i(x_i) ||_\infty$.

3 Acknowledgments

This work was supported by the Flanders Make MultiSysLeCo project.

References

[1] D. Sun, Synchronization and control of multiagent systems, vol. 41. *CRC Press*, 2016.

Extended differential balancing for nonlinear systems

Arijit Sarkar[1] and Jacquelien M.A. Scherpen[1]

I. Introduction

With the growing needs of daily human life sophisticated technologies result into the increasing complexity of systems in numerous fields of science and engineering. However, the increasing complexity leads to high computational burden to design controllers which motivates us to represent the original system using a reduced order model while preserving certain structures of the original system. In this work we investigate nonlinear systems with constant input vector-fields. Generalized differential balanced truncation have been proposed in [1] to find the reduced order model for these kinds of nonlinear systems with a prior error bound and stability guarantees. We extend this idea to extended differential balanced truncation which can provide a tighter apriori error bound than generalized differential balanced truncation as well as can be useful in preserving certain properties, structures in the reduced order model of the system.

II. Extended generalized differential Gramians

Let us consider the system

$$\Sigma : \begin{cases} \dot{x} = f(x) + Bu, \\ y = Cx, \end{cases} \tag{1}$$

where $x \in \mathbb{R}^n$, $u \in \mathbb{R}^m$ and $y \in \mathbb{R}^p$. Now, we can consider the variational system associated with the nonlinear system as

$$d\Sigma : \begin{cases} \delta\dot{x} = \dfrac{\partial f(x)}{\partial x}\delta x + B\delta u, \\ \delta y = C\delta x, \end{cases} \tag{2}$$

where $\delta x \in \mathbb{R}^n$, $\delta u \in \mathbb{R}^m$ and $\delta y \in \mathbb{R}^p$ denote the state, input and output of the variational system respectively.The generalized differential controllability and observability Gramians are defined as the the solutions $P \succ 0$, $Q \succ 0$ of the following differential Lyapunov inequalities

$$\frac{\partial f(x)}{\partial x}P + P\frac{\partial^\top f(x)}{\partial x} + BB^\top \preceq 0, \tag{3}$$

$$Q\frac{\partial f(x)}{\partial x} + \frac{\partial^\top f(x)}{\partial x}Q + C^\top C \preceq 0, \tag{4}$$

for all $x \in \mathbb{R}^n$. The generalized differential Gramians as defined in [1] can be extended to the extended differential Gramians. Extended Gramians have been defined for discrete-time LTI systems in [2] and for continuous-time LTI systems in [3]. Here we define extended differential Gramians for nonlinear systems.

Let us consider the following two LMIs which are the backbone of the definition of extended differential Gramians.

$$\begin{bmatrix} X_o(x) & Q - (\alpha I_n + \frac{\partial^\top f(x)}{\partial x})S \\ Q - S^\top(\alpha I_n + \frac{\partial f(x)}{\partial x}) & (S + S^\top) \end{bmatrix} \succeq 0 \tag{5}$$

$$\begin{bmatrix} -\check{P}\frac{\partial f(x)}{\partial x} - \frac{\partial^\top f(x)}{\partial x}\check{P} & -\check{P} + (\beta I_n + \frac{\partial^\top f(x)}{\partial x})T & -2\check{P}B \\ \check{P} - T^\top(\beta I_n + \frac{\partial f(x)}{\partial x}) & T + T^\top & 2T^\top B \\ -2B^\top\check{P} & 2B^\top T & 4I_m \end{bmatrix} \succeq 0 \tag{6}$$

where $X_0(x) := -Q\frac{\partial f(x)}{\partial x} - \frac{\partial^\top f(x)}{\partial x}Q - C^\top C$, $\check{P} := P^{-1}$. Also consider $X_c(x) := -\check{P}\frac{\partial f(x)}{\partial x} - \frac{\partial^\top f(x)}{\partial x}\check{P} - \check{P}BB^\top\check{P} - \epsilon\check{P}$.

Theorem 1. *The inequality* (4) *has a solution for all* $x \in \mathbb{R}^n$ *if and only if* (5) *has a solution* (Q, S, α) *with* $Q \succ 0$, $(S+S^\top) \succeq 0$ *and* α *large enough for all* $x \in \mathbb{R}^n$. *In addition to that if* X_o *is positive definite, then there exists* α *large enough and* $S = S^\top \succ 0$ *such that* (5) *holds for all* $x \in \mathbb{R}^n$.

Theorem 2. *The inequality* (3) *has a solution* P *if and only if* (6) *has a solution* $(\check{P}, T, \beta)$ *with* $\check{P} \succ 0$. *In addition to that, if* X_c *is positive definite then* $\exists\beta$ *and* $T = T^\top \succ 0$ *such that* (6) *is satisfied.*

Theorem 3. *Suppose the system* (1) *is balanced with the extended differential observability Gramian* (Q, S, α) *and inverse of extended differential controllability Gramian*$(\check{P}, T, \beta)$ *as defined in* (5) *and* (6) *respectively. If the system is in the balanced coordinates,*

$$S = T^{-1} = \Lambda_{ST} = \mathsf{diag}\{\sigma_1, \sigma_2, \cdots, \sigma_n\},$$

where $\sigma_1 \geq \sigma_2 \geq \cdots \geq \sigma_n > 0$. *Then the output of the original and reduced order model satisfy*

$$||y - \hat{y}||_2 \leq 2\sum_{j=r+1}^{n} \sigma_j ||u||_2$$

where $\sigma_r >> \sigma_{r+1}$ *and* $\alpha = \beta$.

References

[1] Y. Kawano and J. M. A. Scherpen, "Model reduction by generalized differential balancing," in *Mathematical Control theory*. Springer-verlag, 2015, vol. I, ch. 19, pp. 349–362.

[2] H. Sandberg, "An extension to balanced truncation with application to structured model reduction," *IEEE Transactions on Automatic Control*, vol. 55, no. 4, pp. 1038–1043, 2010.

[3] P. Borja, J. M. A. Scherpen, and K. Fujimoto, "Extended balancing of continuous-time LTI systems : a structure-preserving approach," *IEEE Transactions on Automatic Control(early access)*, 2022.

[1]Jacquelien M. A. Scherpen and Arijit Sarkar are with Jan C. Willems Cemter for Systems and Control, Engineering and Technology Institute Groningen, Faculty of Science and Engineering, University of Groningen, The Netherlands. {{j.m.a.scherpen, a.sarkar}@rug.nl}

Multirate Performance Quantification using Time-Lifting and Local Polynomial Modeling

Max van Haren[†*], Lennart Blanken[†,‡] and Tom Oomen[†,§]

[†] Control Systems Technology Group, Dept. of Mechanical Engineering, Eindhoven University of Technology, The Netherlands

[‡] Sioux Technologies, Eindhoven, The Netherlands

[§] Delft Center for Systems and Control, Delft University of Technology, Delft, The Netherlands [*]Corresponding author. Email: m.j.v.haren@tue.nl

1 Background

Increasing performance requirements for mechatronic systems leads to continuous-time performance evaluation becoming more important. Continuous-time performance is typically evaluated using a significant higher sampling rate for the plant compared to the sampling rate of the controller, resulting in multirate systems. Similarly to single-rate systems, multirate systems require performance quantification.

2 Problem Formulation

Consider the multirate control structure in Figure 1, where the controller K_l is sampled at a low-rate $\omega_{s,l} = \omega_{s,h}/F$ and P_h at a high-rate $\omega_{s,h} = 2\pi/h_h$. Performance criteria

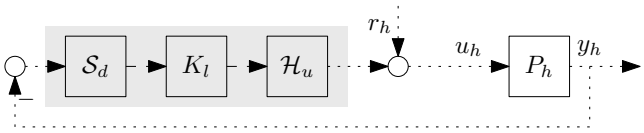

Figure 1: High-rate plant P_h operating in multirate feedback loop with low-rate controller K_l. The signals are up- and downsampled using $\mathcal{H}_u$ and $\mathcal{S}_d$.

for Linear Time Invariant (LTI) systems are typically evaluated using Frequency Response Functions (FRFs). However, since multirate systems are Linear Periodically Time-Varying (LPTV) [1], evaluating frequency domain models is not trivial. Several definitions for FRFs for multirate systems are available [2], requiring multiple experiments. Hence, the aim of this paper is to develop a more time-efficient method to identify multirate FRFs.

3 Approach

This paper considers the Performance Frequency Gain (PFG) definition of multirate FRFs, given by [2]

$$\mathcal{P}\left(e^{j\omega h_h}\right) = \sup_{w_h \neq 0} \frac{\|\zeta_h\|_{\mathcal{P}}}{\|w_h\|_{\mathcal{P}}}, \tag{1}$$

where ζ_h and w_h are chosen by the user, with w_h containing only one frequency component.The PFG represents the maximum response of a system for a single input frequency, hence requiring a multitude of experiments to determine for a frequency grid. An alternative representation of the PFG uses K_l and P_h [2]. To identify P_h, this paper uses the time-lifted representation, translating a SISO LPTV into a MIMO LTI representation [1]. First, define $\underline{J} : \underline{r} \mapsto \underline{y}$ and $\underline{S} : \underline{r} \mapsto \underline{u}$, where $\underline{r} = \mathcal{L}r_h$, $\underline{y} = \mathcal{L}y_h$, $\underline{u} = \mathcal{L}u_h$ and $\mathcal{L}$ the time-lifting operator. $\hat{\underline{J}}$ and $\hat{\underline{S}}$ are estimated with local polynomial modeling, since it identifies MIMO systems in a single experiment [3]. Second, recover the time-lifted original system as $\hat{\underline{P}} = \mathcal{L}\hat{P}_h\mathcal{L}^{-1} = \hat{\underline{J}}\hat{\underline{S}}^{-1}$. The high-rate system $\hat{P}_h$ is found by inverse lifting [1, Section 6.2.1]. Finally, the PFG is calculated by performing the procedure in [2], using $\hat{P}_h$ and K_l.

4 Initial Results

A high-rate fourth-order system P_h with controller K_l is considered with $F = 3$. The PFG is determined based on an estimate of P_h, both using an Emperical Transfer Function Estimate (ETFE) and the developed approach. The estimation error of the PFG for these methods is shown in Figure 2.

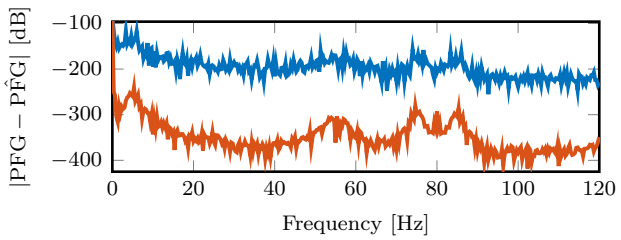

Figure 2: Error for estimating the PFG for ETFE (—) and the developed approach (—).

5 Ongoing Research

Ongoing research is focused at validating the framework in an experimental setting.

Acknowledgments

This research has received funding from the ECSEL Joint Undertaking, grant agreement 101007311 (IMOCO4.E).

References

[1] S. Bittanti and P. Colaneri, *Periodic Systems*. Springer London, 2009.

[2] T. Oomen, M. van de Wal, and O. Bosgra, "Design framework for high-performance optimal sampled-data control with application to a wafer stage," *Int. Journal of Control*, vol. 80, no. 6, pp. 919–934, 2007.

[3] R. Pintelon and J. Schoukens, *System Identification: A Frequency Domain Approach*, 2nd ed. John Wiley, 2012.

Least-squares globally optimal misfit modelling for SISO systems

Sibren Lagauw and Bart De Moor, *Fellow IEEE, SIAM*
Center for Dynamical Systems, Signal Processing, and Data Analytics (STADIUS),
Department of Electrical Engineering (ESAT), KU Leuven, 3001 Leuven, Belgium
sibren.lagauw@esat.kuleuven.be, bart.demoor@esat.kuleuven.be

1 Introduction

Previous work of our research group showed how the least-squares optimal realisation of an autonomous linear time-invariant (LTI) system can be obtained by solving a multiparameter eigenvalue problem (MEVP), the eigen-tuples of which characterise the globally optimal solution(s) [3]. We extend this methodology to the single-input single-output (SISO) setting, resulting in an approach for least-squares globally optimal misfit modelling for SISO systems. Thereby we address a longstanding open problem of least-squares optimality in misfit modelling.

2 Misfit modelling

We parametrise LTI models by means of a rational transfer function $b(z)/a(z)$ in the time-delay operator z^{-1}, which maps the input to output. This model description is a special case (misfit-only) of the more general misfit versus latency framework [4]. The degree n of the numerator and the denominator of the transfer function determines the complexity of the model. Given a sequence of input-output data $\boldsymbol{w} = (\boldsymbol{u}, \boldsymbol{y}) \in \mathbb{R}^N \times \mathbb{R}^N$ and a specified model complexity n, we want to identify the model for which the 2-norm of the corresponding misfit is minimal. The misfit $\tilde{\boldsymbol{w}} = (\tilde{\boldsymbol{u}}, \tilde{\boldsymbol{y}}) \in \mathbb{R}^N \times \mathbb{R}^N$ is the 'modification' that has to be made to the given data such that the resulting sequence $\hat{\boldsymbol{w}} = (\hat{\boldsymbol{u}}, \hat{\boldsymbol{y}}) \in \mathbb{R}^N \times \mathbb{R}^N$ satisfies the model equations of the identified model exactly. A schematic overview is given in Figure 1. Misfit modelling has close links to Willems' behavioural approach [6, 5] on the one hand and (structured) total least-squares on the other [2, 1].

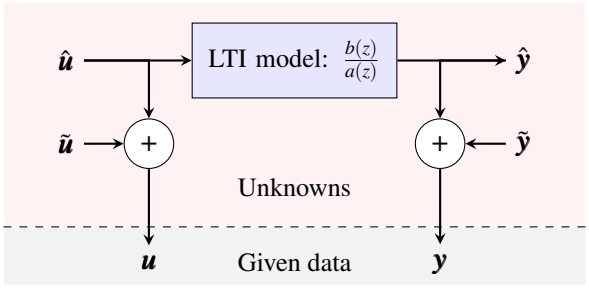

Figure 1: Schematic overview of the identification problem in the misfit setting. The given input-output data $(\boldsymbol{u}, \boldsymbol{y})$ is decomposed in a regular part $(\hat{\boldsymbol{u}}, \hat{\boldsymbol{y}})$ that satisfies the LTI model exactly, and a misfit part $(\tilde{\boldsymbol{u}}, \tilde{\boldsymbol{y}})$, the 2-norm of which should be minimized. In spirit, the misfit idea is close to the dynamic errors-in-variables approach, but we do not presume any a priori statistical assumption.

3 Problem formulation

Several approaches to solve the misfit modelling optimisation problem have been proposed in the literature, both for the parametrisation used here [2, 1], and for a behavioural (isometric) state-space parametrisation [5]. However, these iterative methods remain heuristic, in the sense that convergence to a globally optimal model is not guaranteed.

The misfit modelling problem can be written as:

$$\min_{\tilde{\boldsymbol{u}}, \tilde{\boldsymbol{y}}, a_i, b_i} \quad \sigma^2 = ||\tilde{\boldsymbol{u}}||_2^2 + ||\tilde{\boldsymbol{y}}||_2^2 = \sum_{k=0}^{N-1} (u_k - \hat{u}_k)^2 + \sum_{k=0}^{N-1} (y_k - \hat{y}_k)^2,$$
$$\text{s.t.} \quad \hat{y}_{k+n} + a_1 \hat{y}_{k+n-1} + \ldots + a_n \hat{y}_k = b_0 \hat{u}_{k+n} + b_1 \hat{u}_{k+n-1} + \ldots + b_n \hat{u}_k \quad \forall k \in \{0, \ldots, N-n-1\},$$

with $a_i, b_i \in \mathbb{R}, i = 1, \ldots, n$ the coefficients of $b(z)/a(z)$. Obviously, this optimisation problem is nonlinear, yet, upon closer inspection, its nature is multivariate polynomial: the objective function is a sum of squares, and all unknowns (the $\hat{u}_k$'s, $\hat{y}_k$'s and the transfer function coefficients) also appear as multivariate polynomials in the constraints. Upon invoking Lagrange multipliers, the first order necessary conditions for optimality are also multivariate polynomials, the common roots of which characterise the globally optimal solutions of the identification problem. Rooting such problems is equivalent to solving an MEVP.

We will elaborate on these lines of thought in more detail in our presentation and we will reveal the special properties of the optimal model and associated data sequences, some of which have already been briefly mentioned in [1].

Acknowledgements

This work was supported in part by the KU Leuven: Research Fund (project C16/15/059), and several Leuven Research and Development bilateral industrial projects, in part by Flemish Government agencies: FWO (EOS project G0F6718N (SeLMA), and PhD grants SB/1SA1319N, SB/1S93918, and SB/1S1319N), EWI (Flanders AI Research Program), and in part by the European Commission (EU Research Council under the European Union's Horizon 2020 research and innovation programme (ERC Adv. Grant) under grant 885682).

References

[1] Bart De Moor. Dynamic total linear least squares. *IFAC Symposium on System Identification*, 3(10):159 – 164, 1994.
[2] Bart De Moor. Total least squares for affinely structured matrices and the noisy realization problem. *IEEE Transactions on Signal Processing*, 42(11):3104 – 3113, 1994.
[3] Bart De Moor. Least squares optimal realisation of autonomous LTI systems is an eigenvalue problem. *Communications in Information and Systems*, 20(2):163 – 207, 2020.
[4] Philippe Lemmerling and Bart De Moor. Misfit versus latency. *Automatica*, 37:2057 – 2067, 2001.
[5] Berend Roorda. *Global Total Least Squares - A method for the construction of open approximate models from vector time series*. PhD thesis, Erasmus Universiteit Rotterdam, 1995.
[6] Jan C. Willems. From time series to linear system, Part I: Finite dimensional linear time invariant systems; II: Exact modelling; III: Approximate modelling. *Automatica*, 22/23(5,6,1):561 – 580, 675 – 694, 87 – 115, 1986, 1987.

Globally optimal least-squares misfit identification of multidimensional autonomous systems

Lukas Vanpoucke and Bart De Moor, *Fellow, IEEE, SIAM*
Center for Dynamical Systems, Signal Processing, and Data Analytics (STADIUS),
Department of Electrical Engineering (ESAT), KU Leuven, 3001 Leuven, Belgium
lukas.vanpoucke@esat.kuleuven.be, bart.demoor@esat.kuleuven.be

1 Introduction

For autonomous systems, previous work has shown that the globally optimal least-squares misfit identification can be translated to a multiparameter eigenvalue problem (MEVP). Such an MEVP can be solved using a linear algebra framework, allowing the characterization of the globally optimal solution and its system theoretic properties [1]. We will extend these results to the identification of two-dimensional, and by extension, general multidimensional systems.

2 Multidimensional autonomous systems

Multidimensional autonomous system models contain more than one independent variable, e.g. time and space. We consider two-dimensional, linear, shift-invariant, single output commutative state space models of the form:

$$\mathbf{x}_{k+1,l} = \mathbf{A}_1\mathbf{x}_{k,l},\ \ \mathbf{x}_{k,l+1} = \mathbf{A}_2\mathbf{x}_{k,l},\ \ y_{k,l} = \mathbf{C}\mathbf{x}_{k,l}(0)$$

$$\text{with}\ \ \mathbf{A}_1\mathbf{A}_2 = \mathbf{A}_2\mathbf{A}_1.$$

As a first step towards solving this multidimensional modelling problem, starting from a given output sequence $y_{k,l}$, we confine ourselves to the identification of systems for which $\mathbf{A}_1$ and $\mathbf{A}_2$ are simultaneously diagonizable. More precisely, we assume that $\mathbf{A}_1 = \mathbf{V}\mathbf{\Lambda}_1\mathbf{V}^{-1}$ and $\mathbf{A}_2 = \mathbf{V}\mathbf{\Lambda}_2\mathbf{V}^{-1}$, where the $\mathbf{\Lambda}_i$-matrices are diagonal matrices containing the eigenvalues of the $\mathbf{A}_i$-matrices and the matrix $\mathbf{V}$ has the common eigenvectors as its columns. Note that this is a sufficient, though not a necessary condition for the matrices to commute. Under this assumption, an n-th order autonomous 2-D model can be parameterized by the $2n$ eigenvalues $\lambda_j^{(i)}$ of the $\mathbf{A}_i$-matrices, the n components ξ_j of the initial state $\mathbf{x}_{0,0}$ and the n components c_j of the row vector $\mathbf{C}$. This parameterization can of course be easily extended to even higher dimensional models.

3 Least-squares misfit identification

In the misfit identification framework, the given output sequence $y_{k,l}$ is altered by a misfit sequence $\tilde{y}_{k,l}$ to obtain the so-called 'exact' data $\hat{y}_{k,l} = y_{k,l} - \tilde{y}_{k,l}$. As the name implies, the 'exact' data $\hat{y}_{k,l}$ is required to satisfy the equations of the identified state space model exactly. For some predefined order n, misfit modelling then aims to find the n^{th} order system that minimizes the 2-norm of the misfit sequence. More formally, this corresponds to solving the following nonlinear least-squares problem [2]:

$$\min_{\lambda_j^{(1)},\lambda_j^{(2)},\xi_j,c_j} ||\tilde{\mathbf{y}}||_2^2 = \sum_{k=0}^{N_1}\sum_{k=0}^{N_2}(y_{k,l} - \hat{y}_{k,l})^2$$

$$\text{s.t. } \hat{y}_{k,l} = \textstyle\sum_{j=1}^{n} c_j\xi_j\left(\lambda_j^{(1)}\right)^k\left(\lambda_j^{(2)}\right)^l.$$

Obviously, the misfit modelling optimisation problem is non-linear, yet, upon closer inspection, its nature is multivariate polynomial: the objective function is a sum of squares and all unknowns also appear as multivariate polynomials in the constraints. Upon invoking Lagrange multipliers, the first order necessary conditions for optimality are also multivariate polynomials, the common roots of which characterise all stationary points, including the global optimal solutions. Rooting such problems is equivalent to solving an MEVP. Furthermore, this characterization allows us to describe the system theoretic properties of the globally optimal model and its misfits. In particular, we aim to extend Walsh's theorem to the multidimensional setting [1, 3].

Acknowledgements

This work was supported in part by the KU Leuven: Research Fund (project C16/15/059), and several Leuven Research and Development bilateral industrial projects, in part by Flemish Government agencies: FWO (EOS project G0F6718N (SeLMA), and PhD grants SB/1SA1319N, SB/1S93918, and SB/1S1319N), EWI (Flanders AI Research Program), and in part by the European Commission (EU Research Council under the European Union's Horizon 2020 research and innovation programme (ERC Adv. Grant) under grant 885682).

References

[1] Bart De Moor. Least squares optimal realisation of autonomous LTI systems is an eigenvalue problem. *Communications in Information and Systems*, 20(2):163 – 207, 2020.

[2] Philippe Lemmerling and Bart De Moor. Misfit versus latency. *Automatica*, 37(12):2057–2067, 2001.

[3] Phillip Regalia. *Adaptive IIR filtering in Signal Processing and Control*, page 129. CRC Press, 1994.

A novel aerial robotic swarm hardware

Sinan Oguz, Mary Katherine Heinrich,
Michael Allwright, Weixu Zhu,
Mostafa Wahby, Marco Dorigo
Institut de Recherches Interdisciplinaires et
de Développements en Intelligence Artificielle
Université Libre de Bruxelles (ULB)
Brussels
Belgium
Email: sinan.oguz@ulb.be

Emanuele Garone
Unité d'enseignement en Automatique et
Analyse des Systémes
Université Libre de Bruxelles (ULB)
Brussels
Belgium

1 Abstract

Quadrotors are a versatile and popular category of Unmanned Aerial Vehicles (UAVs). They can take off and land vertically and perform sophisticated maneuvers, while still being relatively small in size with a simple structure and low maintenance costs. They are also easily accessible due to the availability of off-the-shelf components and open-source autopilot solutions that enable fully autonomous flight. Quadrotors are recently becoming more widespread in commercial and civil applications, because of improvements in computational power, battery life, miniaturization, and reduction of sensor complexity. Due to these improvements, combined with many concurrent advances in robotics, swarms of quadrotors are emerging as a suitable technology for complex missions [2].

Designing platforms for real-world swarm applications is challenging [3], for instance because each robot in a swarm must measure information within its immediate environment via its onboard sensors [1]. More onboard sensing capabilities are therefore required than would be needed if the UAV were to be fully controlled by a base station. In the case of quadrotors, a further design challenge is that local failures are unlikely to remain local, because the robots are much more agile and powerful than ground vehicles of similar size. Their failures are likely to cause collisions and damage to neighboring quadrotors and objects in the environment.

On the one hand, overcoming the design challenges of quadrotor swarms by using several expensive sensors and increasing the size of the quadrotors is not optimal in terms of the cost factor. On the other hand, as individual quadrotor size and mass decrease, the ability to sense its local environment also decreases, because each quadrotor can carry only lighter, cheaper (and often less capable) sensors and actuators. A smaller, lighter quadrotor is often less capable of acting on its environment, intensifying design challenges for complex missions. Designing a quadrotor for swarm robotics research requires adequate lab facilities, the ability to build platforms from scratch, and an extensive budget. As real-world experiments with quadrotor swarms consume a lot of resources, most of the current research in swarm robotics instead presents non-realistic simulation results without actual robot implementation [4]. In the limited cases where real UAVs are used, most implementations use commercial off-the-shelf quadrotors that often lack complete documentation and openness and have limited extensibility for allowing researchers to modify them for scientific work.

In this work, we present a novel, well-documented, entirely open-source quadrotor platform to foster and support research involving quadrotors in swarm robotics. The quadrotor can operate both in laboratory settings and outdoor environments, can rely only on onboard processing and sensing without external infrastructure or positioning (e.g., GPS, motion capture system). We are currently validating the hardware and its support software in indoor experiments.

References

[1] Brambilla, M., Ferrante, E., Birattari, M., Dorigo, M.: Swarm robotics: a review from the swarm engineering perspective. Swarm Intelligence **7**(1), 1–41 (2013)

[2] Chung, S.J., Paranjape, A.A., Dames, P., Shen, S., Kumar, V.: A survey on aerial swarm robotics. IEEE Transactions on Robotics **34**(4), 837–855 (2018)

[3] Coppola, M., McGuire, K.N., De Wagter, C., de Croon, G.C.: A survey on swarming with micro air vehicles: Fundamental challenges and constraints. Frontiers in Robotics and AI **7**, 18 (2020)

[4] Schranz, M., Umlauft, M., Sende, M., Elmenreich, W.: Swarm robotic behaviors and current applications. Frontiers in Robotics and AI **7**, 36 (2020)

Distributed MPC for mapping mission with multiple UAVs

Dora Novak[1,2], Alain Vande Wouwer[1], and Sihem Tebbani[2]

[1]Systems, Estimation, Control and Optimization (SECO), University of Mons, Mons, Belgium
[2]Laboratoire des Signaux et Systèmes, Université Paris-Saclay, CentraleSupélec, Gif sur Yvette, France
[1,2]Email:{dora.novak, sihem.tebbani}@centralesupelec.fr , alain.vandewouwer@umons.ac.be

1 Introduction

In recent years, the development of UAVs and their autonomous flight have received significant attention. When planning a multiple UAV flight, coordination among the agents needs to be addressed. In order to prevent collision and perform a mission efficiently, the trajectory of each vehicle should be predicted and tracked in real-time. Model Predictive Control (MPC) has shown promising path planning results for autonomous vehicles. A distributed approach is discussed to ensure computational feasibility in real-time. In distributed MPC, each UAV is an individual subsystem and solves its optimal control problem autonomously while considering the estimated states of other UAVs. The proposed approach should ensure that the entire system converges to the planned destination while avoiding the collision. First, we define a centralized problem, which is later decomposed into distributed cooperative problems for each UAV [1].

2 Problem formulation

The mission consists of multiple agents departing from different starting points in the area of interest. Each agent has an attributed destination, a point of interest where the UAV needs to take a snapshot. Points of interest and their distribution are given *a priori* by the centralized global planner. An example of a mission with 2 UAVs is given in Figure 1. The points are defined in Cartesian coordinates with constant altitude.

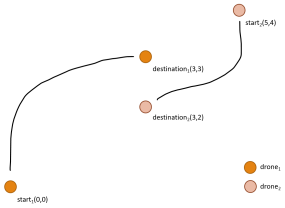

Figure 1: Mapping mission for 2 UAVs

A dynamic model of an UAV is given in (1) and (2). The system states are represented by Cartesian and angular coordinates and are given by $a = \begin{bmatrix} x\ y\ z\ \phi\ \theta\ \psi \end{bmatrix}^\top$ where x, y and z are position coordinates; and ϕ, θ and ψ are angular positions. The inputs are $u = \begin{bmatrix} U\ V\ W\ P\ Q\ R \end{bmatrix}^\top$, where U, V, W are velocities and P, Q, R angular velocities of an UAV [2].

$$\begin{bmatrix} \dot{x} \\ \dot{y} \\ \dot{z} \end{bmatrix} = \begin{bmatrix} C_\theta C_\psi & S_\phi S_\theta C_\psi - C_\phi S_\psi & C_\phi S_\theta C_\psi + S_\phi S_\psi \\ C_\theta S_\psi & S_\phi S_\theta S_\psi + C_\phi C_\psi & C_\phi S_\theta S_\psi - S_\phi C_\psi \\ -S_\theta & S_\phi C_\theta & C_\phi C_\theta \end{bmatrix} \begin{bmatrix} U \\ V \\ W \end{bmatrix} \tag{1}$$

$$\begin{bmatrix} \dot{\phi} \\ \dot{\theta} \\ \dot{\psi} \end{bmatrix} = \begin{bmatrix} 1 & S_\phi T_\theta & C_\phi T_\theta \\ 0 & C_\phi & -S_\phi \\ 0 & S_\phi / C_\theta & C_\phi / C_\theta \end{bmatrix} \begin{bmatrix} P \\ Q \\ R \end{bmatrix} \tag{2}$$

Distributed MPC problem for each vehicle $i \in N$ minimizes the cost function:

$$J_i(t_k, p_i^a, u_i^a) = \int_{t_k}^{t_k+h_p} \gamma_{ai} \|p_i^a(t,t_k)\|^2 + \gamma_{ui} \|u_i^a(t,t_k)\|^2 \, dt + \gamma_{ti} g_i(p_i^a(t_k+h_p, t_k)) \tag{3}$$

subject to constraints:

$$\dot{a}(t;t_k) = f(a(t;t_k), u(t;t_k)), a(t;t_k) \in \mathscr{A}, u(t;t_k) \in \mathscr{U} \tag{4}$$

$$\|p_i(t,t_k) - p_j(t,t_k)\| \geq \alpha, \forall i, j \in N, j \neq i \tag{5}$$

$$v_{min_i} \leq v_i(t) \leq v_{max_i}; |\omega_i(t)| \leq \omega_{max_i} \tag{6}$$

where $p_i^a = \|(x_i, y_i, z_i) - (x_i^d, y_i^d, z_i^d)\|^2$ and u_i^a are distances between desired and actual position and inputs of i-th vehicle, respectively; g_i represents terminal cost and $\gamma_{ai}, \gamma_{ui}, \gamma_{ti}$ are weighting scalars. Constraint (4) represents the system dynamics and constraints on the inputs. Constraint (5) ensures that there is no collision between vehicles i and j, with a minimum safe distance α. Physical constraint (6) bounds velocity and angular velocity of an UAV.

References

[1] F. Mohseni, E. Frisk, and L. Nielsen, "Distributed Cooperative MPC for Autonomous Driving in Different Traffic Scenarios", IEEE Transactions on Intelligent Vehicles, Vol.6, No.2, 299–309, 2020.

[2] S.S. Mansouri, G. Nikolakopoulos, and T. Gustafsson, "Distributed model predictive control for unmanned aerial vehicles", IEEE Workshop on Research, Education and Development of Unmanned Aerial Systems (RED-UAS), 152–161, 2015.

Implementation and Tests of an INDI Control Strategy with the Parrot Mambo Minidrone

G. Delansnay, A. Vande Wouwer
System, Estimation, Control and Estimation (SECO), University of Mons, Belgium
Email: gilles.delansnay@umons.ac.be

1 Introduction

Unmanned Aerial Vehicles takes more and more places in many domains due to their numerous possible applications. Therefore, understanding their inherent dynamics and using them as desired is a key feature in their development. The first approach has been to consider a linear model of the quadrotor and then use linear controllers [1]. Those controllers can handle the quadcopter dynamics under the assumption that they are in almost hovering conditions. However, many applications need to control the aircraft in a larger span of conditions as specific tasks, perturbed environment or loss of control in flight. It is why, nonlinear controller were rapidly considered in this domain.

In this work, we will use a feedback linearization process, the Incremental Nonlinear Dynamic Inversion , to control the Parrot Mambo Drone.

2 Quadcopter model

Quadcopters are 6 degrees of freedom aerial vehicles equipped with four rotors (Figure1). The rotors produce forces and torques that allows moving the body into a 3D environment.

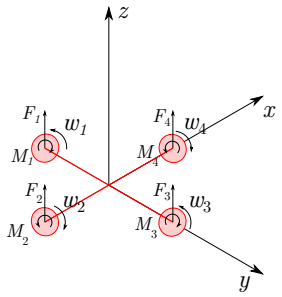

Figure 1: Aircraft with 4 rotors in the body frame

3 Incremental nonlinear dynamic inversion

The Incremental Nonlinear Dynamic Inversion (NDI) controller is a feedback linearization controller [2] which uses derivatives of the system states as an input. Consider a nonlinear model of a drone:

$$\dot{x} = f(x) + g(x)u \tag{1}$$

The idea is to impose that $\dot{x}_n$ behaves according to a virtual input ν in small time increment:

$$\Delta\dot{x}_n = \Delta\nu \approx b(x)\Delta u \tag{2}$$

Then, the input can be computed as :

$$\Delta u(t) = b^{-1}(x)\Delta\nu \tag{3}$$

The virtual input can be selected as a state feedback law :

$$\nu = -k_1x_1 - k_2x_2 - \cdots - k_{n-1}x_{n-1}, \tag{4}$$

and $b(x)$ is the jacobian matrix w.r.t. the input.

4 Simulation Results

Figure 2 shows simulation results.

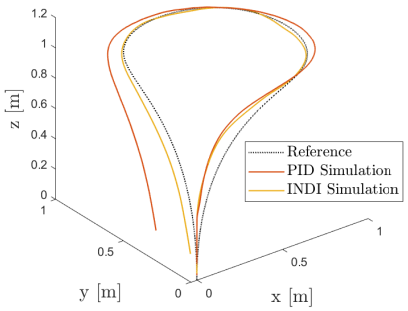

Figure 2: Simulation Results - Trajectory following comparison between the INDI controller and a classic PID structure for the Parrot Mambo Drone

References

[1] L. M. Argentim, W. C. Rezende, P. E. Santos, R. A. Aguiar, Pid, lqr and lqr-pid on a quadcopter platform, in: 2013 International Conference on Informatics, Electronics and Vision (ICIEV), 2013, pp. 1–6. doi:10.1109/ICIEV.2013.6572698.

[2] E. J. J. Smeur, Q. Chu, G. C. H. E. de Croon, Adaptive incremental nonlinear dynamic inversion for attitude control of micro air vehicles, Journal of Guidance, Control, and Dynamics 39 (3) (2016) 450–461. doi:10.2514/1.g001490.

Multi-stage Optimal Motion Planning for Drone Racing

Mathias Bos, Wilm Decré, Jan Swevers, Goele Pipeleers
MECO Research Team, Dept. of Mechanical Engineering, KU Leuven, BE-3001 Heverlee
DMMS-M core lab, Flanders Make, BE-3001 Heverlee
Email: firstname.lastname@kuleuven.be

1 Introduction

This work presents an optimal control problem formulation for online trajectory generation in drone racing through gates and tunnels. Often, state of the art solutions for passing gates rely on predefined waypoints or keyframes in front of and behind the gate with fully determined dynamic state to assure collision free passage [1], or trust that a tradeoff between a progress reward and a safety reward will keep the drone close enough to the gate center in order not to hit the sides [2]. In both cases, the gate geometry is not explicitly taken into consideration. A technique that does explicitly take into account gate geometry by representing the space around it as forbidden area uses the separating hyperplane theorem to avoid collision [3]. This technique, however, scales badly with the number of obstacles, and is not robust against varying configurations of drone and gate poses.

Another issue when planning the motion through a gate is that the time at which the drone passes through the gate is a priori unknown. Often it is manually fixed or decided by a heuristic.

2 Presented approach

The approach presented in this work formulates the motion planning problem as a multi-stage optimal control problem (OCP). This means that the full motion planning problem is split up into stages, each constrained by the same vehicle dynamics, but with their own specific box constraints that delimit the collision free space. For one gate, it considers three stages: an approach stage, a fly-through stage and a fly-away stage. Figure 1 illustrates that the drone position is constrained to the red, yellow and blue area for each of the stages respectively. The formulation is readily extended to multiple gates by adding more stages. For the 3d case, it suffices to add two more constraints in the fly-through stage for the sides of the gate.

3 Results and future work

This approach explicitly takes into account the gate geometry, the advantage of which is clearly observed in Figure 1: the solution takes the fastest route, not the route through the gate center. It also directly tackles the passing time problem by splitting the full motion planning problem up into subsequent stages of which the travel times are minimized together in one OCP.

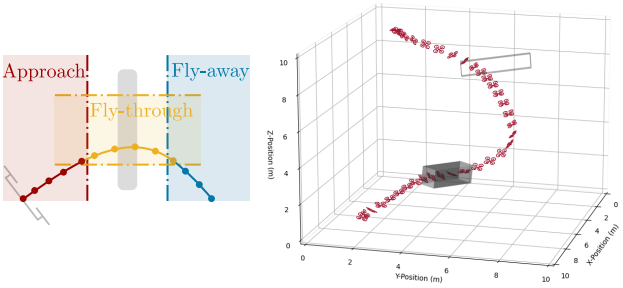

Figure 1: Left: Multi-stage for one gate. Right: Solution of the motion planning problem through a short, stretched gate and a long, narrow gate.

The formulation is succesful in generating feasible trajectories for a large range of gate configurations, unlike the separating hyperplanes approach. Computation times for two gates are in the order of 350 ms on a laptop with powerful CPU. To enable fast onboard computations, several techniques could be explored such as the use of SQP solvers with smart initialization, real time iteration schemes and automatic C-code generation.

Future work includes these techniques for computation speed up, as well as an approach to recede the planning horizon, such that the OCP can be solved in a model predictive control fashion. The approach will be demonstrated in a physical experiment.

References

[1] M. Neunert, C. de Crousaz, F. Furrer, M. Kamel, F. Farshidian, R. Siegwart, and J. Buchli, "Fast nonlinear model predictive control for unified trajectory optimization and tracking," in *2016 IEEE International Conference on Robotics and Automation (ICRA)*, 2016, pp. 1398–1404.

[2] Y. Song, M. Steinweg, E. Kaufmann, and D. Scaramuzza, "Autonomous drone racing with deep reinforcement learning," *CoRR*, vol. abs/2103.08624, 2021.

[3] F. Giulietti, G. Pipeleers, G. Rossetti, and R. Van Parys, "Optimal autonomous quadrotor navigation in an obstructed space," in *2017 Workshop on Research, Education and Development of Unmanned Aerial Systems (RED-UAS)*, 2017, pp. 19–24.

Acknowledgement This work has been carried out within the framework of projects Flanders Make SBO MULTISYSLECO: Multi-System Learning Control and Flanders Make SBO MULTIROB: Rigorous approach for programming and optimal control of multirobot systems. Flanders Make is the Flemish strategic research centre for the manufacturing industry. This work also benefits from project G0C4515N of the Research Foundation - Flanders (FWO - Flanders).

MPC-based Imitation Learning for Autonomous Vehicles Lane Keeping from Human Demonstrations

Flavia Sofia Acerbo[1,2,3], Jan Swevers[1,4], Tinne Tuytelaars[2] and Tong Duy Son[3]
[1] MECO Research Team, Dept. Mechanical Engineering, KU Leuven,
[2] PSI Research Team, Dept. Electrical Engineering, KU Leuven
[3] Siemens Digital Industries Software, Leuven, [4] DMMS-M core lab, Flanders Make
Email: flaviasofia.acerbo@kuleuven.be

1 Introduction

To improve comfort in Autonomous Vehicles (AVs), their control systems can mimic human drivers. Imitation learning algorithms serve this purpose but they usually are fully model-free approaches. On the other hand, Model Predictive Control (MPC) always relies on a (simplified) dynamic model of the vehicle and its surroundings. This work suggests a seamless combination of the two approaches to obtain a human-like AV controller from demonstrations of a desired behavior for a lane keeping control task, exploiting MPC to obtain a model-based version of popular imitation learning algorithms.

2 MPC for End-to-End Differentiable Imitation Learning

In our context, MPC is defined as a deterministic policy, providing a control action based on the current state of the system and on some learnable parameters $a_t = \pi(s_t, \theta)$. To compute the optimal control action, it relies on a predictive differentiable model of the plant $s_{t+1} = f(s_t, a_t)$. To match the human driving behavior, imitation learning algorithms minimize loss functions $L(s_t)$ depending on the states. With a model-free policy, this determines the need of a reinforcement learning step in the loop, while, with our model-based approach, we can exploit the MPC structure to differentiate from s_t to θ. Indeed, in order to compute $\nabla_\theta L(s_t) = (\nabla_s L \nabla_\theta s)_{|s=s_t}$, we can compute $\nabla_\theta s_{|s=s_t}$ in a recursive fashion as:

$$\nabla_\theta s_{|s=s_t} = (\nabla_a f \nabla_\theta a)_{|a=a_{t-1}} + (\nabla_s f \nabla_\theta s)_{|s=s_{t-1}} + (\nabla_a f \nabla_s a \nabla_\theta s)_{|a=a_{t-1}, s=s_{t-1}} \quad (1)$$

The computation of $\nabla_\theta a$ relies on the Karush–Kuhn–Tucker conditions of the MPC.

3 Example: human-like lane keeping control from demonstrations

It has been shown [1] that human lane keeping in curved roads very rarely follows centerline driving. However, that is the common objective for most of lane keeping control algorithms. Therefore, human lane keeping demonstrations are collected on a fixed-base simulator, with constant

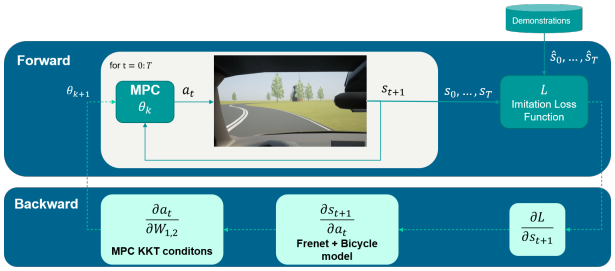

Figure 1: Training loop of MPC-based imitation learning for lane keeping control

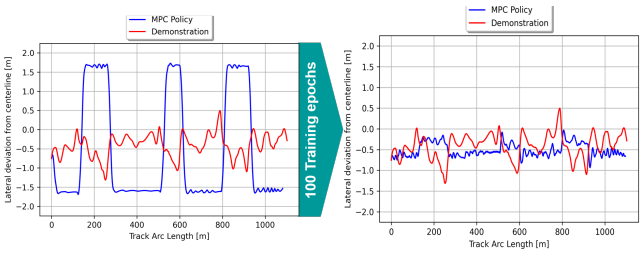

Figure 2: Evolution of the lane centerline deviation d on the whole track from initial condition (left, $\theta_{1,2} = \mathbf{0}$) to learned policy with *state cloning* (right)

50km/h speed. The controlled vehicle is simulated in Simcenter Amesim as a 15DOF high-fidelity model. The MPC policy relies instead on a 6DOF model bicycle model in Frenet coordinates. Its constraints limit the centerline deviation d such that the vehicle stays on its lane. Its cost function is defined as $J(\theta, t) = a_y^2 + (\theta_2 s_t + \theta_1)^2$.
In Figure 2 we show the results obtained by a *state cloning* algorithm, which can be thought of as the model-based adaptation of a behavioral cloning algorithm. Specifically, the loss function is $L(s_t) = \frac{1}{T}\sum_1^T (d_t - \hat{d}_t)^2$, where $\hat{d}$ is the human demonstrated lane centerline deviation.

References

[1] "Modelling Individual Driver Trajectories to Personalise Haptic Shared Steering Control in Curves", S. Barendswaard, 2021

Building a Vehicle Digital Twin for ADAS testing and control

Ludovico Ruga, Tong Duy Son, Theo Geluk
Siemens Digital industries Software, Interleuvenlaan 68, 3001 Leuven, Belgium
ludovico.ruga@siemens.com

1 Introduction

OEMs starting development in ADAS application require the final product to be balancing both comfort and safety attributes. To provide a comprehensive testing, it is needed to develop a methodology that can highlight realistically those attributes while keeping costs and risks at the lowest level. Exclusive real world testing is not affordable, while relying only on simulation data does not guarantee the desired accuracy. To tackle this issue, by intertwining virtual environments with physical measurements a Digital Twin of the ADAS ecosystem is obtained, containing both the ego vehicle and its surroundings.

2 Vehicle Model Identification

This work focuses on the simultaneous identification of two vehicle models with separate functionalities: a Linear Parameter-Varying (LPV) control model and a high-fidelity simulated plant model. Both can help in enhancing control and testing for ADAS comfort applications.

2.1 Single-track LPV model

In modern controllers such as Model-Predictive Control (MPC), a linear single-track model is usually derived, whose parameters are identified using vehicle measurements of constant-speed maneuvers. However, the values of the obtained cornering stiffness parameters C_f, C_r vary severely with the longitudinal speed of the vehicle v_x, so a model identified with data obtained at a certain velocity will not be representative in multiple speeds scenarios. To mitigate this inaccuracy, the identification and use of a single-track LPV model is proposed, using data collected at different velocities with the test vehicle in Figure 2. Figure 1 shows the comparison between the results of an LTI model where C_f and C_r have constant values and a LPV model obtained with the tool presented in [1].

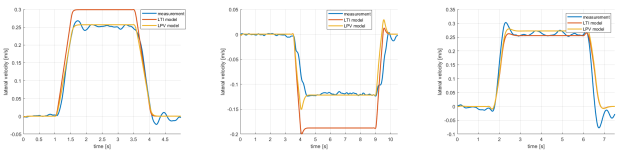

(a) 20 km/h (b) 50 km/h (c) 100 km/h

Figure 1: Comparison between LPV, LTI and physical measurement for the lateral velocity in a step steer maneuver at different speed

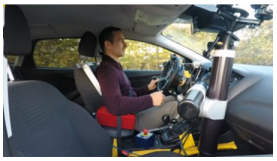

Figure 2: Test vehicle equipped with steering robot used for data collection

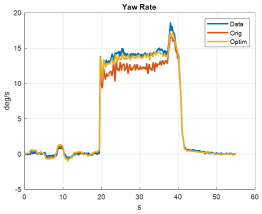

Figure 3: Performance difference between non-optimized and optimized models with respect to real data

2.2 15DOF plant model with optimized tire model

A precise representation of the physical vehicle is of paramount importance to study the dynamical responses of the vehicle to control actions and for the computation of comfort and safety metrics. For these reasons, a model more complex than the LPV one is needed; this work proposes a 15DOF model in Simcenter Amesim coupled with a Pacejka tire model. The 15DOF model has different components that need to be populated with parameters: the chassis, the suspensions and the tire. Of the three of them, the tire parameters are the ones that are more difficult to obtain; moreover, they greatly affect the accuracy of the complete model. To mitigate this issue, an optimization process has been performed with Simcenter HEEDS on the PKY1 and PKY2 parameters of the magic formula, using 250 evaluations and setting as objectives the minimization of the difference between the states of the model and the corresponding data measured on a real vehicle. Figure 3 shows the effect of the optimization on the final performance of the model.

Acknowledgments

This work was supported by the Flanders Make ICON ID2CON (Integrated IDentification for CONtrol) project. The financial support from the Flemish Agency for Innovation and Entrepreneurship (VLAIO) is gratefully acknowledged.

References

[1] Z. Retzler, A. *et al.*, "ReSMILE: Trading off model accuracy and complexity for linear parameter-varying systems," *Proceedings of ISMA 2020 - International Conference on Noise and Vibration Engineering and USD 2020*, 2020.

Implementation of collision avoidance for multi-UAVs system

Oscar Fabian Archila [1,2], Alain Vande Wouwer [1], and Johannes Schiffer [2]
[1]System, Estimation, Control and Optimization (SECO), University of Mons, Mons, Belgium
[2]Control Systems and Network Control Technology, BTU Cottbus-Senftenberg, Cottbus, Germany
[1,2]Co-tutelle BTU and UMONS
Email: archilac@b-tu.de, alain.vandewouwer@umons.ac.be, schiffer@b-tu.de

1 Introduction

One of the most critical issues for ensuring safety and high-quality performance in the control of swarms of unmanned aerial vehicles (UAVs) is collision avoidance. The current collision avoidance systems have satisfactory performance with regards to path planning optimization [1], but the computational cost and the requirements on measurement information increase with the collision avoidance precision. When implementing these algorithms, the embedded collision avoidance system faces hardware restrictions, and measurement errors. The objective of this work is to propose a combination of low-cost strategies based on geometrical rules and potential field forces that require low computational cost, and limited information about the environment.

2 Potential field collision avoidance approach

The potential field approach for collision avoidance problems is a strategy based on a virtual force F_i $(i = 1,...,n)$ with a magnitude and desired direction in order for the UAV to avoid collisions [2]. Specifically, the virtual force consists of an attraction component F_{att} that considers the target and the other drones when a formation is required and a repulsion force F_{rep}, which considers the distance to the other drones and the fixed obstacles in the terrain. The final force F_i is shown in Figure 1.

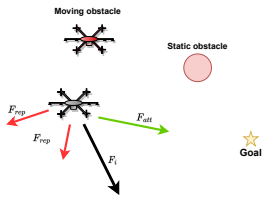

Figure 1: Collision avoidance with obstacles.

3 Geometrical rule

The potential field method sets the direction in which the UAV can avoid collisions. However, it can generate infinite oscillations in some cases when the trajectory is subject to restrictions. One such case occurs when agents fly in front of each other. It is therefore proposed to adapt the target using geometric rules.

4 Simulations results

The first simulation presented in Figure 2 shows the behavior of the algorithm in the presence of two static obstacles. When the UAV enters the critical area the UAV avoids collision. In the second case two problematic scenarios are presented: UAV head to head and UAVs with a cross-shaped path shown in Figure 2 and 3 respectively. The geometrical rule avoids the evident collision in both cases.

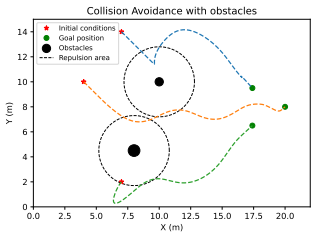

Figure 2: Collision avoidance with static obstacles.

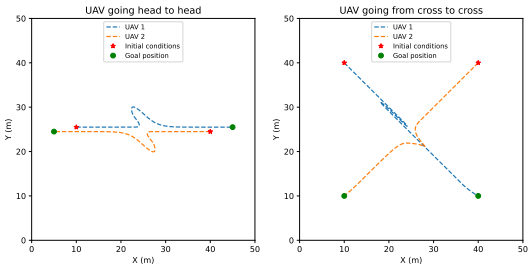

Figure 3: Collision avoidance method in two scenarios: (left) UAVs going head to head, (right) UAVs with a cross-shaped path.

References

[1] Huang, S., Teo, R. S. H., & Tan, K. K. (2019). "Collision avoidance of multi unmanned aerial vehicles: A review". Annual Reviews in Control, 48, 147-164.

[2] L Garcia-Delgado et al. "Quad-rotors formation based on potential functions with obstacle avoidance". In: *IET Control Theory & Applications 6.12 (2012)*, pp. 1787–1802.

Modelling of a Primary Flight Electromechanical Actuator considering Temperature and Production Variability

Benjamin Wauthion, Michel Kinnaert
SAAS, Université Libre de Bruxelles
50, av. Roosevelt, 1050 Bruxelles, Belgique
Email: bewauthi@ulb.ac.be

Paul Alexandre
SociétéAnonyme Belge deConstruction Aéronautique
Chaussée de Haecht 1470, 1130 Bruxelles, Belgium
Email: paul.alexandre@sabca.be

1 Introduction

The development of electrically powered actuators for flight controls has started in the nineties within the framework of the 'more electrical aircraft' trend. The design of the Electro-Hydrostatic Actuators (EHAs) has been a significant step of this evolution since it has granted the suppression of one of the three independent hydraulic systems present on a conventional aircraft [1]. Then, the Electromechanical Actuator (EMA) was presented as an alternative to EHAs since it provides a simpler solution that could improve weight, consumption and reliability figures while decreasing maintenance requirements. Nevertheless, for critical application, the reliability of the EMA technology has not yet been sufficiently demonstrated. In fact, comparing to the other kind of actuators, an EMA contains gear teeth, ball bearings and screw, which makes difficult the prediction of its behaviour over a long-time horizon for the primary flight control application. Particularly, the occurrence of excessive friction or excessive backlash has to be prohibited for safety reason. To understand those phenomena, and to be able to predict them, a model of the EMA has to be built. Based on the afore mentioned model a health monitoring procedure can be used to quantify the degradation of EMA components, and this before that a failure appears.

This abstract introduces the procedure for modelling an EMA. The main challenge is to build a model that fits a large population of EMAs that contain production variability that can be translated into parametric model uncertainty. The industrial partner, SABCA, provides data sets to analyse this production variability as well as test benches to test and validate the EMA model.

2 The approach

The model describes the EMA (constituted of an electric motor, a gear box, a nut/screw mechanism, and a rod) and its environment, namely, the controlled surface (CS) linked to the EMA and the external force applied on the CS. This external part models either an in-flight aerodynamic force or the interaction with the test bench. Figure 1 gives an overview of the system.

In order to describe the friction and backlash phenomena, the model contains on the one hand, a three parameters Stribeck friction model, and on the other hand a three parameters backlash model. The friction model combines stiction and viscous frictions terms and accounts for dependence with respect to the load. The backlash model includes a "Pure backlash" zone (inherent to the mechanical components) and a "stiffness" zones (corresponding to the contraction of the EMA components). A state space model of the EMA can then be written as follow.

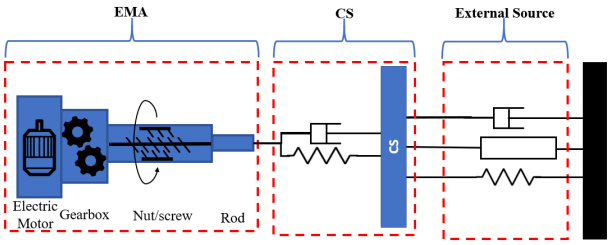

Figure 1: Schematic view of the EMA and its environment

$$\dot{X} = f(X, U, \Phi_0) \tag{1}$$

Where X and U are the states and inputs vectors and Φ_0 is the vector of friction and backlash parameters associated to a healthy EMA. By exploiting the database of produced EMAs, a parameter vector Φ_0 is identified for each EMA. A non-negligible dispersion of the parameter values due to the production variability is found. To approach the probability distribution of the parameters a combination of normal distribution is used. By taking this parameter variability into account, the model is then able to represent the entire SABCA actuator fleet.

In parallel, using the SABCA tests benches, a study of the evolution of the parameters with temperature is performed in order to include a temperature dimension in the model.

3 Acknowledgement

This work is supported by the Brussels-Capital Region (Innoviris) through the MONISA project.

References

[1] D. Van Den Bossche, "The A380 flight control electrohydrostatic actuators, achievements and lessons learnt", 25th Inter. Congress of the Aeronautical Sciences, 2006.

Control in Gravitational Wave detectors

Mathyn van Dael[1,2,*], Gert Witvoet[1,3], Bas Swinkels[2], Tom Oomen[1,4]
[1] Control Systems Technology, Eindhoven University of Technology, Eindhoven, The Netherlands
[2] Nikhef, Amsterdam, The Netherlands
[3] Optomechatronics Department, TNO, Delft, The Netherlands
[4] Delft Center for Systems and Control, Delft University of Technology, Delft, The Netherlands
*Email: m.r.v.dael@tue.nl

1 Introduction

Gravitational Waves are distortions of *spacetime* which are induced by cosmic events such as the merger of black holes. Current generation detectors such as Virgo [1] and LIGO [2] have been able to measure these spatial distortions which are in the order of 1×10^{-18} m. Next generation detectors such as Einstein Telescope [3] aim to measure distortions in the order of 1×10^{-20} m, allowing to look even further into space.

2 Measurement principle

These distortions of space are measured using the concept of interferometry. In Fig. 1, a basic interferometer is shown, which is a simplified configuration of a typical Gravitational Wave detector. The laser on the left emits a beam of light through the Beam Splitter (BS), splitting the beam into two orthogonal directions: to the right and upwards. The individual beams are reflected back by the End Mirrors (EM) and subsequently interfere at the BS. The interference pattern, determined by the relative length difference between the BS and two EMs, is measured by a photodiode (PD). Gravitational Waves have the property that they stretch *spacetime* in a certain direction and simultaneously contract it in the orthogonal direction by the same amount, hence changing the measured interference pattern.

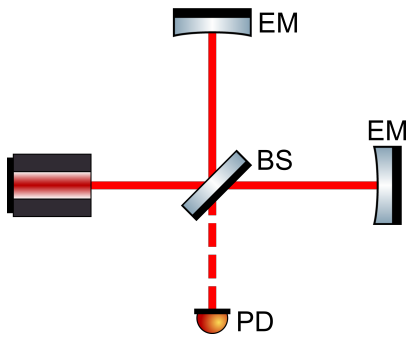

Figure 1: Simplified configuration of an interferometer used in Gravitational Wave detectors.

3 Control challenges

Control systems play a crucial role in the operation and performance of Gravitational Wave detectors. One of their main applications is to actively align the mirrors with respect to each other, both in the longitudinal direction of the beam as well as their angular orientations. The mirrors and other optical components must furthermore also be isolated from environmental disturbances, requiring the use of multi-stage vibration isolation systems. Passive isolation is typically not sufficient, necessitating active control of the isolation stages. Both types of control systems are often MIMO problems that deal with different types of disturbances, yielding a variety of challenges when designing the controllers for these systems.

The sensitivity of the detector is solely determined by a single degree of freedom (DoF), which is the difference in length between the two arms. Each disturbance couples through different subsystems to the differential arm length and many of these disturbances are attenuated on a subsystem level. A more global approach to the control design may yield further improvements in terms of optimizing the detector sensitivity.

4 Technological challenges

Current and next generation Gravitational Wave detectors face a wide variety of technological challenges. Advancements in the control systems can contribute to tackling many of these challenges and therefore lead to improved detection capabilities.

References

[1] F. Acernese *et. al.*, "Advanced Virgo: a second-generation interferometric Gravitational Wave detector," Classical and Quantum Gravity, vol. 32, no. 2, p. 024001, 2014.

[2] J. Aasi *et. al.*, "Advanced LIGO," Classical and Quantum Gravity, vol. 32, no. 7, p. 074001, 2015.

[3] M. Punturo *et. al.*, "The Einstein Telescope: a third-generation gravitational wave observatory," Classical and Quantrum Gravity, vol. 27, no. 19, p. 194002, 2010.

Tool interoperability for efficient model-based system design

Sander Thuijsman
Eindhoven University of Technology, Eindhoven, The Netherlands
s.b.thuijsman@tue.nl

1 Introduction

The design process of Cyber-Physical Systems of Systems (CPSSs) consists of a multi-disciplinary engineering process focusing on functional specification and verification of scenarios and a mono-disciplinary engineering process focusing on the realization of these scenarios in a platform composed of mechanical, optimal, electrical and software components. These engineering disciplines each use a specific set of engineering methods, tools and technologies that are loosely coupled both on a syntactic and on a semantic level. This has a major impact on engineering efficiency; It hampers verification sufficiently early in the development process, especially concerning system-wide (performance and safety) aspects (e.g. throughput and collision avoidance). Additionally, it hinders system evolvability and deployment, i.e. introducing new scenarios or adaptation of existing ones. To significantly improve engineering efficiency seamless syntactic and semantic interoperability between the multi-disciplinary modelling tools need to be established, enabling rapid deployment of (new) machine scenarios and effective prediction and trading-off of key system aspects concerning performance and correctness.

2 Involved tools

The following tools each tackle one or more aspects in the engineering of CPSSs:

1. LSAT[1]***:*** LSAT is short for Logistics Specification and Analysis Tool, and can be used for system specification through resources that consist out of peripherals. These peripherals can execute actions. Activities are aggregations of actions, that describe a piece of behavior in the system, and can be dispatched on the system. LSAT also has visualization techniques such as Gantt charts, movement trajectory plots, and graphical editing to aid the engineer.
2. PLE tool: The Product Line Engineering (PLE) tool is used for variability management in of the system, and can automatically validate and derive product instances within a product line.
3. CIF[2]***:*** CIF, as part of the Eclipse Supervisory Control Engineering Toolkit (Eclipse ESCET^{TM}), is an automata-based tool and language, and is used to specify system behavior, formulate behavioral requirements, and perform supervisory controller synthesis to obtain a correct-by-construction supervisory controller that adheres to the requirements.
4. SDF3[3]***:*** SDF3 is used for makespan analysis, to find the optimal behavior that, for instance, produces products as quickly as possible.
5. mCRL2[4]***:*** mCRL2 is a model checking tool in which properties of system behavior can be specified and verified. This can guarantee particular behaviors in the system, and when a property does not hold a counter-example is given to aid in solving the problem.
6. AEE: The Activity Execution Engine (AEE) is used to go from a model of the system and controller, to deployment of the controller on the physical system. Through the AEE, the timing requirements as specified in LSAT are adhered to.

3 Toolchain and interoperability

The introduced tools all have their own specific functionality. With their combined functionality, they can be used in a workflow for model-based system engineering of CPSSs. An example for such a workflow is as follows:

1. A product line is specified in LSAT.
2. Given a feature configuration, an LSAT product instance can be derived with the PLE tool.
3. Safety requirements are specified, and a supervisory controller is synthesized with CIF.
4. Using the timing information given in the LSAT model, SDF3 is used to select the optimal dispatching sequence of activities from the safe behavior of the supervisory controller.
5. With mCRL2, progress properties are verified for the behavior that results from the obtained dispatching sequence.
6. The obtained control strategy can be deployed on the physical system using the AEE.

Since all tools use their own semantics, automatic model translators have been developed to obtain equivalent models with which the tools can perform their operations. The Arrowhead Framework is used as an Internet Of Things solution to realize seamless integration between the tools. This means that the services from the tools can be used, without unnecessary manual steps. In this way, concept flexible and efficient model based design of CPSSs can be performed.

Research leading to these results has received funding from the EU ECSEL Joint Undertaking under grant agreement n^{o} 826452 (project Arrowhead Tools) and from the partners national programs/funding authorities.

[1] https://esi.nl/research/output/tools/lsat

[2] https://www.eclipse.org/escet/, 'Eclipse', 'Eclipse ESCET' and 'ESCET' are trademarks of Eclipse Foundation, Inc.

[3] https://www.es.ele.tue.nl/sdf3/

[4] https://www.mcrl2.org/

Hardware-in-the-loop testing for the Swalmen tunnel using automatically generated PLC code

L. Moormann
Eindhoven University of Technology
l.moormann@tue.nl

J.M. van de Mortel-Fronczak
Eindhoven University of Technology

W.J. Fokkink
Vrije Universiteit Amsterdam

J.E. Rooda
Eindhoven University of Technology

1 Introduction

Developing supervisory controllers for large-scale cyber-physical systems is becoming increasingly difficult due to large numbers of actuators and sensors involved. Supervisor synthesis, introduced in [1], enables control engineers to automatically derive such a supervisory controller from a model of the plant and a model of the control requirements. Model simulation is often used to validate the controlled system behavior. While simulation is a powerful tool allowing for a quick analysis, it lacks certain aspects of an implemented controller. These aspects include the execution on the control hardware and communication with subsystems and user interfaces (UIs).

To include these aspects in the validation process, hardware-in-the-loop (HIL) simulation can be used, where the supervisory controller is implemented on the control hardware and where it communicates with simulated subsystems and UIs. Real-life case studies that use supervisor synthesis and HIL simulation are, however, few in number. In this work, we present a case study that has been performed for the development of a supervisory controller for the Swalmen tunnel.

2 The Swalmen tunnel

The Swalmen tunnel is a road tunnel in the Netherlands that is 400 meters long and that consists of two traffic tubes and an escape route between them. The northern entrance of the Swalmen tunnel is shown in Figure 1.

Figure 1: Northern entrance of the Swalmen tunnel.

The main function of the supervisory controller is to monitor the situation in the tunnel using sensors, and to correctly handle an emergency when it is detected. A supervisory controller has been synthesized from a plant model consisting of 180 automata and 414 requirement models.

3 HIL simulation

The first step after synthesis is obtaining PLC code from the supervisory controllers. Because of the formal description of the controller model, automatic PLC code generation is possible. The inputs for this generator are the supervisory controller model, and a hardware mapping that connects the events in the controller to the inputs and the outputs of the PLC. For the Swalmen tunnel, PLC code is generated for an ABB PLC containing 17620 lines of code, 260 input signals, and 46 output signals.

To perform HIL simulation, a HIL setup is used. This setup consists of the PLC and two PCs that simulate the UI and the virtual tunnel, respectively. These simulation models are created using the Ignition SCADA software which can read and write the variables in the PLC through an OPC UA server. The simulation models are visualized and connected to the PLC variables, e.g., a button in the UI is connected to the corresponding input variable of the PLC.

HIL simulations have been performed for the Swalmen tunnel to validate the controlled tunnel behavior. In all scenarios, the observed behavior corresponded to the expected behavior. Furthermore, the PLC performance has been analyzed by looking at the PLC cycle time, which was the optimal value of 10ms at all times.

4 Conclusions

In a case study for the Swalmen tunnel, PLC code is automatically generated from a synthesized supervisory controller, and subsequently implemented in a HIL setup. Through HIL simulations, the controlled behavior has been validated and it has been determined that the PLC performance is optimal.

References

[1] P. J. Ramadge and W. M. Wonham. “Supervisory control of a class of discrete event processes”, in SIAM Journal on Control and Optimization, 25(1), pp. 206-230, 1987.

Non-collocated vibration suppression using delayed feedback

Haik Silm and Wim Michiels
Department of Computer Science, KU Leuven
Celestijnenlaan 200A, 3001 Leuven, Belgium
Email: haik.silm@kuleuven.be

Tomáš Vyhlídal
Dept. Instrumentation and Control Engineering
Faculty of Mechanical Engineering, CTU
Technická 4, 160 07 Prague 6, Czechia

1 Introduction

The delayed resonator [1] is an established concept of tuned vibration absorption. It is an peculiar application of a delay, which combined with an accelometer provides a efficient way to turn a passive absorber virtually into a an undamped mass-spring. In the ideal case it provides complete suppression of the vibrations, however it relies on placing the absorber close to the target of suppression.

Recently there has been steps towards the so called non-collocated vibration suppression problem, as represented in the figure for a small lumped mass-spring system. The goal of this work is to extend the delayed resonator design in this general case. The suppression effect cannot rely anymore directly on anti-resonance but instead a more general equilibrium of forces. Consequently, we have to look at the transmission zeros from the vibration force to the displacement of the target mass.

2 Transmission zero assignment

To assign the zeros with the help of a delayed-resonator, we take a state-space view of the model in Figure 1,

$$\dot{x}(t) = Ax(t) + Bf(t) + B_a u_a(t)$$
$$y(t) = Cx(t), \quad y_a(t) = C_a x(t).$$

Here $A \in \mathbb{R}^{n\times n}$ is the dynamics of a mass-spring-damper system, $B \in \mathbb{R}^{n\times 1}$ is the input matrix describing where the vibration force $f(t) = \sin(\omega t)$ acts and $C \in \mathbb{R}^{1\times n}$ specifies the position of the target body to be suppressed. The matrices $B_a \in \mathbb{R}^{n\times 1}$ and $C_a \in \mathbb{R}^{1\times n}$ specify the location of the vibration absorber.

It can be shown that with the delayed feedback law $u_a(t) = g\dot{y}_a(t-\tau)$ a pair of transmission zeros can be placed to the imaginary axis at $\pm j\omega$ by selecting the gain and delay as

$$g = \begin{cases} \frac{1}{|z|} \\ -\frac{1}{|z|} \end{cases} \quad \text{and} \quad \tau = \begin{cases} \frac{\arg(z)}{\omega} & \text{if } \mathrm{Im}(z) \geq 0 \\ \frac{\arg(z)+\pi}{\omega} & \text{if } \mathrm{Im}(z) < 0 \end{cases},$$

where $z = \mathrm{j}\omega \begin{bmatrix} C_a & 0 \end{bmatrix} \begin{bmatrix} \mathrm{j}\omega I - A & -B \\ -C & 0 \end{bmatrix}^{-1} \begin{bmatrix} B_a \\ 0 \end{bmatrix}$. Note that (due to the periodicity) the value for the delay τ is actually not unique, however the solution with the smallest delay is preferable for the sake of overall system stability.

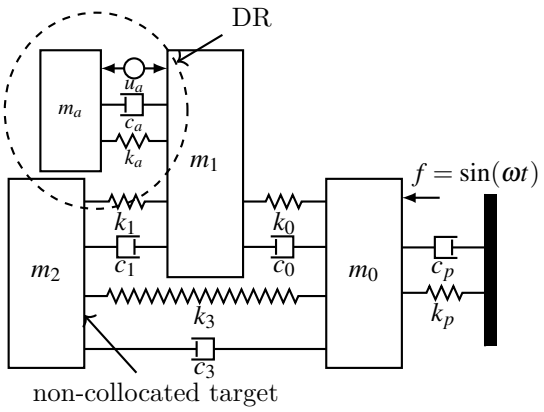

Figure 1: Delayed-resonator (DR) in non-collocated vibration suppression

3 Open problems

A cost of the simplicity in the design of the delayed resonator is that closing the loop using acceleration feedback leads to a *neutral* time-delay system and its detrimental effect on stability is even more critical in the non-collocated case. A further complication comes form the fact that the tuning might be interdependent on a higher-level controller, as in a previous work where an additional controller was assigned the task of stabilization [2].

Finally, in the collocated case the design of vibration absorbers in general and the delayed resonator in specific is well studied [3]. In contrast, questions like where to place the absorber and how to dimension it in the non-collocated case is still open and will be addressed in the talk.

References

[1] N. Olgac and B. T. Holm-Hansen, "A novel active vibration absorption technique: delayed resonator," Journal of Sound and Vibration, vol. 176, no. 1, pp. 93–104, 1994.

[2] H. Silm, W. Michiels, and T. Vyhlídal, "Stabilization with zero location constraints for delay-based non-collocated vibration suppression," IFAC-PapersOnLine, vol. 54, no. 18, pp. 121–126, 2021.

[3] T. Vyhlídal, D. Pilbauer, B. Alikoç, and W. Michiels, "Analysis and design aspects of delayed resonator absorber with position, velocity or acceleration feedback," Journal of Sound and Vibration, vol. 459, p. 114831, 2019.

A first hands-on mechatronics project for engineering students using active magnetic bearings

Laurens Jacobs[1,2], Jan Swevers[1,2] and Goele Pipeleers[1,2]
[1]MECO Research Team, Dept. of Mechanical Engineering, KU Leuven, B-3001 Leuven
[2]DMMS lab, Flanders Make, B-3001 Leuven
laurens.jacobs@kuleuven.be

1 Introduction

Since the recognition of mechatronics as a full-fledged engineering discipline, many researchers, teachers and institutions have been developing dedicated study programs for mechatronic engineering students. The inherent challenges of engineering fields with an interdisciplinary nature, such as mechatronics, are dealt with in many different ways at universities and training centers all over the world [1, 2, 3, 4]. Nevertheless, there is a clear consensus that a sufficient amount of hands-on experience is key to master the design, analysis and implementation aspects of typical mechatronic engineering problems [4, 5].

At KU Leuven, the structure of the mechatronic engineering program is mainly determined by the general blueprint and the broad scope of the Belgian academic engineering curricula, which impose rather strict timing constraints. As a result, students have only recently become familiar with systems modeling and basic control design techniques by the time they are gaining their first hands-on experience with a real mechatronic system. In this presentation, we introduce the assignments of an integrated project on active magnetic bearings (AMBs) which has been tailored for engineering students in this situation. Although AMB systems form an intriguing technology arousing a lot of enthusiasm of these future engineers, rotors supported by AMBs often have fast, nonlinear, highly-coupled dynamics. Therefore, it is important for them to receive clear instructions and guidelines on their approach in order to successfully levitate the rotor of a lab-scale magnetic bearing setup with the standard linear systems and control theory concepts they are acquainted with only.

2 Hardware description

The lab-scale magnetic bearing setup is based on the commercially available MBC500R system by LaunchPoint Technologies [6]. We replaced the high-speed rotor, however, by a symmetric in-house designed shaft, the flexible modes of which are irrelevant for the control design (see Section 3 for the motivation). The 4 radial bearing control currents are considered as inputs, whereas the 4 radial rotor displacements with respect to the bearing center are considered as outputs; see the scheme in Fig. 1. The axial motion of the rotor is constrained by a plain bearing. A standard real-time computer with a high-level user interface is connected through the analog interface of the setup.

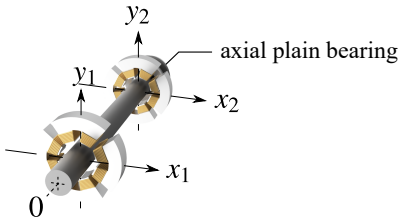

Fig. 1: Conceptual drawing of a rotor radially supported by AMBs

3 Assignment

The assignment is twofold. On the one hand, it comprises the rigid-body modeling of the rotor-bearing system. By only considering rigid-body dynamics, the system's behavior is straightforward to derive from first principles. Flexible dynamics would typically call for finite-element modeling and parameter tuning, which is out of the scope of the project: the system is unstable and the required closed-loop identification approaches to find the actual parameters have not been covered in the students' program yet. On the other hand, the students are asked to design a stabilizing feedback control law, based on their derived model, for levitating a shaft that is not rotating. Reducing the scope of a classic rotordynamic problem as such offers the opportunity of SISO control design: it is well-known that the rigid-body dynamics of a symmetric rotor at standstill can be completely decoupled (diagonalized) by applying appropriate static input-output transformations [7].

References

[1] B. J. Furman and G. P. Hayward. "Asynchronous hands-on experiments for Mechatronics education". *Mechatronics* 12 (2), March 2002.

[2] S. Meek et al. "Mechatronics education in the Department of Mechanical Engineering at the University of Utah". *Mechatronics* 13 (1), February 2003.

[3] V. Giurgiutiu et al. "Mechatronics/microcontroller education for mechanical engineering students at the University of South Carolina". *Mechatronics* 15 (9), November 2005.

[4] Y. Wang et al. "Mechatronics education at CDHAW of Tongji University: Laboratory guidelines, framework, implementations and improvements". *Mechatronics* 19 (8), December 2009.

[5] M. Grimheden. "Mechatronics Engineering Education". PhD thesis, KTH School of Industrial Engineering and Management, November 2005.

[6] LaunchPoint Technologies. "Magnetic Bearing Control System: Engineering Lab Experiment". URL: https://www.launchpnt.com/products/magnetic-bearing-control-engineering-lab-experiment.

[7] G. Schweitzer (ed.) and E. Maslen (ed.). "Magnetic bearings: Theory, design, and application to rotating machinery". Springer, 2009.

Acknowledgement The authors wish to thank Wim Wien and Bart De Schutter of the Delft Center for Systems and Control (DCSC, TU Delft) for making various hardware parts available to us. Laurens Jacobs is a postdoctoral fellow of Flanders Innovation and Entrepreneurship (VLAIO, project HBC.2021.0200).

Model based control of soft robots aiming for trajectory tracking

Mahboubeh Keyvanara
Faculty of Mechanical Engineering
Dynamics and Control Group
Eindhoven University of Technology
The Netherlands
m.keyvanara@tue.nl

Arman Goshtasbi
Faculty of Engineering Technology
University of Twente
The Netherlands
a.goshtasbi@student.utwente.nl

Irene Kuling
Faculty of Mechanical Engineering
Dynamics and Control Group
Eindhoven University of Technology
The Netherlands
i.a.kuling@tue.nl

1 Abstract

Research on dynamic modeling and control of mechanical systems is currently taking on different challenges. The dynamics of mechanical systems play a fundamental role in the design for their operational functionality, meaning, the thorough understanding of the dynamics of engineering systems, including aspects of both modelling and analysis, is a key discipline. In addition, it is an important prerequisite to the automatic control of engineering systems, and, it is tightly connected to the discipline of systems and control, which focuses on the fundamentals of ensuring that mechanical systems can operate safely and with desired performance. Control is also the central factor in making mechanical systems increasingly autonomous.
In this field, designing mechanical devices that can have compliance and mechanical robustness needed for safe and passive interaction with an unknown environment is desired for many applications such as health, agriculture and many others. This goal can be achieved via using softer materials in the design procedure of mechanical systems. Some nonlinearities in a dynamic model can arise from the material characteristics of the system and this can also cause uncertainties and also controlling these systems can become very intricate as model based control might not be achievable any more. For example, traditional rigid robots are made from rigid and dense materials that can guarantee accurate and repeatable motions. Yet, soft robotics is a relatively new subfield of robotics with the aim to improve the motion complexity and environmental robustness that is generally lacking its rigid counterpart [1-3]. Despite numerous beneficial factors of low-compliance [4], this imposes numerous challenges on modeling and control. The dynamics of a continuously deformable soft robot are in theory of the infinite-dimensional nature [5,6]. This paradigm shift has also further emphasized the challenges in control-oriented modeling of soft robots; as their physical description are often more suited for a Partial Differential Equations (PDEs) rather than Ordinary Differential Equations (ODEs).
In this research we investigate a reduced-order ODE model for continuum soft robots with the aim of finding a reasonable balance between the model precision and its applicability for control. This model should also be able to incorporate the hyper-elastic and visco-elastic properties of the robot. Using this model, the goal of controlling the soft robot to track a desired trajectory is explored using control architectures in classic robotics with the aim of accurately controlling the posture of the soft robot.

References

[1] Kriegman S, Blackiston D, Levin M, et al. A scalable pipeline for designing reconfigurable organisms. Proc of the National Academy of Sciences 2020; 117:1853–1859.

[2] Godage I, Medrano-Cerda G, Branson D, et al. Modal kinematics for multisection continuum arms. Bioinspiration Biomimetics 2015; 10:035002.

[3] Falkenhahn V, Mahl T, Hildebrandt A, et al. Dynamic modeling of bellows-actuated continuum robots using the euler-lagrange formalism. IEEE Trans on Robotics 2015; 31:1483–1496.

[4] Galloway K, Becker K, Phillips B, et al. Soft robotic grippers for biological sampling on deep reefs. Soft Robotics 2016; 3:23–33.

[5] Duriez C. Control of elastic soft robots based on real-time finite element method. Proceedings - IEEE International Conference on Robotics and Automation 2013; 3982–3987

[6] Jones B and Walker I, Kinematics for multisection continuum robots, IEEE Transactions on Robotics 2006; 22:43–55.

Wednesday - July 6, 2022
9:00 - 11:00 (WeP)

Hybrid Control Implementation Analysis based on the Finite Set Model Predictive Control Design

Shafaq Gul and Frederik De Belie
Department of Electrical Energy, Metals, Mechanical Constructions & Systems
Ghent University, Member of Flanders Make
Technologiepark 9052 Zwijnaarde
Email: Shafaq.gul@ugent.be ; Frederik.DeBelie@UGent.be

1 Abstract

This paper deals with finite set model predictive control (FS MPC) design for hybrid control analysis. The method is deemed suitable to adapt to variations in the system. It does so by considering the vicinity of the previous control input while searching for a more effective control input. The effectiveness of the technique is explored in tracking the problem of a mass spring damper system.

2 Methodology

Over the last decades, the finite set mpc has gained much attention in the power electronics community due to the discrete nature of the power switches, the low and finite amount of switches besides encompassing benefits of model predictive control [1]. In this paper, in order to improve the performance of the previous controller, a model predictive controller (FS MPC) was designed, to be cascaded in series. The inevitable system variations often deteriorates the previous control performance thus rendering the control input insuffient and there is a need for the modified optimal control input. The designed FS MPC intelligently search for the optional values through an algorithm based on shooting method renowned for the nonlinear problems . Commonly, the shooting method is used in the literature to solve the boundary value problems [2] however, in this study it was used to shoot for the optimum control input, starting from the previous control input, to make the MPC control objective function approach zero. The detailed algorithm is presented in Figure1 and will be elaborated on in the final paper.

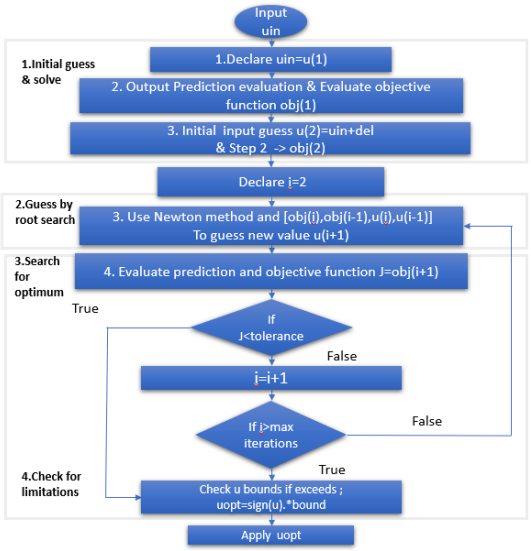

Figure 1.Finite control set mpc based on shooting method

3 Results

The methodology was implemented on a mass spring damper system in matlab/Simulink for the unit step tracking case study. The objective function used in the FS MPC was $\sum_{i=0}^{3}(y_{k+i}-r_k)^2$.In the first case (Figure 2), the linear quadratic integrator controller (LQI) was designed for tracking the step input (blue line).

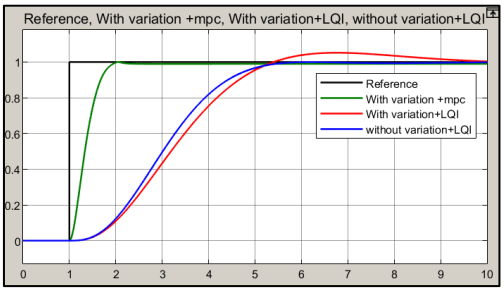

Figure 2. LQI controller response with FS MPC

After system variation introduction, delayed response along with overshoot was observed (red line). In this case, proposed finite set mpc was used in series with LQI with variation (green line) the rise time was increased along with the acceptable overshoot phenomena.

In the second case, instead of LQI, conventional MPC was designed through Simulink mpc block (blue line). In this case, variation was introduced by changing one of the parameters of the system by 20% (red plot), the response badly deteriorated. Afterwards, finite set mpc was added in cascade (green plot) the response settling time was increased without having overshoot.

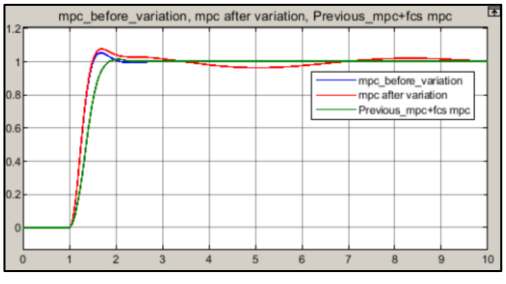

Figure 3. Conventional mpc response with FS MPC

References

[1] B. Yu, W. Song, K. Yang, Y. Guo, and M. S. R. Saeed, "A Computationally Efficient Finite Control Set Model Predictive Control for Multiphase PMSM Drives," *IEEE Trans. Ind. Electron.*, vol. 0046, no. c, 2021, doi: 10.1109/TIE.2021.3131858.

[2] K. S. Sahu and M. K. Jena,"Combining the Shooting Method with an Operational Matrix Method to Solve Two Point Boundary Value Problems," *International Journal of Applied and Computational Mathematics*, vol. 7, no. 2. 2021, doi: 10.1007/s40819-021-00967.

Design Methods for Sampled-Data Systems

L.M. Spin[1] and M.C.F. Donkers[1]
[1] Control Systems Group, Eindhoven University of Technology, Netherlands
Email: l.m.spin@student.tue.nl, m.c.f.donkers@tue.nl

1 Introduction

The vast majority of control algorithms are implemented on digital hardware. In recent years, analysis and synthesis of linear sampled-data (SD) systems has been shifted from using lifting technique, see, e.g. [1], to using jump-flow (JF) systems, see, e.g. [2], that allow for mixed discrete/continuous specifications. However, design methods, such as loop shaping or mixed-sensitivity approaches [3] are not tailored for SD systems. In this work, we aim at providing a more general dissipativity framework for JF systems than in [2], enabling the development of SD performance shaping techniques that use the intuition of well-known LTI shaping techniques [3].

2 Dissipativity-Based Control Synthesis

In this work, we consider a closed-loop (CL) interconnection $\mathscr{T}$ between a generalized SD plant $\mathscr{P}$ and a discrete-time (DT) controller $\mathscr{K}$ with sampling time $t_k = hk$. The CL SD systems has the following JF state-space realization:

$$\mathscr{T}: \begin{cases} \dot{\xi}(t) = \mathscr{A}_c\xi(t) + \mathscr{B}_c w_c(t), & \text{for } t \in (t_k, t_{k+1}] \\ \xi(t_k^+) = \mathscr{A}_d\xi(t_k) + \mathscr{B}_d w_d[k] \\ z_c(t) = \mathscr{C}_c\xi(t) + \mathscr{D}_c w_c(t) \\ z_d[k] = \mathscr{C}_d\xi(t_k) + \mathscr{D}_d w_d[k], \end{cases} \tag{1}$$

where $\xi(t) \in \mathbb{R}^{n_\xi}$, $w_c(t) \in \mathbb{R}^{n_{w_c}}$, $w_d[k] \in \mathbb{R}^{n_{w_d}}$, $z_c(t) \in \mathbb{R}^{n_{z_c}}$ and $z_d[k] \in \mathbb{R}^{n_{z_d}}$ denote the state, continuous-time (CT) disturbance, DT disturbance, CT performance channels and DT performance channel, respectively. In this work, we have developed LMI-based controller synthesis results that minimize the SD $\mathscr{H}_\infty$-norm

$$\|\mathscr{P}\|_{\mathscr{H}_\infty} = \sup_{w_c \neq 0, w_d \neq 0} \frac{\sqrt{\|z_c\|_{\mathscr{L}_2}^2 + \|z_d\|_{\ell_2}^2}}{\sqrt{\|w_c\|_{\mathscr{L}_2}^2 + \|w_d\|_{\ell_2}^2}} \tag{2}$$

and enable the development of controller synthesis design methods for SD systems.

3 Controller Design Methods

The availability of sufficiently general synthesis techniques allow for the development of design methods that are typically formulated as a generalized plant, in which the plant is augmented with LTI filters that encode desired time-domain performance criteria. To enable the design of these filters, we adopt an impulse sampler. This allows for a $\mathscr{L}_2$ time-domain interpretation of the SD system and, hence, a frequency-domain interpretation, using the so-called fundamental frequency analysis. This allows for the development of waterbed effect-like relations for SD systems.

4 Results

Let us consider now the problem of re-designing a CT controller (that satisfies certain closed-loop specifications) as a DT controller. The generalized plant is shown in Figure 1. In Figure 2, we show the step response of the CL system with 1) the CT (non-sampled-data) controller, 2) a Tustin discretization and 3) the DT controller designed using the SD framework. In this figure, where we have taken a large sample interval, it can be observed that sampling leads to performance loss, yet the SD controller performs better than the Tustin discretization.

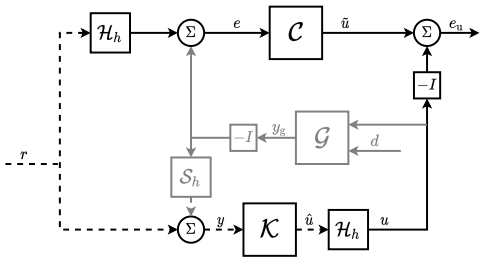

Figure 1: Generalized plant for SD controller redesign.

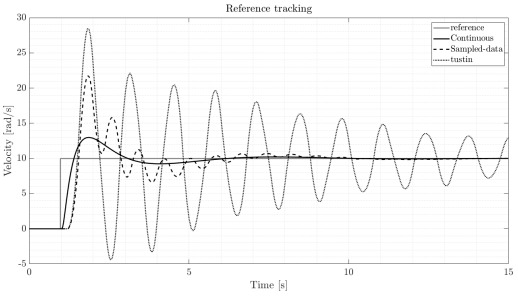

Figure 2: Continuous-time domain interpretation of SD system.

References

[1] T. Chen and B. A. Francis, *Optimal sampled-data control systems*. Springer Science & Business Media, 2012.

[2] H. Dreef and M. Donkers, "$\mathscr{H}_\infty$ and $\mathscr{H}_2$ optimal sampled-data controller synthesis: A hybrid systems approach with mixed discrete/continuous specifications," *Automatica*, vol. 125, p. 109382, 2021.

[3] S. Skogestad and I. Postlethwaite, *Multivariable feedback control: analysis and design*, vol. 2. Wiley, 2007.

On the steady–state behavior of finite–control–set MPC with an application to high–precision switched amplifiers

Duo Xu and Mircea Lazar
Control Systems Group, Eindhoven University of Technology, The Netherlands
Email: {d.xu, m.lazar}@tue.nl

1 Introduction

Motivated by increasing precision demands for switched amplifiers, this paper addresses the problem of model predictive control (MPC) design for discrete–time linear systems with a finite control set (FCS). To improve the steady–state behavior of FCS–MPC, a cost function is formulated to penalize the tracking error with respect to a state and input steady–state limit cycle.

2 Problem description

Switched amplifiers are operated by fast switching among of finite number of switch configurations. The model of switched amplifiers is captured by the following class of discrete–time linear systems with a finite control set:

$$\begin{aligned} x(k+1) &= Ax(k)+Bu(k) \\ y(k) &= Cx(k) \end{aligned} \tag{1}$$

where $x(k) \in \mathbb{R}^n$ is the system state, $u(k) \in \{0,1\}^m$ denotes the discrete system inputs, which represent the switching state and $y(k) \in \mathbb{R}^q$ is the system output. The vector $u(k)$ belongs to a finite control set $\mathbb{U}$. Generally, the system output $y(k)$ cannot be controlled to maintain the exact output reference y_{ref} for the averaged model at steady state; instead, the output will oscillate around y_{ref}, which will generate a periodic trajectory, also known as a limit cycle.

In this work, an optimal limit cycle $\overline{X} := \{\bar{x}(0), \ldots, \bar{x}(p-1)\}$ at steady state with a fixed length $p \geq 1$ is derived [1]. $\overline{X}$ is optimized to generate a suitable trajectory of $y(k)$, while satisfying certain criteria such as least mean deviation with respect to y_{ref} or minimum ripple amplitude. Then, the cost function of FCS–MPC is designed such that the convergence to the optimal limit cycle is achieved.

3 Approach

For a derived optimal limit cycle $\overline{X}$ and its corresponding optimal input $\overline{U}$, the FCS–MPC for tracking this optimal limit cycle can be formulated as the following integer optimization problem:

$$\begin{aligned} \min_{u_{0|k},\ldots,u_{N-1|k}} \quad & J\left(x(k), U_k, \overline{X}, \overline{U}\right) = \|(x_{N|k} - \bar{x}_{N|k}\|_P^2 \\ & + \sum_{i=0}^{N-1} \|x_{i|k} - \bar{x}_{i|k}\|_Q^2 + \|u_{i|k} - \bar{u}_{i|k}\|_R^2 \\ \text{s.t. } & x_{i+1|k} = Ax_{i|k} + Bu_{i|k}, \quad \forall i = 0,\ldots,N-1 \\ & u_{i|k} \in \{0,1\}^m, \quad \forall i = 0,\ldots,N-1 \\ & x_{i|k} \in \mathbb{X}, \quad \forall i = 1,\ldots,N \end{aligned} \tag{2}$$

where

$$\begin{aligned} \bar{x}_{i|k} &= \bar{x}(k+i \bmod p), \quad \forall i = 0,\ldots,N, \\ \bar{u}_{i|k} &= \bar{u}(k+i \bmod p), \quad \forall i = 0,\ldots,N-1, \end{aligned} \tag{3}$$

If the optimization problem (2) is always feasible, the asymptotic convergence is guaranteed if the matrix A is Schur stable and the terminal cost matrix P is chosen a positive definite solution of the linear matrix inequality $-P+Q+A^\top PA \prec 0$.

The limit cycle tracking FCS-MPC has been implemented for one switched amplifier model [2], Figure 1 presents the trajectory of two of the system states. It can be observed that the system states converge to the optimal state limit cycle $\overline{X}$ asymptotically.

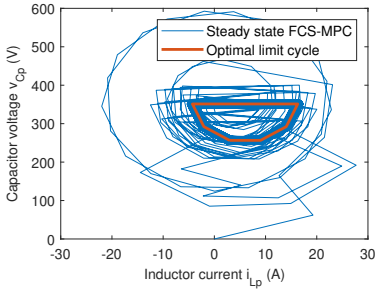

Figure 1: Trajectory of two system states of the amplifier.

4 Outlook

For future work it is of interest to develop more general stabilizing designs for FCS–MPC and to analyze merging of different cost functions with FCS–MPC to improve both transient and steady–state behavior.

References

[1] L. N. Egidio, H. R. Daiha, and G. S. Deaecto, "Global asymptotic stability of limit cycle and H_2/H_∞ performance of discrete-time switched affine systems," Automatica, vol. 116, p. 108927, 2020.

[2] T.T. Nguyen, "State-Feedback Controller Design for Short Stroke and Long Stroke Power Amplifiers" MSc Internship, Eindhoven University of Technology, 2012.

Data-driven distributionally robust iterative risk-constrained model predictive control

Alireza Zolanvari and Ashish Cherukuri
ENTEG, University of Groningen
Email: {a.zolanvari,a.k.cherukuri}@rug.nl

1 Introduction

Practical control systems often operate in uncertain environments. Safe optimal control in such situations can be modeled in many different ways. In this regard, we define an infinite-horizon optimal control problem for a discrete-time deterministic system, where the state is subjected to a conditional value-at-risk constraint. Then, we design a distributionally robust iterative MPC scheme that combines the notions of learning model predictive control [1] and distributionally robust risk constraints [2] to progressively approximates the solution of the infinite-horizon problem.

2 Problem statement and Method

Consider the following discrete-time system:

$$x_{t+1} = f(x_t, u_t), \tag{1}$$

where $f : \mathbb{R}^{n_x} \times \mathbb{R}^{n_u} \to \mathbb{R}^{n_x}$ defines the dynamics. At time t, $x_t \in \mathbb{R}^{n_x}$ and $u_t \in \mathbb{R}^{n_u}$ are the state and control input of the system, respectively, and $x_t \in \mathscr{X}, u_t \in \mathscr{U}$, where $\mathscr{X}$ and $\mathscr{U}$ are assumed to be *compact convex* sets. The aim is to solve an infinite-horizon risk-constrained optimal control problem for system (1) that drives the system to a target equilibrium point $x_F \in \mathscr{X}$. To that end, let $r : \mathscr{X} \times \mathscr{U} \to \mathbb{R}_{\geq 0}$ be a continuous function that represents the *stage cost* associated to the optimal control problem. We assume that

$$\begin{cases} r(x_F, 0) & = 0, \\ r(x, u) & > 0, \quad \forall (x,u) \in (\mathscr{X} \times \mathscr{U}) \setminus \{(x_F, 0)\}. \end{cases} \tag{2}$$

Using this cost function, the risk-constrained infinite-horizon optimal control problem is given as

$$\min \quad \sum_{t=0}^{\infty} r(x_t, u_t) \tag{3}$$

$$\text{s.t.} \quad x_{t+1} = f(x_t, u_t), \quad \forall t \geq 0, \tag{3a}$$

$$x_t \in \mathscr{X}, u_t \in \mathscr{U}, \quad \forall t \geq 0, \tag{3b}$$

$$x_0 = x_S, \tag{3c}$$

$$\mathrm{CVaR}_{\beta}^{\mathbb{P}}[g(x_t, w)] \leq \delta, \quad \forall t \geq 0, \tag{3d}$$

where $x_S \in \mathscr{X}$ is the initial state and constraint (3d) represents the risk-averseness. Here, CVaR stands for the conditional value-at-risk, w is a random variable with distribution $\mathbb{P}$ supported on the compact set $\mathscr{W} \subset \mathbb{R}^{n_w}$, $\delta > 0$ is the risk tolerance parameter, $\beta > 0$ is the risk-averseness coefficient, and the continuous function $g : \mathscr{X} \times \mathscr{W} \to \mathbb{R}$ is referred to as the constraint function.

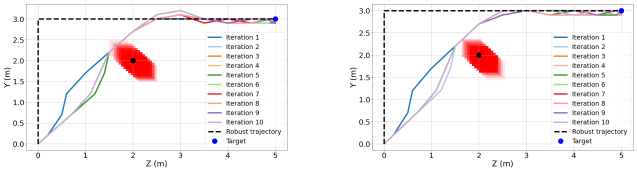

(a) $\theta = 5 \times 10^{-4}$ (b) $\theta = 5 \times 10^{-2}$

Figure 1: Generated trajectories for different radii of the ambiguity set.

The infinite-horizon problem (3) is difficult to solve due to state, input, and risk constraints. Thus, we suggest a procedure to approximate it in which, at each iteration, we generate a trajectory using an MPC scheme, where a DR constrained finite-horizon problem is solved repeatedly. We assume a general class of ambiguity sets that are defined using the data collected in previous iterations. The terminal constraint in the finite-horizon problem enforces the state to lie in a subset of the safe states sampled in previous iterations. Once a trajectory is generated, the samples of the uncertainty collected in the iteration are added to the dataset and the sampled safe set is updated appropriately. The attractive aspect of our iterative algorithm is the fact that safety and cost-performance can be tuned using distributional robustness, irrespective of the number of available samples.

3 Results

Under the assumption that a robustly feasible trajectory is available at the first iteration, we show that each iteration is recursively feasible, and asymptotically converges to the target state. We apply our algorithm to find a risk-averse path for a mobile robot in the presence of an uncertain obstacle.

References

[1] U. Rosolia and F. Borrelli, "Learning model predictive control for iterative tasks. a data-driven control framework," *IEEE Transactions on Automatic Control*, vol. 63, no. 7, pp. 1883–1896, 2017.

[2] A. R. Hota, A. Cherukuri, and J. Lygeros, "Data-driven chance constrained optimization under Wasserstein ambiguity sets," in *American Control Conference*, pp. 1501–1506, July 2019.

Optimal Control and Design of Magnetic Spring-assisted Systems

Branimir Mrak, Jeroen Willems & Edward Kikken
Flanders Make, Belgium. E-mail: firstname.lastname@flandersmake.be

Introduction

In literature, the magnetic spring (MS) [1] has been proposed as an option for energy and peak power reduction in (near) repetitive mechatronic motion systems. It stores energy using magnetic forces instead of alternatives relying on mechanical deformation (i.e., springs) or conversion of mechanical energy to electrical energy (e.g., capacitors), thereby relaxing the downsides (fatigue and conversion losses) of other alternatives. However, the key challenge is how to design and control such MS-assisted mechatronic systems, in order to achieve good performance under variable operational conditions.

Therefore, we have developed a systematic toolchain for the design and control of such magnetic spring assisted drivetrains, addressing the optimization of both the desired torque profile of the magnetic spring (including its physical geometry), as well as the dynamics and controls of the considered drivetrain.

The Magnetic Spring

The rotational variant of the MS, see Fig. 1, consists of a rotor and stator of magnetic material. The relative angle (θ) between these two parts determines the torque applied to the rotor axle. When an MS is added in series with a motor, this magnetic spring torque can be utilized to reduce the oscillating motor torques required for repetitive motions.

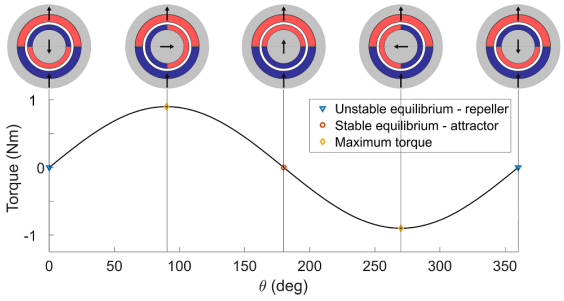

Figure 1: Torsional magnetic spring.

Proposed Magnetic Spring Co-Design Toolchain

The workflow of the toolchain is as follows:

I. Model generation (including the magnetic spring). The system dynamics are modelled in CasADi [2]. These symbolic equations can either be directly formulated as a DAE, or extracted from Simscape using Simscape2CasADi [3].

II. Optimal system and control design. In a single optimization problem (inspired by the methods in [2]), the dynamics and controls of the system will be optimized, along with the desired magnetic spring torque profile $T_{spring}(\theta)$. Alternatively, the MS torque characteristic can be designed using engineering rules, see [1].

III. Optimal component design for magnetic spring. The parameters of the magnetic spring are optimized in a finite element simulation, given a physical parameterization. The goal is to match the torque profile obtained in (2).

IV. Re-computing the optimal controls. If desired, recompute (2) with result of (3).

Experimental Validation on Two Systems

The developed methodology is experimentally validated on two setups: an academic four-bar linkage setup and an industrial parallel delta robot, see Fig. 2. This first setup features a crank-rocker mechanism and is representative of an industrial weaving loom. It is equipped with an adaptive MS and performs repetitive motions. The second setup performs near-repetitive 3D pick and place motions and its MS is designed as a simpler sinusoidal non-adaptive spring. For each of the cases, the performance improvements are shown in Table 1: considerable reductions in energy and / or RMS torques are achieved.

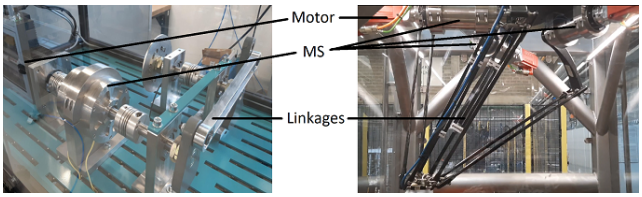

Figure 2: Bar-linkage and delta-robot with MS.

Table 1: Performance improvements for bar-linkage and delta robot.

	No spring	With spring	Red.
Energy bar-linkage	74 J	39 J	47%
RMS torque delta-robot	16.3 Nm	4.9 Nm	70%

Acknowledgements: This work has been carried out within the framework of Flanders Makes ICON project "Torque Ripple Reduction" funded by the agency Flanders Innovation & Entrepreneurship (VLAIO). Flanders Make is the Flemish strategic research centre for the manufacturing industry.

References

[1] Mrak, B., B. Wex, and H. Mitterhofer. "Methodology for Shape Optimization of Magnetic Designs: Magnetic Spring Characteristic Tailored to Application Needs." Actuators. Vol. 11. No. 2. MDPI, 2022.

[2] J. A. E. Andersson, J. Gillis, G. Horn, J. B. Rawlings, and M. Diehl, "CasADi – A software framework for nonlinear optimization and optimal control," 2019.

[3] J. Gillis and E. Kikken, "Symbolic equation extraction from simscape," Benelux Meeting, 2018.

Identifying bang-bang type MPC using Support Vector Machines

Tony Dang, Frederik Debrouwere, and Erik Hostens
Flanders Make,
Lommel, Belgium
Email: tony.dang@flandersmake.be

1 Introduction

Model Predictive Control (MPC) has many desirable characteristics such as its predictive power, its ability to take into account constraints, and being optimal w.r.t. a chosen criteria. However, the computational cost required for solving MPC makes it challenging to deploy it for real-time systems. Additionally, in many cases the resulting optimal control law from the MPC is quite simple, e.g. yielding bang-bang type control. We propose an approach to identify these type of optimal control laws as closed form controllers, which eliminates the need for solving an optimization problem online.

2 Approach

We start from a specific type of MPC problems where no input penalization is considered:

$$\begin{aligned} \min_{x,u} \quad & V(x) = \int_0^T x(t)^\top Q x(t) dt \\ \text{subject to} \quad & \dot{x} = f(x,u) \\ & u \in U. \end{aligned} \tag{1}$$

The optimal control law often yields a bang-bang type controller. In order to identify this nonlinear control law, offline simulations are performed to generate a data set of optimal solutions. This boils down to solving a supervised classification problem. Support Vector Machines (SVMs) [2] are proposed as the model. The dual problem for solving the classification problem is extended with a linear constraint to enforce the switching mode through the origin x^*:

$$\begin{aligned} \max_{\alpha} J_D(\alpha) = \quad & -\frac{1}{2}\sum_{k,l=1}^{N} y_k y_l K(x_k,x_l)\alpha_k\alpha_l + \sum_{k=1}^{N}\alpha_k \\ \text{subject to} \quad & \sum_{k=1}^{N}\alpha_k y_k = 0 \\ & 0 \le \alpha_k \le c,\ k = 1,\ldots,N \\ & \sum_{k=1}^{N}\alpha_k y_k K(x^*,x_k) + b = 0. \end{aligned} \tag{2}$$

Solving this optimization problem results in an identified switching mode for the bang-bang controller.

3 Results

The methodology is applied in practice on a parallel SCARA robot at a frequency rate of 2 kHz. Data is generated by solving a nonlinear input-constrained MPC problem offline (figure 1) for arbitrary point-to-point motions in CasADi [1]. A switching mode is identified using SVMs. The resulting bang-bang controller yielded faster tracking of the setpoints and lower overshoot compared to the PID controller (figure 2).

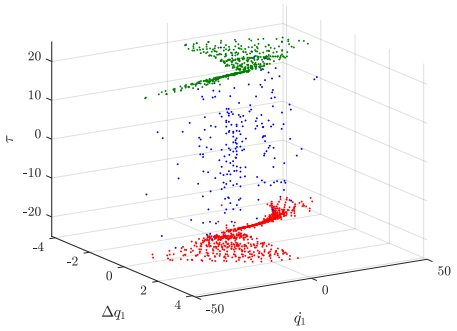

Figure 1: Sampled OCP solutions for motor 1 projected on a 2D slice of the 4D state space. Red and green samples indicate minimum and maximum input torque respectively.

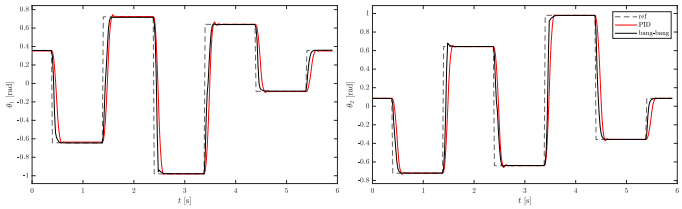

Figure 2: Measured encoder output θ. Serial singularities were reached around 3s and 4s.

References

[1] Joel AE Andersson et al. "CasADi: a software framework for nonlinear optimization and optimal control". In: *Mathematical Programming Computation* 11.1 (2019), pp. 1–36.

[2] Johan AK Suykens et al. *Least squares support vector machines*. World scientific, 2002.

Acknowledgement: This work is supported by Flanders Make project: ICON ID2CON: Integrated Identification to Control.

Modelling Framework and Partitioning of Large-Scale Systems

Alessandro Riccardi, Luca Laurenti and Bart De Schutter
Delft Center for Systems and Control, Delft University of Technology
Email: {a.riccardi, l.laurenti, b.deschutter}@tudelft.nl

1 Introduction

The advancements in computer science and telecommunications of recent years have allowed control engineering to expand its field of application from localized and coherent process plants to interconnected systems. However, even if the computing power and flexibility of processors, and the availability of communication devices to embed in networks have increased, the problem of controlling extended and heterogeneous structures in an optimal and robust fashion remains. This problem is exacerbated by the increasing size and complexity of the networks, leading to the necessity of finding strategies to control Large Scale Systems (LSSs), where 'large' should be interpreted as 'too big to be controlled in a centralized fashion'. Examples of those types of systems can be found in the fields of multi-modal transportation (which may include the use of intelligent vehicles), smart grids (with distributed generation via photovoltaic cells or wind mills), water and gas distribution systems, smart buildings, and supply chains. Promising solutions are sought in Distributed Model Predictive Control (DMPC) strategies, which are by themselves a current field of active research.

2 Modelling Framework for Large-Scale Systems

The nature of LSSs often leads to an intuitive interpretation of their structure through graph theory. In fact a complex system can be converted into a collection of nodes, which represent processing system dynamics and input/output gateways, and links, which are instead transmission channels of a certain 'flow' of information, energy, or material, and which model the relations among the various nodes. This topological structure also occurs at a control and communication level, thus providing multiple superposed graphs that may also vary with time or as a consequence of certain events. Therefore, to extend the modelling capabilities of existing representations of LSSs, it is possible to integrate hybrid models with dynamic graphs and design a framework suitable for the application of DMPC.

3 Partitioning

The application of a DMPC strategy requires the identification of an adequate network partitioning in subsystems that present specific properties to preserve a certain degree of optimality in comparison with a centralized control architecture [1]. Many criteria have been considered in the literature for partitioning a system and often the choice is application-dependent. Moreover, for LSSs this partitioning can be unpractical or too computationally expensive to be performed on-line in a centralized fashion. Therefore, along with the necessity of a non-centralized control approach arises the one of a distributed partitioning strategy to properly allocate the computational burden among control agents, and to allow for an on-line and minimally reconfigurable real-time adaptation of the network partitioning to topology changes.

4 Open Issues and Research Directions

Several works have been proposed for distributed control of LSSs [3]. The initial focus of many studies has been on linear systems, but it remains an open question to consider more complex structures, also allowing for the integration of networks with different physical nature, which are commonly referred to as heterogeneous systems. In particular, our attention, in the context of LSSs, will be devoted to networks with hybrid dynamics, which represent a challenging extension of current works and allow to model a wider class of relevant phenomena [2]. Another research direction concerns the partitioning of LSSs in subsystems, especially regarding networks with dynamic topologies and distributed partitioning strategies. The definition of suitable metrics to capture the relevant features of the network for an optimal partitioning will be one research objective. Finally, a relevant aspect of distributed control approaches applied to LSSs is related to loss of optimality w.r.t centralized control architectures. Quantifying this degree of suboptimality and improving performance of distributed systems is a topic that deserves a specific attention for the evolution of complex systems.

Acknowledgment: This project has received funding from the European Research Council (ERC) under the European Union's Horizon 2020 research and innovation programme (Grant agreement No. 101018826) – Project CLariNet

References

[1] P. Chanfreut, J.M. Maestre, and E.F. Camacho. A Survey on Clustering Methods for Distributed and Networked Control Systems. *Annual Reviews in Control*, 52:75–90, 2021.

[2] W.P.M.H. Heemels, B. De Schutter, and A. Bemporad. Equivalence of hybrid dynamical models. *Automatica*, 37:1085–1091, 2001.

[3] M. Kordestani, A.A. Safavi, and M. Saif. Recent Survey of Large-Scale Systems: Architectures, Controller Strategies, and Industrial Applications. *IEEE Systems Journal*, 15:5440–5453, 2021.

Private Computation of Polynomials over Networks

Teimour Hossienalizadeh, Fatih Turkmen, Nima Monshizadeh

I. Introduction

Distributed computation emerged in the last century mainly because of computation power constraints where by splitting a problem across many parallel threads, researchers were able to reach a solution in a shorter period of time. With the rise of the cloud as a service and broad-band communication, computation power constraint is not the main reason for distributed computation in many fields. Instead, privacy concerns play a significant role in developing distributed algorithms in particular for Cyber-Physical Systems(CPSs). However, a distributed protocol cannot solely solve the privacy issues arising in centralized CPSs since the involved parties still need to share data with each other. Therefore, improving privacy level even in distributed CPSs is of main concern.

II. Problem Formulation

We consider a scenario where, at each time $k = 1, 2, \ldots, K$, agent i in a network is interested in evaluating a polynomial which depends not only on her own private variable x_i but also on the private variables of her neighbours x_j with $j \in \mathcal{N}_i$. In particular, we consider the following class of polynomials:

$$\Phi_i(x_i(k), x_j(k)) := \sum_{j\in\mathcal{N}_i} P_{ij}(x_i(k), x_j(k)) + \prod_{j\in\mathcal{N}_i\cup i} W_j(x_j(k)), \tag{1}$$

where $P_{ij} = \sum_{p,q=0}^{\delta_{ij}} c_{ij}^{(pq)} x_i^p x_j^q$, $W_j = \sum_{q=0}^{\delta_j} c_j^{(q)} x_j^q$, and $i \in V$. The notation x_{-i} is used to indicate the dependency of Φ_i on x_j with $j \neq i$. Notice that P_{ij} is the summation of bivariate polynomials, with x_i and x_j, $j \in \mathcal{N}_i$, being the corresponding two variables. Moreover, the second term on the right hand of (1) collects the multivariate polynomials with more than two variables. As can be seen from (1), we assume that these terms can be written as a product of $|\mathcal{N}_i \cup i| = d_i + 1$ univariate polynomials. This is a large class of polynomials and can accommodate distributed algorithms in control systems with linear or polynomial coupling, as well as distributed optimization algorithms with polynomial constraints.

T. Hosseializadeh and N. Monshizadeh are with the Engineering and Technology Institute; F. Turkmen is with Bernoulli Institute for Mathematics, Computer Science and Artificial Intelligence, University of Groningen, The Netherlands. Email: {t.hosseinalizadeh, n.monshizadeh, f.turkmen}@rug.nl.

Assumption 1. Agents in a network G are honest-but-curious, also known as semi-honest, meaning they follow the required protocol for interacting with other agents but are also interested in determining private values in the network.

Assumption 2. An adversary $\mathcal{A}$ is probabilistic polynomial time, passive, and communications among agents are done in its presence. The adversary $\mathcal{A}$ can be an agent in the network or an external party observing the communication.

The problem we are interested in is to provide a privacy preserving protocol for the evaluation of (1) for agent i. In other words, agent i should be able to obtain the *exact* value of Φ_i without revealing the value of her own private variable x_i to any other agent j and without gaining any privacy-sensitive piece of information other than the result of target function Φ_i.

III. Proposed Algorithm

The solution we provide is based on secret sharing and PHE techniques(see [1] for details of the algorithm). In particular, we use Paillier's scheme to protect the privacy of x_i, and secret sharing for preserving the privacy of x_j, with $j \in \mathcal{N}_i$. Additive secret sharing is used in the summation part of Φ_i, and multiplicative secret sharing is used in the multiplicative term in Φ_i (see (1)).

A. Privacy Analysis

In this subsection, we focus on privacy preserving properties of the proposed algorithm. First, we note that privacy of agent i is preserved throughout the computation of $\Phi_i(\cdot)$ due to the adopted encryption scheme. The situation for privacy preservation of the neighbours of i is different, and their privacy is potentially susceptible to the collusion of agent i with other neighbours. To study such potential collusion, we partition the agents into a set of corrupt V_c and non-corrupt agents V_{nc}, where the corrupt agents may collude with each other and the non-corrupt agents are simply honest-but-curious. In the proposed algorithm, we assume that the distinguished neighbours are *not* corrupt.

Theorem 1. *Assume that $D_i \in V_{nc}$ and consider the computation of $\Phi_i(\cdot)$ following Algorithm 1 in [1]. Let $j \in \mathcal{N}_i$. Then x_j is not inferred uniquely if either $i \in V_{nc}$ or*

$$\mathcal{N}_i \cap (V_{nc} \backslash j) \neq \varnothing, \tag{2}$$

i.e. i has at least one non-corrupt neighbour other than j.

References

[1] T. Hosseinalizadeh, F. Turkmen, and N. Monshizadeh, "Private computation of polynomials over networks," *arXiv preprint arXiv:2104.01369*, 2021.

Abstracted Reduction of Interconnected Structural Models

Luuk Poort
Eindhoven University of Technology*
l.poort@tue.nl

Rob Fey
Eindhoven University of Technology*
r.h.b.fey@tue.nl

Bart Besselink
University of Groningen†
b.besselink@rug.nl

Nathan van de Wouw
Eindhoven University of Technology*
n.v.d.wouw@tue.nl

1 Introduction

To assess their dynamic behaviour, complex structural systems are usually modeled using finite element methods. The large order of these models necessitates the use of model reduction techniques to enable efficient dynamic analysis. These models, represented by the system of linear differential equations $\mathbf{\Sigma}$, often consist of an interconnection of substructures $\mathbf{\Sigma}_j$, $j = 1, \ldots, k$. In practice, model reduction is often performed on individual substructures $\mathbf{\Sigma}_j$, by, e.g., component mode synthesis methods (CMS), because (i) direct reduction of $\mathbf{\Sigma}$ is not computationally tractable and (ii) substructures are typically developed by independent teams. However, if the reduction of a substructure $\mathbf{\Sigma}_j$ to its reduced representation $\hat{\mathbf{\Sigma}}_j$ does not consider the coupling to the other substructure dynamics, the accuracy of the coupled, reduced-order model (ROM), $\hat{\mathbf{\Sigma}}$, cannot be ensured.

2 Research approach

We introduce the idea of reducing $\mathbf{\Sigma}_j$ in interconnection with a low-order approximation of the other substructures, to improve the accuracy of $\hat{\mathbf{\Sigma}}$. Stated differently, instead of considering (and reducing) $\mathbf{\Sigma}_j$ in isolation, we consider the interconnection of $\mathbf{\Sigma}_j$ with an *abstraction* of its environment. This ensures that the reduced $\hat{\mathbf{\Sigma}}_j$ is relevant in the scope of the overall structure. By using only an abstraction instead of the full substructure models, the computational cost of the reduction problem decreases and only a basic, nominal designs of the other substructures are required.

Reduction of the interconnection of $\mathbf{\Sigma}_j$ and the corresponding abstraction using standard reduction methods would destroy the interconnection structure and results in one unified, reduced model. Therefore, structure-preserving reduction methods, such as structure-preserving balanced truncation (SPBT) of [1], are employed to retain the interconnection structure and thus retain access to the reduced subsystems $\hat{\mathbf{\Sigma}}_j$. The combination of SPBT with the use of abstractions is denoted *abstracted* SPBT (ASPBT).

*Dynamics and Control, Mechanical Engineering, Eindhoven University of Technology, P.O. Box 513, 5600 MB Eindhoven, The Netherlands
†Bernoulli Institute for Mathematics, Computer Science and Artificial Intelligence, University of Groningen, P.O. Box 407, 9700 AK Groningen, The Netherlands

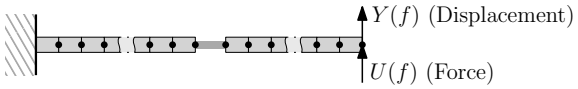

Figure 1: Schematic drawing of the coupled beam model.

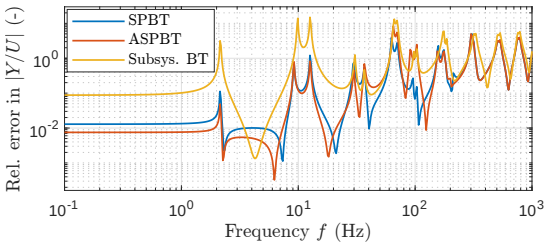

Figure 2: Relative reduction error in $|Y/U|$.

3 Numerical example

Observe the SISO system of two equivalent Euler beams, with 2% modal damping each, in Figure 1. The coupling consists of a translational and rotational spring, with, respectively, 50 and 5 times the left cantilever's translational and rotational stiffness at its end. The discretized cantilever and free beam substructures consist of 60 and 62 degrees of freedom (DoF), respectively, and are reduced to 4 DoF each. Reduction is performed using (i) SPBT, (ii) ASPBT (using CMS-reduced abstractions of 3 DoF) and (iii) subsystem balanced truncation (BT). The resulting relative error magnitudes of the collocated FRF is shown in Figure 2.

4 Conclusion and outlook

Numerical evaluation indicates that ASPBT is superior to subsystem BT in terms of input-output accuracy of the ROM, and is comparable to SPBT. This implies that low-order abstractions are sufficient to capture the relation between $\mathbf{\Sigma}_j$ and $\mathbf{\Sigma}$, while significantly improving computational tractability. In further work, we will formulate error bounds to be able to further compare ASPBT to alternatives.

References

[1] H. Sandberg and R. M. Murray, "Model reduction of interconnected linear systems," *Optimal Control Applications and Methods*, vol. 30, no. 3, pp. 225–245, May 2009.

A priori error bounds for model reduction of interconnected systems

Lars Janssen, TU/e*
Email: l.a.l.janssen@tue.nl

Rob Fey, TU/e*
Email: r.h.b.fey@tue.nl

Bart Besselink, RUG†
Email: b.besselink@rug.nl

Nathan van de Wouw, TU/e*
Email: n.v.d.wouw@tue.nl

1 Introduction

Many complex models of dynamic (multi-)physical systems are naturally based on an interconnection of subsystems. The models of interconnected systems often have a high number of states, which makes controller synthesis, simulation and analysis computationally expensive. This motivates the need for model order reduction (MOR) techniques applicable to such systems. *Subsystem reduction*, where each of the subsystems is reduced individually, is a completely modular approach. Hence, the interconnection structure of the high-order model is preserved and the computationally challenging reduction of one very high-dimensional model is avoided by dividing the problem into multiple smaller problems. However, although subsystem reduction methods will lead to accurate reduced-order representations of the high-order subsystems, this does not directly mean that the reduced-order interconnected system is also accurate. Based on [1], we introduce a method which gives an a priori error bound on the frequency response of the reduced interconnected system based on the a priori error bounds of the reduced subsystems.

2 Preliminaries

We study systems of k linear time-invariant (LTI) subsystems that can be aggregated and represented by block-diagonal transfer function $G = \mathrm{diag}(G_1, \ldots, G_k)$. The subsystems are interconnected via matrix K. The external inputs u and outputs y are connected to the subsystems via external input and output matrix L and M, respectively. In subsystem reduction, each of the subsystems G_j is reduced to an approximate reduced-order subsystem $\hat{G}_j$ and the aggregate is given by $\hat{G} = \mathrm{diag}(\hat{G}_1, \ldots, \hat{G}_k)$. The high-order interconnected system G_c and the reduced-order interconnected system $\hat{G}_c$ with $\hat{y} = \hat{G}_c u$ (Figure 1), are then

$$G_c = MG(I - KG)^{-1}L, \; \hat{G}_c = M\hat{G}(I - K\hat{G})^{-1}L. \quad (1)$$

3 Methodology

For balanced truncation, a widely used MOR method, an upper bound on the $\mathscr{H}_\infty$-norm of the difference between the high-order and reduced-order systems is available a priori.

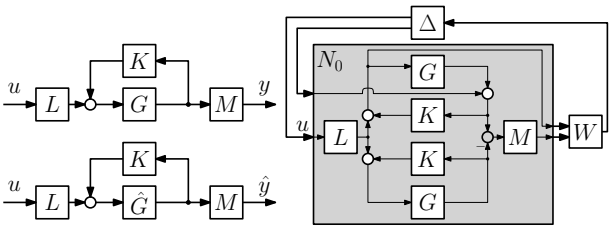

Figure 1: Block diagrams of G_c (top left), $\hat{G}_c$ (bottom left), and $G_c - \hat{G}_c$ represented by N_0, W and Δ (right).

In this work, we extend a priori knowledge of subsystem errors $\|G_j - \hat{G}_j\|_\infty$ to knowledge on $\|G_c - \hat{G}_c\|_\infty$. To do so, we define all subsystem reduction errors as an uncertain system $\Delta := G - \hat{G}$. Then, we can model $G_c - \hat{G}_c$ as a closed loop between N and Δ as shown in Figure 1. Here, the nominal system $N := N_0 W$ is a function of $N_0(G, K, L, M)$ and weighting matrix $W := \mathrm{diag}(w_1 I, \ldots, w_k I, w_c I)$. Using this framework, the structured singular value μ, a powerful tool from robust control, can be used. Namely, if N is internally stable, then

$$\left.\begin{array}{l} \|G_c - \hat{G}_c\|_\infty \leq w_c^{-1}, \text{and} \\ \|G_j - \hat{G}_j\|_\infty \leq w_j \; \forall \; j = 1, \ldots, k \end{array}\right\} \Leftrightarrow \mu_\Delta(N) < 1. \quad (2)$$

Given that an error bound w_j is available a priori for each subsystem, this relation can be used to find an error bound w_c^{-1} on the interconnected system. A less conservative frequency-dependent version of (2) can be used at the cost of increased computation time. In [1], these bounds are illustrated using an example.

4 Conclusion

With (2), we can directly compute the impact of errors in subsystems to the error of the interconnected system. This result is also the first step towards determining a model accuracy specification for the individual subsystems guaranteeing a required overall system accuracy. Therefore, the method can be used as a significant means for the development of accurate modeling of interconnected systems within a completely modular setting.

References

[1] Janssen, L.A.L. et al., "A Priori Error Bounds for Model Reduction of Interconnected Linear Systems using Robust Performance Analysis", ACC 2022 (accepted for publication).

*Dynamics and Control, Mechanical Engineering, Eindhoven University of Technology, P.O. Box 513, 5600 MB Eindhoven, The Netherlands

†Bernoulli Institute for Mathematics, Computer Science and Artificial Intelligence, University of Groningen, P.O. Box 407, 9700 AK Groningen, The Netherlands

Modelling of networks of memristors

Anne-Men Huijzer, Arjan van der Schaft, Bart Besselink
Bernoulli Institute for Mathematics, Computer Science and Artificial Intelligence
CogniGron - Groningen Cognitive Systems and Materials Center
University of Groningen
m.a.huijzer@rug.nl, a.j.van.der.schaft@rug.nl, b.besselink@rug.nl

1 Introduction

The emerging field of neuromorphic computing aims to reduce the energy requirements of computing platforms. For these new neuromorphic technologies dedicated hardware needs to be developed. It is suggested that memristors will play an important role within the hardware of these new neuromorphic technologies. Memristors, originally introduced by Chua in [1], are resistors with a memory storage that can act as non-volatile memory. In this work, we introduce a mathematical framework to study the behavior of networks of memristors. We show that the memristive behavior of such a network is preserved on external branches, i.e. the branches connecting the network to an external source. This result is a generalization of Chua's closure theorem that states that "a one-port containing only memristors is equivalent to a memristor" [1].

2 Main results

We will consider a connected memristor network with N nodes and B branches characterized through the incidence matrix $D \in \mathbb{R}^{N\times B}$, see Figure 1. Let $q \in \mathbb{R}^B$ and $\varphi \in \mathbb{R}^B$ denote the branch charges and fluxes, respectively. We model the memristors through the relation $M \subset \mathbb{R}^B \times \mathbb{R}^B$ as

$$(q,\varphi) \in M, \tag{ML}$$

see [1]. We assume that, for some $\alpha > 0$ and $\beta > 0$,

$$(q-q')^\top(\varphi-\varphi') \geq \alpha|q-q'|^2 + \beta|\varphi-\varphi'|^2$$

for all $(q,\varphi),(q',\varphi') \in M$. Now, we consider B_E external sources, whose distribution over the network is captured in the incidence matrix $D_E \in \mathbb{R}^{N\times B_E}$. We denote the corresponding flux potentials and charges by φ_E and q_E.
We want to show that q_E and φ_E are related by a memristive relationship by utilizing integrated versions of Kirchhoff's voltage and current law, as in [2], and (ML). We note that the integrated version of Kirchhoff's current states that

$$D(q-q_0) = D_E(q_E - q_{E,0}) \tag{KqL}$$

and the integrated version of Kirchhoff's voltage law reads

$$\exists \zeta \in \mathbb{R}^N \text{ s.t. } \begin{bmatrix} \varphi-\varphi_0 \\ \varphi_E - \varphi_{E,0}\end{bmatrix} = \begin{bmatrix} D^\top \\ D_E^\top \end{bmatrix} \zeta. \tag{KφL}$$

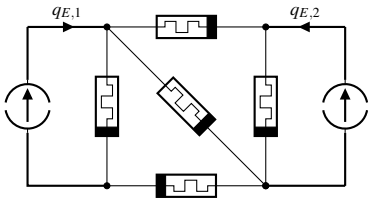

Figure 1: Network of memristors attached to two external sources with corresponding charges $q_{E,1}$ and $q_{E,2}$.

Here, the notation was simplified by omitting time-arguments, e.g. $q_0 = q(0)$ and $\varphi_{E,0} = \varphi_E(0)$.
Now, we can state the following result.

Theorem 2.1 *Let $(q_0,\varphi_0) \in M$ and $q_E - q_{E,0}$ be given. Then, there exists a unique $\varphi_E - \varphi_{E,0}$ such that (KqL), (KφL) and (ML) hold. Moreover, there exist $\alpha_E > 0$ and $\beta_E > 0$ such that*

$$(q_E - q_E')^\top(\varphi_E - \varphi_E') \geq \alpha_E|q_E - q_E'|^2 + \beta_E|\varphi_E - \varphi_E'|^2.$$

3 Discussion

The above result shows that the memristive behavior of a network of memristors is preserved on its external branches. This result enables us to derive an analogous expression for the notions of effective resistance and Kron reduction, see [3], for memristor networks. The inequality in Theorem 2.1 can give information of the influence of the memristors in the network on the memristive behavior measured on its external branches. These topics will be explored further in future research.

References

[1] L. Chua, "Memristor-the missing circuit element," *IEEE Transactions on Circuit Theory*, vol. 18, no. 5, pp. 507–519, 1971.

[2] F. Corinto and M. Forti, "Memristor circuits: Flux—charge analysis method," *IEEE Transactions on Circuits and Systems I: Regular Papers*, vol. 63, no. 11, pp. 1997–2009, 2016.

[3] F. Dörfler and F. Bullo, "Kron reduction of graphs with applications to electrical networks," *IEEE Transactions on Circuits and Systems I: Regular Papers*, vol. 60, no. 1, pp. 150–163, 2013.

Handling sensor and process noise in dynamic network identification[1]

Stefanie Fonken, Karthik Ramaswamy, Paul Van den Hof
Control Systems Group, Department of Electrical Engineering,
Eindhoven University of Technology, The Netherlands
Email: {s.j.m.fonken, k.r.ramaswamy, p.m.j.vandenhof}@tue.nl

1 Introduction

Data-driven modeling suitable for dynamic networks received a great deal of attention in recent years, where dynamic networks refer to widely distributed and spatially interconnect systems that are often large-scale. The interconnecting dynamics (modules) can be estimated using the dynamic network framework. In order to obtain consistent estimates of the modules, the disturbances due to sensor noise need to be incorporated in the estimation procedure. The indirect method in [1] achieves consistent estimates while considering both the sensor and process noise. Direct methods lead to estimates with smaller variance, and have the potential to work with less costly experiments, i.e. less external excitation signals are required. However, most direct methods only consider the process noise [2].

The objective is to obtain accurate (consistent) estimates of the modules in a dynamic network that is influenced by both sensor and process noise, using the multi-step least squares method from [2].

2 Process and sensor noise

The dynamic network framework typically considers a dynamic network influenced by process noise, where the nodes $w = \left[w_1, \cdots, w_L\right]^\top$ are expressed as

$$w = G^0 w + R^0 r + v \tag{1}$$

where G^0 is a hollow matrix, that has the modules G^0_{ji} as its elements, the v is the disturbance related to the process noise that can be represented as filtered white noise $v = H^0 e$. The matrix R^0 and excitation signals r are user manipulated, with r uncorrelated to e.
In practice the measurements of the node signals w are influenced by sensor noise, meaning we can write [3, 1]

$$\tilde{w} = w + s, \tag{2}$$

where $\tilde{w}$ are the measured node signals and s is the disturbance due to sensor noise that is uncorrelated to r and v. Substituting $\tilde{w}$ in (1) results in $\tilde{w} - s = G^0(\tilde{w} - s) + v + Rr$ that can be rewritten to

$$\tilde{w} = G^0 \tilde{w} + \tilde{v} + Rr, \tag{3}$$

where $\tilde{v} = v + (I - G^0)s$, illustrated in Figure 1.

[1]This project has received funding from the European Research Council (ERC), Advanced Research Grant SYSDYNET, under the European Union's Horizon 2020 research and innovation programme (Grant Agreement No. 694504)

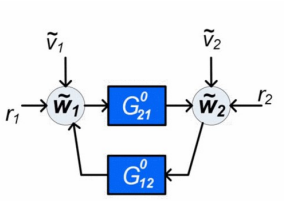

Figure 1: Example of a 2 node network with measured nodes influenced by sensor noise [3], where $\tilde{v} = v + (I - G^0)s$.

3 Multi-step least squares method including sensor noise

The multi-step least squares method of [2] considers a dynamic network that is only influenced by process noise as in (1). The main steps of the method can be summarized as

1. High-order ARX modeling: *this ARX model provides a reconstruction of the innovation signal* ε,
2. Parametric identification: *Use the reconstructed innovation signal* $\hat{\varepsilon}$ *as additional measured input.*

We show that if we add the sensor noise, the algorithm of [2] models the disturbances due to process noise and sensor noise together. Meaning if we reformulate $\tilde{v} = v + (I - G^0)s$ to $\tilde{v} = \tilde{H}^0 \tilde{e}$, our estimated disturbance model is an estimate of $\tilde{H}^0$ and the reconstructed innovation $\hat{\varepsilon}$ is an estimate of $\tilde{e}$. Note that using this approach comes at the cost that additional excitation signals r might be required. As a result we obtain consistent estimates of the dynamic network modules, despite the presence of sensor noise.

References

[1] A.G. Dankers, P.M.J. Van den Hof, X. Bombois, and P.S.C. Heuberger. Errors-in-variables identification in dynamic networks — consistency results for an instrumental variable approach. *Automatica*, 62:39–50, 2015.

[2] S.J.M. Fonken, K.R. Ramaswamy, and P.M.J. Van den Hof. A scalable multi-step least squares method for network identification with unknown disturbance topology, 2022. *To appear in Automatica*, arXiv: 2106.07548.

[3] P.M.J. Van den Hof, A.G. Dankers, and H.H.M. Weerts. From closed-loop identification to dynamic networks: Generalization of the direct method. In *Proc. 56th IEEE Conference on Decision and Control (CDC)*, pages 5845–5850, 2017.

Nonlinear feedforward control for a class of tasks: A Gaussian Process approach applied to a printer

Max van Meer[1] (m.v.meer@tue.nl), Maurice Poot[1], Jim Portegies[2], Tom Oomen[1,3]
Control Systems Technology section[1], Mathematics and Computer Science section[2], Delft Center for Systems and Control[3]
Eindhoven University of Technology, PO Box 513, 5600MB, The Netherlands[1,2], Delft University of Technology, The Netherlands[3]

1 Background

Feedforward control is essential for accurate reference tracking in motion control. For modern systems, feedforward controllers involve the inverse of increasingly complex systems with high order dynamics and dominant nonlinear dynamics of unknown structure. In addition, a large class of tasks must be performed.

2 Problem formulation

The aim is to obtain a nonlinear, noncausal feedforward controller for systems with complex nonlinear dynamics, which is applicable to a range of references. To this end, the system is parametrized as a GP. This allows for high flexibility and the specification of relevant prior information. Gaussian Process (GP) regression has had a major impact on the field of system identification [2] and control [1], as its nonparametric, possibly nonlinear model structure allows for the representation of a large range of systems.

3 Kernel-based inverse model control

Let $G(q)$ denote a discrete-time, nonlinear SISO system, such that G^{-1} characterizes the control effort $u(t)$ solely from past and future outputs $y(t+\tau)$, $t,\tau \in \mathbb{Z}$. In particular, G^{-1} is assumed to be a non-causal nonlinear impulse response (NFIR) system of the form

$$u(t) = f(\mathbf{y}_t), \tag{1}$$

with $\mathbf{y}_t = [y(t+n_{ac}),\ldots,y(t-n_c)]^\top$. Given a stabilizing feedback controller $C(q)$, the aim is to model f from a dataset $\mathcal{D} = \{u(t), y(t)\}$ such that $f(\mathbf{r}_t)$ yields the control effort $u(t)$ that realizes an arbitrary reference sequence $\mathbf{r}_t = [r(t+n_{ac}),\ldots,r(t-n_c)]^\top$.
The key idea is to model f as a GP, i.e.,

$$f(\mathbf{y}_t) \sim \mathcal{GP}(0, k(\mathbf{y}_{t_1} - \mathbf{y}_{t_2})), \tag{2}$$

where k is a kernel function that poses a prior on the smoothness of f with respect to $\mathbf{y}$, e.g., a Matèrn$_{3/2}$ kernel [3]. The expected feedforward signal required to realize reference $R = [\mathbf{r}_1,\ldots,\mathbf{r}_N]^\top$ is then given by the posterior mean of the GP as

$$\mathbb{E}[\mathbf{f}(R)] = K(R,Y)\left[K(Y,Y) + \sigma_n^2 I\right]^{-1}\mathbf{u}. \tag{3}$$

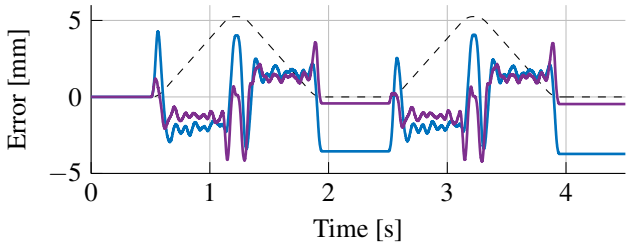

Figure 1: Error $e = r - y$ using linear feedforward (—) and the GP-based feedforward signal (—), along with the scaled reference (- -). With GP-based feedforward, $\|e\|_2$ is reduced by a factor 1.9.

This allows for the synthesis of feedforward signals for different tasks r, given that $\mathcal{D}$ contains observations of similar trajectories y.

4 Experimental results

The developed feedforward approach is applied to an A3 printer with friction. First, 11 closed-loop experiments are performed to obtain a dataset, using standard acceleration and velocity feedforward. In each experiment, a different reference $\tilde{r}_j = a_j r_1$ is used, with r_1 a second order reference and $a_j \in [0.90, 0.92, \ldots, 1.10]$. The data-set is then used to construct a feedforward signal with (3), for a different reference r_2. The result is shown in Figure 1. Even though r_2 is not used as a reference when obtaining the dataset, the error is reduced substantially by the GP-based approach.

5 Conclusion

A feedforward approach is presented that generates feedforward signals for systems with nonlinear dynamics of unknown structure while allowing for task flexibility. Future work aims at the extension towards MIMO systems.

References

[1] M. Deisenroth and C. Rasmussen. PILCO: A Model-Based and Data-Efficient Approach to Policy Search. In *Proceedings of the 28th International Conference on Machine Learning*, pages 465–472, Bellevue, WA, 2011.

[2] G. Pillonetto, F. Dinuzzo, T. Chen, G. De Nicolao, and L. Ljung. Kernel methods in system identification, machine learning and function estimation: A survey. *Automatica*, 50(3):657–682, 2014.

[3] C. Rasmussen and C. Williams. *Gaussian processes for machine learning*. London, England, 2006.

Virtual systems in nonlinear control design

Rodolfo Reyes-Báez, Bayu Jayawardhana
Jan C. Willems Center of Systems and Control, Faculty of Science and Engineering, University of Groningen
{r.reyes.baez, b.jayawardhana}@rug.nl

1 Abstract

We show the potential of a class of dynamical systems, referred to as *virtual systems*, in control design. Roughly speaking, for a given (original) plant, a virtual system can be understood as a system that can produce all plant's trajectories, i.e, the plant is embedded in the virtual one. We provide two examples of control design where a virtual system is used as a target closed-loop system and as an auxiliary system in which the design process is performed.

2 Virtual control systems

We consider a control system Σ_u given by

$$\Sigma_u : \begin{cases} \dot{x} = f(x,t) + \sum_{i=1}^{m} g_i(x,t)u_i, \\ y = h(x,t), \end{cases} \tag{1}$$

evolving on an N-dimensional manifold $\mathscr{X}$ with tangent bundle $T\mathscr{X}$; where $x \in \mathscr{X}$, $u \in \mathscr{U} \subset \mathbb{R}^m$ and $y \in \mathscr{Y} \subset \mathbb{R}^m$. The sets $\mathscr{U}$ and $\mathscr{Y}$ are assumed to be open subsets of $\mathbb{R}^m$.

Definition 1 (Virtual control system [3]) *Consider the system Σ_u in* (1)*. A* virtual control system *associated to Σ_u is defined as the system*

$$\Sigma_u^v : \begin{cases} \dot{x}_v = \Gamma_v(x_v, x, u_v, t), \\ y_v = h_v(x_v, x, t), \qquad \forall t \geq t_0, \end{cases} \tag{2}$$

parametrized by x, with state $x_v \in \mathscr{X}$, and input $u_v \in \mathscr{U}$, where $h_v(x_v,x,t)$ and $\Gamma_v(x_v,x,u_v,t)$ are such that

$$\begin{aligned} \Gamma_v(x,x,u,t) &= f(x,t) + \sum_{i=1}^{n} g_i(x,t)u_i, \\ h_v(x,x,t) &= h(x,t), \qquad \forall u, \forall t \geq t_0. \end{aligned} \tag{3}$$

It follows that any solution $x(t) = \psi_{t_0}(t, x_o)$ of the *original control system* Σ_u in (1), starting at $x_0 \in \mathscr{C}_x$ for a certain input u, generates the solution $x_v(t) = \psi_{t_0}(t, x_0)$ to the virtual system Σ_u^v in (2), starting at $x_{v0} = x_0 \in \mathscr{C}_v$ with $u_v = u$, for all $t > t_0$. However, *not* every virtual system's solution $x_v(t)$ corresponds to an original system's solution. Thus, *for* any *trajectory $x(t)$ of the original system, we may consider* (2) *as a time-varying system with state x_v.*

Example 1 ([1]) *Consider the mechanical system*

$$\begin{aligned} \dot{q} &= v, \\ M(q)\dot{v} + C(q,v)v &= \tau, \end{aligned} \tag{4}$$

with state $x = (\dot{q}, v)$, where $v = \dot{q}$, and input τ. The system

$$\begin{aligned} \dot{q}_v &= v_v, \\ M(q)\dot{v}_v + C(q,v)v_v &= \tau_v - K(v_v - v), \end{aligned} \tag{5}$$

in the state $x_v = (q_v, v_v)$ and parametrized by $x = (q,v)$, is a virtual system associated to (4)*. Indeed, if $(q_v, v_v) = (q,v)$ and $\tau_v = \tau$, then* (5) *can produce the trajectories of* (4)*.*

3 Control design using virtual systems

3.1 Virtual systems as target closed-loop dynamics

System (4) in closed-loop with the following control scheme [4, 3]

$$\tau := M(q)\dot{v}_r + C(q,v)v_r - Kv_r + \tau_v, \tag{6}$$

where $v_r := \dot{q}_d - \Lambda(q - q_d)$ with q_d a desired trajectory and $v_v = v - v_r$, yields precisely the virtual system (5).

3.2 Auxiliary virtual systems in the control design

Consider the following controller for the virtual system (5)

$$\tau_v := M(q)\dot{v}_r + C(q,v)v_r - K_p(q_v - q_d) - K_d(v_v - v_r) + \overline{\tau}_v. \tag{7}$$

It follows that the controller for the original plant in (4) is given by [2, 3]

$$\tau := M(q)\dot{v}_r + C(q,v)v_r - K_p(q - q_d) - K_d(v - v_r) + \overline{\tau}. \tag{8}$$

References

[1] J. Jouffroy and T. I. Fossen. A tutorial on incremental stability analysis using contraction theory. *Modeling, Identification and control*, 31(3):93–106, 2010.

[2] I. R. Manchester, J. Z. Tang, and J.-J. E. Slotine. Unifying robot trajectory tracking with control contraction metrics. In *Robotics Research*, pages 403–418. Springer, 2018.

[3] R. Reyes-Báez. *Virtual contraction and passivity based control of nonlinear mechanical systems: trajectory tracking and group coordination*. PhD thesis, University of Groningen, 2019.

[4] A. van der Schaft. *L2-Gain and Passivity Techniques in Nonlinear Control*. Springer International Publishing, 2017.

Analysis of Sampled-Data Hybrid Integrator-Gain-Based Control Systems

Bardia Sharif, Marcel Heertjes, Henk Nijmeijer, Maurice Heemels
Mechanical Engineering Department, Eindhoven University of Technology,
P.O. Box 513, 5600 MB Eindhoven, The Netherlands.
Email: b.sharif@tue.nl

1 Introduction

Hybrid Integrator-gain systems (HIGS) [1] are hybrid control elements aiming at overcoming (fundamental) performance limitations of linear feedback control. Thus far in the literature, discretization and sampled-data analysis of these control elements are not addressed. In this work, a discrete-time (DT) version of HIGS is presented, which preserves its main characteristics. Furthermore, a discrete-time approach is presented for stability analysis of sampled-data HIGS-controlled systems arising from the interconnection of DT HIGS-based controllers and continuous-time (CT) plants.

2 Discrete-Time HIGS

The proposed DT HIGS element, $\overline{\mathscr{H}}$, is given by

$$\overline{\mathscr{H}}: \begin{cases} x_h[k] = x_h[k-1] + \omega_h T_s e[k], & \text{if } \xi[k] \in \tilde{\mathscr{F}}_1 \\ x_h[k] = k_h e[k], & \text{if } \xi[k] \in \tilde{\mathscr{F}}_2 \\ x_h[k] = 0, & \text{if } \xi[k] \in \tilde{\mathscr{F}}_3 \\ u[k] = x_h[k], \end{cases} \tag{1}$$

where $e[k] \in \mathbb{R}$, $x_h[k] \in \mathbb{R}$, and $u[k] \in \mathbb{R}$ denote the input, state and output of $\overline{\mathscr{H}}$, at sample time $k \in \mathbb{N}$. Moreover, $\omega_h \in \mathbb{R}_{\geq 0}$, $k_h \in \mathbb{R}_{>0}$, and $T_s \in \mathbb{R}_{>0}$, denote the integrator frequency, gain parameter and the sampling time, while the decision as to which mode of operation is followed depends on $\xi[k] = (e[k], x_h[k-1], e[k-1])$. The sets $\tilde{\mathscr{F}}_1, \tilde{\mathscr{F}}_2$, and $\tilde{\mathscr{F}}_3$, are such that the proposed DT HIGS has two important characteristics (i) it produces an output similar to a CT HIGS element (see [1]) and (ii) the input/output (e,u) pair of (1) satisfy a sector constraint similar to that of a CT HIGS [1]. The latter will be exploited in stability of analysis sampled-data HIGS-controlled systems.

3 Proposed Analysis Approach

To analyze stability of sampled-data systems arising from closed-loop interconnection of linear CT plants and DT HIGS-based controllers, the procedure outlined in Fig. 1 is proposed, wherein a DT description of the system is obtained by considering an exact discretization of the plant model. Two methods for stability analysis of this system are presented based on (i) frequency domain conditions that can be verified using frequency response data and (ii) conditions based on linear matrix inequalities (LMIs) guaranteeing input-to-state stability (ISS) using multiple Lyapunov functions. Moreover, it is shown that the inter-sample behavior of the considered class of sampled-data systems can be bounded, and thus, stability of the sampled-data system can be concluded from stability of the studied DT system.

4 Example

Results obtained from the different stability analysis tests applied to an example involving control of a mass-spring-damper system are shown in Fig. 2. It is observed that while the frequency domain conditions can be easily verified based on frequency response data, the proposed LMI-based conditions are significantly less conservative.

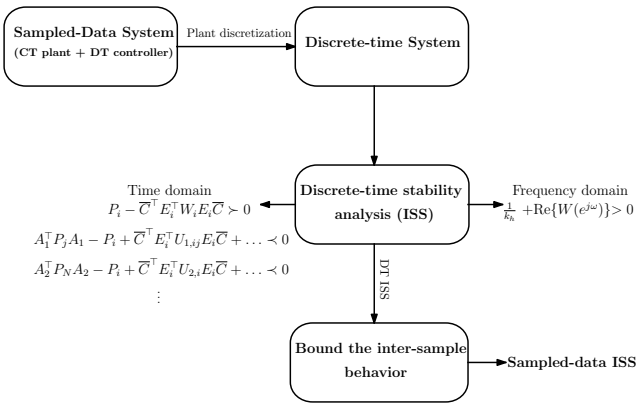

Figure 1: The proposed stability analysis approach.

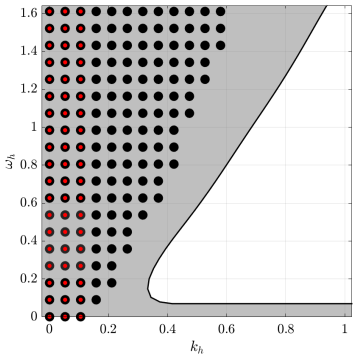

Figure 2: Stable region ■, stable (k_h, ω_h) pairs obtained from LMIs ●, frequency domain criterion ●.

5 Future work

Future work includes reducing the conservatism associated with the stability analysis methods.

References

[1] D. Deenen, B. Sharif, S. van den Eijnden, H. Nijmeijer, M. Heemels, and M. Heertjes. Projection-Based Integrators for Improved Motion Control: Formalization, Well-posedness and Stability of Hybrid Integrator-Gain Systems. *Automatica*, 2021.

Adaptive control without knowing what to adapt to

Rian Beck, Sudarsan Kumar Venkatesan & Bruno Depraetere
† Flanders Make, Belgium. E-mail: firstname.lastname@flandersmake.be

Motivation
Many controllers need to act on a system despite significant changes in the system's dynamics or its environment throughout time. To avoid that the controller then has to be very conservative with limited performance, adaptive control can be used. However, industry often does not trust such controllers, but prefers the non-adaptive controllers they are used to. They can furthermore "validate" those based on understanding into how the behavior will extrapolate.

As an intermediate solution we propose to make an adaptive controller that infrequently switches between a small set of predefined controllers, where each of those is the same controller type as the one currently used, but tuned differently. We will then switch between those controllers based on the observed conditions. The key novelty in this paper is that we will not define those conditions based on insight, but derive them from the data. This way, ideally, we can ***derive from the data what the important conditions are to adapt to***.

Application to hybrid vehicle
We consider as an example the control of a hybrid electrical vehicle, for which we have to control the power split between combustion engine and electromotor. A mature control strategy for this application is an ECMS controller, but the optimal tuning of an ECMS typically depends on the duty cycle. These are however very difficult to predict, so instead robustly tuned ECMS controllers are usually used. We therefore apply the idea outlined above, and look to switch between a small set of pre-defined ECMS controllers, each with their own tuning.

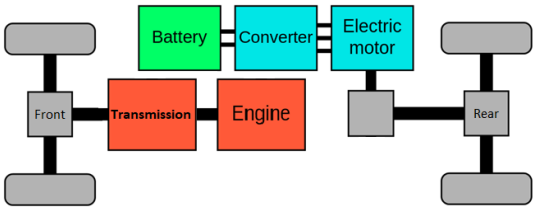

Figure 1: Layout of hybrid vehicle with combustion engine on front wheels, and electromotor on the rear.

To decide when to use which controller, we used a clustering based approach. We first used dynamic programming (DP) to find optimal power split choices for a large and diverse training set. Then we calculated for each point which ECMS parameters yield locally equivalent choices. For each point we also calculated a set of features derived from a window of past data, using the typical sensors available, such as vehicle speed, throttle, etc. As a result, we end up with a big set of points containing "optimal" ECMS parameters, and features that can also be estimated on a vehicle. Then we look for a set of clusters in this combined space, so that (i) each cluster contains a set of points with similar features, and thus hopefully similar conditions, (ii) all the points in the cluster can be controlled with similar ECMS parameters.

Afterwards we assemble the adaptive controller using a classifier to detect cluster membership online based on the same features (but now without including the ECMS parameters), and then online we run that classifier and simply select the ECMS parameters corresponding to the detected cluster.

Results
Performing the clustering using K-means and using 2 clusters, this yields a split as shown in Figure 2. Based on that

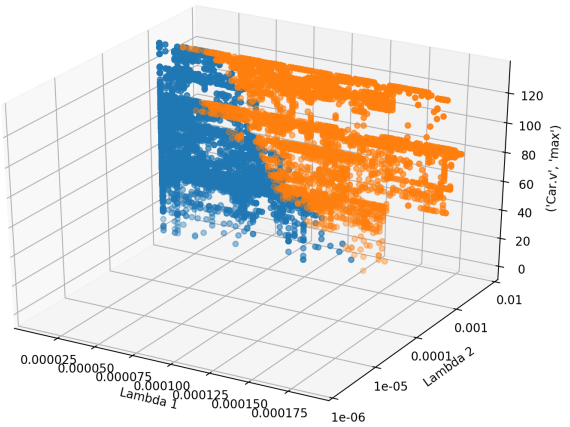

Figure 2: Output of clustering into 2 clusters.

split, we evaluated the resulting adaptive controller for 3 different validation cycles (not included in the training data). Compared to the best possible non-adaptive ECMS we save an additional 0.6-1.3% of fuel, and we approximate the truly optimal DP solutions to within 0.4-0.7%.

Benefits of using this method
Here we used only 2 clusters, and features derived from only a few signals. However, on the long term the problem of deciding which are the key features to adapt to might become more relevant, as more and more possible sources of information to adapt to become available, due to the increasing sensor count and connectedness, and some very rich sensors like camera's and/or LIDARs.

Acknowledgements: This work has been carried out within the framework of Flanders Make's ICON project 'ConACon' (Context Aware Control), funded by the agency Flanders Innovation & Entrepreneurship (VLAIO) and Flanders Make. Flanders Make is the Flemish strategic research centre for the manufacturing industry.

Multi-layered simulation relations for linear stochastic systems

B.C. van Huijgevoort [1] and S. Haesaert[1]

Introduction. Airplanes, cars, drones and power systems are examples of safety-critical control systems. These systems are often best described by stochastic discrete-time models. For these systems, we are interested in the design of controllers that provably satisfy formal specifications. In this work, we focus on the synthesis of controllers for continuous-state stochastic systems that yield guarantees on the satisfaction probability of temporal logic specifications. The synthesis of these controllers crucially depends on approximate finite-state abstractions and their accuracy quantification. This quantification is often performed using approximate stochastic simulation relations with a constant precision. However, for high-dimensional systems and complex formal specifications, this constant precision limits the achievable guarantees of the controllers. Therefore, we define a stochastic simulation relation that contains multiple precision layers, hence allowing a variable precision.

Problem statement. Consider a discrete-time stochastic system M whose behaviour can be described by stochastic difference equations. For this system, we want to design a controller C such that the composed system $M \times C$ satisfies a formal specification ϕ with a high probability. This specification can be given as a temporal formula to represent either simple specifications such as reach-avoid, invariance, liveness or more complex combinations thereof. Given specification ϕ and probability $p \in [0,1]$, the synthesis problem becomes

$$\mathbb{P}(M \times C \vDash \phi) \geq p. \tag{1}$$

However, for continuous-state models there does not exist an analytical solution to this problem.

Approach. In order to perform control synthesis for stochastic models with guarantees, we approximate the continuous-state models by finite-state models $\hat{M}$, for which it is possible to verify certain temporal logic specifications. This method is known as correct-by-design control synthesis [1] and is schematically shown in Figure 1. The top *specification* layer gives the desired behaviour of the controlled system using temporal logic and is used to synthesize an abstract controller over the abstract, finite-state model. This controller is refined from the *finite* layer to the *continuous* layer, leading to controller C. To bound the approximation error caused by using a finite-state model, we use simulation relations [2] that bound deviations in the output ε and in the probability δ. Therefore, the computation of the satisfaction probability of ϕ, $M \times C \vDash \phi$, is replaced by a robust computation [3] that yields a lower bound, that is,

[1]Control Systems group, Eindhoven University of Technology, Email: b.c.v.huijgevoort@tue.nl

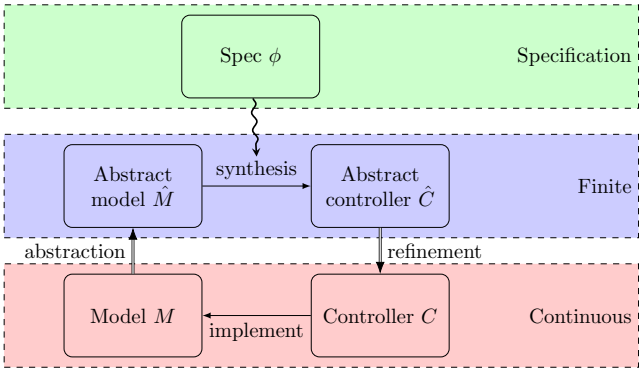

Figure 1: Schematic representation of correct-by-design control synthesis

$\mathbb{P}(M \times C \vDash \phi) \geq \mathbb{R}^{\varepsilon,\delta}(\hat{M} \times \hat{C} \vDash \phi)$. Generally only one simulation relation $\mathcal{R}$ is computed, leading to a constant precision. In ongoing work [4], we allow a variable precision by defining a multi-layered simulation relation $\boldsymbol{\mathcal{R}}$ consisting of multiple simulation relations. Furthermore, we present a method to compute a lower-bound on the probability of 1) staying in simulation relation $\mathcal{R}_i$ and 2) jumping from simulation relation $\mathcal{R}_i$ to $\mathcal{R}_j$ as illustrated in Figure 2. The use of a variable precision increases the achievable guarantees of the controllers and therefore, also the probability in (1).

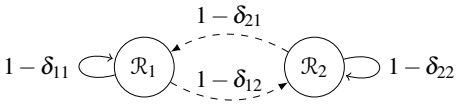

Figure 2: Multi-layered simulation relation $\boldsymbol{\mathcal{R}}$ consisting of two simulation relations $\mathcal{R}_1$ and $\mathcal{R}_2$. The edges are labelled with a lower-bound on the transition probability.

References

[1] M. Mazo, A. Davitian, and P. Tabuada. "Pessoa: A tool for embedded controller synthesis." *International Conference on Computer Aided Verification*, 2010

[2] S. Haesaert, S. Soudjani, and A. Abate. "Verification of general Markov decision processes by approximate similarity relations and policy refinement." *SIAM Journal on Control and Optimization*, 2017

[3] S. Haesaert, S. Soudjani, and A. Abate. "Temporal logic control of general Markov decision processes by approximate policy refinement." *IFAC-PapersOnLine*, 2018

[4] B. C. van Huijgevoort, and S. Haesaert. "Multi-layered simulation relations for linear stochastic systems." *European Control Conference (ECC)*, 2021

Implicit Fixed-Time ISS Safe CBFs

Ming Li and Zhiyong Sun
Department of Electrical Engineering, Eindhoven University of Technology, Eindhoven, The Netherlands
Email: {m.li3; z.sun}@tue.nl

I. Introduction

Fixed-time control barrier functions (FxT-CBFs) are typically designed to satisfy the "eventually-always" type of specifications, which aim to drive the state of a dynamical system to some given sets in specific time intervals and enforce the system trajectories to evolve in some safe sets at all times [1]. However, if external disturbances are present in the dynamical control system, the FxT reachability of the safe sets cannot be guaranteed. To this end, we extend the FxT-CBFs to the functions that are robust to external disturbances, i.e., FxT input-to-state safe CBFs (FxT-ISSf-CBFs). Further, we also propose implicit FxT-CBFs (IFxT-CBFs) and IFxT-ISSf-CBFs based on implicit function theory (IFT) [2], which simplifies the calculations of the derivatives of CBFs.

II. Preliminaries

Consider a control-affine system

$$\dot{\mathbf{x}} = f(\mathbf{x}) + g(\mathbf{x})\mathbf{u}, \tag{1}$$

where $\mathbf{x} \in \mathcal{D} \subseteq \mathbb{R}^n$ and $\mathbf{u} \in \mathcal{U} \subseteq \mathbb{R}^m$, $f : \mathcal{D} \to \mathbb{R}^n$ and $g : \mathcal{D} \to \mathbb{R}^{m\times n}$ are locally Lipschitz. Let a closed convex set $\mathcal{C} \subset \mathbb{R}^n$ be the 0-superlevel set of a continuously differentiable function $h : \mathbb{R}^n \to \mathbb{R}$, and we define $\mathcal{E} \triangleq \{\mathbf{x} \in \mathbb{R}^n : \mathcal{I}(\mathbf{x}) \geq 0\}$, $\partial\mathcal{E} \triangleq \{\mathbf{x} \in \mathbb{R}^n : \mathcal{I}(\mathbf{x}) = 0\}$, $\mathrm{Int}(\mathcal{E}) \triangleq \{\mathbf{x} \in \mathbb{R}^n : \mathcal{I}(\mathbf{x}) > 0\}$, $\mathrm{Out}(\mathcal{E}) \triangleq \{\mathbf{x} \in \mathbb{R}^n : \mathcal{I}(\mathbf{x}) < 0\}$, where the notations ∂, Int and Out on $\mathcal{E}$ denote the boundary, inner and outer regions of $\mathcal{E}$, respectively. Besides, a continuous function $\alpha : (-\tau, \zeta) \to \mathbb{R}$, with $\tau, \zeta > 0$, is an extended class $\mathcal{K}$ function if $\alpha(0) = 0$, and α is strictly monotonically increasing.

Definition 1. *(FxT-CBFs) The continuously differentiable function $h : \mathbb{R}^n \to \mathbb{R}$ is a FxTC-CBF if there exists $a, b > 0$, $p = 1 - \frac{1}{\gamma}$ and $q = 1 + \frac{1}{\gamma}$ for some $\gamma > 1$, such that the following holds:*

$$\sup_{\mathbf{u}\in\mathcal{U}} \mathcal{L}_f h(\mathbf{x}) + \mathcal{L}_g h(\mathbf{x})\mathbf{u} \geq -a\lfloor h(\mathbf{x})\rceil^p - b\lfloor h(\mathbf{x})\rceil^q, \tag{2}$$

where $\mathcal{L}$ denotes the Lie derivative, and the operation $\lfloor\cdot\rceil^s = \mathrm{sgn}(\cdot)|\cdot|^s$, $s > 0$.

Definition 2. *(FxT Reachability) Consider a target set $\mathcal{C}$ and a safe set $\mathcal{S}$, where they are both defined as a set like $\mathcal{I}$, the CBFs $\mathcal{C}$ and $\mathcal{S}$ are denoted by $h(\mathbf{x})$ and $\mathcal{X}(\mathbf{x})$, respectively. Then the target set $\mathcal{C}$ is FxT reachable if the trajectories of the system (1) satisfy the following two conditions: i) if the trajectories start from the safe set $\mathcal{S}$, the target set $\mathcal{C}$ will be visited within time interval $T(\mathbf{x}_0) \leq T_{\max} := \frac{1}{a(1-p)} + \frac{1}{b(q-1)}$; and ii) before reaching the target set $\mathcal{C}$, the system trajectories will always stay in the safe set $\mathcal{S}$.*

Theorem 1. *If there exists a FxTC-CBF $h : \mathbb{R}^n \to \mathbb{R}$ for the system* (1)*, then the target set $\mathcal{C}$ is FxT reachable [1] along the trajectory of the system* (1)*.*

III. IFxT-CBFs and IFxT-ISSf-CBFs

Definition 3. *(IFxTC-CBFs) An implicit function $M : \mathbb{R} \times \mathcal{D} \to \mathbb{R}$, $(h, \mathbf{x}) \mapsto M(h, \mathbf{x})$ is a IFxT-CBF if the following conditions are satisfied:*

1) *M is continuously differentiable on $\mathbb{R} \times \mathcal{D}$;*
2) *for any $\mathbf{x} \in \mathcal{D}$, there exists $M \in \mathbb{R} : M(h, \mathbf{x}) = 0$;*
3) *Let $\xi = \{(h, \mathbf{x}) \in \mathbb{R}\times\mathcal{D} : M(h, \mathbf{x}) = 0\}$. For $(h, \mathbf{x}) \in \xi$, $\mathbf{x} \in \mathcal{C} \Rightarrow h(\mathbf{x}) \geq 0$, $\mathbf{x} \in \partial\mathcal{C} \Rightarrow h(\mathbf{x}) = 0$, $\mathbf{x} \in \mathrm{Int}(\mathcal{C}) \Rightarrow h(\mathbf{x}) > 0$, $\mathbf{x} \in \mathrm{Out}(\mathcal{C}) \Rightarrow h(\mathbf{x}) < 0$;*
4) *$-\infty < \partial_{\mathbf{x}} M(h, \mathbf{x}) < 0$ holds for all $(h, \mathbf{x}) \in \xi$;*
5) *for all $(h, \mathbf{x}) \in \xi$, $\sup_{\mathbf{u}\in\mathcal{U}} \frac{\partial M/\partial \mathbf{x}}{\partial M/\partial h} \cdot (f(\mathbf{x}) + g(\mathbf{x})\mathbf{u}) \leq a\lfloor h(\mathbf{x})\rceil^p + b\lfloor h(\mathbf{x})\rceil^q$,*

Theorem 2. *If there exists a IFxT-CBF $M : \mathbb{R} \times \mathcal{D} \to \mathbb{R}$ for the system* (1)*, then the target set $\mathcal{C}$ is FxT reachable.*

Next, we consider an additive disturbance $d : \mathcal{D} \to \mathbb{R}^n$ to the nominal dynamics (1), i.e.,

$$\dot{\mathbf{x}} = f(\mathbf{x}) + g(\mathbf{x})\mathbf{u} + d(\mathbf{x}). \tag{3}$$

We define a new function $\eta(\mathbf{x}) := h(\mathbf{x}) + \varepsilon$, where ε is the solution of $a \cdot \varepsilon^p + b \cdot \varepsilon^q - \delta = 0$, $\varepsilon > 0$, and δ is dependent on the bound of the disturbance. Then, an updated safe set $\mathcal{C}_d$ is defined as $\mathcal{C}_d \triangleq \{\mathbf{x} \in \mathbb{R}^n : \eta(\mathbf{x}) \geq 0\}$ with $\partial\mathcal{C}_d \triangleq \{\mathbf{x} \in \mathbb{R}^n : \eta(\mathbf{x}) = 0\}$, $\mathrm{Int}(\mathcal{C}_d) \triangleq \{\mathbf{x} \in \mathbb{R}^n : \eta(\mathbf{x}) > 0\}$, $\mathrm{Out}(\mathcal{C}_d) \triangleq \{\mathbf{x} \in \mathbb{R}^n : \eta(\mathbf{x}) < 0\}$.

Assumption 1. *We assume that 1) the safe set $\mathcal{C}$ of the nominal system* (1) *is FxT reachable; 2) there exists $L > 0$ such that $\|\frac{\partial h(\mathbf{x})}{\partial \mathbf{x}}\| \leq L$ for all $\mathbf{x} \in \mathcal{D}$; 3) there exist a positive bound $\bar{d}$ such that $d(\mathbf{x}) \leq \bar{d}$; and 4) the parameters, a, b and δ, follow the inequality $a \leq b$ if $\delta/(2\sqrt{ab}) \geq 1$.*

Definition 4. *(FxT-ISSf-CBFs) The continuously differentiable function $h : \mathbb{R}^n \to \mathbb{R}$ is a FxT-ISSf-CBF for the safe set $\mathcal{C}_d$ if the following holds: $\sup_{\mathbf{u}\in\mathcal{U}} \dot{h}(\mathbf{x}) \geq -a\lfloor h(\mathbf{x})\rceil^p - b\lfloor h(\mathbf{x})\rceil^q - \delta$, where $\delta = L\bar{d}$.*

Theorem 3. *If there exists a FxT-ISSf-CBF $h : \mathbb{R}^n \to \mathbb{R}$ for the system* (3)*, then the safe set $\mathcal{C}_d$ of the system* (3) *is FxT reachable.*

Theorem 4. *Let Assumptions $1 - 4$ hold. If there exists a continuous function $M : \mathbb{R} \times \mathcal{D} \to \mathbb{R}$, $(h, \mathbf{x}) \mapsto M(h, \mathbf{x})$ satisfying the conditions 1), 2), 3), 4) of Definition 3 and the following condition:*

$$\sup_{\mathbf{u}\in\mathcal{U}} \frac{\partial M/\partial \mathbf{x}}{\partial M/\partial h} \cdot (f(\mathbf{x}) + g(\mathbf{x})\mathbf{u}) \leq a\lfloor h(\mathbf{x})\rceil^p + b\lfloor h(\mathbf{x})\rceil^q + \delta, \tag{4}$$

then the target set $\mathcal{C}_d$ is FxT reachable.

References

[1] K. Garg and D. Panagou, "Control- Lyapunov and control-barrier functions based quadratic program for spatio-temporal specifications," in *2019 IEEE 58th Conference on Decision and Control (CDC)*. IEEE, 2019, pp. 1422–1429.

[2] A. Polyakov, "Nonlinear feedback design for fixed-time stabilization of linear control systems," *IEEE Transactions on Automatic Control*, vol. 57, no. 8, pp. 2106–2110, 2011.

Learning-based Control for High-efficient PPC Engines with Gaussian Process

Wang Pan
Control Systems Technology
Eindhoven University of Technology
5612AP Eindhoven
The Netherlands
Email: w.pan@tue.nl

Frank Willems
Control Systems Technology
Eindhoven University of Technology
5612AP Eindhoven
The Netherlands
Email: f.p.t.willems@tue.nl

1 Abstract

In this presentation, an adaptive high-performance control approach for model-based control of Partially Premixed Combustion (PPC) engines is introduced. PPC is a next-generation combustion technology, which has the potential to achieve both ultra-low emissions and high efficiency. Unlike the conventional diesel and gasoline engines, high knock resistance fuel (e.g. Research Octane Number (RON) 70) and high dilution (e.g. Exhaust Gas Recirculation (EGR) 50%) has been exploited in PPC engines to increase the pre-ignition mixing time. Butanol has been used in this study because of it's relative high heat value, proper anti-knock characteristics (RON 98), and can be mixed with commercial diesel under any mass fraction. Also butanol can be produced from bio-mass and has been expected to play a significant role in the future utilization of carbon neutral fuels. As the PPC concept is characterized by a complex chemical-physical process of low temperature kinetic reactions, it lacks direct trigger of ignition and combustion as well as it is sensitive to varying operating conditions. These complex nature of PPC makes it challenging to control the combustion for optimum efficiency and emissions at broad engine operation with low cyclic variability and without exceeding maximum allowed in-cylinder pressure rise rate or peak pressure. The nonlinear relationship between the control input and combustion system response makes that conventional lookup table-based control might need too much maps and calibration effort, thus no longer feasible for real operation scenarios. Model-based control approach is therefore needed to give proper reference for the feed forward combustion control of PPC engines. Furthermore, due to the variation of real driving conditions and the unmodeled dynamics, a fixed model is generally not accurate enough for control during real operation conditions of PPC engines. The current study proposes a learning-based control approach with a hybrid model. A simplified first principal derived model has been first developed to provide a base estimation of the ignition properties. A learning module with Gaussian Process Regression (GPR) has then been added to capture the model errors between the model prediction and in-cylinder pressure measurement data, as shown in figure 1. The aim of this study is to develop a self-learning control oriented model and a model based controller to adjust combustion phasing during steady operation conditions.

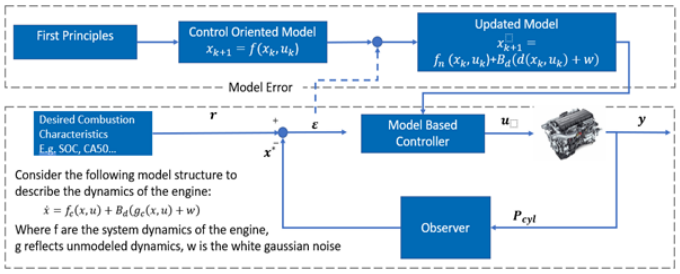

Figure 1 illustration of learning based PPC combustion control concept

This approach has been demonstrated on a single-cylinder heavy-duty diesel engine. BH80 (80 vol% bio-butanol and 20 vol% n-heptane) is blended and tested at 8 bar gross Indicated Mean Effective Pressure (gIMEP) in PPC mode. Inlet heating, inlet boosting and multi-injection strategies have been implemented to simulate the variation of operation conditions. Algorithms were implemented on a Field Programmable Gate Array (FPGA) in order to analyze the heat release using measured cylinder pressure, which is input to next cycle control. As a basis for the combustion control concept a detailed physics-based model was first developed and validated on the engine experiment data. Then, the learning-based control oriented model has been tested on the high fidelity physics-based simulator with Model-In-Loop (MIL) simulation. The results show that without the implementation of the learning model, across a wide range of input conditions, the physics-based model is able to capture the auto-ignition characteristics and predicts the start of combustion within $\pm 2^o$ Crank Angle (CA). After implementation of the learning part, the error bond for the predictions of start of combustion has been reduced to $\pm 1^o$CA. The final results have also been compared with other common used learning approaches (e.g. neural networks, parameter updating). The current approach shows improvement with regard to both prediction accuracy and the extrapolation capacity.

Feedforward Control in the Presence of Input Nonlinearities: A Learning-based Approach

Jilles van Hulst[1,*], Maurice Poot[1], Dragan Kostić[2], Kai Wa Yan[2], Jim Portegies[3], and Tom Oomen[1,4]

[1]Control Systems Technology Group, Dept. of Mechanical Engineering, Eindhoven University of Technology, The Netherlands
[2]Center of Competency, ASM Pacific Technology, The Netherlands
[3]CASA, Dept. of Mathematics and Computer Science, Eindhoven University of Technology, The Netherlands
[4]Delft Center for Systems and Control, Delft University of Technology, The Netherlands
[*]Email: j.s.v.hulst@tue.nl

1 Background

Advanced feedforward control methods often enable mechatronic systems to perform varying motion tasks with extreme accuracy. Many of these developments focus on linear time-invariant systems, either polynomial [1] or rational [2], possibly with friction compensation. In many systems, additional nonlinearities, including actuator saturation, are present that may limit control performance.

2 Problem Formulation

The aim is to achieve low error and high flexibility to varying tasks for motion systems that exhibit dominant linear dynamics, and which contain a static input nonlinearity, i.e., a Hammerstein system. This research aims to learn a parametrized input nonlinearity using data.

3 Approach

A parametrized linear feedforward, i.e., basis functions [1], can compensate the linear component of the described system. In addition, the input nonlinearity can be compensated by inversion in the feedforward, together constituting a Wiener feedforward. The key idea is that norm-optimal iterative learning control (NOILC) is able to compensate nonlinear behavior if it is repetitive. In order to do so, the input nonlinearity is modeled using a parametric model. Then, the NOILC optimization is performed with a repeated reference satisfying persistence of excitation for the nonlinear system. Lastly, the converged NOILC feedforward signal is fitted by the parametrized Wiener feedforward. The fitted parameter values can be used to invert the input nonlinearity.

4 Results

Fig. 1 shows results for positioning of a simulated wire bonder system in one direction, i.e., SISO, with an input nonlinearity. Shown are linear rational basis function (RBF) feedforward [2] and RBF with inversion of the input nonlinearity, obtained using the proposed method. Observe that the proposed method compensates the input nonlinearity, which results in a lower error 2-norm and higher performance directly after a task change compared to strictly linear parametrized feedforward.

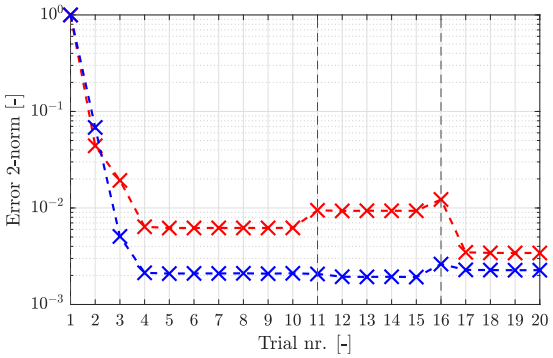

Figure 1: Comparison of the error 2-norm per trial for linear parametrized feedforward (-) and the proposed method (-). In order to show the flexibility of the methods, the motion task is changed at trials 11 and 16. This task change is indicated by vertical dashed lines.

5 Conclusion and Outlook

This research introduces a method for identification and compensation of input nonlinearities by exploiting a norm-optimal ILC signal. Results indicate that performance in terms of both tracking error and flexibility to task variations are improved.

References

[1] S. H. van der Meulen, R. L. Tousain, and O. H. Bosgra, "Fixed Structure Feedforward Controller Design Exploiting Iterative Trials: Application to a Wafer Stage and a Desktop Printer," *Journal of Dynamic Systems, Measurement, and Control*, vol. 130, no. 5, sep 2008.

[2] J. Bolder and T. Oomen, "Rational basis functions in iterative learning control - With experimental verification on a motion system," *IEEE Transactions on Control Systems Technology*, vol. 23, no. 2, pp. 722–729, 2015.

MPC Informed Control via Neural Networks

M. Bahadir Saltik Bayu Jayawardhana
Discrete Technology and Production Automation
University of Groningen
Nijenborgh 4
9747 AG Groningen
The Netherlands
Email: {m.b.saltik,b.jayawardhana}@rug.nl

Ashish K. Cherukuri
Optimization and Decision Systems
University of Groningen
Nijenborgh 4
9747 AG Groningen
The Netherlands
Email: a.k.cherukuri@rug.nl

1 Introduction

The aim of this work is to develop a neural network (NN) based learning algorithm which robustly and optimally controls an nonlinear system along a trajectory without applying variational calculus tools. An industrially accepted (sub)optimal control method adhering the constraints is the model predictive control (MPC) approach. Here we develop a technique to make use of recently proposed learning algorithms ([1]) in approximating the MPC controllers via NNs.

The need for learning an MPC controller is due the online optimization step inherent in the MPC setup. Restricted number of MPC iterations can lead to suboptimal control actions due to real time requirements, especially for large scale systems. Instead, we make use of the achievements in the physics informed neural network (PINN) approach to effectively learn and generalize the control actions obtained from the MPC controlled closed-loop data to elevate online solution of the optimization problem.

2 Optimization Problem for Learning Controllers

We consider the reference tracking problem for nonlinear systems in the form of MPC problem $\mathscr{P}$:

$$\mathscr{P}: \begin{cases} \min & J^{MPC}, \\ J^{MPC} = & \sum_{j=0}^{N_p-1} \varepsilon_{j|k}^\top Q \varepsilon_{j|k} + \Delta u_{j|k}^\top R \Delta u_{j|k}, \\ x_{j+1|k} = & f(x_{j|k}, u_{j|k}),\ y_{j|k} = h(x_{j|k}), \\ \varepsilon_{j|k} = & y_{j|k} - r_{k+j},\ u_{j+1|k} = u_{j|k} + \Delta u_{j|k}, \\ & c_j(x_{j|k}, u_{j|k}) \leq 0. \end{cases} \tag{1}$$

We assume that state and MPC control actions are available for different reference settings. For the learning problem we construct a NN with the cost function

$$J^{NN} = J^{data} + \lambda_1 J^{MPC},$$

where $J^{data} = \sum_{i=0}^{N_{\text{data}}} \|u_i^{MPC} - u_i^{NN}\|_2^2$ corresponds to squared sum of the difference between the control actions predicted via the NN u^{NN} and the training sample u^{MPC}, while the cost term J^{MPC} is as given in Eq. (1) and parametrized with respect to the NN. The tuning, or regulatization, parameter λ_1 allows the user to weight the terms corresponding the respective cost terms.

3 A Case Study and Future Work

We consider the problem of a 4-tank system with MPC parameters as in [2]. The NN consists of one hidden layer with 12 ELUs, two output nodes for two control inputs, and inputs as the state and the reference signal parameters (amplitude and frequency). Low learning rate ($\eta = 0.01$) and high dropout value is required to reduce the noisy NN output. The reference signal, constraints and trajectories are given in Figure 1. We train the NN with the state and MPC input trajectories generated from stochastic initial conditions and reference signals that are not used in the evaluation.

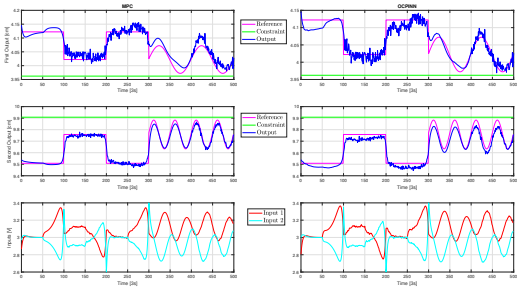

Figure 1: Output trajectories for system controlled with MPC and neural network induced control actions.

The results indicate that both of the controlled systems are in close alignment. However the NN based controller does not back off the operating point sufficiently. Future directions are better parameterization of reference signals for long prediction horizons, guarantees on the constraint satisfaction and control performance properties.

References

[1] Chen, Steven W., et al. Large scale model predictive control with neural networks and primal active sets. Automatica 135 (2022): 109947.

[2] M.B. Saltık, L. Özkan, S. Weiland. Moment Based Model Predictive Control for Linear Systems: Additive Perturbations Case. International Journal of Robust and Nonlinear Control (Under Review).

Multi-System Iterative Learning Control: extending ILC towards Interconnected Systems.

Daniele Ronzani, Armin Steinhauser and Jan Swevers
MECO Research Team, Dept. Mechanical Engineering, KU Leuven
DMMS lab, Flanders Make
Celestijnenlaan 300B, 3001 Heverlee, Belgium
firstname.lastname@kuleuven.be

1 Introduction

Traditionally, iterative learning control (ILC) is employed to improve the performance of a repetitive task by learning on a single system. However, in the context of Cyber-Physical Systems (CPS) and Industry 4.0, mechatronic systems are interconnected and could therefore exploit knowledge learned by other machines systematically. For instance, the commissioning of a new fleet of similar machines, that has to learn how to optimally perform the same task, or the addition of a new system to a tuned fleet, are possible scenarios where learning and sharing a common model could lead to an improvement of performance and/or reduction of commissioning time.
This work present the Multi-System Iterative Learning Control (MSILC) algorithm that aims to extend traditional ILC towards multiple systems.

2 Algorithm

The MSILC approach is based on a generic nonlinear norm-optimal ILC method that, as shown in [1], can be interpreted as a two-step procedure: first compute an explicit model correction and subsequently invert the corrected system dynamics. Specifically, the MSILC further exploit the model correction step by calculating a common correction—shared between all systems—and a correction specific to each system, as shown in Figure 1. The MSILC algorithm, is implemented as a custom class of RoFaLT [2], `MultiSystemsILC`, and is available on GitLab [1]. The software provide a and generic tool for an optimization, model-based nonlinear ILC.
The approach is theoretically analyzed and categorized in the field of linear ILC through the well known framework of filter design. The MSILC iteration-domain dynamics can be equivalently represented by the update law (1) for the next iteration $i+1$ of a system k belonging to a fleet of K systems. The parameter ϕ, resulting from the regularization in the delta correction step, provide a tuning knob to trade-off between a single-system

[1] https://gitlab.mech.kuleuven.be/meco-software/multisystem-ilc

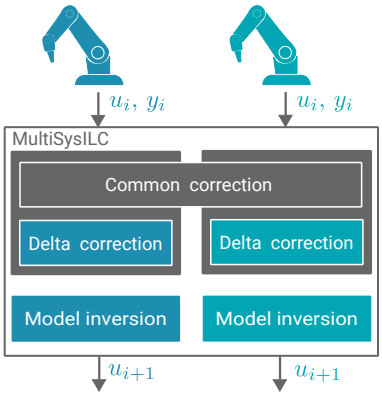

Figure 1: Illustration of the MSILC algorithm.

norm-optimal update law (1a) and a common norm-optimal update law. The filters $\mathcal{L}$ and $\mathcal{Q}$ are designed by means of the regularization parameter in the model inversion step of the algorithm.

$$u_{i+1}^k = \phi\, \mathcal{Q}\big(u_i^k + \mathcal{L}\, e_i^k\big) \tag{1a}$$

$$+ (1-\phi)\frac{1}{K}\sum_{j}^{K} \mathcal{Q}\big(u_i^j + \mathcal{L}\, e_i^j\big), \tag{1b}$$

3 Numerical study

The functioning of the approach is discussed through a numerical study of a fleet of positioning stages with measurement affected by iteration-varying disturbances. The results demonstrate the increase of the fleet performance achieved by using a trade-off between a single-system and common update law.

References

[1] M. Volckaert, J. Swevers, and M. Diehl, A Two Step Optimization Based Iterative Learning Control Algorithm, ASME 2010 Dyn. Syst. Control Conf. Vol. 1, pp. 579-581, Jan. 2010.

[2] A. Steinhauser, T. D. Son, E. Hostens, and J. Swevers, RoFaLT : An Optimization-based Learning Control Tool for Nonlinear Systems, 2018 IEEE 15th Int. Work. Adv. Motion Control, pp. 198-203, Mar. 2018.

Acknowledgement This work has been carried out within the framework of Flanders Make's SBO project 'MultiSysLeCo' (Multi-System Learning Control) funded by the agency Flanders Innovation & Entrepreneurship (VLAIO) and Flanders Make. Flanders Make is the Flemish strategic research centre for the manufacturing.

Reduction in calibration effort of diesel engine transient control by using LSTM-based methodology

Prasoon Garg* Emilia Silvas*,† Frank Willems*,†
*Dept. of Mechanical Eng., Eindhoven University of Technology, The Netherlands
†TNO Traffic and Transport, Helmond, The Netherlands (p.garg.1@tue.nl)

Abstract

Large development times and costs are required in calibration of transient control of diesel engines. Existing control calibration approach for engines follows a two-step approach: base calibration at steady-state conditions and expert intensive calibration for transients operation. This approach is unsystematic, requires large expert effort and the calibrated control settings usually result in sub-optimal engine performance in transients [1].

In this paper, a Machine Learning-based methodology is proposed, where a Long Short-term Memory (LSTM) neural network (NN) model can learn in a supervised manner the transients control policy and reference trajectories as a function of external inputs to the control system. This study focuses on transient control of diesel engine air-path subsystem. The objective is to develop a systematic approach to accurately model transient control policy, reduce the expert effort with minimal computational and memory complexity for real-time implementation on engine control unit (ECU).

The proposed model-based calibration approach comprises: 1) off-line optimization to determine transients control policy and 2) efficient modeling of this policy for ECU implementation. This work focuses on the second step of this proposed approach. The proposed model $\mathcal{M}$ input-output structure is defined as,

$$\mathcal{M} : \boldsymbol{w} \rightarrow \begin{bmatrix} \boldsymbol{u}_0 \\ \boldsymbol{r} \end{bmatrix} \tag{1}$$

where the model learns to predict the control signals $\boldsymbol{u}_0$ and $\boldsymbol{r}$ as a function of external inputs $\boldsymbol{w}$ in supervised learning manner as shown in Figure 1. Here, $\rightarrow$ refers to mapping from inputs to output.

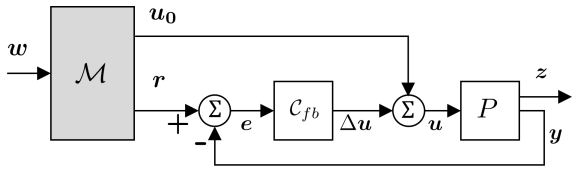

Figure 1: Proposed control system design

For this data-driven modeling, the input-output data has to be generated using off-line optimization as described above. However, for the model development in this study the training data-set $(\boldsymbol{w}, [\boldsymbol{u}_0 \ \boldsymbol{r}]^\top)$ is generated from an existing calibrated engine model-in-the-loop environment.

The proposed input-output relationship is modeled using a LSTM NN, which is a gated recurrent neural network (RNN) [2]. LSTM NNs are efficient in learning long-term time dependencies between inputs and outputs. In order to determine the LSTM model parameters, numerical optimization method is applied. The optimization problem is to minimize the expected empirical loss between the true data labels $\boldsymbol{o} = [\boldsymbol{u}_0 \ \boldsymbol{r}]^\top$ and the LSTM model predictions $\hat{\boldsymbol{o}}(\boldsymbol{w}; \boldsymbol{\Theta}) = [\hat{\boldsymbol{u}}_0 \ \hat{\boldsymbol{r}}]^\top$, where $\boldsymbol{\Theta}$ are the model parameters.

In this presentation, we will present the LSTM model development approach, which includes experiment design and data acquisition, data-set generation, choice of input history length to the LSTM model, NN hyper-parameter tuning and model validation. The choice of best LSTM model architecture is motivated by trade-off analysis as shown in Figure 2 between the system performance accuracy and calibration effort with varying LSTM model complexity.

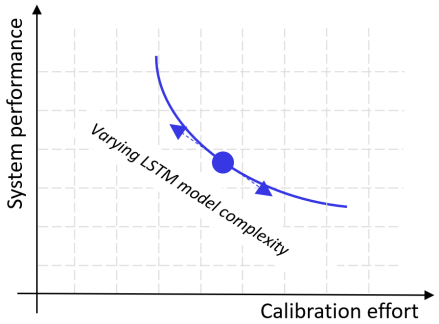

Figure 2: Illustration of the trade-off

Acknowledgement

We thank DENSO for providing financial support and the Powertrain R&D team at DENSO Aachen Engineering Centre (AEC) for the constructive discussions for this study.

References

[1] P. Garg, E. Silvas, and F. Willems, "Potential of machine learning methods for robust performance and efficient engine control development," *6th IFAC Conference on Engine Powertrain Control, Simulation and Modeling E-COSM*, vol. 54, no. 10, pp. 189–195, 2021.

[2] S. Hochreiter and J. Schmidhuber, "Long short-term memory," *Neural computation*, vol. 9, no. 8, pp. 1735–1780, 1997.

Safe Learning-Based Model Predictive Control

Filippo Airaldi Bart De Schutter Azita Dabiri
Delft Center for Systems and Control, Delft University of Technology
Mekelweg 2, 2628 CD Delft, The Netherlands
{f.airaldi,b.deschutter,a.dabiri}@tudelft.nl

1 Introduction

Recent successes in Reinforcement Learning (RL) and the rising abundance of data have led to a growing interest in learning-based control methodologies [1], which strive to learn different elements of the controller framework in order to reduce conservativeness and improve closed-loop performance. However, ensuring *safety* and *constraint satisfaction*, paramount aspects in the majority of control applications, remains a challenge, particularly during the learning process. A purely data-driven solution to this issue, Safe RL [2] encourages safety in the long term by appropriately modifying the optimality criterion or the exploration process by, for instance, penalizing dangerous behaviours or integrating knowledge from a teacher. Nonetheless, few or no formal guarantees on constraint satisfaction are currently available in literature. An alternative approach is offered by Learning-Based Model Predictive Control (LBMPC) [3], which has also been gaining substantial attention thanks to its ability to structurally take safety constraints into account and to provide formal tools for the analysis of stability and feasibility.

In this presentation we review recent works on LBMPC, identify open issues in the field, and suggest a set of possible research directions addressing these issues.

2 Approaches

Model Predictive Control (MPC) has established itself as a powerful control methodology able to explicitly handle hard constraints and deliver an (sub)optimal policy even with a possibly inaccurate model of the underlying system. In recent years, particular focus has been dedicated to the integration of learning within this framework. The various approaches in LBMPC can be classified by what elements, e.g., the model dynamics, the controller design parameters, or the disturbance set, are learned [3].

Learning the system dynamics to improve performance is an obvious direction, since MPC relies on a nominal model to formulate predictions on the state trajectories. A frequent assumption in this line of research is to collect the unknown errors affecting the nominal model as an additive term, which is learnt based on data collected online. Gaussian Processes (GPs) are commonly employed as they seamlessly allow for the treatment of model uncertainties, though assumptions on the shape of the disturbance set are often made to be able to establish stability and safety.

Another direction is to learn the controller parameters, such as the stage cost, the terminal cost, terminal set constraint, as well as the disturbance set. In this context, noteworthy is the combination of Safe RL with robust MPC [4], where the MPC controller acts as a parametric function approximation that can structurally handle safety, while the RL agent is tasked with tuning the parameters of the controller. Here, care during the parameter update must be taken to avoid jeopardizing stability and feasibility of the MPC.

3 Open issues & research directions

We highlight the following open challenges: *(i)* several studies have shown promising theoretical and practical results in the integration of robust MPC with learning techniques, but a concern is that its conservativeness may adversely affect the efficiency: can less conservative formulations, such as stochastic and scenario-based MPC in particular, be employed to yield higher performance? Additionally, *(ii)* can we use the tools from scenario-based optimization to obtain a probabilistic certification for safety? Lastly, *(iii)* exploration of the safe action space is mostly implemented passively. Is it possible to adapt the theory from Multi-Armed Bandit (MAB) and RL to actively ensure sufficient and efficient exploration in LBMPC as well?

Acknowledgements: This research is part of a project that has received funding from the European Research Council (ERC) under the European Union's Horizon 2020 research and innovation programme (Grant agreement No. 101018826 - CLariNet).

References

[1] L. Brunke, M. Greeff, et al. Safe Learning in Robotics: From Learning-Based Control to Safe Reinforcement Learning. *arXiv preprint arXiv:2108.06266*, 2021.

[2] J. Garcia, F. Fernández. A Comprehensive Survey on Safe Reinforcement Learning. *Journal of Machine Learning Research*, 16(1):1437-1480, 2015.

[3] L. Hewing, K. P. Wabersich, et al. Learning-Based Model Predictive Control: Toward Safe Learning in Control. *Annual Review of Control, Robotics, and Autonomous Systems*, 3:269–296, 2020.

[4] M. Zanon, S. Gros. Safe reinforcement learning using robust MPC. *IEEE Transactions on Automatic Control*, 66(8):3638–3652, 2021.

Optimal motion planning sped up with LogSumExp for obstacle avoidance

Joris Gillis Goele Pipeleers Jan Swevers
MECO Research Team, Department Mechanical Engineering, KU Leuven
DMMS lab, Flanders Make, Leuven, Belgium
Email: {firstname}.{lastname}@kuleuven.be

1 Optimal motion planning

Optimal control problems (OCP) offer a versatile methodology for solving optimal motion planning of mechatronic systems over a continuous state space $x(t) \in \mathbb{R}^{n_x}$ and control space $u(t) \in \mathbb{R}^{n_u}$. Using a direct transcription, one can transform such an OCP into a nonlinear program. A popular multiple shooting transcription results in:

$$\begin{aligned} \underset{\substack{x_1,x_2,\ldots,x_{N+1},\\ u_1,u_2,\ldots,u_N}}{\text{minimize}} \quad & \textstyle\sum_{i=1}^{N} l(x_k,u_k) + e(x_{N+1}), \\ \text{subject to} \quad & x_{k+1} = F(x_k,u_k), \quad k = 1\ldots N \\ & B(x_1,x_{N+1}) = 0, \\ & h(x_k,u_k) \geq 0, \quad k = 1\ldots N \end{aligned} \tag{1}$$

with $l(\cdot,\cdot)$ and $e(\cdot)$ representing cost, $F(\cdot,c\dot{)}$ representing discretized system dynamics, $B(\cdot,\cdot)$ representing boundary conditions, and $h(\cdot,\cdot)$ representing path constraints.

2 Obstacle avoidance

In an environment littered with convex obstacles $O_1,\ldots,O_{n_o}$, obstacle avoidance of a convex self S with those obstacles can be readily mapped to the above path constraints with a signed distance function:

$$\text{dist}(S(x_k),O_i) \geq 0, \quad k = 1\ldots N, \quad i = 1,\ldots,n_o. \tag{2}$$

As an example, consider a circular self at position $p(x)$ with radius R and circular obstacles with positions p_i and radii r_i. Equation (2) becomes:

$$\|p(x_k) - p_i\|_2 - (R + r_i) \geq 0, \quad k = 1\ldots N, \quad i = 1,\ldots,n_o.$$

When using an efficient modeling tool such as CasADi[1], the computational bottleneck in numerical solution for large n_o is to be found in the numerical algebra ("linalg") of a solver as opposed to evaluations of objective and constraint functions including its derivatives ("fun_eval").

3 Use of LogSumExp

To reduce matrix dimensions, we propose to replace the i-enumeration in Equation (2) with a smooth approximation to the minimum distance based on LogSumExp, i.e.

$$\text{lse}(y) := \log(e^{y_1} + \ldots + e^{y_n}), \quad \text{with } y \in \mathbb{R}^n. \tag{3}$$

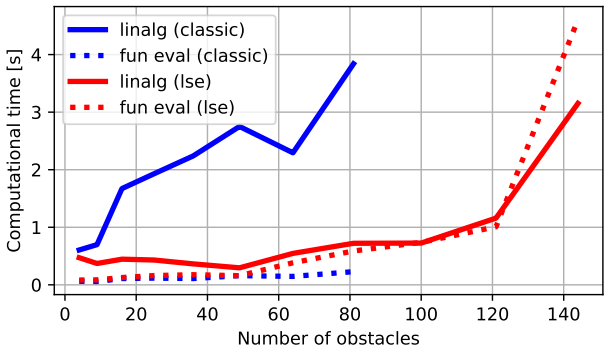

Figure 1: Benchmark results

Its approximation error is one-sided and quantifiable: introducing α as scalar scaling factor, $\frac{1}{\alpha}\text{lse}(\alpha\cdot)$ is never smaller than the true maximum and at most $\log(n)/\alpha$ larger.

Dismissal of LogSumExp for obvious overflow and accuracy issues appears unfounded [2]; a robust computational recipe, still continuously differentiable is given by:

$$\text{lse}(y) = \max(y) + \text{log1p}\left(\sum_{\substack{i=1 \\ i \neq \text{argmax}(y)}}^{n} e^{y_i - \max y}\right). \tag{4}$$

4 Results

Adding LogSumExp as differentiable component in CasADi, we present in Figure 1 a simple benchmark of time-optimal point-to-point motion of a bicycle model through a grid of circular obstacles, solved with Ipopt.

References

[1] Joel A. E. Andersson, Joris Gillis, Greg Horn, James B. Rawlings, and Moritz Diehl. CasADi: a software framework for nonlinear optimization and optimal control. *Mathematical Programming Computation*, Jul 2018.

[2] Pierre Blanchard, Desmond J Higham, and Nicholas J Higham. Accurately computing the log-sum-exp and softmax functions. *IMA Journal of Numerical Analysis*, 41(4):2311–2330, 08 2020.

Acknowledgement. This work has been carried out within the framework of projects WorkDrive: Flanders Make SBO, Modular, autonomous work-drive architectures, DIRAC: Flanders Make SBO, Deterministic and Inexpensive Realizations of Advanced Control. Flanders Make is the Flemish strategic research centre for the manufacturing industry.

An adaptive MPC scheme for systems with variable topologies

Tony Dang, Taranjitsingh Singh, and Frederik Debrouwere
Flanders Make
Lommel, Belgium
Email: tony.dang@flandersmake.be

1 Introduction

An adaptive Model Predictive Control (MPC) scheme is proposed for the control of systems with time-varying topologies. Such systems are relevant for e.g. heating control in buildings where connections between different rooms can be closed and opened, pneumatic networks where states of valves can change, etc. Such dynamically changing systems are often too complex for classical control strategies. In many cases, these systems are also MIMO systems. Hence, MPC is a potentially suitable strategy for such problems.

An adaptive MPC scheme is proposed by modelling the system using graph theory [2]. The introduction of the Laplacian matrix $\mathscr{L} = \mathscr{D} - \mathscr{A} = [L_{ij}]$ as a parameter in the system allows us to adaptively switch the topology during the MPC loop, without the need for rewriting all system equations. $\mathscr{D}$ is the Degree matrix and $\mathscr{A}$ the Adjacency matrix, and undirected communication is assumed.

2 Modelling approach

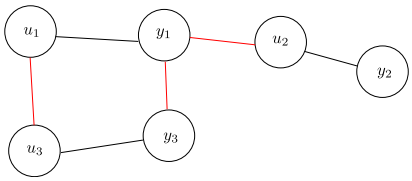

Figure 1: Three subsystems in an arbitrary topology. Communication dynamics are indicated by the red edges. The black edges indicate the internal dynamics of the individual subsystems.

The communication dynamics between different subsystems enter each individual subsystem as an additional input. E.g. for the system given in figure 1, the full system dynamics are modelled as follows:

$$\begin{aligned} \dot{y}_1 &= f(y_1,u_1) - \boldsymbol{l}_1/\tau_c \begin{bmatrix} y_1 & u_1 & y_2 & u_2 & y_3 & u_3 \end{bmatrix}^\intercal \\ \dot{u}_1 &= f(u_1,y_1) - \boldsymbol{l}_2/\tau_c \begin{bmatrix} y_1 & u_1 & y_2 & u_2 & y_3 & u_3 \end{bmatrix}^\intercal \\ &\dots \end{aligned} \tag{1}$$

with τ_c the time constant for the communication dynamics and $\boldsymbol{l}_i$ the row vectors of the Laplacian matrix $\mathscr{L}$. For the given system in figure 1, the Laplacian takes the following form:

$$\mathscr{L} = \begin{bmatrix} 2 & 0 & 0 & -1 & -1 & 0 \\ 0 & 1 & 0 & 0 & 0 & -1 \\ 0 & 0 & 0 & 0 & 0 & 0 \\ -1 & 0 & 0 & 1 & 0 & 0 \\ -1 & 0 & 0 & 0 & 1 & 0 \\ 0 & -1 & 0 & 0 & 0 & 1 \end{bmatrix}. \tag{2}$$

The Laplacian $\mathscr{L}$ enters the system equations as an adaptive parameter in the MPC scheme, as shown in equation 1.

3 Results

Simulation results in CasADi [1] of the adaptive MPC scheme are applied to a pneumatic system (figure 2). An input-bounded MPC is defined with $V(x,u) = \sum_{k=1}^{N}(y_{2,k} - y_{\text{ref}})^2$. The topology is identical to the topology described in figure 1. Around 150 seconds, a topology change is induced: a disconnection between y_1 and y_3 occurs.

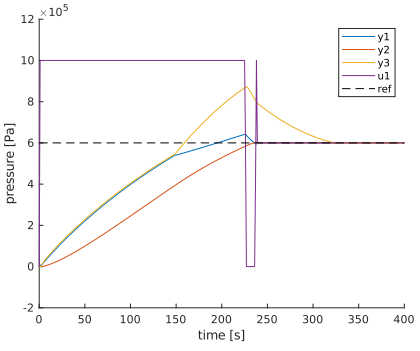

Figure 2: Simulation results of the adaptive MPC.

References

[1] Joel AE Andersson et al. "CasADi: a software framework for nonlinear optimization and optimal control". In: *Mathematical Programming Computation* 11.1 (2019), pp. 1–36.

[2] Guangming Xie and Long Wang. "Consensus control for a class of networks of dynamic agents". In: *International Journal of Robust and Nonlinear Control: IFAC-Affiliated Journal* 17.10-11 (2007), pp. 941–959.

Acknowledgement: This work is supported by Flanders Make project: ICON ID2CON: Integrated Identification to Control.

Reformulating Collision Avoidance Constraints for Multi-DOF Robotic Planning

Dries Dirckx, Jan Swevers, Wilm Decré, Goele Pipeleers
MECO Research Team, Department of Mechanical Engineering, KU Leuven
DMMS-M Core Lab, Flanders Make, Leuven, Belgium
Celestijnenlaan 300, B-3001 Heverlee
Belgium
Email: dries.dirckx@kuleuven.be

1 Introduction

Collision-free trajectory planning of robotic systems in a cluttered environment has attracted a lot of attention in industry and the robotics research community over the last few years. Applications can be found in a variety of domains such as aerial vehicles, forklifts driving in a warehouse, assistive robots in medical environments, etc. Motion planners create a feasible trajectory that satisfies certain constraints such as robot joint and actuation limits, and avoids collision. This work describes a novel, computational-cost reducing collision avoidance constraint for trajectory planning of robotic systems by adopting a smooth approximation of the maximum function. The proposed method reduces the number of constraints in a trajectory planning problem by expressing a number of constraints as one single constraint that is approximately equivalent to the most critical constraint and still has a continuous derivative over its whole domain.

2 Smooth reformulation

In multi-DOF robotic optimization based motion planning, all possible collisions are formulated as a set of separate constraints in an Optimal Control Problem. These are generally formulated as

$$d(O_{ki},R_{kj}) \geq 0 \quad i = 1,\ldots,N_{obs}, j = 1,\ldots,N_{obj} \qquad (1)$$

where $d(O_{ki},R_{kj})$ is the distance between obstacle O_{ki} and robot primitive R_{kj} and N_{obs}, N_{obj} are the number of obstacle and robot primitives. The amount of collision constraints becomes substantial for a cluttered environment with a lot of possible collisions and allows for a possible reduction.

A smooth maximum reformulation, called the Logarithmic-Sum-of-Exponentials (LSE) definition [**?**], computes a single approximated minimal distance d_k on a point p_k on the trajectory

$$d_k = a_d - \frac{1}{\alpha}\log\Big(\sum_{i=1}^{N_{obs}}\sum_{j=1}^{N_{obj}} e^{-\alpha(d(O_{ki},R_{kj})-a_d)}\Big) \qquad (2)$$

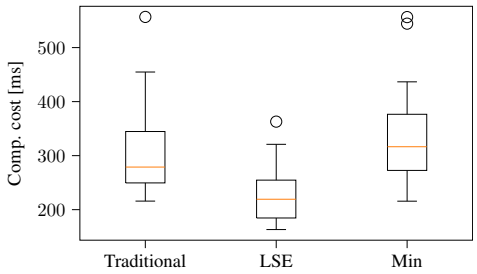

Figure 1: Boxplot comparing three formulations for 25 different configurations of the 3D robotic arm example with five iterations per configuration.

where a_d is the actual minimal distance between all robot and obstacle pairs at point p_k, α is a scaling factor determining the maximal approximation error $\log(N_{obs}N_{obj})/\alpha$.

3 Numerical validation

Figure **??** shows the decrease in computation times in a 3D robot motion planning task with 36 primitives. The proposed reformulation clearly speeds up planning algorithms by combining several constraints. A reduction of 28% of the median computation time over several configurations can be noted. The gain in computation time clearly outweighs the cost due to an increase in iterations, even in complex planning cases.

References

[1] P. Blanchard, D.J. Higham, N.J. Higham, "Accurate Computation of the Log-Sum-Excp and Softmax Function", IEEE 2019

Acknowledgement

This research is supported by Flanders Make ICON FROGS: Flexible and Robust Robotic Gripping Solutions able to deal with product variability. Flanders Make is the Flemish strategic research centre for the manufacturing industry.

Learning From Demonstration for Leader-Follower Robotic Configurations

Busra Sen[1], Elena Torta[1], Marco Alonso[2], Henry Stoutjesdijk[2], and M.J.G. van de Molengraft[1]

[1] Control Systems Technology Group, Department of Mechanical Engineering, Eindhoven University of Technology, Gemini Room PO Box 513 5600 MB Eindhoven, The Netherlands,
[2]Philips Medical Systems International B.V. Veenpluis 6, 5684 PC Best Eindhoven , The Netherlands ,
Email: b.sen@tue.nl

1 Introduction

Interventional procedures, such as catheter-based operations, represent the state-of-the-art for the treatment of some heart and neurological diseases. The execution of these procedures requires taking multiple X-ray images of a patient's body from multiple angles in different phases of the procedure. Imaging is facilitated by a robot that moves in a cluttered and dynamically changing environment shared with the surgical team. Previous research has focused on increasing the degree of dexterity of such medical robots [1]. In this research we focus on improving how the surgical team can personalize robots' trajectories by adopting a Learning from Demonstration (LfD) approach. The system is composed by multiple robots that together perform imaging. Since it is not efficient neither effective to request users to teach each single robot, we focus the learning from demonstration approach on the following research question: How can users teach one robot and the teaching be automatically propagated to all robots composing the system such that the task can be performed according to user preferences? In this study, the main purpose is to complete a collaborative task shared among two medical manipulators, namely a leader and a follower. LfD based on a probabilistic approach is chosen [2] as the key method to teach the desired trajectories to the leader robot. The follower robot knows only the task constraints such as relative position and relative velocity from the leader robot. The experimental setup is reported in Fig. 1.

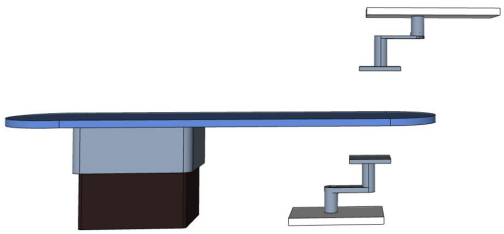

Figure 1: Considered configuration of the leader-follower setup from the doctoral thesis of van Pixteren [1]

2 Method

Demonstrations are shown to the leader robot in a simulation environment via a teleoperation device (i.e. a joystick). This reduces collision risks since the physical robot is very large in size. The trajectory of the leader robot is recorded in the form of joint angles and end-effector positions. After several demonstrations with different initial positions, the joint probability distribution of the input and the output is fitted by a Gaussian Mixture Models (GMM). Gaussian Mixture Regression (GMR) [2] is then used to encode the robot's motion. In the reproduction stage, a similarity metrics [2] is chosen such that:

$$\begin{aligned} &\underset{\dot{x}^L,\dot{\theta}^L}{\text{minimize}} \quad (\dot{\theta}^L-\hat{\dot{\theta}}^L)^T W^\theta (\dot{\theta}^L-\hat{\dot{\theta}}^L)+(\dot{x}-\hat{\dot{x}}^L)^T W^x (\dot{x}^L-\hat{\dot{x}}^L) \\ &\text{subject to} \quad \dot{x}^L = J\dot{\theta}^L \end{aligned}$$

where the semi-definite positive matrices W^θ, W^x can be selected according to the importance of the constraints on the joint angles (θ^L) and end-effector positions (x^L). The purpose of this equation is to keep the actual joint position or the end-effector position close to the demonstrated data. The follower robot is allowed to move while satisfying the task's constraints. During the demonstration, the end-effector position of the leader robot with respect to the target position is recorded (x_T^L) and the desired distance between the leader and the follower robot can be calculated by a function such that:

$$x^F = f(x_T^L, d). \tag{1}$$

3 Conclusion and Future Studies

We argue that, in a multi-robot setup with known task's constraints, the task can be taught to only one robot. In this approach, the follower adapts to the leader, and it is responsible to satisfy coordination constraints. In the next steps, the orientation between the end-effectors of the two robots will be taken into account in the reproduction stage. In order to be responsive to dynamic obstacles, reinforcement learning will be used to generalize the motion of the system. We expect to show that when the leader reacts to obstacles, the follower also learns how to best modify its trajectory. Alongside, when the follower encounters obstacles, the leader will learn how to adapt its motion to compensate for unexpected motion of the follower.

References

[1] van Pinxteren, J. A. W. (2021). Novel mechatronic architectures for interventional X-ray systems. Eindhoven University of Technology.

[2] Calinon, S., Guenter, F., Billard, A. (2007). On learning, representing, and generalizing a task in a humanoid robot. IEEE Transactions on Systems, Man, and Cybernetics, Part B (Cybernetics), 37(2), 286-298.

Exploiting Plant Dynamics in Robotic Fruit Localization

Jordy Senden[1], Lars Janssen, Robbert van der Kruk, Herman Bruyninckx, René van de Molengraft

Department of Mechanical Engineering
Eindhoven University of Technology
the Netherlands

1 Introduction

The task of harvesting a tomato truss requires the truss to be separated from the stem by severing the peduncle. Challenges to perform this task with an autonomous robotic system include ripeness detection of the truss and localizing the peduncle, which is often done using only a vision system. Occlusion by leaves, stems and other trusses generally hamper vision-based detection. This study proposes a supplementary method to reach the peduncles, based on vibration feedback.

2 Approach

When mechanically exciting the tree at the stem, at a certain frequency the truss will resonate to the excitation. A visualization of this is shown in Figure 1. When traveling along the stem, while exciting it, the shift of this resonance frequency indicates the progress towards the peduncle.

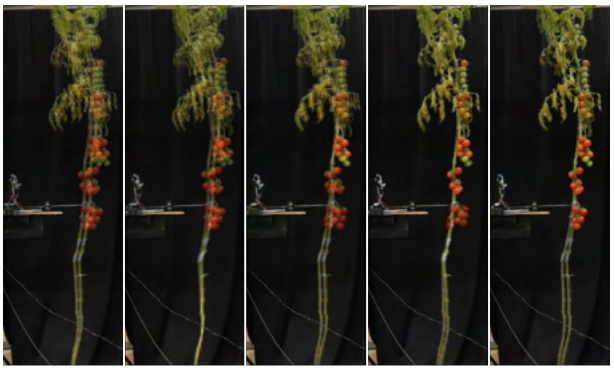

Figure 1: Resonance of a tomato plant at increasing frequencies, visualized by overlaying multiple frames in a video. Blur indicates movement, while sharpness indicates that the plant part is standing still. A consecutive decoupling of the trusses is observed at increasing frequencies.

3 Results

It is demonstrated that the resonance frequency increases when the distance to the peduncle decreases, which is attributed to a change of the mechanical stiffness of the stem part between the location of excitation and the location of the peduncle. The closest truss has the highest resonance frequency of $3-4Hz$. Similar to the mock-up plant, it is shown that these frequencies increase when approaching the peduncle, with approximately $0.7Hz/m$, shown in Figure 2. The change of the frequencies should be used to track the progress towards a truss, rather than predicting an exact location. This approach is independent of the exact parameters of the plant, resulting in a promising proof-of-concept as extra sensor modality.

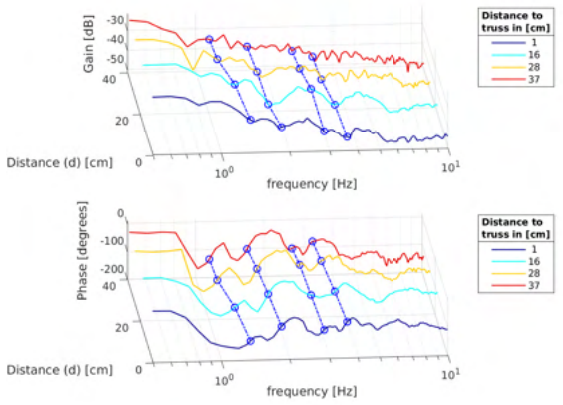

Figure 2: Measured frequency responses, where the stem is excited at different distances below the first truss. The blue circles indicate the anti-resonance frequencies, indicated by a phase increase, of the four trusses at different distances.

4 Conclusion

The dynamic response of the plant to an excitation force can be used track the progression towards the truss, while traveling up the stem. This relative truss localization method is complementary to vision based fruit localization techniques. This method works without the need of exact model parameter. Instead, the resonance frequencies need to be determined at different actuation positions. Tracking if these frequencies increase or decrease give enough information to know whether we are approaching a tomato or moving farther from it.

[1]EMAIL: j.p.f.senden@tue.nl

Remote Control of a Two-Wheeled Robot: Evidences from Experiments over Wi–Fi

Matthias Pezzutto
Department of Information Engineering
University of Padova
via Gradenigo 6B, Padova, Italy.
matthias.pezzutto@phd.unipd.it

Emanuele Garone
Service d'Automatique et d'Analyse des Systèmes
Université Libre de Bruxelles
avenue Franklin Roosevelt 50, Bruxelles, Belgium.
egarone@ulb.ac.be

1 Introduction

Wireless networks play an important role in many cutting-edge control applications like large-scale systems, multi-agent systems, and mobile robotics. When the feedback loop is closed over wireless, the links cannot be assumed ideal but they are affected by packet losses and delays. We aim to experimentally test how the wireless network affects the satisfaction of constraints on the system evolution.

2 Experimental setup

The tests presented in the following involve experimental communication data from a Wi-Fi network and accurate simulated dynamics of a two-wheeled robot. The network experiments consist of the transmission of time-stamped packets from a host PC to a target board (Raspberry Pi 3) over a Wi-Fi network (IEEE 802.11n standard), and the other way around, with a given periodicity (T=5ms). This setup mimics the periodic communications between a plant and a remote controller. The packet loss sequences obtained in the experiment have been included in a Simulink model together with the plant model and the control algorithm. We accurately simulate the nonlinear unstable dynamics, the sensing devices (encoders and MPU), and the actuator saturation. In the following, we compare 4 control strategies: the RG over Lossy Networks [1], the MPC for Tracking over Lossy Networks [2], the Networked MPC [3] with an inner stabilizing controller, and the Networked MPC [3] directly applied to the unstable system. Among these 4 solutions, only the last one does not need a reliable link between the sensor and the actuator, thus it is the most general. However, the setup with reliable sensor-actuator link is not restrictive in several applications, e.g. in robotics, where the system can be locally controlled but the on-board computational capabilities are not sufficient to implement high-performing control strategies and to enforce constraints.

3 Results

We test the considered strategies on a reference tracking task and we require the tilt angle to be less than 0.1rad. Under good channel conditions, all the strategies achieve the same performances, without noticeable differences with respect to the case with dedicated ideal cables. Under bad channel conditions, an explicative result is reported in the figure. We can see that [3] is not able to enforce the constraints. When the robot is pre-stabilized, the violations are modest, but still up to 0.05rad on a limit of 0.1rad. If the local controller is not implemented, the consequences are catastrophic: the robot falls down and cannot proceed anymore. This is due to the fact that the bound on the number of consecutive packet losses, required by [3], is violated by the Wi-Fi network. Conversely, strategies [1] and [2] succeed in reaching the desired set-point while satisfying the constraints.

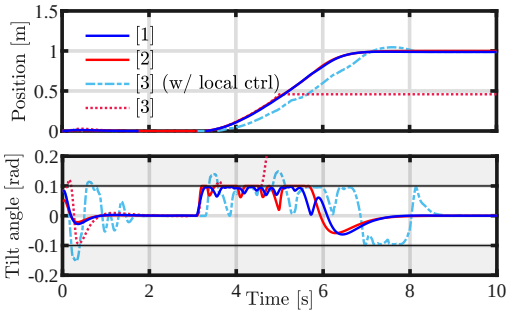

4 Discussion and conclusion

From the outcomes of the experiments, we think that, under average channel conditions, [1] and [2] are able to achieve the same performances as classic solutions relying on wired cables. Under bad channel conditions, we believe that [1] and [2] can still guarantee constraint satisfaction. These results suggest that using a local simple controller to stabilize the system and a wireless controller to enforce constraints is a promising direction for advanced control applications.

References

[1] M. Pezzutto, E. Garone, L. Schenato. "Reference Governor for Constrained Control over Lossy Channels." IEEE Control Systems Letters (2019)

[2] M. Pezzutto, M. Farina, R. Carli, L. Schenato. "Remote MPC for Tracking over Lossy Networks." IEEE Control Systems Letters (2021)

[3] G. Pin, T. Parisini. "Networked predictive control of uncertain constrained nonlinear systems: Recursive feasibility and input-to-state stability analysis." IEEE TAC (2010)

Simulation-aided Verification of SLAM Algorithms

Anoosh Anjaneya Hegde, Michael Phillips, Herman Van der Auweraer, Tong Duy Son
Siemens Digital Industries Software
3001, Leuven, Belgium
Email: anoosh.hegde@siemens.com

1 Introduction

State estimation plays an important role in the functioning of autonomous vehicles and, is usually coupled with the construction of the environment model (map-building), generally known as SLAM. The map is not only used to fine tune the state estimation, but also serve as an input to the motion planning module in an autonomous vehicle.
Development of state estimation and map building algorithms are often driven by a combination of factors such as choice of robot, the environment of operation and performance requirement. However, subtle changes in these factors, such as operation of the robot in rainy weather condition/highly dynamic environment can result in poor performance of the algorithms, if they're not originally designed for such changes. Therefore, the robustness and reliability of the SLAM algorithm needs to be quantified. This often requires expensive physical testing.
Simulation environments can help address some of the reliability and robustness issues, since they allow testing the SLAM algorithm, in different weather conditions (rainy, windy, sunny), dynamic environments and also induce different uncertainties. However, simulation environments often have the issue that the data from the sensor models are not rich when compared with physical sensors.
Simcenter Prescan is a simulation environment that provides high fidelity Physics-based lidar, radar and camera models (based on Unreal engine), based on accurate energy propogation, motion computation and modelling of beam shape. Here, the SLAM algorithms can be verified and, also validated for a certain performance requirement.

2 Simulation-aided Algorithm Development and Validation

In this work, we look at how high fidelity simulation environments like Simcenter Prescan, can aid in the development of SLAM algorithms and also help quantify their operating conditions (robustness).

For this we begin by first verifying a state-of-the-art SLAM algorithm, Lego-Loam [1] to accurately localize and map the environment using only a lidar sensor, in both virtual and physical environments. We not only make use of rotating lidar like velodyne VLP16, but also adapt the algorithm to work with solid-state lidars like Xenomatix. We first test the efficacy of the algorithm in a virtual environment constructed on Prescan (shown in Figure 1).

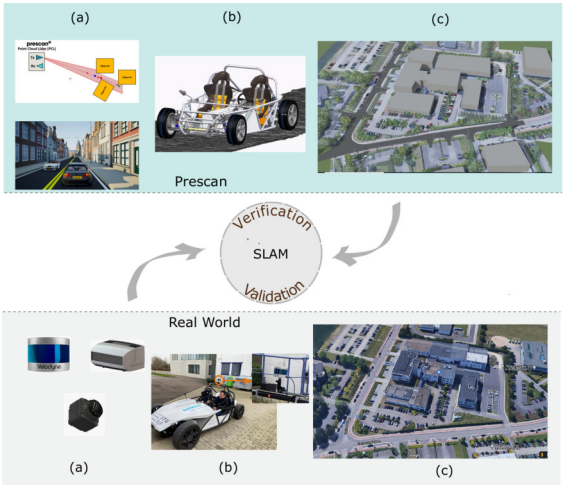

Figure 1: Development of SLAM based on both Real and Simulation environments: (a) Lidar and Camera (b) Autonomous Vehicle Platform: Simrod (c) Scenario used for SLAM verification

Most of the state-of-the-art algorithms for SLAM are tested on real physical data, where in the SLAM results are often validated with data from GPS, which is also prone to error. However, in a virtual environment like Prescan, ground truth is known making it easier to validate the algorithms. We also validate the performance of the algorithm on real data, using both Xenomatix and Velodyne on the Autonomous vehicle platform at Siemens (Simrod) as shown in Figure 1.

In the future, we'll also look at how to leverage this simulation capability not only to verify the SLAM algorithms but also aid in other activities such as maximizing SLAM performance by identifying the placement of multiple sensors.

3 Acknowledgements

This work was supported by the Flanders Make ICON MARLOC (Mixed absolute and relative localization) project. The financial support from the Flemish Agency for Innovation and Entrepreneurship (VLAIO) is gratefully acknowledged.

References

[1] T. Shan and B. Englot, "Lego-loam: Lightweight and ground-optimized lidar odometry and mapping on variable terrain," in *IEEE/RSJ International Conference on Intelligent Robots and Systems (IROS)*. IEEE, 2018, pp. 4758–4765.

Hybrid Vehicle Models for Control of Evasive Maneuvers

Leila Gharavi, Bart De Schutter
Delft Center for Systems and Control
Delft University of Technology
Email: L.Gharavi@tudelft.nl

Simone Baldi
Southeast University
Email: S.Baldi@tudelft.nl

1 Introduction

Despite the progress in recent decades, autonomous driving still faces significant challenges in terms of reaching high levels of automation. Evasive maneuvers in hazardous scenarios are prime examples requiring further research should be conducted. First, due to the lack of sufficient and reliable experimental data in hazardous driving scenarios, the available methods for motion planning and control are limited to model-based approaches. Second, during aggressive maneuvers, the vehicle's dynamics and the tire behavior exceed their linear ranges. Therefore, more accurate dynamics should be taken into account for better closed-loop performance. Meanwhile, acting swiftly is crucial. Hence, the main challenge will be finding the right balance between the accuracy of the vehicle model and the computation time. Different approaches to using hybrid representations of the vehicle dynamics model are discussed here.

2 Vehicle Dynamics Models

The coupling between longitudinal and lateral dynamics, as well as the tire-force behavior, contribute to a highly nonlinear vehicle model. One control design option is to utilize nonlinear control design techniques. Alternatively, the model may be simplified in order to use linear control design techniques while still capturing some of the nonlinear phenomena: representative techniques in this directions are the Linear Parameter-Varying (LPV) and PieceWise-Affine (PWA) approximations.

The LPV formulation transforms a nonlinear system into a parametrized linear system with measurable varying parameters. Due to the fact that this transformation is not always possible, there are three methods to approximate a nonlinear system as an LPV system [1]: the polytopic approach, the grid-based approach, and the linear fractional transformation approach, all of which use linear time-invariant models at different operating points. Atoui et al. have compared these approaches for single-track modeling of the vehicle's lateral dynamics [1]: the conclusion is that the grid-based method has the best performance in terms of computation cost and accuracy. When all or a subset of the varying parameters are also states of the system, the resulting formulation is called quasi-LPV, for which two other techniques have been introduced [2]: state transformation and function substitution.

In PWA approximation, the state space is divided into polytopes, and the nonlinear system is approximated by an affine function in each polytopic region. Several methods have been proposed for providing such approximations and determining an error bound based on them [3]. In finding a PWA approximation, there are two main considerations: how should the state space be divided and how should the approximated function be calculated. State space partitioning is particularly important since it determines the computational complexity, the accuracy, and potential numerical issues of the resulting controller. In general, a higher number of partitions reduces the error bound in each region, but leads to frequent switches among regions.

3 Future Research

LPV and PWA are seldom applied to highly complicated models, but rather to simpler ones with mild nonlinearities. Planning and control of evasive maneuvers for automated vehicles in critical scenarios requires a systematic analysis of different vehicle models and their computational performance and requirements, which — to the best of our knowledge — has not yet been conducted. Our future research will therefore focus on developing a comparison benchmark for selecting a model for trajectory planning and vehicle control in hazardous driving scenarios.

This research is supported by the Dutch Science Foundation NWO-TTW within the EVOLVE project (nr. 18484).

References

[1] H. Atoui, O. Sename, V. Milanés, and J. J. Martinez. LPV-based autonomous vehicle lateral controllers: A comparative analysis. Technical Report hal-03197895, 2021.

[2] O. Sename, P. Gáspár, and J. Bokor. *Robust Control and Linear Parameter Varying Approaches: Application to Vehicle Dynamics*. Springer, 2013.

[3] N. Groot, B. De Schutter, and H. Hellendoorn. Integrated model predictive traffic and emission control using a piecewise-affine approach. *IEEE Transactions on Intelligent Transportation Systems*, 14(2):587–598, 2013.

Traffic control for AGVs on a grid layout

Karlijn Fransen[1,2], Joost van Eekelen[1,2], and Michel Reniers[1]
[1]Eindhoven University of Technology - [2]Vanderlande
Email: {k.j.c.fransen, j.a.w.m.v.eekelen, m.a.reniers}@tue.nl

1 Introduction

Automated guided vehicles (AGVs) are increasingly popular for transport and sortation in intralogistic systems. Controlling a dense fleet of vehicles such that system level performance requirements are met, is challenging. The main functionalities in the system level controller are *job assignment*, *path planning* and *traffic control*, see Figure 1. We present a traffic control approach for AGVs on a grid layout.

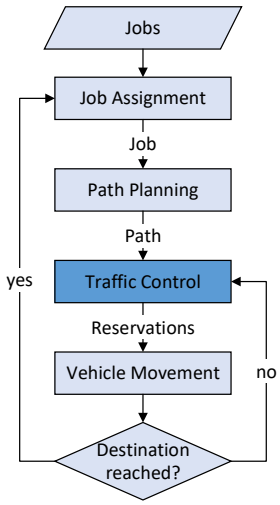

Figure 1: Generic AGV workflow, based on [1].

2 Grid based AGV traffic control

On a grid layout, AGVs move from tile to tile. Tiles do not overlap and need to be reserved for a vehicle exclusively before the vehicle may enter the tile. An example is given in Figure 2. Four AGVs are shown with intended paths (arrows) and currently reserved tiles (colored shading). AGVs A, C, and D compete for tile 1, and AGVs C and D compete for tile 2. Which AGVs get to drive these tiles first?

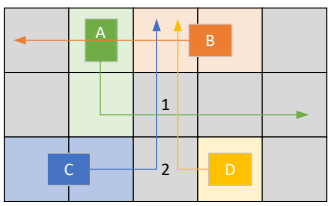

Figure 2: Grid example with four AGVs.

The proposed traffic controller reserves tiles for AGVs using a periodically executed workflow (Figure 3), that consists of a *happy flow* part and a *starvation avoidance* part. The happy flow allows for AGV prioritization, and the execution of *hard checks* and *soft checks*. Hard checks include e.g. tile availability and deadlock avoidance, while soft checks include e.g. hinder avoidance due to priorities. The checks jointly produce a precedence graph in which each AGV is represented by a vertex (see the right hand side of the figure). If the precedence graph contains strongly connected components (i.e. vehicles prevent each other from driving), then the starvation avoidance strategy can be applied to the graph such that at least one vehicle that did not pass all soft checks gets a tile to drive. This ensures global system progress.

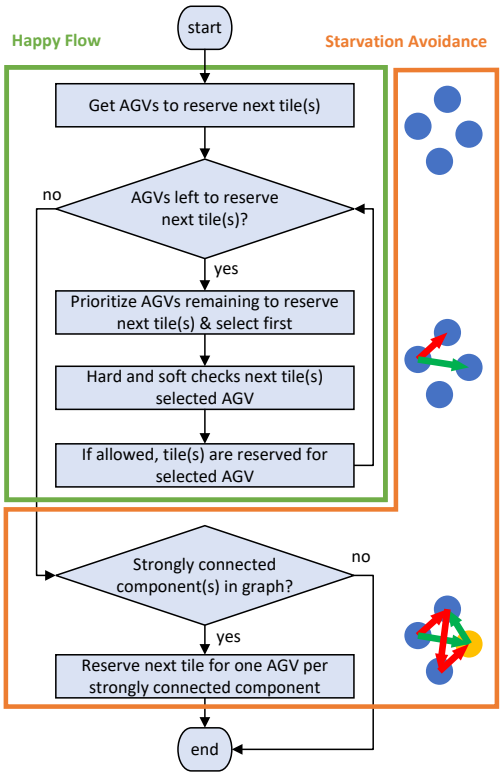

Figure 3: Workflow for reserving tiles for AGVs.

References

[1] M. De Ryck, M. Versteyhe, and F. Debrouwere, "Automated guided vehicle systems, state-of-the-art control algorithms and techniques", Journal of Manufacturing Systems, vol. 54, pp. 152–173, 2020.

A Closed-Form Solution to Control Allocation in the Framework of Constrained Navigation of Autonomous Ships

Xavier Jordens, Emanuele Garone
SAAS, Université libre de Bruxelles
50, av. F.D. Roosevelt, CP 165/55
1050 Bruxelles
Belgium
Email: xavier.jordens@ulb.be
Email: emanuele.garone@ulb.be

1 Introduction

The general framework of this research concerns the constrained navigation of autonomous ships. The aim is to deal with the navigation of ships in narrow ways (e.g. a harbor), as depicted in Fig. 1. The type of ship considered in this work is a two-azimuth thrusters ship (Fig. 2). The ability of such ships to produce lateral forces adapts to this kind of navigation environment.

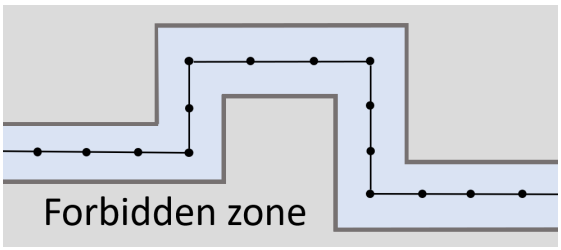

Figure 1: Example of constrained navigation path.

2 Model predictive control

We propose to tackle this problem by using a Model Predictive Control (MPC) as it is widely reported for ship navigation to deal with inherent vehicle constraints such as actuator saturation [1]. In addition, narrow ways navigation adds constraints on the ship position and velocity, which can also be handled by MPC scheme. Prestabilizing the system with a control law allows to simulate an infinite prediction horizon, and hence, ensure the feasibility of the MPC, increase its robustness, and simplify the computational burden.

3 Two-azimuth thrusters ship

The dynamics of surface marine vehicles is usually reduced to a 3 degrees of freedom model: surge, sway, and yaw motion. A two-azimuth thrusters ship has four control signals (the thrust F and the orientation θ of each thruster) that produce together a resulting x-oriented thrust F_x, y-oriented thrust F_y and z-oriented torque τ.

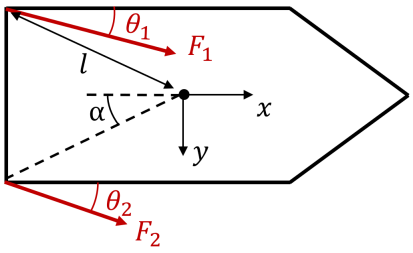

Figure 2: Two-azimuth thruster ship model.

4 Control allocation

Control schemes for ships navigation usually compute the desired F_x, F_y, and τ based on position or velocity reference. Control allocation aims at finding the mapping from the desired thrusts and torque to an optimal configuration in terms of thrusters orientations and thrusts [2]. This is usually done by solving an optimization problem to minimize the total thrusters power and accounting for some constraints such as thrusters singularities. Since MPC already requires online optimization, it is interesting in terms of computational efforts to avoid online optimization for control allocation. Our objective is therefore to find if it exists, a closed-form solution to control allocation, i.e. to find a continuous function φ such that:

$$\varphi : \mathbb{R}^3 \to \mathbb{R}^4 : \beta = \begin{bmatrix} F_x \\ F_y \\ \tau \end{bmatrix} \to \delta = \begin{bmatrix} F_1 \\ F_2 \\ \theta_1 \\ \theta_2 \end{bmatrix}.$$

References

[1] V. Codesseira and E. Tannuri, "Path Following Control For Autonomous Ship using Model Predictive Control," IFAC PapersOnLine, 2021.

[2] T. Johansen, T. Fossen, and S. Berge, "Constrained Nonlinear Control Allocation With Singularity Avoidance Using Sequential Quadratic Programming," IEEE Trans Control Syst Technol, 2004.

Motion Planning and Control for Autonomous Vehicles in Lane Merging Scenarios

Merlijne Geurts[1,*], Emilia Silvas[1,2], Alexander Katriniok[3], Maurice Heemels[1]
[1]Eindhoven, University of Technology, Mechanical Engineering, Control Systems Technology, 5612 AZ, Eindhoven, The Netherlands
[2]TNO, Integrated Vehicle Safety, Automotive Campus 30, 5708 JZ, Helmond, The Netherlands
[3]Ford Research & Innovation Center (RIC), Süsterfeldstraße 200, 52072 Aachen, Germany
[*]Corresponding author
Email: {m.e.geurts, e.silvas, m.heemels}@tue.nl, akatrini@ford.com

1 Introduction

Automated and cooperative driving holds the promise to improve road traffic by reducing traffic accidents, congestion, saving time and money for drivers and transportation companies, and by reducing pollution. The main functionalities that are needed in automated driving vehicles, as shown in Figure 1, need to cope with more complexity, for example dealing with mixed traffic, multiple road users, prediction uncertainty and interactions with drivers. These challenges are observed in virtually all scenarios including lane merging scenarios.

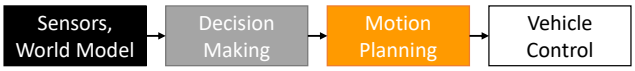

Figure 1: Example of autonomous vehicle elements.

2 SOTA in motion planing and control

Driving and merging in a dense high-speed traffic flow is a challenging task for drivers and autonomous vehicles, due to the need to perform multiple tasks at once (see Figure 2) [2]. Current (merging) algorithms, using machine learning or optimization methods, are not always able to proactively make proper decisions, as they often only exploit current knowledge they have. This calls for new and safer solutions [1].

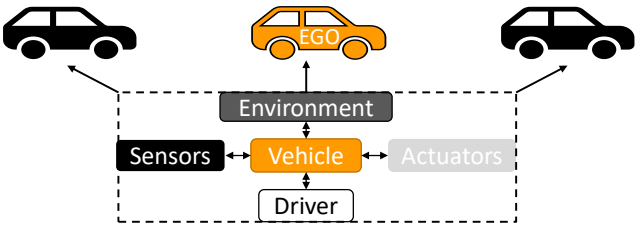

Figure 2: High overview of challenges in autonomous vehicles.

3 Lane merging scenario in mixed traffic

In order to develop safe trajectory generation and control algorithms for merging (see Figure 3), in this presentation a distributed model predictive controller will be presented based on generalizing the idea of collision points [3]. This will lead to convex optimization programs to be run online.

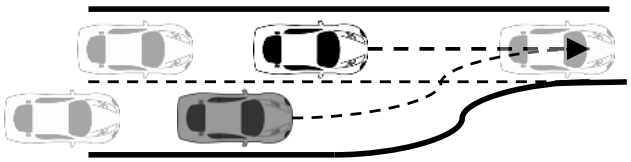

Figure 3: Example lane merging scenario.

4 Summary and future work

In summary, this presentation will show the trends and future needs for safe and comfortable motion planning and control, based on an extensive literature review. Through a simulation based benchmark study for merging scenario we will show preliminary results regarding the potential of including (uncertain) predicted information in the model predictive controller. Furthermore, the first steps in developing trajectory generation and control are shown for a merging scenario in mixed traffic. Future work will focus on a more realistic inclusion of prediction *uncertainty* in trajectory generation and control.

Acknowledgment

This work is part of the research program AMADeuS with project number 18489, which is partly financed by the Netherlands Organisation for Scientific Research (NWO).

References

[1] M. Bouton, A. Nakhaei, D. Isele, K. Fujimura, & M.J. Kochenderfer (2020). Reinforcement Learning with Iterative Reasoning for Merging in Dense Traffic. In arXiv:2005.11895v1 [cs.AI] 25 May 2020.

[2] W. Cao, M. Mukai & T. Kawabe (2019). Merging trajectory generation method using real-time optimization with enhanced robustness against sensor noise. In Artificial Life and Robotics (2019) 24:527–533.

[3] A. Katriniok, P. Kleibaum, & M. Joševski (2017). Distributed Model Predictive Control for Intersection Automation Using a Parallelized Optimization Approach. In IFAC-PapersOnLine, 50(1), 5940–5946.

Safety Shell: Reducing performance-limits in autonomous vehicles

Caspar Hanselaar[1], Emilia Silvas[1,2], Andrei Terechko[3] and Maurice Heemels[1]
[1]Department of Mechanical Engineering, CST group, Eindhoven University of Technology
P.O. Box 513, 5600 MB Eindhoven, NL, Email[1]: c.a.j.hanselaar@tue.nl
[2]TNO, Dutch Organization for Applied Scientific Research, P.O. Box 756, 5700 AT Helmond, NL
[3]NXP Semiconductors N.V, High Tech Campus 46, 5656 AG Eindhoven, NL

1 Introduction

Traffic accident related deaths are the 8th cause of death worldwide. Autonomous Driving (AD) vehicles are expected to significantly reduce these deaths, yet to attain full AD several challenges still remain. For example, due to either *faults* (e.g, temporary hardware failures) or *performance-limits* (e.g, false negative detection of objects) AD vehicles still cause collisions and, consequently, require supervision from human drivers or tightly controlled environments. To ensure AD vehicles are safe enough, they must be able to detect and mitigate faults and performance-limits during operation, without reducing AD availability.

2 Current Limitations in AD architectures

Detection of performance-limits and faults is generally based on a redundant channel with a heterogeneous safety *World Model* (WM) in a *Monitor-Actuator* architecture [1], which improves upon single channel systems (Fig. 1.a) by allowing detection of performance-limits of the primary channel (Fig 1.b). To allow performance-limit detection in secondary channels a cross-channel checking architecture is required (Fig. 1.c).

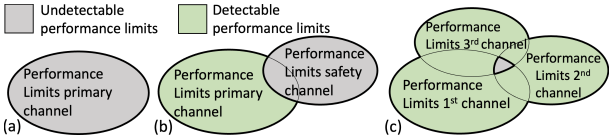

Figure 1: Diagram of detectability of performance-limits of architectures: (a) single channel, (b) Monitor-Actuator, (c) scalable cross-channel checking

Existing mitigation strategies rely on *transition of control* to drivers or emergency stop *Motion Planners* (MP). This reduces the availability of AD functions and can create dangerous situations due to short transition of control times or sudden braking. To address these issues, we propose a scalable cross-channel checking architecture.

3 Safety Shell multi-channel architecture

The Safety Shell computes the *last safe intervention time* (τ_L) via cross-comparisons of the selected channel to all WMs (Fig. 2). The τ_L represents when an emergency manoeuvre is expected to be needed to avoid unreasonable risk, as adapted from the MP appraoch by [2]. By continuing with the selected channel if τ_L permits, we avoid premature disruptive intervention due to performance-limits of the channels' WM or MP. This increases AD time without sacrificing safety or comfort. If the selected channel doesn't replan to a safe trajectory or the risk assessment isn't reduced, the arbiter may switch to a safer channel, maintaining the availability of AD functions.

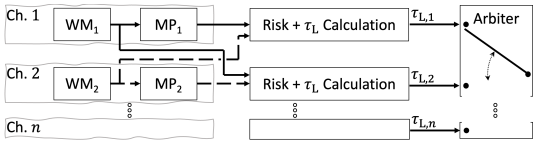

Figure 2: Abstract overview of the proposed Safety Shell scalable multi-channel architecture and arbitration concept

4 Simulation results

In a false-negative object detection test, the Safety Shell architecture reduces collision probability compared to both single channel and a Monitor-Actuator architecture with autonomous emergency braking functionality (Fig. 3). In a false-positive object detection test our method continues in the majority of cases where the Monitor-Actuator architecture triggers braking to standstill or a transition of control. These results confirm the potential of the Safety Shell.

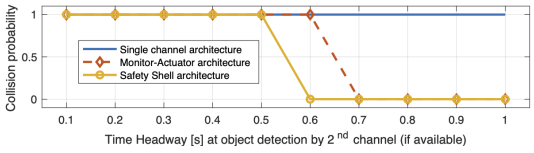

Figure 3: Results of false-negative detection use-case

References

[1] A. Mehmed, W. Steiner, and A. Čaušević, "Systematic False Positive Mitigation in Safe Automated Driving Systems," Int. Symposium on Industrial Electronics and Applications, 2020, pp. 1-8

[2] F. Damerow and J. Eggert, "Risk-aversive behavior planning under multiple situations with uncertainty," IEEE Int. Conference on Intelligent Transportation Systems, 2015, pp. 656-663

An online optimization approach to the random coordinate descent algorithm in open multi-agent systems

Charles Monnoyer de Galland[1] Renato Vizuete[2,3] Julien M. Hendrickx[1] Paolo Frasca[3]
Elena Panteley[2]

[1]ICTEAM, UCLouvain, Belgium: {charles.monnoyer,julien.hendrickx}@uclouvain.be
[2]L2S CentraleSupélec, France: {renato.vizuete,elena.panteley}@l2s.centralesupelec.fr
[3]GIPSA-lab, France: paolo.frasca@gipsa-lab.fr

1 Introduction and problem formulation

The optimal resource allocation is a well-known optimization problem where a budget must be distributed among agents in an optimal way. Such problems arise, *e.g.*, in the distribution of computation power (budget) among computing entities (agents): each agent i has a fixed amount of tasks to be computed d_i (called *demand*) and actually computes some quantity x_i, such that the total amount of computed tasks $\sum_i x_i$ matches the total demand $\sum_i d_i$, *i.e.*,

$$\min_{x\in\mathbb{R}^n} \sum_{i=1}^n f_i(x_i) \quad \text{subject to} \quad \sum_{i=1}^n x_i = \sum_{i=1}^n d_i, \qquad (1)$$

where each function $f_i : \mathbb{R} \to \mathbb{R}$ is α-strongly convex and β-smooth, and corresponds to the local cost held by agent i.

Many existing analyses around such problem stand for systems where the set of agents is fixed during the process. Yet, arrivals and departures of agents can occur at a time-scale similar to that of the process, *e.g.*, with agents experiencing faults or joining the process for a limited period of time. This gives rise to *open* multi-agent systems, where the set of agents may change with the time, resulting in the system size n_k, the local cost functions f_i^k and the demands d_i^k potentially changing at each iteration k. In particular, the solution of (1), denoted as $x^{*,k}$, also evolves with k.

We analyze the performance of the Random Coordinate Descent algorithm (RCD) introduced in [1] in open systems. This algorithm allows for solving (1) with low computational complexity, as agents update their estimates in a pairwise fashion by following each other's gradient. The convergence of the RCD algorithm in open systems of fixed size has been already analyzed in [2]. However, in this work, we use tools inspired from online optimization to study this algorithm in a system of potentially variable size, by comparing its performance x^k with that of the *optimal solution* $x^{*,k}$ and the *selfish strategy* $x_i^{s,k} = d_i^k$, which amounts to the total absence of collaboration between the agents.

2 Methodology and preliminary results

Following the online optimization approach used *e.g.*, in [3], we define the *dynamical regret* Reg_T which we will use to characterize the performance of the algorithm, but also the *benefit* Ben_T and *potential benefit* Pot_T as follows:

$$Reg_T := \sum_{t=1}^T \left(f^t(x^t) - f^t(x^{*,t})\right); \quad Ben_T := \sum_{t=1}^T \left(f^t(x^{s,t}) - f^t(x^t)\right),$$

and $Pot_T = Reg_T + Ben_T = \sum_{t=1}^T \left(f^t(x^{s,t}) - f^t(x^{*,t})\right)$. The regret thus corresponds to the accumulation of errors with respect to the optimal solution, and the benefit to the advantage of performing the RCD algorithm instead of doing nothing. We derive upper and lower bounds on the evolution of these quantities in expectation to highlight how the RCD behaves as compared to the optimal and selfish strategies. We show that these bounds grow linearly with T, and therefore their exact value does as well, as illustrated in Figure 1.

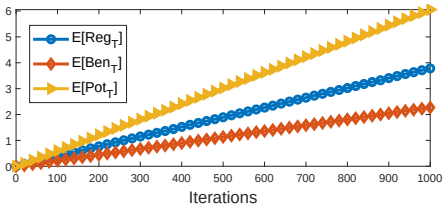

Figure 1: Evolution of $\mathbb{E}Reg_T$, $\mathbb{E}Ben_T$ and $\mathbb{E}Pot_T$ simulated in a system of 5 agents subject to frequent replacements.

3 Acknowledgements

C. Monnoyer de Galland is a FRIA fellow (F.R.S.-FNRS). This work is supported by the "RevealFlight" ARC at UCLouvain and in part by ANR via grant HANDY, number ANR-18-CE40-0010.

References

[1] I. Necoara, "Random coordinate descent algorithms for multi-agent convex optimization over networks," *IEEE Transactions on Automatic Control*, 2013.

[2] C. Monnoyer de Galland, R. Vizuete, and et. al., "Random coordinate descent algorithm for open multi-agent systems with complete topology and homogeneous agents," in *IEEE 60th Conference on Decision and Control*, 2021.

[3] S. Shahrampour and A. Jadbabaie, "Distributed online optimization in dynamic environments using mirror descent," *IEEE Transactions on Automatic Control*, 2018.

Towards Memory-Optimal Traversal of Expression Graphs of Atomic Operations in CasADi

Alejandro Astudillo[1*], Joris Gillis[1], Goele Pipeleers[1], Wilm Decré[1], Jan Swevers[1]
[1]MECO Research Team, Dept. of Mechanical Engineering, KU Leuven, Leuven, Belgium.
[1]DMMS Lab, Flanders Make, Leuven, Belgium.
[*]Email: alejandro.astudillovigoya@kuleuven.be

1 Introduction

CasADi [1] is a numerical optimization framework that implements algorithms to solve (non)convex optimal control problems. It uses expression graphs to handle the evaluation and differentiation of functions and algorithms. Every node in such graphs represents an atomic operation and the traversal order, i.e., the order in which the nodes are visited and evaluated, is defined by using the depth-first search (DFS) algorithm. Such traversal order sets the foundation for automatic code generation and determines the amount of memory to be allocated for evaluating an expression graph. The DFS algorithm, together with breadth-first search (BFS), is one of the most generally used traversal order algorithms. However, neither of them guarantees an evaluation with minimum memory usage. This poses a problem for the implementation of algorithms in embedded systems, as they have very limited memory, and in standard CPUs, as a high memory usage would represent cache misses (and larger evaluation times) during the evaluation of the expression graph.

2 Methodology

The MinMemTraversal algorithm [2] is a traversing order algorithm that guarantees the memory-optimal evaluation of expression *trees* (instead of graphs) with nodes of non-atomic objects. This algorithm considers the maximum memory usage during the evaluation of each node and the memory usage upon completion of such evaluation to define indivisible sequences of nodes with memory-optimal traversal. We have extended the MinMemTraversal algorithm to compute the memory-optimal traversal order of expression graphs of atomic operations. This extended algorithm exploits two properties of such expression graphs: (i) every node can have more than one child and (ii) every node has unit size in memory. The first property indicates that a node should be kept in memory until all its children have been evaluated, while the second property indicates that in-place evaluation, i.e., a node can overwrite one of its parents in memory, is possible.

3 Results

We show the effectiveness of our algorithm by means of an example where the forward sensitivity of an expression is computed. Let us define an expression $f(\mathbf{x})$ that is built iteratively as

$$f(\mathbf{x}) := z_n = \begin{cases} \mathbf{x}, & \text{if } n = 0, \\ z_{n-1}\sin(z_{n-1}), & \text{otherwise}, \end{cases} \tag{1}$$

where $\mathbf{x}$ is a symbolic variable of unit size and $n \in \mathbb{Z}_{\geq 0}$ is the number of iterations. Using the Leibniz chain rule, one can compute the forward sensitivities of $f(\mathbf{x})$ with a forward seed $\mathbf{y}$ as $\frac{\partial f(\mathbf{x})}{\partial \mathbf{x}}^{\top}\mathbf{y}$, where

$$\frac{\partial f(\mathbf{x})}{\partial \mathbf{x}} := \frac{\partial z_n}{\partial \mathbf{x}} = \begin{cases} 1, & \text{if } n = 0, \\ \sin(\mathbf{x}) + \mathbf{x}\cos(\mathbf{x}), & \text{if } n = 1, \\ \frac{\partial z_n}{\partial z_{n-1}}\frac{\partial z_{n-1}}{\partial \mathbf{x}}, & \text{otherwise}, \end{cases} \tag{2}$$

and $\frac{\partial z_n}{\partial z_{n-1}} = \sin(z_{n-1}) + z_{n-1}\cos(z_{n-1})$.
Both DFS and BFS return a traversal order whose evaluation has a space complexity of $O(n)$. However, please note that the computation of $\frac{\partial z_n}{\partial \mathbf{x}}^{\top}\mathbf{y}$ $\forall n > 1$ depends only on z_{n-1} and $\frac{\partial z_{n-1}}{\partial \mathbf{x}}^{\top}\mathbf{y}$, i.e., the immediately preceding iteration. Therefore, the evaluation of $\frac{\partial z_n}{\partial \mathbf{x}}^{\top}\mathbf{y}$ $\forall n > 1$ does not require to store values from previous iterations in memory and has an optimal space complexity of $O(1)$, which is achieved with our algorithm. Since the original MinMemTraversal algorithm is not able to handle expression graphs, its traversal reordering cannot be compared against our algorithm.
The next research step involves the assessment of our extended algorithm in (i) the reduction of the memory requirements of functions and algorithms within a model predictive control framework, and (ii) the effect of such reduction on the speed-up of the solution of the underlying optimal control problem.

Acknowledgement This research is supported in part by the FWO project G0A6917N of the Research Foundation - Flanders (FWO - Flanders) and in part by Flanders Make SBO MULTIROB: "Rigorous approach for programming and optimal control of multi-robot systems".

References

[1] J. Andersson, J. Gillis, G. Horn, J.B. Rawlings, and M. Diehl, "CasADi: a software framework for nonlinear optimization and optimal control," in Mathematical Programming Computation, 11 (1), pp. 1-36, 2019.

[2] C. Lam, T. Rauber, G. Baumgartner, D. Cociorva, and P. Sadayappan, "Memory-optimal evaluation of expression trees involving large objects," in Computer Languages, Systems and Structures, 37 (2), pp. 63-75, 2011.

Extension of the Performance Estimation framework via a novel approach for convex interpolation

Anne Rubbens and Julien Hendrickx
ICTEAM institute, UCLouvain, 1348 Louvain-la-Neuve, Belgium.
Email: {anne.rubbens, julien.hendrickx} @uclouvain.be

1 Introduction

The *Performance Estimation Problem* (PEP) was recently developed to automatically compute tight worst-case bounds on the performance of a wide class of first-order optimization algorithms designed for given classes of functions [1].
A key step in the PEP framework is to render the infinite-dimensional problem of computing the worst-case function of the given class tractable. It relies on the derivation of necessary and sufficient interpolation conditions, i.e. for some $n \in \mathbb{N}, d \in \mathbb{R}$, given a set $\{x_i, g_i, f_i\} \in (\mathbb{R}^d \times \mathbb{R}^d \times \mathbb{R})^n$, the existence of a function f of a given class, and of a quantity g depending on f (for instance its gradient) interpolating (x_i, g_i, f_i) is ensured if and only if the set satisfies some condition. In [1], an interpolation framework for classes of functions such as smooth strongly convex functions has been derived, based on Legendre conjugates.
We propose a novel approach to derive interpolation conditions for various classes of functions, allowing to extend the field of applications of the PEP framework. This approach is related to the question of whether or not a function defined on a small domain possesses an extension guaranteed to have some properties, for instance continuity [2] [3].

2 Contribution

Suppose a function f is defined on a (possibly finite) subset $A \subset R^d$ and satisfies, for all $x, y \in A$, a pairwise constraint, for instance

$$f(y) \geq f(x) + \langle g(x), y - x \rangle \text{ where } g(x) \in \partial f(x). \quad (1)$$

We define this constraint to be *interpolable* if and only if there exists an extension F of f, defined on $\mathbb{R}^d$, such that $F(x) = f(x)$ for all $x \in A$ and F satisfies the constraint for all $x, y \in \mathbb{R}^d$. An interpolable constraint defining a class of functions, such as the constraint (1) for the class of convex functions, is an interpolating condition for this class.
Our novel approach to derive interpolable constraints relies on the following definition:

Definition 1. Suppose a function f is defined on a (possibly finite) subset $A \subset R^d$ and satisfies, for all $x, y \in A$, a pairwise constraint. This constraint is *extensible* if and only if for all $x_+ \in \mathbb{R}^d$, there exist $f_+ \in \mathbb{R}, g_+ \in \mathbb{R}^d$ such that the pairwise constraint is satisfied for all $x, y \in A \cup \{x_+\}$, i.e. if f can be extended to any point in such a way that the extension satisfies the constraint at all points of its domain.

It holds that infinitely extensible and finitely extensible constraints enforcing the local boundedness of f and g are equivalent to interpolable constraints. Hence, instead of deriving extensions valid on $\mathbb{R}^d$, we now simply prove the existence of a single-point extension. Moreover, proving that a constraint is not interpolable can be done straightforwardly by providing a counterexample to its extensibility. For instance, consider this constraint defining L-smooth functions:

$$|f(x) - f(y) - \langle g(y), x - y \rangle| \leq \frac{L}{2}||x - y||^2.$$

The two triples $(x, g, f)) = \{(0, -1, 0), (-1, -2, 1)$ satisfy the constraint with $L = 1$. However, there exists no f_+, g_+ extending the constraint to $x_+ = \frac{-1}{2}$. Hence, this constraint cannot serve as an interpolation condition for the class of L-smooth functions. Using the extension technique, we prove the following:

Theorem 1. The family of constraints defined by

$$\begin{aligned} f(x) \geq & f(y) + A||g(x) - g(y)||^2 + B(||g(x)||^2 - ||g(y)||^2) \\ & + C||x - y||^2 - 4\frac{AC}{D}\langle g(x), x - y \rangle + D\langle g(y), x - y \rangle \end{aligned}$$

where $A, B \geq 0$ and $D \neq 0$, is extensible and interpolable.

Note that letting $A = \frac{1}{4L}, B = 0, C = -\frac{L}{4}$ and $D = \frac{1}{2}$ provides an interpolation condition for the class of L-smooth functions. Similarly, letting $A = \frac{1}{2(L-\mu)}, B = 0, C = \frac{\mu L}{2(L-\mu)}$ and $D = \frac{L}{L-\mu}$ provides an interpolation condition for μ-strongly L-smooth convex functions.

3 Acknowledgments

A. Rubbens is supported by the French Community of Belgium through a FNRS fellowship.

References

[1] A. B. Taylor, J.M. Hendrickx, F. Glineur, "Smooth strongly convex interpolation and exact worst-case performance of first-order methods", *Math. Prog.*, 2017.

[2] H. Whitney, "Analytic extensions of differentiable functions defined in closed sets", *Transactions of the American Mathematical Society*, 1934.

[3] D. Azagra and C. Mudarra, "An extension theorem for convex functions of class C1,1 on Hilbert spaces", *J. Math. Anal. Appl. 446*, 2017.

Towards Performance Estimation Problems on Quadratic Functions

Nizar Bousselmi, Julien M. Hendrickx and François Glineur
ICTEAM, UCLouvain, 1348 Louvain-la-Neuve, Belgium.
Email: {nizar.bousselmi, julien.hendrickx, francois.glineur}@uclouvain.be

1 Introduction

The *Performance Estimation Problem* (PEP) methodology has been recently introduced [1, 2] to compute the exact worst-case performance of a first-order optimization method on a given class of function, e.g. L-smooth μ-strongly convex functions. In this work, we propose to solve PEP for the class of quadratic functions of the form $f(x) = \frac{1}{2}x^T Qx$ with $\mu I \preceq Q \preceq LI$ for given parameters μ and L, i.e. L-smooth μ-strongly convex homogeneous quadratic functions.

2 Problem statement

PEP can be formulated as semidefinite programs where the matrix variable is the $2N \times 2N$ Gram matrix $G = P^T P$ with $P = \begin{pmatrix} x_1 & \cdots & x_N & g_1 & \cdots & g_N \end{pmatrix}$. In the PEP context, the x_i's and g_i's are, respectively, the iterates and the gradient at the iterates, produced by the N iterations of the given method. However, in this work, we will consider for simplicity that the x_i's and g_i's are just given.

We define a Gram matrix associated to a quadratic function.
Definition 1. A symmetric matrix $G \in \mathbb{S}^{2N}$ is a (μ, L, N)-*quadratic-Gram matrix* if and only if there exist a dimension $d \in \mathbb{N}$, a symmetric matrix $Q \in \mathbb{S}^d$ with $\mu I \preceq Q \preceq LI$ and a sequence $x_i \in \mathbb{R}^d$ for $i = 1, \ldots, N$ such that $G = P^T P$ with

$$P = \begin{pmatrix} x_1 & \cdots & x_N & \overbrace{Qx_1}^{g_1} & \cdots & \overbrace{Qx_N}^{g_N} \end{pmatrix} \in \mathbb{R}^{d \times 2N}. \tag{1}$$

The set of all (μ, L, N)-quadratic-Gram matrices is denoted $\mathscr{G}_{\mu,L,N}$. It can be shown that any conic combination of (μ, L, N)-quadratic-Gram matrices is also a (μ, L, N)-quadratic-Gram matrix, thus, the set $\mathscr{G}_{\mu,L,N}$ is a convex cone.
Theorem 1. The set of all (μ, L, N)-quadratic-Gram matrices $\mathscr{G}_{\mu,L,N}$ is a convex cone.

Since the set $\mathscr{G}_{\mu,L,N}$ is convex, we seek an explicit convex description of it in order to add the constraints to PEP.

3 Case with $N = 1$ point

First, we look at the case $N = 1$ where we only have one point x_1 and its gradient g_1. It can be shown that the set of $(\mu, L, 1)$-quadratic-Gram matrices of one point is exactly described by three convex inequalities.

Theorem 2. Given a symmetric matrix $G = \begin{pmatrix} g_{11} & g_{12} \\ g_{12} & g_{22} \end{pmatrix}$, the conditions

$$g_{11} \geq 0 \tag{2}$$
$$g_{12}^2 \leq g_{11} g_{22} \tag{3}$$
$$g_{22} \leq -\mu L g_{11} + (\mu + L) g_{12} \tag{4}$$

are necessary and sufficient conditions for $G \in \mathscr{G}_{\mu,L,1}$.

4 Case with N points

Now, we consider the general case $N \geq 1$. First of all, we can write a quadratic-Gram matrix under the following form

$$G = \begin{pmatrix} X^T X & X^T QX \\ X^T QX & X^T Q^2 X \end{pmatrix} \tag{5}$$

where $X = \begin{pmatrix} x_1 & \cdots & x_N \end{pmatrix} \in \mathbb{R}^{d \times N}$. In addition to the global symmetry and positive semidefiniteness of G, hence of diagonal blocks $X^T X$ and $X^T Q^2 X$, we observe that off diagonal block $X^T QX$ is also symmetric and positive semidefinite. Actually, it is possible to find several necessary characterizations of a quadratic-Gram matrix (see for example Theorem 3 in [3] in a different context). However, it appears to be much less straightforward to check or prove the sufficiency, which is the question we are investigating.

5 Conclusion and perspectives

Theorem 1 ensures that the set of quadratic-Gram matrices is convex. Therefore it is likely that there exists a way to describe the set with an explicit list of convex constraints. Once these constraints are identified and we are able to solve PEP on quadratic functions, it will be possible to measure and quantify the gap between the worst-case performance of a given first-order optimization method on general L-smooth μ-strongly convex functions and on quadratic functions.

N. Bousselmi is supported by the French Community of Belgium through a FRIA fellowship (F.R.S.-FNRS).

References

[1] A.B. Taylor, J.M. Hendrickx, F. Glineur *Smooth strongly convex interpolation and exact worst-case performance of first-order methods*. Mathematical Programming, 2017, vol. 161, no 1, p. 307-345.

[2] Y. Drori, M. Teboulle *Performance of first-order methods for smooth convex minimization: a novel approach*. Mathematical Programming, 2014, vol. 145, no 1, p. 451-482.

[3] S. Colla, J.M. Hendrickx *Automated Worst-Case Performance Analysis of Decentralized Gradient Descent*. 2021

Advances in Feasible SQP Methods for NMPC

David Kiessling, Joris Gillis, Jan Swevers
MECO Research Team, KU Leuven, Leuven, Belgium
DMMS-M lab, Flanders Make, Leuven, Belgium
Email: david.kiessling@kuleuven.be

Moritz Diehl
Department of Mathematics
Department of Mircosystems Engineering
University of Freiburg, Freiburg, Germany

1 Introduction

In Nonlinear Model Predictive Control (NMPC) a nonlinear program (NLP) resulting from an optimal control problem (OCP) is solved in every sampling period. The first input of the optimal solution is applied to the system, the time horizon is shifted by one sampling time, and the procedure is repeated. We consider NLPs of the form:

$$\begin{aligned} \min_{\substack{x_0,\dots,x_N \\ u_0,\dots,u_{N-1}}} \quad & \sum_{k=0}^{N-1} l(x_k,u_k)+e(x_N) \\ \text{s.t.} \quad & x_0-\bar{x}_0=0 \\ & x_{k+1}=f(x_k,u_k), \quad \forall k=0,\dots,N-1 \\ & g(x_k)\le 0, \quad \forall k=0,\dots,N \end{aligned} \tag{1}$$

where $x_k\in\mathbb{R}^{n_x}$, $u_k\in\mathbb{R}^{n_u}$ describe the states and controls, respectively. $l\colon \mathbb{R}^{n_x}\times\mathbb{R}^{n_u}\to\mathbb{R}$, $e\colon \mathbb{R}^{n_x}\to\mathbb{R}$ denote the stage and terminal cost functions. $f\colon \mathbb{R}^{n_x}\times\mathbb{R}^{n_u}\to\mathbb{R}^{n_x}$ describes the dynamics of the system and $g\colon \mathbb{R}^{n_x}\times\mathbb{R}^{n_u}\to\mathbb{R}^{n_h}$ describe the stage constraints. Current state-of-the-art NMPC algorithms face several challenges. Firstly, the NLP should be solved within every sampling time in order to guarantee a reliable feedback controller. If the solution time exceeds the sampling period it is advantageous to stop the solver at a suboptimal, but feasible iterate and using that control input as next input. Secondly, current NMPC solvers mainly rely on local convergence properties, but particularly in path planning problems of mechatronic systems highly nonlinear constraints can require global convergence of the underlying solver.

Our research aims at overcoming these two bottlenecks in current NMPC practice. Sequential Quadratic Programming (SQP) methods are especially advantageous in solving a sequence of optimization problems. Keeping every iterate feasible can be exploited for early termination in the NMPC context. Moreover, equipping the SQP method with a globalization strategy, such as a merit function or a filter combined with a trust-region or linesearch mechanism is necessary to guarantee global convergence and therefore solve hard problems arising, for instance, in motion planning.

2 Feasible SQP Methods

The SQP subproblem consists of the linear approximation of the constraints in (1) and a quadratic approximation of the Lagrangian function, respectively. For ease of notation we summarize the variables of (1) in $w\in\mathbb{R}^w$, the cost function in $F(w)$, the equality constraints in $H(w)$, and the inequality constraints in $G(w)$. For a given matrix $H_k\in\mathbb{R}^{(n_w\times n_w)}$ and an iterate w_k the QP subproblem is given by

$$\begin{aligned} \min_{\Delta w\in\mathbb{R}^{n_w}} \quad & \nabla F(w_k)^\top \Delta w+\frac{1}{2}\Delta w^\top H_k \Delta w \\ \text{s.t.} \quad & H(w_k)+\nabla H(w_k)^\top \Delta w=0 \\ & G(w_k)+\nabla G(w_k)^\top \Delta w\le 0. \end{aligned} \tag{2}$$

Denoting the solution of (2) by Δw_k, the new iterate $w_{k+1}=w_k+\Delta w_k$ is in general not feasible with respect to the constraints of (1). Projecting w_{k+1} onto the feasible set of (1) yields a feasible step $\tilde{w}_{k+1}$. We call such a combination of QP step and projection a *feasible SQP method*. In [3] an algorithmic framework is described that combines a trust-region approach with a projection on the feasible set. Independent of the applied projection the method converges globally as long as the projection satisfies certain conditions. A particular projection is described in [2]. The main idea of this approach is to repeatedly correct the higher order terms of $h(w_{k+1})$, $g(w_{k+1})$ until feasibility is obtained at the point $\tilde{w}_{k+1}$. This technique is known as *zero-order iterations*.

3 Outlook

In the future, we will focus on advancing the results of [2, 3] towards a fast and reliable solver for NMPC problems. Zero-order iterations converge towards the solution of a perturbed version (1). Fast convergence of these iterations is crucial for an efficient SQP algorithm. Improving the globalization strategy of [3] in combination with zero-order iterations can yield faster overall convergence. Furthermore, [1] points out a direct connection between the algorithmic framework of [3] and optimization on manifolds, which might be explored in future research.

References

[1] P.-A. Absil, J. Trumpf, R. Mahony, B. Andrews "All roads lead to Newton: feasible second-order methods for equality-constrained optimization" *Technical Report UCL-INMA-2009.024*, 2009.

[2] H. Bock, M. Diehl, E. Kostina, and J. Schlöder, "Constrained optimal feedback control of systems governed by large differential algebraic equations", *Real-Time and Online PDE-Constrained Optimization, pages 3–22. SIAM*, 2007.

[3] S. Wright, M. Tenny "A feasible trust-region sequential quadratic programming algorithm" *SIAM Journal on Optimization*, 2004.

Acknowledgement: This work has been carried out within the framework of Flanders Make SBO DIRAC: DIRAC - Deterministic and Inexpensive Realizations of Advanced Control. Flanders Make is the Flemish strategic research centre for the manufacturing industry.

Performance Estimation Problem for Decentralized Optimization Methods

Sebastien Colla and Julien M. Hendrickx
ICTEAM Institute, UCLouvain, 1348 Louvain-la-Neuve, Belgium.
Email: { sebastien.colla, julien.hendrickx } @uclouvain.be

1 Introduction

We develop a methodology that automatically provides nearly tight performance bounds for first-order decentralized methods on convex functions and we demonstrate its usefulness on different existing methods [1]. Decentralized optimization has received an increasing attention due to its useful applications in large-scale machine learning and sensor networks, see e.g. [2] for a survey. In decentralized methods for separable objective functions, we consider a set of agents $\{1,\dots,N\}$, working together to solve the following optimization problem:

$$\underset{x\in\mathbb{R}^d}{\text{minimize}} \quad f(x)=\frac{1}{N}\sum_{i=1}^{N} f_i(x),$$

where $f_i:\mathbb{R}^d\to\mathbb{R}$ is the private function locally held by agent i. Each agent i holds its own version x_i of the decision variable x, performs local computations and exchanges local information with its neighbors to come an agreement on the minimizer x^* of the global function f. Exchanges of information often take the form of an average consensus on some quantity, e.g., on the x_i. These consensuses can be represented using a multiplication by a matrix $W\in\mathbb{R}^{N\times N}$, typically assumed symmetric and doubly stochastic.

One of the simplest decentralized optimization method is the distributed (sub)gradient descent (DGD) [2] where agents successively perform an average consensus step (1) and a local gradient step (2). We have, for all $i\in\{1,\dots,N\}$,

$$y_i^k=\sum_{j=1}^{N} w_{ij}x_j^k; \tag{1}$$

$$x_i^{k+1}=y_i^k-\alpha\nabla f_i(x_i^k), \tag{2}$$

where $\alpha>0$ is a constant step-size.

2 Contributions and results

In general, the quality of an optimization method is evaluated *via* a worst-case guarantee. Obtaining theoretical worst-case performance bounds for decentralized algorithms can often be a challenging task, requiring combining the impact of the optimization component and the interconnection network. This can result in performance bounds that are complex and not very tight. For example, we have empirically shown that the existing performance bounds for DGD are significantly worse than the actual worst-cases. However, accurate performance bounds are important to correctly understand the impact of the network topology and algorithm parameters on the performance of the algorithm.

In this work, we follow an alternative computational approach that finds a worst-case performance guarantee of an algorithm by solving an optimization problem, known as the performance estimation problem (PEP). The PEP approach has led to many results in centralized optimization, see e.g. [3], but it has never been applied to decentralized optimization methods. The current PEP framework lacks for ways of representing the communications between the agents. We therefore propose two formulations of the average consensus steps that can be embedded in a solvable PEP [1].

The first formulation uses a given averaging matrix W to directly incorporate the updates of the chosen method as constraints over the iterates. This leads to performance bounds that are tight, but specific to the given matrix.
The second formulation is a relaxation that considers entire spectral classes of possible symmetric matrices. This allows PEP to provide spectral upper bounds on the performance that are valid over an entire class of networks and can thus be compared with the bounds of the literature. This also allows looking for the worst communication network from the given class. This formulation is a relaxation because it replaces the set of consensus steps (e.g. (1)) with a set of constraints that are only proven to be necessary for having an averaging matrix in the given class. Although it is a relaxation, the performance guarantees it provides for the decentralized algorithms we have experimented, such as DGD and DIGing, significantly improve on the theoretical existing ones and are numerically tight. They are also independent of the number of agents in the problem and they help for better tuning of the parameters of the algorithms.

Using our two new formulations, the PEP approach can be applied directly to many decentralized algorithms.

Acknowledgements

S. Colla is supported by the French Community of Belgium through a FRIA fellowship (F.R.S.-FNRS).

References

[1] S. Colla, J. M. Hendrickx, "Automated Worst-Case Performance Analysis of Decentralized Gradient Descent", *60th IEEE Conference on Decision and Control*, 2021.

[2] A. Nedić, A. Olshevsky and M. G. Rabbat, "Network Topology and Communication-Computation Tradeoffs in Decentralized Optimization," 2018.

[3] A. B. Taylor, J. M. Hendrickx and F. Glineur, "Exact Worst-Case Performance of First-Order Methods for Composite Convex Optimization," 2015.

Wednesday - July 6, 2022
16:00 - 18:00 (WeE)

On designing distributed consensus protocol for multi- Energy Storage Unit (ESU) system in a microgrid

Taranjitsingh Singh, Tony Dang, and Frederik Debrouwere
Flanders Make, Lommel, Belgium
Email: firstname.lastname@flandersmake.be

1 Introduction

In order to mitigate the power balancing burden from the main powergrid, the Energy Storage Units (ESUs) provide smooth power fluctuation due to change in power demand at the point of common coupling. It is required that the total active power of the microgrid is regulated to its reference value at the point of common coupling. For achieving this power balancing, control of State of Charge (SOC) of ESUs are required to avoid depletion and saturation of ESUs. So, it is required that all the ESUs maintain same SOCs or reach a certain consensus. Considering each ESU as an agent, which are interacting with each other, the problem is deduced to a distributed consensus control problem for a multi-agent system.

For the interaction among agents, consider an undirected graph $\mathscr{G} = (\mathscr{V}, \mathscr{E}, \mathscr{A})$, with the set of vertices $\mathscr{V}$, where ith vertex represent ith agent, the set of edges $\mathscr{E} \subseteq \mathscr{V} \times \mathscr{V}$, and weighted adjacency matrix $\mathscr{A} = [a_{ij}]$ with non-negative adjacency elements a_{ij}. The degree for an agent is defined as $d_i \triangleq \sum_{j=1}^{N} a_{ij}$ to form the degree matrix $\mathscr{D} \triangleq \text{diag}(d_1, \cdots d_N)$ to give the Laplacian matrix $\mathscr{L} = \mathscr{D} - \mathscr{A} = [L_{ij}]$.

2 Problem Formulation

Consider the following m^{th} order dynamics in a multi-agent system:

$$\dot{p}_i^{(1)}(t) = \dot{p}_i^{(2)}(t),\ \dot{p}_i^{(m-1)}(t) = \dot{p}_i^{(m)}(t),\ \cdots,\ \dot{p}_i^{(m)}(t) = u_i \quad i = 1, ..., N \text{ agents} \tag{1}$$

where $\dot{p}_i^{(k)} \in \mathbb{R}^n$ are the states of the i^{th} node. The consensus protocol for each agent is defined as [1]:

$$u_i = -\sum_{j=1, j\neq i}^{N} a_{ij} \sum_{k=1}^{m} K_{ik}(p_j^k(t) - p_i^k(t)). \tag{2}$$

where K_i is the state feedback matrix to be designed for each agent. We consider an application of homogeneous ESUs in a microgrid, where each ESUs are modelled as second-order agents with SOC and Rate of Power (RoP) as their states [2]. We consider a virtual leader at the point of common coupling to solve the active power balancing problem. The control objective is to track the SOC trajectory of the virtual leader and the cooperative control formulation (2) for multi-agents is used to achieve this control objective.

3 Results

A certain load profile defines the virtual leader trajectory, with 50% initial SOC as shown in the figure 1. Six ESUs with different initial SOCs are considered follow the trajectory of the virtual leader. Two communication graphs are considered, namely, $\mathscr{G}_1$ and $\mathscr{G}_2$ as shown in the figure 1.

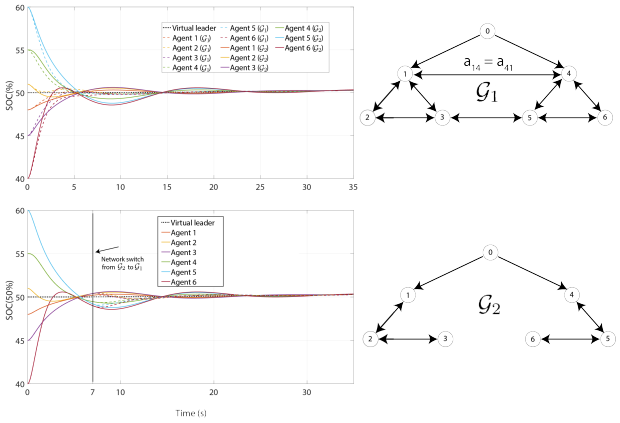

Figure 1: (Top-left) ESUs following virtual leader for two communication networks $\mathscr{G}_1$(top-right) and $\mathscr{G}_2$(bottom-right). (Bottom-left) ESUs following virtual leader for $\mathscr{G}_2$ and switching to $\mathscr{G}_1$ after 7s.

With simulations performed separately with $\mathscr{G}_1$ and $\mathscr{G}_2$, it is observed that the followers converge faster with stronger communication and the ability of the protocol to converge in case of a switching network topology. These results will allow us to further accommodate time-varying network topologies to gracefully achieve consensus in case of failures in a microgrid.

References

[1] W. Yu, G. Chen, W. Ren, J. Kurths, and W. X. Zheng, "Distributed higher order consensus protocols in multiagent dynamical systems," *IEEE Transactions on Circuits and Systems I: Regular Papers*, vol. 58, no. 8, pp. 1924–1932, 2011.

[2] C. Huang, S. Weng, D. Yue, S. Deng, J. Xie, and H. Ge, "Distributed cooperative control of energy storage units in microgrid based on multi-agent consensus method," *Electric Power Systems Research*, vol. 147, pp. 213–223, 2017.

Acknowledgement: This work is supported by Flanders Make project: ICON ID2CON: "Integrated Identification to Control" funded by the agency Flanders Innovation & Entrepreneurship (VLAIO) and Flanders Make.

Industrial DC grids using MPC tweaked to be charge sustaining

Bruno Depraetere, Taranjitsingh Singh & Jeroen Willems
Flanders Make, Belgium. E-mail: firstname.lastname@flandersmake.be

Motivation

Whereas there is a strong trend towards actively controlled power nets on city/neighborhood level (smart grids) and household level (microgrids), industrial nets are mostly still lagging behind. They are usually grown over time, and not designed in a coordinated manner. Each machine typically has its own rectifier or front end, which means each front end has to be able to deliver peak power. There usually also are no significant storage elements, making it impossible to balance varying loads. As a result, high peak powers are often obtained, and outages and reliability issues do occur.

Approach

In this paper we instead consider an industrial DC grid, wherein all machines are driven from a single shared DC grid. This is fed using a small set of *shared* rectifiers or front ends, and a set of *shared* DC storage elements such as batteries or super caps are added.

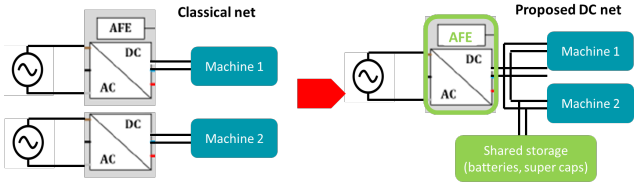

Figure 1: Layout of classical nets (left), using a front end per machine, and without storage elements, compared to that of the proposed DC net (right), using a (set of) shared front end(s) and shared DC storage.

A controller is then added to actively decide when power should be drawn or fed to the net through the front ends, and when to or from the storage elements. For simple cases rule-based controllers can be developed, but when for example variable pricing and uncertain predictions are included, MPC quickly becomes the best choice. This MPC is then set up to choose the optimal flow of powers, taking into account a model for the losses, and a prediction of upcoming events. For a simple case with 1 active front end (AFE) with efficiency η_1, 1 super cap (SC) with state of charge SOC and efficiency $\eta_2 > \eta_1$, and 1 load, the resulting MPC optimizing over a horizon of N samples, becomes:

$$\min_{P^{\mathrm{AFE}},\, P^{\mathrm{SC}}} \quad \sum_{k=1:N} \Big((1-\eta_1)\big|P_k^{\mathrm{AFE}}\big| + (1-\eta_2)\big|P_k^{\mathrm{SC}}\big| \Big)$$

$$\begin{aligned}
\textbf{s.t.} \quad & P_k^{\mathrm{AFE}} + P_k^{\mathrm{SC}} = P_k^{\mathrm{load}}, && k = 1:N \\
& \mathrm{SOC}_{k+1} = \mathrm{SOC}_k + T_s\, P_k^{\mathrm{SC}}, && k = 1:N \\
& 0 \le \mathrm{SOC}_k \le 1 && k = 1:N \\
& \mathrm{SOC}_N = 0.5
\end{aligned}$$

wherein P^{X} denotes the power delivered by source X.

Results

In simulations as well as on an experimental setup we have shown that this approach can significantly reduce the peak power and thus the purchase cost of the front ends, and furthermore reduce losses by avoiding the use of the less efficient components. A simulation example for the simple case above using full horizon MPC is shown in Figure 2, wherein the peak AFE power is reduced with almost 50% compared to the AC case without SC, and losses are reduced by 1-5% by using the less efficient AFE less. More complex cases can yield more savings in installation cost (smaller total front end capacity to be traded off with price of storage) as well as running costs (less losses). There they will furthermore provide more flexibility to actively control power flows, which allows to react more easily to issues popping up (e.g. failures) and in doing so avoid outages.

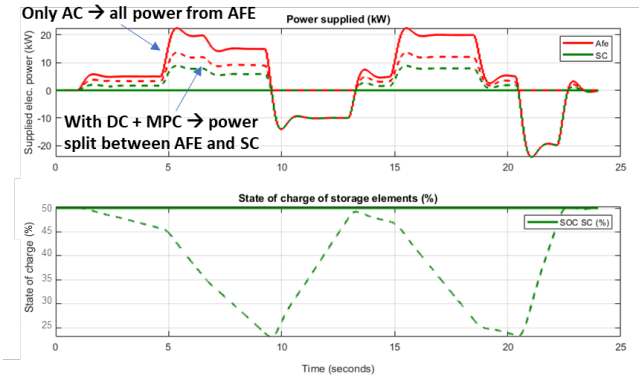

Figure 2: Result of full horizon MPC comparing AC without SC (full line), vs DC with SC (dashed).

Remaining challenges

However, in order to achieve these for realistic applications, the main difficulty in the MPC problem is to, despite imperfect predictions, **ensure long term charge sustainability**. Otherwise the state of charge can drains or fills completely at the wrong times, thereby reducing the ability to actively control and balance loads. We will present several options, among which an approach relying on augmenting the prediction horizon with a **virtual horizon**. This virtual horizon contains a typical load pattern, so it basically leads the MPC to consider what control actions to make now, given the typical loads to be expected in the future.

Acknowledgements: This work has been carried out within the framework of Flanders Make's ICON project 'Multi-DC' (Multi-machine energy management, facilitated by DC links), funded by the agency Flanders Innovation & Entrepreneurship (VLAIO) and Flanders Make. Flanders Make is the Flemish strategic research centre for the manufacturing industry.

Computing an FIR controller using an efficient iterative scheme

R. Haasjes[1] r.haasjes@utwente.nl
A.P. Berkhoff[1,2] a.p.berkhoff@utwente.nl
B. Rosić[1] b.rosic@utwente.nl

[1]University of Twente ET-AMDA, Drienerlolaan 5, 7522 NB Enschede (NL)
[2]TNO Acoustics and Sonar, Oude Waalsdorperweg 63, 2597 AK Den Haag (NL)

1 Introduction

Acoustic anechoic chambers are used to conduct measurements and experiments under free-field conditions. In the ideal case, all acoustic waves are absorbed at the walls, such that no reflections exist. In reality low frequency sound will be reflected by the walls, due to limitations of passive absorption measures [1]. Active noise control is effective at lower frequencies, which makes this a promising addition to the passive wall absorption. Because of the typical large dimensions of the chamber, a large number of sources and sensors is required for satisfactory performance. The computation of a controller for such a large-scale system is computationally expensive. This work shows a scheme to efficiently obtain a finite impulse response (FIR) controller, demonstrated by a single-channel simulation in a duct.

2 Approach

Following the approach in [2], both a preconditioner/decoupler of the secondary path ($\hat{G}_{mi}(z)$ and $\hat{G}_{ai}(z)$) and a prewhitening/decorrelation filter ($\hat{F}_w(z)$) are derived via the frequency-domain. The filters are delayed to ensure causality. The delay to be added is found by minimizing errors due to wrap-around and truncation effects. The adaptive part of the algorithm used in the simulation incorporates normalization of the input by its power.

3 Simulation

A duct with a single-channel control setup is used to simulate the control performance. The setup is schematically shown in Fig. 1, where $d_1 = 0.8575m$, $d_2 = 0.343m$, $d_3 = 0.1715m$, $d_4 = 1.3720m$ and $R_0 = 0.90$, $R_L = -0.95$ are the reflection coefficients at $x = 0$ and $x = L$ respectively.

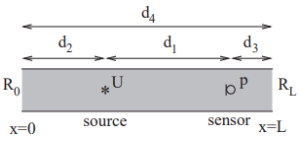

Figure 1: Simulation setup: single-channel control in a duct.

The FIR filters corresponding to the decomposition are shown in Fig. 2. All FIR filters are truncated after $J = 128$ samples. A delay of 20, 10 and 50 samples is added to $\hat{F}_w(z)$, $\hat{G}_{\text{mi}}(\text{z})$ and $\hat{G}_{\text{ai}}(\text{z})$ respectively. A normalized tolerance of 0.0137 is used to truncate 68 of 513 singular values to compute $\hat{G}_{\text{mi}}(\text{z})$.

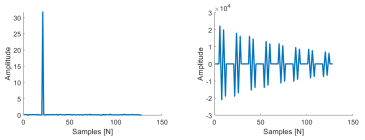

(a) FIR of $\hat{F}_w(z)$. (b) FIR of $G(z)$.

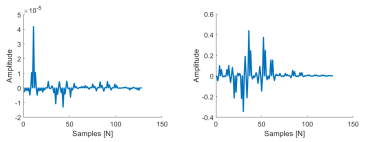

(c) FIR of $\hat{G}_{mi}(z)$. (d) FIR of $\hat{G}_{ai}(z)$.

Figure 2: FIR filters used in the iterative algorithm.

The algorithm is compared to a normalized filtered-error LMS algorithm. The results are shown in Fig. 3, from which can be concluded that the preconditioned algorithm has improved convergence speed.

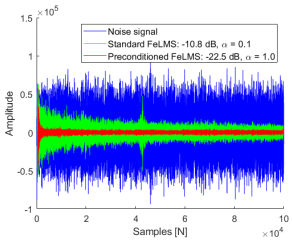

Figure 3: Convergence of the algorithms.

4 Acknowledgements

This research is funded by TNO. The support and funding from TNO are gratefully acknowledged.

References

[1] S. Schneider and C. Kern. "Acoustical Behavior of the Large Anechoic Chamber at the Laboratoire de Mécanique et d'Acoustique in the Low Frequency Range". In: *Acta Acustica united with Acustica 94* (2008), pp. 141-147.

[2] M.R. Bai, S.J. Elliott. "Preconditioning multichannel adaptive filtering algorithms using EVD- and SVD-based signal prewhitening and system decoupling". In: *Journal of Sound and Vibration 270* (2004), pp. 639-655.

Disturbance estimation to avoid the model mismatch effects in Model Predictive Control

Alvaro Florez and Jan Swevers
MECO Research Team, Dept. Mechanical Engineering, KU Leuven
DMMS lab, Flanders Make
Email: alvaro.florez@kuleuven.be

1 Introduction

Model predictive control (MPC) is a control methodology that considers the system model to predict the future output, this interval is known as prediction horizon. An optimization problem is usually constrained is solved to find the control sequence that minimizes a cost function defined. The first sequence value is applied, and the process starts again, moving forward the prediction horizon one sample time.

MPC uses a system model and a cost function that the user defines, usually, it is a regulator problem or track a changing set point, but also any other objective could be defined. Track a reference without error is a commonly required task, but, in the presence of persistent disturbances or model mismatches achieve zero offset is not always possible. Just adding an integrator to the plant could not eliminate the offset [2]. In this work, the unknown information from the model is lumped in disturbance variables, the MPC problem can take it into account and achieve a perfect tracking of the reference.

2 Problem formulation and results

Consider a discrete nonlinear system which is defined by

$$\begin{aligned} \boldsymbol{x}_{k+1} &= \boldsymbol{f}\left(\boldsymbol{x}_k, \boldsymbol{u}_k\right) & \boldsymbol{x}_{real\ k+1} &= \boldsymbol{f}_{real}\left(\boldsymbol{x}_k, \boldsymbol{u}_k\right) \\ \boldsymbol{y}_k &= \boldsymbol{h}(x_k) & \boldsymbol{y}_{real\ k} &= \boldsymbol{h}_{real}(\boldsymbol{x}_k) \end{aligned} \tag{1}$$

where $\boldsymbol{x} \in \mathbb{R}^{n_x}$ is the state vector, $\boldsymbol{u} \in \mathbb{R}^{n_u}$ the input vector, and, $\boldsymbol{y} \in \mathbb{R}^{n_y}$ the system output. The model from the left side (known) could be slightly different from the real one on the right side (unknown), it could be because of some unmodeled dynamics or unmeasured disturbances in the system. To address this, the system must be augmented with a disturbance model for the estimation process, and assuming these disturbances as constant ($d_{k+1} = d_k$) we have

$$\begin{aligned} \boldsymbol{x}_{k+1} &= \boldsymbol{f}_{aug}\left(\boldsymbol{x}_k, \boldsymbol{d}_k, \boldsymbol{u}_k\right) \\ \boldsymbol{y}_k &= \boldsymbol{h}_{aug}(\boldsymbol{x}_k, \boldsymbol{d}_k) \end{aligned} \tag{2}$$

Inside the function $\boldsymbol{f}_{aug}$ is defined the influence of the disturbance in the states. Inside the function $\boldsymbol{h}_{aug}$ is defined the effect of the disturbance to the output. Using the measurements, the states and disturbances are estimated using a Kalman filter, therefore the optimization problem solved each sample time is defined as [1]

$$\begin{aligned} \underset{\boldsymbol{x},\,\boldsymbol{u}}{\text{minimize}} \quad & \sum_{t=0}^{N-1} \ell(\boldsymbol{x}_t - \boldsymbol{x}_s, \boldsymbol{u}_t - \boldsymbol{u}_s) + F(\boldsymbol{x}_N - \boldsymbol{x}_s) \\ \text{subject to} \quad & \boldsymbol{x}_0 = \hat{\boldsymbol{x}}_k, \;\; \boldsymbol{d}_0 = \hat{\boldsymbol{d}}_k, \\ & \boldsymbol{x}_{t+1} = \boldsymbol{f}_{aug}(\boldsymbol{x}_t, \hat{\boldsymbol{d}}_k, \boldsymbol{u}_t) \end{aligned} \tag{3}$$

where $\boldsymbol{x}_s = \boldsymbol{f}_{aug}(\boldsymbol{x}_s, \hat{d}_k, \boldsymbol{u}_s), \quad \boldsymbol{r}_k = \boldsymbol{h}_{aug}(\boldsymbol{x}_s, \hat{d}_k)$.
The functions ℓ and F are commonly as the linear quadratic regulator functions, this will reduce error terms to zero.
The second order model of a DC-motor with a spring connected to the rotor is considered. The model is linear, but the measurements come from a nonlinear friction motor model. The motor should track a position reference while a constant disturbance is applied.

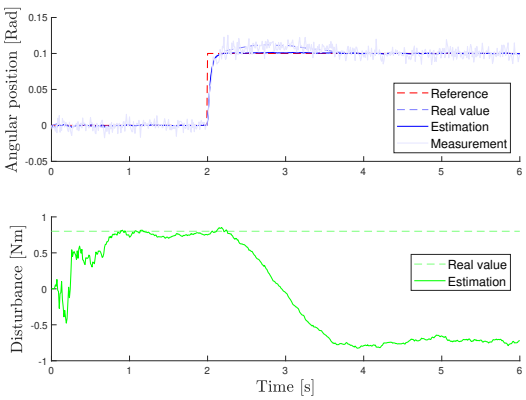

Acknowledgement This work is supported in part by Flanders Make SBO DIRAC "Deterministic and Inexpensive Realizations of Advanced Control" and in part by KUL-C1: KU Leuven Research project C14/15/067 "B-spline based certificates of positivity with applications in engineering".

References

[1] M. Morari and U. Maeder. Nonlinear offset-free model predictive control. *Automatica*, 48(9):2059–2067, 2012.

[2] Gabriele Pannocchia and James B. Rawlings. Disturbance models for offset-free model-predictive control. *AIChE Journal*, 49(2):426–437, 2003.

Offset-free model predictive control of the electron density profile in a tokamak

T.O.S.J. Bosman[1,2,*], M. van Berkel[1], M.R de Baar[1,2]
[1] DIFFER - Dutch Institute for Fundamental Energy Research, Eindhoven, the Netherlands
[2] Eindhoven University of Technology, Control Systems Technology, Eindhoven, the Netherlands
[*] *t.o.s.j.bosman@differ.nl*

1 Introduction

The tokamak is at the moment the most promising design for a thermonuclear fusion reactor (see [1] for a control-oriented introduction). In such a reactor, energy is produced by harvesting the energy released when deuterium and tritium atoms fuse together. The generated fusion power, and thus the performance of the reactor, depends on the spatial electron density distribution, referred to as electron density profile. However, the electron density is also subject to limits that can lead to detrimental instabilities when violated. Consequently, reliable control of the plasma density profile is essential for high-performance and safe operation of tokamaks.
On contemporary experimental reactors, gas injection or the injection of a single pellet type (mm-sized body of frozen fuel) are the actuators used for this purpose. On future commercials reactors, pellet injection is regarded as the only viable option for core density control as gas injection will be ineffective. Since multiple pellet types will have to be used, a controller that can control the density distribution with multiple actuators is required. In this work, an offset-free model predictive control (MPC) setup is proposed for this purpose.

2 Problem formulation

The evolution of the electron density profile $n_e(\rho,t)$ in a tokamak on the spatial domain $\rho \in [0,1]$ can be described by the 1D partial differential equation

$$\frac{1}{V'}\frac{\partial}{\partial t}(n_e(\rho,t)V') + \frac{1}{V'}\frac{\partial \Gamma(\rho,t)}{\partial \rho} = S(\rho,t) + \Lambda(\rho)u^c(t), \tag{1}$$

where Γ is radial electron transport flux (often represented by a drift-diffusion model), S are uncontrolled particle source terms, Λ the spatial deposition profile of the control inputs u^c, and V' the time derivative of the plasma volume (assumed known). The aim of the controller is to change the control inputs such that: (i) a high-performance reference density profile is tracked in a region of interest; (ii) the line-integrated density stays below the Greenwald density limit [2]; and (iii) a favorable ratio is maintained between the logarithmic gradients of the ion temperature profile and the electron density profile.

3 Approach

In [3], a control-oriented model for the particle transport in a tokamak called RAPDENS was proposed where the density profile is approximated using finite elements. The resulting states $x(t)$ are the time-varying spline coefficients that parameterize the profile. RAPDENS computes the local linearization of the transport dynamics at each time step. The resulting linear model is augmented with a disturbance state $d(t)$ that is estimated at each time step with a Kalman filter. The augmented linear model is used to derive the offset-free MPC controller as follows

$$\min_{u_0^c,\ldots,u_N^c,\varepsilon} \quad \|x_N - \bar{x}_N\|_P^2 + \sum_{k=0}^{N-1} \|x_k - \bar{x}_k\|_Q^2 + \|u_k^c - \bar{u}_k^c\|_R^2 + W_\varepsilon \varepsilon^2 \tag{2}$$

$$\text{subj. to} \quad A_{\text{ineq}} U_k \leq b_{\text{ineq}}, \tag{3}$$

$$g_1(x_k, u_k^c, d_k, \varepsilon) \leq 0, \tag{4}$$

where N is the prediction horizon, P, Q, R, W_ε are weights, and $\bar{x}$, $\bar{u}^c$ the desired steady-state state and inputs. A_{ineq} and b_{ineq} are matrices used to account for the limit on the line-integrated density using the hard linear constraint (3). The function g_1 is used in the soft nonlinear constraint (4) to account for the favorable ratio of logarithmic gradients [4] as discussed in Section 2. Violation of the soft constraint is penalized with the parameter ε.

4 Results

The designed offset-free MPC controller has been tested in control simulations using the control-oriented model RAPDENS. The simulations show that the controller is capable of regulating the density profile with multiple pellet actuators. However, for large pellets that can only be injected at low frequencies, the discrete pellet dynamics become dominant and limit the achievable performance. This serves as motivation for further hybrid controller development.

References

[1] Pironti et al., IEEE Control Systems **25**, (2005)
[2] Greenwald, Plasma Phys. Control. Fusion **44**, (2002)
[3] Blanken et al., Fusion Eng. Des. **126**, (2018)
[4] Bosman et al., J. Phys. Commun. **5**, (2021)

Detection of Floor Surface Transitions using a SNIS Consistency Test

Bastiaan Vandewal Goele Pipeleers Jan Swevers
MECO Research Team, Department of Mechanical Engineering, KU Leuven, Belgium
Core Lab DMMS-M, Flanders Make, Leuven, Belgium
Email: bastiaan.vandewal@kuleuven.be

1 Introduction

The accurate estimation of wheel slip properties on changing floor surfaces can improve the driving behavior and positional accuracy of vehicles. In this abstract we focus on detecting a change in the floor surface online, using the Summed Normalized Innovation Squared (SNIS) consistency check, which is a measure to statistically check if the innovations of a Kalman Filter are still consistent with the model [1].

2 Summed Normalized Innovation Squared

The Normalized Innovation Squared (NIS) values can be calculated as a weighted version of the squared innovations, where the weighting is done with a covariance matrix S_j which is a measure for the expected uncertainty on the innovations. The SNIS test checks consistency by using the last m NIS values and is given by:

$$SNIS_k = \sum_{j=k-m+1}^{k} \nu_j^\top S_j^{-1} \nu_j. \tag{1}$$

SNIS values are χ^2-distributed for a linear system subject to Gaussian model uncertainty. Checking if a NIS or SNIS value is above a given boundary value allows for testing the consistency of the measurement. If the innovation cannot be explained by the expected uncertainty on the measurement, an inconsistency is detected, stating that either the model (parameters) or measurement is erroneous. Changing the parameter m allows for a trade-off between fast detection of surface changes and the number of false alarms.

3 Use case and approach

A model of an omnidirectional vehicle with four independently driven Mecanum wheels is used, applying the wheel slip model as discussed in [2]. Within the extended Kalman Filter we assume that the surface friction parameter is time invariant in order to easily detect a changing surface. Once this occurs, the SNIS values show peak values, an inconsistency is reported and the estimation error covariance for this parameter is enlarged in order to allow for fast convergence towards a new constant parameter value. Depending on this enlargement the convergence speed can be reduced drastically.

4 Detecting contact transitions

Figure 1 shows the simulation of a lemniscate-shaped motion trajectory five times in a row. After each trajectory the motion is repeated with the same control inputs but with a different friction surface parameter, except for the transition between the third and fourth movement, where the friction coefficient stays constant. The different levels for this friction coefficient and convergence towards this value is shown in green and red respectively. The velocity of one of the wheels is shown in blue to keep track of the evolution of the trajectory. The second part of this figure shows how the SNIS value is evolving over time and the threshold above which an inconsistency is detected.

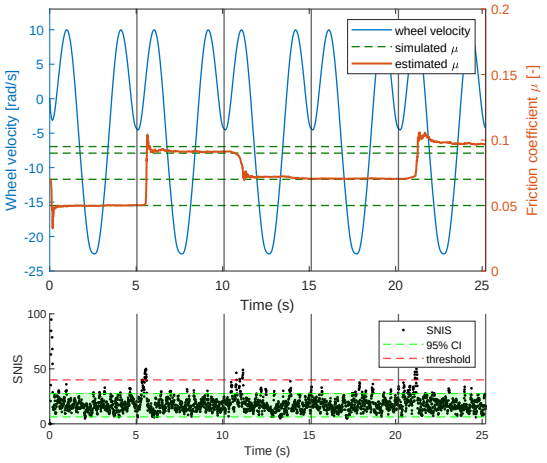

Figure 1: Convergence behavior of the friction surface parameter with changing surface properties.

Acknowledgement This work has been carried out within the framework of Flanders Make's SBO project MultiSysLeCo (Multi-System Learning Control). Flanders Make is the Flemish strategic research centre for the manufacturing industry.

References

[1] T. Lefebvre, H. Bruyninckx and J. De Schutter, "Polyhedral contact formation modeling and identification for autonomous compliant motion," in IEEE Transactions on Robotics and Automation, vol. 19, no. 1, pp. 26-41, Feb. 2003, doi: 10.1109/TRA.2002.805677.

[2] B. Vandewal, J. Gillis, G. Pipeleers and J. Swevers, "Simplified Wheel Slip Modeling and Estimation for Omnidirectional Vehicles," in 2022 IEEE 17th International Conference on Advanced Motion Control (AMC), Feb. 2022.

A short review of finite-sample error analysis of linear system identification for control [1]

Shengling Shi, Bart De Schutter
Delft Center for Systems and Control, Delft University of Technology, The Netherlands
Email: {s.shi-3, B.DeSchutter}@tudelft.nl

1 Introduction

The error quantification of an identified model is important, e.g., for robust control and analyzing the effect of the error on the closed-loop performance when the model is used for control. While the classical asymptotic analysis provides error quantification when the data length approaches infinity, there is a growing interest from the machine learning and system identification communities in non-asymptotic analysis to provide error bounds for a finite data length [1]. This talk provides a short introduction and review of these results and their application in control.

2 Non-asymptotic identification with measured states

Consider a linear state-space model:

$$x_{t+1} = Ax_t + Bu_t + w_t, \tag{1}$$

where $x_t \in \mathbb{R}^n$, $u_t \in \mathbb{R}^p$, and w_t is a sub-Gaussian distributed white noise. For simplicity, we assume $B = 0$ and $x_0 = 0$ for now. Then given the measurements $\{x_t\}_{t=1}^N$, the problem is to obtain the estimate $\hat{A}$ of A in (1), and more importantly, to provide an error bound of the following type: With high probability and for any finite N larger than some lower bound, it holds that $\|A - \hat{A}\|_2 \leqslant \varepsilon_A(N)$, where $\|\cdot\|_2$ denotes the spectral norm, and the error also depends on the identification approach and the unknown A.

The least squares estimator $\hat{A}$ of (1) has been considered in [2] when A is stable, and it is shown that $\varepsilon_A = \mathcal{O}\big(\sqrt{(n\log n)/[N\lambda_{\min}(\Gamma_\infty)]}\big)$, where, for any positive integer t, $\Gamma_t \triangleq \sum_{k=0}^{t-1} A^k (A^k)^\top$ is the finite-time controllability Gramian. Therefore, the error has a decay rate $\mathcal{O}(1/\sqrt{N})$ with respect to the data length, which is the optimal rate as shown in the lower bound of [2]. It can also be found that a larger minimum eigenvalue of the infinite-time controllability Gramian leads to a smaller estimation error. This bound is further extended in [3] to consider marginally stable A and unstable A. When all the eigenvalues of A are outside the unit circle, an exponential decay rate $\mathcal{O}(|\lambda_{\min}(A)|^{-N})$ can be achieved for the error ε_A. The analysis can also be trivially extended to systems with inputs, which has been addressed in the literature.

[1] This research has received funding from the European Research Council (ERC) under the European Union's Horizon 2020 research and innovation programme (Grant agreement No.101018826 - CLariNet).

3 Non-asymptotic identification with unmeasured states

When only the output is measured with the output equation $y_k = Cx_t + \eta_t$, where $y_t \in \mathbb{R}^m$ and η_t is white noise, a subspace identification method can be employed to obtain estimates $\hat{A}$ and $\hat{C}$ from $\{y_t\}_{t=1}^N$. More importantly, if the model order is known, a finite-sample error bound $\|TAT^\top - \hat{A}\| \leqslant \varepsilon$, for some orthonormal matrix T, can be derived, which shows that $\varepsilon = \mathcal{O}(\log N/N)$ when A is marginally stable [4]. An error bound for subspace identification when the model order is unknown has also been developed in the literature.

4 Connection to control

The finite-sample error bounds have been employed to analyze the performance of robust LQR or LQR for the nominal model with the uncertainty ignored. As an example, consider (1) with states measured and then the least square estimate $(\hat{A}, \hat{B})$ of the system. Denote the optimal performance of an infinite-horizon LQR controller by $J^\star$ when the true system is known, and let $\hat{J}$ be the performance of an infinite-horizon robust LQR controller applied to the estimated nominal model with the finite-sample error bound. Then the performance error can be bounded as $(\hat{J} - J^\star)/J^\star = \tilde{\mathcal{O}}((n+p)/N)$ [1], where $\tilde{\mathcal{O}}$ suppresses a logarithmic factor. The bound shows a clear dependence of the control performance on the state, input dimensions, and the data length.

References

[1] B. Recht, "A tour of reinforcement learning: The view from continuous control," *Annual Review of Control, Robotics, and Autonomous Systems*, vol. 2, pp. 253–279, 2019.

[2] M. Simchowitz, H. Mania, S. Tu, M. I. Jordan, and B. Recht, "Learning without mixing: Towards a sharp analysis of linear system identification," in *Conference on Learning Theory*. PMLR, 2018, pp. 439–473.

[3] T. Sarkar and A. Rakhlin, "Near optimal finite time identification of arbitrary linear dynamical systems," in *International Conference on Machine Learning*. PMLR, 2019, pp. 5610–5618.

[4] A. Tsiamis and G. J. Pappas, "Finite sample analysis of stochastic system identification," in *2019 IEEE 58th Conference on Decision and Control (CDC)*. IEEE, 2019, pp. 3648–3654.

Parameter estimation of multiple poles by subspace-based methods

Prabhu Vijayan[1,2], Mariya Ishteva[1], Ivan Markovsky[2]
[1] KU Leuven - Campus Geel, Department of Computer Science, 2440 Geel, Belgium
[2] Vrije Universiteit Brussel, dept. ELEC, Pleinlaan 2, 1050 Brussels, Belgium
Email: {prabhu.vijayan, mariya.ishteva}@kuleuven.be
ivan.markovsky@vub.be

1 Introduction

In this work, the harmonic retrieval of the sum of complex exponentials is considered. Numerous techniques to estimate the parameters are available, such as linear prediction methods [1], subspace-based methods [2]-[4]. The discrete-time signal, x_n, is given as a sum of K complex damped exponentials, corrupted by white Gaussian noise b_n:

$$x_n = \sum_{k=1}^{K} a_k e^{j\phi_k} e^{\{(-\alpha_k + j2\pi f_k)\Delta t\}n} + b_n, \quad n = 0, 1, ..., N-1.$$

The parameters defining the model are frequency f_k, damping factor α_k, amplitude a_k and phase ϕ_k. This paper focuses on the signal sequence, that has multiple signal poles, where the harmonic retrieval problem results in high error [5]. This issue is addressed by a more generalized signal model, $\tilde{x}_n$, that considers the multiplicity of poles.

$$\tilde{x}_n = \sum_{k=1}^{r} \sum_{l=1}^{M_k} a_k e^{j\phi_k} n^{l-1} e^{\{(-\alpha_k + j2\pi f_k)\Delta t\}n} + b_n.$$

Here, r is the number of unique poles whose multiplicity is $M_k, k = 1, 2, ..., r$. More compactly,

$$\tilde{x}_n = \sum_{k=1}^{r} \sum_{l=1}^{M_k} c_k n^{l-1} z_k^n + b_n,$$

where $c_k = a_k e^{j\phi_k}$, $z_k = e^{\{(-\alpha_k + j2\pi f_k)\Delta t\}}$ are the k^{th} complex amplitude and signal pole, respectively, to be estimated.

2 Harmonic Retrieval

Various methods namely, Hankel Total Least Square (HTLS), Kung's methods, linear prediction and model order reduction are used to estimate the signal poles $\hat{z}_k$, from the signal sequence $\tilde{x}_n$ of given model order K. In the former two methods, $\tilde{x}_n$ is arranged in a Hankel matrix $\boldsymbol{H}$ of size $L \times M$, $L > K$, where L is hyperparameter and $M = N - L + 1$, $M > K$. The frequencies and damping factors are determined from the signal pole estimates $\hat{z}_k$, $k = 1, ..., K$. For the estimation of complex amplitudes $\hat{c}_k$, given in $\boldsymbol{c}$, by least square method, a modified Vandermonde matrix $\boldsymbol{T}$ of size $N \times K$ is proposed, that is constructed using $\hat{z}_k$ and their multiplicities.

$$\boldsymbol{T}\boldsymbol{c} = \tilde{x}_n, \quad n = 0, 1, ..., N-1,$$

$$\boldsymbol{T} = \begin{bmatrix} \begin{bmatrix} \hat{z}_1^n \\ n\hat{z}_1^n \\ \vdots \\ n^{M_1-1}\hat{z}_1^n \end{bmatrix}^T & \cdots & \begin{bmatrix} \hat{z}_r^n \\ n\hat{z}_r^n \\ \vdots \\ n^{M_r-1}\hat{z}_r^n \end{bmatrix}^T \end{bmatrix}.$$

r - number of unique poles, $M_1, .., M_r$ are their multiplicities. The amplitude and phase are determined from the estimated complex amplitudes $\hat{c}_k$.

3 Numerical Examples and Conclusions

The effect of hyperparameter L on the performance of the HTLS and Kung's realization methods for $\tilde{x}_n$ is studied here. From experiments, the estimates are better for a (nearly) square Hankel matrices, i.e. $\frac{N}{3} \leq L_{optimal} \leq \frac{N}{2}$. The algorithms were tested for signal with and without noise. HTLS and Kung's realization method resulted in better estimates, as they involve numerically stable SVD, whereas linear prediction and model order reduction determine poles through state matrix, constructed by coefficients of recurrence relation of the polynomial function, leading to numerically unstable results. The parameter estimation is limited to signal sequence with poles of multiplicities 3. The signal model is numerically unstable for higher multiplicity.

References

[1] Kumaresan, R., Tufts, D.W.: Estimating the Parameters of Exponentially Damped Sinusoids and Pole-Zero Modeling in Noise, IEEE Trans. of Acous., Vol.30, No.6, 1982.

[2] Bhaskar Rao, D.V., Arun, K.S.: Model-based processing of signals: a state-space approach. Proc. IEEE 1992, 80, p. 283–309.

[3] Kung, S.Y., Arun, K.S., Bhaskar Rao, D.V.: State-space and singular value decomposition-based approximation methods for the harmonic retrieval problem. J. Opt. Soc. Am. 198, 73(12), p. 1799–1811.

[4] Markovsky, I., Vaccaro, R.J., Van Huffel, S.: System identification by optimal subspace estimation, Dept. EE, K.U.Leuven, 2006.

[5] Papy, J.-M., De Lathauwer, L., Van Huffel, S.: Exponential data fitting using multilinear algebra: the decimative case, Journal of Chemometrics, DOI:10.1002/cem.1212, p. 341–351.

Spectral network identification with generalized diffusive coupling

Marvyn Gulina and Alexandre Mauroy
Namur Institute for Complex Systems (naXys) and Department of Mathematics,
University of Namur, Rue de Bruxelles 61, B-5000 Namur, Belgium
Email: marvyn.gulina@unamur.be and alexandre.mauroy@unamur.be

1 Spectral identification of networks

Spectral network identification aims at estimating the eigenvalues of the Laplacian matrix L of the network from data. This allows to infer global information on the network structure from local measurements at a few number of nodes **Mauroy2017**.

2 Scalar diffusive coupling framework

We consider a dynamical system defined over a network. The local dynamics of the unit attached to node k are directly influenced by its neighbors through input and output signals. In the particular case of n identical units with diffusive coupling, the dynamics of node k are described by

$$\begin{cases} \dot{x}_k = F(x_k) + G(x_k)u_k & \in \mathbb{R}^m \\ u_k = \sum_{j=1}^n W_{kj}(y_k - y_j) & \in \mathbb{R}^r \\ y_k = H(x_k), & \in \mathbb{R}^r \end{cases} \tag{1}$$

with the (continuously differentiable) functions $F : \mathbb{R}^m \to \mathbb{R}^m$, $G : \mathbb{R}^m \to \mathbb{R}^{m\times r}$ and $H : \mathbb{R}^m \to \mathbb{R}^r$. Note that the coupling coefficients W_{kj} are the entries of the adjacency matrix $W \in \mathbb{R}^{n\times n}$ of the network. The network Laplacian matrix is given by $L = D - W$, where D denotes the degree matrix defined by $d_i = \sum_{k=1}^n W_{ik}$. We further assume that the units asymptotically reach a synchronized state $x_1 = \cdots = x_n = x^*$, *i.e.* $\lim_{t\to\infty} x_k(t) = x^*$.

The Jacobian matrix associated with the whole system (1) and evaluated at x^* writes

$$J = I_n \otimes A - L \otimes BC^T, \tag{2}$$

with $A = \partial F/\partial x(x^*)$, $B = G(x^*)$ and $C = \nabla H(x^*)$. In the previous work **Mauroy2017**, it was proved that the relationship between the spectrum of the Jacobian matrix $\sigma(J)$ and the spectrum of the Laplacian matrix $\sigma(L)$ is one-to-one when $r = 1$ and satisfies

$$(A - \mu I_m)w = \lambda BC^T w, \tag{3}$$

where $\mu \in \sigma(J)$ and $\lambda \in \sigma(L)$. It follows that one can retrieve the spectrum of L from the spectrum of J. Moreover, states measurements can be used to compute the spectrum of the Jacobian matrix through the DMD algorithm **Schmid2010**.

It is noticeable that the results of **Mauroy2017** are limited to the case $r = 1$ in (1). This corresponds to scalar-valued input and output signals, a condition that is not satisfied in many situations, such as reaction-diffusion networks. If $r > 1$, the rank of the matrix BC^T can be larger than 1 and the one-to-one relation between μ and λ obtained from (3) does not hold. In this context, the main contribution of the present work is to provide a generalized framework for spectral identification, which is valid for the case of vector-valued inputs and outputs ($r > 1$).

3 Generalization of the framework

We will show that the spectral identification problem is feasible under a mild assumption based on the spectral moments of BC^T. More precisely, one can obtain a linear system of equations which allows to compute the spectral moments of L from those of J. Finally the spectrum of L can be recovered from its spectral moments. However, this process might lead to significant numerical errors on the individual eigenvalues and should therefore be avoided.

We will propose an alternative method for solving the spectral identification problem, which is based on the properties of the characteristic polynomial of the generalized eigenvalues problem (3). This method will be illustrated with numerical simulations.

Sparse Learning in System Identification: Debiasing and Infinite-Dimensional Algorithms [1]

M. Tolga Akan[1], Mingzhou Yin[2], Andrea Iannelli[2], Mohammad Khosravi[2]
[1] Eindhoven University of Technology, [2] ETH Zurich
Email: {m.t.akan}@tue.nl, {myin, iannelli, khosravm}@control.ee.ethz.ch

1 Introduction

Recent developments in the identification techniques propose to use regularized optimization methods to decouple the experimental data adherence maximization term and a low-order model promoting term. Recently, a state of the art, sparsity recovery regularizer technique, the *atomic norm regularization*, has been developed by Chandraskearan et al. in [2] and it is applied to system identification problems by Shah at al. in [3], as a low-order model promoting method. This technique approximates the infinite dimensional atomic set via the discretization and solves an ℓ_1 norm regularized, convex optimization problem to obtain the poles and the residues (i.e. numerator) of the first order transfer functions that composes the estimated model as a linear combination. However, a potential drawback in such a technique is having biased estimations of the residues and not accurate representations of the poles of the atoms.

2 Proposed Identification Approach

In this study, novel identification methods are developed by extending the atomic norm regularization based system identification technique. For this purpose, a new definition of the atomic set is introduced to ensure the responses of the atoms are real valued.

The proposed first method extends the atomic norm regularized identification with the group Lasso (GL) regularizer, with the aim to impose the constraint on the special coefficients structure arising from the newly defined atomic set. Unfortunately, to obtain a convex program, the group Lasso penalizes large coefficients more compared to small coefficients since the same penalization parameter, λ, is used for all variables similarly to ℓ_1-norm regularization. This results in high biased estimations for the large coefficients, a problem which constitutes the main motivation of this study to implement further techniques in the field of high-dimensional statistics.

For a nearly unbiased sparse estimation, firstly the regularization function should be singular at the origin to promote the sparsity, and secondly, it must be bounded by a constant to avoid the bias at the large coefficients. Under these constraints, we extend the grouped atomic norm regularized identification via DC programming based non-convex penalization framework of Gasso et. al in [4]. Hence, we approximate Log and ℓ_q penalties as iterative reweighted Lasso problems by adaptively penalizing the parameters.

Iteratively solving Eq.1 by initializing $w_\omega^{(0)} = 1$ presents DC-based non-convex extension of the atomic norm-regularized identification problem, while the first step is the group Lasso problem.

$$\begin{aligned} &\hat{\beta}^{(k)} = \arg\min_\beta \tfrac{1}{2}\|y - \textstyle\sum_\omega \mathbf{X}_\omega \beta_\omega\|_2^2 + \\ &\lambda \textstyle\sum_\omega w_\omega^{(k-1)} \sqrt{\mathbf{p}_\omega}\, \|\beta_\omega\|_2, w_\omega^{(k)} = 1 - \dfrac{h'\left(\left\|\hat{\beta}_\omega^{(k)}\right\|_2\right)}{\lambda} \end{aligned} \quad (1)$$

where $\mathbf{X}_\omega$ is truncated response vector of the atoms under input sequence, $\mathbf{p}_\omega = 2$ for $\omega \in \mathscr{H}$, $\mathbf{p}_\omega = 1$ for $\omega \in R_{(-1,1)}$, $h' = \lambda(1 - \frac{q}{|\beta_j|^{1-q}})$ for ℓ_q-penalty, $h' = \lambda(1 - \frac{1}{|\beta_j|+\varepsilon})$ for *Log*-penalty, $\mathscr{H}$ is the discretized set of the upper half of unit disc and $R_{(-1,1)}$ is the discretized set of the natural number in the range of (-1,1).

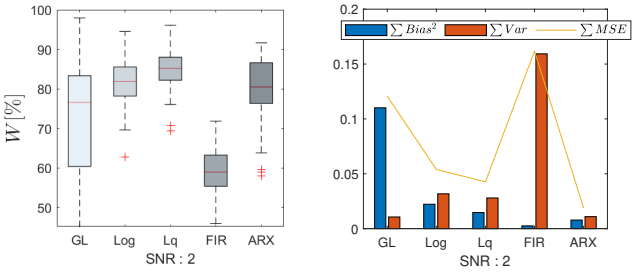

Figure 1: Simulations for fitting metric (W) and bias-variance comparison of the proposed methods and the baseline algorithms

References

[1] M. T. Akan., "Sparse Learning in System Identification: Debiasing and Infinite-Dimensional Algorithms," *ETH Zurich*, 2021.

[2] V. Chandrasekaran, et al., "The Convex Geometry of Linear Inverse Problems," *Found. of Comp. Math.*, pp. 805-849, 2012.

[3] P. Shah et al., "Linear system identification via atomic norm regularization," *IEEE 51st IEEE CDC)*, 2012.

[4] G. Gasso et al., "Recovering Sparse Signals With a Certain Family of Nonconvex Penalties and DC Programming," *IEEE Trans. on Sig. Proc.*, pp. 4686-4698, 2009.

Parameter estimation under periodic disturbances using the Maximum Likelihood algorithm

D.M.E. Kruijver[1], W.B.J. Hakvoort[1], and M.A. Beijen[2]

[1]Department of Mechanics of Solids, Surfaces, and Systems (MS3), University of Twente, P.O. Box 217, 7500 AE Enschede, The Netherlands
[2]DEMCON Advanced Mechatronics, Institutenweg 25, 7521 PH Enschede, The Netherlands
Email: d.m.e.kruijver@utwente.nl

1 Introduction

Real-time parameter estimation is used to fit an actuated second-order mass-spring-damper system on a small set (few seconds, 4096 Hz) of measured frequency response data. Previously the parameters were estimated by the Linear Least Square (LLS) estimator, which resulted in biased estimates in the presence of periodic disturbances. This can be seen in Figure 1, where the exact second order model, the measured data and the Bode plot from the LLS estimate are shown. The periodic disturbance at 60Hz is seen as natural frequency and has a negative effect on the performance of the estimator. In this research a new estimation algorithm is proposed to improve the accuracy of the estimation when a periodic disturbance is disturbing the system.

2 Improved algorithm

To improve the estimation, three adjustments have been made to the algorithm: (a) using the Maximum Likelihood (ML) algorithm such that frequency points with a large uncertainty contribute less to the solution than frequency points with a small uncertainty [1], (b) using random excitations and (c) adding initial and final conditions to the transfer function model [1] [2]. The ML estimator does improve the accuracy in case of random disturbances but not in case of periodic disturbances. The estimation accuracy in case of periodic disturbances can be improved by the second adjustment. This can be explained by looking into more detail to the weighting function of the maximum likelihood algorithm which is the inverse of the output error variance and is calculated with the cross- and auto-power spectra of the input-output signals:

$$\sigma_Y^2(k) = S_{YY}(j\omega_k) - S_{YU}(j\omega_k)S_{UU}^{-1}(j\omega_k)S_{YU}^H(j\omega_k). \quad (1)$$

A periodic disturbance will be correlated with a periodic excitation, while with a non-periodic excitation, there is no correlation between the input and the output signal which results in a small value for the cross-power. As a result, the output error mainly depends on the power spectrum S_{YY} which has a high value at the periodic disturbance and a low weighting will be assigned to the disturbed frequency by the ML algorithm. This results in a more accurate parameter estimation as can be seen in Figure 1, where the estimated Bode plot with the ML algorithm is approximately the same as the exact Bode plot. However, due to the random excitation, the excitation is different for every second and the variance in the estimates is slightly increased. When using random excitations, it is important to apply the third adjustment. Initial and final conditions should be added to the transfer function because the signals are not measured over an infinite time period and sampling is applied to measure discrete time signals.

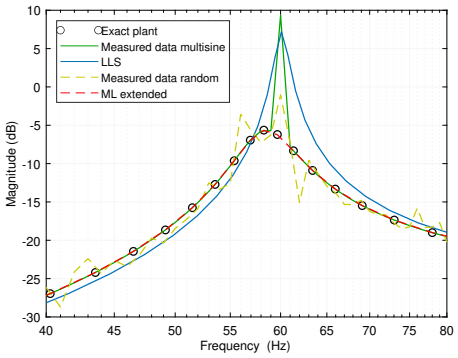

Figure 1: Bode plot of the measured data, real data and estimated models

3 Results

From this research it is concluded that in case of non-periodic and periodic disturbances, the use of the ML estimator in combination with a non-periodic excitation signal and an extended transfer function model the accuracy of the estimation is improved. The variance in the estimation is increased by using the random excitation, but the overall accuracy is improved.

References

[1] R. Pintelon and J. Schoukens, *System Identification: A Frequency Domain Approach*. John Wiley Sons, 2012.

[2] R. Pintelon, J. Schoukens, and G. Vandersteen, "Frequency domain system identification using arbitrary signals," 1997.

Identifying a highly nonlinear MIMO Volterra system including Bayesian confidence bounds in seconds on a laptop

Eva Memmel, Clara Menzen, Kim Batselier
DCSC, TU Delft,
Mekelweg 2, 2628 CD Delft
{e.m.memmel, c.m.menzen, k.batselier}@tudelft.nl

MIMO Volterra system Identification

When it comes to nonlinear system identification, Volterra series are a commonly used model structure. Being an extension to the linear FIR model, Volterra series have the following characteristics: the outputs $y(t)$ are expanded as a combination of past inputs $u(t)$, weighted by the Volterra coefficients w_i. A Volterra series is usually truncated at a degree D and memory M, which results in the following relationship for a single input, single output (SISO) system:

$$y(t) = w_0 + \sum_{d=1}^{D} \sum_{m_1,\dots,m_d=0}^{M-1} w_d(m_1,\dots,m_d) \prod_{j=1}^{d} u(t-m_j) + e(t).$$

Unfortunately, the number of Volterra coefficients scales exponentially with the order of nonlinearity D. This is known as the Curse of Dimensionality.
Generally, two attractive features of a system identification algorithm are a quick run-time and trustworthy, informative results. First, a system identification cycle usually requires many iterations to tune hyperparameters like M and D. Therefore, it is advantageous to have a short computation time. Second, system identification is used in various applications (as for example designing control systems), where confidence bounds can be useful to estimate how much trust can be placed into the predictions.
Due to the Curse of Dimensionality, the feasible order of nonlinearity for Volterra Series is limited to 3 or 4. Otherwise, the storage costs are too high to perform the system identification on a standard laptop. Switching to a cluster is unfortunately not a lasting solution either. Due to the exponentially growing storage demand, the cluster will also quickly reach its limits. As a result, we cannot rely on hardware to solve this issue.
Classically, the identification problem is rewritten as ordinary-least-squares problem and validated with a test-data set by looking at some scalar metric like the root mean squared error. This has two major drawbacks: Assumptions on the model are made implicitly and the evaluation of the trustworthiness of the model relies on a single number.

Bayesian Inference in a Volterra Tensor Network

These drawbacks can be alleviated with the following ideas: The key idea to lift the Curse of Dimensionality is to trade storage for computation. By decomposing the Volterra model into a tensor network, the computational complexity scales now linear in the order of nonlinearity [1].
Implementing Bayesian framework for the system identification offers three benefits: explicit assumptions, confidence bounds for the estimation and including prior knowledge about the system. These advantages are preserved when applying tensor networks [2].
In this work, we want to discuss the following research question: Is it possible to apply a Bayesian framework to a multiple input, multiple output (MIMO) Volterra tensor network? As a preview on the results, we consider an academic example. It consists of a 10th order nonlinear Volterra system with $8^{10} = 1.073.741.824$ coefficients. The system is subject to white, Gaussian noise. The computation was done on an IntelCore i7-10610U @ 1.80GHz with 16GB RAM in 19 s. The mean prediction with 99% confidence bounds of the validation output are depicted in Figure 1.

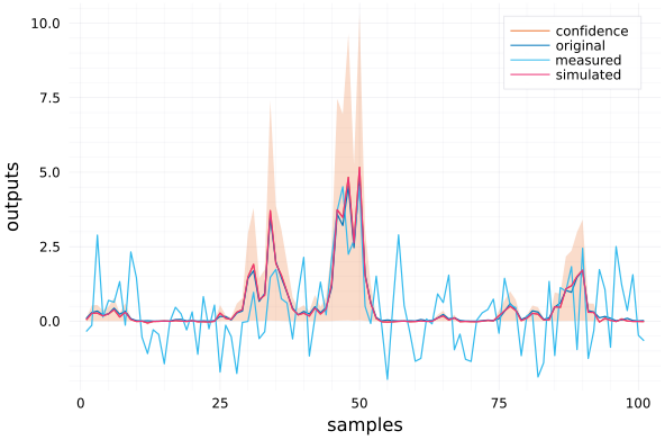

Figure 1: Test data with Bayesian Volterra tensor network

References

[1] Kim Batselier, Zhongming Chen, and Ngai Wong. Tensor network alternating linear scheme for mimo volterra system identification. *Automatica*, 84:26–35, 2017.

[2] Clara Menzen, Manon Kok, and Kim Batselier. Alternating linear scheme in a bayesian framework for low-rank tensor approximation. *arXiv preprint arXiv:2012.11228*, 2020.

Towards advanced model based control of bioprocesses

Satyajeet Bhonsale*
satyajeetsheetal.bhonsale@kuleuven.be

Wannes Mores*
wannes.mores@kuleuven.be

Jan Van Impe*
jan.vanimpe@kuleuven.be

*BioTeC+, Department of Chemical Engineering, KU Leuven, Technology Campus Ghent

1 Abstract

In last decade, the production of speciality products through biochemical process has gained traction. Amongst other products, microorganisms have been used to produce artificial sweeteners, biopharmaceutics, etc. Such a biochemical process is governed by a multitude of reactions within a single microbial cell, as well as the interaction between the cell and the reactor medium. Metabolic networks summarise all the reactions and within the cell and the interactions of the cell with the surroundings. The different metabolites act as the nodes of the network and the reactions or fluxes between the different metabolites act as the edges. The entire network can be summarised in the stoichiometric matrix **S**, whose elements $S_{i,j}$ correspond to the stoichiometric coefficient of the *i*th metabolite in the *j*th reaction. The main disadvantage of using a metabolic network model is the limitation on the size of the network that can be used. Genome scale models constitute of hundreds of metabolites and reactions leading to a large number of differential states. Thus, control and optimisation of bioprocesses is based on the macroscopic mass balance based models.

The state of the art in bioprocess control, the nonlinear model predictive control (NMPC) uses the model to solve an dynamic optimisation problem over a prediction horizon. The optimal inputs computed are applied only till a new measurement is obtained, at which point the model is reinitialised and the dynamic optimisation problem solved again by shifting the prediction horizon forward. Recently, [1] demonstrated the use of a metabolic network based nonlinear model predictive control to regulate a bioprocess. However, a very small scale metabolic network with four metabolites and seven fluxes was used. The free fluxes in the network were estimated from the extracellular metabolites in a moving horizon estimation (MHE) framework.

In this paper, we aim to compare the metabolic network based NMPC with the traditional macroscopic model based NMPC. The biochemical plant is assumed to follow a metabolic network (Figure 1) with known flux distribution. The case study considers a continuous bioprocess with two substrates. The two substrates are mixed before they are fed into the bioreactor. This flow rate of the feed is constant, but the composition can be be altered by manipulating the weight fraction in the mixing step. Thus, the control input in this case is the weight fraction. Based on the simulated data, a macroscopic mass balance model is identified describing the biomass growth, the substrate consumption, and the product formation.

The traditional NMPC uses the macroscopic model to compute the optimal input sequence, and apply it to the plant. As all the external metabolites are assumed to be measured, a estimator scheme is not required. In the metabolic network based NMPC, the free fluxes need to be estimated from the available measurements, i.e., the extracellular metabolites. Following [1] and [2], an MHE framework is utilised to estimate the three free fluxes. The tracking performance both these control schemes is compared and the influence of parameters such as prediction horizon and measurement noise is elucidated.

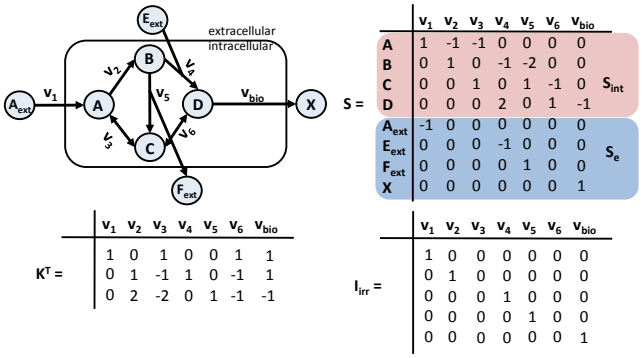

Figure 1: Metabolic network used in the case study

References

[1] P. Nimmegeers, D. Vercammen, S. Bhonsale, F. Logist, and J. Van Impe. Metabolic reaction network-based model predictive control of bioprocesses. *Applied Sciences*, 11(20), 2021.

[2] D. Vercammen, F. Logist, and J. Van Impe. Dynamic estimation of specific fluxes in metabolic networks using non-linear dynamic optimization. *BMC Systems Biology*, 8(132), 2014.

Assessment of microbial food safety risks due to climate change

Lydia Katsini[1], Satyajeet Bhonsale[1], Carlos Andre Muñoz López[1], Styliani Roufou[2], Sholeeem Griffin[3], Vasilis Valdramidis[3], Simen Akkermans[1], Monika Polanska[1], Jan Van Impe[1*]

[1]KU Leuven, Department of Chemical Engineering,
BioTeC+ Chemical & Biochemical Process Technology & Control,
Gebroeders De Smetstraat, 9000 Ghent, Belgium
[2]University of Malta, Department of Food Sciences and Nutrition, MSD 2080, Malta
[3]University of Malta, Department of Food Sciences and Nutrition,
Centre of Molecular Medicine and Biobanking, MSD 2080, Malta
*Email: jan.vanimpe@kuleuven.be

1 Abstract

Microbial food safety is both directly and indirectly affected by climate and climate change, placing public health at risk. This contribution presents a modelling framework to assess the effects of climate change on microbial food safety. The dairy sector is considered as a case study. At the stage of raw milk, the microbial food safety of dairy is directly associated with the total mesophilic microbial count, or Total Bacterial Count, TBC, measured in CFU/mL. TBC serves as an indicator for the milk contamination levels at the environment of the farm.

Climate change impact assessments are usually based on impact models [1]. These models describe the effect of climate variables on the system under study. The first objective of this contribution is the development of such an impact model, that characterizes the effect of climate variables on the TBC levels of raw cow milk. For this, TBC data of raw milk from 123 dairy farms in the Maltese islands is used. The data covers a timespan of 6 years, namely from January 2015 to December 2020 and has a weekly sampling frequency. The climate data used, originates from the AGRI4CAST Resources Portal, from the Joint Research Center (JRC) of the European Commission. Data-driven modelling methods, such as partial least squares, are utilized.

The second objective of this contribution is associated with the input of impact models during the impact assessment, namely, climate change projections. These are the output from established climate models, which are developed by multiple climate science institutions worldwide [2]. They describe the atmosphere of the Earth along with its interactions with other compartments of the climate system, e.g., water bodies, and the incoming solar radiation. Climate projections are generated by considering several different alternative scenarios for future climate mitigation, e.g., business as usual, strong collaboration to mitigate, etc. As there is no single 'best performing' climate model, a group of models, called multi-model ensemble, has to be considered for each future scenario [3]. Thus, the second aim of this contribution is to obtain climate change projections that account for multiple climate mitigation scenarios in the form of multi-model ensemble trajectories. This involves: (1) screening of the available climate models, based on their ability to simulate the temperature conditions of the area under study, (2) performing bias adjustment using a suitable method that ensures biological consistency on the output of the impact model, and (3) downscaling the projections to the appropriate scale [4].

By initializing the developed impact model with the obtained climate projections possible food safety risks associated with climate change are identified. Propagating these risks, from the stage of raw milk, along the farm-to-fork continuum is useful to evaluate possible threats related to different dairy products.

2 Acknowledgements

This work was supported by the European Union's Horizon 2020 Research and Innovation Programme [Marie Skłodowska-Curie grant agreement number 813329]. SA was supported by the Research Foundation – Flanders (FWO), under grant 1224620N. CAML holds a VLAIO-Baekeland [HBC.2017.0239] grant.

References

[1] L. Katsini, S. Bhonsale, S. Akkermans, S. Roufou, S. Griffin, V. Valdramidis, O. Misiou, K. Koutsoumanis, C.A. Munoz Lopez, M. Polanska, and J. Van Impe. Trends in Food Science and Technology, 2021.

[2] C. Liu, N. Hofstra, and R. Leemans, Food Research International, 68(31), 2015.

[3] A. Doslo, Journal of Geophysical Research: Atmospheres, 121(5488), 2016.

[4] A.F. Lutz, H.W. ter Maat, H. Biemans, A.B. Shrestha, P. Wester, and W.W. Immerzeel, International Journal of Climatology, 36(3988), 2016.

Experimental modeling of a beer fermentation process

Jesús Miguel Zamudio Lara[1,2], Laurent Dewasme[1], Héctor Hernández Escoto[2], Alain Vande Wouwer[1]
[1]Systèmes, Estimation, Commande et Optimisation (SECO)
Université de Mons, 7000 Mons, Belgium
Email: (jesusmiguel.zamudiolara, laurent.dewasme, alain.vandewouwer)@umons.ac.be
[2]División de Ciencias Naturales y Exactas
Universidad de Guanajuato, Guanajuato 36050, México, Email: hhee@ugto.mx

1 Introduction

During beer brewing, the fermentation stage is crucial to guarantee beer quality. Beside, the complex behavior of the involved components makes beer fermentation an interesting candidate application for advanced monitoring and control, which require a mathematical model. To this end, Gee and Ramirez [1] proposed a complete fermentation model, which however would imply a complex instrumentation for control purposes. Andrés-Toro et al. [2] derived later on a simpler model validated with various temperature profiles and measurements from industrial breweries. This model however involves biomass, which is difficult to measure online in common fermentors. A more practical and control-oriented description was proposed by Trelea et al. [3], based on the carbon dioxide dynamics instead of biomass, also considering total sugar and ethanol concentrations.

In this work, the model of [3] is slightly adapted, with among other changes, the introduction of a logistic kinetic structure for the CO_2 production. Structural and local identifiability analyses are also achieved to avoid possible over-parametrization and provide parameter estimation accuracy assessment.

2 Mathematical model

The dynamic model is obtained by mass balancing based on reaction scheme (1) where sugars (S) are consumed by yeast (X) to produce, ethanol (E), carbon dioxide (CO_2), and among the byproducts, vicinal diketones (VDK) which are later converted into other products (P). Stoichiometry is normalized with respect to carbon dioxide, replacing the biomass as main variable to monitor the status of the fermentation process.

$$\begin{aligned} K_S\mathrm{S} &\xrightarrow{\mu_X \mathrm{X}} k_E\mathrm{E} + k_V\mathrm{VDK} + \mathrm{CO_2} \\ \mathrm{VDK} &\xrightarrow{r_{Ab}} \mathrm{P} \end{aligned} \tag{1}$$

3 Results

A set of experimental runs have been achieved using a 30L batch fermentor, producing a kölsch (Ale) beer, and varying the initial concentrations, and the operating temperature. The resulting data sets are used for model identification and validation. The parameter identification procedure is based on a weighted least-squares criterion. Minimization is achieved using a combination of the MATLAB® optimizers fminsearch and lsqnonlin, in order to reach the best local minimum and evaluate the parametric sensitivity Jacobian, which can be further used to compute the fisher Information Matrix and assess parameter local identifiability and confidence intervals.

Figure 1 shows the resulting model fitting with the experimental data.

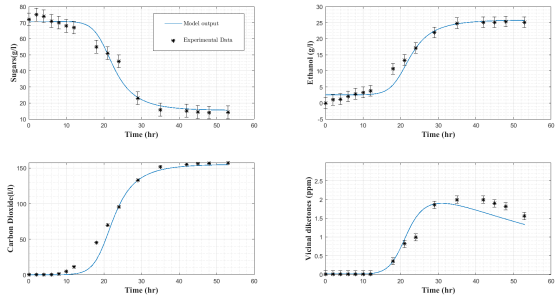

Figure 1: Experimental data and model prediction.

The model is in good agreements with the experimental data. Ongoing research considers the dependency of the latency phase to temperature.

References

[1] D.A. Gee, and W.F. Ramirez, "A flavour model for beer fermentation", J. Ins. Brew., 100, 321-329, 1994.

[2] B. de Andrés-Toro, J.M. Girón-Sierra, J.A. López-Orozco, J.M. Fernández-Conde, J.M. Peinado, and F. García-Ochoa, "A kinetic model for beer production under industrial operational conditions", Mathematics and computers in simulation, 48, 65-74, 1998.

[3] I.C. Trelea, M. Titica, and G. Corrieu, "Dynamic optimization of the aroma production in brewing fermentation", Journal of process control, 14(1), 1-16, 2003.

Towards large-scale observer design for Magnetic Resonance Thermometry in hyperthermia cancer treatments

S.A.N. Nouwens
TU Eindhoven
5600 MB, Eindhoven
s.a.n.nouwens@tue.nl

M.M. Paulides
TU Eindhoven
5600 MB, Eindhoven

B. de Jager
TU Eindhoven
5600 MB, Eindhoven

W.P.M.H. Heemels
TU Eindhoven
5600 MB, Eindhoven

1 Introduction and problem description

Hyperthermia treatments are successful adjuvants to conventional cancer therapies in which the tumor is sensitized by heating. To monitor the treatment, the clinical practice heavily relies on invasive sparse probes that are uncomfortable for the patient. Magnetic Resonance Thermometry (MRT), is proposed as a solution to this problem as it allows for three-dimensional temperature measurements using an MRI scanner. However, clinical integration is hampered by a low signal-to-noise ratio and measurement bias. To advance the clinical integration, we consider the problem of estimating the internal patient temperature using MRT.

MRT measurements exploit temperature dependent parameters in Magnetic Resonance Imaging (MRI). For example, the widely used PRFS MRT exploits the temperature dependent magnetic shielding coefficient of the hydrogen nucleus in water molecules [1]. In this paper, we represent MRT measurements by the following output model,

$$y_i(\boldsymbol{r}) = C_i(\boldsymbol{r})T(\boldsymbol{r}) + \eta_i, \qquad \eta_i \sim \mathcal{N}(a_i(\boldsymbol{r}), \Sigma_i(\boldsymbol{r},\boldsymbol{r}')), \quad (1)$$

for $i = 1,\ldots,N$. In (1), y_i, $\boldsymbol{r}$, C_i, T, a_i, Σ_i denote the MRT, position vector, tissue-dependent sensitivity, temperature, bias, and covariance, respectively. For multi-echo MRI scans N is typically $\sim 10^1$. As a result, at each sample time, we receive $\sim 10^7$ data points. To solve the problems that arise in large-scale data acquisition, we are interested in fusing (1) into a single output given by $y(\boldsymbol{r}) = \sum_{i=1}^{N} L_i(\boldsymbol{r},\boldsymbol{r}') * y_i(\boldsymbol{r})$ using simple kernel functions $L_i(\boldsymbol{r},\boldsymbol{r}')$, where $[*]$ denotes the convolution operator. A general overview of the proposed state estimation pipeline is shown in Fig. 1.

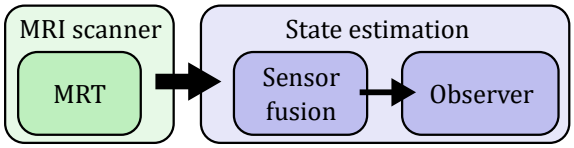

Figure 1: Estimation pipeline with distributed sensor fusion and state observer for tractable temperature estimation.

2 Methods and results

As briefly mentioned, we are interested in fusing N MRT measurements given by (1). More specifically, we will focus on two MRT principles, namely, PRFS (P) and T1-relaxation (T1) based MRT [1]. These measurements are denoted by $y_{\mathrm{P}}(\boldsymbol{r})$ and $y_{\mathrm{T1}}(\boldsymbol{r})$, respectively, with

$$C_{\mathrm{P}}(\boldsymbol{r}) = C_{\mathrm{T1}}(\boldsymbol{r}) = \begin{cases} 1, & \text{for } \boldsymbol{r} \text{ in aqueous tissue,} \\ 0, & \text{otherwise,} \end{cases} \quad (2a)$$

$$\eta_{\mathrm{P}} \sim \mathcal{N}(a(\boldsymbol{r}), \Sigma(\boldsymbol{r},\boldsymbol{r}')), \quad \eta_{\mathrm{T1}} \sim \mathcal{N}(0, \beta\Sigma(\boldsymbol{r},\boldsymbol{r}')), \quad (2b)$$

where $\beta > 1$. Loosely speaking, $y_{\mathrm{P}}(\boldsymbol{r})$ is impaired by measurement bias and $y_{\mathrm{T1}}(\boldsymbol{r})$ by a low signal-to-noise ratio. Our goal is to exploit the observation that the bias $a(\boldsymbol{r})$ is well-described by low-order polynomials [1, 2]. Hence, we propose complementary low and high-pass filter that satisfy $L_{\mathrm{HP}}(\boldsymbol{r},\boldsymbol{r}') * a(\boldsymbol{r}) \approx 0$ and $L_{\mathrm{LP}}(\boldsymbol{r},\boldsymbol{r}') := \delta(\boldsymbol{r},\boldsymbol{r}') - L_{\mathrm{HP}}(\boldsymbol{r},\boldsymbol{r}')$, where δ denotes the Dirac-delta kernel, as inspired by [2]. Both filters are implemented by projecting the MRT onto a polynomial basis and discarding the low and high order polynomials, respectively.

The complementary filter sensor fusion is validated using a heated phantom experiment. The corresponding PRFS, T1, and fused MRT are shown in Fig. 2. From Fig 2, the bias in the PRFS MRT is clearly visible by the overall lower temperature, as well as the low signal-to-noise ratio of T1 MRT. Observe that the fused MRT is both bias corrected, while the noise is comparable to PRFS MRT.

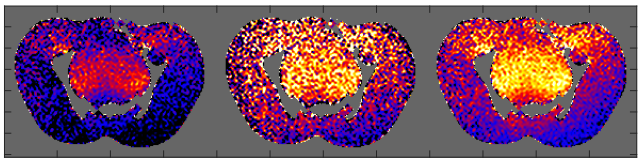

Figure 2: MRT from a phantom mimicking the pelvic region. Gray regions correspond to $C_{\mathrm{P/M}}(\boldsymbol{r}) = 0$. **Left**: biased low noise PRFS MRT. **Middle**: unbiased high noise T1 MRT. **Right**: Unbiased and low noise fused MRT.

3 Conclusions and future work

Complementary low and high-pass filters are shown to be a successful strategy in fusing PRFS and T1 MRT. Overall, fusing multiple measurements is a promising strategy to distribute the complexity of the observer design while being robust to the limitations of each MRT principle.

We believe further improvements can be realized by modeling and simultaneous estimation of the measurement bias and including additional MRT principles. Finally, online estimation of the patient-specific output sensitivity, as seen in some MRT principles, could result in more MRT measurements that are available for sensor fusion.

References

[1] Rieke, V. and Butts Pauly, K. (2008) *MR thermometry* J. Magn. Reson. Imaging, 27: 376-390

[2] Shiva K. Das, James Macfall, Robert McCauley, Oana Craciunescu, Mark W. Dewhirst and Thaddeus V. Samulski (2005) *Improved magnetic resonance thermal imaging by combining proton resonance frequency shift (PRFS) and apparent diffusion coefficient (ADC) data* Int. J. Hyperthermia, 21:7, 657-667

Using ANNs in dynamical systems to improve asynchrony detection in mechanical ventilation

Lars van de Kamp[1,2], Joey Reinders[2], Bram Hunnekens[2], Tom Oomen[1,3], and Nathan van de Wouw[1]
1 Department of Mechanical Engineering, Eindhoven University of Technology, Eindhoven
2 Demcon Advanced Mechatronics, Best
3 Delft Center for Systems and Control, Delft University of Technology, Delft, The Netherlands
Email: l.g.j.v.d.kamp@tue.nl

Mechanical ventilation

Mechanical ventilation is used in Intensive Care Units (ICUs) to save lives of patients who are not able to breath on their own. Mechanical ventilation supports patients by ensuring adequate oxygenation and carbon dioxide elimination. Mechanical ventilators attached to the patient are used to ensure airflow in and out of the lungs. This is challenging for spontaneously breathing patients because it potentially leads to ventilators disrespecting the demands of the patient, i.e., Patient-Ventilator Asynchrony (PVA). Different types of PVA can be characterized based on the delay during inspiration Δt_{insp} and expiration Δt_{exp} between patient and ventilator. In practice, currently asynchronies can only be detected by real-time inspection of pressure and flow waveforms as depicted in Figure 1. However, clinicians lack time and/or knowledge to effectively detect asynchrony based on pressure and flow waveforms [1], therefore an automatic detection approach is pursued.

Detection problem

Using first principle modelling, it is found that PVA can be detected from pressure and flow curves based on nonlinear dynamical models with unknown parameters and logical rules that are patient and ventilator specific. From a system identification point of view, the goal is identify the dynamical models for a wide variety of plants (different patients) and inputs (available pressure and flow curves).

General approach

The general approach consists of experiment design, a model set choice and a fit criterion choice. In the experiment design, prior knowledge, in the form of first principle models, is used to generate synthetic data from a simulation environment. The set of models that we consider are artificial neural networks (ANNs). Subsequently, by choosing a fit criterion the dynamical model can be identified using the generated data and a particular model choice. In this way, the data-driven identified dynamical model contains implicit knowledge about the underlying first principle models. In case of the PVA detection, a dynamical model based on a recurrent neural network is trained using a cross-entropy loss function [2]. In the next section, the detection performance of the model is shown using synthetic patient data.

Results

Through a simulated case-study the performance of the detection model is shown in Figure 2. The figure shows all the

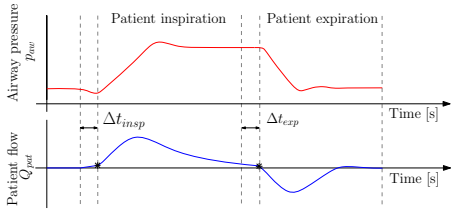

Figure 1: Typical pressure supported patient breath, where the ventilator supports the patient inspiration after Δt_{insp} seconds and cycles off Δt_{exp} seconds after the patient's expiration.

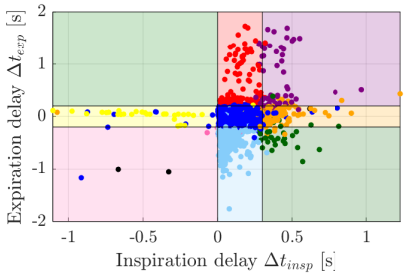

Figure 2: Results of the asynchrony detection model. Each data point represents patient breath combined with a ventilator breath that is characterized based on the inspiration delay Δt_{insp} and the expiration delay Δt_{exp}. An asynchrony is detected correctly if the data point has the same color as the background, which is the case for 93.3% of the breaths.

different patient breaths represented by a single data point and their detected asynchrony type. The asynchrony type of a breath is detected correctly if the colour matches the background colour. The total detection accuracy is 93.3%, which is a significant improved compared to clinicians, which do often not have the time or ability to detect asynchronies in practice at all. In a larger context, this shows that data-driven models, such as ANNs, have the potential to represent complex dynamical systems if the models are trained with synthetic data that is generated with a first principle model-based simulation environment.

References

[1] D. Colombo, G. Cammarota, M. Alemani, L. Carenzo, F. Barra, R. Vaschetto , A.S. Slutsky, F. Della Corte, P. Navalesi, "Efficacy of ventilator waveforms observation in detecting patient-ventilator asynchrony", in *Critical Care Medicine*, Vol. 39, Issue 11, p. 2452-2457, 2011.

[2] J. Reinders, L. van de Kamp, B. Hunnekens, T. Oomen, and N. van de Wouw, "Automatic patient-ventilator asynchrony detection and classification framework using objective asynchrony definitions, 2022.

Dynamic model development for prediction of intracellular trehalose accumulation in baker's yeast

Antoine Huet Mihaela Sbarciog Philippe Bogaerts
3BIO-BioControl, Université Libre de Bruxelles
CP 165/61, 50, Av. F.-D. Roosevelt, B-1050 Brussels, Belgium
Email: antoine.huet@ulb.be; mihaela.iuliana.sbarciog@ulb.be
philippe.bogaerts@ulb.be

1 Introduction

In the agro-food industry, it is essential to reach high cell viability rate when forming dry yeast. However, during the various processes, cells encounter several stress-inducing environments, which increase the mortality rate of the yeast cells. The intracellular accumulation of trehalose, a sugar naturally synthesized within insects, plants and yeasts, rises the resistance to stress and improves yeast cells viability in industrial bioprocesses. This paper describes the extension of a baker's yeast growth model to account for the intracellular trehalose storage and mobilization.

2 Model development

The model is an extension of the yeast growth with the coordinated uptake of glucose and nitrogen introduced in [1], which includes the overflow metabolism as described by [2] to account for the Crabtree effect. New reactions characterizing the storage and mobilization of trehalose are added. Hence, the model is based on the reaction network:

$$G \xrightarrow{r_1} k_1 X \tag{1}$$

$$G \xrightarrow{r_2} k_2 X + k_4 E + k_7 A \tag{2}$$

$$E \xrightarrow{r_3} k_3 X \tag{3}$$

$$N + A \xrightarrow{r_4} k_8 X \tag{4}$$

$$G_{int} \underset{r_{mT}}{\overset{r_{sT}}{\rightleftharpoons}} \frac{1}{2} T \tag{5}$$

where X, G, N, E, A, G_{int} and T respectively denote the biomass, extracellular glucose, ammonium, ethanol, intracellular α-ketoglutarate, intracellular glucose and intracellular trehalose. $k_1 \dots k_8$ represent the pseudo-stoichiometric coefficients. The reactions included in the network (1)-(5) express: i) biomass growth on glucose through respiration; ii) biomass growth on glucose through fermentation, with ethanol production and α-ketoglutarate accumulation; iii) biomass growth on ethanol through respiration, which is only possible if the global glucose uptake is inferior to the maximum respiratory capacity and occurs only in the presence of ethanol; iv) formation of biomass on ammonium as well as coordinated consumption of α-ketoglutarate, therefore boosting the fermentation as α-ketoglutarate is considered an inhibitor of the fermentation; v) storage of trehalose by consumption of the intracellular glucose and trehalose mobilization with release of intracellular glucose. The mass balance on each component results in a set of delay-differential equations, due to the delayed dependence of trehalose storage on the extracellular glucose uptake rate and the delayed dependence of trehalose mobilization on ethanol respiration rate.

3 Parameter estimation

All model parameters are estimated from experimental data. The estimation of the parameters corresponding to the reactions (1)-(4) is reported in [1]. The focus here is on the estimation of five parameters corresponding to the trehalose storage and mobilization rates. These parameters are identified using MATLAB 'lsqnonlin' function, which applies the trust-region-reflective optimization algorithm to minimize a least-squares criterion. This criterion consists of the sum of squared differences between model predictions and the experimental values. A multistart approach is used. For each parameter, pseudo-random values over given ranges were used for the initialization of the optimization algorithm. The estimated parameters are reported in Table 1.

Table 1: Estimated parameters

Parameter	Value	95% Confidence
μ_{sTmax} [gT/gG]	0.0500	[0.0416, 0.0584]
μ_{mTmax} [gT/gE]	0.4796	[0.3262, 0.6330]
K_{IsN} [gN/L]	0.3317	[0.1658, 0.4976]
τ_s [h]	6.080	[6.0797, 6.0803]
τ_m [h]	3.3905	[3.3558, 3.4251]

Acknowledgement This research has been funded by the Wallonia Region (SPW Recherche) and supported by Wagralim, the agri-food innovation cluster in Wallonia Region, within the framework of the WA-SuNuP project.

References

[1] A. Richelle, P. Fickers, and Ph. Bogaerts, "Macroscopic modelling of baker's yeast production in fed-batch cultures and its link with trehalose production", Comput. Chem. Eng. 61, 220–233, 2014.

[2] B. Sonnleitner, and O. Käppeli, "Growth of *Saccharomyces cerevisiae* is controlled by its limited capacity: formulation and verification of a hypothesis", Biotechnol. Bioeng. 28, 927–937, 1986.

Reinforcement learning for optimal control of linear systems with constraints via piecewise affine/quadratic approximation

Kanghui He, Ton van den Boom, Bart De Schutter
Delft Center for Systems and Control
Delft University of Technology
(K.He, A.J.J.vandenBoom, b.deschutter)@tudelft.nl

1 Introduction

Reinforcement learning (RL) provides powerful tools for the synthesis of controllers due to its strong interactions with the environment. When RL is applied to physical systems, model-based RL, also known as (approximate) dynamic programming, has received more attention since it can make effective use of the state transition information provided by the model. However, most of the RL explorations in optimal control problems do not consider constraints that commonly exist in safety-critical systems. Based on this observation, we consider an RL formulation in optimal control of linear systems, specifically, linear quadratic regulation (LQR), and intend to enforce the learning-based controller to satisfy linear constraints, involving states, inputs, or even multi-time step constraints.

2 Constrained LQR and model predictive control

As for the constrained LQR problem, the existing literature often considers a finite-horizon problem with a terminal cost to approximate the original infinite-horizon LQR problem. With the optimal value function of the unconstrained LQR problem as the terminal cost, the finite-horizon problem will be equivalent to the infinite-horizon problem if the horizon is sufficiently long. Such constrained LQR algorithm can be executed online in a receding horizon manner, known as model predictive control (MPC). MPC is a multi-step rollout algorithm and is related to policy iteration methods in RL [1]. However, the determination of the horizon N is time-consuming: usually one needs to solve an extra convex program or iteratively increase its value. Moreover, some tight constraints will make the minimum admissible value of N very large, and consequently impose more computational burden on the online MPC implementation.

3 RL for constrained systems

Compared with MPC, RL methods do not need multi-step policy optimization and can thus be more computational inexpensive. They can be divided into policy-based and value-based methods. In constrained cases, however, neither the optimal policy nor the value function is readily available, even for the most basic LQR problems. Although explicit MPC can provide analytical solutions to constrained LQR problems, it often suffers from high computational complexity and memory requirements. These observations motivate researchers to employ approximate RL. Approximation in policy space uses, e.g. neural networks, to learn unconstrained policies and leverages projection or safety filter-based methods to modify the policies. These policy-based designs, however, sometimes fail to capture the optimal solution of the constrained problem and lack stability guarantees. In comparison, approximation in value space, which uses approximation architectures to represent the value function and produces the policy through online solving a constrained optimization problem, is an indirect approach. [2] first investigates this approach, although it is limited to searching for the best linear feedback control law. Applying RL to approximate the constrained LQR controller with feasibility and stability guarantees is still an open issue.

4 Intended approaches

It has been proved that the optimal control law for the constrained LQR problem is piecewise affine (PWA), and the corresponding optimal value function is convex and piecewise quadratic. With this knowledge, we can (i) construct a PWA neural network to learn the control law, or (ii) design a piecewise quadratic neural network to approximate the value function. Fed with different initial states, the constrained LQR algorithm can be performed offline to collect enough training data. When interacting with the system online, the policy-based method needs a feasibility certificate, while the value-based method solves a convex constrained policy optimization problem. The main benefits of these methods are that they move lots of computational tasks to offline and do not require an initial stabilizing policy.

References

[1] D. P. Bertsekas, *Reinforcement learning and optimal control*. Athena Scientific, 2019.

[2] A. Chakrabarty, et al, "Approximate dynamic programming for linear systems with state and input constraints," European Control Conference, 2019, pp. 524-529.

Acknowledgement This paper is part of a project that has received funding from the European Research Council (ERC) under the European Union's Horizon 2020 research and innovation programme (Grant agreement No. 101018826 - CLariNet).

Physics-Guided Neural Networks for Feedforward Control: An Orthogonal Projection-Based Approach

Johan Kon[1,*], Dennis Bruijnen[2], Jeroen van de Wijdeven[3], Marcel Heertjes[1,3], and Tom Oomen[1,4] [1]

1 Background

Feedforward control can significantly improve the performance of dynamic systems [1]. It aims at finding the input to a dynamic system such that this system's output tracks a desired reference. Typically both high performance and flexibility to varying references are desired. An extensive feedforward control framework that addresses these requirements has been developed for linear time-invariant (LTI) systems, based on system identification and inversion [2], or direct identification of the inverse in a learning setting [3]. Extensions to nonlinear dynamics typically require the dynamics to be fully known [4].

2 Problem Formulation

Increasing performance requirements in industrial applications, such as precision mechatronics, lead to a situation in which the LTI assumption is no longer satisfied. These nonlinear dynamics do not fit the LTI feedforward parametrization and subsequently limit the performance.

The goal is to develop a feedforward control framework that integrates physical models containing prior knowledge together with universal function approximators, e.g., neural networks, to compensate the unknown nonlinear dynamics in an explainable manner.

3 Approach

The developed feedforward framework is a class of nonlinear finite impulse response (FIR) parametrizations, i.e.,

$$f(k) = \sum_{i=0}^{\ell} \theta_i q^{-i} r(k) + \mathscr{C}_\phi \left(r(k), q^{-1} r(k), \ldots, q^{-\ell} r(k) \right),$$

which is a parallel combination of a linear FIR model and a function approximator $\mathscr{C}_\phi$ acting on the reference and its ℓ lags, parametrized as a neural network with coefficients ϕ.

The parameters θ, ϕ are optimized using an orthogonal-projection based cost function, in which the neural network output in the subspace of the model is penalized through orthogonal projection. This results in uniquely identifiable model coefficients θ.

[1]This work is supported by Topconsortia voor Kennis en Innovatie (TKI), and ASML and Philips Engineering Solutions.
[1]Control Systems Technology Group, Eindhoven University of Technology, P.O. Box 513, 5600 MB Eindhoven, The Netherlands. [2]Philips Engineering Solutions, High Tech Campus 34, 5656 AE Eindhoven, The Netherlands. [3]ASML, De Run 6501, 5504 DR Veldhoven, The Netherlands. [4]Delft University of Technology, P.O. Box 5, 2600 AA Delft, The Netherlands. *Email: j.j.kon@tue.nl

4 Results

Figure 1 shows the application of this feedforward framework to a system with nonlinear friction. It illustrates that the developed parallel parametrization (middle) is able to capture the unknown nonlinear dynamics, resulting in high performance, whereas the an LTI parametrization (top) is not able to. The non-uniqueness of the developed parallel parametrization results in opposing contributions, and is removed by the orthogonal-projection based cost function (bottom), such that the neural network captures only the unknown dynamics.

Future research focuses on extending the feedforward parametrization to (nonlinear) zero dynamics for flexible modes, and its application to CT scanners and wafer stages.

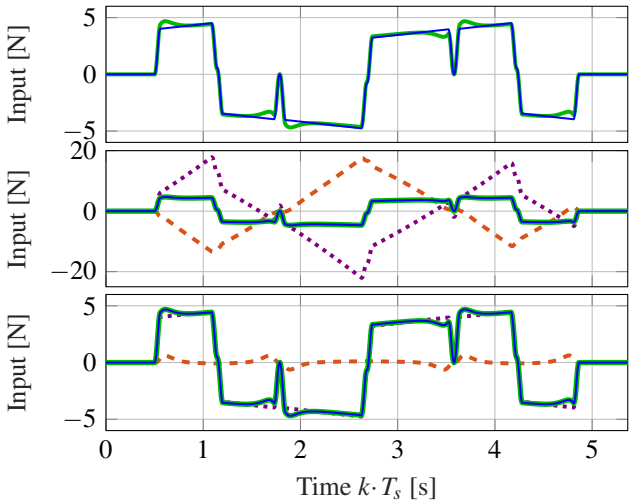

Figure 1: Optimal (—) and generated (—) feedforward with model (····) and neural network (- - -) for LTI (top) and developed parallel parametrization without (middle) and with (bottom) orthogonal-projection based cost function.

References

[1] J. A. Butterworth, L. Y. Pao, and D. Y. Abramovitch, "A comparison of control architectures for atomic force microscopes," *Asian J. Control*, vol. 11 (2), pp. 175–181, 2009.

[2] L. R. Hunt, G. Meyer, and R. Su, "Noncausal inverses for linear systems," *IEEE Trans. Automat. Contr.*, vol. 41 (4), pp. 608–611, 1996.

[3] J. Bolder, T. Oomen, and M. Steinbuch, "Exploiting rational basis functions in iterative learning control," in *52nd IEEE Conf. Decis. Control*, 2013, pp. 7321–7326.

[4] S. Devasia, D. Chen, and B. Paden, "Nonlinear inversion-based output tracking," *IEEE Trans. Automat. Contr.*, vol. 41 (7), pp. 930–942, 1996.

Simple Learning Control for Smooth Dog Clutch Engagements

Jeroen Willems[†], Stijn Goossens[*], Bruno Depraetere[†] & Sorin Bengea[†]

[†] Flanders Make, Belgium, firstname.lastname@flandersmake.be

[*] Dana Incorporated, Bruges, Belgium, firstname.lastname@dana.com

Introduction

Dog clutches are widely used in the automotive industry, where they can for example be embedded in gearboxes or power transfer units (PTUs). PTUs allow switching from 2WD to 4WD, but are also relevant for e-axles and drivelines of the future. They can use dog clutches since they are more cost-effective than e.g., friction clutches, however, (dis-)engagements cause more noise, potentially leading to NVH issues. In this paper, we present a simple learning-based control algorithm to ensure smooth engagements of a dog clutch embedded in a PTU.

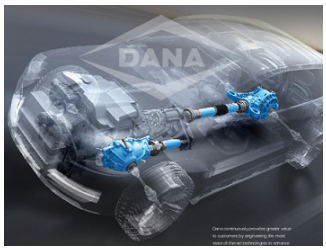

Considered System and Challenges

As represented in Fig. 1 [1], a dog clutch connects two gears running at nearly the same speed. If the teeth are well aligned and the speed difference is small, the dog clutch can be actuated, causing a left to right displacement, and the teeth to nicely mesh. With speed differences that are too high, or teeth that are misaligned, the teeth will first bounce. There will then be a delay while the gears rotate further, after which the actuation can finally mesh the teeth correctly.

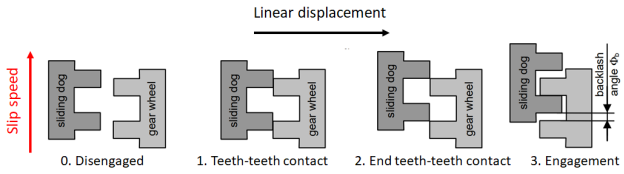

Figure 1: The states in the engagement of the dog clutch.

In this work we will focus on the controls of the linear displacement, which is actuated by a highly non-linear solenoid. A voltage can be commanded, after which current will be built up in the solenoid, causing the gear to move if enough force is built up. Several challenges are present:

- Non-linearity and stochasticity of the PTU, including the influence of external conditions such as temperature and battery voltage, but also the teeth alignment which is a function of initial (random) slip angle and slip speed.
- Limited sensing, as for estimation and control only command voltage and measured current can be used (position & speed were only measured for validation).
- Only very approximate models are available.
- Solenoid time constant is similar to the typical engagement time, limiting achievable feedback bandwidth.

Proposed Control Framework

We have developed a simple speed-based controller relying on a speed observer, which requires only approximate model knowledge (e.g., constant resistance and inductance of the solenoid's coil) and limited measurements, yielding $\hat{v}$ [2]. The control approach consists of the following steps:

1. Command a block-wave current reference signal I_{ref}, causing a voltage V to be sent (via a PI controller), building up force on the gear. When enough force is built up, the gear will start moving.
2. When motion is detected using the estimator, i.e., $\hat{v} > v_{threshold}$, we switch to a speed-based feedback controller: $V = K\hat{v}$, which commands a voltage to build up current (and thus force) in the *opposing* direction, braking the actuator before it hits the end stop.
3. Engagement.

The optimal value of the control gain K (and thus how hard we brake) is determined using a simple rule-based learning controller. The control approach has further been extended to cases where the teeth are not yet aligned.

Experimental Results

We applied the developed controls to an experimental PTU. The results for a single condition are shown in Fig. 2: when the controller is applied, significantly smoother engagements are achieved. Averaged over multiple conditions, the (weighted) vibrations recorded with an accelerometer are reduced with on average 45-80%, thereby improving NVH significantly.

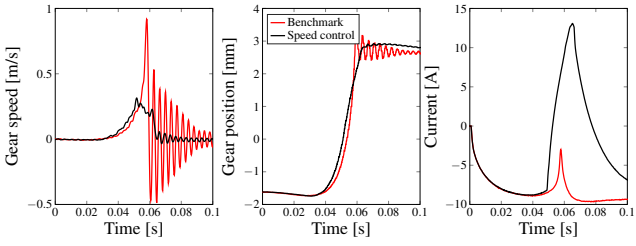

Figure 2: Proposed speed control algorithm vs. benchmark.

Acknowledgements: This work has been carried out within the framework of Flanders Make's SBO project 'MultiSysLeCo' (Multi-System Learning Control), funded by the agency Flanders Innovation & Entrepreneurship (VLAIO) and Flanders Make. Flanders Make is the Flemish strategic research centre for the manufacturing industry.

References

[1] V. Jeyaraman, "Gearshift simulation model of a dog clutch", 2019.

[2] Braun, Tristan, Johannes Reuter, and Joachim Rudolph. "A novel observer approach for self sensing of single-coil digital valves." IFAC-PapersOnLine 50.1 (2017): 782-787.

Integrated optimization-based and learning-based control for PWA systems

Caio Fabio Oliveira da Silva Azita Dabiri Bart De Schutter
Delft Center for Systems and Control, Delft University of Technology, The Netherlands
Email: {c.f.oliveiradasilva,a.dabiri,b.deschutter}@tudelft.nl

1 Introduction

Our daily lives depend on the proper functioning of many complex large systems, such as energy, water, and transportation networks. Ensuring that the societal ever increasing demands are fulfilled in a safe, efficient, and sustainable fashion is definitely not a simple task. From a mathematical standpoint, analysis and control design of such systems are very challenging due to their large scale and fast dynamics. Furthermore, these networks often have a combination of continuous and discrete dynamics, i.e., hybrid dynamics, which makes the problem even more challenging.

In order to tackle the control problem of networks with hybrid dynamics, we aim to integrate model predictive control (MPC) and model-based reinforcement learning (RL) with the intent of bringing the advantages of both approaches, i.e., the outcome of such integration should have formal guarantees and be of low on-line computational complexity. These model-based techniques are explored under the light of piecewise affine (PWA) models for their simplicity, tractability, and capacity of representing hybrid phenomena. In order to break down the problem, initial attention is devoted to small-scale PWA systems.

2 Background

In what follows, we motivate the integration of MPC and model-based RL by exposing the main benefits and drawbacks of each technique separately.

MPC is an optimization-based control approach that is well-established method in the control community for its success in process control industries and its capacity to handle complex systems and constraints. Moreover, there is an abundance of results concerning formal guarantees such as stability, safety, and performance. However, these guarantees come often at the price of intense on-line computational requirements.

RL is a general learning framework where the agent learns a control policy based on its interaction with the environment. Due to recent success in applications such as backgammon, chess, and the game of Go, this area has received a considerable amount of interest. The main advantage of RL lies in its capacity to learn complex policies and its low on-line computational requirements. On the other hand, formal guarantees are scarce, and, consequently, it is hard to ensure safety and stability.

Past work that concerns the combination of MPC and learning-based approaches can be divided in three main groups: (i) on-line adaptation of the MPC prediction model; (ii) use of MPC, as a backup controller, to provide safety for an RL controller; and (iii) tuning of the cost and constraint functions of MPC with RL methods to improve the controller's performance [1]. However, there is little work done on the integration of MPC and RL for constrained hybrid systems and networks. Hence, we aim to explore this research gap, i.e., the intersection of MPC, RL, and small-scale constrained PWA systems.

3 Methods

Next, we discuss possible manners of accomplishing the research objective. The first research direction concerns the direct integration of MPC and RL. In this setting, MPC is used to decide the continuous actions and RL is employed to determine the discrete actions. Alternatively, we present other approaches that are either sequential or indirect. The second research direction aims to reduce to the on-line computational burden by dividing of the prediction horizon in two parts: a shorter control horizon, controlled by MPC, and a remaining horizon, driven by RL. As a result, the number of optimization variables and on-line computational complexity are reduced. The third alternative is to enhance the training efficiency of RL by employing a fast MPC method to provide initial maps from states to suboptimal inputs. Initially, the system is controlled by the MPC controller, but one could gradually shift from the MPC to the RL controller as the performance of the latter improves.

Acknowledgement: This research has received funding from the European Research Council (ERC) under the European Union's Horizon 2020 research and innovation programme (Grant agreement No. 101018826 - CLariNet)

References

[1] L. Hewing, K. P. Wabersich, M. Menner, and M. N. Zeilinger, "Learning-Based Model Predictive Control: Toward Safe Learning in Control," In: Annual Review of Control, Robotics, and Autonomous Systems 3.1, pp. 269–296, 2020.

Flexible learning with prior knowledge: iterative learning control with sampled-data characterized basis functions

Masahiro Mae[1,2,*], Max van Haren[2], Wataru Ohnishi[1], Tom Oomen[2,3], Hiroshi Fujimoto[1]
[1]Graduate School of Engineering, The University of Tokyo, Japan. *Email: mmae@ieee.org
[2]Department of Mechanical Engineering, Eindhoven University of Technology, The Netherlands.
[3]Delft Center for Systems and Control, Delft University of Technology, The Netherlands.

1 Background

Performance and flexibility are typical trade-offs in mechatronic systems. Linearly parameterized feedforward control has both performance and flexibility [1]. The choice of parameterization should be determined by prior knowledge such as sampled-data characteristics.

2 Problem formulation

The controlled system is shown in Figure 1. The goal is to minimize the continuous-time tracking error $e(t)$ using the feedforward signal $f[k] = \Psi[k]\theta$ with parameter θ. For instance, Ψ is parameterized as $\Psi = [r, \xi r, \xi^2 r]$ for a mass-damper-spring system with a differentiator ξ. Typically, n^{th} order backward difference is used as n^{th} order differentiator ξ_{BD}^n to design the feedforward parameterization [2] as

$$\xi_{BD}^n = \left(\frac{1-z^{-1}}{T_s}\right)^n. \tag{1}$$

This does not explicitly address the zero-order-hold characteristic of the step-like input shape restriction.

3 Approach

The aim is to develop flexible feedforward control with intersample consideration. The approach considers the feedforward parameterization with basis functions for flexibility that are designed with sampled-data characteristics such as zero-order-hold and multirate state tracking [3].

4 Results

The stable inversion of the n^{th} order integrator discretized by zero-order-hold is used as n^{th} order differentiator ξ_{SI}^n to design the feedforward parameterization as

$$\xi_{SI}^n = \left\{\mathscr{Z}\left(\frac{1-e^{-sT_s}}{s}\cdot\frac{1}{s^n}\right)z\right\}^{-1}. \tag{2}$$

The experimental result in the single inertia system $G(s) = \frac{1}{Js^2}$ with the acceleration feedforward parameterization is shown in Figure 2. The sampling time is $T_s = 20\,\text{ms}$. It shows that the feedforward parameterization using stable inversion $\Psi_{SI}[k] = \xi_{SI}^2 r[k+1]$ outperforms that using backward difference $\Psi_{BD}[k] = \xi_{BD}^2 r[k+1]$.

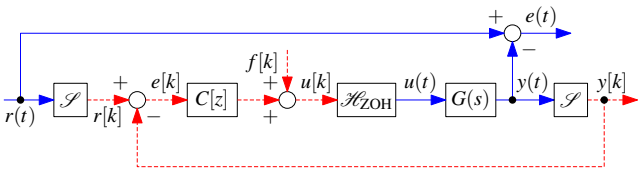

Figure 1: Controlled system discretized by zero-order-hold $\mathscr{H}_{\text{ZOH}}$ and sampler $\mathscr{S}$. The discrete-time signal (- - -) can be controlled and the continuous-time signal (——) is the performance variable.

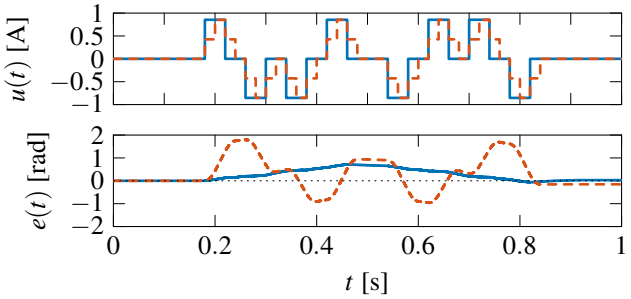

Figure 2: Experimental result of a reference tracking problem, with a parametric feedforward using stable inversion (——), that outperforms backward difference (- - -), reducing RMS and MAX errors by a factor of two.

5 Ongoing research

The ongoing research focuses on extending the feedforward parameterization that considers higher-order characteristics.

Acknowledgements

This research is granted from Tateishi Science and Technology Foundation.

References

[1] M. Boerlage, R. Tousain, and M. Steinbuch, "Jerk derivative feedforward control for motion systems," in *Proceedings of the 2004 American Control Conference*, vol. 5. IEEE, 2004, pp. 4843–4848 vol.5.

[2] P. Lambrechts, M. Boerlage, and M. Steinbuch, "Trajectory planning and feedforward design for electromechanical motion systems," *Control Engineering Practice*, vol. 13, no. 2, pp. 145–157, feb 2005.

[3] W. Ohnishi, N. Strijbosch, and T. Oomen, "Multirate State Tracking for Improving Intersample Behavior in Iterative Learning Control," in *2021 IEEE International Conference on Mechatronics (ICM)*, no. 2. IEEE, mar 2021, pp. 01–06.

A Privacy Preserving Federated Learning Framework

Haleh Hayati[1], Carlos Murguia[2]
Department of Mechanical Engineering, Eindhoven University of Technology
Emails: [1]h.hayati@tue.nl, [2]c.g.murguia@tue.nl

1 Introduction and problem statement

In recent years, Machine Learning (ML) has been successfully used in various applications. In traditional ML, training data is centrally held by one server executing the learning algorithm. Federated learning (FL) has been recently presented as a decentralized ML algorithm that can scale to thousands of participants [1]. Its core concept is to train models on separate datasets distributed across clients, which preserves local data privacy to a certain extent. The idea behind FL is to train local models on clients' devices and then exchange models instead of raw data among clients and servers to achieve a global model. Servers then aggregate clients' models and send the aggregation back to clients to iterate the learning algorithm. The process is repeated until convergence is reached. Although FL provides some privacy level for clients' data, information about clients can still be inferred from the model updates.
In recent years, various privacy-preserving schemes have been used to address privacy leakage in FL. However, they often provide privacy at the expense of model performance or system efficiency, and balancing these tradeoffs, is a crucial issue in implementing private FL.

2 Methodology

To address aforementioned issues, in this work, we propose a Privacy-Preserving Federated Learning (PPFL) framework that it is computationally efficient, provides the same level of accuracy and convergence rate as the standard FL, and reveals no information about the clients' data.
The idea is to design a multiplicative random encoding matrix that extends the dimension of the parameter space of the global model (an immersion) and develop a modified learning algorithm that uses the distorted global model and converges to an affine transformation of the original training model. We also add randomness by exploiting the kernel of the encoding matrix, and recover the undistorted optimal model by using the left invertibility of the transformation.

Let w^t be the global model at the t-th iteration of FL and w_i^t the local updating model of i-th client. Consider a full rank matrix $M \in \mathbb{R}^{n\times m}(m > n)$, with right inverse $G \in \mathbb{R}^{m\times n}$ ($MG = I$), and a matrix $N \in \mathbb{R}^{m\times(m-n)}$ expanding the kernel of M ($MN = 0$). The distorting multiplicative random matrix A^t for t-th iteration is defined as $A^t = G + NR^t$, for some random matrix R^t. Then, for every A^t, we can conclude that $MA^t = I$. Server uses matrix A^t to encode the global model w^t, as $\tilde{w}^t = A^t w^t$, and then, in the next iteration, multiply it by M to decode it.

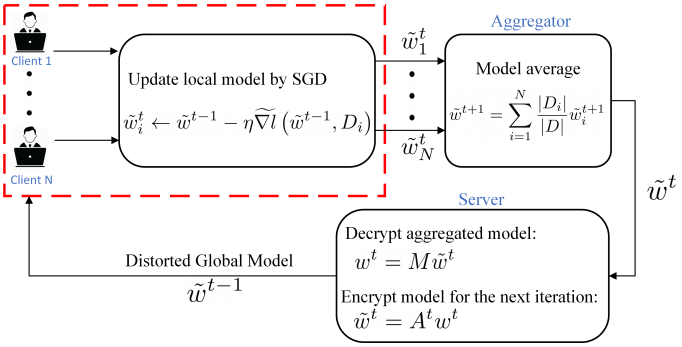

Figure 1: Flowchart of proposed PPFL.

Generally, in FL clients employ distributed Stochastic Gradient Descent (SGD) for training local ML models. We also distort the loss function used in SGD by output regulation such that it uses the distorted global model and converge to an affine transformation of the original trained model. Furthermore, we consider a third party as an aggregator that interfaces between clients and the server. The aggregator takes the average of the updated models from clients and sends it to the server so that server cannot access any local models. Besides, since the aggregator does not have access to the original updated models, it is not required to be trusted.
The flowchart of the algorithm is shown in Figure 1. The algorithm is summarized in four steps:
1) In the hand-shaking phase, server sends the modified SGD algorithm and the random initial model to clients. Also, in each iteration, server encodes the global model as $\tilde{w}^t = A^t w^t$ and sends it to clients to update.
2) Clients employ the modified SGD to update the distorted model $\tilde{w}^t$. They send the updated models to the aggregator.
3) Aggregator takes average of updated models from clients and send the aggregated model to the server.
4) Finally, server decodes the model by multiplying it by M.
The process is repeated until convergence is reached. In the last iteration, the server has access to the exact model with a non-privacy-preserving federated learning model.
Therefore, this mechanism provides privacy for local and global models in all iterations of FL without degrading the final model and convergence rate of FL.

References

[1] J. e. a. Konečnỳ, "Federated learning: Strategies for improving communication efficiency," 2016.

Learning MPC for Interaction-Aware Autonomous Driving: A Game-Theoretic Approach

Brecht Evens, Mathijs Schuurmans, Panagiotis Patrinos
KU Leuven, BE-3001 Heverlee, Belgium
Department of Electrical Engineering (ESAT-STADIUS)
Email: { brecht.evens,mathijs.schuurmans,panos.patrinos} @kuleuven.be

1 Background

Despite many efforts in recent years, safe autonomous navigation in the presence of humans remains a highly challenging task. Traditionally, this problem is tackled by separating it into a forecasting problem and a planning problem. However, this strategy may lead to overly conservative and defensive behavior, commonly referred to as the *frozen robot problem* [1]. In dense traffic situations, for instance, such a vehicle will struggle to merge into lanes efficiently or be unable to cross a condensed junction.

2 Methodology

Early work on social navigation has shown that the frozen robot problem can be solved by modelling vehicles as a team of cooperative players engaging in joint collision avoidance. Following this line of research, we have introduced a novel framework in [2] for controlling autonomous vehicles in general traffic situations which accounts for the mutual interactions between the controlled vehicle and other road users. More specifically, the navigation problem is modelled as a game consisting of M players, where each player $\nu \in \mathcal{A} := \{1, 2, \dots, M\}$ is assumed to optimally decide upon their input variables $u^\nu \in \mathbb{R}^{n_\nu}$ with respect to a receding horizon optimal control cost $J^\nu(u^\nu, u^{-\nu})$ subject to coupled constraints $u^\nu \in \mathcal{U}^\nu(u^{-\nu})$, i.e., each road user is assumed to solve

$$\underset{u^\nu \in \mathcal{U}^\nu(u^{-\nu})}{\textbf{minimize}}\, J^\nu(u^\nu, u^{-\nu}), \qquad \nu \in \mathcal{A}, \tag{1}$$

where $u^{-\nu} := (u^i)_{i \in \mathcal{A}\setminus\{\nu\}}$ represents the input variables of all other players. In autonomous driving, these coupled constraints naturally consist of shared (collision avoidance) constraints and additional player-specific constraints. By imposing some additional structure on the cost functions of the different interacting players, this problem can be specialized to a *generalized potential game*, for which a continuous potential function $\mathcal{P}$ exists representing the preferences of all players. As a result, an optimal solution of the game, i.e., a *generalized Nash equilibrium*, can be obtained by solving a single optimization problem

$$\underset{u \in \mathcal{U}}{\textbf{minimize}}\, \mathcal{P}(u), \tag{2}$$

where $u := (u^i)_{i \in \mathcal{A}}$ represents the input variables of all players. By solving optimization problem (2) repeatedly within a model predictive control scheme, this game-theoretical formulation allows the controlled vehicle to efficiently cooperate with other road users, while safety guarantees follow from the imposed collision avoidance constraints.

The controlled vehicle is required to have access to the (implicit) objective function and constraints of the other road users. However, this information is in general unknown. Moreover, different drivers behave differently on the road, and the behavior of a single driver might even change over time. This issue is adressed in a data-driven manner: the human objective function and constraints are parametrized, and the parameters are updated in an online fashion by adapting standard inverse optimal control methodologies such as [3] to the considered game-theoretical framework. More specifically, the parameters are updated by minimizing the residual of the optimality conditions of the game given human observations. This approach enables the controlled vehicle to learn not only cost function but also constraint parameters from expert demonstrations, as opposed to traditional inverse reinforcement learning strategies [4].

3 Numerical experiments

To verify the practical usability of the developed methodologies, extensive numerical simulations in various traffic scenarios have been performed. The source code of the driving simulator and videos of a merging experiment are available at https://brechtevens.github.io/GPG-drive/.

References

[1] P. Trautman and A. Krause, "Unfreezing the robot: Navigation in dense, interacting crowds," in *2010 IEEE/RSJ International Conference on Intelligent Robots and Systems*, pp. 797–803, 2010.

[2] B. Evens, M. Schuurmans, and P. Patrinos, "Learning MPC for Interaction-Aware Autonomous Driving: A Game-Theoretic Approach," *arXiv:2111.08331 [math]*, 2021.

[3] K. Hatz, J. P. Schlöder, and H. G. Bock, "Estimating parameters in optimal control problems," *SIAM Journal on Scientific Computing*, vol. 34, no. 3, pp. 1707–1728, 2012.

[4] D. Sadigh, N. Landolfi, S. S. Sastry, S. A. Seshia, and A. D. Dragan, "Leveraging effects on human actions for planning and active information gathering over human internal state," *Autonomous Robots*, vol. 42, no. 7, pp. 1405–1426, 2018.

Stochastic stability of perturbed best-response dynamics for networked coordination games

Bo Jin
Faculty of Science and Engineering
University of Groningen
Nijenborgh 4
9747 AG Groningen
The Netherlands
Email: b.jin@rug.nl

Ming Cao
Faculty of Science and Engineering
University of Groningen
Nijenborgh 4
9747 AG Groningen
The Netherlands
Email: m.cao@rug.nl

1 Abstract

We study the stochastic stability of perturbed best-response dynamics for networked coordination games on tree graphs. Consider a network of agents adopting a strategy from their given strategy sets following perturbed best response dynamics. When the network topology is a tree, we show that each Nash equilibrium of a networked coordination game is a stochastically stable state of the corresponding perturbed best response dynamics.

2 Problem Formulation

Consider a network of N agents and denote the network by an undirected graph $\mathscr{G} = (\mathscr{I}, \mathscr{E})$ with $\mathscr{I} := \{1, 2, \cdots, N\}$ and $\mathscr{E}$ being the node set and edge set respectively. Each agent i, when activated, plays a 2-player coordination game with each of its neighbors by choosing a strategy from the binary strategy set $\mathscr{X} = \{0, 1\}$ and receives respectively a payoff according to the payoff matrix

$$E^i := \begin{array}{c} \\ 0 \\ 1 \end{array} \begin{array}{c} \begin{array}{cc} 0 & 1 \end{array} \\ \begin{pmatrix} 1 & 0 \\ 0 & 1 \end{pmatrix} \end{array}$$

For this activation event, its payoff is the sum of those earned against all its neighbors and we denote this payoff relationship by $r^i : \mathscr{X}^N \to \mathbb{R}$.

2.1 Best response decision rule

At each time t, one agent is chosen from $\mathscr{I}$ at random to update its strategy according to the best response decision rule. More specifically, denote the strategy of agent i and the joint strategy of all the agents at time t by $x^i(t)$ and $x(t)$ respectively; the asynchronous best response dynamics can be represented by

$$\begin{cases} x^i(t+1) = x^i(t) & \text{if} \quad i \notin \Delta(t) \\ x^i(t+1) \in \underset{x^i \in \mathscr{A}^i}{\arg\max}\, u^i(x^i, x^{-i}(t)) & \text{if} \quad i \in \Delta(t) \end{cases} \tag{1}$$

where $\{\Delta(t)\}_{t \geq 0}$ is a sequence of random subsets of $\mathscr{I}$, and $x^{-i}(t) := (x^1(t), \cdots, x^{i-1}(t), x^{i+1}(t), \cdots, x^N(t))$ represents the joint strategy of all the agents other than i.

Denote the neighborhood of agent i by $\mathscr{N}^i$ and define $n^i = |\mathscr{N}^i|$. The number of i's neighbors choosing strategy 0 is denoted by n_0^i. According to its payoff matrix E^i, i's payoff is calculated by

$$\begin{cases} u^i(0, x^{-i}) = n_0^i \\ u^i(1, x^{-i}) = n^i - n_0^i \end{cases} \tag{2}$$

We assume that in the special scenario when agent i receives the same payoff no matter which strategy is chosen, this agent sticks to its previous strategy. Then, the argmax computation in (1) can be rewritten as

$$x^i(t+1) = \begin{cases} 0 & \text{if} \quad \frac{n_0^i(t)}{n^i(t)} > \frac{1}{2} \\ 1 & \text{if} \quad \frac{n_0^i(t)}{n^i(t)} < \frac{1}{2} \\ x^i(t) & \text{if} \quad \frac{n_0^i(t)}{n^i(t)} = \frac{1}{2} \end{cases} \tag{3}$$

2.2 Perturbed best-response dynamics

Suppose that at each time, when an agent is chosen to update its strategy, there exists a small probability $\varepsilon > 0$ with which the agent chooses a strategy randomly. This is sometimes referred to as *mutation* or *perturbation*. Then, the perturbed best-response dynamics define a Markov chain. Assume there is a unique stationary distribution for the Markov chain. When the probability ε becomes arbitrarily small, the joint actions, which can still be observed with positive probability in the long run, are called *stochastically stable*.

3 Result

Theorem 1 *For the networked coordination game on a tree, every Nash equilibrium is stochastically stable.*

A passivity approach for displacement-based and rigid formation

Ningbo Li[1] , J.M.A. Scherpen[1] , A.J. van der Schaft[1], and Zhiyong Sun[2]
1. Jan C. Willems Center for Systems and Control, University of Groningen, the Netherlands
2. Department of Electrical Engineering, Eindhoven University of Technology, the Netherlands.
ningbo.li@rug.nl, j.m.a.scherpen@rug.nl and a.j.van.der.schaft@rug.nl, and z.sun@tue.nl

1 Motivation

In [1], the notion of passivity is used for group coordination. The control objective is to steer the differences of output variables of neighboring agents to a prescribed compact set. By extending this idea to formation control, this work proposes a passivity approach in port-Hamiltonian (pH) form for formation stabilization and velocity tracking. The control law consists of two parts, where the internal feedback is to track the velocity and the external feedback is to achieve formation stabilization. A necessary condition to achieve convergence to the target set is the linear independence of the columns of the incidence matrix of an underlying interaction graph. However, for formation control, this condition is often not satisfied, for example in the displacement-based formation of cyclic graphs. Also in the case of rigid formations, the underlying graph usually contains cycles. The objective of this work is to extend the passivity approach to displacement-based formation and rigid formation in case of cyclic graphs.

2 Main results

We consider a group of N agents coupled by an underlying graph with M edges, while each agent is modeled in pH form as a single point mass in $\mathbb{R}^d$.

$$\begin{pmatrix} \dot{q} \\ \dot{p} \end{pmatrix} = \begin{pmatrix} 0 & I_{Nd} \\ -I_{Nd} & -D^r \end{pmatrix} \begin{pmatrix} \frac{\partial H}{\partial q}(p) \\ \frac{\partial H}{\partial p}(p) \end{pmatrix} + \begin{pmatrix} 0 \\ I_{Nd} \end{pmatrix} u \qquad (1)$$
$$y = \frac{\partial H}{\partial p}(p)$$

where $q \in \mathbb{R}^{Nd}$, $p \in \mathbb{R}^{Nd}$, $u \in \mathbb{R}^{Nd}$, and $y \in \mathbb{R}^{Nd}$ is the position, momentum, input, and output, respectively. $D^r \in \mathbb{R}^{Nd \times Nd}$ is a positive semi-definite dissipation matrix. The Hamiltonian consists of the kinetic energy associated with the movement of the mass and takes the following form $H = \frac{1}{2}\sum_{i=1}^{N} p_i^T M_i^{-1} p_i$, where $M_i = m_i I_d$.

The coordination objective for the group behavior consists of two parts. One is that the velocity of each agent converges to a prescribed common value, i.e.,

$$\lim_{t\to\infty} |\dot{q}_i(t) - v^*(t)| = 0.$$

The other is that the position difference variables associated with the edges

$$z = (B^T \otimes I_d)q \qquad (2)$$

converge to a prescribed compact set $\Xi \subset \mathbb{R}^{M\times d}$, where $\Xi = \{z_1^*, z_2^*, ..., z_M^*\}$ and $z_j^*, j = 1, 2, ..., M$ is the prescribed difference variable associated with edges j. B is the incidence matrix.

For displacement-based formation, the velocity tracking is achieved by internal feedback, which is given by

$$u_i^v = -D_i^r v^* - D_i^t M_i^{-1} \bar{p}_i. \qquad (3)$$

Furthermore, the formation stabilization is achieved by external feedback, following directly as

$$u^f = -(B \otimes I_d)\bar{z} - (B \otimes I_d)D^f(B^T \otimes I_d)M^{-1}p. \quad (4)$$

The control law for velocity tracking of the rigid formation is the same as (3). Here, we only give the control law for formation stabilization. For distance-based formation, it takes the form as

$$\begin{aligned} u^d &= -(B \otimes I_d)\frac{\partial H^d}{\partial z} \\ &= -(B \otimes I_d)(blkdiag(z_1^T, z_2^T, ..., z_M^T))^T e^d. \end{aligned} \qquad (5)$$

For bearing-based formation, it is given by

$$\begin{aligned} u^b &= -(B \otimes I_d)\frac{\partial H^b}{\partial z} \\ &= -(B \otimes I_d)blkdiag(\frac{P_{s_1}}{||z_1||}, ..., \frac{P_{s_M}}{||z_M||})(s - s^*) \end{aligned} \qquad (6)$$

3 Conclusion

In this work, a passivity approach in pH form for formation stabilization and velocity tracking is proposed. For displacement-based formation, by choosing the proper Hamiltonian function for formation stabilization, the proposed approach can be applicable for not only the acyclic graphs but also the cyclic graphs. For distance-based formation, by establishing the relationship between infinitesimal rigidity and time derivative of the Hamiltonian, the local convergence of the proposed formation system is guaranteed. For bearing-based formation, the almost global convergence can be obtained since the infinitesimal bearing rigidity is sufficient to global bearing rigidity.

References

[1] M. Arcak, "Passivity as a design tool for group coordination," *IEEE Transactions on Automatic Control*, vol. 52, no. 8, pp. 1380–1390, 2007.

Using dynamic norms to facilitate innovation diffusion in networks

Lorenzo Zino
University of Groningen
lorenzo.zino

Mengbin Ye
Curtin University, Perth, Australia
mengbin.ye@curtin.edu.au

Ming Cao
University of Groningen
m.cao@rug.nl

1 Introduction

Innovation diffusion is a fundamental phenomenon in human societies. Network coordination games have been extensively used to capture salient features of such diffusion processes and study their time evolution [1]. Through these studies, two notable factors have been identified as key to allowing successful innovation diffusion: *relative advantage* of the innovation with respect to the status quo and presence of a sufficiently large number of *innovators*. However, many important innovations lack these two key ingredients [2].

Dynamic norms have recently emerged as a powerful method to encourage individuals to adopt an innovation by highlighting a growing trend in its uptake, and have been extensively studied in the social-psychology literature [3] and observed in experimental evidence [4]. Here, we propose a novel mathematical model for innovation diffusion that incorporates dynamic norms, and use it to gain analytical insights into how such an individual-level mechanism can be key to collectively unlock social diffusion. Some preliminary results are in [5], while further developments are in [6].

2 Innovation Diffusion Model

The game is played by a set $\mathcal{V} = \{1,\dots,n\}$ of $n \geq 2$ players. At each discrete time-step, each player $i \in \mathcal{V}$ revises their strategy $x_i(t) \in \{0,1\}$, choosing between the *status quo* (0), and the *innovation* (1). We denote by $z(t) = \frac{1}{n}\sum x_i(t)$ the total fraction of *adopters* of the innovation at time t. The revision follows a stochastic mechanism. With probability γ, individual i follows *dynamic norms*, selecting the strategy whose fraction of adopters has increased in the previous time-step; otherwise, i will play a *coordination game* with k other individuals selected uniformly at random in the population, denoted as $\mathcal{N}_i(t)$, receiving a unit payoff for coordinating to the status quo and a payoff $1+\alpha$ for coordinating to the innovation. Here, α captures the *advantage* (if positive) or disadvantage (if negative) of the innovation with respect to the status quo. Then, the individual follows the best-response dynamics, that is,

$$x_i(t+1) = \begin{cases} 1 & \text{if } \sum_{j\in\mathcal{N}_i(t)} (1+\alpha)x_j(t) > \sum_{j\in\mathcal{N}_i(t)} (1-x_j(t)), \\ 0 & \text{otherwise}. \end{cases} \tag{1}$$

The parameter γ captures the individual's *sensitivity* to dynamic norms.

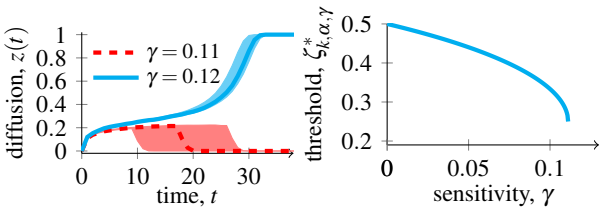

Figure 1: (a) Simulations with γ below and above the threshold; (b) $\zeta^*_{k,\alpha,\gamma}$ as a function of γ. Parameters: $k = 3$, $\alpha = 0$.

3 Results

We consider a scenario in which the system is initialized in a status quo consensus ($x_i(0) = 0, \forall i \in \mathcal{V}$), and a fixed fraction of *innovators* $\zeta \in (0,1]$ starts adopting the innovation at $t = 1$. Given the random times $S_\varepsilon := \inf\{t > 0 : z(t) \geq 1-\varepsilon\}$ and $F_\varepsilon := \inf\{t > 0 : z(t) \leq \varepsilon\}$, we say that *social diffusion is guaranteed* if $P[S_\varepsilon < F_\varepsilon] \to 1$ as $n \to \infty$, for any $\varepsilon > 0$; while, if the opposite occurs, we say that *status quo is maintained*.

Through a rigorous analysis of the dynamical system, we demonstrate that sensitivity to dynamic norms is indeed key in favoring social diffusion. Specifically, we prove that if γ trespasses a threshold that can be analytically characterized as a function of α and k (see [5]), than social diffusion is guaranteed for any fraction of initial adopters (Fig. 1a). Below this threshold, social diffusion is guaranteed only if $\zeta > \zeta^*_{k,\alpha,\gamma}$, where the threshold with respect to the fraction of innovators $\zeta^*_{k,\alpha,\gamma}$ is monotonically decreasing in γ (Fig. 1b).

References

[1] A. Montanari and A. Saberi. The spread of innovations in social networks. *Proc. Natl. Acad. Sci. USA*, 107(47):20196–20201, 2010.

[2] E. M. Rogers. *Diffusion of Innovations*. 2003.

[3] G. Sparkman and G. M. Walton. Dynamic Norms Promote Sustainable Behavior, Even If It Is Counternormative. *Psychol Sci.*, 28(11):1663–1674, 2017.

[4] M. Ye, L. Zino, Ž. Mlakar *et al.*. Collective patterns of social diffusion are shaped by individual inertia and trend-seeking. *Nat. Comm.*, 12:5698, 2021.

[5] L. Zino, M. Ye, and M. Cao. On modeling social diffusion under the impact of dynamic norms. In *Proc. 60th IEEE Conf. Decis. Control.*, 2021.

[6] —. Facilitating innovation diffusion in social networks using dynamic norms. *Under Review*, 2022.

Aggregating distributed energy resources for grid flexibility services: A distributed game theoretic approach

Xiupeng Chen[1], Jacquelien M. A. Scherpen[1,2], Nima Monshizadeh[1]
[1]Engineering and Technology Institute Groningen, University of Groningen, Groningen, the Netherlands
[2]Jan C. Willems Center for Systems and Control, University of Groningen, Groningen, the Netherlands
Email:{xiupeng.chen,j.m.a.scherpen,n.monshizadeh}@rug.nl

1 Motivation

Designing energy management mechanisms for distributed energy resources in the smart grid has been considered as a potential solution for a renewable-power future. The smart grid is typically composed of a variety of new participants, such as micro-grid, aggregator, prosumer, and so on. This heterogeneous nature of the smart grid motivates the adoption of game theory as an analytical tool to model the behaviors of these participant [1]. Another important problem is to design algorithms that enable these participants to reach a certain desired game result. In the control community, designing algorithms for equilibrium-seeking problems has gained high research interest. Even though these algorithms perform well in efficiency and convergence, some key technical issues should be emphasized when implementing them into the smart grid, such as privacy and robustness issues.

2 Problem Formulation

We consider a scenario where there is a supply deficit or surplus in power system and distributed energy resources can be utilized to meet this mismatch between power supply and demand. A fully decentralized energy management framework is designed to aggregate these resources for grid flexibility services, as shown in Fig.1.

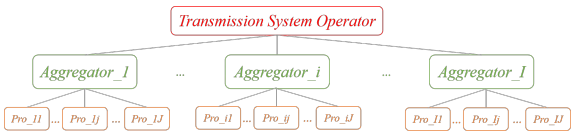

Figure 1: The decentralized energy management framework

The set of aggregators is denoted by $\mathscr{I} = \{1,2,...,I\}$, each aggregator aims to maximize revenue of providing flexibility in wholesale electricity market,

$$\max_{0\le x_i\le \bar{x}_i} J_i(x_i,p_i,x_{-i}) = -x_i p_i + l(s)x_i \qquad (1)$$

where x_i is the flexibility response of aggregator i, $l(s)$ is the price paid by wholesale market to aggregators with $s = \frac{1}{N}\sum_{i\in\mathscr{I}} x_i$, p_i is the price paid by aggregator i to prosumers, $\bar{x}_i$ is the maximum available flexibility.

Each prosumer's goal is to maximize its revenue by altering its demand or supply given the price p_i proposed by aggregator i.

$$\max_{x_{ij}\ge 0} U_{ij}(x_{ij}) = x_{ij}p_i - f_{ij}(x_{ij}) \qquad (2)$$

where x_{ij} is the flexibility response of prosumer j, $f_{ij}(x_{ij})$ is cost function.

3 Main result

We propose a fully distributed algorithm in discrete-time that steers the players to the Nash Equilibrium(NE) with fixed step sizes. Each player exchanges and maintains only an estimate of the aggregate, but not their true action information.

Algorithm 1 Distributed algorithm

Initialization: All aggregators $i \in \mathscr{I}$ initializes p_i^0, $\sigma_i^0 \in \mathbb{R}^n$, $\psi_i^0 \in \mathbb{R}^n$, broadcast p_i^0 to prosumers and get the initial response flexibility x_i^0

Iterate until convergence:

$p_i(k+1) = p_i(k) - \frac{\tau_i k_i f_i(x_i(k),\sigma_i(k))}{\alpha_i}$
$x_{ij}(k+1) = arg\max U_{ij}(x_{ij}) = x_{ij}p_i(k+1) - f_{ij}(x_{ij})$
$x_i(k+1) = \sum x_{ij}(k+1)$
$\psi_i(k+1) = \psi_i(k) + v_i(\sum(\sigma_i(k) - \sigma_j(k)))$
$\sigma_i(k+1) = \sigma_i(k) + \beta_i(-\sigma_i(k) + x_i(k) - 2\psi_i(k+1) + \psi_i(k))$

where $f_i(x_i,\sigma_i) = \nabla_{x_i} J_i(x_i,y)|_{y=\sigma_i} + \frac{1}{N}\nabla_y J_i(x_i,y)|_{y=\sigma_i}$

Theorem 1 *If the mapping $x_i \to f_i(x_i,\sigma_i)$ is μ_i-strongly monotone and ℓ_i-Lipschitz continuous, and the mapping $u \to f_i(x_i,\sigma_i)$ is $\bar{\ell}_i$-Lipschitz continuous, $\mu_i > \bar{\ell}_i$, the graph of information sharing network between aggregators is connected, then there exit parameters k_i, τ_i, v_i, β_i such that the algorithm1 converges to the unique NE of the game.*

References

[1] W. Saad, et al, "Game-theoretic methods for the smart grid: An overview of microgrid systems, demand-side management, and smart grid communications," IEEE Signal Processing Magazine 29.5 (2012): 86-105.

Inverse Learning for Linear-quadratic Zero-sum Differential Games

Emin Martirosyan
Engineering and Technology Institute Groningen
University of Groningen
P.O. Box 72, 9700 AB Groningen
The Netherlands
Email: e.n.martirosyan@rug.nl

Ming Cao
Engineering and Technology Institute Groningen
University of Groningen
P.O. Box 72, 9700 AB Groningen
The Netherlands
Email: m.cao@rug.nl

1 Introduction

Non-cooperative differential games were first introduced in [1] within the framework of zero-sum games. The application of differential games is far-reaching. Although most of the literature has focused on determining the outcome of a game given its objective, recently, an increasing interest appeared in the inverse problem, where, given the behavior, the objective of a player needs to be found. In our work, we introduce an algorithm that generates an objective function for an equivalent game in the sense that it shares one of the NE feedback laws with the original game. The algorithm combines both inverse optimal control and reinforcement learning methods in the form of gradient descent updates.

2 Problem Formulation

Consider a pair of trajectories $(x_s, u_{1,s})$ where x_s is a state trajectory and $u_{1,s}$ is a control input trajectory of player 1, i.e., $u_{1,s} = F_{1,s}x_s$; $x_s \in \mathbb{R}^n$ and $u_{i,s} \in \mathbb{R}^{m_i}$ for $i = 1,2$. $F_{1,s}$ is known to be a feedback law that constitutes the NE pair for the game with the *known* dynamics

$$\dot{x}_s(t) = Ax_e + B_1u_{1,s}(t) + B_2u_{2,s}(t) \tag{1}$$

with $A \in \mathbb{R}^{n\times n}$, $B_i \in \mathbb{R}^{n\times m_i}$ and *unknown* cost functions

$$J_{1,s}(x_0,u_1,u_2) = \int_0^\infty \{x^\top(t)Q_sx(t) + u_1^\top(t)R_{1,s}u_1(t) - \\ - u_2^\top(t)R_{2,s}u_2(t)\}dt = -J_{2,s}(x_0,u_1,u_2), \tag{2}$$

where $Q_s = Q_s^\top \in \mathbb{R}^{n\times n}, R_{1,s} = R_{1,s}^\top \in \mathbb{R}^{m\times m}$ and $R_{2,s} \in \mathbb{R}$ are positive definite. Then, from Corollary 8.6 in [2], it follows that for $i = 1,2$

$$u_{i,s}(t) = F_{i,s}x(t) = (-1)^iR_{i,s}^{-1}B_i^\top K_sx_s(t), \tag{3}$$

where K_s is a unique symmetric solution of

$$-A^\top K_s - K_sA + K_s(B_1R_{1,s}^{-1}B_1^\top - B_2R_{2,s}^{-1}B_2^\top)K_s - Q_s = 0, \tag{4}$$

such that $A - B_1R_{1,s}^{-1}B_1^\top K_s + B_2R_{2,s}^{-1}B_2^\top K_s$ is stable.
Assumptions: (A,B_1) in (1) is controllable.
Inverse RL Goal: using the given trajectories $(x_s,u_{1,s})$ and the system dynamics A,B_1,B_2, one aims to provide Q,R_1,R_2 of a cost function, that together with the given dynamics to form a game where $F_{1,s}$ is a feedback law that constitutes the NE pair.

3 Algorithm

The algorithm below has proven convergence and generates a linear-quadratic zero-sum differential game with Q,R_1,R_2 where $F_{1,s}$ is a stabilizing feedback law that constitutes linear feedback NE pair.

Algorithm 1

1. Initialize $R_1 = R_1^\top > 0$ and $R_2 > 0$. Initialize $Q^{(0)} = Q^{(0)\top} > 0$ such that $(A, \sqrt{Q^{(0)}})$ is observable for *known* A and set $i = 0$. Solve (4) with respect to $K^{(0)}$.
2. Estimate F_o using the observed trajectories as
$$\hat{F}_o = -\hat{u}_o\hat{x}_o^T(\hat{x}_o\hat{x}_o^T)^{-1}.$$
3. Compute
$$F^{(i)} = -R^{-1}B^\top K^{(i)}, \quad s^{(i)} = F^{(i)} - F_o.$$
4. Update $K^{(i)}$ to $\bar{K}^{(i)}$ as
$$\bar{K}^{(i)} = K^{(i)} + \alpha\left(s^{(i)\top}R^{-1}B^\top + BR^{-1}s^{(i)}\right) = K^{(i+1)}.$$
5. Perform evaluation of $Q^{(i+1)}$ as
$$Q^{(i+1)} = -A^T\bar{K}^{(i)} - \bar{K}^{(i)}A + \bar{K}^{(i)}(BR^{-1}B^\top - \gamma^{-2}DD^\top)\bar{K}^{(i)}.$$
6. Set $i = i+1$. Perform steps 3-5 till $s^{(i)\top}s^{(i)} < \varepsilon$ where $\varepsilon > 0$ is a small constant.

References

[1] R. Isaacs, Karreman Mathematics Research Collection, Society for Industrial, and Applied Mathematics. *Differential Games: A Mathematical Theory with Applications to Warfare and Pursuit, Control and Optimization*. SIAM series in applied mathematics. Wiley, 1965.

[2] J.C. Engwerda. *LQ Dynamic Optimization and Differential Games*. John Wiley & Sons, 2005.

Stochastic barrier functions for safety verification of autonomous vehicles and human agents

[1]Frederik Baymler Mathiesen, [1]Luca Laurenti, [2]Simeon Calvert
[1]Delft Center for Systems and Control [2]Department of Transport & Planning
Delft University of Technology, The Netherlands
{f.b.mathiesen, l.laurenti, s.c.calvert}@tudelft.nl

1 Introduction

One major bottleneck for the wide-spread adoption of autonomous vehicles is the lack of safety guarantees, with existing approaches either requiring an enormous amount of data or being overly conservative [1]. This problem is made extremely challenging by the presence of human-driven vehicles because humans are neither deterministic functions nor reward-maximizing agents. To give non-trivial safety guarantees with humans-in-the-loop, we model humans probabilistically and compute probably approximately correct-like bounds [2]: with a given level of confidence δ, synthesize a controller π such that the probability of safety $P(x_k \in X_s, \forall k \in [0,H])$ where x_k and X_s denote the state and the safe set is larger than $1-\varepsilon$ in a finite horizon H.

2 Method

Consider the merging scenario in Figure 1. The two vehicles are one human h and one autonomous agent a where the state of each vehicle is position and velocity $[p,v]^T$, denoted x^h and x^a respectively, and the action u is the acceleration. The discrete-time dynamics $g(x^e,u_k)$, $e \in \{h,a\}$ are

$$p_{k+1} = p_k + v_k \cdot \Delta t + u_k \cdot \Delta t^2 \quad (1)$$
$$v_{k+1} = v_k + u_k \cdot \Delta t \quad (2)$$

The safe set is the set of states where the distance between the vehicles $d(x) = |p^a - p^h|$ is larger than a threshold d_s.

$$X_s = \{x \mid d(x) \geq d_s\} \quad (3)$$

To determine the action u_k for the autonomous vehicle, we synthesize a deterministic controller $\pi(x)$. The human behavior is modeled with a Bayesian Neural Network (BNN) $f(x,w)$ to predict the action. The weights in a BNN are probability distributions, hence the human behavior is probabilistic. We let $F(x,w)$ denote the composition of the autonomous controller, human behavior, and vehicle dynamics

$$F(x,w) = \begin{bmatrix} g(x^h, f(x,w)) \\ g(x^a, \pi(x)) \end{bmatrix} \quad (4)$$

To compute a lower bound $1-\varepsilon$ for the probability $P(x_k \in X_s, \forall k \in [0,H])$, we find a barrier function $B(x)$ satisfying [3]

$$\frac{1}{N}\sum_{i=1}^{N} B(y_i) \leq \frac{B(x)}{\alpha} + \beta \qquad \forall x \in X_s \; \forall y_i \in Y_i \quad (5)$$

where α, β are decision variables and the variable y_i represents the next state given a BNN weight sample w_i. The set $Y_i = \{y_i \mid A_i^l x + b_i^l \leq y_i \leq A_i^u x + b_i^u\}$ over-approximates the next states where the affine bounds are piecewise linear relaxations on $F(x,w)$ using linear bound propagation [4]. The empirical mean $\frac{1}{N}\sum_{i=1}^{N} B(y_i)$ approximates $\mathbb{E}[B(F(x,w)) \mid x]$, and this approximation introduces the confidence level δ and is affected by the number of samples N.

By modeling human behavior with a BNN and finding a stochastic barrier function, we can guarantee a lower bound for the safety probability $1-\varepsilon$ with the given confidence δ.

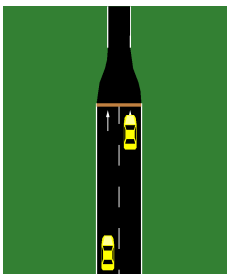

Figure 1: Mixed-autonomy two vehicle merge scenario.

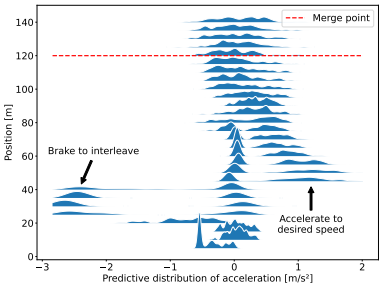

Figure 2: Predictive distribution of BNN as the human agent travels down the lane.

References

[1] D. Isele, A. Nakhaei, and K. Fujimura, "Safe reinforcement learning on autonomous vehicles," in *IROS*, 2018.

[2] M. Mitzenmacher and E. Upfal, *Probability and computing: Randomization and probabilistic techniques in algorithms and data analysis*. Cambridge university press, 2017.

[3] H. J. Kushner, *Stochastic Stability and Control*, ser. Mathematics in Science and Engineering. 1967.

[4] K. Xu, Z. Shi, H. Zhang, *et al.*, "Automatic perturbation analysis for scalable certified robustness and beyond," in *NeurIPS*, 2020.

Sim2real for Autonomous Vehicle Control using Executable Digital Twin

Jean Pierre Allamaa [1,2], Panagiotis Patrinos [2], Herman Van der Auweraer [1], Tong Duy Son [1]
[1] Siemens Digital Industries Software, 3001, Leuven, Belgium
[2] Dept. Electr. Eng. (ESAT) - STADIUS research group, KU Leuven, 3000 Leuven, Belgium
Email: jean.pierre.allamaa@siemens.com

1 Introduction

With the advancement of control and planning algorithms for autonomous driving, a challenge still remains in the transfer from simulation to the real world. Manual tuning to validate the control design requirements in a physical environment is time-consuming and expensive. However, simulations are often fast to validate the algorithms. Nevertheless, this often comes at the expense of over tuning in simulation hindering transferability to the real world. In this work, we propose a sim2real method to transfer and adapt a nonlinear model predictive control (NMPC) from simulation to the real target system based on an executable digital twin (xDT). The DT is the high fidelity simulator of the vehicle dynamics, executable online in the control parameter randomization and learning process. Control parameters adapt 1) to a changing real-world environment and 2) towards improved performance. The performance metric is not required to be differentiable nor analytical with respect to the control parameters and dynamics are not linearized.

2 Automatic control tuning using xDT

We first exploit the Unscented Kalman Filter (UKF) to generate multiple sample points with a Gaussian distribution around the estimated parameter's mean [1]. We use this method to estimate the control parameters resulting in a quantifiable improved performance in a highly non-linear environment. State evolution dynamics are replaced by the xDT. The DT is sampled with the same control architecture as on the real car, but with the distributed sample points. The algorithm compensates for model mismatches and noise by calculating a Kalman gain K_k pointing in the direction of parameters that improves the real vehicle performance. New set of parameters θ_{K+1} are computed with new measurements:

$$\theta_{K+1} = \theta_K + K_k(h_{ref} - h_{meas}(\theta_K)). \quad (1)$$

h_{ref} and h_{meas} are vector valued reference and measured performance. For example, with $h_{meas} = [10e_{Vel}, 10e_{LAT}, T_{exec,NMPC}]$, the algorithm adapts the controller parameters such that deviation from reference velocity and centerline, and NMPC execution time are reduced. The xDT is randomized with different parameters than the real car, and adaptation is online and on-the-go.

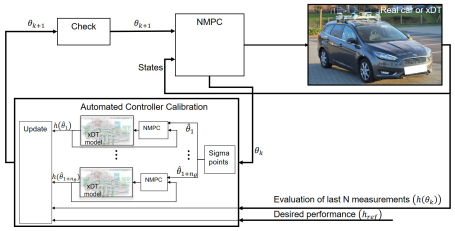

Figure 1: Control parameter adaptation on an xDT

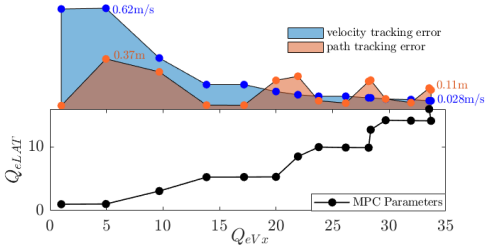

Figure 2: Parameter evolution and Infinity norm of tracking error

3 Test case on a double lane change

We test the algorithm on 4 successive double lane changes of 12s each, at 80 kph. We formulate a path following NMPC, in presence of model mismatches and output noise. The parameters to be updated, every 3s, are the Q and R matrices in the optimal control problem cost term:

$$l_k(x_k, u_k) = (x(k) - x_{ref}(k))^T Q(x(k) - x_{ref}(k)) + u(k)^T Ru(k) \quad (2)$$

Different to prior work, we adapt the covariance matrices on the go, as well as the Gaussian spread such that the Q and R matrices used in sampling the xDT are positive definite, and the Gaussian distribution around the mean is conserved. In Figure 2, peaks in path tracking error occur as the car performs the lane change, but both norms follow a decreasing trend with time (left to right). The weights on lateral deviation Q_{eLAT} and velocity error Q_{eVx} adapt on-the-go.

Acknowledgements

This project has received funding from the European Union's Horizon 2020 research and innovation programme under the Marie Skłodowska-Curie grant agreement ELO-X No 953348

References

[1] M. Menner, K. Berntorp, and S. Di Cairano, "Automated controller calibration by kalman filtering," 2021. URL https://arxiv.org/abs/2111.10832.

Are we there yet? An Overview of Open Challenges in Trajectory Prediction for Autonomous Driving

Manuel Muñoz Sánchez[1], Emilia Silvas[1,2], Jos Elfring[1,3], René van de Molengraft[1]
[1]Department of Mechanical Engineering, Control Systems Technology Group,
Eindhoven University of Technology, Eindhoven, The Netherlands
[2]Department of Integrated Vehicle Safety, TNO, Helmond, The Netherlands.
[3]Product Unit Autonomous Driving, TomTom, Amsterdam, The Netherlands
Email: m.munoz.sanchez@tue.nl

1 Introduction

Automated vehicles (AVs) have become widely popular since they have several potential benefits such as increased safety, efficiency, and comfort. To reach full automation, an AV must anticipate other road user's motions in the driving environment through *motion prediction*. The term *motion* is often used interchangeably to refer to different types of motion, as summarized in Fig. 1. To build motion prediction models, the adoption of deep learning methods has led to significant improvements in the field [1, 2], yet many open challenges still remain.

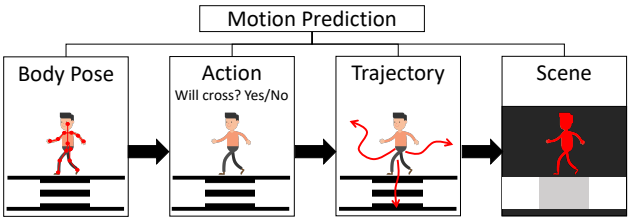

Figure 1: Overview of motion prediction types

2 Open Challenges in Trajectory Prediction

Current challenges in trajectory prediction can be grouped in three categories: *method*, *data*, and *evaluation* challenges.

Method Challenges. Depending on the modeling approach, trajectory prediction methods can be classified into *physics-*, *pattern-*, and *planning-based* methods, each with their own strengths and weaknesses [1].

Data Challenges. Despite the existence of several public datasets [1, 2], various limiting factors persist, such as semi-automatic annotations potentially leading to noisy ground truth, trajectory length being insufficient to evaluate long-term predictions, data for uncommon driving behavior being scarce, and often lacking relevant contextual information.

Evaluation Challenges. With current evaluation practices it is not possible to assess a model's suitability for different situations due to the lack of a standardized benchmarking procedure [1], among other difficulties such as the plethora of existing metric names and formulations [2], or the exclusion of relevant evaluation criteria (e.g. run-time, robustness, and generalization). Additionally, predictions are often evaluated over all trajectories, hindering the identification of a model's shortcomings as exemplified in Fig. 2, where predictions that are highly accurate in most cases fail in a safety-critical scenario.

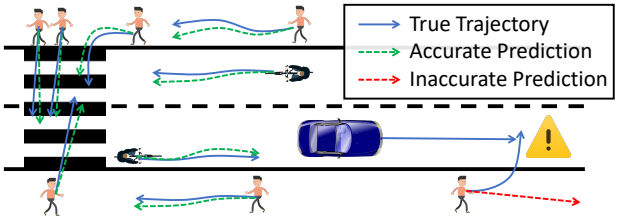

Figure 2: Example scenario where a model that is accurate on average fails in a safety-critical situation.

3 Results & Future Work

After a review of the main open challenges in trajectory prediction, we will present preliminary results on scenario-based assessment of prediction models for autonomous driving, addressing the issue shown in Fig. 2 and allowing a transparent assessment of a model's suitability for different situations. Future work will focus on the development of a benchmarking procedure for motion prediction models that covers all relevant aspects. To that end, we will focus on relevant scenarios currently underrepresented in available datasets, fair comparison of models of different natures, relevant prediction horizons, and additional metrics to evaluate a model's robustness and generalization capabilities.

Acknowledgement: This work was supported by the SAFE-UP project under EU's Horizon 2020 research and innovation programme, grant agreement 861570.

References

[1] A. Rudenko, A. et al., "Human motion trajectory prediction: a survey". The International Journal of Robotics Research, 39(8), 895–935, 2020

[2] A. Rasouli, "Deep Learning for Vision-based Prediction: A Survey", *arXiv preprint arXiv:2007.00095*, 2020.

Link manipulation of mixed-vehicle cyclic platoon: A stability perspective

Woohyun Jeong[1,2], Yoonsoo Kim[1], Alain Vande Wouwer[2]

[1]Graduate School of Mechanical and Aerospace Engineering
Gyeongsang National University, Repulic of Korea

[2]System, Estimation, Control and Optimization (SECO)
University of Mons, Belgium

1 Introduction

This paper discusses about the network stability margin of several vehicles (including human vehicles (HVs) and an autonomous vehicle (AV)) moving on a ring roadway or a cyclic platoon. This cyclic platoon has an information-exchange structure such that the $(i+1)$th vehicle can use the information of its predecessor (the ith vehicle), where $i = 1,2,\ldots,N$, $N+1 = 1$, and N is an odd number. The stability of cyclic platoon or ring stability is considered in [1], where the concept of strong/weak ring stability is proposed. However, the quantitative degree of ring stability is still unclear. Motivated by the concept of network stability margin introduced in [2], we consider in this study link manipulation to improve the network stability margin of a cyclic platoon. By link manipulation, we mean rewiring a link (altering a direction of information-flow) and adding an extra link to the platoon, for the purpose of minimizing the change to the existing information flow. Furthermore, we also consider the effect of AV location on the stability of the platoon. As a result, a link manipulation scheme minimizing the largest cycle length improves the network stability margin the most.

2 Problem statement and Method

As shown in Figure 1, a cyclic platoon C is initially given which has an information-exchange structure L_C or Laplacian matrix such that a vehicle receives and utilizes the information of its predecessor. It is assumed that each of the vehicles' dynamic characteristics in the platoon can be described by an identical transfer function $T_{veh}(s)$. This study then considers finding an optimal link manipulation scheme (adding an extra link after rewiring a link) that modifies the information-exchange structure, so that the network stability margin α^* defined in [2] is maximized. This α^* can be interpreted as gain and phase margins for SISO (Single-Input-Single-Output) systems, and it is in general determined by both L_C and $T_{veh}(s)$ for MIMO (Multi-Input-Multi-Output) systems. Examples of link manipulation are shown in Figure 1.

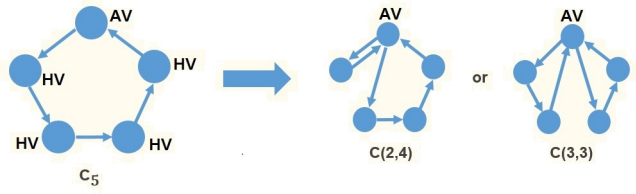

Figure 1: Link manipulation of a cyclic platoon with $N = 5$.

3 Result

It can be shown that α^* decreases with the number of vehicles N in the platoon, so do λ_2 and $1/|C|$. Here, λ_2 and $|C|$ denote the second smallest eigenvalue of L_C and the largest cycle length in C, respectively. Therefore, it is desired to minimize λ_2 or $|C|$ for the purpose of maximizing α^*, which can be achieved via the link manipulation, resulting in two symmetric HV-cycles of length $(N-1)/2$ sharing one node at which the single AV is located (e.g. $C(3,3)$ in Figure 1).

4 Acknowledgement

This research was supported by the National Research Foundation of Korea (NRF) funded by the Ministry of Science and ICT, Republic of Korea (Grant No. 2021R1A2C1004547 and 2017R1A5A1015311).

References

[1] V. Giammarino, S. Baldi, P. Frasca and M. L. Delle Monache "Traffic Flow on a Ring With a Single Autonomous Vehicle: An Interconnected Stability Perspective," *IEEE Transactions on Intelligent Transportation Systems*, Vol. 22, No. 8, pp. 4998-5008, 2021.

[2] Y. Kim, "On the Stability Margin of Networked Dynamical Systems," *IEEE Transactions on Automatic Control*, Vol. 62, No. 10, pp. 5451-5456, 2017.

Autonomous Driving of Articulated Vehicles at Distribution Centre

Viral Gosar
Gemini(Z) -1.132,
5612 AE, Netherlands
v.v.gosar@tue.nl

Mohsen Alirezaei
m.alirezaei@tue.nl

I.J.M. Besselink
I.J.M.Besselink@tue.nl

1 Abstract

This abstract discusses the requirement of autonomous driving of commercial vehicle specifically at distribution centers and outlines how a lab setup is further used to test such autonomous driving application.

2 INTRODUCTION

Within the logistic sector, heavy vehicles have been widely used for road freight transport due to their capability of carrying large cargo loads. The business in the logistic sector can further take competitive advantage of the rapid innovations in connected and autonomous transport by implementing autonomous driving of commercial vehicles in a confined environment, e.g. a distribution centre (DC), ship yards, etc; where handling of goods can be made more effective and efficient. Additionally, at these constrained environment drivers experience tedious manoeuvring task and are prone to accidents due to space limitation. Thus, automation of these vehicles specifically for parking/docking manoeuvre is necessary [1].

3 Low Speed Autonomous Driving Tractor Semi-trailer

The main layers of autonomous vehicles (AV) are the planning, perception and control, where in system modelling is an important phase necessary before all the above mentioned layers (Figure 1).

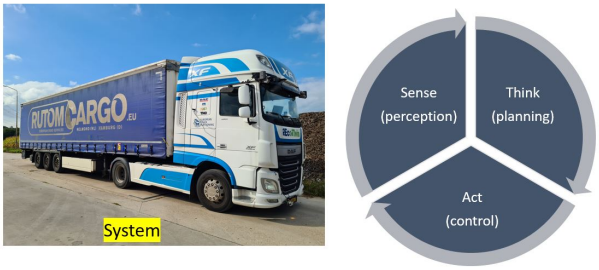

Figure 1: steps toward automated driving

The system under consideration in this study is a complex vehicle, of the type tractor semi-trailer (Figure 1). The complexity of the vehicle is due to the mechanical joint (articulation point) present between the tractor and semi-trailer, that creates large swept path while driving forward and causes semi-trailer instability while driving in reverse. Specifically, at the DC where driving space is limited and the accuracy requirement while reversing the vehicle between the docking aisle are quite high, these vehicles need to be driven at large steering angle which lead to tire scrubbing. Hence, the requirement to understand the behaviour of these vehicle on position level is crucial.

4 Testing and Lab Application

In order to understand the behaviour of the vehicle for low speed and large steering manoeuvre, real world test were conducted at DPD distribution in Oirschot, the Netherlands. Pre- defined forward driving and reverse driving manoeuvres were performed at low speed and special emphasis was given to docking and parking manoeuvres. All the tests were performed with both an unloaded and loaded (12 ton) semi-trailer.

Figure 2: TU/e Lab setup

Testing the vehicle for every small development can be time consuming and require a lot financial investment, additionally, testing autonomous controller in live environment can be dangerous. Hence, to test autonomous driving application, a 1:13 scaled setup of a distribution centre and tractor semi-trailers at the Eindhoven University of technology is used (Figure 2).

References

[1] "CATALYST Living Lab," [Online]. Available: https://dutchmobilityinnovations.com/spaces/1182/catalyst-living-lab/about/.

The effects of varying demand on Breass's paradox in traffic networks

J. Verbree, A.K. Cherukuri
University of Groningen
ENgineering and TEchnology institute Groningen
Optimization and Decision Sytems(ODS)
Nijenborgh 4, 9747 AG, Groningen
The Netherlands
j.verbree@rug.nl, a.k.cherukuri@rug.nl

1 Introduction

Congestion on the road is a problem that most of us know all too well, and that should be avoided if at all possible. Ideally road networks are designed in such a way that congestion, and consequently travel time, is minimized for all users. Breass's paradox(BP) is the phenomenon that occurs when removal of one or more roads from a network decreases the travel time experienced by the users of the network. Worsening performance by addition of a road to the network is truly the epitome of innefficiency, and we would of course want to prevent this from happening. Unfortunately, the question of whether or not a network suffers from BP is complex, and computationally hard to answer. Finding the subset of roads in a network that minimizes travel time is for instance an NP problem [1]. Furthermore, The occurence of BP depends on the total amount of traffic, called the *demand*, traversing the network. A network subject to BP at one level of demand may not be subject to BP at a different level [2]. In our work we focus on this last aspect of BP. We look at the effects of varying demand, which is the total amount of traffic traversing the network, on the paradox, and try to leverage these results to find sufficient conditions for the occurence of BP.

2 Model

The model we use is that of a *routing game*. The network is described by a directed, acyclic graph $\mathscr{G} = (\mathscr{V}, \mathscr{E})$, with an associated origin-destination(OD) pair $(v_o, v_d) \in \mathscr{V} \times \mathscr{V}$. The set of all paths from v_o to v_d we denote $\mathscr{P}$. Any driver enters the network at v_d and needs to choose a path $p \in \mathscr{P}$ in order to arrive at v_d. A total demand $D \geq 0$ must be routed in this way, leading to a flow vector $f \in \mathscr{F}_D := \{f \in \mathbb{R}^{|\mathscr{P}|}_{\geq 0} \mid \sum_{r \in \mathscr{P}} f_r = D\}$. Letting f_p denote the amount of traffic traversing path p, the amount of traffic traversing edge e_k is given by $\sum_{r \in \mathscr{P}}(f_r)$. To each edge $e_l \in \mathscr{E}$ we associate a non-decreasing, continuous cost function $C_{e_k}(\cdot)$. The cost of traversing e_k is then given by $C_{e_k}(f_{e_k})$. The cost of traversing the path p is subsequently given by $C_p(f) := \sum_{e_k \in p} C_{e_k}(f_{e_k})$. We assume that the routed flow is in Wardrop equilibrium(WE):

Definition 2.1. *Let $\mathscr{P}$, $\{C_{e_k}\}_{e_k \in \mathscr{E}}$ and $D \geq 0$ be given. A flow $f \in \mathscr{F}_D$ is said to be in Wardrop equilibrium if for all $p \in \mathscr{P}$ such that $f_p > 0$ we have*

$$C_p(f) \leq C_r(f), \quad \forall r \in \mathscr{P}.$$

An essential step in our work is characterizing how the WE changes as the demand increases. This we will discuss in more detail during the talk.

3 Results

The following result allows us to identify paths which are in some way either 'useless' meaning that no flow ever traverses that path, or 'harmful' in that they cause BP.

Theorem 3.1. *For a given $\mathscr{P}$ and $\{C_{e_k}\}_{e_k \in \mathscr{E}}$, let $\mathscr{W}_D$ denote the set of WE when the demand on the network is $D \geq 0$. If for some $p \in \mathscr{P}$ and all $f^D \in \mathscr{W}_D$ we have $f_p = 0$, then either $f^T_p = 0$ for all $T \in [0, D]$ and all $f^T \in \mathscr{W}_T$, or the path p causes Breass's paradox for some $0 < T < D$.*

We have also proven the following results, which is a generalization of earlier results obtained for a specific network, the *Wheatstone* network, which is the quintessential example of a network subject to Breass's paradox.

Theorem 3.2. *Let $\mathscr{P}$ be given, and the functions $\{C_{e_k}\}_{e_k \in \mathscr{E}}$ be affine. There is a lower bound $D^- > 0$ and an upper bound $D^+ < \infty$ such that BP can only occur on the interval (D^-, D^+).*

References

[1] T. Roughgarden, "On the severity of Braess's paradox: Designing networks for selfish users is hard," *Journal of Computer and System Sciences*, vol. 72, no. 5, pp. 922–953, 2006.

[2] E.I. Pas, S.L. Principio, "Braess' paradox: Some new insights", *Transportation Res. Ser. B*, vol. 31, no. 3, 265—276, 1997.

Joint Design and Operation of an Electric Autonomous Mobility-on-Demand System

Fabio Paparella
Eindhoven University of Technology
De Rondom 70, 5612 AP Eindhoven, The Netherlands
f.paparella@tue.nl

Theo Hofman
Eindhoven University of Technology
t.hofman@tue.nl

Mauro Salazar
Eindhoven University of Technology
m.r.u.salazar@tue.nl

1 Abstract

Mobility-as-a-Service (MaaS) is an emerging type of service that allows users to plan, book and pay for multiple types of mobility services through a common digital channel [1]. Newly developed algorithms can compute a wide variety of instances. [2] proposes an algorithm to route in real-time vehicles for thousands of daily requests; [3] shows a method to optimize the fleet sizes and vehicles distribution. Due to a strong coupling between AMoD systems and charging infrastructure, charging stations siting is investigated in [4] through a Linear Programming approach. In [5] Salazar et al. explore intermodal AMoD systems, where AMoD operators are coupled with public transport. Usually, vehicles that are adopted to provide this service are commercial vehicles. Few papers in literature focus on the optimization of the design of a fleet specifically for AMoD applications. In [6], the authors show a method to jointly optimize the number of vehicles in a fleet and their class capacity (i.e., number of seats) in an AMoD ride-sharing environment. To the best of the authors' knowledge, no optimization model exists that studies the trade-off between number of vehicles in a fleet and their battery size, while taking into account the surrounding charging infrastructure. When optimizing the number and composition of electric vehicles of a fleet, there is a clear trade-off between the number of vehicles and their autonomy. Intuitively, the larger the battery, the lower the daily charging trips, the higher the daily availabilty, but the higher the consumes due to heavier vehicles. Moreover this decision is strictly coupled with the presence of charging infrastructures in the area. The contributions of this paper are twofold. First, we present a linear formulation to jointly optimize the number of electric vehicles in a fleet, their battery size and the operational costs. In fact, the objective function is expressed as a linear combination of operational costs of the fleet, as well as initial costs, and profits generated by serving requests. Thanks to the linear formulation, optimality is guaranteed and the problem can be solved with commercial solvers. Second, we display a real-world case study of New York City (NYC) and yellow taxi data, which allows us to quantify the general benefits of jointly optimized E-AMoD with respect to the surrounding charging infrastructure. In particular, we show that a vehicle's range heavily affects operation and routing decisions and, thus, system efficiency. Our studies reveal that a balance between battery size, fleet size and presence of charging stations can yield significant benefits compared to a system that was not jointly optimized.

References

[1] G. Smith, "Making mobility-as-a-service: Towards governance principles and pathways" 06 2020.

[2] J. Alonso-Mora, S. Samaranayake, A.Wallar, E. Frazzoli, and D. Rus, "On demand high-capacity ride-sharing via dynamic trip-vehicle assignment," Proceedings of the National Academy of Sciences, vol. 114, DOI 10.1073/pnas.1611675114, no. 3, pp. 462–467, 2017. https://www.pnas.org/content/114/3/462

[3] A. Wallar, J. Alonso-Mora, and D. Rus, "Optimizing vehicle distributions and fleet sizes for shared mobility-on-demand," in Proceedings of the International Conference on Robotics and Automation, ICRA 2019, DOI 10.1109/ICRA.2019.8793685, pp. 3853–3859. United States: IEEE, 2019.

[4] J. Luke, M. Salazar, R. Rajagopal, and M. Pavone, "Joint optimization of autonomous electric vehicle fleet operations and charging station siting," in Proc. IEEE Int. Conf. on Intelligent Transportation Systems, Indianapolis, IN, Sep. 2021, in press. http://arxiv.org/abs/2107.00165

[5] M. Salazar, N. Lanzetti, F. Rossi, M. Schiffer, and M. Pavone, "Intermodal autonomous mobility-on-demand," IEEE Transactions on Intelligent Transportation Systems, 2019. https://ieeexplore.ieee.org/document/8894439

[6] A. Wallar, W. Schwarting, J. Alonso-Mora, and D. Rus, "Optimizing multi-class fleet compositions for shared mobility-as-a-service," in 2019 IEEE Intelligent Transportation Systems Conference (ITSC), DOI 10.1109/ITSC.2019.8916904, pp. 2998–3005, 2019.

Tightening ambiguity set characterizations for data-driven distributionally robust optimization

Lotfi Mustapha Chaouach[1], Dimitris Boskos[1], and Tom Oomen[1,2]

[1]Delft Center for Systems and Control, 2628CD, Delft, the Netherlands (e-mail: l.chaouach@tudelft.nl)
[2]Eindhoven University of Technology, the Netherlands

1 Introduction

Real-world systems are always uncertain. Their increasing complexity, sophistication, and connectivity generate further sources of uncertainty that is characterized by deterministic (worst-case) or stochastic models. The latter assume existence of a probability distribution, which is typically inferred from data. To build such data-driven models, we need to account for limitations induced by the fact that data may be corrupted or only available at small amounts. These aspects influence the accuracy of inferences about the underlying probability distributions and their usefulness for decision making. To overcome these issues, it is required to derive reliable probabilistic models of the uncertain components from the available data under the least possible amount of conservativeness.

2 Problem formulation

The central problem in stochastic optimization is to take optimal decisions in problems affected by randomness. A typical stochastic optimization problem has the form

$$\inf_{x\in\mathscr{X}} \mathbb{E}_{P_\xi}\left[f(x,\xi)\right] \tag{1}$$

where f is the objective function, x is the decision variable, and $\xi \in \mathbb{R}^d$ is a random variable with distribution P_ξ. In practice, as P_ξ is often unknown, it is approximated by the empirical distribution $P_\xi^N := \sum_{i=1}^N \delta_{\hat{\xi}_i}$ of i.i.d. samples. Yet, for small amounts of data, this approach may become insufficient, as the approximation P_ξ^N may exhibit significant deviations from P_ξ. To address this issue, uncertainty in the distribution is considered as

$$\inf_{x\in\mathscr{X}} \max_{P_\xi\in\mathscr{P}^N} \mathbb{E}_{P_\xi}\left[f(x,\xi)\right], \tag{2}$$

which is a distributionally robust optimization problem [1, 2, 3], where $\mathscr{P}^N$ is an ambiguity set of distributions that is informed by the samples and contains plausible models for the true distribution. A convenient choice of ambiguity sets for such problems are balls in the Wasserstein metric centered at the empirical distribution P_ξ^N. For compactly supported distributions, choosing the radius

$$\varepsilon_N(\beta,\rho) := \left(\frac{\ln(C\beta^{-1})}{c}\right)^{\frac{1}{q}} \frac{\rho}{N^{\frac{1}{q}}},\quad q := \max\{2p,d\}, \tag{3}$$

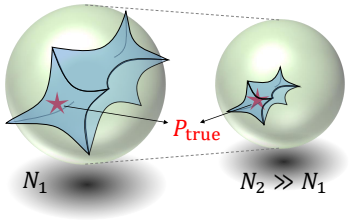

Figure 1: High-dimensional hyperrectangles shrink much faster with the number of samples compared to Wasserstein ambiguity balls.

where $d \neq 2p$ and ρ is the diameter of the support of P_ξ, guarantees that the ambiguity ball contains the true distribution with probability at least $1-\beta$. However, (3) implies that for high-dimensional random variables, the radius decreases with the excessively slow rate of the order of $N^{-\frac{1}{d}}$.

3 Ambiguity hyperrectangles

To address the conservative decrease rate in (3), we exploit independence of lower-dimensional components of the random variable $\xi = (\xi_1,\ldots,\xi_n)$. We build a lower-dimensional ambiguity ball for each component and construct an ambiguity hyperrectangle by taking all product measures across the individual distributions from the n balls. Such a rectangle shrinks at the faster rate $N^{\frac{-1}{q^\star}}$ with the number of samples, where $q^\star := \max\{q_k, k=1,\ldots,n\}$, $q_k := \max\{2p,d_k\}$ for $d_k \neq 2p$ and d_k is the dimension of ξ_k. The ambiguity hyperrectangle is much smaller than the original ambiguity ball and contains the true distribution with the same confidence (cf. Figure 1).

References

[1] P. M. Esfahani and D. Kuhn, "Data-driven distributionally robust optimization using the Wasserstein metric: performance guarantees and tractable reformulations," Mathematical Programming, vol. 171, no.1-2, pp. 115–166, 2018.

[2] R. Gao and A. Kleywegt, "Distributionally robust stochastic optimization with Wasserstein distance,"arXiv preprint arXiv:1604.02199, 2016.

[3] J. Blanchet and K. Murthy, "Quantifying distributional model risk via optimal transport," Mathematics of Operations Research, vol. 44, no. 2, pp. 565–600, 2019.

A Pareto ellipsoids based algorithm for multiobjective optimisation under parametric uncertainty

Wannes Mores[1] Satyajeet S. Bhonsale[1] Ihab Hashem[1] Philippe Nimmegeers[1]
Jan Van Impe[1,2]

1 Introduction

Multi-objective model-based optimization is a useful tool in chemical process design since different conflicting objectives are usually present (e.g. maximal productivity and minimal energy consumption). Solving such problems increases the computational cost of the optimization significantly. Robustification of constraints regarding parametric uncertainty is important as safe operating conditions are desired in these processes. Uncertainty propagation will also contribute to a higher computational cost. The methodology provided will attempt to reduce the overall computational cost by integration of the uncertainty into existing scalarization techniques for multi-objective optimization. The constructed ellipsoids will also serve as a visualization of the uncertainty on objective performance.

2 Pareto ellipsoid criterion

The scalarization method used in the novel Pareto based algorithm is based on NBI [2]. Significance of the Pareto points is guarantueed using the Divide and Conquer concept presented in [1]. We expand upon this D&C concept by using the expectation and covariance matrices for model outputs. These matrices can be generated using uncertainty propagation methods. In this study, the sigma points method [3] is used.

Pareto ellipsoids are defined for a given confidence level using a backoff parameter derived from a χ^2 distribution. The expectation gives the location, the covariance matrix gives the size and rotation of the ellipsoids. With these ellipsoids, a new significance criterion can be defined within the D&C concept. The Pareto ellipsoid significance criterion is defined as follows:
A Pareto point is considered insignificant if the Pareto point falls within the Pareto ellipsoid of a neighboring Pareto point ***or*** *if one of its neighboring Pareto points falls within the Pareto ellipsoid of the Pareto point.*

Using this new criterion, a new Pareto ellipsoids based algorithm is defined and implemented for (bio-)chemical case studies.

[1]BioTeC+, KU Leuven, Belgium
[2]jan.vanimpe@kuleuven.be

3 Results

The proposed algorithm is used within four case studies. For comparison purposes, the D&C and NBI methods are also implemented. One of the case studies using the Pareto ellipsoid significance criterion is shown in Figure 1 as an example. All case studies show a reduction in Pareto points when

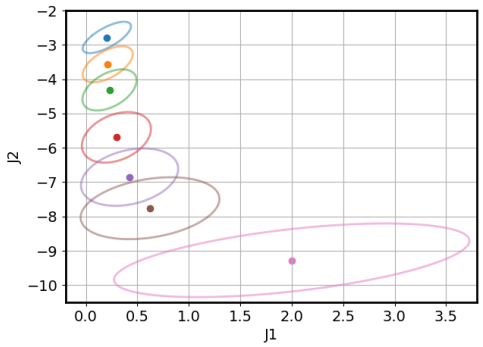

Figure 1: Example of Pareto ellipsoids

using the Pareto ellipsoids based algorithm, which therefore result in a lower computational cost. The uncertainty is also visualised, to be interpreted by a decision maker.

References

[1] Hashem, I., Telen, D., Nimmegeers, P., Logist, F., Van Impe, J. (2017). A novel algorithm for fast representation of a Pareto front with adaptive resolution: Application to multi-objective optimization of a chemical reactor. Computers and Chemical Engineering, 106, 544–558. https://doi.org/10.1016/j.compchemeng.2017.06.020

[2] Das, I., Dennis, J. E. (1998). Normal-boundary intersection: A new method for generating the Pareto surface in nonlinear multicriteria optimization problems. SIAM journal on optimization, 8(3), 631-657.

[3] Julier, S., Uhlmann, J. K. (1996). A General Method for Approximating Nonlinear Transformations of Probability Distributions. 1–27.

Computational Use of an Artificial Bee Colony approach for Model Predictive Control

Jhonny de Sá Rodrigues
FEUP - Univ. do Porto (Portugal)
jsrodrigues@inegi.up.pt

Alejandro Goldar
SAAS - ULB
alejandro.goldar.davila@ulb.be

Abstract

A Model Predictive Control (MPC) is a model-based control framework that enforces constraints satisfaction by computing, at each time instant, a sequence of future control actions. Such a computation is based on a receding-horizon minimization problem, whose computational complexity can be intense for nonlinear applications where neither global optimally nor feasibility can be ensured. Instead of implementing an MPC that resorts to "common" algorithms to find a minimal solution, this work proposes the use of a modified Artificial Bee Colony approach to solve such a complex optimal problem.

In the case of linear systems subject to convex constraints such minimization is quite straightforward and requires to find a gradient at each time instant. However, for a nonlinear system, finding a global optimum is not ensured and solving algorithm can be quite time-consuming due to the intensiveness of such an optimal problem. In this case, one can solve the optimization problem by making use of an Artificial Bee Colony (ABC) approach [1].

An ABC consists of a swarm-based zero-order technique that is able to find the optimal value of a function based on a "search" algorithm that makes use of 3 sets of bees, namely: *Employed* bees, *Onlooker* bees and *Scout* bees. The *Employed* bees, are randomly assigned as possible solutions of the system, x_{ij}, such that

$$x_{ij}^{k}=x_{min,j}^{k}+random[0,1]\left(x_{max,j}^{k}-x_{min,j}^{k}\right) \tag{1}$$

where i stands for the solution and j for the parameter of such solution at time k.

Upon all the Employed bees have proposed a solution, those solutions are evaluated J_i until time $k+1$.

$$\begin{aligned} J_i=&\sum\left(Ref-f\left(x_{ij}\right)\right)W_1\left(Ref-f\left(x_{ij}\right)\right)^T \\ &+\sum\left(\Delta x_{ij}\right)W_2\left(\Delta x_{ij}\right)^T \end{aligned} \tag{2}$$

where Ref stands for the reference of each parameter j, $f(x_{ij})$ stands for the function which defines the problem, and W_1 and W_2 stands for weight matrices for the error and control effort respectively. Then, a fitness relation between all the evaluated *Employed* solutions determines a probability of obtaining a minimum

$$fit_i=\frac{1}{1+J_i} \tag{3}$$

$$P_i=fit_i/\sum_{i=1}^{N}fit_i \tag{4}$$

Once a minimum is selected, *Onlooker* bees are sent towards that solution to explore the surroundings. By sending the *Onlooker* bees, the algorithm verifies whether the solutions provided by the *Employed* bees can be further improved or not, thus aiming at finding a global minimum. It is also worth highlighting that in this step one can consider an hybrid method, if the computational capabilities allow it, that accelerates the convergence of the Onlooker bees solutions by calculating the function gradient using the *Onlooker* bees definition as:

$$v_{ij}^{+}=x_{ij}+\Delta x_{ij} \tag{5}$$

$$v_{ij}^{-}=x_{ij}-\Delta x_{ij} \tag{6}$$

where superscript "+" stands for the proposed solution i of the parameter j plus a fixed variation in parameter j, and the superscript "−" stands for the proposed solution i of the parameter j plus a fixed variation in parameter j. This modification to the classical *Onlooker* bee definition proposed by [1] allows to create a gradient vector around solution i. It is worth to mention that to generate the gradient it is required to evaluate (2) $2n+1$ times using the solutions generated by the *Onlooker* bees, where n is the amount of parameters j of the solution. Once all *Onlooker* bees are evaluated, a greedy selection is performed where a new *Employed* bee is selected as the best as the best *Onlooker* bee found and new *Onlooker* bees are defined using (5) and (6). This process for the *Onlooker* bees stops when a minimum variation of J_i is reached or a maximum number of iterations.

The last set of bees (*Scout*), create a new group of solutions using (1) while replacing all the Employed bees that did not meet the probability (4) in order to repeat the process until a tolerance limit is achieved. Hence, the ABC approach requires to solve several time the same problem, which can be computationally expensive but easier to implement in devices with reduced computational capabilities. Furthemore, one of the main appeals of this approach is that the computational burden can be reduced by distributing the calculations of the *Employed* and *Onlooker* between different processing devices or cores.

ALPAQA: A matrix-free solver for nonlinear MPC and large-scale nonconvex optimization

Pieter Pas, Mathijs Schuurmans and Panagiotis Patrinos
KU Leuven, Department of Electrical Engineering (ESAT),
STADIUS Center for Dynamical Systems, Signal Processing and Data Analytics,
Kasteelpark Arenberg 10, 3001 Leuven, Belgium
{pieter.pas,mathijs.schuurmans,panos.patrinos}@kuleuven.be

1 Introduction

The increasing complexity of the models used in disciplines such as model predictive control necessitates optimization solvers that can handle large and usually nonconvex optimization problems. This work proposes such a solver, with a focus on nonlinear model predictive control (NMPC).

2 Solution techniques for NMPC

Popular traditional techniques for solving NMPC problems are sequential quadratic programming (SQP) and interior point (IP) methods. In the context of model predictive control, where each time step requires the solution of a minimization problem, SQP can be advantageous because of its warm starting capabilities: the solution of the previous time step (or a shifted version thereof) can be used as the initial guess for the current problem. Given that the solutions of successive time steps are often quite similar, faster convergence can be achieved compared to random or fixed initial guesses. Interior point methods are harder to warm start, but robust state-of-the-art implementations such as IPOPT make it an attractive general-purpose solver.
A third class of algorithms for constrained optimization are the augmented Lagrangian methods (ALM) [1], where a subset of the constraints are replaced by an exact penalty term. The result is the so-called augmented Lagrangian function. When successively minimized by an inner solver, and by appropriately updating the Lagrange multipliers and penalty factors, convergence to a solution of the original problem can be achieved under mild conditions. Augmented Lagrangian methods inherit many of the favorable properties of the inner solver, and can take advantage of warm starting.

3 Contributions

This work presents ALPAQA [2], a new software package for constrained nonconvex optimization. The algorithms used by ALPAQA are based on the matrix-free PANOC algorithm [3], which handles nonconvex optimization problems with constraints that allow efficient computation of the proximal operator, such as box constraints. An augmented Lagrangian method is used to allow for more general constraints. PANOC combines the global convergence properties of first-order methods with the superlinear convergence of quasi-Newton methods. Thanks to the matrix-free, limited memory BFGS implementation, it is applicable to both large-scale problems and in real-time embedded environments. Concretely, ALPAQA solves general nonconvex nonlinear programs of the form

$$\begin{aligned} \underset{x}{\text{minimize}} \quad & f(x) \\ \text{subject to} \quad & \underline{x} \le x \le \overline{x} \\ & \underline{z} \le g(x) \le \overline{z}, \end{aligned} \tag{P}$$

with the objective function $f : \mathbb{R}^n \to \mathbb{R}$ and the constraints function $g : \mathbb{R}^n \to \mathbb{R}^m$ possibly nonconvex.

ALPAQA is published as an open-source C++ library and is accessible through an easy-to-use Python interface that provides integration with the CasADi package for the computation of derivatives and the formulation of optimal control problems and other NLPs.

Furthermore, the authors propose two modifications to improve the practical performance and robustness of the PANOC algorithm [4]: the first improvement exploits the structure of the derivatives of the objective function when applied to box-constrained problems; the second improvement modifies the PANOC line search condition to be able to reject quasi-Newton steps that harm practical convergence.

Experiments demonstrate the effectiveness of these modifications for model predictive control problems and a larger set of NLP benchmarks.

References

[1] E. G. Birgin and J. M. Martínez, *Practical Augmented Lagrangian Methods for Constrained Optimization*, N. J. Higham, Ed. SIAM, 2014.

[2] P. Pas, ALPAQA, GitHub: https://github.com/kul-optec/alpaqa, 2021.

[3] L. Stella, A. Themelis, P. Sopasakis, and P. Patrinos, "A simple and efficient algorithm for nonlinear model predictive control," in *2017 IEEE 56th Annual Conference on Decision and Control (CDC)*, 2017, pp. 1939–1944.

[4] P. Pas, M. Schuurmans, and P. Patrinos, ALPAQA*: A matrix-free solver for nonlinear MPC and large-scale nonconvex optimization*, 2021. arXiv: 2112.02370.

Towards Tight Convergence Rates of the Gradient Method on Hypoconvex Functions

Teodor Rotaru
ESAT-STADIUS
KU Leuven
Kasteelpark Arenberg 10, bus 2446
B-3001 Leuven, Belgium
teodor.rotaru@kuleuven.be

François Glineur
ICTEAM-INMA
UCLouvain
Avenue Georges Lemaître 4, bte L4.05.01
B-1348 Louvain-la-Neuve, Belgium
francois.glineur@uclouvain.be

Panagiotis Patrinos
ESAT-STADIUS
KU Leuven
Kasteelpark Arenberg 10, bus 2446
B-3001 Leuven, Belgium
panos.patrinos@esat.kuleuven.be

1 Introduction

We perform the first tight convergence analysis of the gradient method with fixed step sizes applied to the class of smooth hypoconvex (weakly-convex) functions, i.e., smooth nonconvex functions whose curvature (i.e., maximum Hessian eigenvalue) belongs to the interval $[\mu, L]$, where $\mu < 0$. The results fill the gap between convergence rates for smooth nonconvex and smooth convex functions.

The convergence rates were identified with the help of the performance estimation framework (PEP) [1, 2] adapted to hypoconvex functions. We provide mathematical proofs for a large range of step sizes and prove that the convergence rates are tight when all step sizes are smaller or equal to $1/L$. Finally, we identify the optimal constant step size that minimizes the worst-case of the gradient method applied to hypoconvex functions.

2 Contributions

Let h_i be the i-th (normalized) step size of the gradient method (1), which is known to converge for all $h_i \in (0,2)$.

$$x_{i+1} = x_i - \frac{h_i}{L}\nabla f(x_i) \tag{1}$$

We prove:

- **the first upper bounds** of the convergence rates for the gradient method on hypoconvex functions with step sizes in $(0,\bar{h}]$, where $\bar{h} \in [\frac{3}{2}, 2)$ is a threshold with an analytical expression depending on the ratio κ between μ and L.

Theorem 1. *Let $f \in \mathcal{F}_{\mu,L}(\mathbb{R}^d)$ be a smooth hypoconvex function, with $L > 0$ and $\mu \in (-\infty, 0)$. Let $\kappa := \mu/L$, $\bar{h}(\kappa) := \frac{1+\kappa-\sqrt{1-\kappa+\kappa^2}}{\kappa}$ and N iterations of the gradient method (1) with $h_i \in \left(0, \bar{h}(\kappa)\right]$, $i \in \{0,\dots,N-1\}$, generating the sequence $x_1,\dots,x_N$ starting from x_0. Assume that f has a global minimum f_* and $f(x_0) - f_* \leq \Delta$, where $\Delta > 0$. Then*

$$\min_{0\leq i\leq N} \|\nabla f(x_i)\|^2 \leq \frac{2L(f(x_0)-f_*)}{1+\sum_{i=0}^{N-1}\left[2h_i - h_i^2 \frac{-\kappa}{2\min\left(1,\frac{1}{h_i}\right)-(1+\kappa)}\right]}$$

- **the tightness** of the upper bounds for step sizes $h_i \in (0,1]$, by constructing a worst-case function example.
- **the tight convergence rate** for the gradient method on smooth convex functions with step sizes $h_i \in (0, \frac{3}{2}]$.

From our findings we deduce:

- **the optimal constant step size** recommendation, which minimizes the worst-case upper bound with respect to κ.
- **the existence of three worst-case regimes** with respect to intervals of a constant step size h:
(i) $h \in (0,1]$, (ii) $h \in \left(1, \bar{h}\right]$ and (iii) $h \in \left(\bar{h}, 2\right)$.

Following extensive numerical simulations, we conjecture:

- **the upper bound** for the gradient method on convex functions with constant step size $h \in (\frac{3}{2}, 2)$.
- **a partial description of the upper bound** of the third regime corresponding to $h \in (\bar{h}, 2)$.

Our results complement and extend the recent analysis of [3], also performed using the performance estimation framework, that establishes tight rates for the gradient method in the case of smooth nonconvex functions (corresponding to the special case of hypoconvex functions $\mu = -L$).

References

[1] Y. Drori and M. Teboulle, "Performance of first-order methods for smooth convex minimization: a novel approach," *Mathematical Programming*, vol. 145, pp. 451–482, June 2014.

[2] A. B. Taylor, J. M. Hendrickx, and F. Glineur, "Performance estimation toolbox (PESTO): Automated worst-case analysis of first-order optimization methods," in *2017 IEEE 56th Annual Conference on Decision and Control (CDC)*, pp. 1278–1283, Dec. 2017.

[3] H. Abbaszadehpeivasti, E. de Klerk, and M. Zamani, "The exact worst-case convergence rate of the gradient method with fixed step lengths for L-smooth functions," *Optimization Letters*, Nov. 2021.

Thursday - July 7, 2022
10:50 - 11:50 (ThP)

Low frequency isolation of a six degrees of freedom platform using high precision inertial sensors

Mouhamad Haidar Lakkis
Precision Mechatronics Laboratory, University of Liege, Université Libre de Bruxelles
mhlakkis@uliege.be

Jennifer Watchi
Precision Mechatronics Laboratory, Université Libre de Bruxelles
jennifer.watchi@ulb.be

Rasa Jamshidi
Precision Mechatronics Laboratory, University of Liege
R.jamshidi@uliege.be

Ameer Sider
Precision Mechatronics Laboratory, University of Liege
asider@uliege.be

Christophe Collette
Precision Mechatronics Laboratory, University of Liege, Université Libre de Bruxelles
christophe.collette@uliege.be

1 Abstract

After the first detection of gravitational waves in 2015, a new window in scientific exploration was widely open. This detection was only possible with gravitational-wave detectors operating in ultra-stable environments. Moreover, to guarantee good performance of such detectors ground motion active isolation is a *must*. An active isolation approach was successfully implemented in LIGO's positioning platforms[1][2] where it was possible to obtain amplitude spectral densities lower than $10^{-12}\ m/\sqrt{Hz}$ for vertical and longitudinal seismic isolation at frequencies around 1Hz. However, actively isolating in lower frequencies is still remarkably challenging. Precision Mechatronics Laboratory (PML) in University of Liege (ULiege) and Université Libre de Bruxelles (ULB) is addressing theoretically and validating experimentally this low frequency active control problem.

High precision displacement vacuum inertial sensors[3] are placed on top of a six degree of freedom platform. Six inertial sensors are used for measuring displacement in the vertical direction and three for displacement in horizontal direction. Resonance frequencies of vertical and horizontal sensors are 0.3 Hz and 0.7 Hz respectively with resolution of $2 \times 10^{-13}\ m/\sqrt{Hz}$ at 1 Hz for the two kind of sensors. Sensors' signals are then feedbacked into six voice coil actuators (three horizontal and three vertical) integrated below the platform. Actuators and sensors are placed in a quasi-collocated architecture facilitating the controllability of the plant. Low resonance frequencies and noise-to-signal ratios of the developed inertial sensors are allowing active control in frequencies as low as 0.01 Hz.

References

[1] F. Matichard, B. Lantz, K. Mason, R. Mittleman, B. Abbott, S. Abbott, E. Allwine, S. Barnum, J. Birch, S. Biscans et al. Advanced LIGO two-stage twelve-axis vibration isolation and positioning platform. Part 1: Design and production overview, *Precision Engineering*,40:273-286, 2015.

[2] F. Matichard, B. Lantz, K. Mason, R. Mittleman, B. Abbott, S. Abbott, E. Allwine, S. Barnum, J. Birch, S. Biscans et al. Advanced LIGO two-stage twelve-axis vibration isolation and positioning platform. Part 2: Experimental investigation and tests results, *Precision Engineering*,40:287-297, 2015.

[3] B. Ding. *Development of High Resolution Interferometric Inertial Sensors.* PhD thesis, Université libre de Bruxelles, 2021.

Wind farm power reserve for secondary frequency regulation through distributed yaw optimization

Younes OUDICH[1], Michel KINNAERT[1] &
Johan GYSELINCK[2]
Depart. SAAS[1] & Depart. BEAMS[2]
Université Libre de Bruxelles
CP 165/55, 50 Av.F.D. Roosevelt B-1050 Brussels
Belgium
Emails: younes.oudich@ulb.be
michel.kinnaert@ulb.be

Frederik DE BELIE[3]
Depart. ESME[3] & Flanders Make[3]
Ghent University
Sint-Pietersnieuwstraat 33
9000 Ghent
Belgium
johan.gyselinck@ulb.be[2]
frederik.debelie@ugent.be[3]

1 Introduction

The ability to significantly participate in the frequency regulation and provide valuable ancillary services to the Transmission System Operator (TSO) is one of the present wind farm (WF) challenges, due to imprecision in wind speed forecasting and insufficient power reserve in certain operating conditions notably. In this work, the feasibility of WFs to participate in the utility grid through yaw control, is assessed. First, an advanced wake model is developed and a systematic approach is proposed to estimate its parameters from data generated via the FAST.Farm simulator. Next, a distributed yaw optimization algorithm is proposed so that an adequate trade-off between precision and computing time is reached. Following, the power gain resulting from yaw control is assessed for all the wind directions through simulations using the wake model. Finally, the worse duration of the wake transient associated to yaw control is evaluated.

The novel approach of this research is to view the wake redirection through yaw optimization as a surplus power reserve, enabling WF operators to be part of the grid frequency regulation. But each TSO has its own frequency control specifications. Since this work is part of the Belgian PhairywinD project[1], the specifications of the Belgian TSO, named ELIA, are considered. Besides, only the requirements of the secondary frequency regulation are taken into account, because the yaw actuator is not fast enough for the primary frequency regulation. There are two key requirements: the power bid must be higher than $1MW$, and it must be delivered at latest after $15min$ of response time.

2 Application and results

The investigation of the possibility to succeed ELIA requirements through yaw optimization control is performed based on the layout of the Belgian Mermaid offshore WF made of 28 wind turbines (WTs), with $5MW$ nominal power each. Thanks to the wake model and the proposed yaw optimization algorithm, the WF produced power can be maximized by controlling the yaw angle of each WT for a given wind speed and direction. Figure 1 depicts the power gain through yaw optimization for the wind speed range $U_0 \in [7.85; 10.24] m/s$ corresponding to the operation zone 2 of the WT, in all the wind directions. Zone 2 is considered because the wfake model has been validated only in the maximum power point tracking (MPPT) zone. The results show that the requirement for secondary frequency control defined by ELIA can be accomplished through yaw optimization in terms of power reserve, in almost all the wind speeds and directions. Finally, assessing the duration of the wake transient associated to yaw control, it has been shown that the yaw system is fast enough for ELIA time response requirement.

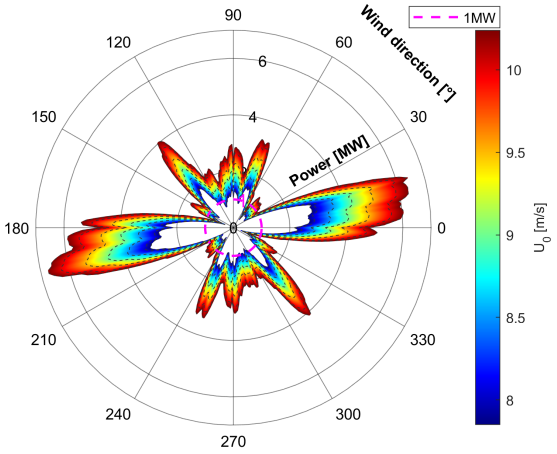

Figure 1: Mermaid power gain rose in MW, depending on the wind speed

3 Acknowledgement

This research is part of the Belgian PhairywinD project, funded by the Belgian FPS Economy.

References

[1] PhairyWind, 2020, [online] Available at: https://www.phairywind.be/.

On discretization of continuous-time LPV control solutions

Yorick Broens[1], Hans Butler[1,2] and Roland Tóth[1,3]
[1] Control Systems Group, Eindhoven University of Technology, Eindhoven, The Netherlands
[2] ASML, Veldhoven, The Netherlands
[3] Systems and Control Laboratory, Institute for Computer Science and Control, Budapest, Hungary
Email: Y.L.C.Broens@tue.nl

1 Introduction

In recent years, the Linear Parameter-Varying (LPV) framework has become increasingly useful for analysis and control of time-varying systems. Generally, LPV control synthesis is performed in the continuous-time (CT) domain due to significantly more intuitive performance shaping methods in CT, see [1]. However, the main complication of CT synthesis approaches is the successive implementation of the resulting CT control solutions on physical hardware. In the literature, several discretization methods have been developed for LPV systems, see [2]. However, most of these approaches necessitate heavy nonlinear operations introduced by the discretization of these time-varying matrices or can introduce significant approximation error, thereby severely limiting implementation capabilities of CT LPV control solutions. Alternatively, the w' discretization approach has been introduced in the LTI case to allow for preservation of the CT control, see [3]. Based on these observations, this paper aims at extending the w' discretization approach to LPV systems, such that implementation of CT LPV control solutions on physical hardware is simplified.

2 Approach

Consider a CT LPV state-space (SS) representation, denoted by G, which is given by:

$$\begin{bmatrix} \dot{x}(t) \\ y(t) \end{bmatrix} = \begin{bmatrix} A(p(t)) & B(p(t)) \\ C(p(t)) & D(p(t)) \end{bmatrix} \begin{bmatrix} x(t) \\ u(t) \end{bmatrix}, \tag{1}$$

where $p : \mathbb{R} \to \mathbb{P} \subseteq \mathbb{R}^{n_p}$ corresponds to the scheduling vector, $x : \mathbb{R} \to \mathbb{X} \subseteq \mathbb{R}^{n_x}$ is the state variable, $u : \mathbb{R} \to \mathbb{U} \subseteq \mathbb{R}^{n_u}$ denotes the control input and $y : \mathbb{R} \to \mathbb{Y} \subseteq \mathbb{R}^{n_y}$ corresponds to the output signal. In order to transform the CT LPV SS representation (1) to the w' domain, the frequency domain filter:

$$w' = \frac{2}{T_s}\frac{z-1}{z+1}, \tag{2}$$

is reformulated into an equivalent time-domain operator r:

$$r = \frac{2}{T_s}\frac{q-1}{q+1}, \tag{3}$$

where q corresponds to the shift operator and T_s is the sampling time. Moreover, the system represented by (1) is expressed in the w' domain as:

$$\begin{bmatrix} rx(k) \\ y(k) \end{bmatrix} = \begin{bmatrix} A(p(k)) & B(p(k)) \\ C(p(k)) & D(p(k)) \end{bmatrix} \begin{bmatrix} x(k) \\ u(k) \end{bmatrix}, \tag{4}$$

where the CT LPV SS matrices are preserved by defining the r^{-1} operator, see Figure 1, which corresponds to:

$$\begin{bmatrix} \xi(k+1) \\ x(k) \end{bmatrix} = \begin{bmatrix} I & 2I \\ \frac{T_s}{2}I & \frac{T_s}{2}I \end{bmatrix} \begin{bmatrix} \xi(k) \\ rx(k) \end{bmatrix} \tag{5}$$

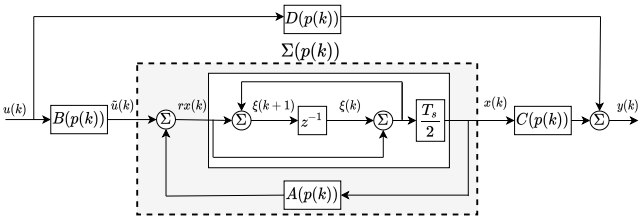

Figure 1: Block interconnection of the w' implementation, where the white area denotes the r^{-1} operator and $\Sigma(p(k))$ corresponds to the equivalent dynamics, which is used to remove the algebraic loop that is introduced by the r^{-1} operator.

From the structure of the r^{-1} operator, it is observed that it is identical to the Tustin operator, see [2]. Nonetheless, the proposed approach allows for discrete-time implementation using the CT LPV system matrices, thereby both preserving physical insight and simplification of the implementation procedure of CT LPV control solutions on physical hardware. In order to remove the algebraic loop that is introduced by the r^{-1} operator, see Figure 1, subsystem $\Sigma(p(k))$ is introduced, which is given by:

$$\begin{bmatrix} \xi(k+1) \\ x(k) \end{bmatrix} = \begin{bmatrix} I+\Phi(p(k))A(p(k))T_s & 2\Phi(p(k)) \\ \Phi(p(k))\frac{T_s}{2} & \Phi(p(k))\frac{T_s}{2} \end{bmatrix} \begin{bmatrix} \xi(k) \\ \tilde{u}(k) \end{bmatrix}, \tag{6}$$

where $\Phi(p(k)) = [I - A(p(k))\frac{T_s}{2}]^{-1}$. Moreover, the full discretized system, denoted by G_d, is given by:

$$G_d = C(p(k)) \cdot \Sigma(p(k)) \cdot B(p(k)) + D(p(k)), \tag{7}$$

where $\det\left(I - A(p(k))\frac{T_s}{2}\right) \neq 0 \; \forall \; p \in \mathbb{P}$.

3 Conclusions

It is observed that application of the w' discretization is equivalent with the Tustin discretization using the CT LPV SS matrices. Furthermore, implementing the w' discretization via the r^{-1} operator simplifies the implementation process of CT LPV control solutions on physical hardware while the physical interpretation of the CT LPV control solution is preserved.

References

[1] K. Zhou and J. C. Doyle, *Essentials of robust control*, vol. 104. Prentice hall Upper Saddle River, NJ, 1998.

[2] R. Tóth, *Modeling and identification of linear parameter-varying systems*, vol. 403. Springer, 2010.

[3] R. Whitbeck and L. Hofmannf, "Digital control law synthesis in the w'domain," *Journal of Guidance and Control*, vol. 1, no. 5, pp. 319–326, 1978.

A Frequency Domain Maximum Likelihood Approach to Estimate Space-Dependent Parameters in Heat and Mass Transport

Ricky van Kampen[1,2], Siep Weiland[3], Hans Zwart[4,5], Matthijs van Berkel[1]
[1] Energy Systems and Control Group, DIFFER, Eindhoven, the Netherlands
[2] Control Systems Technology Group, Eindhoven University of Technology, Eindhoven, the Netherlands
[3] Control Systems Group, Eindhoven University of Technology, Eindhoven, the Netherlands
[4] Dynamics and Control Group, Eindhoven University of Technology, Eindhoven, the Netherlands
[5] Mathematical Systems Theory, University of Twente, Enschede, the Netherlands
R.J.R.vanKampen@differ.nl

1 Introduction

Scalar transport (e.g. heat or mass) plays an important role in many different fields, such as physics and chemistry. For example, the efficiency of a nuclear fusion reactor is mainly determined by how much heat the core plasma (fuel) loses to the reactor wall [1]. Therefore, engineers and physicist are interested in reducing the transport. Another example is given in the field of hydrology, where heat is used as a tracer to determine the magnitude and direction of vertical ground water fluxes across streambeds to identify hot spots for contaminants and nutrients [2]. Typically, these transport phenomena are modeled around an operating point by a linear one-dimensional parabolic partial differential equation (PDE), commonly known as the advection-diffusion-reaction equation. However, in most physical systems the (exact) parameters dictating the transport are unknown. Hence, data-driven estimation of the unknown physical parameters is necessary to complete the model such that it can be used for simulation, analysis, prediction, and control. Here, our goal is to estimate these unknown physical parameters utilizing uncertain measurement data.

2 Problem Formulation

Consider the following 1D linear parabolic partial differential equation

$$\frac{\partial T}{\partial t} = D(x)\frac{\partial^2 T}{\partial x^2} + V(x)\frac{\partial T}{\partial x} + K(x)T + P(x)s(t), \qquad (1)$$

that governs the temperature $T(x,t)$ in the spatial domain $x \in [0,L]$ and time t. The functions $D(x)$, $V(x)$ and $K(x)$ represent the unknown physical parameters for the diffusivity, convectivity and reactivity. The input consists of the unknown spatial deposition profile $P(x)$ and the known modulation signal $s(t)$. Furthermore, the *boundary* and *initial* conditions are considered to be unknown.

The goal is to simultaneously estimate $D(x)$, $V(x)$, $K(x)$ and $P(x)$ based on $s(t)$ and the uncertain measurements $y(t) = \mathrm{col}\big(T(x_1,t),\ldots,T(x_M,t)\big) + v(t)$ on $M > 2$ locations, where $v(t)$ is a sequence of zero mean, identically distributed, independent random variables.

3 Methodology

In [3], we introduce a method to estimate spatially varying transport parameters by rewriting the problem as a linear least squares problem. This brings the advantage of a closed-form solution, thus a low computational cost, but the disadvantage of a high sensitivity to measurement uncertainty resulting in biased estimates. To properly deal with measurement uncertainty, a maximum likelihood approach has been developed.

We mainly follow the methodology from [3] that now results in a linear errors-in-variables problem. Then, the maximum likelihood solution is obtained by optimizing a nonlinear cost function using minimization techniques such as Gauss-Newton or Levenberg-Marquardt. In this way, we keep the advantage of the linearity of the problem as we have simple analytic expression for the derivatives, but also handle uncertainty in an optimal way.

4 Results

Using the maximum likelihood solution significantly reduces the error of the estimated transport parameters with respect to the closed-form solution, albeit with a significantly higher computational cost.

References

[1] M. van Berkel *et al. Automatica*, vol. 50, pp. 2113–2119, aug 2014.

[2] R. J. R. van Kampen *et al. Water Resources Research*, vol. 58, no. 3, p. e2021WR030886, 2022.

[3] R. J. R. van Kampen *et al. IEEE Control Systems Letters*, vol. 5, pp. 1681–1686, nov 2021.

Flux fit method for estimating transport parameters in nuclear fusion reactors based on perturbation analysis

J. H. Slief[1,2], R. J. R. van Kampen[1,3], M. W. Brookman[4], M. van Berkel[1]
[1] Energy Systems and Control group, DIFFER, Eindhoven, the Netherlands
[2] Science and Technology of Nuclear Fusion, Eindhoven University of Technology, Eindhoven, the Netherlands
[3] Control Systems Technology, Eindhoven University of Technology, Eindhoven, the Netherlands
[4] General Atomics, San Diego, USA
j.h.slief@differ.nl

Introduction

The transport of scalar quantities such as heat or mass is a process relevant in many fields of study. In 1D, this transport is governed by the following equation:

$$\frac{\partial}{\partial t}z(r,t) = -\nabla_r q(r,t) + s(r,t), \tag{1}$$

where z represents a (vector of) physical parameter(s) as a function of space r and time t, q represents the corresponding flux(es) and s is the collection of sources and sinks [2]. We use this equation to model the transport of heat in the core of a nuclear fusion reactor since the efficiency of the reactor depends strongly on the rate of heat loss from the reactor core. Hence, we wish to gain insight in the heat flux $q(r,t) = -D(r)\nabla_r z(r,t) - V(r)z(r,t)$, where z represents temperature and the heat flux is described in terms of a diffusive-convective model with diffusivity D and convectivity V. Note that our approach is also applicable to mass transport or any other scalar transport.

Problem statement

The specific problem we are interested in is to find spatial profiles for D and V based on spatially and temporally resolved measurements of z. For our application, we can assume that the distributed input is time-independent. Hence, it can be described by $s(r,t) = P(r)u(t)$. Since, in practice, $P(r)$ is not known exactly, we will also resolve $P(r)$ from the measurements of z. Our approach to resolve the spatial dependencies of D, V and P revolves around reformulating (1) in terms of the flux q and fit this to a diffusive-convective formulation of the flux. Hence, we call our method the 'flux fit' method [1].

Method

Our approach is based on the following: (i) we apply perturbation analysis to linearize the system by modulating a source term $\tilde{u}$ in time with a well known waveform and frequency; (ii) the resulting fluctuations $\tilde{z}$ are measured with sufficiently high spatial and temporal resolution; (iii) we analyze the measurements in the frequency domain; (iv) we assume cylindrical geometry, with r the radius of the cylinder; and (v) we parametrize the unknown profiles P, D and V in terms of a set of parameters $\beta = \left[\beta^P, \beta^D, \beta^V\right]$. This allows us to reformulate (1) in terms of a perturbed flux:

$$\tilde{Q}_{\mathrm{S}}(r,\omega,\beta^P) = \frac{1}{r}\int_0^r r'\left(P(r',\beta^P)\tilde{U}(\omega) - i\omega\tilde{Z}(r',\omega)\right)dr', \tag{2}$$

where the source modulation $\tilde{U}(\omega) = \mathcal{F}\{\tilde{u}(t)\}$ and $\tilde{Z}(r,\omega) = \mathcal{F}\{\tilde{z}(r,t)\}$ are well known (measured) quantities. $\mathcal{F}$ represents the Fourier transform. The diffusive-convective model for the flux is written as:

$$\tilde{Q}_{\mathrm{T}}(r,\omega,\beta^{D,V}) = -D(r,\beta^D)\frac{\partial}{\partial r}\tilde{Z}(r,\omega) - V(r,\beta^V)\tilde{Z}(r,\omega). \tag{3}$$

The unknown parameters β can be found through the minimum of the cost function, given by:

$$\chi^2 = \min_{\beta}\left|\left|\tilde{Q}_{\mathrm{S}}(r,\omega,\beta^P) - \tilde{Q}_{\mathrm{T}}(r,\omega,\beta^{D,V})\right|\right|^2, \tag{4}$$

where the residual is denoted by χ^2.

Results

We have applied and compared this method to other numerical methods to resolve D, V and P from measurements within the context of nuclear fusion. We show that estimates of P with our flux fit method are in remarkable agreement with the other methods. We also show that the accuracy of the estimation of P is crucial to the accuracy of the estimations of D and V.

References

[1] J. H. Slief *et al.* Phys. Plasma **29** 010703 (2022)
[2] M. W. Brookman *et al.* Phys. Plasma **28** 042507 (2021)

Subnetwork identification in diffusively coupled linear networks[1]

E.M.M. Kivits and P.M.J. Van den Hof
Control Systems Group, Department of Electrical Engineering
Eindhoven University of Technology, P.O. Box 513, 5600 MB Eindhoven, The Netherlands.
Email: e.m.m.kivits@tue.nl and p.m.j.vandenhof@tue.nl

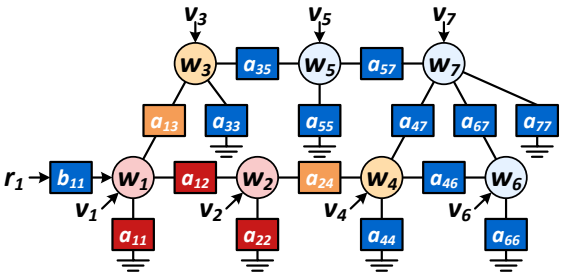

Figure 1: A diffusively coupled network with a target subnetwork (red) and its neighbour dynamics (orange).

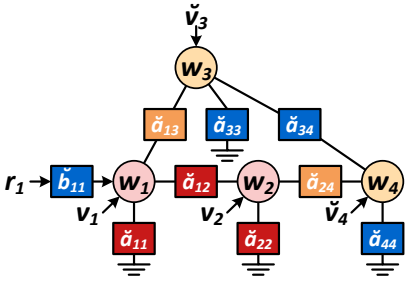

Figure 2: The immersed network resulting from immersing the blue nodes from the network in Figure 1.

1 Diffusively coupled network

A diffusively coupled network is characterized by symmetric interconnections and therefore, it is typically depicted by an undirected graph. This network is described by the polynomial model

$$A(q^{-1})w(t) = B(q^{-1})r(t) + v(t), \quad v(t) = F(q)e(t), \quad (1)$$

with node signals $w(t)$; excitation signals $r(t)$; white noise process $e(t)$; symmetric polynomial matrix $A(q^{-1}) = \sum_{k=0}^{n_a} A_k q^{-k}$ with A_0 full rank (typically not equal to I) and $A^{-1}(q^{-1})$ stable; polynomial matrix $B(q^{-1}) = \sum_{k=0}^{n_b} B_k q^{-k}$; and monic, stable and stably invertible rational matrix $F(q)$ [1]. The symmetry of the diffusive couplings is incorporated in the model (1) by the symmetry of $A(q^{-1})$.

A *subnetwork* contains the full information on how a selected set of node signals interacts. Figure 1 shows a diffusively coupled network with a subnetwork indicated in red.

2 Identification set-up

The identification of a subnetwork really becomes a local problem as only the node signals of the subnetwork and their neighbour node signals need to be measured. The unmeasured node signals can be discarding from the network model by eliminating them from the representation through an *immersion* procedure that preserves the network model structure [1]. This means that the $A(q^{-1})$-polynomial of the immersed network, indicated by $\breve{A}(q^{-1})$, remains to be symmetric. Figure 2 shows the immersed network corresponding to the network in Figure 1.

[1]This project has received funding from the European Research Council (ERC), Advanced Research Grant SYSDYNET, under the European Union's Horizon 2020 research and innovation programme (grant agreement No 694504).

3 Consistent subnetwork identification

The complete immersed network is consistently identified by the convex multi-step algorithm for full network identification in [1] if the following conditions are satisfied:

1. The true system is in the model set.
2. At least one excitation signal is present.
3. $\Phi_r(\omega) \succ 0$ for a sufficient number of frequencies.
4. The polynomials $\breve{A}(q^{-1})$ and $\breve{B}(q^{-1})$ are left coprime.
5. There exists a permutation matrix P such that $\begin{bmatrix}\breve{A}_0 & \breve{A}_1 & \cdots & \breve{A}_{\breve{n}_a} & \breve{B}_0 & \breve{B}_1 & \cdots & \breve{B}_{\breve{n}_b}\end{bmatrix} P = \begin{bmatrix} D & R \end{bmatrix}$, with D a square and diagonal matrix.
6. There is a parameter constraint on $\breve{A}(q^{-1})$ or $\breve{B}(q^{-1})$.

Here, we can choose a custom parameter constraint, which means that we identify a scaled version of the immersed network. This scaling is corrected in the identification of the target subnetwork by an additional parameter constraint.

The target subnetwork is consistently identified from the identified immersed network under the condition that

7. There is a parameter constraint on $A(q^{-1})$ or $B(q^{-1})$ of the target subnetwork.

Result: Conditions and an algorithm for consistent identification of a subnetwork.

References

[1] E.M.M. Kivits and P.M.J. Van den Hof, "Identification of diffusively coupled linear networks through sructured polynomial models," Submitted to IEEE Transactions on Automatic Control, 2022, ArXiv: 2106.01813.

Concurrent design of an electric fleet powertrain

Maurizio Clemente, Mauro Salazar,Theo Hofman
Eindhoven University of Technology
PO Box 513, 5600MB
Eindhoven, The Netherlands
m.clemente@tue.nl

1 Abstract

The transition to sustainable energy and mobility is not progressing fast enough to meet objectives set by world leaders. The NEON research program (New Energy Outlook for the Netherlands [1]) aims to address this problem by investing in innovative methods to accelerate this process in The Netherlands. Our focus is on electric mobility, which helps keep our cities less polluted and significantly reduces CO_2 emissions. Despite their growing number, electric vehicles still account for a small share of the total amount of cars [2] due to a larger upfront cost compared to petrol cars. In an effort to speed up the transition, we seek to reduce the vehicles' total cost of ownership (TCO), composed of the initial cost of the vehicle, and the cost of operations during its lifetime (energy usage and maintenance). In order to reach this goal, we employ a concurrent design optimization methodology that combines module-based product-family strategies with powertrain design. In particular, we leverage modularity and standardization of components in a fleet of electric vehicles to lower their production costs, while simultaneously minimizing consumption.

Module-based product-family strategies have been widely studied and employed by many industrial players to generate savings in research and development, quality control, interface design and integration. Besides, they allow for a more efficient development of differentiated products, increasing flexibility and responsiveness in manufacturing processes, reducing testing and certification times [3]. Traditionally, in a module-based product family, new products are instantiated by adding, substituting, and removing one or more functional modules [4], such as the battery pack or the electric motor. We speak of horizontal leveraging when more products share the same module for different applications while vertical leveraging involves scaling components to attack different market niches (Fig. 1).

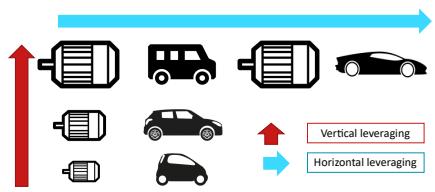

Figure 1: Leveraging strategies in a family of vehicles.

We introduce a framework consisting in designing optimal single-sized modules for the whole family of vehicles, using multiple copies of the same module instead of scaling in order to take full advantage of economy-of-scale strategies (Fig. 2). The module size is determined by employing a convex model of the vehicle consumption, taking into account the impact of changing components' sizes and multiplicity to find the optimal compromise between component and operational costs. The problem is framed as a convex second-order conic program, providing a solution that is guaranteed to be globally optimal.

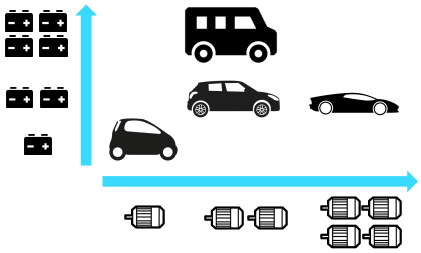

Figure 2: Concurrent design optimization of electric motor and the battery size in a fleet of battery electric vehicles.

Preliminary results show that the sum of component and operational cost, without considering benefits introduced by economy-of-scale and learning curves, only account for an increase of 3% of the TCO: a small percentage, compared to the potential savings. This is due to the fact that a module may be slightly oversized for one of the vehicles to satisfy the whole fleet at best. However, this comes together with an increase in performances, like shorter acceleration time or higher top speed. For these reasons, we believe this methodology has the potential to cut down production costs and accelerate the transition to electric vehicles.

References

[1] "NEON Research - Lighting the way to zero emission energy and mobility." Available online at https://neonresearch.nl/. (2021).

[2] "Global ev outlook 2020." Available online at https://www.iea.org/reports/global-ev-outlook-2020. (2020).

[3] D. Robertson and K. Ulrich, "Planning for product platforms," *Sloan Management Review*, 1998.

[4] T. Simpson, Z. Siddique, and R. J. Jiao, *Product Platform and Product Family Design Methods and Applications*. Springer US, 2006.

Modeling and State-Of-Health Prediction of Lithium-Ion batteries under dynamic, high-current applications

Francis le Roux
Control Systems Group
Eindhoven University of Technology
De Groene Loper 19, 5612 AP Eindhoven
The Netherlands
Email: f.a.l.le.roux@tue.nl

Ernst Ferg
Department of Chemistry
Nelson Mandela University
University Way, 6019 Gqeberha
South Africa
Email: ernst.ferg@mandela.ac.za

1 Introduction

In recent years, Lithium-Ion (Li-Ion) battery technologies have been implemented in various applications including Battery Electric Vehicles, Hybrid Electric Vehicles, power tools and, the replacement of the traditional Lead-acid Starting, Lighting, Ignition battery with a Li-Ion equivalent. The implementation of a Li-Ion SLI battery brings about a set of requirements that ensure performance as well as safety in application [1].
Upon implementing a Li-Ion battery under dynamic, high-current applications, the response of the battery becomes complex in comparison to conventional batteries used in energy storage solutions or Battery Electric Vehicles. This makes estimating the State-Of-Health (SOH) more challenging. In this work, we will apply Incremental Capacity Analysis (ICA) and Gaussian Process Regression for estimating the SOH.

2 Battery Simulation Model

Commercial software solutions were compared to model the Li-Ion battery on which SOH estimation would be applied, namely Siemens Simcenter Amesim and BaSiS Battery Simulation Software. To develop a SOH estimation algorithm, a Li-Ion battery model was developed in Siemens Simcenter Amesim. Cycling data was generated for a single cell under dynamic, high-current applications, at varying operating temperatures.
In order to test the developed SOH algorithm, a 12V Li-Ion battery was simulated in Siemens Simcenter Amesim. The model consisted of four series connected cells, with a thermal super-component connected to each cell. The battery was charged under a Constant-Current Constant-Voltage charge regime and underwent dynamic, high-current discharge.

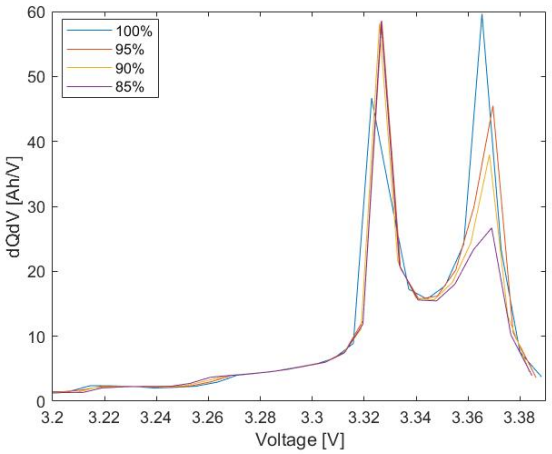

Figure 1: Incremental Capacity Analysis performed on charge data of simulated 12V Li-Ion battery

3 State-Of-Health Algorithm

ICA is the ratio of the change in capacity to change in voltage. ICA (Figure 1) was performed on the charge data of the simulated cell after which significant features were extracted. The features utilised to indicate the ageing of the cells were peak height, peak position and peak area. By training and testing the SOH model using Siemens Simcenter Amesin, the SOH model was found to estimate battery SOH efficiently at a temperature range of 25°C to 45°C [2].

References

[1] E. E. Ferg, F. Schuldt, and J. Schmidt. The challenges of a Li-ion starter lighting and ignition battery: A review from cradle to grave. *Journal of Power Sources*, 423:380–403, 5 2019.

[2] F A Le Roux. Modelling and State-Of-Health prediction of Lithium-Ion Batteries under Dynamic High-Current Applications, 2021.

Combined Cell-Level Estimation of State-of-Charge and Temperature in Battery Packs

B.A.C. van de Ven, R.W.H. Sneijders, F.S.J. Hoekstra, H.J. Bergveld, M.C.F. Donkers
Control Systems Group - Eindhoven University of Technology, The Netherlands
Email: {b.a.c.v.d.ven,f.s.j.hoekstra,h.j.bergveld,m.c.f.donkers}@tue.nl.

1 Introduction

Given the explosive demand for the electrification that currently exists, cell-level measurements, such as cell voltage and temperature, and estimations of the states inside battery packs, such as the State of Charge (SoC), are increasingly important. As these quantities are used for monitoring the operational limits of the battery pack, an accurate value is required for these by the battery management system. However, measuring all individual cell temperatures in a large battery pack can be an involved and costly procedure due to the required electronics. Furthermore, estimating the SoC without taking the temperature of each cell into account can lead to a errors in case of a non-uniform spread of temperatures inside the battery pack, so the accuracy of SoC estimation can be improved by knowing the temperatures on every individual cell. The downside of such an approach however is that this can be computationally heavy when using the approach normally used for SoC estimation [1].

2 Combined Estimation

A solution for this is to estimate both SoC and temperature using a combined thermal and electrical model for every individual cell inside the battery pack. This combined approach makes use of an empirical model to represent the electrical behaviour of the battery cells, this model is dependent on both SoC and temperature. Coupled to this, is a battery-pack thermal model, which uses a lumped-parameter model that represents the heat generation from the cells, as well as thermal conduction, convection and heat transport between cells. Together these models are embedded in an Extended Kalman Filter with Cross-correlated noise and Forgetting (EKF-CF), in which the model residual is used as noise covariance [2].

3 Results

Through the presented approach, we have estimated SoC and temperature using experimental data. This experimental data was acquired on a scaled-down battery pack with 9 parallel-connected cells using a realistic load profile, coming from a vehicle drive cycle, that excites the battery pack both electrically and thermally. Different cases have been considered in this work, ranging from completely ignoring temperature effects in the estimation (Case 0), measuring all cell temperatures (Case 1), estimating all cell temperatures (Case 2 and 3) and partial temperature estimation of cell temperatures with a limited number of measurements (Cases 4 and 5) [2]. The results are summarised in Table 1 and Figure 1. From these results, it can be concluded that both SoC an temperature can be reliably estimated with only a limited number or no temperature sensors. As a result of this, the presented approach could be used to reduce the number of required sensors, or to increase the fault tolerance of the battery pack.

Table 1: Estimation error of the estimation scenarios

Case	Scenario	SoC RMSE	T RMSE
0	No T Dependency	1.54	-
1	All Cell T Measured	0.73	-
2	All Cell T Estimated, No Model	0.74	4.17
3	All Cell T Estimated	0.69	1.26
4	Hybrid 1: Centre Cell Meas.	0.75	0.50
5	Hybrid 2: Diagonal Cells Meas.	0.72	0.45

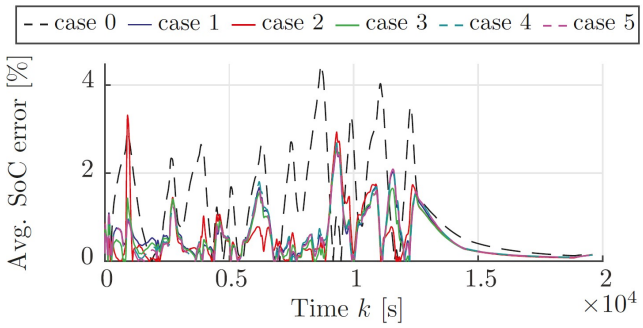

(a) SoC errors

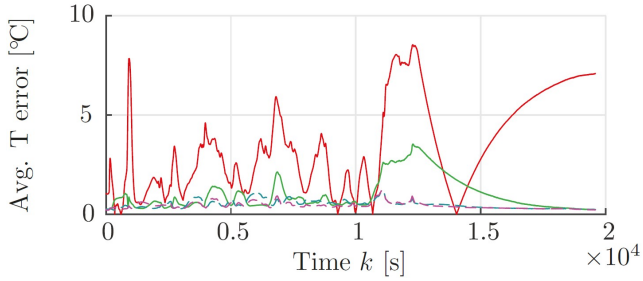

(b) Temperature errors

Figure 1: Averaged estimation (SoC, T) errors for Estimator variants 0 to 5.

References

[1] D. Zhang, L. D. Couto, P. Gill, S. Benjamin, W. Zeng, and S. J. Moura, "Interval observer for soc estimation in parallel-connected lithium-ion batteries," in *2020 American Control Conference (ACC)*. IEEE, 2020, pp. 1149–1154.

[2] B. A. C. van de Ven, R. W. H. Sneijders, F. S. J. Hoekstra, H. J. Bergveld, and M. C. F. Donkers, "Combined Cell-Level Estimation of State-of-Charge and Temperature in Battery Packs."

Tuning the stability margin for passivity-based controllers for standard mechanical systems

Carmen Chan-Zheng [1] , Pablo Borja [2], and Jacquelien M.A. Scherpen[3]

1 Introduction

The passivity-based control (PBC) is a well-established technique that offers a constructive approach for stabilizing a large class of complex systems [1]. Customarily, the control parameters of PBC approaches are selected such that its closed-loop system is stable. For instance, in [1, 2, 3] we find results on $\mathscr{L}_2$ stability, asymptotic stability, and input-to-state (ISS) stability. However, certain applications require other specific performance indices rather than stability. For instance, it is essential to ensure a prescribed performance (e.g., overshoot, gain margin, rate of convergence) to solve a task from applications involving mechanical systems that require high precision (e.g., aerospace, biomedics, semiconductor, among other industries).

In this abstract, we briefly summarize a tuning methodology for a class of PBC approaches which in closed-loop with a standard mechanical system result in some particular target dynamics that preserve the mechanical structure.

2 The tuning approach

Define $x := col(q,p)$, where $q,p \in R^n$ are the generalized positions and momenta vectors, respectively. Moreover, assume that a perturbed mechanical system has the following port-Hamiltonian structure

$$\dot{x} = (J_d(x) - R_d(x))\nabla H_d(x) + d(t,x) \tag{1}$$

with $d : R_{\geq 0} \times R^n \times R^n \to R^{2n}$ being the disturbance vector and

$$\begin{aligned} J_d(x) &:= \begin{bmatrix} 0_{n\times n} & M^{-1}(q)M_d(q) \\ -M_d(q)M^{-1}(q) & J_2(x) \end{bmatrix} \\ R_d(x) &:= \begin{bmatrix} 0_{n\times n} & 0_{n\times n} \\ 0_{n\times n} & D_d(q,p) \end{bmatrix} \\ H_d(x) &:= \frac{1}{2}p^\top M_d^{-1}(q)p + U_d(q), \end{aligned} \tag{2}$$

where $M_d : R^n \to R^{n\times n}$ is the desired inertia matrix that is positive definite; $U_d : R^n \to R_+$ is the desired potential energy which has a *strict minimum* at $q_\star \in R^n$; $H_d : R^n \times R^n \to R_+$ is the desired Hamiltonian with a *strict minimum* at $(q_\star, 0_n)$; $D_d : R^n \times R^n \to R^{n\times n}$ is the desired damping matrix that is positive semi-definite; and $J_2 : R^n \times R^n \to R^{n\times n}$ is skew symmetric.

Some PBC methodologies encountered in the literature that obtains the target dynamics in (1)-(2) can be found in [2, 4, 5].

We aim to exploit the ISS property (see [6]) in a quantitative manner. In other words, we provide an expression, obtained via a ISS analysis of (1)-(2), for the stability gain margin that is in terms of the *control parameters*, i.e., $M_d(q,p)$, $J_2(q,p)$, $D_d(q,p)$, $H_d(q,p)$. Here, we define the stability gain margin $g_m \in R_+$ as the maximum permissible growth of the norm of the disturbance with respect to the norm of the trajectories in which the closed-loop system remains ISS, i.e.,

$$\frac{\|d\|}{\|x\|} \leq g_m$$

We expect to apply the tuning methodology to prescribe the desired gain margin for an underactuated mechanical system.

[1]The work of C. Chan-Zheng is sponsored by the University of Costa Rica.

[2]P. Borja is with the department of Cognitive Robotics (COR), Faculty of Mechanical, Maritime and Materials Engineering, at TU Delft, 2628 CD Delft, The Netherlands (email: l.p.borjarosales@tudelft.nl).

[3]C. Chan-Zheng and J.M.A. Scherpen are with the Jan C. Willems Center for Systems and Control, and Engineering and Technology institute Groningen (ENTEG), Faculty of Science and Engineering at the University of Groningen, 9747 AG Groningen, The Netherlands (email: c.chan.zheng@rug.nl, j.m.a.scherpen@rug.nl).

References

[1] A.J. van der Schaft. *L2-Gain and Passivity Techniques in Nonlinear Control*. Springer International Publishing, 2017.

[2] P. Borja, R. Ortega, and J. M. A. Scherpen. New Results on Stabilization of port-Hamiltonian Systems via PID Passivity-based Control. *IEEE Transactions on Automatic Control*, pages 1–1, 2020.

[3] A. Donaire and T. Perez. Dynamic positioning of marine craft using a port-Hamiltonian framework. *Automatica*, 48(5):851–856, May 2012.

[4] F. Gómez-Estern and A.J. van der Schaft. Physical damping in IDA-PBC controlled underactuated mechanical systems. *European Journal of Control*, 10(5):451–468, 2004.

[5] T.C. Wesselink, P. Borja, and J.M.A. Scherpen. Saturated control without velocity measurements for planar robots with flexible joints. In *2019 IEEE 58th Conference on Decision and Control (CDC)*, pages 7093–7098, 2019.

[6] E. Sontag and Y. Wang. On characterizations of the input-to-state stability property. *Systems & Control Letters*, 24(5):351–359, 1995.

On Robust Fault Diagnosis of Complex Mechatronic Systems

Koen Classens[1], W.P.M.H. (Maurice) Heemels[1] and Tom Oomen[1,2]

[1]Dept. of Mechanical Engineering, Eindhoven University of Technology, The Netherlands
[2]Delft Center for Systems and Control, Delft University of Technology, The Netherlands
{K.H.J.Classens,W.P.M.H.Heemels,T.A.E.Oomen}@tue.nl

1 Background

The economic value of high-tech production equipment is proportional to its productivity. A key enabler for high productivity in manufacturing machines are positioning systems. The accuracy and speed of these positioning systems rely on an excellent and refined mechanical design in conjunction with effective control algorithms. Despite excellent mechanical system design and advanced control strategies, high-tech production equipment still undergoes a significant amount of downtime. To minimize this downtime, fault diagnosis systems are essential which facilitate effectively scheduled and targeted maintenance such that productivity is maximized [1].

2 Problem

Many fault diagnosis systems are based on parametric first principle models of the system. However, a complete and perfectly accurate mathematical model is never available, and the characteristics of the disturbances and noise are typically unknown. Hence, there is always a mismatch between the actual process and its mathematical model, even in the absence of faults. These discrepancies cause fundamental difficulties in fault detection and isolation (FDI) applications. The effect of modeling uncertainties is therefore a crucial point in the model-based FDI concept, and the solution of this problem is the key for its practical applicability. The aim is to explicitly take model uncertainty into account, such that a robust FDI system can be designed that provides performance guarantees when implemented on the true system.

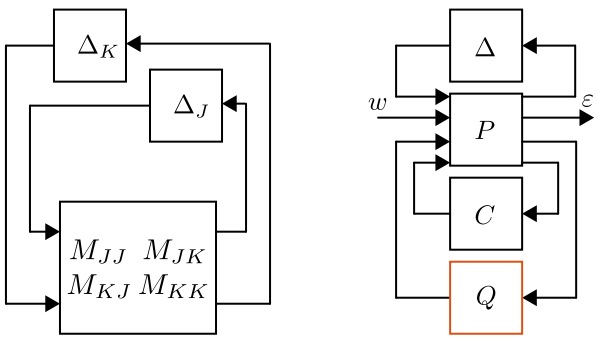

Figure 1: Generalized structured singular value, μ_g, analysis test (left) and closed-loop configuration for fault detection by means of the residual signal ε (right).

3 Approach

The proposed approach integrates prior information, i.e., models that are available from controller design, with posterior information in the form of experimental input/output data during normal operating conditions. The fault diagnosis system is designed by explicitly taking uncertainty and disturbances into account, while guaranteeing a specified fault sensitivity. To this end, the problem is posed as an $\mathscr{H}_\infty/\mathscr{H}_-$ optimization problem, which builds upon well-established theory adopted from the field of advanced motion control, i.e., the generalized structured singular value μ_g [2] and μ synthesis [3], see Figure 1. The approach is evaluated through a numerical analysis.

4 Results

It is shown that effective robust fault diagnosis systems can be synthesized by means of LMI optimization, solving the $\mathscr{H}_\infty/\mathscr{H}_-$ problem. By means of a numerical case study, resembling a next-generation positioning system, its effectiveness is illustrated. The fault diagnosis system guarantees specified performance criteria, which are analyzed using the generalized structured singular value μ_g [2].

5 Outlook

The main focus of this abstract lies in the generation of useful residual signals. In the future, more emphasis will be put on fault isolation. In addition, the proposed robust fault diagnosis filters will be implemented on a next-generation wafer stage.

References

[1] K. Classens, W. P. M. H. Heemels, and T. Oomen, "Digital Twins in Mechatronics: From Model-based Control to Predictive Maintenance," in *2021 IEEE International Conference on Digital Twins and Parallel Intelligence*, Beijing, China, 2021.

[2] M. Newlin and R. Smith, "A generalization of the structured singular value and its application to model validation," *IEEE Transactions on Automatic Control*, vol. 43, no. 7, pp. 901–907, 1998.

[3] S. Skogestad and I. Postlethwaite, *Multivariable Feedback Control Analysis and Design*, Second Edition. John Wiley & Sons, 2001.

This work is supported by Topconsortia voor Kennis en Innovatie (TKI), and is supported by ASML Research, Veldhoven, The Netherlands.

A Saturation-Aware Trajectory-Based Explicit Reference Governor for a Robotic Manipulator

M. Ambrosino [1], A. Cotorruelo[1], and E. Garone[1]

[1]Service d'Automatique et d'Analyse des Systèmes, Université Libre de Bruxelles, Brussels, Belgium.
[1]Email corresponding author: Michele.ambrosino@ulb.be

1 Problem Statement

Consider the general n-degree-of-freedom serial rigid robot manipulator, whose dynamics are modeled as

$$B(q)\ddot{q}+C(q,\dot{q})\dot{q}+g(q)=\tau, \tag{1}$$

where q, $\dot{q}$, $\ddot{q}\in\mathbb{R}^n$ are the vector of joint positions, velocities and accelerations, respectively; $B(q)\in\mathbb{R}^{n\times n}$ is the inertia matrix, $C(q,\dot{q})\in\mathbb{R}^{n\times n}$ is the centripetal-Coriolis matrix, $g(q)\in\mathbb{R}^n$ is the gravity vector, and $\tau\in\mathbb{R}^n$ is the control input vector. Typically, these systems are subject to joint range constraints and maximum joint velocity constraints. Typically, actuator saturation has been modeled as a constraint on the input, *i.e.* $\tau_{min,i}\leq\tau_i\leq\tau_{max,i}$, $i=1,\dots,n$, for some lower and upper actuator limits $\tau_{min,i}$, $\tau_{max,i}\in\mathbb{R}$, $i=1,\dots,n$. However, as proven in [2], modeling input saturation as a constraint entails a loss of performance in some cases, and should instead be modeled as intrinsic nonlinearities of the system. Doing so, allows us to re-write (1) as

$$B(q)\ddot{q}+C(q,\dot{q})\dot{q}+g(q)=\sigma(\tau), \tag{2}$$

where $\sigma:\mathbb{R}^n\to\mathbb{R}^n$ is a generalized saturation function.

In this work we propose a saturation-aware trajectory-based Explicit Reference Governor (ERG) scheme to control the system (2).

2 Control Scheme

The control scheme proposed in this work decouples the stabilization of the system and the satisfaction of the constraints [1]. An *inner loop controller* pre-stabilizes the system, in this paper we use a PD with gravity compensation. A *governing unit* modifies the reference fed to the system in such a way that constraints are fulfilled at all times by continuously manipulating the derivative of the applied reference as the product of two terms: the Navigation Field (NF) ρ, and the Dynamic Safety Margin (DSM) Δ. More formally.

3 Results

To show the efficency of our approach, we compare the proposed control strategy with constraints control strategies proposed in [2] and in [1]. As shown in Fig.1, the proposed control scheme is able to drive the robot from the initial to the desired configurations while fulfilling the velocity and position constraints. Moreover, it can be seen that our scheme outperformed the Constrained ERG implemented in [1] both in performance and computational times, Tab.1. However, even if the study shows that the RG strategies exhibit a higher performance than the ERG strategies, from a computational point of view, the ERG schemes provide a significant lower cost.

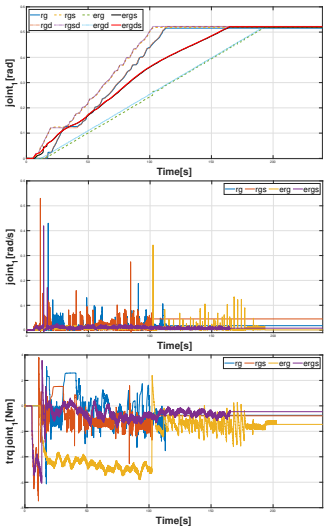

Figure 1: Time evolution of the position/velocity/torque joint #1.

Control Strategy	Avg. Time [ms]
Constrained RG [2]	0.1768
Saturated RG [2]	0.1627
Constrained ERG [1]	0.0152
Saturated ERG	**0.0141**

Table 1: Average computational times

References

[1] Merckaert, Kelly, et al. "Real-time motion control of robotic manipulators for safe human–robot coexistence." Robotics and Computer-Integrated Manufacturing 73 (2022).

[2] Cotorruelo, Andres, Daniel Limon, and Emanuele Garone. "Output admissible sets and reference governors: Saturations are not constraints!." IEEE Transactions on Automatic Control 65.3 (2019): 1192-1196.

Spectrum optimization of time-delay systems applied to non-collocated vibration suppression

Adrian Saldanha, Haik Silm, and Wim Michiels
NUMA, Department of Computer Science, KU Leuven,
Celestijnenlaan 200a, 3001 Leuven, Belgium
Email: adrian.saldanha@kuleuven.be

Tomas Vyhlidal
Faculty of Mechanical Engineering,CTU,
166 36 Prague 6, Czechia

1 Background

In this work, a control design method is proposed for simultaneous shaping of poles and zeros of a linear time-invariant system, motivated by the application of non-collocated vibration suppression in multibody systems. The phenomenon of non-collocated suppression arises in situations, wherein it is either not possible or infeasible to attach an absorber directly onto the target mass whose vibrations are to be suppressed. The control effort must instead be applied remotely from the target mass, which explains the term 'non-collocated suppression'. In the spring-mass-damper system model shown in Figure 1, the system is excited by an external harmonic force f of frequency ω and the target mass is m_1. This is a typical case of non-collocated suppression since the control input u for suppressing vibrations at m_1 is not applied locally but instead applied remotely at m_2. This requirement of completely suppressing vibrations of a prescribed frequency at a target location, coupled with achieving any higher level control task, thereby leads to a multi-objective controller design problem.

2 Mathematical Formulation

Consider the state-space model of an LTI system as:

$$\begin{aligned} \dot{x}(t) &= Ax(t) + Bf(t) + B_1 u(t) \\ y(t) &= Cx(t). \end{aligned} \tag{1}$$

where $u(t) = Ky_1(t-\tau)$ and $y_1(t) = C_1 x(t)$. Here, $A \in \mathbb{R}^{n\times n}$ is the system matrix, $B \in \mathbb{R}^{n\times 1}$ is the input matrix describing where the excitation force $f(t)$ acts and $C \in \mathbb{R}^{1\times n}$ is the matrix corresponding to the position of the target. The matrices $B_1 \in \mathbb{R}^{n\times p}$ and $C_1 \in \mathbb{R}^{q\times n}$ denote the controller input matrix and the sensor output matrices respectively, $K \in \mathbb{R}^{p\times q}$ represents the controller gain matrix to be determined and $\tau > 0$ represents a non-negligible delay due to measurement lag.

A complete suppression of vibrations at the target can be translated into the presence of zeros of the transfer function from f to y. This requirement, along with maximizing the decay rate of the solutions to improve the stability margin of the closed-loop system can be translated into a constrained

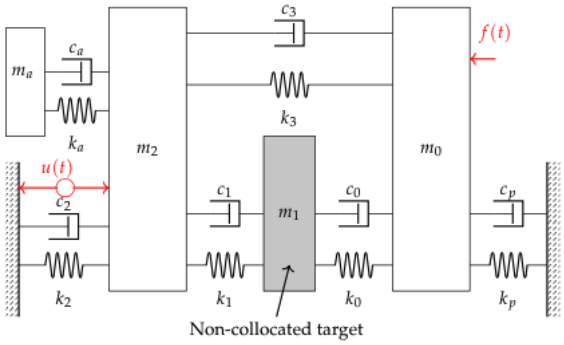

Figure 1: Force $f(t)$ is the external excitation force of frequency ω and mass m_1 is the target mass.

optimization problem in K:

$$\begin{aligned} &\min_{K\in\mathbb{R}^{p\times q}} \ \alpha(K) \\ &\text{s.t.} \quad h_i(K) = 0, \quad i = 1,\dots,m \end{aligned} \tag{2}$$

where $\alpha(K)$ is the spectral abscissa function,

$$\alpha(K) := \sup\left\{\Re(\lambda) : \left|\lambda I - A - B_1 K C_1 e^{-\lambda\tau}\right| = 0\right\}$$

and the constraints $h_i(K) = 0$ impose zeros at the target frequencies.

3 Solution

Problem (2) is challenging since the objective function is in general a non-smooth, non-convex function, while the constraint functions are multi-variable polynomial functions in K. This work presents a method for solving the above optimization task by converting the constrained optimization problem into an unconstrained one by elimination. Due to the polynomial equation in K, the constraints cannot be eliminated easily. To circumvent this difficulty, two methods are presented here, which exploit the property that in general, the constraints are affine in a *subset* of the controller parameters.

References

[1] W. Michiels, T. Vyhlídal, and P. Zítek, "Control design for time-delay systems based on quasi-direct pole placement," Journal of Process Control, vol. 20, no. 3, pp. 337–343, Mar. 2010.

Constrained Optimal System Design for Active Vibration Isolation Systems.

Sil Spanjer, Wouter Hakvoort
Department of Mechanics of Solids, Surfaces and Systems (MS3), University of Twente
Email: {s.t.spanjer, w.b.j.hakvoort}@utwente.nl

1 Introduction

Vibration isolation systems are designed to attenuate the sensitivity to direct and indirect disturbances on a vibration sensitive payload. Direct disturbances act on the sensitive payload, and indirect disturbances work through the vibration isolation system on the sensitive payload. For passive vibration isolation systems with a fixed mass, there is a trade-off between the sensitivity to these direct and indirect disturbances, which is determined by the suspension frequency and relative damping [1].
A major justification for the use of active vibration isolation systems (AVIS) is the circumvention of this trade-off [1]. However, the performance of AVIS is still depending on the suspension frequency when taking into account the sensor and actuator noise [2]. These additional noise sources affect performance though the system dynamics as well as the controllers, which motivates the development of a combined optimization method for both mechanical and control design. This method extends on [2] by implementing a constrained H_2 controller.

2 Method

The AVIS can be described with the following state space model in generalized plant format

$$\begin{bmatrix} \dot{F}_a \\ \dot{\varepsilon} \\ \ddot{\varepsilon} \end{bmatrix} = \begin{bmatrix} -\omega_a & 0 & 0 \\ 0 & 0 & 1 \\ \frac{1}{m_1} & \frac{-k}{m_1} & \frac{-d}{m_1} \end{bmatrix} \begin{bmatrix} F_a \\ \varepsilon \\ \dot{\varepsilon} \end{bmatrix} + \left[\begin{array}{ccc|cc} 0 & \omega_a & 0 & 0 & \omega_a \\ 0 & 0 & 0 & 0 & 0 \\ -1 & 0 & 0 & 0 & 0 \end{array}\right] \begin{bmatrix} a_0 \\ V_d \\ n_0 \\ n_1 \\ V_a \end{bmatrix}$$

$$\begin{bmatrix} a_1 \\ \varepsilon \\ V_a \\ \tilde{a}_0 \\ \tilde{a}_1 \end{bmatrix} = \left[\begin{array}{ccc} \frac{1}{m_1} & \frac{-k_1}{m_1} & \frac{-d_1}{m_1} \\ 0 & 1 & 0 \\ 0 & 0 & 0 \\ \hline 0 & 0 & 0 \\ \frac{1}{m_1} & \frac{-k_1}{m_1} & \frac{-d_1}{m_1} \end{array}\right] \begin{bmatrix} F_a \\ \varepsilon \\ \dot{\varepsilon} \end{bmatrix} + \left[\begin{array}{ccccc} 0 & 0 & 0 & 0 & 0 \\ 0 & 0 & 0 & 0 & 0 \\ 0 & 0 & 0 & 0 & 1 \\ \hline 1 & 0 & 1 & 0 & 0 \\ 0 & 0 & 0 & 1 & 0 \end{array}\right] \begin{bmatrix} a_0 \\ V_d \\ n_0 \\ n_1 \\ V_a \end{bmatrix}, \tag{1}$$

where x_1 is the position of the sensitive payload, x_0 the position of the floor, $\varepsilon = x_1 - x_0$, V_d the direct (voltage) disturbance, n_0 and n_1 the sensor noises of the accelerometers which measure $\ddot{x}_0$ and $\ddot{x}_1$ respectively. The system is parametrized by the suspension stiffness k_1, damping d_1, mass of the sensitive payload m_1, and actuator pole ω_a. Further, V_a is the actuator voltage, being the controlled input, and the $\tilde{\cdot}$ symbol is used for a measured signal.
A frequency dependent input scaling matrix is used to impose the relevant input spectra for noise sources and floor vibration. The constraints are implemented by using relative weighing of the output channels $[a_1,\ \varepsilon,\ V_a]^T$. The optimal weights are iteratively determined using a bisection algorithm. The constraints are based on the thermal limit of the actuator, and the allowable stress in a parallel leafspring setup.

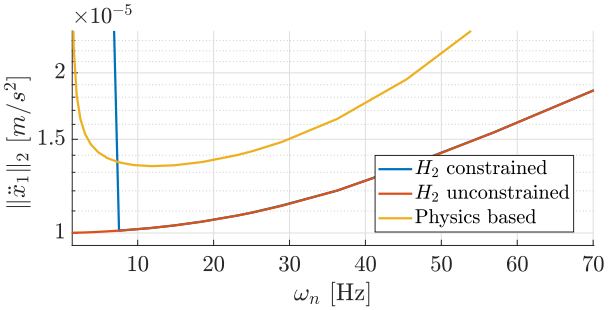

Figure 1: $\|x_1\|_2$ for three controllers and varying ω_n.

3 Results and Conclusion

An illustrative example of the optimal design method is given as a variation over the suspension frequency ω_n. Here, the relative damping of the system is kept constant. In figure 1, $\|\ddot{x}_1\|_2$ is given for the constrained H_2 controller, and is compared to the unconstrained H_2 and a physics based controller [2]. The physics based controller consists of a disturbance feedforward and a skyhook damper feedback controller, where the relative damping of the closed loop suspension is kept constant. In figure 1, the optimal mechanical design depends on the used control method. Taking into account this interaction yields a significant performance improvement.

References

[1] M. Beijen, M. Heertjes, H. Butler, and M. Steinbuch, "H_∞ feedback and feedforward controller design for active vibration isolators," *IFAC-PapersOnLine*, vol. 50, no. 1, pp. 13384–13389, 2017.

[2] S. T. Spanjer and W. Hakvoort, "Optimal active vibration isolation systems for multiple noise sources," in *2021 European Control Conference (ECC)*, pp. 2473–2478, IEEE, 2021.

Active Metamaterial Vibration Suppression in Flexure Mechanisms

Bram Seinhorst, Wouter Hakvoort
chair of Precision Engineering, University of Twente
P.O. Box 217, 7500 AE Enschede, The Netherlands
Email: {b.seinhorst/w.b.j.hakvoort}@utwente.nl

1 Introduction

The inherent lack of backlash and friction in flexure mechanisms makes them ideal for high precision applications. However, these flexure mechanisms also have low internal damping, resulting in undamped vibrations. These vibrations do not only occur in the desired movement direction of the mechanism, but also in support directions. In this work we propose to include active material in the flexure mechanism, such that the support vibrations can be damped.

2 A cross hinge case

We consider a model of a cross-hinge that has been designed as an actuator suspension, inspired by [1]. An aluminium payload is suspended between two cross flexure pivot hinges, as shown in Figure 1. The payload is actuated by a moment τ and the rotation θ is measured. The rotation of the hinge is controlled by a PID-controller with a crossover of 300 rad/s and a phase margin of 45°. The center of mass of payload is slightly offset from the rotation axis of the hinges. As a result, actuation of the rotation of the hinge also results in slight excitation of a modeshape corresponding to translational movement of the end-effector mass. The corresponding modeshape is shown in Figure 1.

By adding piezoelectric patches to either side of the leaf springs, we can use active damping to suppress the unwanted modeshape. In figure 1 the patches are drawn with a pink color. Due to the limited allowable strain in the patches, they are only included at the base of the leaf springs. For each pair of patches, we use a positive position feedback controller [2]. The controllers are tuned to 630 rad/s, the resonance frequency of the unwanted parasitic modeshape under 15° rotation.

3 Results

In order to investigate the excitation of these parasitic modes, we take a look at the linearised closed-loop transfer from reference θ_{ref} to vertical position of the center of mass of the hinge z_{com}, for various nominal rotations. The resulting vibration transfer with and without active control are visualised in figure 2. It can be seen that with larger nominal deflection, the resonance peak is increasingly suppressed. Hence, supression of the problematic resonance in deflected state is achieved.

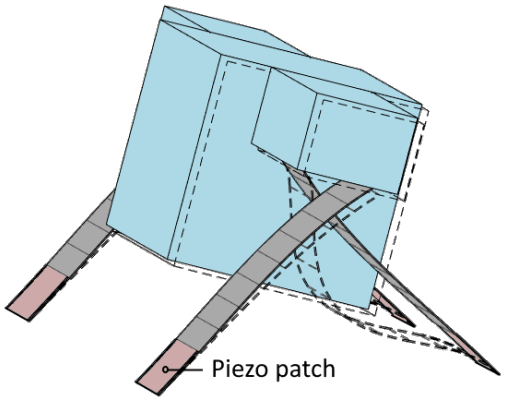

Figure 1: The flexure suspended mass under 15° deflection. The dashed lines indicate a vibration mode that has dropped significantly in frequency due to deflection.

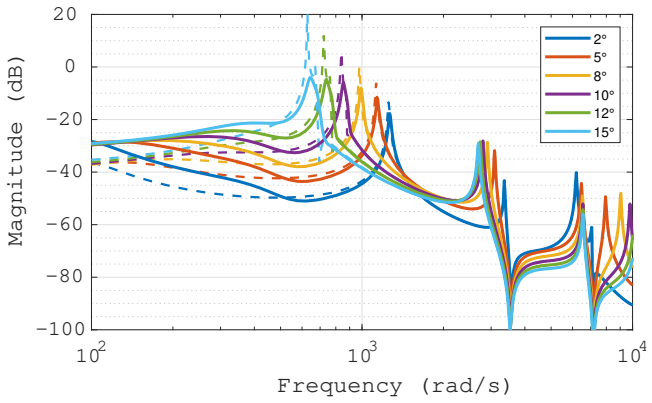

Figure 2: Transfer from θ_{ref} to z_{com} for various nominal rotations. The dashed lines indicate the response without active vibration control and the solid lines with active vibration control.

References

[1] M. Naves et al. “Flexure-based 60 degrees stroke actuator suspension for a high torque iron core motor” Precision Engineering, 2020.

[2] H. Syed, “Comparative study between positive position feedback and negative derivative feedback for vibration control of a flexible arm featuring piezoelectric actuator” International Journal of Advanced Robotic Systems, 2017.

On a sliding mode observer for a reaction-convection-diffusion model

Judicaël Mohet[a], Anthony Hastir[a], Habib Dimassi[b], Joseph J. Winkin[a] and Alain Vande Wouwer[c]
a: Namur Institute for Complex Systems (naXys) and Department of Mathematics,
University of Namur, Rue de Bruxelles 61, B-5000 Namur, Belgium
b: High Institute of applied sciences and technology of Sousse,
University of Sousse, Cité Taffala (Ibn Khaldoun), 4003 Sousse, Tunisia
c: Laboratoire d'Automatique, University of Mons, Boulevard Dolez 31, B-7000 Mons, Belgium
Email: judicael.mohet@unamur.be, anthony.hastir@unamur.be,
dimassihabib2013@gmail.com, joseph.winkin@unamur.be
and alain.vandewouwer@umons.ac.be

In this work, we build an observer for a linear reaction-convection-diffusion (RCD) system subject to a bounded disturbance $\phi(t)$, on the basis of a single measurement $y(t) = z(0,t)$. Due to the external disturbance, a sliding mode control law is used, [4]. In this talk, we deal with a continuation and improvements of the results obtained in [1]. In particular, we consider a new control law in order to avoid the on-line computation problem of the control. With $e = z - \hat{z}$ denoting the state estimation error, the errors dynamics are described by the partial differential equation

$$e'_t = De''_{xx} - e'_x - k_0 e + \phi - u,\ x \in [0,1],\ t \geqslant 0,$$

with initial condition $e(x,0) = e_0(x)$ and boundary conditions $De'_x(0,t) = e(0,t)$ and $e'_x(1,t) = 0$.

Our main contributions are the proof of the generation of a strongly continuous (C_0) and compact semigroup on the Sobolev space $\mathscr{H}^1(0,1)$ and the proof of the sliding movement (for a given initial error profile), despite the perturbation and the discontinuity of the input. We also improve the control law and prove the exponential stability of the error dynamics thanks to a new Lyapunov function. Finally, a comparison between the early and late lumping approaches is carried out.

We work on the space of absolutely continuous scalar and square integrable functions on $[0,1]$ whose first derivative is square integrable. This is the Sobolev space denoted by $\mathscr{H}^1(0,1)$. Since $\mathscr{H}^1(0,1) \subset L^2(0,1)$, we are able to prove that the RCD dynamics operator

$$-A = D\frac{d^2}{dx^2} - \frac{d}{dx} - k_0 I$$

is the infinitesimal generator of a C_0 and compact semigroup on $\mathscr{H}^1(0,1)$. Thanks to [3, Corollary 3.1], it follows that, for all initial errors $e_0 \in D(-A) \cap \ker C$, where C is the observation operator given by $Ch = h(0)$ for all $h \in \mathscr{H}^1(0,1)$, there exists a viable generalized solution in the sense of [3, Definition 2.1], for the error dynamics of the RCD system, whenever e_0 is in the ball of radius $\frac{\rho - L}{\alpha}$, where $\alpha > 0$, L is a bound on the disturbance and ρ is a design parameter of the sliding mode input $u(t) = \rho \frac{e(0,t)}{|e(0,t)|}$.

It is reported that the function

$$V(t) = \frac{D}{2}\left(e'_z(0,t)\right)^2 + \frac{1}{2}\int_0^1 \left(e'_z(s,t)\right)^2 ds$$

is a Lyapunov function for the RCD error model. Moreover, we establish the exponential stability of the RCD error system and show that the error trajectory tends to 0 uniformly and exponentially fast.

From the numerical point of view, the early lumping approach consists in an approximation of the PDE before designing the control law, whereas the discretization is done at the end of the process for the late lumping approach. The method described in [2], which is based on early lumping, was used for numerical simulations. It turns out that the results obtained in both case are very close. Finally, each method exhibits the exponential stability of the errors dynamics.

References

[1] Dimassi H., J.J. Winkin and A. Vande Wouwer, A sliding mode observer for a linear reaction–convection–diffusion equation with disturbances. Systems and control Letters **124** 40-48, 2019

[2] Edwards, C. and S.K. Spurgeon, Sliding mode control: theory and applications. CRC Press, 1998

[3] Levaggi L., Sliding modes in banach spaces. Differential an Integral Equation **15** 167-189, 2002

[4] Mohet J. et. al., Infinite-dimensional sliding mode state observer design for a disturbed linear reaction-convection-diffusion equation, in preparation.

Sampling-free Linear Iterative Bayesian Updating of Non-linear Model States

W. van Dijk, W.B.J. Hakvoort, B. Rosic
Department of Mechanics of Solids, Surfaces, and Systems (MS3), University of Twente
P.O. Box 217, 7500 AE Enschede, The Netherlands
{w.vandijk/w.b.j.hakvoort/b.rosic}@utwente.nl

1 Introduction

For highly non-linear dynamics and/or non-Gaussian distributed states, standard filters for state estimation lose their optimality or in extreme cases, fail altogether. In this work, a sampling-free filter is proposed that iteratively linearises the non-linear observation function without explicitly deriving the Jacobian.

2 Iterative Bayesian updating

Assume a continuous non-linear dynamical system,

$$\dot{\boldsymbol{x}} = f(\boldsymbol{x},t), \tag{1}$$

which is observed at discrete time moments k with an observation function $h(\cdot)$,

$$\boldsymbol{y}^k = h(\boldsymbol{x}^k) + w^k. \tag{2}$$

A general version of the Kalman filter is based on the conditional expectation of the random variable $\boldsymbol{x}^k$ given a measurement $\boldsymbol{y}^k$ [1], and can be written as:

$$\boldsymbol{x}_a^k(\omega) = \boldsymbol{x}_f^k(\omega) + \phi(\hat{\boldsymbol{y}}^k) - \phi(\boldsymbol{y}(\boldsymbol{x}_f^k(\omega))), \tag{3}$$

in which the map ϕ approximates the previously mentioned conditional expectation, $\phi(\boldsymbol{y}) \approx \mathbb{E}(\boldsymbol{x}|\boldsymbol{y})$, and $\boldsymbol{x}_f^k(\omega)$ represents our prior knowledge (i.e. uncertainty) on the state estimate.

Further assumptions on the map ϕ, such as linearity, as well as possible approximations of the highly nonlinear functions $f(\cdot)$ and $h(\cdot)$ in equations (1) and (2) will result in different types of filters. Two special cases of this are the classical and the ensemble Kalman filters [1], although many more exist.

In this work, a linear approximation of the observation function is made using an ensemble, i.e. $\hat{H} \approx h(\cdot)$. Subsequently, this approximation is updated by iteratively adjusting its linearisation point such that an unbiased filter is obtained.

Furthermore, the sampling based approximation of $h(\cdot)$ can be replaced using polynomial chaos expansions [3]. This results in a sampling-free filter, suitable for non-linear dynamics and non-Gaussian distributed states.

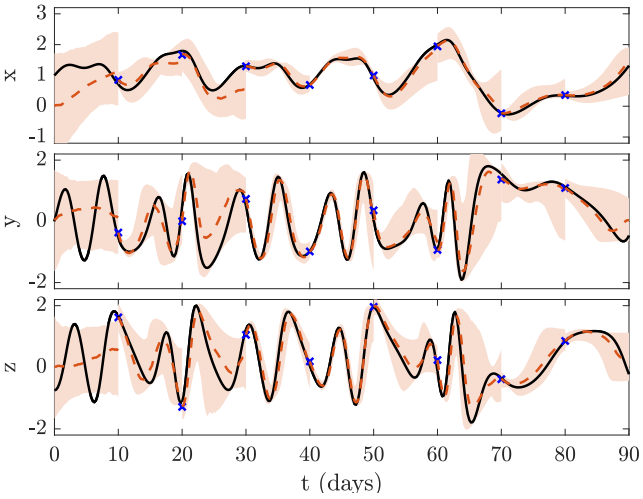

Figure 1: State estimation of the Lorenz 84 problem. (▬) Truth; (▪ ▪) Estimated mean; (▬) 90% confidence interval; (×) Linearisation point.

3 Results

The sample based iterative filter is applied on the Lorenz 84 [2] problem with nonlinear observations (Figure 1). As can be seen, the filter is able to track the the states of the system. Similar results are obtained for the sampling-free iterative filter, however, this filter requires more frequent measurements for accurate approximation of the observation function.

References

[1] B. Rosić, A. Kučerová, J, Sýkora, O. Pajonk, A. Litvinenko, H.G. Matthies, 2011. "Parameter Identification in a Probabilistic Setting", Engineering Structures, 50, (179-196).

[2] E.N. Lorenz, 1984, "Irregularity: a fundamental property of the atmosphere". Tellus A, 36(2), (98–110).

[3] O. Pajonk, B. Rosić, H.G. Matthies, 2013, "Sampling-free linear Bayesian updating of model state and parameters using a square root approach", Computers & Geosciences, 55, (70-83).

Real-time Fault Estimation for a Class of Discrete-Time Linear Parameter-Varying Systems

C. van der Ploeg[1,2], E. Silvas[1,2], N. van de Wouw[2], P. Mohajerin Esfahani[3]

[1] Netherlands Organisation for Applied Scientific Research, Integrated Vehicle Safety Group, 5700 AT Helmond, The Netherlands

[2]Department of Mechanical Engineering, Technische Universiteit Eindhoven, P.O. Box 513, 5600 MB Eindhoven, The Netherlands

[3]Delft Center for Systems and Control, Delft University, Mekelweg 2, 2628 CD Delft, The Netherlands

Email: C.J.v.d.Ploeg@tue.nl

1 Introduction

The detection, isolation, and/or estimation of faults is a crucial functionality to ensure the safety and efficiency of automated systems. Linear parameter-varying (LPV) fault detectors/estimators are often used to detect, isolate and estimate faults occurring in non-linear systems, for which the non-linearity can be captured in scheduling parameters. By approaching fault diagnosis of the non-linear system through linear systems theory, a generic and computationally efficient approach can be developed, making it highly relevant for safety-critical applications.

2 Problem statement

Consider a parameter-varying model as follows:

$$H(w_k,\mathfrak{q})[x]+L(w_k,\mathfrak{q})[z]+F(w_k,\mathfrak{q})[f]=0,$$

where $\mathfrak{q}$ represents the shift operator (i.e., $\mathfrak{q}[x(k)]=x(k+1)$) and x,z,f,w represent discrete-time signals indexed by the discrete time counter k. Here, x contains unknown signals (e.g., disturbances and unmeasured states), z represents the known signals (e.g., inputs/measurements) and f represents the fault(s) of interest. The matrices $H(w_k,\mathfrak{q}),L(w_k,\mathfrak{q}),F(w_k,\mathfrak{q})$ are parameter-varying polynomial functions in the variable $\mathfrak{q}$, depending on the parameter signal w. Finally, w represents a scheduling parameter of which the explicit relationship with time is unknown a priori, but the parameter is measurable in real-time. The main research challenge is formulated as finding a polynomial function $N(w_k,\mathfrak{q})$, which maps the known signal z to the fault(s) of interest, f, while decoupling any effect of the unknown signal x.

3 Proposed solution

To find the polynomial $N(w_k,\mathfrak{q})$, the following three contributions have been proposed [1]:

(i) **Parameter-varying filter synthesis:** We propose a novel parameter-varying polynomial decomposition for LPV dynamical systems, which paves the way for a convex reformulation of the isolation/estimation filter at each time instance.

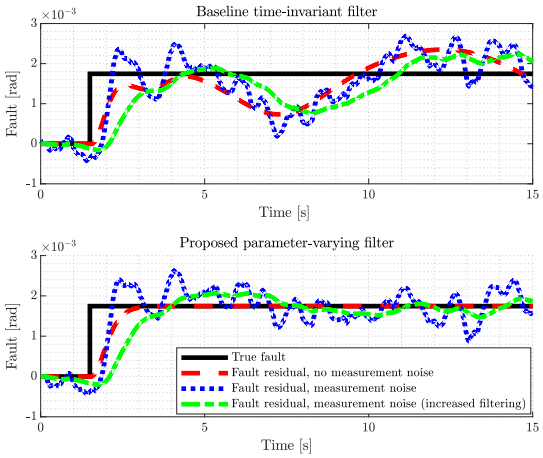

Figure 1: Performance of the baseline time-invariant and the proposed parameter-varying filter.

(ii) **Isolability conditions:** We offer the *existence* conditions of an isolation filter via a novel polynomial time-varying matrix construction. This allows for a *tractable* evaluation of isolability for LPV systems.

(iii) **Analytical solution:** We further propose an arbitrarily accurate approximation for the original program of the filter design whose solution is analytically available. This allows for *implementable* real-time filter synthesis while using valuable practical considerations in the context of LPV systems.

The estimation filter is demonstrated on offset estimation for the steering system of an automated vehicle. The results (Fig. 1) show that the LPV filter outperforms a time-invariant baseline and decouples the effect of the parameter variations and disturbances while performing well under the presence of noise.

References

[1] C. Van Der Ploeg, E. Silvas, N. Van De Wouw, and P. Mohajerin Esfahani. “Real-Time Fault Estimation for a Class of Discrete-Time Linear Parameter-Varying Systems”. In: *IEEE Control Systems Letters* 6 (2022), pp. 1988–1993.

On contraction analysis of switched systems with mixed contracting-noncontracting modes via mode-dependent average dwell time

Hao Yin, Bayu Jayawardhana, and Stephan Trenn
Jan C. Willems Center for Systems and Control, University of Groningen, 9747 AG Groningen, The Netherlands.
hao.yin@rug.nl, b.jayawardhana@rug.nl and s.trenn@rug.nl

1 Introduction

This paper studies contraction analysis of switched systems that are composed of a mixture of contracting and noncontracting modes. The first result pertains to the equivalence of the contraction of a switched system and the uniform global exponential stability of its variational system. Based on this equivalence property, sufficient conditions for a mode-dependent average dwell-time based switching law to be contractive are established. Correspondingly, LMI conditions are derived that allow for numerical validation of contraction property of switched linear systems, which include those with all unstable modes.

2 Problem formulation

Consider switched systems in the form of

$$\dot{x}(t) = f_{\sigma(t)}(x(t),t), \quad x(t_0) = x_0, \tag{1}$$

where $x(t) \in \mathscr{X} \subseteq \mathbb{R}^n$ is the state vector, $t_0 \in \mathbb{R}$ is the initial time and $x_0 \in \mathscr{X}$ is the initial value. For a switched system given by (1), it is called contracting if there exists positive numbers c and α such that for all solutions $x_1(t)$, $x_2(t)$ of (1) we have $\|x_1(t) - x_2(t)\| \leq ce^{-\alpha t}\|x_1(t_0) - x_2(t_0)\|$. The objective of this paper is to propose a sufficient condition that guarantees the switched system (1) is contracting with respect to switching law $\sigma(t)$ when not all modes of (1) are contracting, including the case where none of the modes is contracting.

3 Main Result

The family of (time-varying) linear switched system

$$\dot{\xi}(t) = F_{\sigma(t)}(x(t),t)\xi(t), \quad \xi(t_0) = \xi_0 \in \mathbb{R}^n \tag{2}$$

with $F_p(x(t),t) = \nabla_x f_p(x(t),t)$ and $x(\cdot)$ be any given solution trajectory of (1) is called uniformly globally exponentially stable (UGES), if there exist positive numbers c, α (independently of the chosen solution $x(\cdot)$) such that for every solution $\xi(t)$ of (2) the following inequality holds $\|\xi(t)\| \leq ce^{-\alpha t}\|\xi(t_0)\|$.

Proposition 1 *For a given switching signal $\sigma(t)$, the system* (1) *is contracting if, and only if, the family of systems* (2) *is UGES.*

Theorem 1 *Consider switched nonlinear system* (1) *with switching signal $\sigma : [0,\infty) \to \mathscr{M}$ and corresponding switching times $\mathscr{S} := \{t_0, t_1, \ldots, t_i, \ldots\}$. Assume that we can classify each mode p as being either stable or unstable, i.e. assume $\mathscr{M} = \mathscr{S} \dot{\cup} \mathscr{U}$ and, correspondingly, assume the switching signal σ has a MDADT $\tau_{ap} > 0$ for each stable mode $p \in \mathscr{S}$ and a MDALT $\tau_{ap} > 0$ for each unstable mode $p \in \mathscr{U}$. Furthermore, assume that for each mode $p \in \mathscr{M}$ there exist $\bar{\nu}_p \geq \underline{\nu}_p \geq 0$ and a continuously differentiable function $V_p : \mathbb{R}^n \times \mathbb{R}^n \times \mathbb{R}_{\geq 0} \to \mathbb{R}_{\geq 0}$ such that for all (x,ξ,t), $\underline{\nu}_p\|\xi\|_2^2 \leq V_p(x,\xi,t) \leq \bar{\nu}_p\|\xi\|_2^2, \forall p \in \mathscr{M}$, and $\dot{V}_p(x,\xi,t) \leq \eta_p V_p(x,\xi,t), \forall p \in \mathscr{M}$, with $\eta_p \geq 0$ if $p \in \mathscr{U}$ or $\eta_p < 0$ otherwise. Finally, assume that for every $p \in \mathscr{M}$, there exists $\mu_p > 0$ such that $V_{\sigma(t_i)}(x,\xi,t_i) \leq \mu_{\sigma(t_i^-)} V_{\sigma(t_i^-)}(x,\xi,t_i), \forall t_i \in \mathscr{S}$. Then the switched nonlinear system* (1) *is contracting if*

$$\left.\begin{aligned} \tau_{ap} > \underline{\tau}_{ap} &:= -\frac{\ln \mu_p}{\eta_p}, \quad \forall p \in \mathscr{S}, \\ \tau_{ap} < \overline{\tau}_{ap} &:= -\frac{\ln \mu_p}{\eta_p}, \quad \forall p \in \mathscr{U}. \end{aligned}\right\} \tag{3}$$

4 Simulation Results

In this numerical example, we apply our main results to the synchronization problem of one-way coupled identical oscillators, whose dynamics take the form

$$\dot{w} = f(w(t),t), \tag{4}$$

$$\dot{x} = f(x(t),t) + u_{\sigma(t)}(w(t)) - u_{\sigma(t)}(x(t)), \tag{5}$$

where $w(t), x(t) \in \mathbb{R}^n$ is the state vector, $f(w(t),t)$ is the dynamics of the uncoupled oscillators, and $u_{\sigma(t)}(w(t)) - u_{\sigma(t)}(x(t))$ is the switched coupling force.

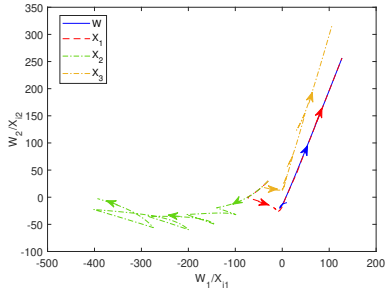

Efficient Abstraction of Switched Stochastic Systems Driven by Neural Networks

Steven Adams
TU Delft
S.J.L.Adams@tudelft.nl

Luca Laurenti
TU Delft
L.Laurenti@tudelft.nl

Morteza Lahijanian
University of Colorado Boulder
Morteza.Lahijanian@colorado.edu

1 Introduction

With the explosive growth of available data and computing resources, data-driven system identification has yielded impactful results across diverse disciplines, including control. Nevertheless, it is an open problem how to control with provable guarantees unknown non-linear dynamical systems against complex temporal logic specifications. Existing data-driven frameworks are generally limited to linear systems.

An approach to formal verification relies on the abstraction of the continuous-space stochastic models into discrete-space Markov processes. This approach requires well specified systems and lacks scalability to complex models, moreover, it is unclear how to derive abstractions of dynamical systems driven by neural networks. This paper introduces a scalable theoretical and computational synthesis framework for switched stochastic systems driven by neural networks (NN) in the continuous dynamics.

2 Problem Formulation

We consider the following continuous-domain, discrete-time switched stochastic process

$$x_{k+1} = f_{u_k}(x_k) + Gw_k, \tag{1}$$

where $x_k \in \mathbb{R}^n$, $u_k \in U$, and U is a finite set of modes. For every $u \in U, f_u : \mathbb{R}^n \to \mathbb{R}^n$ is a feed-forward NN. The noise term w_k is a vector of independent random normal distributed variables. The combination of NNs, known to be universal function approximators, and the inclusion of noise, make Process (1) a rich model.

We are interested in solving the following problem: Given a stochastic process of the form (1) and a linear temporal logic formula defined over finite traces (LTL$_f$) [1], find an optimal switching strategy that guarantees satisfaction of the LTL$_f$ formula with a probability greater than a given threshold.

3 Overview Approach

We approach the above problem by abstracting Process (1) using a finite-state Interval Markov decision process (IMDP) [2], whose interval-valued transition probabilities enable formal stochastic modeling. Due to the NNs highly non-linear nature, bounding the transition kernel of a NN-driven system is non-trivial and potentially computational expensive. We develop an efficient bounding procedure in which we employ Interval- and Linear Bound Propagation (IBP/LBP) techniques [3] and use the linearity of the additive Gaussian noise to evaluate in parallel the bounds for sorted batches of states per dimension. Next, we synthesize a strategy on the IMDP that maximizes the satisfaction probability of the LTL$_f$ specification.

4 Experimental Validation

Figure 1 provides an illustration of the control synthesis problem for a 4 mode system learned from a non-linear data set with additive noise. The LTL$_f$ is, 'eventually reach the black box' with a probability threshold $\varepsilon = 0.05$. We plot in green all states that satisfy the specification (lower bound $> 1-\varepsilon$), in red those with a probability smaller than ε (upper bound $< \varepsilon$) and in yellow states for which, due to uncertainty, we cannot claim if they satisfy or not the specification with a confidence epsilon.

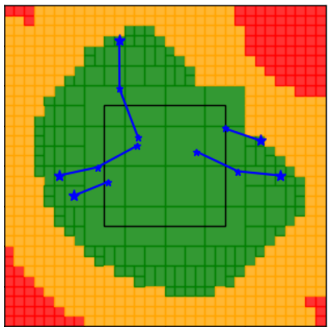

Figure 1: State classification for a system learned from a nonlinear data set under optimal switching strategy.

References

[1] G. De Giacomo and M. Y. Vardi, "Linear Temporal Logic and Linear Dynamic Logic on Finite Traces," *Twenty-Third International Joint Conference on Artificial Intelligence*, 2013.

[2] R. Givan, S. Leach, and T. Dean, "Bounded-parameter Markov decision processes," *Artificial Intelligence*, vol. 122, pp. 71–109, 2000.

[3] H. Zhang, T.-W. Weng, P.-Y. Chen, C.-J. Hsieh, and L. Daniel, "Efficient Neural Network Robustness Certification with General Activation Functions," *NeurIPS*, pp. 4939–4948, 11 2018.

The one-step function for discrete-time nonlinear switched singular systems

Sutrisno
Bernoulli Institute for Mathematics, CS and AI
University of Groningen
Nijenborgh 9, 9747 AG Groningen
The Netherlands
Email: s.sutrisno@rug.nl

Stephan Trenn
Bernoulli Institute for Mathematics, CS and AI
University of Groningen
Nijenborgh 9, 9747 AG Groningen
The Netherlands
Email: s.trenn@rug.nl

1 Introduction

Consider the class of switched systems where each mode is a discrete-time nonlinear singular system without input of the form

$$E_{\sigma(k)}x(k+1) = F_{\sigma(k)}(x(k)), \tag{1}$$

where $k \in \mathbb{N}$ is the time instant, $x(k) \in \mathbb{R}^n$ is the state, $\sigma : \mathbb{N} \to \{0,1,2,...,\mathtt{p}\}$ is the switching signal determining which mode $\sigma(k)$ is active at time instant k, $E_i \in \mathbb{R}^{n\times n}$ are singular with a constant rank i.e. $\operatorname{rank} E_i = r < n$, and $F_i(x) = (f_{1,i}(x), f_{2,i}(x), ..., f_{n,i}(x))^\top$ are vector valued functions of nonlinear functions with $f_{j,i} : \mathbb{R}^n \longrightarrow \mathbb{R}$. Define $\mathscr{S}_i := \{x \in \mathbb{R}^n : F_i(x) \in \operatorname{im} E\}$. From basic algebra, there exist invertible matrices $S_i, T_i \in \mathbb{R}^{n\times n}$ such that $S_i E_i T_i = \left[\begin{smallmatrix} I_r & 0 \\ 0 & 0 \end{smallmatrix}\right]$. By using the state transformation $T^{-1}_{\sigma(k)}x(k) = \binom{v(k)}{w(k)}$, $v \in \mathbb{R}^r$, $w \in \mathbb{R}^{n-r}$, system (1) can be rewritten as

$$\begin{aligned}\begin{bmatrix} I & 0 \\ 0 & 0 \end{bmatrix}\begin{pmatrix} v(k+1) \\ w(k+1) \end{pmatrix} &= S_{\sigma(k)}F_{\sigma(k)}\left(T_{\sigma(k)}\begin{pmatrix} v(k) \\ w(k) \end{pmatrix}\right) \\ &=: \begin{pmatrix} G_{\sigma(k)}(v(k),w(k)) \\ H_{\sigma(k)}(v(k),w(k)) \end{pmatrix}\end{aligned} \tag{2}$$

Inspired by the one-step map for linear switched singular systems in [1], in this study, we formulate the one-step function for nonlinear switched singular systems under the following assumptions:

Assumption 1.1. *For each $i \in \{0,1,...,\mathtt{p}\}$, $\mathscr{S}_i$ is a subspace.*

Assumption 1.2. $\mathscr{S}_i \cap \ker E_j = \{0\}$ $\forall i, j \in \{0,1,...,\mathtt{p}\}$.

Remark 1.3. Since $\mathscr{S}_i$ is a subspace, the nonlinear algebraic constraint $H_i(v,w) = 0$ is equivalent to a linear algebraic constraint. Hence, the nonlinearity appears now only on $G_i(v,w)$. However, we believe that the one-step function proposed in this study could be generalized for cases with $\mathscr{S}_i$ is not necessarily a subspace; this is our ongoing work.

2 Nonswitched Systems

We discuss in this section the solution for nonswitched cases of (1) of the form

$$Ex(k+1) = F(x(k)),\ k = 0,1,... \tag{3}$$

where $E \in \mathbb{R}^{n\times n}$ is singular. Recall $\mathscr{S} = \{x \in \mathbb{R}^n : F(x) \in \operatorname{im} E\}$, and suppose that Assumptions (1.1)-(1.2) hold.

Lemma 2.1. *System* (3) *has a solution with initial condition $x(0) = x_0 \in \mathbb{R}^n$ if, and only if, $x_0 \in \mathscr{S}$. Its solution is unique and satisfies*

$$x(k+1) = \Phi_(x(k)) = \Pi^{\ker E}_{\mathscr{S}} E^+ F(x(k))\ \forall k \in \mathbb{N}. \tag{4}$$

where E^+ is a generalized inverse of E and $\Pi^{\ker E}_{\mathscr{S}}$ is the (unique) projector onto $\mathscr{S}$ along $\ker E$.

Proof sketch: By a state transformation as in (2), system (3) can be rewritten as

$$\begin{pmatrix} I & 0 \\ 0 & 0 \end{pmatrix}\begin{pmatrix} v(k+1) \\ w(k+1) \end{pmatrix}(k+1) = \begin{pmatrix} G(v(k),w(k)) \\ H(v(k),w(k)) \end{pmatrix}$$

and by Assumption 1.2, $0 = H(v(k),w(k))$ has a solution, and thus (3) has a solution. From (3),

$$x(k+1) \in E^{-1}(F(x(k))) = \{E^+F(x(k))\} + \ker E \tag{5}$$

and $x(k+1)$ must also satisfy

$$x(k+1) \in \{x \in \mathbb{R}^n : F(x) \in \operatorname{im} E\} = \mathscr{S}. \tag{6}$$

By Assumption 1.2 and the projector lemma in [1], $x(k+1)$ satisfies (4) uniquely. □

3 Switched Systems

Based on the one-step function for nonswitched systems, we have the following theorem about the the one-step function for switched systems of the form (1).

Theorem 3.1. *System* (1) *under Assumptions 1.1-1.2 has a solution with initial condition $x(0) = x_0 \in \mathbb{R}^n$ if, and only if, $x_0 \in \mathscr{S}_{\sigma(0)}$. Its solution is unique and satisfies*

$$x(k+1) = \Phi_{\sigma(k+1),\sigma(k)}(x(k)),\ \forall k \in \mathbb{N} \tag{7}$$

where $\Phi_{i,j}$ is the one-step function from mode-j to mode-i given by

$$\Phi_{i,j}(x(k)) := \Pi^{\ker E_j}_{\mathscr{S}_i} E_j^+ F_j(x(k)) \tag{8}$$

where E_j^+ is a generalized inverse of E_j and $\Pi^{\ker E_j}_{\mathscr{S}_i}$ is the (unique) projector onto $\mathscr{S}_i$ along $\ker E_j$.

Proof sketch: The proof is a straightforward generalization from the proof for nonswitched systems by replacing (5)-(6) with

$$x(k+1) \in E_j^{-1}(F_j(x(k))) = \{E_j^+F_j(x(k))\} + \ker E_j,$$
$$x(k+1) \in \{x \in \mathbb{R}^n : F_i(x) \in \operatorname{im} E_i\} = \mathscr{S}_i$$

respectively. □

References

[1] Pham Ky Anh, et al. "The one-step-map for switched singular systems in discrete-time." *Proc. 58th IEEE Conf. Decision Control (CDC) 2019.*

Part 3
List of Participants

Leontine Aarnoudse
Dept. of Mechanical Engineering
Eindhoven University of Technology
l.i.m.aarnoudse@tue.nl

Flavia Sofia Acerbo
Engineering Services
Siemens Digital Industries Software
flavia.acerbo@siemens.com

S.J.L. Adams
Delft Center for Systems and Control
Delft University of Technology
s.j.l.adams@tudelft.nl

Filippo Airaldi
Delft Center for Systems and Control
Delft University of Technology
f.airaldi@tudelft.nl

MT Akan
Electrical Engineering
Eindhoven University of Technology
m.t.akan@tue.nl

Jean Pierre Allamaa
Engineering Services RTD
Siemens Digital Industries Software
jean.pierre.allamaa@siemens.com

MICHELE AMBROSINO
SAAS
UNIVERSITE LIBRE DE BRUXELLES
pascale.lathouwers@ulb.be

Anahita Amiri
Mechanical Engineering
Eindhoven University of Technology
a.amiri@tue.nl

Pieter Appeltans
Computer Science
KU Leuven
pieter.appeltans@kuleuven.be

Oscar Fabian Archila
SECO/Cntrol Sys. and Network Control Techno.
UMons/BTU Cottbus-Senftenberg
archilac@b-tu.de

Alejandro Astudillo
Department of Mechanical Engineering
MECO Research Team, KU Leuven
alejandro.astudillovigoya@kuleuven.be

Adrien Banse
ICTEAM
UCLouvain
adrien.banse@student.uclouvain.be

Rian Beck
DecisionS
Flanders Make
rian.beck@flandersmake.be

Gerben Beintema
Electrical Engineering
Eindhoven University of Technology
g.i.beintema@tue.nl

R.M. Beumer
Dept. of Mechanical Engineering
Eindhoven University of Technology
r.m.beumer@tue.nl

Satyajeet S. Bhonsale
BioTeC+
KU Leuven
jan.vanimpe@kuleuven.be

Lennart Blanken
Mechatronic System Design
Sioux Technologies B.V.
lennart.blanken@sioux.eu

Max Bolderman
Electrical Engineering
Eindhoven, University of Technology
m.bolderman@tue.nl

NICOLAS BONO ROSSELLO
SAAS
UNIVERSITE LIBRE DE BRUXELLES
pascale.lathouwers@ulb.be

Olaf Borsboom
Mechanical Engineering
Eindhoven University of Technology
o.j.t.borsboom@tue.nl

Mathias Bos
Dept. of Mechanical Engineering
KU Leuven
mathias.bos@kuleuven.be

Dimitris Boskos
DCSC
Delft University of Technology
d.boskos@tudelft.nl

Thomas Bosman
Energy Systems and Control
DIFFER
t.o.s.j.bosman@differ.nl

Nizar Bousselmi
Mathematical Engineering department
Université catholique de Louvain
nizar.bousselmi@uclouvain.be

Y.L.C. Broens
Electrical Engineering
Eindhoven University of Technology
Y.L.C.Broens@tue.nl

Michiel Busschaert
Department of Chemical Engineering
KU Leuven
michiel.busschaert@kuleuven.be

Sonveaux Candy
Dept. of Mathematics
University of Namur
candy.sonveaux@unamur.be

Carmen Chan
Engineering and Technology institute Groningen
University of Groningen
c.chan.zheng@rug.nl

Carmen Chan-Zheng
Engineering and Technology institute Groningen (ENTEG)
University of Groningen
c.chan.zheng@rug.nl

Hamin Chang
Mathematics, Computer Science and Artificial Intelligence
Bernoulli Institute
hmchang@cdsl.kr

Lotfi Chaouach
Delft Center for Systems and Control
TU Delft
l.m.chaouach@gmail.com

Xiupeng Chen
Engineering and technology institute
University of Groningen
xiupeng.chen@rug.nl

Valentin P. Chernev
Systems, Estimation, Control and Optimization
University of Mons
valentinplamenov.chernev@umons.ac.be

Koen Classens
Mechanical Engineering
Eindhoven University of Technology
k.h.j.classens@tue.nl

Maurizio Clemente
Control System Technology
University of Eindhoven
m.clemente@tue.nl

Sébastien Colla
ICTEAM
UCLouvain
sebastien.colla@uclouvain.be

Peter Coppens
Electrical Engineering
KU Leuven
peter.coppens@kuleuven.be

ANDRES COTORRUELLO
SAAS
UNIVERSITE LIBRE DE BRUXELLES
pascale.lathouwers@ulb.be

Tony Dang
DecisionS
Flanders Make
tonydangct@gmail.com

LUIS DANIEL COUTO MENDONCA
SAAS
UNIVERSITE LIBRE DE BRUXELLES
pascale.lathouwers@ulb.be

Sonia De Santis
Mechanical Engineering
KULeuven
jan.swevers@kuleuven.be

Wilm Decre
Mechanical Engineering
KU Leuven
wilm.decre@kuleuven.be

Delansnay Gilles
System, Estimation, Control and Estimation (SECO)
University of Mons
gilles.delansnay@umons.ac.be

Bruno Depraetere
DecisionS
Flanders Make
bruno.depraetere@flandersmake.be

Dries Dirckx
Mechanical Engineering
KU Leuven
dries.dirckx@kuleuven.be

Sadegh Ebrahimkhani
ELEC deptartment
Vrije Universiteit Brussel
Sadegh.Ebrahimkhani@vub.be

MHW Engelaar
Dept. of Electrical Engineering
Eindhoven University of Technology
m.h.w.engelaar@tue.nl

Brecht Evens
ESAT
KU Leuven
brecht.evens@kuleuven.be

Arash Farnam
Department of Electromechanical, Systems and Metal Engineering
Ghent University
arash.farnam@ugent.be

Rafael Fernandes Cunha
DTPA
University of Groningen
r.f.cunha@rug.nl

Alvaro Florez
Mechanical Engineering
MECO research team, KU Leuven
alvaro.florez@kuleuven.be

Stefanie Fonken
Electrical Engineering
Eindhoven University of technology
s.j.m.fonken@tue.nl

Joshua A. Foster
Engineering Technology
Vrije Universiteit Brussel
joshua.aiden.foster@vub.be

Karlijn Fransen
Systems Architecture
Vanderlande Industries B.V.
karlijn.fransen@vanderlande.com

Kathinka Frieswijk
Discrete Technology & Production Automation
University of Groningen
k.frieswijk@rug.nl

Prasoon Garg
Mechanical Engineering
PhD Student
p.garg.1@tue.nl

CVC Geelen
Biometris
Wageningen University
caspar.geelen@wur.nl

M.E. Geurts
Dept. of Mechanical Engineering
Eindhoven University of Technology
m.e.geurts@tue.nl

Farhad Ghanipoor
Mechanical Engineering Department,
Eindhoven University of Technology
f.ghanipoor@tue.nl

Leila Gharavi
Delft Center for Systems and Control
Delft University of Technology
L.Gharavi@tudelft.nl

J Gillis
Dept. of Mechanical Engineering
KU Leuven
joris.gillis@kuleuven.be

ALEJANDRO GOLDAR DAVILLA
SAAS
UNIVERSITE LIBRE DE BRUXELLES
pascale.lathouwers@ulb.be

Carlos Jose Gonzalez Rojas
Electrical Engineering Control Systems group
TUe
c.j.gonzalez.rojas@tue.nl

Viral Gosar
Mechanical Engineering
Eindhoven University of Technology
v.v.gosar@tue.nl

Shafaq Gul
Department of Electrical Energy, Metals, Mechanical Constructions & Systems
Ghent University, Member of Flanders Make
shafaq.gul@ugent.be

Marvyn Gulina
Dept. of Mathematic
University of Namur
marvyn.gulina@unamur.be

Rick Haasjes
Mechanical Engineering
University of Twente
r.haasjes@utwente.nl

Wouter Hakvoort
Department of Mechanics of Solids, Surfaces & Systems
University of Twente
w.b.j.hakvoort@utwente.nl

Noel Hallemans
Department ELEC
Vrije Universiteit Brussel
Noel.Hallemans@vub.be

Caspar Hanselaar
Mechanical Engineering
Eindhoven Technical University
c.a.j.hanselaar@tue.nl

Anthony Hastir
Department of mathematics
University of Namur
anthony.hastir@unamur.be

Haleh Hayati
Department of Mechanical Engineering
Eindhoven University of Technology
h.hayati@tue.nl

Kanghui He
Delft Center for Systems and Control
Delft University of Technology
K.He@tudelft.nl

Guillermo Legarda Herranz
IRIDIA-CoDE
Université libre de Bruxelles
guillermo.legarda.herranz@ulb.be

Marcel Heertjes
Mecahnical Engineering
Eindhoven University of Technology
m.f.heertjes@tue.nl

Anoosh Anjaneya Hegde
Engineering Services
Siemens Digital Industries Software
anoosh.hegde@siemens.com

Y.J.J. Heuts
Electrical Engineering
University of Technology Eindhoven
y.j.j.heuts@tue.nl

Teimour Hosseinalizadeh
Engineering and technology institute
University of Groningen
t.hosseinalizadeh@rug.nl

Antoine Huet
3BIO-BioControl
ULB
Antoine.Huet@ulb.be

B.C. van Huijgevoort
Control systems
Eindhoven University of Technology
b.c.v.huijgevoort@tue.nl

Anne-Men Huijzer
Bernoulli Institute for Mathematics, Computer Science and Artificial Intelligence and CogniGron
University of Groningen
m.a.huijzer@rug.nl

L.C. Iacob
Dept. of Electrical Engineering
Eindhoven University of Technology
l.c.iacob@tue.nl

Laurens Jacobs
Dept. of Mechanical Engineering
KU Leuven
laurens.jacobs@kuleuven.be

L.A.L. Janssen
Dept. of Mechanical Engineering
Eindhoven University of Technology
l.a.l.janssen@tue.nl

Bayu Jayawardhana
Engineering and Technology Institute Groningen
University of Groningen
b.jayawardhana@rug.nl

Woohyun Jeong
Graduate School of Mechanical and Aerospace Engineering
Gyeongsang National University,
woohyun.jeong@gnu.ac.kr

Bo Jin
Faculty of Science and Engineering
University of Groningen
b.jin@rug.nl

Dominique Joubert
Mathematical and Statistical Methods
Wagenignen University & Research
dominique.joubert@wur.nl

XAVIER JORDENS
SAAS
UNIVERSITE LIBRE DE BRUXELLES
pascale.lathouwers@ulb.be

Lydia Katsini
BioTeC+
KU Leuven
jan.vanimpe@kuleuven.be

Karel Keesman
Mathematical and Statistical Methods
Wageningen University
karel.keesman@wur.nl

Twan Keijzer
Delft Center for Systems and Control
Delft University of Technology
t.keijzer@tudelft.nl

Mahboubeh Keyvanara
Mechanical engineering
Postdoctoral researcher
m.keyvanara@tue.nl

David Kiessling
Mechanical Engineering
MECO Research Team, KU Leuven
david.kiessling@kuleuven.be

Edward Kikken
DecisionS lab
Flanders Make
edward.kikken@flandersmake.be

E.M.M. (Lizan) Kivits
Department of Electrical Engineering
Eindhoven University of Technology
e.m.m.kivits@tue.nl

Jesse Koenders
Energy Systems and Control Group
DIFFER
j.t.w.koenders@differ.nl

Krishna Dheeraj Kommuri
Mechanical Engineering
Technical University of Eindhoven
k.d.kommuri@tue.nl

Johan Kon
Dept. of Mechanical Engineering
Eindhoven University of Technology
j.j.kon@tue.nl

Danielle Kruijver
Department of Mechanics of Solids, Surfaces and Systen
University of Twente
d.m.e.kruijver@utwente.nl

Sibren Lagauw
ESAT
KU Leuven
sibren.lagauw@esat.kuleuven.be

Mouhamad Haidar Lakkis
Aerospace and Mechanical Engineering
University of Liege, Université Libre de Bruxelles
mhlakkis@uliege.be

Pau Lapiedra Carrasquer
BioTeC+
KU Leuven
jan.vanimpe@kuleuven.be

Jesús M. Zamudio Lara
SECO
Université de Mons
jmzl05@hotmail.com

John Lataire
Department ELEC
Vrije Universiteit Brussel
John.Lataire@vub.be

Francis le Roux
Dept of Electrical Engineering
Eindhoven University of Technology
f.a.l.le.roux@tue.nl

Ningbo Li
DTPA
University of Groningen
ningbo.li@rug.nl

Tinghua Li
Discrete Technology & Production
Automation (DTPA)
University of Groningen
t.li@rug.nl

Ming Li
Department of Electrical Engineering
Eindhoven University of Technology
m.li3@tue.nl

Xiaoyu Liu
Delft Center for Systems and Control
Delft University of Technology
x.liu-20@tudelft.nl

Masahiro Mae
Electrical Engineering and Information Systems
The University of Tokyo
mmae@ieee.org

Asala Mahajna
Discrete Technology and Production Automation
University of Groningen
a.mahajna@rug.nl

Emin Martirosyan
Engineering and Technology Institute Groningen
University of Groningen
e.n.martirosyan@rug.nl

Frederik Baymler Mathiesen
Delft Center for Systems and Control
Delft University of Technology
f.b.mathiesen@tudelft.nl

Maxime Maton
Systems, Estimation, Control and Optimization (SECO)
University of Mons (FPMs)
Maxime.MATON@umons.ac.be

Babak Mehdizadeh Gavgani
Electromechanical, Sys. and Metal Engineering
Ghent University
babak.mehdizadehgavgani@ugent.be

Tomas Meijer
Department of Mechanical Engineering
Eindhoven University of Technology
t.j.meijer@tue.nl

Eva Memmel
DCSC
Delft University of Technology
e.m.memmel@tudelft.nl

Joram Meskens
DecisionS
Flanders Make
joram.meskens@flandersmake.be

Judicaël Mohet
Department of mathematics
University of Namur and naXys
judicael.mohet@unamur.be

Charles Monnoyer de Galland
ICTEAM
UCLouvain
charles.monnoyer@uclouvain.be

Lars Moormann
Control Systems Technology
Eindhoven University of Technology
l.moormann@tue.nl

Sarvin Moradi
Dept. of Electrical Engineering
Eindhoven University of Technology
s.moradi@tue.nl

Wannes Mores
BioTeC+
KU Leuven
jan.vanimpe@kuleuven.be

Christian Mugisho Zagabe
Department of Mathematics
University of Namur
christian.mugisho@unamur.be

Manuel Muñoz Sánchez
Mechanical Engineering
Eindhoven University of Technology
m.munoz.sanchez@tue.nl

Branimir Mrak
MotionS lab
Flanders Make
branimir.mrak@flandersmake.be

M Nijenhuis
Faculty of Engineering Technology
University of Twente
m.nijenhuis@utwente.nl

S.A.N. Nouwens
Mechanical Engineering
TU/e
s.a.n.nouwens@tue.nl

Dora Novak
Laboratoire des Signaux et Systèmes
Université Paris-Saclay
dora.novak@centralesupelec.fr

SINAN OGUZ
IRIDIA
ULB
sinan.oguz@ulb.be

Caio Fabio Oliveira da Silva
Delft Center for Systems and Control
Delft University of Technology
C.F.OliveiradaSilva@tudelft.nl

Tom Oomen
Mechanical Engineering
Eindhoven University of Technology
t.a.e.oomen@tue.nl

YOUNES OUDICH
SAAS
UNIVERSITE LIBRE DE BRUXELLES
pascale.lathouwers@ulb.be

Nick Paape
Mechanical Engineering
Eindhoven University of Technology
n.paape@tue.nl

Wang Pan
CST
TU/e
w.pan@tue.nl

Fabio Paparella
Mechanical Engineering
TU Eindhoven
f.paparella@tue.nl

Pieter Pas
ESAT
KU Leuven
pieter.pas@kuleuven.be

Ralf Peeters
Data Science and Knowledge Engineering
Maastricht University
ralf.peeters@maastrichtuniversity.nl

Dries Peumans
Department ELEC
Vrije Universiteit Brussel
Dries.Peumans@vub.be

MATTHIAS PEZZUTTO
SAAS
UNIVERSITE LIBRE DE BRUXELLES
pascale.lathouwers@ulb.be

Armin Piratehzad
Bernoulli Institute for Mathematics, Computer Science and Artificial Intelligence
University of Groningen
a.pirastehzad@rug.com

Luuk Poort
Dept. of Mechanical Engineering
Eindhoven University of Technology
l.poort@tue.nl

Maurice Poot
Dept. of Mechanical Engineering
Eindhoven University of Technology
m.m.poot@tue.nl

András Retzler
Department of Mechanical Engineering
KU Leuven
andras.retzler@kuleuven.be

V.D. Reyes Dreke
Control System Deparment
Eindhoven University of Technology
v.d.reyes.dreke@tue.nl

Rodolfo Reyes-Báez
Jan C. Willems Center of Systems and Control
University of Groningen
r.reyes.baez@rug.nl

Alessandro Riccardi
Delft Center for Systems and Control
Delft University of Technology
a.riccardi@tudelft.nl

Jhonny Rodrigues
Mechanical Engineering
Faculdade de Engenharia da Universidade do Porto
jsrodrigues@inegi.up.pt

Daniele Ronzani
Mechanical Engineering
KU Leuven
daniele.ronzani@kuleuven.be

Bojana Rosic
MS3
University of Twente
b.rosic@utwente.nl

Edwin Ross
Mathematical and Statistical Methods - Biometris
Wageningen University and Research
edwin.ross@wetsus.nl

Teodor Rotaru
Dept. of Electrical Engineering (ESAT)
KU Leuven
teodor.rotaru@kuleuven.be

Wim Van Roy
Dept. of Mechanical Engineering
KU Leuven
wim.vanroy@kuleuven.be

Anne Rubbens
INMA
Rubbens
anne.rubbens@outlook.be

Ludovico Ruga
Engineering Services
Siemens Digital Industries
ludovico.ruga@siemens.com

Adrian Saldanha
Department of Computer Science
KU Leuven
adrian.saldanha@kuleuven.be

M.B. SALTIK
DTPA
University of Groningen
m.b.saltik@rug.nl

Santiago Sanchez-Escalonilla Plaza
DTPA
University of Groningen
santiago.sanchez@rug.nl

Arijit Sarkar
Discrete Technology and Production Automation
University of Groningen
a.sarkar@rug.nl

Ajay Sathya
Mechanical Engineering
KU Leuven
ajay.sathya@kuleuven.be

Jacquelien Scherpen
DTPA
University of Groningen
j.m.a.scherpen@rug.nl

Maarten Schoukens
Electrical Engineering
Eindhoven University of Technology
m.schoukens@tue.nl

Mathijs Schuurmans
Dept. Electrical Engineering (ESAT-STADIUS)
KU Leuven
mathijs.schuurmans@kuleuven.be

Bram Seinhorst
Department of Mechanics of Solids, Surfaces
& Systems
University of Twente
b.seinhorst@utwente.nl

Busra Sen
Dept. of Mechanical Engineering
Eindhoven University of Technology
b.sen@tue.nl

Jordy Senden
Control Systems Technology
Eindhoven University of Technology
j.p.f.senden@tue.nl

Haik Silm
Departement of Computer Science
KU Leuven
haik.silm@kuleuven.be

Brayan M. Shali
Bernoulli Institute
University of Groningen
b.m.shali@rug.nl

Bardia Sharif
Mechanical Engineering
Eindhoven University of Technology
b.sharif@tue.nl

Shengling Shi
Delft Center for Systems and Control
Delft University of Technology
s.shi-3@tudelft.nl

Taranjitsingh B. Singh
DecisionS
Flanders Make
taranjitsingh.singh@flandersmake.be

Jelle Slief
ESC group
DIFFER
j.h.slief@differ.nl

Sil Spanjer
Mechanics of Solids Surfaces and Systems
University of Twente
s.t.spanjer@utwente.nl

Luuk Spin
Department of Electrical Engineering
Eindhoven University of Technology
l.m.spin@student.tue.nl

M. Steinbuch
ME/CST
Eindhoven University of Technology
m.steinbuch@tue.nl

Zhiyong Sun
Department of Electrical Engineering
Eindhoven University of Technology
z.sun@tue.nl

D. Sun
Delft Center for Systems and Control
Delft University of Technology
D.Sun-1@tudelft.nl

Sutrisno Sutrisno
Bernoulli Institute for Mathematics, Computer Science and Artificial Intelligence
University of Groningen
s.sutrisno@rug.nl

Jan Swevers
Mechanical Engineering
KU Leuven
jan.swevers@kuleuven.be

Paul Tacx
dept mechanical engineering
Eindhoven University of Technology
p.j.m.m.tacx@tue.nl

Sander Thuijsman
Mechanical Engineering
Eindhoven University of Technology
s.b.thuijsman@tue.nl

Koen Tiels
Dept. of Mechanical Engineering
Eindhoven University of Technology
k.tiels@tue.nl

R. Toth
Dept. of Electrical Engineering
Eindhoven University of Technology
r.toth@tue.nl

Matthijs van Berkel
Energy Systems & Control
DIFFER
m.vanberkel@differ.nl

Mathyn van Dael
Mechanical Engineering
Eindhoven University of Technology
m.r.v.dael@tue.nl

Lars van de Kamp
Department of mechanical Engineering
Eindhoven University of technology
l.g.j.v.d.kamp@tue.nl

Bjorn van de Ven
Dept. of Electrical Engineering
Eindhoven University of Technology
bjornvdven@kpnplanet.nl

Bart van den Boorn
Solar Fuels
DIFFER
b.f.h.vandenboorn@differ.nl

Paul Van den Hof
Dept. of Electrical Engineering
Eindhoven University of Technology
p.m.j.vandenhof@tue.nl

Robbert van der Kruk
Mechanical Engineering
Technical University of Eindhoven
r.j.v.d.kruk@tue.nl

C.J. van der Ploeg
Mechanical Engineering
Eindhoven University of Technology
c.j.v.d.ploeg@tue.nl

Wouter van Dijk
Department of Mechanics of Solids, Surfaces & Systems
University of Twente
w.vandijk@utwente.nl

Max van Haren
Mechanical Engineering
Eindhoven University of Technology
m.j.v.haren@tue.nl

Jilles van Hulst
Dept. of Mechanical Engineering
Eindhoven University of Technology
j.s.v.hulst@tue.nl

Ricky van Kampen
Energy Systems and Control
DIFFER
R.J.R.vanKampen@differ.nl

Max van Meer
Dept. of Mechanical Engineering
Eindhoven University of Technology
m.v.meer@tue.nl

Wim Van Roy
Dept. of Mechanical Engineering
KU Leuven
wim.vanroy@kuleuven.be

Roy van Zuijlen
Dept. of Mechanical Engineering
Eindhoven University of Technology
r.a.c.zuijlen@tue.nl

Bastiaan Vandewal
Mechanical Engineering
KU Leuven
bastiaan.vandewal@kuleuven.be

Lukas Vanpoucke
ESAT
KU Leuven
lukas.vanpoucke@kuleuven.be

JJ Verbakel
Mechanical Engineering
Eindhoven University of Technology
j.j.verbakel@tue.nl

J Verbree
ENgineering and TEchnology institute Groningen
University of Groningen
j.verbree@rug.nl

Elise Verhees
Mechanical Engineering
Eindhoven University of Technology
e.d.t.verhees@tue.nl

P. C. N. Verheijen
Dept. of Electrical Engineering
Eindhoven University of Technology
p.c.n.verheijen@tue.nl

Chris Verhoek
Dept. of Electrical Engineering
Eindhoven University of Technology
c.verhoek@tue.nl

Prabhu Vijayan
ELEC
VUB
prabhu.vijayan@vub.be

Maarten Vlaswinkel
Dept. of Mechanical Engineering
Eindhoven University of Technoology
m.g.vlaswinkel@tue.nl

Renzi Wang
STADIUS, ESAT
KU Leuven
rwang@esat.kuleuven.be

BENJAMIN WAUTHION
SAAS
UNIVERSITE LIBRE DE BRUXELLES
pascale.lathouwers@ulb.be

Raphaël Widdershoven
ESAT
STADIUS
raphael.widdershoven@kuleuven.be

Paul Wijnbergen
Bernoulli institute
University of Groningen
p.wijnbergen@rug.nl

Jeroen Willems
DecisionS lab
Flanders Make
jeroen.willems@flandersmake.be

J.J. Winkin
Mathematics
University of Namur
joseph.winkin@unamur.be

Hao Yin
Faculty of Science and Engineering
University of Groningen
hao.yin@rug.nl

Duo Xu
Dept. of Electrical Engineering
Eindhoven University of Technology
d.xu@tue.nl

Lorenzo Zino
Faculty of Science and Engineering
University of Groningen
lorenzo.zino@rug.nl

Alireza Zolanvari
Faculty of science and engineering
University of Groningen
a.zolanvari@rug.nl

Part 4
Organizational Comments

Welcome

The Organizing Committee has the pleasure of welcoming you to the 41^{st} Benelux Meeting on Systems and Control, at ULB, Brussels, Belgium.

Aim

The aim of this meeting is to promote research activities and cooperation between researchers in Systems and Control. It is the forty-first in a series of annual conferences that are held alternately in Belgium and The Netherlands. The meeting is organized by UMons and ULB.

Scientific Program Overview

1. A plenary lecture by David Howey (University of Oxford, UK) on Data-driven battery health diagnosis in real-world applications.

2. A plenary lecture by Nicanor Quijano (Universidad de los Andes, Colombia) on The Role of Population Games and Evolutionary Dynamics in Control.

3. A plenary lecture by Ilya Kolmanovsky (University of Michigan, USA) on Perspectives, Challenges and Opportunities in Control of Systems with Constraints.

4. A Mini-course by Mouhacine Benosman (Mitsubishi Electric Research Laboratories (MERL)) on A hybrid approach to control: classical control theory meets machine learning theory.

5. Contributed short lectures. See the list of sessions for the titles and authors of these lectures.

Directions for speakers

For a contributed lecture, the available time is 20 minutes. Please leave five minutes for discussion and room changes, and adhere to the indicated schedule. In each room beamers are available. When using a beamer, you have to provide a notebook yourself and you have to start your lecture with the notebook up and running and the external video port switched on.

Registration

The registration fee includes:

- Admission to all sessions.
- The final programme and plenaries booklet.
- Coffee and tea during the breaks.
- In the case of an accommodation arrangement: lunch and dinner on Tuesday, breakfast, lunch, and dinner on Wednesday, and breakfast and lunch on Thursday.
- In the case of a "one day" arrangement: lunch, reception and dinner on Tuesday, lunch and dinner on Wednesday, and lunch on Thursday.
- Free use of a wireless Internet connection (WiFi) wherever technically available.

The registration fee does not include:

- Cost of phone calls
- Special ordered drinks during lunch, dinner, in the evening, etc.

Organizing Committee

The Organizing Committee of the 41^{st} Benelux Meeting consists of

- Alain Vande Wouwer
  UMons
- Michel Kinnaert
  ULB
- Emanuele Garone
  ULB
- Laurent Dewasmes
  UMons
- Guilherme A. Pimentel
  UMons
- Erjen Lefeber
  TU/e
- Pascale Lathouwers
  ULB
- William Van Hoeck
  UMons
- Laurent Catoire
  ULB

Scientific Committee

The Scientific Committee of the 41st Benelux Meeting consists of

- Pierre-Antoine ABSIL
  UCLouvain
- Bart DE SCHUTTER
  TUDelft
- Julien HENDRICKX
  UCLouvain
- Clara IONESCU
  UGent
- Karel KEESMAN
  WUR
- John LATAIRE
  VUB
- Mia LOCCUFIER
  UGent
- Ivan MARKOVSKY
  VUB
- Alexandre MAUROY
  UNamur
- Wim MICHIELS
  KULeuven
- Henk NIJMEIJER
  TU/e
- Jacquelien SCHERPEN
  RUG
- Jan SWEVERS
  KULeuven
- Paul VAN DEN HOF
  TU/e
- Arjan VAN DER SCHAFT
  RUG
- Jan VAN IMPE
  KULeuven
- Holger VOOS
  UNI LU
- Steffen WALDHERR
  KULeuven
- Joseph WINKIN
  UNamur

Sponsor

The meeting is supported by the following organizations:

- Fonds de la Recherche Scientifique - FNRS
- Fondation Wiener Anspach
- UMons/SECO
- ULB

Conference location

The address of ULB is

Université Libre de Bruxelles
Campus du Solbosch, Bâtiment U
Brussels - Belgium

Best Junior Presentation Award

Continuing a tradition that started in 1996, the 41st Benelux Meeting will close with the announcement of the winner of the Best Junior Presentation Award. This award is given for the best presentation, given by a junior researcher, and it consists of a trophy that may be kept for one year and a certificate. The award is specifically given for quality of presentation rather than quality of research, which is judged in a different way. At the meeting, the chairs of sessions will ask three volunteers in the audience to fill out an evaluation form. After the session, the evaluation forms will be collected by the Prize Commissioners who will then compute a ranking. The winner will be announced on Thursday, July 7, in room UB5.132, at 13:00. The evaluation forms of each presentation will be returned to the junior researcher who gave the presentation. The Prize Commissioners are Dr. Mihaela Sbarciog and Prof. Maarten Schoukens.

The organizing committee counts on the cooperation of the participants to make this contest a success.

Website

An electronic version of the Book of Abstracts can be downloaded from the Benelux Meeting website.

Tuesday July 5, 2022

11:00 - 11:20	Coffee						
11:20 - 11:25	UB5.132 *Welcome and Opening*						
11:30 - 12:30	UB5.132 Plenary 1 : Ilya Kolmanovsky *Perspectives, Challenges and Opportunities in Control of Systems with Constraints*						
12:30 - 14:00	Lunch						
Room TuP	UB5.132 TuP01 *System Theory 1*	UB5.230 TuP02 *System Ident. 1*	UB4.132 TuP03 *Energy 1*	UB4.136 TuP04 *Robotics 1*	UB2.147 TuP05 *Koopman Operator-Deep Learning*	UB4.151 TuP06 *State Observers 1*	UA4.222 TuP07 *Optimization 1*
14:00 - 14:20	Banse	Peeters	Koenders	Kruk	Iacob	Ross	Astudillo
14:20 - 14:40	Engelaar	Tiels	Singh	Tinghua Li	Zagabe	Geelen	Widdershoven
14:40 - 15:00	Appeltans	Foster	Dreke	Herranz	Beintema	Meijer	Van Roy
15:00 - 15:20	Pirastehzad	Ebrahimkhani	Couto	Verhees	Verhoek	Beumer	Heuts
15:20 - 15:40	Wijnbergen	Tacx	Goldar	Gavgani	Retzler	Keijzer	Borsboom
15:40 - 16:10	Coffee Break						
Room TuE	UB5.132 TuE01 *Med. Bio. Sys 1*	UB5.230 TuE02 *Data Driven Tech.*	UB4.132 TuE03 *Process Control*	UB4.136 TuE04 *Learning-Based Ctrl 1*	UB2.147 TuE05 *System Theory 2*	UB4.151 TuE06 *Vehicles 1*	UA4.222 TuE07 *Electromechanical Appl. 1*
16:10 - 16:30	Maton	Schuurmans	Chernev	Moradi	Shali	Oguz	Wauthion
16:30 - 16:50	Rossello	Rojas	Meskens	Plaza	Farnam	Novak	Dael
16:50 - 17:10	Sonveaux	Vlaswinkel	Carrasquer	Bolderman	Sarkar	Delansnay	Thuijsman
17:10 - 17:30	Boorn	Poot	Busschaert	Aarnoudse	Haren	Bos	Moormann
17:30 - 17:50	Frieswijk	Coppens	Paape	Kikken	Lagauw	Acerbo	Silm
17:50 - 18:10	Joubert	Verheijen	Liu	Sun	Vanpoucke	Ruga	Jacobs
18:10 - 18:30				Ghanipoor		Archila	Keyvanara
18:40 - 19:40	Reception						
19:45 - 21:45	Dinner						

Wednesday July 6, 2022

Room	UB5.132	UB5.230	UB4.132	UB4.136	UB2.147	UB4.151	UA4.222
WeP	WeP01	WeP02	WeP03	WeP04	WeP05	WeP06	WeP07
	Optimal Control 1	*Interconnected Sys.*	*Nonlinear Control*	*Learning-Based Control 2*	*Robotics 2*	*Vehicles 2*	*Optimization 2*
9:00 - 9:20	Gul	Riccardi	Meer	Pan	Gillis	Hegde	Galland
9:20 - 9:40	Spin	Hosseinalizadeh	Reyes-Baez	Hulst	Dang	Gharavi	Astudillo
9:40 - 10:00	Xu	Poort	Sharif	Saltik	Dirckx	Fransen	Rubbens
10:00 - 10:20	Zolanvari	Janssen	Beck	Ronzani	Sen	Jordens	Bousselmi
10:20 - 10:40	Mrak	Huijzer	Huijgevoort	Garg	Senden	Geurts	Kiessling
10:40 - 11:00	Dang	Fonken	Ming Li	Airaldi	Pezzutto	Hanselaar	Colla
11:00 - 11:30	Coffee Break						
11:30 - 12:30	UB5.132 Plenary 2 : David Howey *Data-driven battery health diagnosis in real-world applications*						
12:30 - 14:00	Lunch						
14:00 - 15:30	UB5.132 Mini-course 1: Mouhacine Benosman *A hybrid approach to control: classical control theory meets machine learning theory*						
15:30 - 16:00	Coffee Break						
Room	UB5.132	UB5.230	UB4.132	UB4.136	UB2.147	UB4.151	UA4.222
WeE	WeE01	WeE02	WeE03	WeE04	WeE05	WeE06	WeE07
	Optimal Control 2	*System Identification 2*	*Med. Bio Sys. 2*	*Learning-Based Control 3*	*Game Theory*	*Vehicles 3*	*Optimization 3*
16:00 - 16:20	Dang	Shi	Bhonsale	He	Evens	Mathiesen	Paparella
16:20 - 16:40	Depraetere	Vijayan	Katsini	Kon	Jin	Allamaa	Chaouach
16:40 - 17:00	Haasjes	Gulina	Lara	Willems	Ningbo Li	Sánchez	Mores
17:00 -17:20	Florez	Akan	Nouwens	da Silva	Zino	Jeong	Rodrigues
17:20 - 17:40	Bosman	Kruijver	Kamp	Mae	Chen	Gosar	Pas
17:40 - 18:00	Vandewal	Memmel	Huet	Hayati	Martirosyan	Verbree	Rotaru
18:00 - 18:15	Break						
18:15 - 19:15	UB5.132 In memoriam Rik Pintelon						
19:30 - 21:00	Dinner						

Thursday July 7, 2022

9:00 - 10:30	UB5.132 Mini-course 2: Mouhacine Benosman *A hybrid approach to control: classical control theory meets machine learning theory*					
10:30 - 10:50	Coffee Break					
Room ThP	UB5.132 ThP01 *Electromechanical Appl. 2*	UB5.230 ThP02 *System Indetification 3*	UB4.132 ThP03 *Energy 2*	UB4.136 ThP04 *Mechatronics*	UB2.147 ThP05 *Vibration*	UB4.151 ThP06 *State Observers 2*	UA4.222 ThP07 *Switched Systems*
10:50 - 11:10	Lakkis	Kampen	Clemente	Chan-Zheng	Saldanha	Mohet	Yin
11:10 - 11:30	Oudich	Slief	Le Roux	Classens	Spanjer	Dijk	Adams
11:30 - 11:50	Broens	Kivits	de Ven	Ambrosino	Seinhorst	Ploeg	Sutrisno
11:50 - 12:00	Break						
12:00 - 13:00	UB5.132 Plenary 3: Nicanor Quijano *The Role of Population Games and Evolutionary Dynamics in Control*						
13:00 - 13:15	UB5.132 *Announcement of the Best Junior Presentation Prize & Closure of the 41st Benelux Meeting*						
13:15 - 14:30	Lunch						

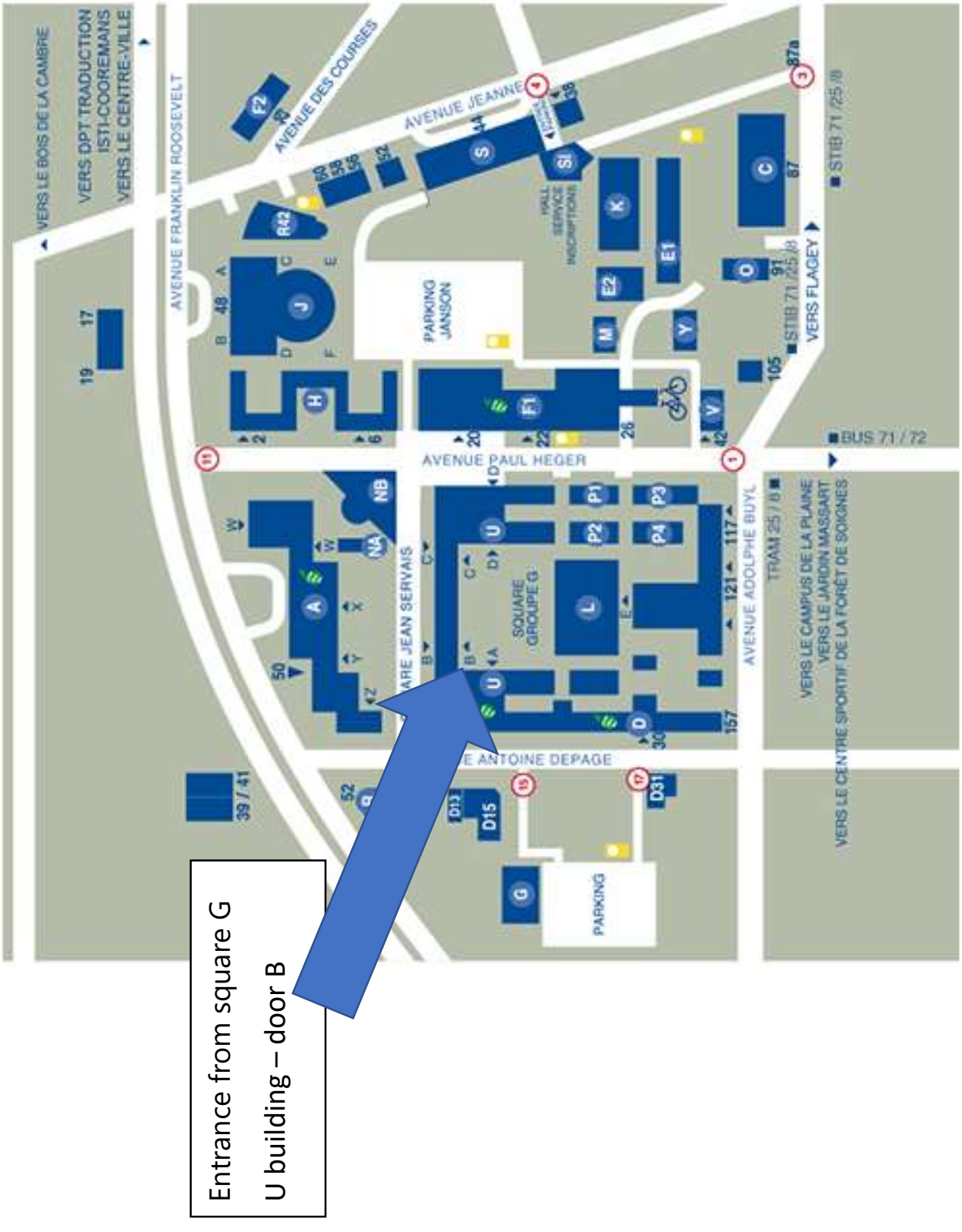
VERS LE BOIS DE LA CAMBRE
VERS DPT TRADUCTION ISTI-COOREMANS
VERS LE CENTRE-VILLE
AVENUE FRANKLIN ROOSSEVELT
AVENUE DES COURSES
AVENUE JEANNE
PARKING JANSON
AVENUE PAUL HEGER
AVENUE ADOLPHE BUYL
SQUARE GROUPE G
PARKING
VERS FLAGEY
BUS 71 / 72
STIB 71 /25 /8
TRAM 25 / 8
VERS LE CAMPUS DE LA PLAINE
VERS LE JARDIN MASSART
VERS LE CENTRE SPORTIF DE LA FORÊT DE SOIGNES
Entrance from square G
U building – door B

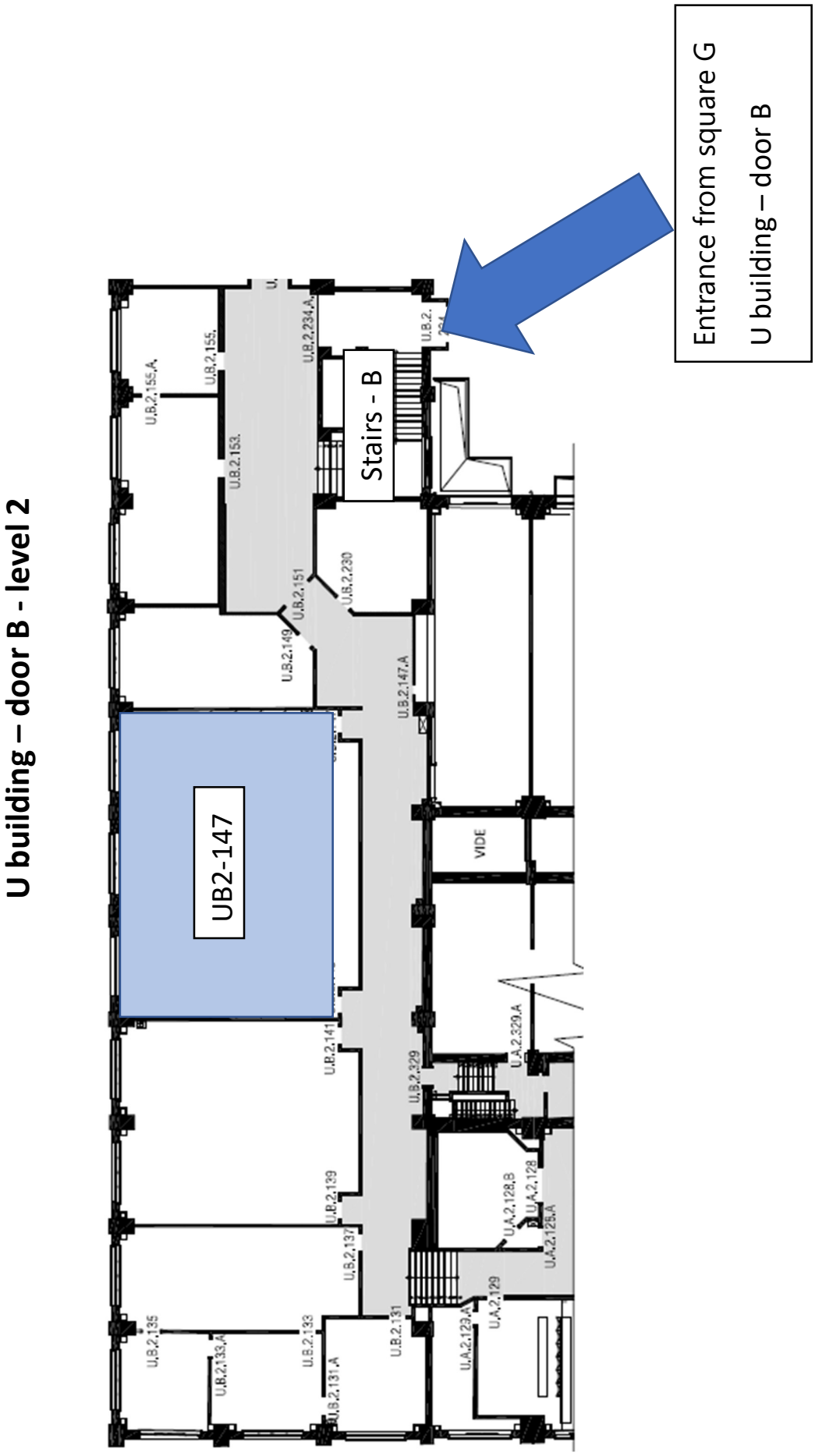
U building – door B - level 2
Entrance from square G
U building – door B
Stairs - B
UB2-147
VIDE
U.B.2.155.A
U.B.2.155.
U.B.2.153.
U.B.2.234.A
U.B.2.230
U.B.2.151
U.B.2.149
U.B.2.147.A
U.B.2.141
U.B.2.139
U.B.2.137
U.B.2.135
U.B.2.133.A
U.B.2.133
U.B.2.131.A
U.B.2.131
U.B.2.329
U.A.2.329.A
U.A.2.128.B
U.A.2.128
U.A.2.128.A
U.A.2.129
U.A.2.129.A

U building – door B - level 4

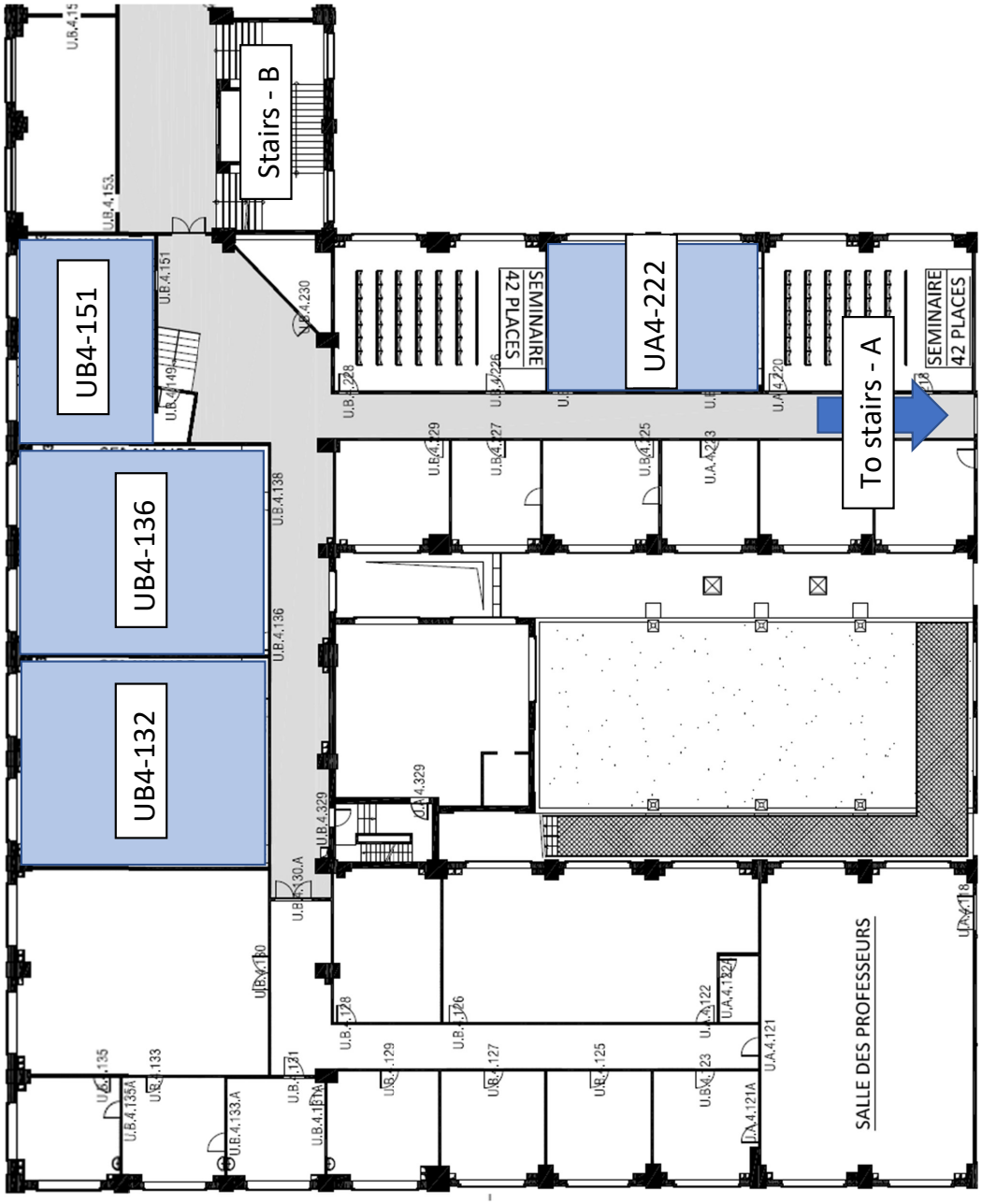

U building – door B - level 5

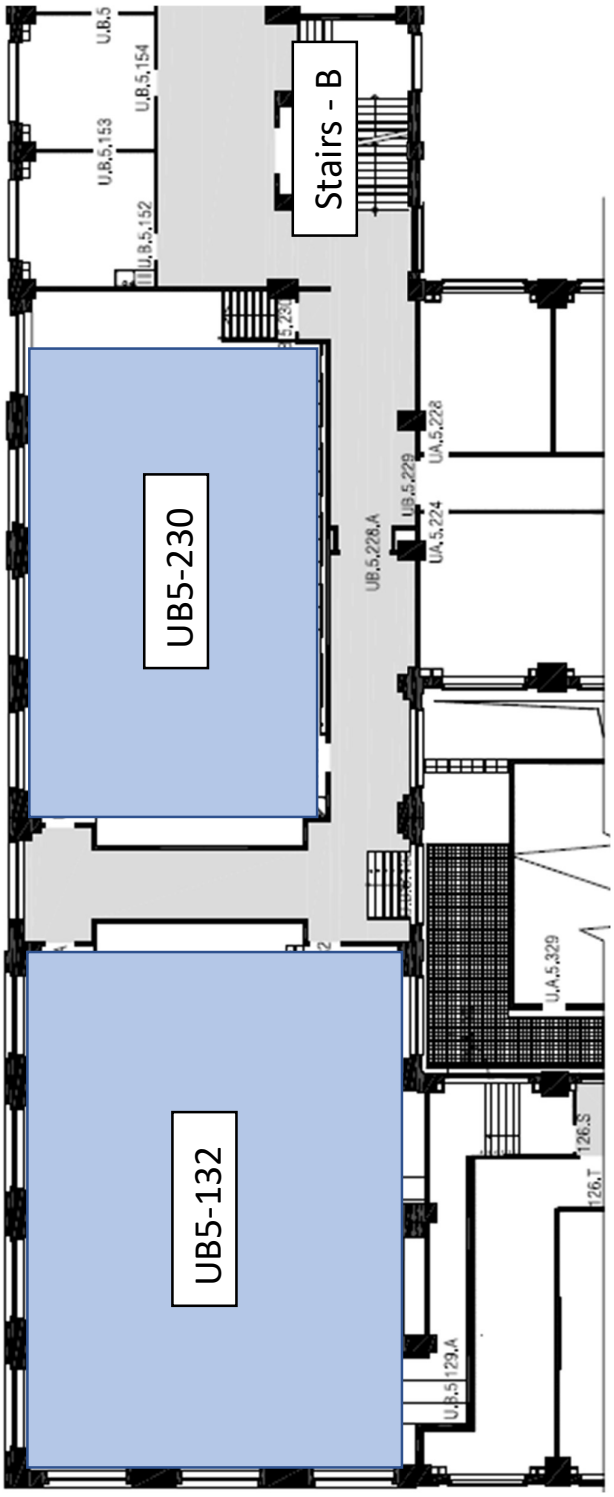

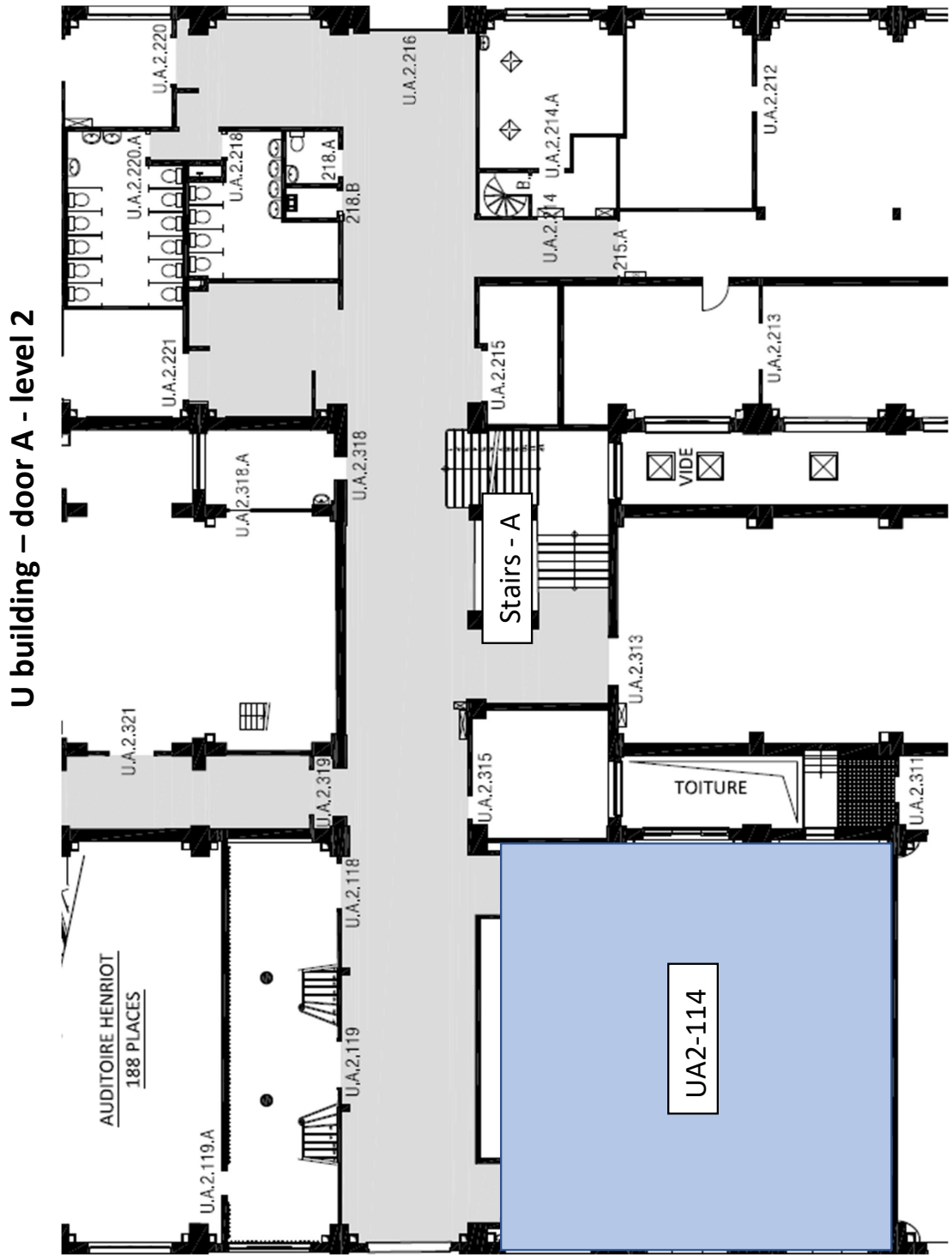
U building – door A - level 2
U.A.2.220
U.A.2.220.A
U.A.2.218
218.A
218.B
U.A.2.216
U.A.2.214.A
U.A.2.212
215.A
U.A.2.221
U.A.2.215
U.A,2.213
U.A.2.318.A
U.A.2.318
VIDE
Stairs - A
U.A.2.313
U.A.2.321
U.A.2.319
U.A.2.315
TOITURE
U.A.2.311
U.A.2.118
AUDITOIRE HENRIOT
188 PLACES
U.A.2,119
U.A.2.119.A
UA2-114